IDENTIFICATION	REVISION
FS1-0014159	11.0

Framatome Fuel

TOTAL NUMBER OF PAGES: 636

Framatome TN-B1
Docket No. 71-9372
Safety Analysis Report

ADDITIONAL INFORMATION:

This is the non-proprietary version of FS1-0014159-11.0

PROJECT	
HANDLING	None
CATEGORY	TEP - Technical Report
STATUS	

DISTRIBUTION TO	PURPOSE OF DISTRIBUTION

This document is electronically approved. Records regarding the signatures are stored in the fsanpexp Documentum docbase. Any attempt to modify this file may subject employees to civil and criminal penalties.

EDRMS object Id. : **0901216781515030**
Released date (Western EU time) : **2023/01/31 15:37:30**

Role	Name	Date (YYYY/MM/DD)	Organization
Writer	**FLANAGAN Bryan**	**2023/01/31 01:32:15**	**Framatome Inc.**
Reviewer	**MANNING Calvin**	**2023/01/31 01:40:06**	**Framatome Inc.**
Reviewer	**ELLIOTT Kevin**	**2023/01/31 01:44:56**	**Framatome Inc.**
Approver	**TATE Timothy**	**2023/01/31 15:37:30**	**Framatome Inc.**

RELEASE DATA:

SAFETY RELATED DOCUMENT: Y

CHANGE CONTROL RECORDS:
This document, when revised, must be reviewed or approved by following regions:
France: N
USA: Y
Germany: N

REVISIONS

REVISION	DATE	EXPLANATORY NOTES
11.0	See 1st page release date	Revised document to increase enrichment to less than or equal to 8.0 wt.% ^{235}U. Section 1.1, Identified higher enrichment value within introduction. Section 1.2, Identified two enrichment ranges within package description. Section 1.2.1.2.3, Included varying size and quantity of vibroisolator rubber for vibration performance (per drawing FS1-0042700-2.0 change). Section 1.2.3, Identified the two enrichment ranges within the package contents. New Table 1-4 for higher enrichment content. Renumbered tables in Section 1.0 Expanded Table 1-5 to include higher enrichment content. New Table 1-6 for Gadolinia content requirements. Section 1.2.3.4.1, editorial clarification in reference to Table 1-7. Section 1.4.1.1, drawings, replaced 105E3739 Rev. 4 with FS1-0042699-1.0 to allow multiple rubber options (see revision 10 changes) and new number and layout reflects current drawing standards. FS1-0042700-2.0 revised to include new Note 4 regarding optional vibroisolator size and quantity to optimize vibration absorption options. Section 2.11, added discussion for higher enrichment content and new 17x17 Type 3 PWR fuel rod criteria. Section 3.1.2, added discussion of decay heat for the new contents and a new Table 3-1. Revised table numbering in Section 3. Section 4.2.2, updated leak rate information with higher enrichment contents. Section 4.4, updated leak rate information with higher enrichment contents. Section 5.0, included a shielding discussion for the higher enrichment contents. Section 6.0, added description for the location of the various criticality evaluations. Section 6.1, included the ≤ 8.0 wt.% ^{235}U description and information in Tables 6-1 and 6-2. Table 6-2, added missing loose rod information for CANDU and generic PWR rods. Added new column for PWR 17x17 Type 3 rods. Table 6-3, new section added for the ≤ 8.0 wt.% ^{235}U configurations.

REVISION	DATE	EXPLANATORY NOTES
11.0 continued		Section 6.1.3, additional CSI values included for the ≤ 8.0 wt.% ^{235}U configurations Section 6.2 and Table 6-5, included the ≤ 8.0 wt.% ^{235}U information. Section 6.12, Clarified section heading and first paragraph as applying to ≤ 5.0 wt.% ^{235}U. New Section 6.13 added as an appendix for the ≤ 8.0 wt.% ^{235}U evaluation. Red change text and change bars not included in margin for this section for clarity. Section 6.15 renumbered and included additional references from new Section 6.13.
10.0	1/27/2022	Section 1.4, Updated multiple drawings to include optional use of synthetic rubber within inner container and shock isolation system and make some exterior rubber parts optional. Allow material options (rubber or neoprene) for inner and outer container gaskets. Revised drawings updated to current Framatome drafting standards. Sections 1.2.1, 1.2.1.1, 2.2.1, 2.2.2.1, 3.5, and 7.4, included rubber in discussion of the polyethylene foam used in the inner container. Removed the term “natural” from natural rubber to imply all rubber material as applicable. Section 2.2.2, Updated material reactions associated with multiple rubber types to show no excessive corrosion will occur. Section 2.6.5, Added discussion for vibration isolation rubber material and inner container cushioning material changes with no effect to package performance. Section 2.12.3, Added note for synthetic rubber having no effect on the sealing ability of the package. Section 6, Updated criticality evaluation for the following items: • Fuel assembly orientation within the package • Increased fuel channel side thickness to ≤ 0.320 cm • SCALE code errors for H1-Poly cross section • Added consideration of material change (rubber) for inner container liner • Added explicit consideration of preferential flooding in the NCT array configuration • Criticality safety index was revised. Tables 6-3 and 6-59, Updated results for multiple criticality cases.

REVISION	DATE	EXPLANATORY NOTES
10.0 continued		Tables 6-1 and 6-56, Updated 11x11 fuel channel side thickness to ≤ 0.320 cm. Sections 6.1.3 and 6.12.1.3, Updated CSI evaluations. 11x11 fuel assembly CSI is now 1.5. Section 6.12, added clarification that the 0.320 cm fuel channel thickness and additional items are evaluated in Section 6.12.11. Section 6.12.1.2, Updated limiting array sizes for 11x11 fuel assemblies. Section 6.12.11, New section documenting additional criticality analyses mentioned in Section 6 above. Section 6.13, Added two references.
9.0	2/14/2019	Changed the document to Proprietary for drawings in Section 1.4.1.1 Section 1.2.1, first paragraph, clarified the packaging containment boundary. Section 1.2.3.3 • First paragraph. Clarified maximum enrichment of 5 wt% ^{235}U. • Second paragraph. New paragraph clarifying the use of sintered pellet additives.
8.0	3/27/2018	Update template and company name.
		Section 1.2.2 • First paragraph. Updated fuel rod end closure verification methods. • First paragraph. Clarified maximum fuel rod internal pressure limits. • Second paragraph. Clarified that bounding cladding parameters are used for the safety analysis evaluations.
		Sections 2.6.1.1, 3.1.4 and 3.4.2, first paragraph, clarified the fuel rod design parameters reported for NCT.
		Section 3.1.4, second paragraph, clarified that the maximum fuel rod internal pressure at HAC was used for determining the limiting cladding stress to evaluate the maximum allowed pressure for all rod types.
		Section 4.1.1 • Second paragraph. Revised the second sentence to remove X-ray inspection and ultrasonic testing; these techniques are no longer used to inspect rod closure welds. • Third paragraph. Completely rewritten to add the specific inspection techniques used for qualifying of 11x11 fuel rod welds.

REVISION	DATE	EXPLANATORY NOTES
8.0 continued		• Fourth paragraph. New to add the specific inspection techniques used for in-process inspection of 11x11 fuel rod welds. Also the reference to ASTM B811 13 was removed. ASTM B811 13 is applicable to burst testing cladding, Framatome uses a proprietary burst test to verify the integrity of sample closure rod closure welds. • Fifth paragraph. New, added the burst test frequency. • Sixth paragraph. New, added the critical welding parameters that are monitored. • Seventh paragraph. Revised last sentence to clarify that it applies to each individual rod of any design.
		Section 4.7 Add References 1 and 2
		Section 6.12.6.1, last paragraph corrected typographical error.
		Section 8.2.2 • This section was completely rewritten to include the rod welding qualification inspection and in-process inspection requirements for the 11x11 fuel rods from Section 4.1.1 per the NRC's request.
		Section 8.4 Added References 1 and 2.
7.0	12/21/2017	Section 2.6.9 • Corrected typographical error.
		Section 3.2.2 Corrected typographical error of three occurrences where the Fahrenheit temperatures do not have the degree symbol (°)
		Section 4.4 • Section header changed typographical error.
		Section 6 • Updated Table 6-3 • Updated Table 6-59 • Additional changes were made on pages 402, 414, 415, 424, 461, and 469 to support the changes in Table 6-3 and Table 6-59 • Page 506, format change to Reference 20 These changes were made in response to a NRC RAI
		Section 8.2.2 paragraph was revised to provide a description of the qualification and acceptance tests for the ATRIUM 11 fuel rod and end caps in response to a NRC RAI.

REVISION	DATE	EXPLANATORY NOTES
6.0	8/31/2017	Section 1 • Section 1. Line four in first paragraph change page number for Glossary of Terms and Acronyms from “15” to “23” • Section 1.2 Line two in first paragraph changed “real” to “distinct” and in first line of fifth paragraph added “are” • Section 1.2.3. Deleted “primarily as” and “and U_3O_8” in fourth sentence of first paragraph. • Table 1-3 Corrected footnote 1
		Section 2 • Corrected Figure 2-13 number to Figure 2-12 and renumbered subsequent figure numbers. • Section 2.7.4.1. Corrected typographic error
		Section 3 • Section 3.4.2. Corrected number to "1.1145" in first sentence • Section 3.5.2. Correct typographic error in third paragraph • Section 3.5.3.2. Changed "perfect" to "ideal" in third sentence of first paragraph and changed "psia" to "psi" in second equation on page 167 • Table 3-5 Updated table and Note
		Section 4 • Section 4.1.1. Update to section • Section 4.2.2. Numbers changed • Section 4.4. Numbers changed and added sentence to fourth paragraph
		Section 6 • Table 6-3 Updated “Fuel Assembly Package Array HAC” information and added new footnote a and renumbered existing footnote to b • Table 6-59 Updated “Fuel Assembly Package Array HAC” information and added new footnote a and renumbered existing footnote to b

REVISION	DATE	EXPLANATORY NOTES
6.0 continued		Section 6 • Table 6-3 Updated "Fuel Assembly Package Array HAC" information and added new footnote a and renumbered existing footnote to b • Table 6-59 Updated "Fuel Assembly Package Array HAC" information and added new footnote a and renumbered existing footnote to b • Section 6.12.3.1.1. added "(single package)" to bullet item eight and added bullet item nine. Updated last two paragraphs in this section on page 402 • Figure 6-52 added "5 wt%" to captions for first two figures and added "5 wt% (NCT, HAC single package)" caption to third figure and added fourth figure with caption "3.3 wt% (HAC package array)" • Section 6.12.3.2. Updated second and fourth paragraph • Table 6-60 Added footnotes a and b • Updated bullet five on page 414 • Section 6.12.3.4.1. Updated number in last paragraph • Section 6.12.3.5.11. Added last paragraph on page 426 • Table 6-79 Added last row to table and footnote a • Section 6.12.4.1. Added new last paragraph on page 460 • Section 6.12.4.2. Added new last paragraph on page 461 • Section 6.12.5.1. Added "with axial uniform enrichment" in second paragraph and added last paragraph on page 466 • Section 6.12.6.1. Added "for the uniform axial enrichment" to last bullet item, added "with uniform axial enrichment" to second, and fourth paragraph; fifth paragraph deleted "worst" from the second and third sentence and fourth sentence; and added new last paragraph (all changes on page 468) • Section 6.12.10.1. added reference to Section 6.12.3.2. and Table 6-60 Section 6.12.10.2. added reference to Section 6.12.3.2. and Table 6-60
5.0	2/15/2017	Section 1.2.3.4.7. "Fuel Rods in a Protective Case" – changed "polyethylene" to "polyurethane" to reflect actual configuration. Corrections to Tables 6-1, 6-56, and 6-61. Sections 7.1.2.4. and 7.1.2.6. paragraph 3 added"11x11 or".
4.0	11/17/2016	Section 1 • Section 1.2.3 "Contents" Added 11x11 arrays. • Table 1-2 Updated to include Type 11x11. Table reformatted to improve readability. • Table 1-3 Updated to reflect the higher uranium dioxide weight of a 11x11 fuel assembly. • Table 1-4 Updated to reflect an 11x11 fuel assembly. • Section 1.2.3.4.7 "Fuel Rods in a Protective Case" – changed "polyurethane" to "polyethylene" to reflect actual configuration. • Table 1-5 Deleted as information is available in other tables and sections.

REVISION	DATE	EXPLANATORY NOTES
4.0 continued		• Table 1-5 Added “and Zirconium alloy” to the list of structural material for nuts to reflect current fuel assembly designs. • Section 1.41. The pages for the drawings on these pages were changed to a 11x17 size in order to improve readability. The drawings are unchanged from revision 3.
		Section 3 • Table 3-5 was updated to include the ATRIUM 11 and updated other designs to the current limiting design requirements. Section 6 Added Appendix B, Section 6.12, for the criticality analysis of 11x11 fuel assemblies and rods Other Changes Include: • Table 6-1, replaced theoretical density limit with a gram density, added 11x11 fuel assembly information • Table 6-2, replaced theoretical density limit with a gram density, added 11x11 fuel rod information • Section 6.1.1.1, added an option for using 9 pcf foam for the FANP 10x10 and 11x11 assemblies • Table 6-3, added the 11x11 fuel assembly and rod results • Table 6-4, added the 11x11 fuel assembly information • Section 6.1.3, added headers for clarification • Table 6-41, corrected typographical error • Table 6-44, corrected typographical error • Table 6-48, corrected typographical error • Table 6-51, corrected typographical error • Table 6-54, corrected typographical error
3.0	4/2/2014	Revisions in Sections 1.2.3.4.6 and 1.2.3.4.7 have been changed in response to a NRC RAI.
		Revisions in Section 2.5.1 have been changed in response to a NRC RAI.
		Correction in Table 6-8 have been changed in response to a NRC RAI.
		Revisions in Section 8.1.2 have been changed in response to a NRC RAI.
2.0	3/14/2014	Added 3 figures on pages 49, 50, and 51p per NRC RAI.
1.0	1/28/2014	New document

SIGNATURE BLOCK

Name and Title/Discipline	Document Role	P/LP, R/LR, A-CRF, A	Pages/Sections Prepared/Reviewed/ Approved or Comments
Bryan Flanagan	Lead Author	LP	All
Kevin Elliott	Lead Reviewer	LR	All
Calvin Manning	Reviewer	R	All
Timothy Tate	Approver	A	All

Note: P/LP designates Preparer (P), Lead Preparer (LP)
R/LR designates Reviewer, Lead Reviewer (LR)
A-CRF designates Project Manager Approver of Customer Required Format (A-CRF)
A designates Approver/RTM – Verification of Reviewer Independence

TABLE OF CONTENTS

LIST OF TABLES

LIST OF FIGURES

Glossary of Terms and Acronyms

ASME – American Society of Mechanical Engineers

ASME B&PVC – ASME Boiler and Pressure Vessel Code

ASNT – American Society for Non-destructive Testing

CG – Center of Gravity

CTU – Certification Test Unit

BWR – Boiling Water Reactor

HAC – Hypothetical Accident Condition

IC – Inner Container

IC Inner Thermal Insulator (Aluminum Silicate) – The Alumina Silicate thermal insulation between the inner and outer walls of IC container to provide added margin to criteria set forth for HAC fire condition in 10 CFR 71.73(c)(4)

IC Lid – The lid of the inner container

IC Body – The body of the inner container consisting of the outer wall the thermal insulation, the inner wall, the polyethylene liner and the shock absorbing system along with the fuel securement system

JIS – Japanese Industrial Standards

JSNDI – Japanese Society for Non-destructive Inspection

LDPE – Low Density Polyethylene

NCT – Normal Conditions of Transport

NDIS – Non-destructive Inspection Society

OC – Outer Container

OC Body – The assembly consisting of the OC lower wall, and the internal shock absorbing material

OC Lid – The lid for the outer container.

Packaging – The assembly of components necessary to ensure compliance with packaging requirements as defined in 10 CFR 71.4. Within this SAR, the packaging is denoted as the TN-B1 packaging

Package – The packaging with its radioactive contents, as presented for transportation as defined in 10 CFR 71.4. Within this SAR, the package is denoted as the TN-B1 package.

Payload – Unirradiated fuel assemblies and fuel rods.

RAM – Radioactive Material

SAR – Safety Analysis Report (this document)

TI – Transport Index

USL – Upper Safety Limit

1. GENERAL INFORMATION

This chapter of the Safety Analysis Report (SAR) presents a general introduction and description of the TN-B1 package. The major components comprising the TN-B1 package are presented in Figure 1-1 through Figure 1-4. Detailed drawings presenting the TN-B1 packaging design are included in Appendix 1.4.1. Terminology and acronyms used throughout this document are presented in the Glossary of Terms and Acronyms on page 25. This package is intended to be used to transport Boiling Water Reactor (BWR) fuel assemblies containing both Type A and Type B fissile material.

1.1. INTRODUCTION

The model TN-B1 package is derived from the RAJ-II package (NRC CoC 9309) and has the same structural design. The only distinct difference between the TN-B1 and the RAJ-II will be the allowed contents.

The model TN-B1 package has been developed to transport unirradiated fuel for Boiling Water Reactors. The cladding of the fuel provides the primary containment for the radioactive material. The inner and outer containers provide both thermal protection as well as mechanical protection from drops or accident conditions. There are two ^{235}U enrichment ranges analyzed separately which greatly affect the criticality evaluations. Chapter 6 details the criticality evaluations as they are presented for multiple designs. Section 6.12 evaluates the 11x11 fuel assembly array with an enrichment value up to and including 5.0 weight percent ^{235}U. Section 6.13 evaluates the 11x11 fuel assembly array and loose rod configuration for an enrichment value up to and including 8.0 weight percent ^{235}U. The differences between these ranges are thoroughly discussed throughout this document.

The integrity of the fuel is maintained by the protective outer package, the insulated inner package and the fuel rod cladding through both Normal Conditions of Transport (NCT) and Hypothetical Accident Conditions (HAC) deformations. A variety of full-scale engineering development tests were included as part of the certification process. Ultimately, two full-scale Certification Test Units (CTUs) were subjected to a series of free drops and puncture drops.

The payload within each TN-B1 package consists of a maximum of two unirradiated Boiling Water Reactor (BWR) fuel assemblies or individual rods (BWR, Uranium Carbide, or generic Pressurized Water Reactor (PWR)) contained in a cylinder, protective case or bundled together and positioned in one or both sides of the inner container. See Table 6-1 TN-B1 Fuel Assembly Loading Criteria. See Table 6-2 TN-B1 Fuel Rod Loading Criteria. The containment is provided by the leak tested cladding making up the fuel rods.

The shielding and criticality assessments are provided in Chapter 5.0 and Chapter 6.0. The Criticality Safety Index (CSI) for the TN-B1 package is defined in Chapter 6.0.

The TN-B1 package is designed for shipment by truck, ship, or rail as either a Type B(U) fissile material or Type A fissile material package per the definition in 10 CFR 71.4 and 49 CFR 173.403.

Dimensions of the packaging identified in the text, tables, figures, etc. of this SAR, are intended to be nominal. The drawings provided in Appendix 1.4.1 contain the dimensions and the tolerances.

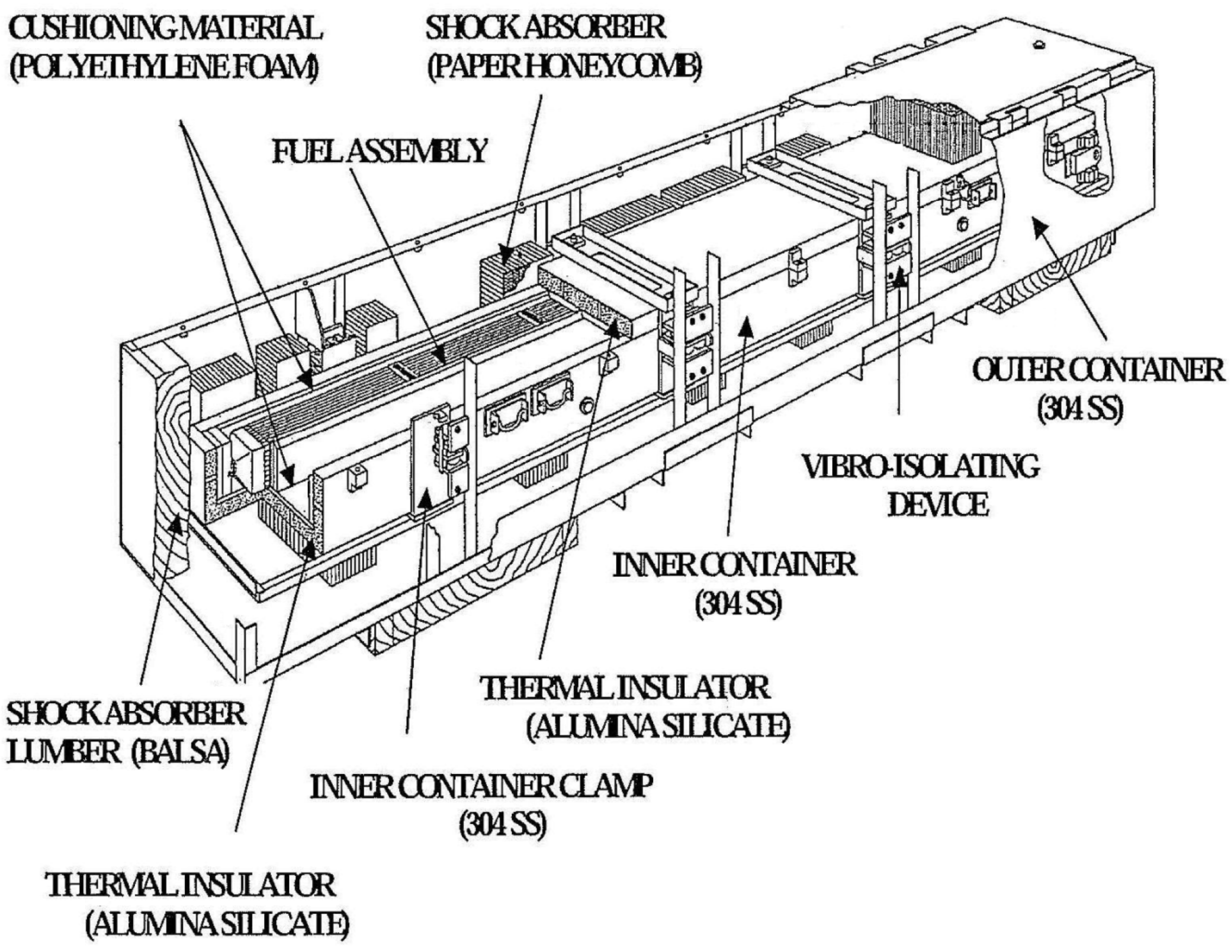

Figure 1-1 TN-B1 PACKAGE ASSEMBLY

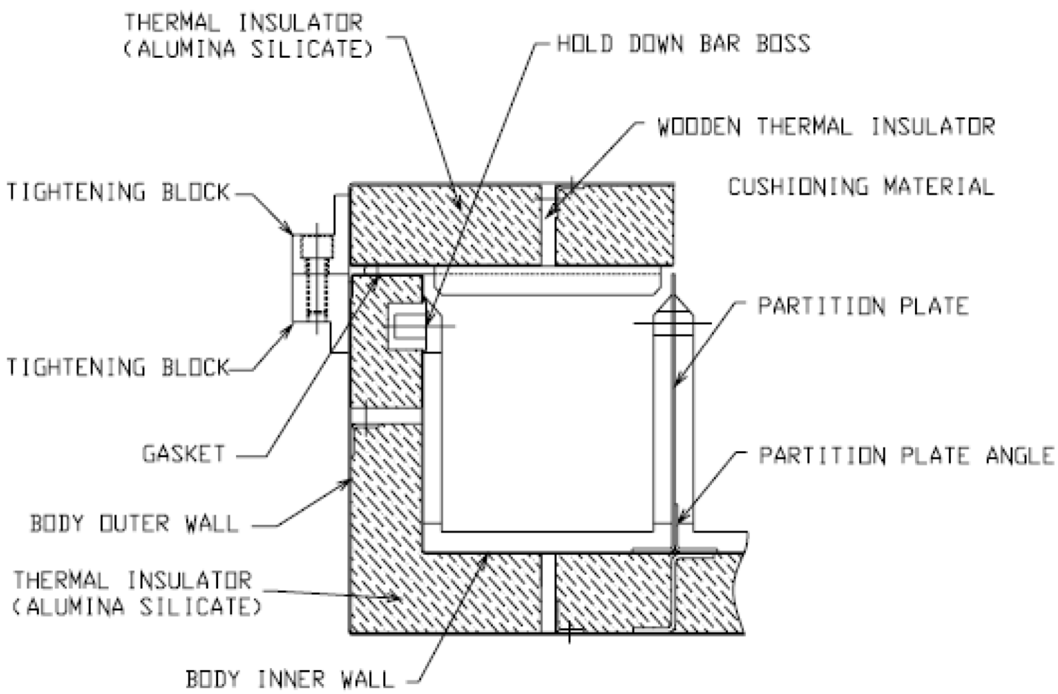

Figure 1-2 Cross-Section of Inner Container

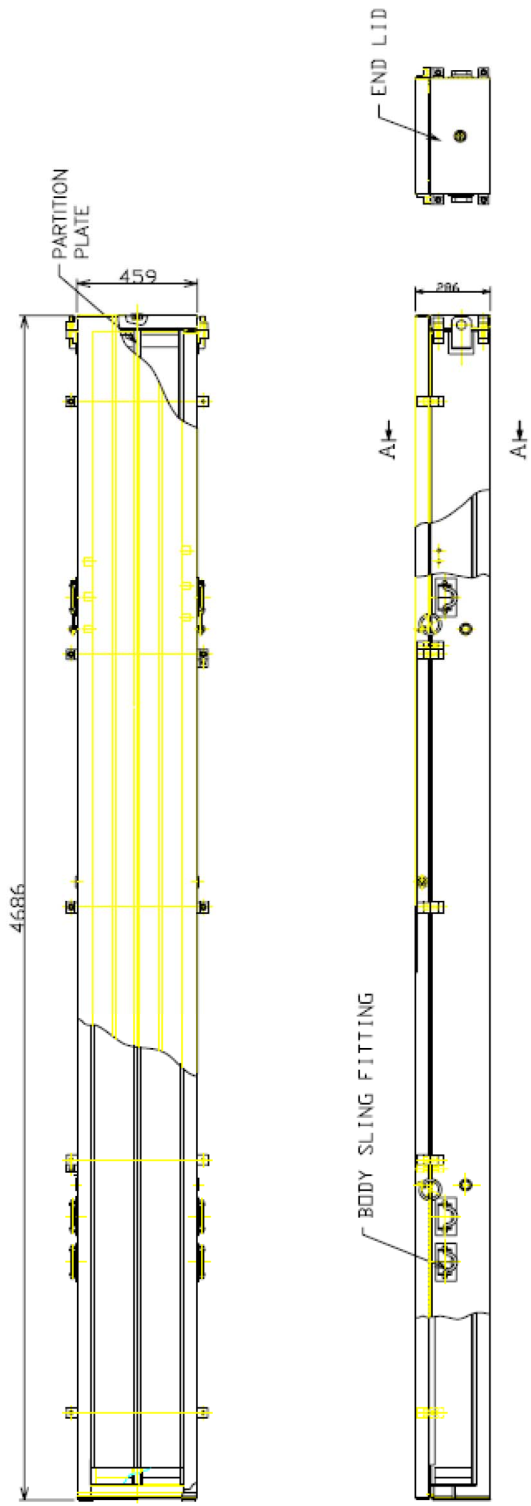

Figure 1-3 Inner Container

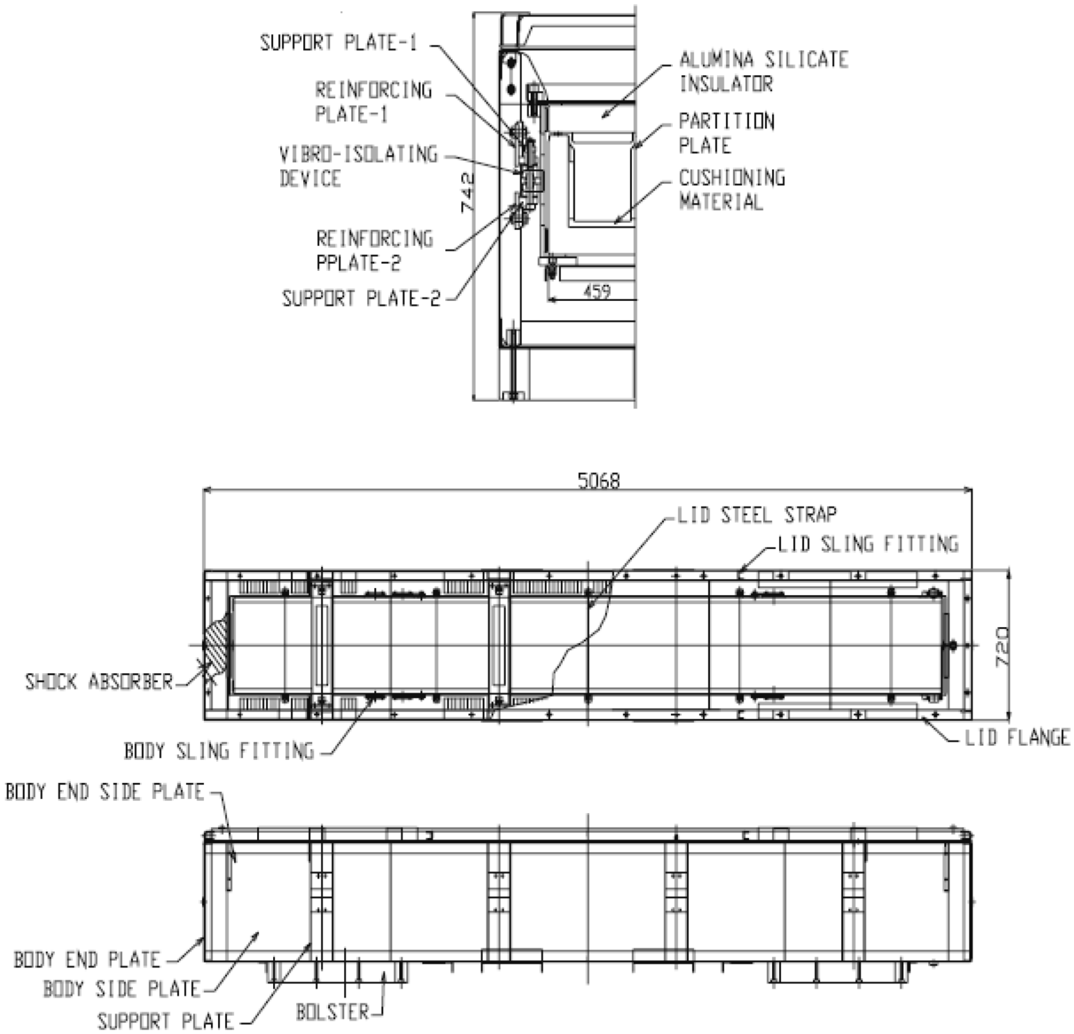

Figure 1-4 Inner and Outer Container

1.2. PACKAGE DESCRIPTION

This section presents a basic description of the model TN-B1 package. General arrangement drawings of the TN-B1 package are presented in Appendix 1.4.1. The Transport Index (TI) for this package is based on shielding and criticality assessments provided in Chapter 5.0 and Chapter 6.0. There are two ^{235}U enrichment ranges analyzed separately which affect the criticality evaluations. The differences between these ranges are thoroughly discussed throughout this document

1.2.1. *Packaging*

The packaging is comprised of one inner container and one outer container both made of stainless steel. The inner container is comprised of a double-wall stainless steel sheet structure with alumina silicate thermal insulator filling the gap between the two walls to reduce the flow of heat into the contents in the event of a fire. Foam polyethylene or rubber cushioning material is placed on the inside of the inner container for protection of the fuel assembly. The outer container is comprised of a stainless steel angular framework covered with stainless steel plates. Inner container clamps are installed inside the outer container with a vibro-isolating device between to alleviate vibration occurring during transportation. Additionally, wood and a honeycomb resin impregnated kraft paper (hereinafter called "paper honeycomb") are placed as shock absorbers to reduce shock due to a drop of the package. In addition to the packaging described above, the primary containment boundary is the fuel rod clad and the ceramic nature of the fuel pellets minimizes potential dispersion of the radioactive material.

The design details and overall arrangement of the TN-B1 packaging are shown in Appendix 1.4.1 TN-B1 General Arrangement Drawings.

1.2.1.1. **Inner Container (IC)**

The structure of the inner container is shown in Figure 1-2 and Figure 1-3. The inner container is comprised of three parts: an inner container body, an inner container end lid (removable), and an inner container top lid (removable). These components are fastened together by bolts made of stainless steel through tightening blocks. The inner container body is fitted with six sling fittings and the inner container lid is fitted with four sling fittings as shown in Figure 2-2 Inner Container Sling Locations. The inner container body has a double wall structure made of stainless steel. Its main components are an outer wall, inner wall and alumina silicate thermal insulator.

The outer wall is made of a 1.5 mm (0.0591 in) thick stainless steel sheet formed to a U-shape that constitutes the bottom and sides of the inner container body. A total of 14 stainless steel tightening blocks are attached on the sides of the outer wall, seven per side, to fasten the inner container lid and the inner container end lid by bolts. Additionally, six stainless steel sling fittings are attached on the sides (three on each side) for handling.

The inner wall of the inner packaging is formed into U-shape with 1.0 mm (0.0391 in) thick stainless steel sheet. The inner packaging is partitioned down the center with 2.0 mm (0.0787 in) thick stainless steel sheet welded to the bottom of the packaging. Foam polyethylene or rubber is placed on the inner surface of the inner wall where the fuel assemblies are seated. The void space between the outer and inner steel sheeting is filled with an alumina silicate thermal insulation 48 mm (1.89 in) thick.

1.2.1.2. **Outer Container (OC)**

The structure of the outer container is shown in Figure 1-4. The outer container is comprised of three parts: a container body, a container lid and inner container hold clamps made of stainless steel and fastened together using stainless steel bolts.

Two tamper-indicating device attachment locations are provided, one on each end, of the outer container.

1.2.1.2.1. ***Outer Container Body***

The outer container is made from a series of stainless steel angles (50mm x 50mm x 4mm)(1.97 inch x 1.97 inch x 0.157 inches) that make the framework. Welded to the framework are a bottom plate and side plates made of 2 mm (0.079 inch) thick stainless steel.

Sling holding angles for handling with a crane and protective plates for handling with a forklift are welded on the outside of the container body.

A total of eight sets of support plates are welded on the inside of the outer container body for installing the inner container hold clamps. Additionally, shock absorbers made of 146 mm (5.75 in) wood are attached to each end and paper honeycomb shock absorbers are attached to the bottom and sides for absorbing shock due to a drop. The geometry of the shock absorber is shown in Figure 1-5. The shock absorbers are 157 mm (6.18 in) thick and 108 mm (4.25 in) thick.

1.2.1.2.2. ***Outer Container Lid***

The outer container lid is comprised of a lid flange and a lid plate made of stainless steel.

Stainless steel lid sling fittings are welded four places on the top surface of the outer container lid. A paper honeycomb shock absorber, 157 mm (6.18 in) thick by 160 mm (6.30 in) wide and 380 mm (14.96 in) long is attached to the bottom side of the lid similar to the attachment at the bottom of the container.

The outer container lid has holes for bolts in its flange so that it can be fastened to the outer container body by the stainless steel bolts.

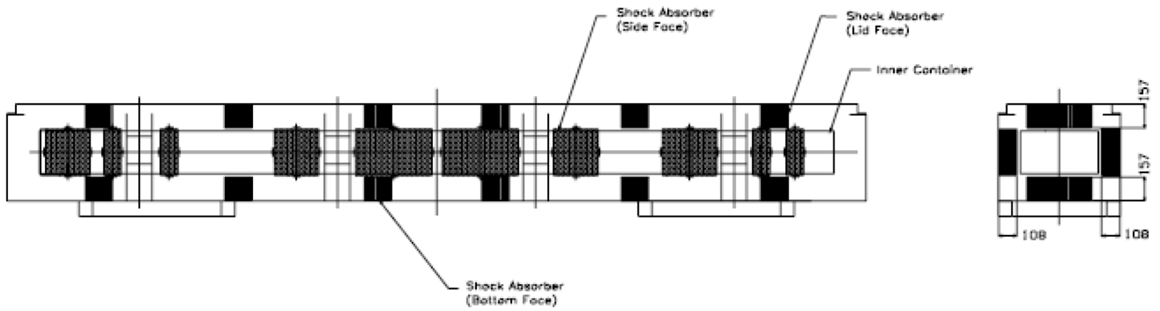

Figure 1-5 Shock Absorber Geometry

1.2.1.2.3. *Inner Container Hold Clamp (Located on Outer Container)*

The inner container hold clamp consists of an inner container receptacle and a vibro-isolating device.

The inner container receptacle consists of an inner container support plate, a support frame, a bracket and an inner container hold clamp fastener made of stainless steel. The receptacle guides the inner container to the correct position. The inner container receptacle is fitted with the vibro- isolating device through the gusset attached to the bracket.

The vibro-isolating material is attached on the upper and lower side of the gusset. These vibro-isolating parts may be of varying size and quantity to optimize vibration reduction characteristics of the rubber material during transport with the function of maintaining fuel assembly quality. Shock mount fastening bolts go through the vibro-isolating rubber to secure the assembly. The bolts at both ends are tightened so that the vibro-isolating rubber pieces press the gusset to the optimum compression.

There are four sets (eight pieces) of the vibro-isolating devices mounted on the outer container. Finally, a variety of stainless steel fasteners are used as specified in Appendix 1.4.1.

1.2.1.3. **Gross Weight and Dimensions**

The maximum gross shipping weight of a TN-B1 package is 1,614 kg (3,558 pounds) maximum. A summary of the major component weights and dimensions are given in Table 1-1.A summary of overall component weights is delineated in Table 2-1.

Table 1-1 Maximum Weights and Outer Dimensions of the Packaging

Item	Weight and outer dimensions
Maximum weight of inner	308 kg (679 lb)
Maximum weight of outer	622 kg (1,371 lb)
Maximum weight of packaging	930 kg (2,050 lb)
Dimensions of inner container	Length: 4,686 mm (184.49 in) Width: 459 mm (18.07 in) Height: 286 mm (11.26 in)
Dimensions of outer container	Length: 5,068 mm (199.53 in) Width: 720 mm (28.35 in) Height 742 mm (29.21 in) (including bolsters)

1.2.1.4. **Materials and Component Dimensions**

1.2.1.4.1. ***Inner Container***

The materials and component dimensions of the inner container are shown in Appendix 1.4.1.

1.2.1.4.2. ***Outer Container***

The materials and component dimensions of the outer container are shown in Appendix 1.4.1.

1.2.1.5. **Criticality Control Features**

The TN-B1 package does not require specific design features to provide neutron moderation and absorption for criticality control. The contents of the package rely on gadolinia loading for criticality control based on enrichment. Gadolinia loading requirements are provided in Table 6-1 TN-B1 Fuel Assembly Loading Criteria. There are no spacers required for criticality control. Fissile materials in the payload are limited to an amount that ensures safely sub-critical packages for both NCT and HAC. Further discussion of criticality control features is provided in Chapter 6.0.

1.2.1.6. **Heat Transfer Features**

The unirradiated fuel has negligible decay heat, therefore, the TN-B1 package is not designed for dissipating heat. The packaging is designed to protect the fuel and its containment by providing containment during the Hypothetical Accident Conditions (HAC). A more detailed discussion of the package thermal characteristics is provided in Chapter 3.0

1.2.1.7. Coolants

Due to the passive design of the TN-B1 package with regard to heat transfer, there are no coolants utilized within the TN-B1 package.

1.2.1.8. Protrusions

The only significant protrusions on the TN-B1 packaging exterior are those associated with the lifting features on the outer container exterior. These are the sling holding angles and the bolsters at the bottom of the packaging. The bolsters protrude the furthest at 80 mm (3.15 in).

The only significant protrusions on the inner container exterior are the lifting sling fittings and the tightening blocks that are used for securing the lid. There are lifting sling fittings on the body and the main lid. Each of the sling fittings fold down so they protrude only the thickness of the lifting rod or bail.

1.2.1.9. Lifting and Tie-down Devices

The lifting devices for the TN-B1 consist of the sling holding angles on the outer container which keep the slings from moving when used to sling the container during handling. The loaded container is designed to use four slings that form basket hitches under the container. The empty container is handled with two slings. The package may also be handled by the use of a forklift. The sling hold angles are designed so that even if they failed it would not affect the performance of the package.

The inner container is handled by the use of a series of lifting sling fittings. They are attached in a manner that even if they fail it will not compromise the performance of the inner container. On both the inner and outer containers, the lid lifting devices are marked to ensure proper use. A detailed discussion of lifting and tie-down designs, with corresponding structural analyses, is provided in Section 2.4.1 and 2.4.2.

1.2.1.10. Shielding

Due to the nature of the unirradiated fuel payload, no biological shielding is necessary or provided by the TN-B1 packaging.

1.2.1.11. Packaging Markings

The packaging will be marked with its model number, serial number, gross weight and also with the package identification number assigned by the NRC.

1.2.2. *Containment System*

The containment system components are identified above in Section 1.2.1 and accompanying figures. The primary containment boundary of this package is the fuel rod cladding as shown in example Figure 1-6 Example Fuel Rod (Primary Containment). The fuel rod is completed by loading the uranium dioxide pellets into a zirconium alloy cladding tube. The tubes are pressurized with helium and zirconium end plugs are welded to the tube which effectively seals and contains the radioactive material. Welds of the fuel rods are verified for integrity by such means as visual inspection, burst test samples and process control. The maximum internal pressure of fuel rods at room temperature is conservatively limited by an allowable clad stress of 10.18 Mpa as determined by testing of representative cladding samples (Section 3.5.3.2). Therefore, fuel rod designs must have a maximum pressure times the maximum clad inside radius to thickness ratio of 10.18 MPa or less to meet the HAC requirements.

The fuel rod cladding can optionally have a thin liner on the inside diameter that may have a lower material strength in comparison to non-liner clad. As the fuel rod clad is the primary containment boundary, the least bounding clad design is evaluated as part of the safety analyses. The requirements applicable for the evaluation are contained within Sections 2.7.4.3 and 2.7.4.4 for the structural analysis and Section 3.5.3.2 for the thermal analysis. For the criticality evaluation (Section 6.0), the presence of a liner in the fuel rod clad has no significant impact on the analysis.

The TN-B1 package cannot be opened unintentionally. Both the OC and IC lids are attached to their respective bodies with socket-headed cap screws. There are twenty-four bolts holding the outer lid in place. There are no other openings in the outer container. The inner container has ten bolts holding the main lid in place and four bolts holding the end closure in place. Thus, the requirements of 10 CFR 71.43(c) are satisfied.

Figure 1-6 Example Fuel Rod (Primary Containment)

1.2.2.1. **Pressure Relief System**

There are no pressure relief systems included in the TN-B1 package design to relieve pressure from within either the inner or outer containers or the fuel rod. Fire-consumable fusible plugs are used on the exterior surface of both the outer and inner containers to prevent pressure build up from the insulating and shock absorbing material during a fire event. These fusible plugs may be made of plastic. Two plugs are installed in the outer container body and two in the outer container lid. Four are installed in the inner container body, one in the end lid and two in its main lid.

1.2.3. *Contents*

A maximum of two fuel assemblies are placed in each packaging. The packaging is designed and analyzed to ship fuel configured either in 8x8, 9x9,10x10 or 11x11 arrays or as loose rods contained in a cylinder, protective case or positioned in one or both sides of the inner container. Fuel assemblies may also be shipped in the BWR fuel channel. The nuclear fuel pellets located in rods and contained in the packaging are uranium oxide (UO_2).

The fuel assembly enrichment criteria for less than or equal to 5.0 wt.% ^{235}U and less than or equal to 8.0 wt.% ^{235}U is evaluated separately in Section 6.0. For enrichments less than or equal to 8.0% ^{235}U (the fuel rod maximum enrichment is less than or equal to 8.0% ^{235}U), the criticality evaluation is provided in Appendix C beginning in Section 6.13. In addition to the shipment of fuel assemblies, Section 1.2.3.4.5, Section 1.2.3.4.6 and Section 1.2.3.4.7 describe contents configurations for shipping individual fuel rods not contained in a fuel assembly.

Table 1-2 provides a listing of the type, form and mass of material that may be shipped in the TN-B1. Both Type A and Type B materials are allowed for shipment of materials meeting the isotopic requirements listed in Tables 1-3 and 1-4. The fuel assemblies may be of various model and type as long as they meet the specified requirements delineated in Section 6.0.

Where fuel rods are referenced as being loaded with uranium dioxide mixed with gadolinium oxide (hereinafter gadolinia) the pellets in the gadolinia fuel rods contain a minimum of 2.0% or 4.0% gadolinium depending on the ^{235}U enrichment as shown in Table 1-6.

1.2.3.1. **Type A contents**

Where the contents of the packaging is commercial grade uranium or other uranium materials where the A_2 value is not exceeded, the packaging may be considered to contain Type A quantities.

1.2.3.2. **Type B contents**

Where the contents of the packaging is enriched reprocessed uranium or other origin uranium not exceeding the values in Table 1-3, the packaging is considered to contain Type B quantities.

1.2.3.3. **Quantity of Radioactive Materials of Main Nuclides**

The fuel assemblies in this packaging are loaded with low enrichment uranium dioxide containing less than or equal to 8.0 wt% ^{235}U. Where the content of the packaging consists of Type B quantities of material, the main nuclides are treated as shown in Tables 1-2 through 1-4 to calculate total activity, activity fractions and A_2 for the mixture.

Fuel rods assembled into the fuel assemblies are those loaded with sintered pellets of uranium dioxide and/or with sintered pellets of uranium dioxide mixed with various additives (e.g., Chromia, Gadolinia, and Silica). Additives with insignificant neutron absorbing properties (i.e., Chromia and Silica), are not credited in the safety basis. Gadolinia requirements are evaluated and included in Table 6-1.

Table 1-2 Quantity of Radioactive Materials (Type A and Type B)

Characteristic	Fuel Assembly Materials			
	Type 8×8	Type 9×9	Type 10×10	Type 11×11
Main nuclides	Low enriched uranium less than or equal to 5% U-235			
State of uranium	Uranium oxide ceramic pellet (Solid)			
Fuel assembly average enrichment	5.0% maximum			
Fuel rod maximum enrichment	5.0% maximum			
Number of fuel rods containing gadolinia	See Table 6-1			
Weight of uranium dioxide pellets (per fuel assembly)	235 kg	240 kg	275 kg	281 kg

Table 1-3 Type B Quantity of Radioactive Material (Type A and B) for ≤ 5.0 wt.% ^{235}U

Isotope	Maximum content[1]	Maximum mass, g	Specific Activity[2], TBq/g	Total Activity, TBq	Total Activity, Ci
U-232	2.00E-09 g/gU	9.92E-04	0.83	8.23E-04	2.23E-02
U-234	2.00E-03 g/gU	9.92E+02	2.30E-04	2.28E-01	6.17E+00
U-235	5.00E-02 g/gU	2.48E+04	8.00E-08	1.98E-03	5.36E-02
U-236	2.50E-02 g/gU	1.24E+04	2.40E-06	2.98E-02	8.04E-01
U-238	9.23E-01 g/gU	4.58E+05	1.20E-08	5.49E-03	1.48E-01
NP-237	1.66E-06 g/gU	8.23E-01	2.60E-05	2.14E-05	5.79E-04
PU-238	6.20E-11 g/gU	3.08E-05	6.30E-01	1.94E-05	5.24E-04
PU-239	3.04E-09 g/gU	1.51E-03	2.30E-03	3.47E-06	9.37E-05
PU-240	3.04E-09 g/gU	1.51E-03	8.40E-03	1.27E-05	3.42E-04
Gamma Emitters [3]	5.18E+05 MeV-Bq/kgU	N/A	N/A	2.57E-02	6.94E-01
			Total	2.92E-01	7.89E+00

1. Based on a maximum payload of 281 kg UO_2 per assembly, 248 kg U (562 kg UO_2, 496 Kg U total).
2. 10CFR71, Appendix A
3. Assuming gamma energy of 0.01 MeV to maximize total content.

Table 1-4 Type B Quantity of Radioactive Material (Type A and B) for ≤ 8.0 wt.% ^{235}U

Isotope	Maximum content[4]	Maximum mass, g	Specific Activity[5], TBq/g	Total Activity, TBq	Total Activity, Ci
U-232	1.10E-07g/gU	1.10E-07	0.83	4.53E-02	1.20E+00
U-234	7.65E-03g/gU	7.65E-03	2.30E-04	8.73E-01	2.35E+01
U-235	8.00E-02 g/gU	8.00E-02	8.00E-08	3.17E-03	8.73E-02
U-236	2.50E-02 g/gU	2.50E-02	2.40E-06	2.98E-02	8.06E-01
U-238	8.87E-01 g/gU	8.87E-01	1.20E-08	5.28E-03	1.50E-01
NP-237	1.66E-06 g/gU	1.66E-06	2.60E-05	2.14E-05	5.85E-04
PU-238	6.20E-11 g/gU	6.20E-11	6.30E-01	1.94E-05	5.23E-04
PU-239	3.04E-09 g/gU	3.04E-09	2.30E-03	3.47E-06	9.35E-05
PU-240	3.04E-09 g/gU	3.04E-09	8.40E-03	1.27E-05	3.47E-04
Gamma Emitters [6]	5.18E+05 MeV-Bq/kgU	N/A	N/A	2.57E-02	6.94E-01
			Total	2.82E-01	2.65E+01

4. Based on a maximum payload of 281 kg UO_2 per assembly, 248 kg U (562 kg UO_2, 496 Kg U total).
5. 10CFR71, Appendix A
6. Assuming gamma energy of 0.01 MeV to maximize total content.

Table 1-5 Mixture A_2 Calculation for Type B Payload

Isotope	Maximum Radioactivity content (Ci)	10CFR71 A_2 per isotope (Ci)	Activity Fraction	A_2 Fraction
≤ 5.0 wt.% ^{235}U				
U-232	2.23E-02	0.0270	2.75E-03	1.68E-01
U-234	6.17E+00	0.1600	7.63E-01	5.56E+00
U-235	5.36E-02	Unlimited	-	
U-236	8.04E-01	0.1600	9.94E-02	1.90E-01
U-238	1.48E-01	Unlimited	-	
Np-237	5.79E-04	0.0540	7.18E-05	4.09E-04
Pu-238	5.24E-04	0.0270	6.50E-05	7.32E-04
Pu-239	9.37E-05	0.0270	1.16E-05	1.31E-04
Pu-240	3.42E-04	0.0270	4.23E-05	4.85E-04
Gamma Emitters	6.94E-01	0.5400	8.59E-02	1.59E-01
Total	**2.65E+01**	-	**Sum of A_2 fractions**	**5.65E+00**
Mixture A_2				**0.18 Ci**
> 5.0 to ≤ 8.0 wt.% ^{235}U				
U-232	1.20E+00	0.0270	3.24E-02	1.68E-01
U-234	2.35E+01	0.1600	3.76E+00	5.56E+00
U-235	8.73E-02	Unlimited	-	
U-236	8.06E-01	0.1600	1.29E-01	1.90E-01
U-238	1.50E-01	Unlimited	-	
Np-237	5.85E-04	0.0540	3.16E-05	4.09E-04
Pu-238	5.23E-04	0.0270	1.41E-05	7.32E-04
Pu-239	9.35E-05	0.0270	2.52E-06	1.31E-04
Pu-240	3.47E-04	0.0270	9.36E-06	4.85E-04
Gamma Emitters	6.94E-01	0.5400	8.59E-02	1.59E-01
Total	**2.65E+01**	-	**Sum of A_2 fractions**	**7.59E+00**
Mixture A_2				**0.13 Ci**

Table 1-6 Gadolinia Loading Requirements

Parameter	Loose Rods		Type				
Fuel Assembly Type	11x11	17x17 Type 3	8x8	9x9	FANP 10x10	GNF 10x10	11x11
Gadolinia Requirements Lattice Average Enrichment							
≤ 8.0 wt % U-235	No Gd Req.	No Gd Req.	Not Eval.	Not Eval.	Not Eval.	Not Eval.	21 @ 4 wt.%
≤ 7.5 wt % U-235							19 @ 4 wt.%
≤ 7.0 wt % U-235							17 @ 4 wt.%
≤ 6.5 wt % U-235							15 @ 4 wt.%
≤ 6.1 wt % U-235							13 @ 4 wt.%
≤ 5.8 wt % U-235							13 @ 2 wt.%
Values below are the # of Gadolina rods required based on a minimum 2 wt.% Gadolinia							
Gadolinia Requirements Lattice Average Enrichment	BWR/PWR Rods						
≤ 5.0 wt % U-235	No Gd Req.		7	10	12	12	13
≤ 4.8 wt % U-235			7	10	12	12	12
≤ 4.7 wt % U-235			6	8	12	12	12
≤ 4.6 wt % U-235			6	8	10	10	11
≤ 4.4 wt % U-235			6	8	10	10	10
≤ 4.3 wt % U-235			6	8	9	9	10
≤ 4.2 wt % U-235			6	6	8	8	9
≤ 4.1 wt % U-235			4	6	8	8	8
≤ 3.9 wt % U-235			4	6	6	6	7
≤ 3.8 wt % U-235			4	4	6	6	6
≤ 3.7 wt % U-235			2	4	6	6	6
≤ 3.6 wt % U-235			2	4	4	4	5
≤ 3.5 wt % U-235			2	2	4	4	4
≤ 3.3 wt % U-235			2	2	2	2	3
≤ 3.2 wt % U-235			2	2	2	2	2
≤ 3.1 wt % U-235			None	2	2	2	2
≤ 3.0 wt % U-235			None	None	2	2	2
≤ 2.9 wt % U-235			None	None	None	None	None

1.2.3.4. Physical Configuration

1.2.3.4.1. *Fuel Assembly*

The configuration of typical fuel assemblies is shown in Figure 1-8 Fuel Assembly with Optional Packing Materials. The fuel assemblies may be of various model and type as long as they meet the requirements listed. The materials of the main components in the fuel assemblies are listed in Table 1-7. The maximum weight of contents including fuel and packing material is 684 kg (1,508 lb).

1.2.3.4.2. *Chemical Properties*

Example of structural materials of the fuel assembly is shown in Table 1-8. Zirconium alloy, stainless steel and Ni-Cr-Fe alloy are chemically stable materials, and they are excellent in heat resistance and corrosion resistance.

1.2.3.4.3. *Density of Materials*

The density for the fuel assembly materials is presented in Table 1-8.

1.2.3.4.4. *Packing Materials*

A number of packing materials may be used to guard the fuel assembly (e.g., cluster separators, and polyethylene bags). An example of the packing materials and their use is shown in Figure1-8.

1.2.3.4.5. *Bundled Fuel Rods*

In addition to the fuel assembly configuration described above, fuel rods may be shipped bundled together in groups of rods up to 25 total rods. Fuel rods are fixed together using ring clamps. The criticality safety case for loose rods that shows that as many as 25 fuel rods per side can be arranged in any configuration within the volume of the inner container. Based on this criticality safety analysis the ring clamps are not relied on or needed for maintaining the configuration of the fuel rods.

1.2.3.4.6. *Fuel Rods In a 5-Inch Pipe*

Another physical configuration is the use of a 5-inch diameter schedule 40 stainless steel pipe. The physical configuration of the pipe is shown in drawing 0028B98. The number of fuel rods shipped in this configuration is limited by the quantities in Table 6-2. See Section 6.3.1.3.1 and 6.3.1.3.2 for other descriptions of the pipe.

1.2.3.4.7. *Fuel Rods in a Protective Case*

Figure 1-7 shows the configuration of the protective case. The protective case is a stainless steel box comprised of a body, lid, wood spacer absorber and end plate. In addition to the figure below, detailed drawings of the protective case are provided in Appendix 1.4.1. The protective case is surrounded by polyurethane foam cushioning material, which provides a snug fit within the inner container. Depending on the rod type, the protective case may be used to transport any number of authorized fuel rods up to a maximum of 30 rods. See Table 6-2.

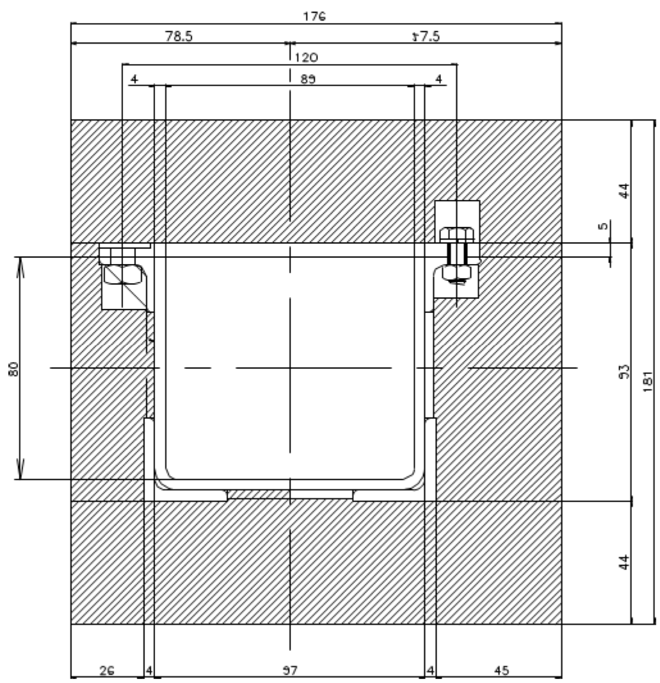

Figure 1-7 Protective Case

Table 1-7 Example of Fuel Structural Materials

Component parts	Structural materials
Pellets	Uranium dioxide sintered (in some cases uranium dioxide blended with gadolinia)
Cladding tube	Zirconium alloy, metallic zirconium
Internal spring	Stainless steel
Getter	Zirconium alloy and stainless steel
Upper and Lower end plug	Zirconium alloy
Water rod	Zirconium alloy
Upper and Lower tie plate	Stainless steel
Spacer	Zirconium alloy
Finger spring	Ni-Cr-Fe alloy
Expansion spring	Ni-Cr-Fe alloy
Nut	Stainless steel and Zirconium alloy
Locking tab washer	Stainless steel

Table 1-8 Density of Structural Materials

Main structural materials	Density
Zirconium alloy metallic zirconium	Approximately 6.5 g/cm³ (0.235lb/in^3)
Uranium dioxide pellet	Approximately 10.4 g/cm³ (0.376 lb/in^3)
Stainless steel	Approximately 7.8 g/cm³ (0.282 lb/in^3)
Ni-Cr-Fe alloy	Approximately 8.5 g/cm³ (0.307 lb/in^3)

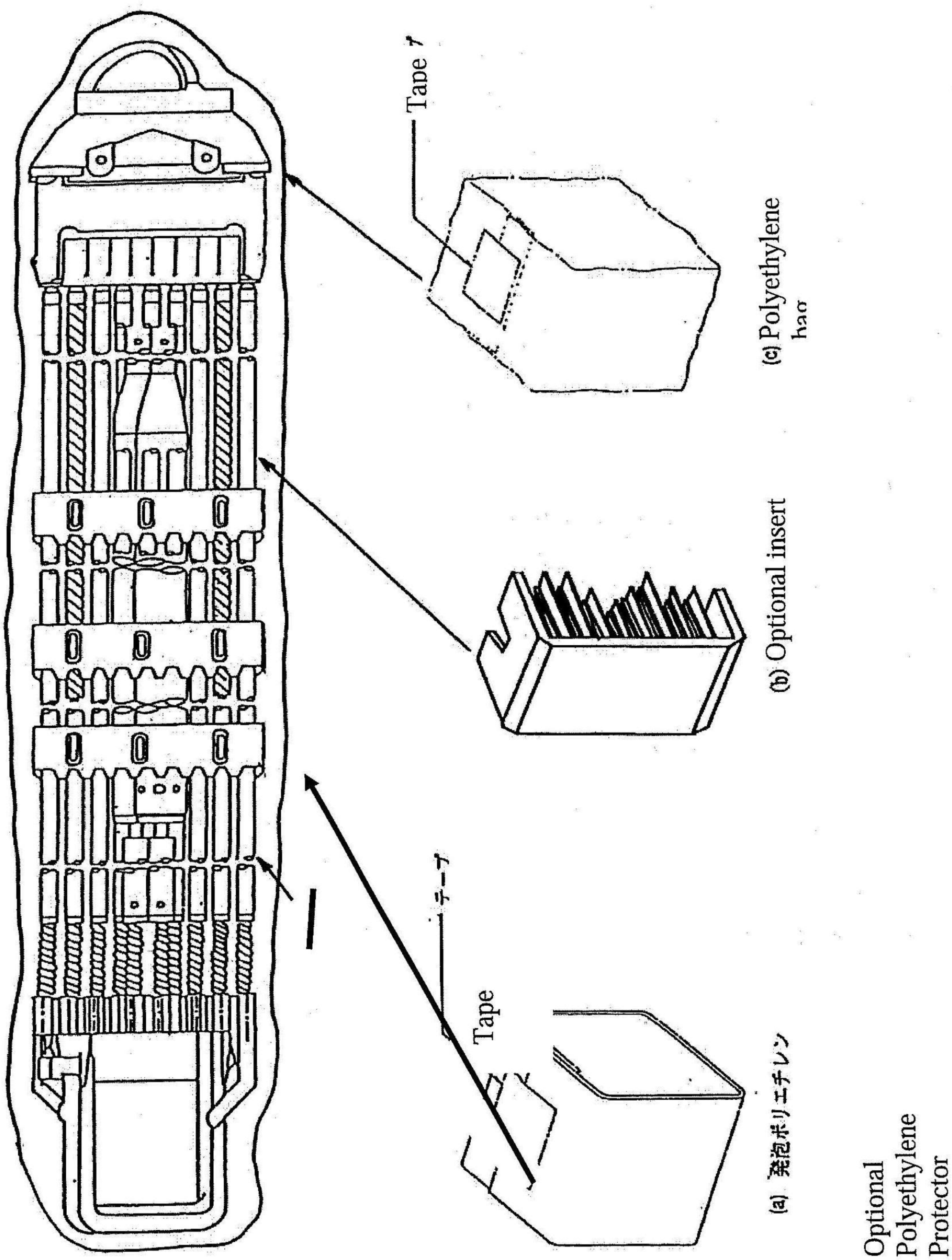

Figure 1-8 Assembly with Optional Packing Materials

1.2.4. *Operational Features*

The TN-B1 packaging is not considered operationally complex. Operational features are readily apparent from an inspection of the drawings provided in Appendix 1.4.1 and the previous discussions presented in Section 1.2.1. Operational procedures and instructions for loading, unloading, and preparing empty TN-B1 packages for transport are provided in Chapter 7.0

1.3. GENERAL REQUIREMENTS FOR ALL PACKAGES

1.3.1. *Minimum Package Size*

The TN-B1 package is a rectangular box that is 742 mm (29.21 in) high by 720 mm (28.35 in) wide by 5,068 mm (199.53 inches) long. Thus, the requirement of 10 CFR 71.43(a) is satisfied.

1.3.2. *Tamper-Indicating Feature*

Seal pins are provided at each end of the outer container body and lid for the use of tamper indicating seals. A tamper indicating seal is attached at each end of the loaded outer container by inserting the seal through the holes in the body and lid seal pins and securing the seal. The tamper indicating seal is not readily breakable and would provide evidence of tampering or opening by an unauthorized person. Thus, the requirement of 10 CFR 71.43(b) is satisfied.

1.4. APPENDIX

1.4.1. *TN-B1 General Arrangement Drawings*

This section presents the TN-B1 packaging general arrangement drawing consisting of 15 drawings entitled, *TN-B1 SAR Drawing,* see drawing list below. Within the packaging general arrangement drawing, dimensions important to the packaging safety are dimensioned and toleranced. Other dimensions are provided as a reference dimension, and are toleranced in accordance with the JIS (Japan Industrial Std.) B 0405. See 2.1.4.1 and 2.1.4.2.

1.4.1.1. **Drawing List**

Table 1-9 Outer Container Drawings

Drawing number	Number of Sheets	Revision #	Name
105E3737	1	6	Outer/Inner Container Assembly Licensing Drawings
FS1-0042698	4	1.0	TN-B1 Outer Container Main Body Assembly Licensing Drawings
FS1-0042699	2	1.0	Outer Container Fixture Assembly Licensing Drawings
FS1-0042700	1	2.0	TN-B1 Outer Container Fixture Assembly Installation Licensing Drawings
105E3741	1	1	Outer Container Shock Absorber Assembly Licensing Drawings
105E3742	1	3	Outer Container Bolster Assembly Licensing Drawings
FS1-0042703	1	1.0	TN-B1 Outer Container Lid Assembly Licensing Drawings
02-9162717	1	1	Outer Container Marking Licensing Drawings

Table 1-10 Inner Container Drawings

Drawing number	Number of Sheets	Revision #	Name
FS1-0042705	4	1.0	TN-B1 Inner Container Main Body Assembly Licensing Drawings
105E3746	1	1	Inner Container Parts Assembly Licensing Drawings
FS1-0042707	2	1.0	TN-B1 Inner Container Lid Assembly Licensing Drawings
FS1-0042708	1	1.0	TN-B1 Inner Container End Lid Assembly Licensing Drawings
02-9162722	1	1	Inner Container Marking Licensing Drawings

Table 1-11 Contents Drawings

Drawing number	Number of Sheets	Revision #	Name
105E3773	1	1	Protective Case
0028B98	1	1	Shipping Container Loose Fuel Rods

2. STRUCTURAL EVALUATION

This section presents evaluations demonstrating that the TN-B1 package meets applicable structural criteria. The TN-B1 packaging, consisting of unirradiated fuel assemblies that provide containment, an inner container, and an outer container with paper honeycomb spacers, is evaluated and shown to provide adequate protection for the payload. Normal Conditions of Transport (NCT) and Hypothetical Accident Condition (HAC) evaluations, using analytic and empirical techniques, are performed to address 10 CFR 71 performance requirements.

Numerous tests were successfully performed on the RAJ-II package during its initial qualification in Japan that provided a basis for selecting the certification tests. RAJ-II certification testing involved two full-scale Certification Test Units (CTU) at Oak Ridge, TN. The RAJ-II CTUs were subjected to a series of free drop and puncture drop tests. The RAJ-II CTUs protected the simulated fuel assemblies, allowing them to remain undamaged and leak tight throughout certification testing. Since the RAJ-II and TN-B1 structural designs are identical, the RAJ-II tests are completely applicable to the TN-B1 package. Details of the certification test program are provided in Appendix 2.12.1.

2.1. DESCRIPTION OF STRUCTURAL DESIGN

2.1.1. *Discussion*

A comprehensive discussion on the TN-B1 packaging design and configuration is provided in chapter 1.0. Drawings provided in Appendix 1.4.1 show the construction of the TN-B1 and how it protects the fuel assemblies. The containment is provided by the fuel cladding and welded end fittings of the fuel rods. The fuel is protected by an inner container that provides thermal insulations and soft foam that protects the fuel from vibration. The inner container is supported by vibration isolation system inside the outer container that has shock absorbing blocks of balsa and honeycomb made of resin impregnated kraft paper (hereinafter called "paper honeycomb"). Specific discussions relating to the aspects important to demonstrating the structural configuration and performance to design criteria for the TN-B1 packaging are provided in the following sections. Standard fabrication methods are used to fabricate the TN-B1 package.

Detailed drawings showing applicable dimensions and tolerances are provided in Appendix 1.4.1.

Weights for the various components and the assembled packaging are provided in Section 2.1.3.

2.1.1.1. Containment Structures

The primary containment for the radioactive material in the TN-B1 is the fuel rod cladding, which is manufactured to high standards for use in nuclear reactors. The fabrication standards for the fuel are in excess of what is needed to provide containment for shipping of the fuel. The fuel rod cladding is designed to provide containment throughout the life of the fuel, prior to loading, in transportation, and while used in the reactor where it operates at higher pressures and temperatures, and must contain fission products as well as the fuel itself.

The cladding tubes for the fuel are high quality seamless tubing. The clad fuel is verified leaktight before shipment.

2.1.1.2. **Non-Containment Vessel Structures**

The TN-B1 is made up of two non-containment structures, the inner container, and the outer container that are designed to protect the fuel assemblies and clad rods which serve as the containment. The inner container design provides some mechanical protection although its primary function is to provide thermal protection. The outer container consists of a metal wall with shock absorbing devices inside and vibration isolation mounts for the inner container. Section 1.2.1 provides a detailed description of the inner and outer container. Non-containment structures are fabricated in accordance with the drawings in Appendix 1.4.1.

Welds for the non-containment vessel walls are subjected to visual inspection as delineated on the drawings in Appendix 1.4.1.

2.1.2. ***Design Criteria***

Proof of performance for the TN-B1 package is achieved by a combination of analytic and empirical evaluations. The acceptance criteria for analytic assessments are in accordance with 10 CFR 71 and the applicable regulatory guides. The acceptance criterion for empirical assessments is a demonstration that both the inner and outer container are not damaged in such a way that their performance in protecting the fuel assemblies during the thermal event is not compromised and the fuel itself is not damaged throughout the NCT and HAC certification testing. Additionally, package deformations obtained from certification testing are considered in subsequent thermal, shielding, and criticality evaluations are validated.

2.1.2.1. **Analytic Design Criteria (Allowable Stresses)**

The allowable stress values used for analytic assessments of TN-B1 package structural performance come from the regulatory criteria such as yield strength or 1/3 of yield or from the ASME Code for the particular application. Material yield strengths, taken from the ASME Code, used in the analytic acceptance criteria, Sy, and ultimate strengths, Su, are presented in Table 2-2 of Section 2.2.

2.1.2.2. **Containment Structures**

The fuel cladding provides the primary containment for the nuclear fuel.

2.1.2.3. Non-Containment Structures

For evaluation of lifting devices, the allowable stresses are limited to one-third of the material yield strength, consistent with the requirements of 10 CFR 71.45(a). For evaluation of tie-down devices, the allowable stresses are limited to the material yield strength, consistent with the requirements of 10 CFR 71.45(b).

2.1.2.4. Miscellaneous Structural Failure Modes

2.1.2.4.1. *Brittle Fracture*

By avoiding the use of ferritic steels in the TN-B1 packaging, brittle fracture concerns are precluded. Specifically, most primary structural components are fabricated of austenitic stainless steel. Since this material does not undergo a ductile-to-brittle transition in the temperature range of interest (above -40 ºF), it is safe from brittle fracture.

The closure bolts used to secure the inner and outer container lids are stainless steel, socket head cap screws ensuring that brittle fracture is not of concern. Other fasteners used in the TN-B1 packaging assembly provide redundancy and are made from stainless steel, again eliminating brittle fracture concerns.

2.1.2.4.2. *Extreme Total Stress Intensity Range*

Since the response of the TN-B1 package to accident conditions is typically evaluated empirically rather than analytically, the extreme total stress intensity range has not been quantified. Two full- scale certification test units (see Appendix 2.12.1) successfully passed free-drop and puncture testing. The CTUs were also fabricated in accordance with the drawings in Appendix 1.4.1, thus incurring prototypic fabrication induced stresses. Exposure to these conditions has demonstrated leak tight containment of the fuel, geometric configuration stability for criticality safety, and protection for the fuel. Thus the intent of the extreme total stress intensity range requirement has been met.

2.1.2.4.3. *Buckling Assessment*

Due to the small diameter of the containment boundary (the fuel rod cladding) and the fact that its radial deflection is limited by the internal fuel pellets, radial buckling is not a failure mode of concern for the containment boundary. Axial buckling deflection is also limited by the inner wall of the inner container and lid. The applied axial load to the fuel is also limited by the wood at the end of the packaging. The limited horizontal movement of the fuel during an end drop limits the ability of the fuel to buckle as demonstrated in tests performed on CTU 2 (see Appendix 2.12.1).

It is also noted that 30-foot drop tests performed on full-scale models with the package in various orientations produced no evidence of buckling of any of the fuel (see Appendix 2.12.1). Certification testing does not provide a specific determination of the design margin against buckling, but is considered as evidence that buckling will not occur. In addition buckling is a potential concern to ensure adequate geometric configuration control of the post accident package for criticality control. This involves not only the internal configuration of the package but the potential spacing between packages as well. Deformation of the TN-B1 is limited by its redundant structure. The wall of the package acts to stiffen the support plates that carry the load of the inner container via the vibration isolating mechanism. Part of the redundant system to minimize deformation of the fuel is the paper honeycomb that absorbs shocks that would impart side loading to the fuel. The inner container, consisting of an inner wall separated from an outer wall by thermal insulation, is lined with cushioning material that supports the fuel. Regardless of the specific failure mechanism of the support plates, the total deformation is limited by the shock absorbers (paper honeycomb). These blocks immediately share the load. Hence, even if the support plates would buckle allowing the outer wall to plastically deform, the amount of deformation is limited by the shock absorbing material. This has been demonstrated by test to allow only 118 mm (4.7 inches) of deformation of the shock absorbing blocks. The criticality evaluation takes into consideration this deformation. The redundant support system combined with the vibro-isolation and shock absorption system prevents the deformation of the inner container and the fuel.

The axial deformation resulting from an end drop is controlled in a similar manner. The end of the outer container has a wood shock absorber built in that carries the load from the inner container to the outer wall after the vibro-isolation device deflects. This reduces the load carried by the outer wall and support plates. It prevents large loads and deformations that could contribute to buckling of the fuel. The inner container constrains the fuel from large deformations or buckling.

Therefore, the support system prevents buckling of the packaging or fuel that would affect the criticality control or containment.

2.1.3. *Weights and Centers of Gravity*

The maximum gross weight of a TN-B1 package, including a maximum payload weight of 684 kg (1,508 pounds) is 1,614 kg (3,558 pounds). The maximum vertical Center of Gravity (CG) is located 421 mm (16.57 inches) above the bottom surface of the package for a fully loaded package. A maximum horizontal shift of the horizontal CG is 92 mm (3.62 inches). This is allowed for in the lifting and tie-down calculations presented in Section 2.5.1. Figure 2-1 shows the locations of the center of gravity for the major components and the location of the center of gravity for the assembled. A detailed breakdown of the TN-B1 package component weights is summarized in Table 2-1.

2.1.3.1. **Effect of CG Offset**

The shift of the CG of the package 92 mm (3.6 inches) has very little effect on the performance of the package due to the length of the package, 5,068 mm (199.53 in). This results in a small shift of the weight and forces from one end of the package to the other. The actual total shift is:

$$3.6\% = 1 - \frac{(2)\left(\left(5068/2\right) - 92\right)}{5068}$$

The offset of the CG is taken into account in the lifting and tie down calculations. The effect of this relatively small offset can be neglected.

2.1.4. *Identification of Codes and Standards for Package Design*

The radioactive isotopic content of the fuel is primarily U-235 with small amounts of other isotopes that make it Type B. Using the isotopic content limits shown in Section 1.2.3 the package would be considered a Category II. As such the applicable codes that would apply are the ASME Boiler and Pressure Vessel Code Section III, Subsection ND for the containment boundary which is the fuel cladding and Section III, Subsection NG for the criticality control Structure and the Section VIII for the non-containment components.

The fuel cladding, due to its service in the reactor and need for high integrity, is designed to and fabricated to standards that exceed those required by ASME Section III Subsection ND. The structure used to maintain criticality control is demonstrated by test. The packaging capabilities are verified by test and the codes used in fabrication are called out on the drawings in Appendix 1.4.1. The sheet metal construction of the packaging requires different joint designs and manufacturing techniques that would normally be covered by the above referenced codes.

2.1.4.1. **JIS/ASTM Comparison of Materials**

The Certification Test Units (CTUs) were manufactured in Japan using material meeting JIS specifications. The fuel cladding and ceramic pellets were manufactured in the US to US specifications. The future manufacturing of TN-B1 packages may be performed using American standards (ASTM or ASME) that are appropriate substitutes for the Japanese standards (JIS) material comprising the CTUs. In order to assure that the packaging manufactured in the future meets the performance requirements demonstrated for the RAJ-II CTUs a detailed review of the differences between the American and Japanese standards was performed. The scope of the study included the: stainless steel products, wood products, rubber, paper honeycomb, and polyethylene foam. The study concluded that American standards material is available and compatible to the JIS standards. Future manufacturing of these packages for domestic use may be to American or Japanese specifications meeting the tolerances specified in the general arrangement drawings.

2.1.4.2. JIS/ASME Weld Comparison

Based upon an evaluation, it is concluded that the following standards are equivalent for the purposes of fabrication of the TN-B1 container in the United States:

Japanese Specification	American Specification
JIS Z 3821 Standard qualification procedure for welding technique of stainless steel	ASME Section IX
JIS Z 3140 Method of inspection for spot weld	ASME Section IX
JIS Z 3145 Method of bend test for stud weld	ASME Section IX

2.1.4.3. JIS/JSNDI/ASNT Non-destructive Examination Personnel Qualification and Certification Comparison

The following standards are considered equivalent for Non-destructive Examination Personnel Qualification and Certification. Personnel with these qualifications and certifications are authorized to perform examinations of the fabrication inspection requirements for the TN-B1 container in the United States. Although these documents cover other disciplines, this comparison only applies to Liquid Penetrant Examination.

Japanese Specification	American Specification
JIS Z 2305 Qualification and Certification for NDT Personnel	SNT-TC-1A* Recommended Practice
Certification NDIS 0601	SNT-TC-1A Recommended Practice
Certification NDIS J001	SNT-TC-1A Recommended Practice

*Society of Non-destructive Testing – Technical Council

Table 2-1 TN-B1 Weight

Contents	Number of assemblies per package	Maximum 2 Assemblies
	Number of fuel rods per package	See section 1.2.3
	Total weight	684 kg (1,508 lb)
Inner container	Body	200 kg (441 lb) (including bolts)
	Lid	101 kg (223 lb)
	End lids	7 kg (15.4 lb)
	Total weight	308 kg (679 lb)
Outer container	Body	485 kg (1,069 lb) (including bolts)
	Lid	137 kg (302 lb)
	Total weight	622 kg (1,371 lb)
Total weight of package		1,614 kg (3,558 lb)

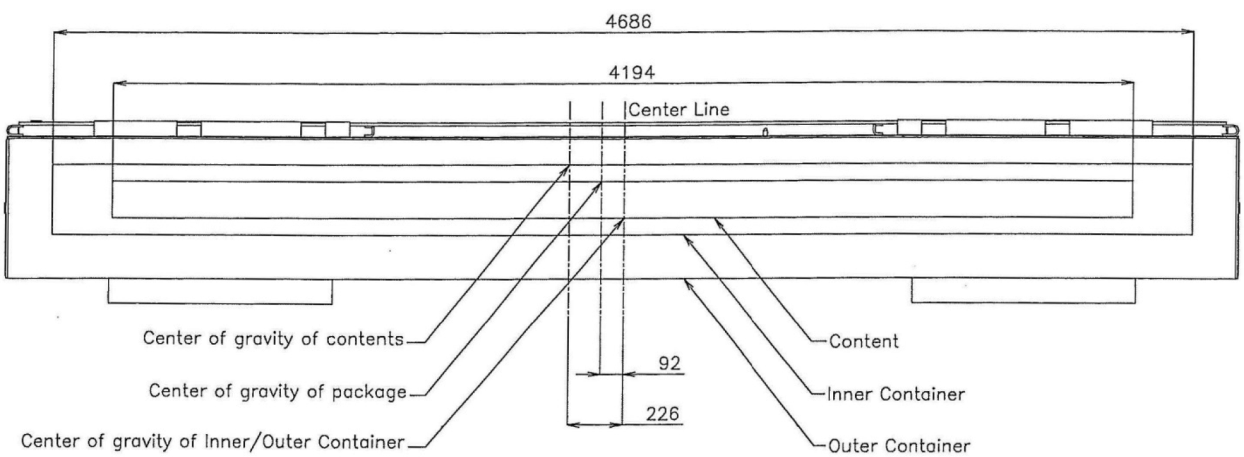

(unit: mm)

Figure 2-1 Center of Gravity of Package Components

2.2. MATERIALS

2.2.1. *Material Properties and Specifications*

The major structural components, i.e., the Outer Container (OC) and Inner Container (IC) walls, supports, and attachment blocks are fabricated from austenitic stainless steel. Other materials performing a structural function are lumber (bolster), balsa (shock absorber), paper honeycomb (shock absorber), alumina silicate (thermal insulator), polyethylene foam (cushioning material), rubber (cushioning material), and zirconium alloy (fuel rod cladding). The drawings presented in Appendix 1.4.1 delineate the specific material(s) used for each TN-B1 packaging.

The remainder of this section presents and discusses pertinent mechanical properties for the materials that perform a structural function. Both the materials that are used in the analytics and those whose function in the package is demonstrated by test such as the shock absorbing material are presented. In general the analytics covering the lifting and tie down capabilities of the package and some normal condition events are limited to the stainless steel structure of the packaging.

Table 2-2 presents the bounding mechanical properties for the series 300 stainless steel used in the TN-B1 packaging. Each of the representative mechanical properties is those of Type 304 stainless steel and is taken from Section II, Parts A and D, of the ASME Boiler and Pressure Vessel Code. These properties are applicable to both packages that may have been made in Japan to Japanese specifications, Japanese Industrial Standards (JIS) or using ASME specification material. The density of stainless steel is taken as 0.29 lb/in3 (8.03E3 kg/m3), and Poisson’s Ratio is 0.3.

Table 2-3 presents the mechanical properties of the main non-stainless steel components of the package necessary for the structural analysis.

Table 2-2 Representative Mechanical Properties of 300 Series Stainless Steel Components

① **Minimum Elongation (%)**	**Temperature** **°C (°F)**	② **Yield Strength, S_y MPa (×10^3 psi)**	③ **Ultimate Strength, S_u MPa (×10^3 psi)**	④ **Elastic Modulus, e GPa (×10^6 psi)**	⑤ **Thermal Expansion Coefficient, α x 10^{-6} mm/mm/°C (×10^{-6} in/in/°F)**
35	-29 (-20)	206.8 (30.0)	517.1 (75.0)	-----	-----
40	21 (70)	206.8 (30.0)	517.1 (75.0)	195.1 (28.3)	-----
30	38 (100)	206.8 (30.0)	517.1 (75.0)	-----	15.39 (8.55)
25	93 (200)	172.4 (25.0)	489.5 (71.0)	190.3 (27.6)	15.82 (8.79)
30	149 (300)	155.1 (22.5)	455.1 (66.0)	186.2 (27.0)	16.2 (9.00)
40	204 (400)	142.7 (20.7)	444.0 (64.4)	182.7 (26.5)	16.54 (9.19)
40⑥	23°C ⑥	205 MPa Min⑥	520 MPa Min⑥	-----	-----
40⑦	21°C ⑦	205 MPa Min⑦	515 MPa Min⑦	-----	-----

Notes:
① ASME Code, Section II, Part A
② ASME Code, Section II, Part D, Table Y-1
③ ASME Code, Section II, Part D, Table U
④ ASME Code, Section II, Part D, Table TM-1, Material Group G
⑤ ASME Code, Section II, Part D, Table TE-1, 18Cr-8Ni, Coefficient B
⑥ JIS Handbook Ferrous Materials and Metallurgy I, Sections G4303, G4304, G4305 Material Specifications
⑦ ASTM A240, A666 & A276 Material Specifications

Table 2-3 Mechanical Properties of Typical Components

Materials (Usage)	Yield stress or yield strength	Tensile strength	Compressive strength	Bending strength	Static initial peak stress	Modulus of longitudinal elasticity	Density (g/cm^3)
Lumber (bolster)	56.3 MPa Nominal	–	50.5 MPa Nominal	72.0 MPa Nominal	–	7.85 GPa Nominal	0.53 Nominal
Balsa (shock absorber)	–	–	16 MPa Nominal	–	–	–	0.18 Nominal
Paper honeycomb (shock absorber)	–	–	–	–	2.35 MPa Nominal	–	0.06 Nominal
Alumina Silicate (thermal insulator)	–	–	294 kPa Nominal	314 kPa Nominal	–	–	0.25 Nominal
Foam polyethylene (cushioning mat'l)	–	–	Approx. 0.2MPa @ 50% strain	–	0.69 MPa Nominal	–	0.068 Nominal
Zirconium alloy (fuel rods) ASTM B811	241 MPa (35,000psi)	413 MPa (60,000psi)	–	–	–	97.1 GPa Nominal	6.5 Nominal
300 Series Stainless Socket Headed Cap screw	241 MPa (35,000psi) (Min)	379 MPa (75,000psi) (Min)	–	–	–	–	–

2.2.2. *Chemical, Galvanic, or Other Reactions*

The major materials of construction of the TN-B1 packaging (i.e., austenitic stainless steel, polyurethane foam, alumina thermal insulator, resin impregnated paper honeycomb, lumber (hemlock and balsa), and rubber) will not have significant chemical, galvanic or other reactions in air, inert gas or water environments, thereby satisfying the requirements of 10 CFR 71.43(d). These materials have been previously used, without incident, in radioactive material (RAM) packages for transport of similar payload materials. A successful RAM packaging history combined with successful use of these fabrication materials in similar industrial environments ensures that the integrity of the TN-B1 package will not be compromised by any chemical, galvanic, or other reactions.

The TN-B1 packaging is primarily constructed of series 300 stainless steel. This material is highly corrosion resistant to most environments. The metallic structure of the TN-B1 packaging is composed entirely of this material and compatible 300 series weld material. Since both the base and weld materials are 300 series materials, they have nearly identical electrochemical potential thereby minimizing any galvanic corrosion that could occur.

The stainless steel within the IC cavity between the inner and outer walls is filled with a ceramic alumina silicate thermal insulator. This material is non-reactive with either the wood or the stainless steel, both dry or in water. The alumina silicate is very low in free chlorides to minimize the potential for stress corrosion of the IC structure.

The polyethylene foam that is used in the IC for cushioning material has been used previously and is compatible with stainless steel. The polyethylene foam in is very low in free halogens and chlorides.

Resin impregnated paper honeycomb is used in the TN-B1 packaging as cushioning material. The impregnated paper is resistant to water and break down. It is low in leachable halides.

Synthetic rubber is added as an option to supplement the existing natural rubber previously authorized within the packaging. The term rubber is used to bound both natural rubber and synthetic type rubbers. Multiple rubber types are listed to allow many vibration absorbing solutions for the best fuel assembly performance characteristics. Neoprene is also identified as an option for the inner and outer container gaskets. The most common types of synthetic rubber used in industry for vibration absorption include the following:

- Natural rubber
- Neoprene
- Silicone
- SBR (styrene-butadiene rubber)
- EPDM (ethylene propylene diene monomer rubber).

Other than SBR, the above synthetic rubbers are also regularly used as gaskets and seals in the packaging industry. SBR type rubber is best known for its use in pneumatic tires. These types of rubbers are very stable and unreactive in the intended use of the TN-B1 package.

Since the primary materials of construction mentioned in this section are relatively unreactive, no excessive corrosion or other reactions will occur during normal use. The package is normally transported on a flatbed trailer and is not subject to immersion or exposure to water or chemical other than occasional precipitation or mild cleaning agents. If unusual corrosion or reactions of the stainless steel or other material components occur, it will be readily detected during pre-use inspections of the packaging prior to loading. The other packaging components are not subject to chemical degradation or corrosion during normal use. All the components located near any rubber are open to inspection and visually inspected prior to each use.

2.2.2.1. **Content Interaction with Packaging Materials of Construction**

The materials of construction of the TN-B1 packaging are checked for compatibility with the materials that make up the contents or fuel rods that are to be shipped in the TN-B1. The primary materials of construction of the fuel assembly that could come in contact with the packaging are the stainless steel and the zirconium alloy material that is used for the cladding of the fuel rods. Zirconium alloy (including metal zirconium), stainless steel, and Ni-Cr- Fe alloy, which form a passivated oxide film on the surface under normal atmosphere with slight moisture, are essentially stable. The contact of the above three kinds of metals with polyethylene is chemically stable. These materials are compatible with the stainless steel, polyethylene, and rubber that could come in contact with the contents.

2.2.3. *Effects of Radiation on Materials*

Since this is an unirradiated fuel package, the radiation to the packaging material is insignificant. Also, the primary materials of construction and containment, austenitic stainless steel and the zirconium alloy cladding of the fuel are highly resistant to radiation.

2.3. FABRICATION AND EXAMINATION

2.3.1. *Fabrication*

The TN-B1 is fabricated using standard fabrication techniques. This includes cutting, bending and welding the stainless steel sheet metal. As shown on the drawing the welding is done to AWS D1.6 Welding of Stainless Steel. The process may also be controlled by ASME Section IX or other international codes. The containment, the cladding of the fuel rods is fabricated to standards that exceed the required Section VIII of the ASME Boiler and Pressure vessel code due to the service requirements of the fuel in reactors.

2.3.2. *Examination*

The primary means of examination to determine compliance of the TN-B1 to the design requirements is visual examination of each component and the assembled units. This includes dimensional verification as well as material and weld examination. The materials will also be certified to the material specifications. Shock absorbing material such as the paper honeycomb will also have verified material properties.

2.4. LIFTING AND TIE-DOWN STANDARDS FOR ALL PACKAGES

For analysis of the lifting and tie-down components of the TN-B1 packaging, material properties from Section 2.2 are taken at a bounding temperature of 75°C (167 ºF) per Section 2.6.1.1. This is the maximum temperature that the container reaches when in the sun. The primary structural material is 300 series stainless steel that is used in the Outer Container (OC).

A loaded TN-B1 package can be lifted using either a forklift or by slings. The gross weight of the package is a maximum of 1,614 kg (3,558 lb). Locating/protection plates for the forklift and locating angles for the sling locate the lift points for the package. In both cases the package is lifted from beneath. The failure of these locating/protective features would not cause the package to drop nor compromise its ability to perform its required functions.

The inner container may be lifted empty or filled with the contents using the sling fittings that are attached at the positions shown in Figure 2-2. The details of the sling fittings are as shown in Figure 2-3. Since the center of gravity depends on existence of the contents, the sling fittings for the filled container and the empty container are marked respectively as "Use When Loaded" and "Use When Empty" to avoid improper operations. Also, the sling fittings on the lid of inner container to lift the lid only are marked as "Use for Lifting Lid" similar to the outer container.

The sling devices are mechanically designed to be able to handle the package and the inner container filled with the fuel assemblies in safety; they can lift three times the gross weight of the package, or three times the gross weight of the filled inner container respectively, so that they can with stand rapid lifting.

Properties of 300 series stainless steel are summarized below.

Table 2-4 Properties of 300 Series Stainless Steel

Material Property	Value	Reference
At 75ºC (167 ºF)		
Elastic Modulus, E	191.7 GPa (27.8×10^6 psi)	Table 2-2
Yield Strength, σ_y	184.7 MPa (26,788 psi)	
Shear Stress, equal to (0.6) σ_y	110.8 MPa (16,073 psi)	

2.4.1. *Lifting Devices*

This section demonstrates that the attachments designed to lift the TN-B1 package are designed with a minimum safety factor of three against yielding, per the requirements of 10 CFR71.45 (a).

The lifting devices on the outer container lid are restricted to only lifting the outer container lid, and the lifting devices in the inner lid are restricted to only lifting the inner container lid. Although these lifting devices are designed with a minimum safety factor of three against yielding, detailed analyses are not specifically included herein since these lifting devices are not intended for lifting a TN-B1 package.

The outer container can be handled by either forklift or slings in a basket hitch around the package, requiring no structural component whose failure could affect the performance of the package.

2.4.1.1. **Lifting of Inner Container**

The inner container is lifted when loaded with fuel from the outer container with sling fittings attached to the body of the inner container. Three pairs (six in total) of the sling fittings are attached to the inner container as shown in Figure 2-2. The center of gravity depends upon whether the container is filled or not. Since the six sling fittings are the same, the stress in the sling fittings are evaluated for the case of at the maximum weight condition that occurs when the inner container is filled with fuel assemblies.

The stress on the sling fitting when lifting the inner container filled with contents is evaluated by determining the maximum load acting on any given fitting.

The maximum load, Pv, (see Figure 2-9) acting on one of the sling fitting vertically when lifting is given by the following equation:

$$P_v = \frac{(W_2 + W_3)}{n} \cdot g$$

Where:

P_v: maximum load acting to sling fitting in vertical direction	N
W_2: mass of inner container	308 kg (679 lb)
W_3: mass of contents	684 kg (1,508 lb)
n: number of sling fittings	4
g: acceleration of gravity	9.81 m/s^2

Accordingly, the maximum load acting on the sling fitting vertically is calculated as:

$$P_v = \frac{684 + 308}{4} x9.81 = 2.433x10^3 N\ (546.9lbf)$$

The load, P, acting to the sling fitting when the sling is at a minimum angle of 60° is calculated as:

$$P = \frac{P_v}{\sin\theta} = \frac{2.433x10^3}{\sin 60°} = 2.809\ \times\ 10^3\ \mathrm{N}\ (631\ \mathrm{lbf})$$

Also, the maximum load, PH, acting on the sling fitting horizontally is calculated as:

$$P_H = \frac{P_v}{\tan\theta} = \frac{2.433x10^3}{\tan 60°} = 1.405\ \times\ 10^3\ \mathrm{N}\ (316\ \mathrm{lbf})$$

Each sling fitting is made up of a hooking bar which is a 12mm diameter bent rod and a perforated plate that is made up of two pieces of angle that are welded together. The perforated plate of the sling fitting is welded to a support of that is welded to the body of the inner container.

The shearing stress in the hooking bar (see Figure 2-6) is given by the following equation:

$$\tau_N = \frac{Px\emptyset}{A}$$

Where

τ_N: shearing stress on hooking bar of sling fitting	MPa
P: maximum load	2.809×10^3 N (631 lbf)
A: cross-section of hooking bar of sling fitting	$\pi/4 \times 12^2 = 113$ mm^2 (0.175 in^2)
Ø: load factor	3

Accordingly, the shearing stress on the hooking bar of the sling fitting at its center is calculated as:

$$\tau_N = \frac{2.809x10^3x3}{113} = 74.58MPa(10{,}820psi)$$

The yield stress for stainless steel is 184.7 MPa (26,790 psi) and the shear allowable is 0.6 x184.7 = 110.8 MPa (16,070 psi) at the maximum normal temperature, hence the margin (MS) is

$$MS = \frac{110.8}{74.58} - 1 = 0.48$$

Therefore, the sling fitting can withstand three times the load without yielding in shear.

The strength of the perforated plate of a sling fitting is evaluated for failure by shearing. The shear stress on a perforated plate (see Figure 2-7) of the sling fitting by the total load is given by the following equation:

$$\tau_N = \frac{Px\emptyset}{A}$$

Where:

τ_N: shearing stress on the perforated plate of a sling fitting	MPa
P: maximum load	2.809×10^3 N (631 lbf)
A: cross-section of the upper part of the perforated plate:	$2x\frac{50-14}{2}\,x\,6 = 216mm^2(0.33in^2)$
Ø: load factor	3

Accordingly, the shearing stress, $\tau_{N,}$ on the perforated plate of sling fitting is calculated as:

$$\tau_N = \frac{2.809x10^3x3}{216} = 39.01 \text{ MPa } (5{,}658 \text{ psi})$$

The allowable shearing stress for stainless steel is 110.8 MPa (16,073 psi). Then the margin of Safety (MS) is:

$$MS=\frac{110.8}{39.01} - 1 = 1.84$$

Therefore, the shear strength of the plate meets the requirement of not yielding under three times the load.

Next, the strength of welds of the sling fittings is evaluated for the torsional loads applied. Torsional loads are applied to the welds of sling fitting per Figure 2-8.

The moment of inertia of area, $I_{P,}$ to the welds of sling fittings is given by the following equation:

$$I_P = I_X + I_Y$$

$$I_X = I_{X2} - I_{X1}$$

$$I_Y = \Sigma I_{Yi}$$

Where

I_P : moment of inertia of area to welds	mm^4
I_X : moment of inertia of area to welds for X-axis	mm^4
I_Y : moment of inertia of area to welds for Y-axis	mm^4
I_{X1} : moment of inertia of area to inside of weld for X-axis	mm^4
I_{X2} : moment of inertia of area to outside of weld for X-axis	mm^4
I_{Y1} : moment of inertia of area to each weld for Y-axis	mm^4

The moment of inertia of area, I, to a cross-sectional area of width, b, and height, h, is given by:

$$I = \frac{1}{12}bh^3$$

Conservatively only the outside welds not including any corner wrap around that attach the sling fitting to the support plate are considered. Thus, the moment of inertia of area, I_X and I_Y to the welds for X-axis and Y-axis are calculated as:

$$I_x = \left(\frac{1}{12}\ x\ 88\ x\ 54^3\right) - \left(\frac{1}{12}\ x\ 88\ x\ 50^3\right) = 2.38\ x\ 10^5\ mm^4\ (0.57\ in^4)$$

$$I_y = 2I_{Y1} = 2\ x\ \frac{1}{12}\ x\ 2\ x\ 88^3 = 2.27\ x\ 10^5\ mm^4\ (0.55\ in^4)$$

Accordingly, the moment of inertia of area, IP, to the welds is calculated as

$$I_p = (2.38\ x\ 10^5\ ) + (2.27\ x\ 10^5\ ) = 4.65\ x\ 10^5 mm^4\ (1.12\ in^4)$$

The shearing stress, $S_{d,}$ on the weld due to the load acting on the sling fitting is given by the following equation:

$$s_d = \frac{P\ \cdot\ \phi}{A}$$

Where:

S_d shearing stress on welds due to the load to sling fitting	MPa
P: maximum load acting to one of sling fitting	2.809×10^3 N (631 lbf)
A: overall cross-section of welds	$2 \times 88 = 176$ mm^2 (0.273 in^2)
ϕ: load factor	3

Accordingly, the shearing stress on welds due to the load acting to the sling fitting is calculated as:

$$S = \frac{2.809\ x\ 10^3\ x\ 3}{176} = 47.9 MPa\ (6{,}950\ psi)$$

The maximum bending moment acting to the sling fitting is given by the following equation from Figure 2-9.

$$M_{max} = P \cdot l$$

Where:

M_{max}: maximum bending moment acting to sling fitting	N · mm
P: maximum load acting to one of sling fitting	2.809×10^3 N (631 lbf)
l: distance from fulcrum to load point	17 mm (0.67 in)

Therefore, the maximum bending moment acting to the sling fitting is calculated as:

M_{max} = 2.809 × 10^3 × 17

= 4.8 × 10^4 N·mm (424.8 in·lbf)

The stress due to this bending moment is given by the following equation:

$$S_m = \frac{M_{max} \cdot r \cdot \phi}{I_p}$$

Where:

S_m: Stress acting to a point at r from center of gravity due to bending moment MPa

r: distance from center of gravity to end of welds $\sqrt{44^2 + 25^2} = 50.6\ mm\ (1.99\ in)$

M_{max}: maximum bending moment acting to sling fitting 4.8 × 10^4 N·mm (424.8 in·lbf)

I_P: moment of inertia of area to welds 4.65 × 10^5 mm^4 (1.12 in^4)

ϕ: load factor 3

From this equation, the maximum bending moment, S_m, acting to the sling fitting is calculated as:

$$S_m = \frac{4.8\ x\ 10^4 x\ 50.6\ x\ 3}{4.65\ x\ 10^5} 15.6 MPa\ (2{,}260\ psi)$$

In addition, the composite shearing stress, S, on the welds is given by the following equation:

$$S = \sqrt{S_d^2 + S_m^2 + 2 S_d S_m \cos\theta}$$

Where

Cos θ = 25/50.6

From this equation, the composite shearing stress, S, is calculated as

$$S = \sqrt{47.9^2 + 15.5^2 + 2\ x\ 47.9\ x\ 25/50.6}$$

= 57.2 MPa (8,300 psi)

Meanwhile, the allowable shearing stress for 300 series stainless steel is 110.8 MPa (16,073 psi).

Then the margin (MS) is:

$$MS = \frac{110.8}{57.2} - 1 = 0.94$$

The welds are capable of carrying 3 times the expected load without yielding.

Likewise the welds of the support plates for sling fittings are evaluated in the same manner. Since the welds of the support plates (see Figure 2-10) receive the same load as mentioned above in the case of the welds of the sling fittings, it is evaluated by same analytic method as mentioned above. The symbols used here shall have same meaning.

The moment of inertia of area, IP, to the welds of support plate is given by the following equation:

$$I_P = I_X + I_Y$$

Where:

IX = Ix2 – Ix1

IY = Iy2 – Iy1

The moment of inertia of areas I_X and I_Y to the welds for X-axis and Y-axis are calculated as:

$$I_X = \frac{1}{12} \times 153 \times 83^3 - \frac{1}{12} \times 150 \times 80^3$$

$$= 8.903 \times 10^5 \text{ mm}^4 \ (2.14 \text{ in}^4)$$

$$I_Y = \frac{1}{12} \times 83 \times 153^3 - \frac{1}{12} \times 80 \times 150^3$$

$$= 2.273 \times 10^6 \text{ mm}^4 \ (5.46 \text{ in}^4)$$

Accordingly, the moments of inertia of areas to the welds for the support plates are calculated as:

$$I_P = 8.903 \times 10^5 + 2.273 \times 10^6$$

$$= 3.163 \times 10^6 \text{ mm}^4 \ (7.60 \text{ in}^4)$$

The overall cross-section, A, of welds of the support plate is:

$$A = (153 \times 83) - (150 \times 80)$$

$$= 699 \text{ mm}^2 \ (1.08 \text{ in}^2)$$

The shearing stress, S_d, on the welds of the support plate for the sling fitting is calculated by a similar equation as the welds of the sling fitting.

$$S_d = \frac{2.809 \, x \, 10^3 x \, 3}{699} = 12.1 \text{ MPa (1,760 psi)}$$

In addition, the stress, S_m, on the welds of the support plate due to the bending moment is calculated as:

Where:

$$r = \sqrt{75^2 + 40^2} = 85 \text{ mm (3.35 in)}$$

$$S_m = \frac{5.9 \times 10^4 \times 85 \times 3}{3.163 \times 10^6} = 4.76 \text{ MPa (690 psi)}$$

Accordingly, the composite shearing stress S on the welds of support plate is calculated as:

$$S = \sqrt{S_d^2 + S_m^2 + 2 S_d S_m \cos\theta}$$

Where:

$$\cos\theta = 40/85$$

$$S = \sqrt{12.1^2 + 4.76^2 + \left(2 \times 12.1 \times 4.76 \times (40/85)\right)}$$

$$= 14.9 \text{ MPa (2,160 psi)}$$

Meanwhile, the allowable shearing stress for 300 series stainless steel is 110.8 MPa (16,073 psi). Then the margin of safety (MS) is:

$$MS = \frac{110.8}{14.9} - 1 = 6.4$$

Therefore, the support plate welds are capable of carrying three times the normal load and not yielding.

As indicated by the margins of safety calculated for each component, the hook bar has the lowest margin; therefore, in case of an overload the hook bar will fail prior to any other component. This ensures that, at failure, the rest of the packaging is capable of performing its function of protecting the fuel.

2.4.1.2. Package Lifting Using the Outer Container Lid Lifting Lugs

The outer container lid is lifted by four (4) Ø8-mm (Ø0.315 in.) Type 304 stainless steel bars that are welded to the 50 × 50 × 4 stainless steel lid flange angle. Under a potential excessive loading condition, such as lifting the entire loaded package, these four lifting lugs are required to fail prior to damaging the outer container lid structure.

The outer container lid is also equipped with the four (4) Ø6-mm (Ø0.236 in.) Type 304 stainless steel bar handles, which may be used to manually lift the lid. These bars are welded to the vertical leg of the lid flange angle with single-sided flare-bevel welds for an approximate length of 13 mm, as shown in View G-G on General Arrangement Drawing 105E3743. Since the handles have smaller cross-section (Ø6-mm vs. Ø8-mm), and have smaller and shorter attachment welds, the analysis of the lid lifting bars bounds the handles.

The four lifting bars will be used for this analysis with an assumed lifting angle of 45 degrees. From Table 2-1, the TN-B1 package weighs 1,614 kg [15,827 N] (3,558 lb). For the assumed lifting arrangement, the maximum load on the bar is:

$$F = 1/4\left[\frac{15{,}827}{\sin 45^\circ}\right] = 5{,}596 \text{ N } (1{,}258 \text{ lbs})$$

Assuming that the lift point is centered above the midpoint of the package (located 1,025 mm longitudinally and 318 mm laterally from lifting bar), the resultant forces on the lifting bar will be:

$$F_{horizontal} = F_{vertical} = F \cos 45^\circ = 3{,}957 \text{ N } (890 \text{ lbs})$$

$$F_{//} = F_{horizontal}\, sin\left(\tan^{-1}\left(\frac{1{,}025}{318}\right)\right) = 3{,}779 \text{ N } (850 \text{ lbs})$$

$$F_{\perp} = F_{horizontal}\, cos\left(\tan^{-1}\left(\frac{1{,}025}{318}\right)\right) = 1{,}173 \text{ N } (264 \text{ lbs})$$

where: $F_{horizontal}$ = Force in horizontal plane
$F_{//}$ = Force parallel to longitudinal axis of package
$F_{\perp}$ = Force perpendicular to longitudinal axis of package

These reaction loads will develop both bending and shear stresses in the bar, shear stresses in the attachment welds, and tensile stresses in the flange angle. Each of these stress components will be analyzed separately.

Bending of Bar

The maximum reaction load on the lifting bar will be bending stresses in the bar. Treating the bar as a fixed-fixed beam, the maximum bending stress, σ_b, will be:

$$\sigma_b = \frac{M_{max}}{Z_{Bar}}$$

where: $M_{max} = 1/8[(F_{vertical})^2 + (F_{//})^2]^{1/2}(l) = 1/8(5,472)(76) = 51,984$ N-mm (460 lb_f-in) $Z_{bar} = \pi(d^3)/32 = \pi(8^3)/32 = 50.3$ mm^3 (0.003 in^3)

$l = 2(46-8) = 76$ mm (2.99 in) [assumed equal to bent free length of bar]

Substituting these values results in a maximum bending stress of 1,033 MPa (149,824 psi). The allowable bending stress for the Type 304 material is equal to Sy = 184.7 MPa (26,788 psi). Therefore, the margin of safety against yielding in bending is:

$$MS = \frac{184.7}{1,033} - 1.0 = -0.8$$

Shear of Bar

The maximum reaction load on the lifting bar will result in shear stresses in the bar. For the shearing the bar, the maximum shear stress will be:

$$\tau_{bar} = \frac{\left[(F_{Vertical})^2 + \left(F_{//}\right)^2\right]^{1/2}}{Area} = \frac{5,472}{(\pi/4)(8)^2} = 108.9 \text{ MPa } (15,795 \text{ psi})$$

The allowable shear stress for the Type 304 material is equal to 0.6Sy = 0.6(184.7) = 110.8 MPa (16,070 psi). Therefore, the margin of safety against yielding in shear is:

$$MS = \frac{110.8}{108.9} - 1.0 = 0.02$$

Tension in Bar

Since the bending stress is well beyond the yield strength, the bar will bend until the reaction load will be reacted as pure tension in the bar. For this condition, the tensile stress, $\sigma_{t\text{-}bar}$, in the bar will be:

$$\sigma_{t-bar} = \frac{F}{2(Area)} = \frac{5,596}{2\left[\left(\frac{\pi}{4}\right)(8^2)\right]} = 55.7 MPa (8,079 psi)$$

The allowable tensile stress for the Type 304 material is equal to the minimum yield strength, 184.7 MPa (26,788 psi). The margin of safety for this condition is then:

$$MS = \frac{184.7}{55.7} - 1.0 = 2.3$$

Attachment Welds

As shown in View F-F on General Arrangement Drawing 105E3743, the lifting bars are welded to the lid flange angle with double-sided flare-bevel welds for an approximate length of 28 mm (1.10 in.) on each leg of the bar. The ends of the bar are welded with a seal fillet weld, which has minimal strength and hence, will be ignored. Since the bar is relatively small, the flare-bevel weld will be treated as an equivalent fillet weld with a 4-mm leg. For this assumption, the maximum primary shear stress, τ_{weld}, in the weld will be:

$$\tau_{weld} = \frac{\left[(F_{vertical})^2 + (F_{//})^2\right]^{1/2}}{Shear\ area\ of\ welds} = \frac{5,472}{4(4Cos45°)(28)} = 17.3MPa\ (2,509psi)$$

Due to the off-set, there will also be a secondary (torsion) shear stress, τ'_{weld}, component:

$$\tau'_{Weld} = \frac{\mathrm{Mr}}{\mathrm{J}}\frac{Mr}{J}$$

where: M = applied moment to weld group

= $[(F_{vertical})^2 + (F_{//})^2]^{1/2}$(distance from centroid + bend radius + ½ bar diameter)

= 5,472(14 + 8 + 4) = 142,272 N-mm (1,259 lb_f - in)

r_{max} = distance from centroid of weld group to farthest point in weld

= $[(1/2(46-8))^2 + (14)^2]^{1/2}$ = 23.6 mm (0.929 in)

J = second polar moment of inertia of weld group, mm^4

Since the four flare-bevel welds are the same size and location, the second polar moment of inertia for the weld group is determined treating the welds as a line*. For this case, the second polar moment of inertia is:

$$J = 0.707(h)\frac{d(3b^2 + d^2)}{6}$$

* Shigley, Joseph E., and Mischke, Charles R., *Mechanical Engineering Design, Fifth Edition*, McGraw-Hill, Inc., 1989.

where:

h = leg length of weld = 4 mm

d = length of weld = 28 mm

b = distance between weld groups = (462 + 462)1/2 = 65.1 mm

Substituting these values results in a secondary polar moment of inertia of 178,138 mm^4 (0.428 in^4). The secondary shear stress then becomes:

$$\tau'_{weld} = \frac{(142{,}272)(23.6)}{178{,}138} = 18.8 \text{ MPa } (2{,}727 \text{ psi})$$

The total shear stress in the weld is then the square root of the sum of the squares of the primary shear and secondary shear:

$$\tau_{total} = [(\tau_{weld})^2 + (\tau'_{weld})^2]^{1/2} = 25.5\ MPa\ (3{,}698\ psi)$$

The allowable shear stress for the Type 304 material is equal to 110.8 MPa (16,070 psi). Therefore, the margin of safety against yielding in shear for the welds is:

$$MS = \frac{110.8}{25.5} - 1.0 = 3.3$$

Shear Tearout of Base Metal

Shear tearout of the 4-mm thick base metal is evaluated by conservatively considering only the area of a section equal to the weld length of the two welds. The 2-mm thick sheet that is attached to the vertical leg of the flange angle is ignored for this calculation. The total tensile area, A_t, will be:

$$A_{shear} = 2[4(28)] = 224 \text{ mm}^2\ (0.347 \text{ in}^2)$$

For this case, the shear stress of the base metal, $\tau_{base\ metal}$, is:

$$\tau_{base\ matal} = \frac{F}{A_{Shear}} = \frac{5{,}596}{224} = 25.0 \text{MPa } (3{,}624 \text{ psi})$$

The allowable shear stress for the Type 304 material is equal to 110.8 MPa (16,070 psi). The margin of safety for this condition is then:

$$\text{MS} = \frac{110.8}{25.0} - 1.0 = 3.4$$

Summary

As demonstrated by these calculations, the minimum margin of safety for the outer container lid lifting lugs is -0.8, which results in failure of the bar in bending for lifting the complete loaded package. The largest positive margin of safety (+3.4) occurs in the base metal of the lid flange angle, which demonstrates that the outer container lid structure would not fail in an excessive load condition. All other margins of safety in the load path are positive, but are lower than the base metal. Therefore, potentially lifting the complete package by these lid lifting lugs will fail the lifting bar and have no detrimental effect on the effectiveness of the TN-B1 package.

2.4.2. *Tie-Down Devices*

There are no tie-down features that are a structural part of the TN-B1 package. The packages are transported either in container vans or on flatbed trucks. When transported in container vans, blocking and bracing is provided that distributes any loads into the packages. This bracing and blocking is customized to address individual shipping configurations and the specific container van being used. When transported on a flatbed trailer, straps going over the package are used to secure it to the trailer. Therefore, the requirements of 10 CFR 71.45(b) are satisfied since no structural part of the package is used as a tie-down device.

An evaluation is performed on the ability of the package to withstand loadings of 2 g vertical and 5 g laterally when restrained by strapping. The worst-case loading situation for the packages is when they are stacked in groups of 9 on a flatbed trailer and secured with a minimum of 3 straps. Although the packages may be shipped in other configurations such as 2x3 the greatest strap loading that would be applied to the package when secured in a 3x3 configuration. Between each adjacent column of packages 2 × 4 wood shoring may be placed where the straps will be applied. The evaluation below is conservatively performed without the 2 × 4 shoring in place.

As a bounding evaluation, it is assumed that the outside corners of the top outside packages carry all the vertical loads that would result from the vertical acceleration and the vertical load required to resist the over-turning moment from the horizontal acceleration. The corners of all top packages would actually carry the vertical load. See Figure 2-11.

For modeling purposes, the matrix of nine packages is treated as a rigid body. By summing moments, the vertical force required to prevent the over-turning of the stack by the horizontal loads is determined. This load is conservatively applied to one edge of one container

The key dimensions and weights for each package are:

Width	w = 720 mm (28.3in)
Total Height	h = 742 mm (29.2in)

CG height	cgy = 421 mm (16.6 in)
Mass of each package	m = 1,614 kg (3,558 lb) Gravitational
acceleration	$g = 9.81\ m/sec^2$
Vertical acceleration factor	$g_V = 2$
Horizontal acceleration factor	$g_h = 5$

The vertical center of gravity of the 9-package matrix is:

$$CGy = 3mg(2h + cgy)/9mg + 3mg(h + cgy)/9mg + 3mg(cgy)/9mg = 1.163 \times 10^3 \text{ mm (45.8 in)}$$

Summing the forces in the vertical direction due to the 2 g loading, the strap load applied at the two locations can be determined for this load condition.

$$R_{st} = 9\ g_v\ m\ g/2 = 1.425 \times 10^5 \text{ N } (3.202 \times 10^4 \text{ lb}_f)$$

Summing moments about one of the bottom corners of the stack will determine the strap force required to resist overturning due to the horizontal loading.

$$R_s = \frac{(g_h(CG_y)9mg)}{(3w)} = 3.835 \times 10^5 \text{ N } (8.621 \times 10 \text{ lb}_f)$$

Total vertical strap load is:

$$R_t = R_{st} + R_s = 5.260 \times 10^5 \text{ N } (1.182 \times 10^5 \text{ lb}_f)$$

Checking the support plate carrying capability:

There are eight (8) 5mm × 55mm support plates in groups of two (2) that carry the vibro-isolation frame inside the outer container. These are skipped welded to the wall, plus have two thick (10 and 15 mm) by 80 mm and 70 mm wide plates welded between them. These plates are in addition to the body straps and the body struts (angles) in corners that provide vertical stiffening to the side panels. On top of the side panel, there are two angles that make up the flange in both the body and the lid that provide load distribution capability to the side wall and the internal structure. In addition these angles are stiffen at the ends by the bolster support angle that further distributes the end strap loads to the end structure of the package reducing load in the sides of the package.

Since the eight support plates are assembled together in groups of two with the reinforcement plates connecting the plates along with the welding to the wall, each two-plate section is considered as a column that is capable of carrying the tie-down loads. Addressing the support plates as a channel section, which is 140 mm wide and 57 mm deep, its properties can be determined.

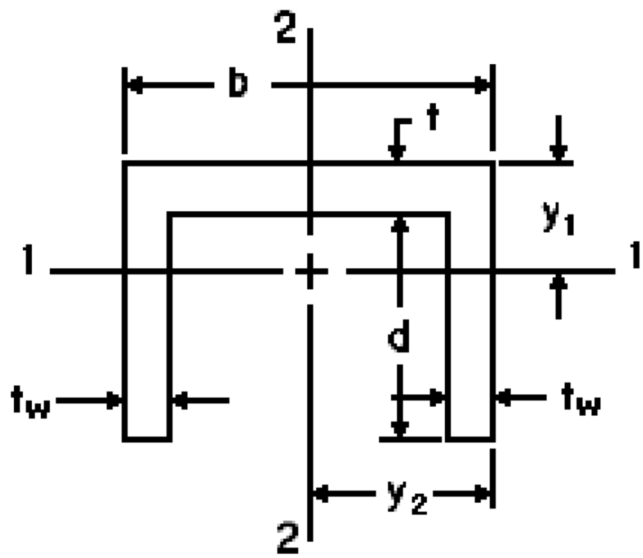

Channel section	
Length of web	b = 140 mm (5.5 in)
Length of flange	d = 55mm (2.2 in)
Web thickness	t = 2 mm (0.08 in)
Flange thickness	t_w = 5 mm (0.2 in)
Area	$A = t_b + 2t_wd = 830.3\ mm^2\ (1.287\ in^2)$

Since there are four of these assemblies to a side the total area is:

$$A_{spt} = 4A = 3{,}321\ mm^2\ (5.148\ in^2)$$

The compressive stress is

$$\sigma_c = R_t/A_{spt} = 158.4\ MPa\ (23.0\ ksi)$$

This is less than the yield stress of the Type 304 stainless steel S_y = 206.8 MPa (30.0 ksi).

The resistance of the plate to buckling is also evaluated. The equation to obtain the moments of inertia of area of the support plate which are subject to buckling is:

$$y_1= (bt^2+2t_wd(2t+d))/2(tb+2t_wd) = 19.9\ mm\ (0.783\ in)$$

$$y_2 = b/2 = 70\ mm\ (2.756\ in)$$

Moments of Inertia

$$I_1 = b(d+t)^3/3 + d^3(b-2t_w)/3-A(d+t-y_1)^2 = 2.894 \times 10^5 mm^4\ (0.695\ in^4)$$

$$I_2 = (d+t)b^3/12 – d(b-2t_w)^3/12 = 2.110 \times 10^7 \text{ mm}^4 \ (7.122 \text{ in}^4)$$

The radius of gyration can then be calculated for each axis:

$$r_1 = \sqrt{\frac{I_1}{A}} = 18.7 \text{ mm } (0.736 \text{ in}) \qquad r_2 = \sqrt{\frac{I_2}{A}} = 59.7 \text{ mm } (2.35 \text{ in})$$

The minimum radius of gyration indicates the weakest orientation for buckling:

$k = r_1 = 18.7$ mm (0.736 in)

ℓ: Length of support plate = 160 mm (6.3 in)

Also, the slenderness ratio, $\frac{L}{k}$ is:

$$\frac{L}{k} = \frac{160}{18.7} = 8.6$$

As the ends are fixed, the coefficient “n” becomes 4, so the limit value of the slenderness ratio becomes:

$$85\sqrt{n} = 85\sqrt{4} = 170$$

Because the slenderness ratio of this material is less than the limit value slenderness ratio, Euler's equation is not applicable, and the secant formula for buckling is used. The equation to obtain the support plate's buckling strength is:

$$\frac{P}{A} = \frac{S_y}{1 + \frac{ec}{k^2} sec\left[\frac{C\ell}{2k}\sqrt{\frac{P}{AE}}\right]}$$

Where:

P: Buckling strength (load) of support column N

A: Area of column = 830.3 mm^2 (1.287 in^2)

Sy: Minimum yield strength of Type 304 stainless steel = 206.8 MPa (30.0 ksi)

C: Coefficient to the long support fixed at both ends = 1.2

E: Elastic modulus of Type 304 stainless steel = 1.95 × 105 MPa (Table 2-2 at 40°C)

e: Eccentricity small since the strap load is centered = 5 mm (0.2 in)

ℓ: Unsupported length of the support column = 160 mm (6.3 in) c: Shortest distance to an outside side edge from the centroid = 19.9 mm (0.783 in)

Substituting these values in the above equation and solving for P iteratively results in a buckling strength of the support plate column of:

$$P = 1.332 \times 10^5 \text{ N } (29{,}945 \text{ lb}_f)$$

There are four support columns to a side, which results in the sidewall frame having a minimum capacity of:

$$P_t = 4P = 5.328 \times 10^5 \text{ N } (119{,}780 \text{ lb}_f)$$

Since this load capacity is greater than the applied load ($R_t = 5.259 \times 10^5$ N (1.182×10^5 lb_f)), the supports will not buckle when the worst-case tie-down loads are applied to a package. This capacity approaches the force required to yield the columns in compression (i.e., $A_{spt}S_y = 6.868 \times 10^5$ N (1.544×10^5 lb_f).

By considering the stiffening of the support plates with the reinforcement plates used to carry the inner support frame, it has been demonstrated that the support plates have sufficient capacity to react the tie-down load if the package experiences a 5 g lateral and a 2 g vertical loading simultaneously. This evaluation does not take into consideration the large carrying capability of the ends of the package where there are corner angles, end plates, and wood overlay plates that further strengthen the package's buckling capability. The use of three or more straps ensures that the load is distributed along the package so that the load can be reacted by the support plates and other internal structure. The stiffness of the OC lid, when the bolster support angles are considered with the reinforced edge of the OC body, ensures that the load is distributed to the internal structure of the package.

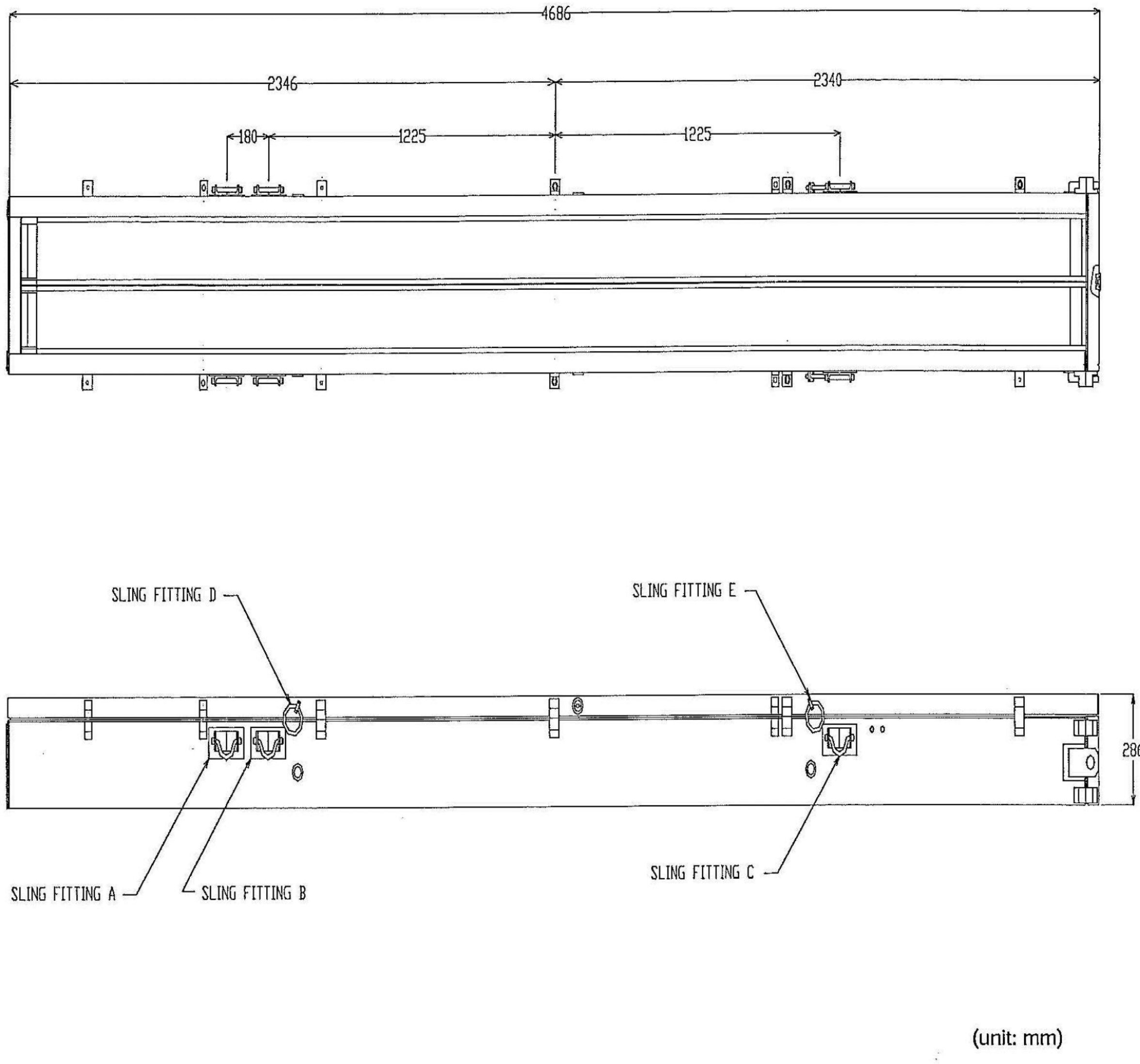

Combination of sling fitting	Used for
A and C	Lifting a Loaded Container
B and C	Lifting an Empty Container
D and E	Lifting a Lid

Figure 2-2 Inner Container Sling Locations

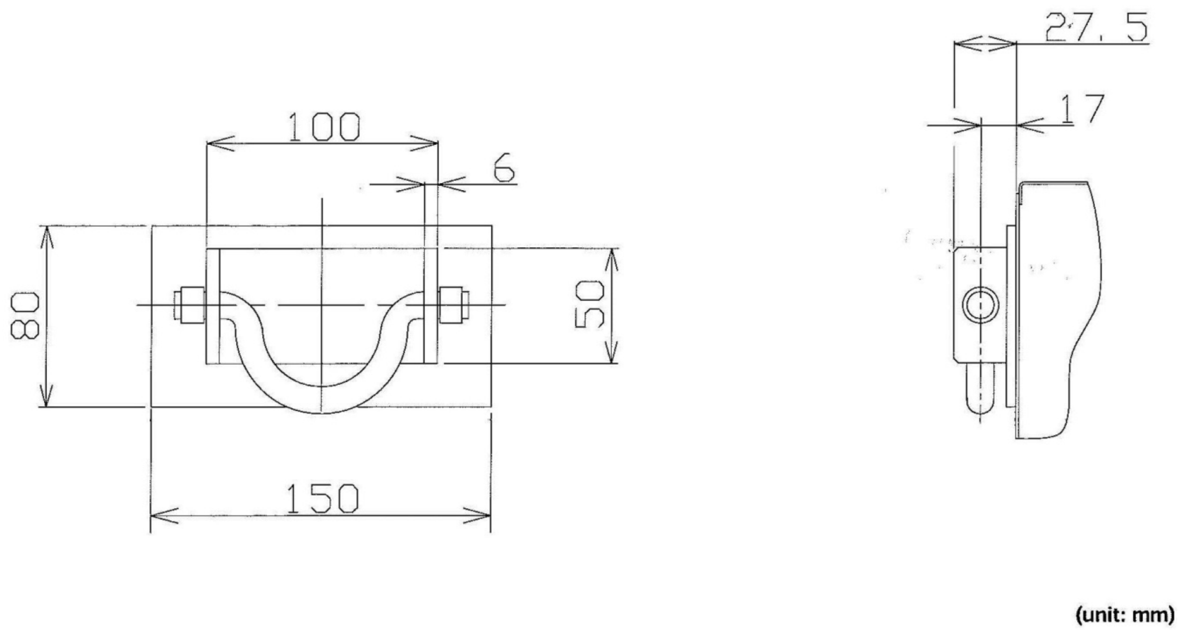

Figure 2-3 Sling Attachment Plate Detail

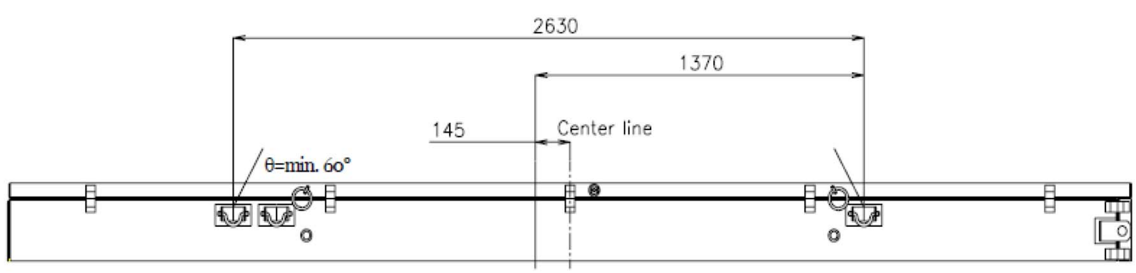

Figure 2-4 Lifting Configuration of Inner Container

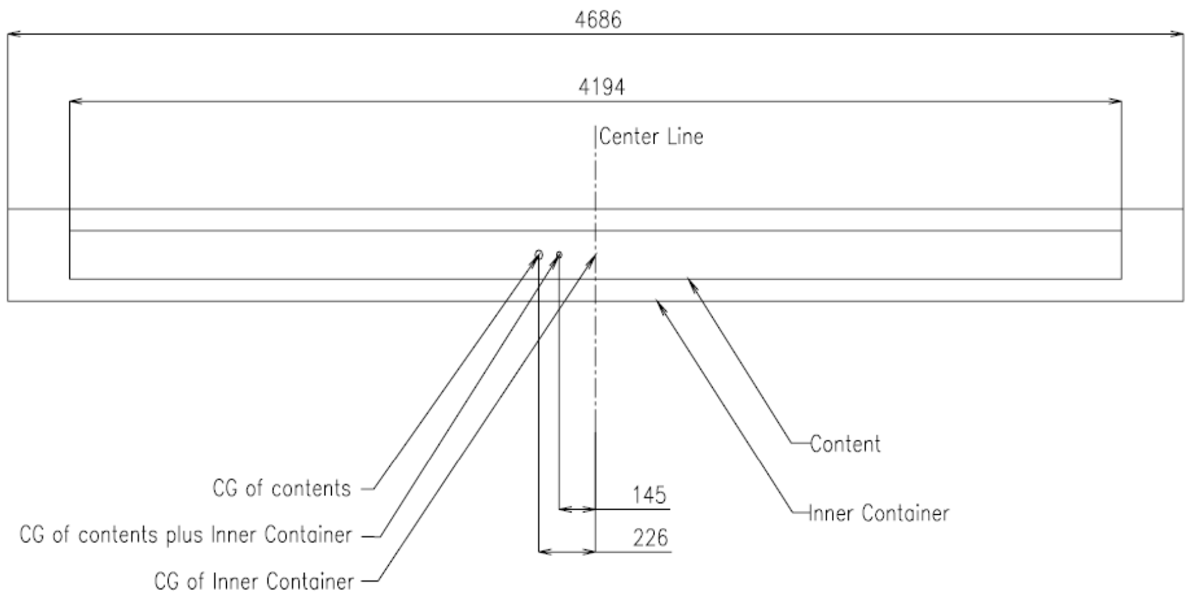

(unit: mm)

Figure 2-5 Center of Gravity of Loaded Inner Container

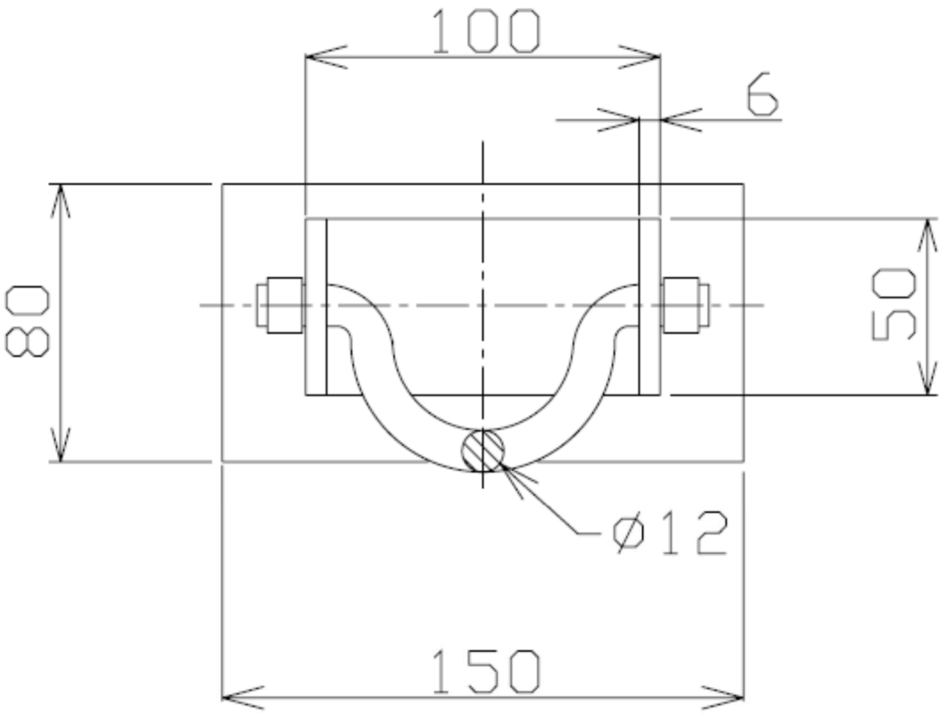

(unit: mm)

Figure 2-6 Hooking Bar of Sling Fitting

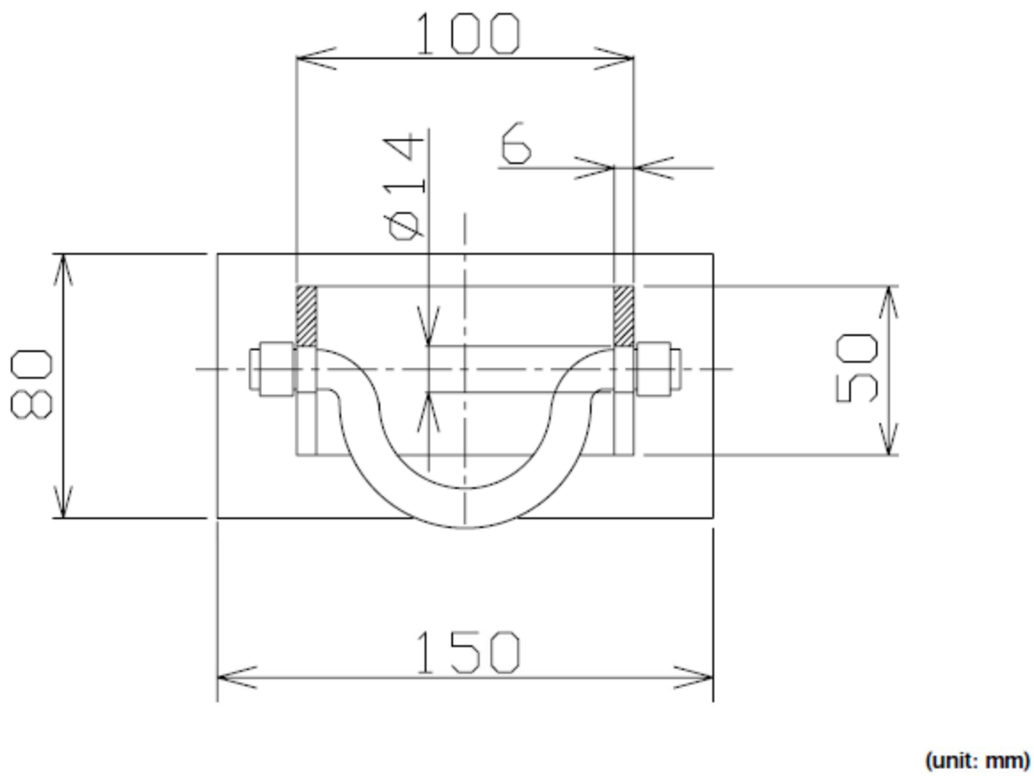

Figure 2-7 Perforated Plate of Sling Fitting

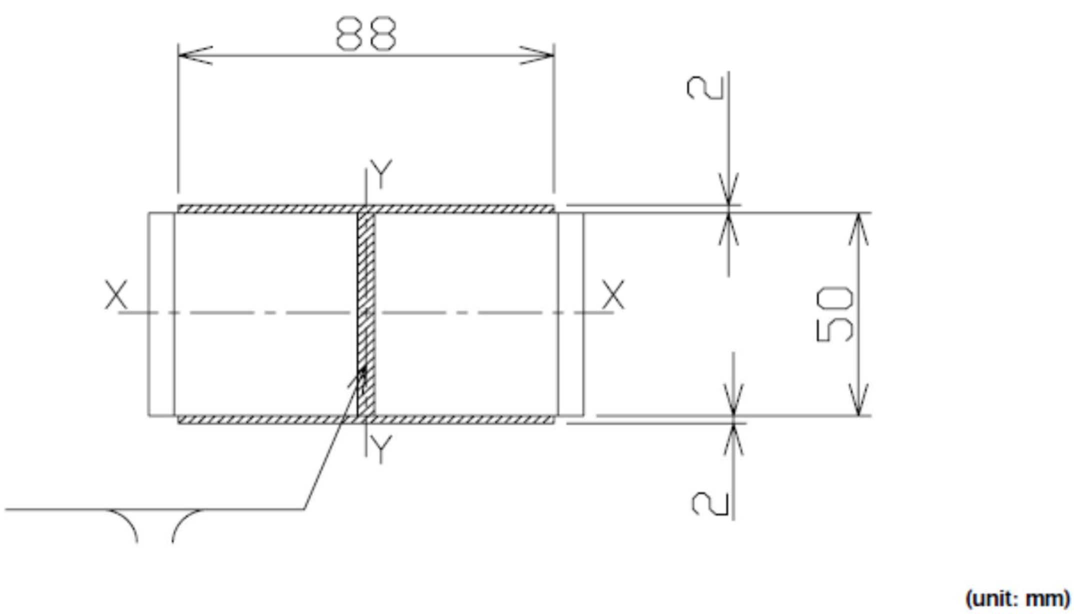

Figure 2-8 Sling Fitting Weld Geometry for Attachment to Support Plate

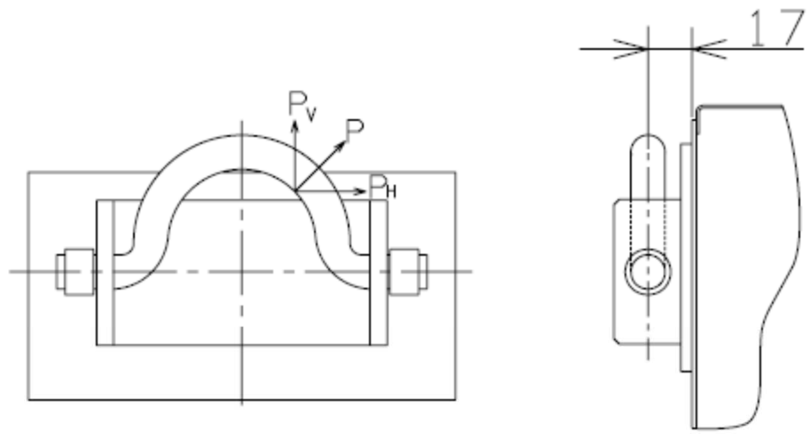

(unit: mm)

Figure 2-9 Loads on Sling Fitting

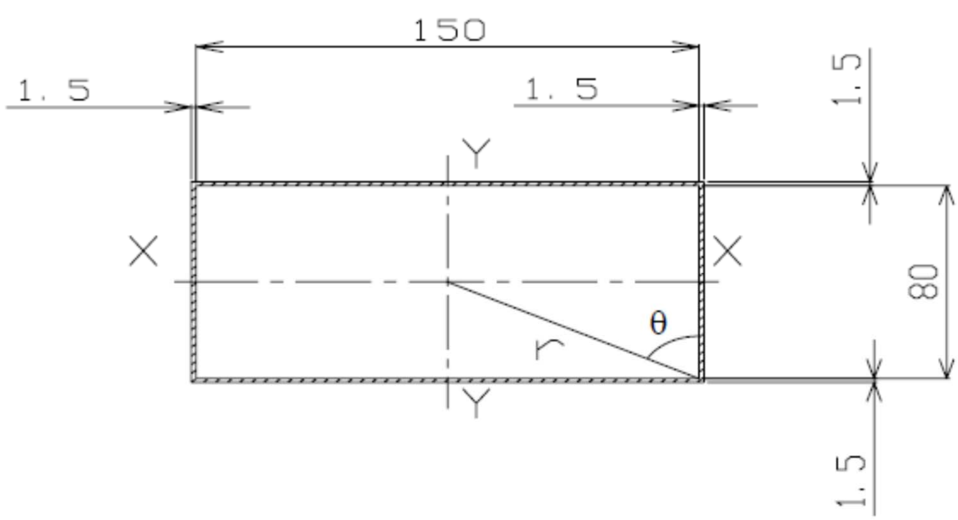

(unit: mm)

Figure 2-10 Welds for Support Plate Attachment to Body

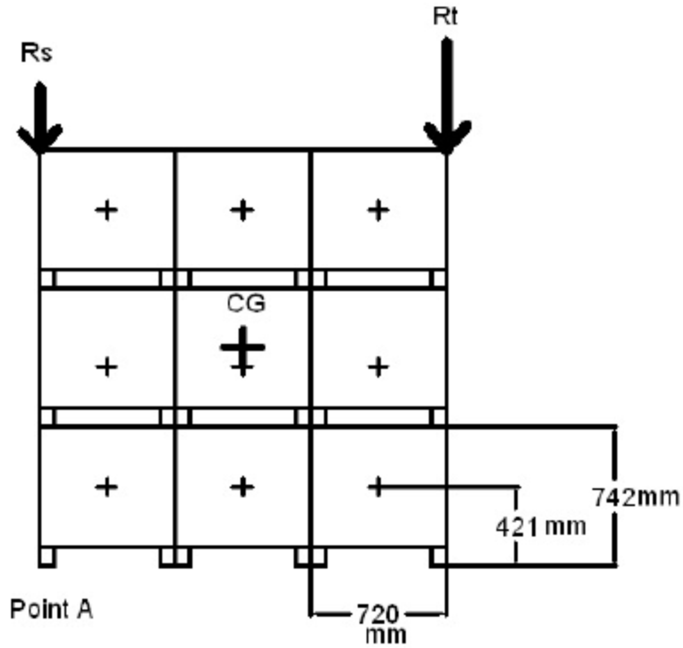

Figure 2-11 Tie-Down Configuration

2.5. GENERAL CONSIDERATIONS

2.5.1. *Evaluation by Test*

The primary means of demonstrating that the package meets the regulatory accident conditions was by test. The package was tested full-scale by dropping four full-scale certification test units (CTUs) from 9 meters in different orientations. (Two of the test units were dropped as part of the Japanese certification process.)

Within the GNF-A CTUs, the fuel was mocked up by a metal boxed section that provided the representative weight in one fuel assembly shipping location. The steel section was segmented to prevent the mockup from adding unrealistic stiffness to the package. In the other fuel assembly shipping position a mockup fuel assembly was used. This had the same cross-sectional properties of the actual fuel. The rods were filled with lead to represent the actual fuel. Weights were added along side of the assembly to provide the correct mass for the fuel that may be shipped with channels as well as allowing for the different density between lead and the uranium oxide pellets.

The units tested in Japan had a simulated 8X8 fuel assembly and weights representing the other fuel assembly in each test unit. The weight and dimensions of the mockup fuel approximated the weight of the fuel to be shipped in the container.

Details of the prototypes in the drop can be found in Section 2.7 and Appendix 2.12.

The damage caused by the test was evaluated in each of the affected sections, Section 3.0, Section 4.0, and Section 6.0. Both the inner and outer lids stayed in place, although damaged. The inner container holding frame deformed but restrained the inner container. Due to the end drop there was some plastic deformation of the fuel but well within the limits of the criticality evaluation. After the testing, the GNF-A fuel rods passed a helium leakage rate test demonstrating containment.

(Note that the TN-B1 and the RAJ-II are structurally identical so that the results from both the GNF-J and GNF-A tests apply to the TN-B1.)

2.5.2. *Evaluation by Analysis*

The normal conditions of transport were evaluated by analysis and by comparison to the accident testing. The primary analysis was done for the compression loading. The material properties are taken from Table 2-4, which is based on published ASME properties. A static analysis was performed in Section 2.6.9 Compression.

Since the normal condition pressure and temperatures are well below the design conditions for the fuel cladding no separate analysis was performed.

2.6. NORMAL CONDITIONS OF TRANSPORT

The TN-B1 package, when subjected to the Normal Conditions of Transport (NCT) specified in 10 CFR 71.71, is shown to meet the performance requirements specified in Subpart E of 10 CFR 71. As discussed in the introduction to this chapter, with the exception of the NCT free drop, the primary proof of NCT performance is via analytic methods. Regulatory Guide 7.6 criteria are demonstrated as acceptable for NCT analytic evaluations presented in this section. Specific discussions regarding brittle fracture and fatigue are presented in Sections 2.1.2.4 and 2.6.5 and are shown not to be limiting cases for the TN-B1 package design. The ability of the welded containment fuel rod cladding to remain leak-tight is documented in Section 4.0.

Properties of Type 304 stainless steel as representative of those properties for 300 series stainless steel are summarized below.

Table 2-5 Material Properties

Material Property	Material Property Value (psi)			Reference
	-40 ºC (-40 ºF)	21ºC (70 ºF)	75ºC (167ºF)	
	Type 304 Stainless Steel			
Elastic Modulus, E	198.6GPa (28.8×10^6psi)	195.1GPa (28.3×10^6psi)	191.7GPa (27.8×10^6psi)	Table 2-2
Design Stress Intensity, S_m	137.9MPa (20,000 psi)	137.9MPa (20,000 psi)	137.9MPa (20,000 psi)	
Yield Strength, S_m	206.8MPa (30,000psi)	206.8MPa (30,000psi)	184.7MPa (26,788psi)	
Tensile Strength	517.1MPa (75,000psi)	517.1MPa (75,000psi)	498.6MPa (72,300)	

The TN-B1 package's ability to survive HAC, 30-foot free drop, 40-inch puncture drop, and 30-minute thermal event also demonstrated the packages ability to also survive the NCT. Evaluations are performed, when appropriate, to supplement or expand on the available test results. This combination of analytic and test structural evaluations provides an initial configuration for NCT thermal, shielding and criticality performance. In accordance with 10 CFR 71.43(f), the evaluations performed herein successfully demonstrate that under NCT tests the TN-B1 package experiences "no substantial reduction in the effectiveness of the packaging". Summaries of the more significant aspects of the full-scale free drop testing are included in Section 2.6.7, with details presented in Appendix 2.12.1.

2.6.1. ***Heat***

The NCT thermal analyses presented in Section 3.0, consist of exposing the TN-B1 package to direct sunlight and 100 ºF still air per the requirements of 10 CFR 71.71(b). Since there is negligible decay heat in the unirradiated fuel, the entire heating came from the solar insolation. The maximum temperature of 77°C (171°F) was located on the lid of the outer container.

2.6.1.1. **Summary of Pressures and Temperatures**

The fuel assembly exhibits negligible decay heat. The TN-B1 package and internal components, when loaded with the required 10 CFR 71.71(c) (1) insulation conditions, develop a maximum temperature of 77 ºC (171 ºF). The resulting pressure at the maximum temperature is 1.33 MPa (192.9 psia) when the fuel rods are pressurized with helium to a maximum pressure of 1.1145 MPa (absolute pressure) (161.7 psia) at ambient temperature.

2.6.1.2. **Differential Thermal Expansion**

With NCT temperatures throughout the packaging being relatively uniform (i.e. no significant temperature gradients), the concern with differential expansions is limited to regions of the TN-B1 packaging that employ adjacent materials with sufficiently different coefficients of thermal expansion. The IC is a double-walled, composite construction of alumina silicate thermal insulator between inner and outer walls of stainless steel. The alumina silicate thermal insulator is loosely packed between the two walls and does not stress the walls. Differential thermal expansion stresses are negligible in the OC for three reasons: 1) the temperature distribution throughout the entire OC is relatively uniform, 2) the OC is fabricated from only one type of structural material, and 3) the OC is not radially or axially constrained within a tight-fitting structure due to the relatively low temperature differentials and lack of internal restraint within the TN-B1 package.

The cladding of the fuel which serves as containment is not stressed due to differential thermal expansion since a gap remains between the fuel pellet and the cladding at both the cold temperature -40°C and the highest temperature the fuel could see due to the HAC which is 800°C. This is demonstrated as follows:

The nominal fuel pellet and cladding dimensions and the resulting radial gap (0.00335 inches) is shown below based on a temperature of 20°C:

As-Built Dimensions (inches)		
Nominal Clad OD	D_{co}	0.3957
Nominal Clad ID	D_{ci}	0.348
Nominal Pellet OD	D_{fo}	0.3413
Nominal Radial Pellet/Clad	g_n	0.00335

The strain due to thermal expansion or contraction in the Zr cladding is equal to*

$$\left(\frac{\Delta D}{D}\right)_{Clad} = 7.4\ x\ 10^{6}\ (\Delta T)$$

Where ΔT is positive for an increase in temperature and negative for a decrease in temperature.

* Framatome ANP MOX Material Properties Manual 51-5010288-03

The strain due to thermal expansion or contraction in the fuel pellet is equal to*:

$$\left(\frac{\Delta D}{D}\right)_{Clad} = -3.28\times10^{-3} + 1.179\times10^{-5}T - 2.429\times10^{-9}T^2 + 1.219\times10^{-12}T^3$$

Where T is the absolute final temperature in degrees Kelvin (K).

The following table summarizes the thermal strain and the thermal growth in the cladding and pellets with a temperature change from 20°C to -40°C (ΔT = −60o C, T = 233K). All dimensions are expressed in inches.

Table 2-6 Thermal Contraction at -40°C

	Strain at -40°C $\left(\frac{\Delta D}{D}\right)$	Thermal Expansion at -40°C $\left(\frac{\Delta D}{D}\right)D$	Dimension at -40°C D+ $\left(\frac{\Delta D}{D}\right)$D
Pellet OD	-6.49×10^{-4}	-2.22×10^{-4}	0.3411
Cladding ID	-4.44×10^{-4}	-1.55×10^{-4}	0.3478

This results in a radial gap at -40°C of:

$$g_{-40} = \frac{0.3478 - 0.3411}{2} = 0.0034\ in$$

The following table summarizes the thermal strain and the thermal growth in the cladding and pellets with a temperature change from 20°C to 800°C (ΔT = 780°C, T = 1,073K). All dimensions are expressed in inches.

Table 2-7 Thermal Expansion at 800°C

	Strain at 800°C $\left(\frac{\Delta D}{D}\right)$	Thermal Expansion at 800°C $\left(\frac{\Delta D}{D}\right)D$	Dimension at 800°C D+ $\left(\frac{\Delta D}{D}\right)$D
Pellet OD	8.08×10^{-3}	2.76×10^{-3}	0.3441
Cladding ID	5.77×10^{-3}	2.01×10^{-3}	0.3500

* Framatome ANP MOX Material Properties Manual 51-5010288-02

This results in a radial gap at 800°C of:

$$g_{800} = \frac{0.3500 - 0.3411}{2} = 0.0030\ in$$

2.6.1.3. **Stress Calculations**

Since the temperatures and pressures generated under normal conditions of transport are well below the design conditions for the boiling water reactor fuel no specific calculations were performed for the fuel containment.

2.6.1.4. **Comparison with Allowable Stresses**

The normal conditions of transport conditions are well below the operating conditions of the fuel no comparison to allowable stresses was performed.

2.6.2. ***Cold***

The NCT cold condition consists of exposing the TN-B1 packaging to a steady-state ambient temperature of -40 ºF. Insulation and payload internal decay heat are assumed to be zero. These conditions will result in a uniform temperature throughout the package of -40 ºF. With no internal heat load (i.e., no contents to produce heat), the net pressure differential will only be reduced from the initial conditions at loading.

For the containment, the principal structural concern due to the NCT cold condition is the effect of the differential expansion of the fuel to the zirconium alloy tube. During the cool-down from 20 ºC to -40 ºC, the tube could shrink onto the fuel because of difference in the thermal expansion coefficient. However, the clearance between the fuel and the cladding is such that even if the fuel did not shrink, there would still be clearance. Differential thermal expansion stresses are negligible in the package for three reasons: 1) the temperature distribution throughout the entire package is relatively uniform, 2) the package is fabricated from only one type of structural material, and 3) the package is not radially or axially constrained.

Brittle fracture at -40 ºF is addressed in Section 2.1.2.4.1.

2.6.3. ***Reduced External Pressure***

The effect of a reduced external pressure of 25 kPa (3.5 psia) per 10 CFR 71.71(c)(3) is negligible for the TN-B1 packaging. The TN-B1 package contains no pressure-tight seal and therefore cannot develop differential pressure. Therefore, the reduced external pressure requirement of 3.5 psia delineated in 10 CFR 71.71(c)(3) will have no effect on the package. Compared with the 1.115 MPa (161.7 psia) internal pressure in the fuel rods, a reduced external pressure of 3.5 psia will have a negligible effect on the fuel rods.

2.6.4. *Increased External Pressure*

The TN-B1 package contains no pressure-tight seal and, therefore, cannot develop differential pressure. Therefore, the increased external pressure requirement of 140 kPa (20 psia) delineated in 10 CFR 71.71(c)(4) will have no effect on the package. The pressure-tight cladding of the fuel rods is designed for much higher pressures in its normal service in a reactor and is not affected by the slight increase in external pressure.

The containment is provided by the cladding tubes of the fuel. These tubes, designed for the conditions in an operating reactor, have the capability of withstanding the increased external pressure. The failure mode of radial buckling is not a plausible failure mode since the fuel pellets would prevent any significant deformation due to external pressure.

2.6.5. *Vibration*

The TN-B1 packaging contains an internal shock mount system and, therefore, cannot develop significant vibratory stresses for the package's internal structures. Therefore, vibration normally incident to transportation, as delineated in 10 CFR 71.71(c)(5), will have a negligible effect on the package. Due to concerns of possibly damaging the fuel so it cannot be installed in a reactor after transport, extreme care is taken in packaging the fuel using cushioning material and vibration isolation systems. These systems also ensure that the fuel containment boundary also remains uncompromised. The welded structure of the lightweight TN-B1 package is unaffected by vibration. However, after each use the packaging is visually examined for any potential damage.

The vibration isolation system is sized, and rubber materials selected for specific fuel assembly requirements, to absorb normal transportation vibration and not impact type loads that quickly exceed the small compression range of the vibro-isolators. The primary purpose of the vibration isolation system is to maintain fuel quality (for reactor purposes) with changes to the rubber and vibration absorbing properties having no effect on the existing tests and analysis to the impact performance of the packaging.

The fuel assembly cushioning material within the inner container is to maintain the quality of the fuel assembly design for use in-reactor against vibrations during transport. The ability of the cushioning material to absorb impacts is severely limited by its thickness and small compression range. Material changes allowing alternate rubber cushioning material has no effect on the existing tests and analysis.

2.6.6. *Water Spray*

The materials of construction of the TN-B1 package are such that the water spray test identified in 10 CFR 71.71(c)(6) will have a negligible effect on the package.

2.6.7. *Free Drop*

Since the maximum gross weight of the TN-B1 package is 1,614 kg (3,558 lb), a 1.2 m or four-foot free drop is required per 10 CFR 71.71(c)(7). The Hypothetical Accident Condition (HAC), 9 m (30 foot) free drop test required in 10 CFR 71.73(c)(1) is substantially more damaging than the 1.2 m (4 foot) NCT free drop test. Section 2.7.1 demonstrates the TN-B1 package's survivability and bounds the free drop requirements of 10 CFR 71.71(c)(7). Due to the relatively fragile nature of the fuel assembly payload in maintaining its configuration for operational use, any event that would come close to approximating the NCT free drop would cause the package to be removed from service and re-examined prior to continued use.

As part of the effort to obtain package certification in Japan by GNF-J, certification testing of the package, which included both an end drop and a lid-down horizontal drop, was performed. In each case a 0.3-meter (1-foot) and a 1.2 meter (4-foot) drop was performed prior to the 9-meter (30-foot) drop. In both cases the test package was slightly damaged but the damage had no significant effect on the performance of the package in relation to either the containment or the ability of the package to meet the requirements of 10 CFR 71. The GNF-J certification testing is discussed in Appendix 2.12.2.

Therefore, the requirements of 10 CFR 71.71(c)(7) are met.

2.6.8. *Corner Drop*

This test does not apply, since the package weight is in excess of 100 kg (220 pounds), and the structural materials used in the TN-B1 are not primarily wood or fiberboard, as delineated in 10 CFR 71.71(c)(8).

2.6.9. *Compression*

Since the package weighs less than 5,000 kg (11,000 pounds), as delineated in 10 CFR 71.71(c)(9), the package must be able to support five times its weight without damage.

The load to be given as the test condition is the load (W_1) times five of the weight of this package or the load (W_2) which is obtained through multiplying the package's vertical projected area by 13 kPa, whichever is heavier. In the case of this package, the equations to obtain each load are:

$$W_1 = 5 \times m \times g$$

$$W_2 = 13\ \text{kPa} \times L \times B$$

Where:

m: Mass of package	1,614 kg (3,558 lb)
g: Gravitational acceleration	9.81 m/s^2

L: Length of package 5,068 mm (199.53 in)

B: Width of package 720 mm (28.35 in)

From this

W_1 = 5 × 1,614 × 9.81 = 79.16 kN (17,800 lbf)

$W_2 = 13 \times 10^{-3} \times 5{,}068 \times 720$ = 47.4 kN (10,660 lbf)

Therefore, as W1>W2, the stacking load is assumed as W = 79.16 kN (17,800 lbf).

The stacking of these packages is as shown in Figure 2-12, so the outer container only sustains the stacking load. In this case, it is assumed that loads are carried by a total of eight support plates positioned in the center of the bolster out of sixteen support plates of the outer container body positioned at the lowest layer. This assumption makes the load sustaining area smaller, so the evaluation is conservative. The compressive load given to the support plate is the above-mentioned stacking load plus the weight of the outer container's lid.

The equation to obtain the support plate's compressive load is:

$$W_c = W_1 + W_3$$

W_c: Compressive load	N
W_1: Stacking load	79.16 kN (17,800 lbf)
W_3: Load by the outer container's lid	1.34 kN (301 lbf)
m_F: Mass of outer container lid	137 kg (302 lb)
g: Gravitational acceleration	9.81m/s^2

From this, the 80.5 kN (18,100 lbf)

When the fuel assemblies are packed, the gravity center of the outer container is shifted longitudinally, so the load acting on the support plate, which is closer to the gravity center, becomes larger.

Therefore, the equation to obtain the vertical maximum load given to one support plate, which is closer to the gravity center, is:

$$P = \frac{W}{4} \frac{\ell_2}{\ell_0}$$

Where:

P: Maximum load acting on one support plate which is nearer to the gravity center N

W: Compressive load given to the support plate 80.5 kN (18,100 lbf)

ℓ_0: Longitudinal support plate space 3,510 mm (138.2 in)

ℓ_2: Distance from the package's gravity center position to the support

$$\frac{3{,}510}{2} + 92 = 1{,}847 \text{ mm (73.76 in)}$$

From this, the maximum load P acted to one support plate, which is nearer to the gravity center, is:

$$P = \frac{80.5 \times 10^3 \times 1{,}847}{4 \times 3{,}510} = 10.6 \times 10^3 \text{ N (2,380 lbf)}$$

The resistance of the plate to buckling is also evaluated. The equation to obtain the moment of inertia of area of the support plate which is subject to buckling is:

$$I_Z = \frac{1}{12} hb^3$$

Where:

I_Z: Moment of inertia of area of support plate mm^4

b: Thickness of support plate 5 mm (0.2 in)

h: Width of support plate 55 mm (2.2 in)

From this, the moment of inertia of area, I_Z, of the support plate is:

$$I_Z = \frac{1}{12} \times 55 \times 5^3 = 572.9 \text{ mm}^4 \ (1.376\text{x}10^{-3} \text{ in}^4)$$

Also, the equation to obtain the radius of gyration of the area of the support plate is:

$$k = \sqrt{\frac{I_z}{A}}$$

Where:

k: Radius of gyration of area of support plate mm

I_Z: Moment of inertia of area of support plate 572.9 mm^4 (1.376x10^{-3} in^4)

A: Cross-sectional area of support plate $5 \times 55 = 275$ mm^2 (0.426 in^2)

ℓ: Length of support plate 559 mm (22.4 in)

From this, the radius of gyration of area k of the support plate is:

$$k = \sqrt{\frac{572.9}{275}} = 1.44 \text{ mm } (0.0568 \text{ in})$$

Also, the slenderness ratio $\frac{\ell}{k}$ is:

$$\frac{\ell}{k} = \frac{559}{1.44} = 388$$

As the ends are fixed, the coefficient n becomes 4, so the limit value of the slenderness ratio becomes as below.

$$85\sqrt{n} = 85\sqrt{4} = 170$$

Because the slenderness ratio of this material, 388, exceeds the limit value of slenderness, Euler's equation is used. The equation to obtain the support plate's buckling strength is:

$$P_k = \frac{n\pi^2 E I_z}{\ell^2}$$

Where:

P_k: Buckling strength (load) of support plate N

n: Coefficient to the long support fixed at both ends 4

E: Longitudinal elasticity modulus of Gr304 stainless steel 1.94×10^5 MPa (at 40°C)

I_Z: Moment of inertia of area of support plate 572.9 mm^4 (1.376x10^{-3} in^4)

ℓ: Length of the support plate 559 mm (22.4 in)

From this, the buckling strength P_k of the support plate is:

$$P_k = \frac{4x3.14^2x1.94x10^5x572.9}{559^2} = 14\times10^3 \text{N } (3{,}050 \text{ lb})$$

Therefore, $P_k > P$, so the body support plate will not buckle.

2.6.10. *Penetration*

The one-meter (40-inch) drop of a 6 kg (13-pound), hemispherical-headed, 3.2 cm (1.3-inch) diameter, steel cylinder, as delineated in 10 CFR 71.71(c)(10), is of negligible consequence to the TN-B1 package. This is due to the fact that the TN-B1 package is designed to minimize the consequences associated with the much more limiting case of a 40-inch drop of the entire package onto a puncture bar as discussed in Section 2.7.3. The drop of the 6 kg bar will not damage the outer container.

Table 2-8 Temperatures

Location	Maximum temperature
Environment (Open air)	38°C
Package's external surface	77°C
Inner container	<77°C

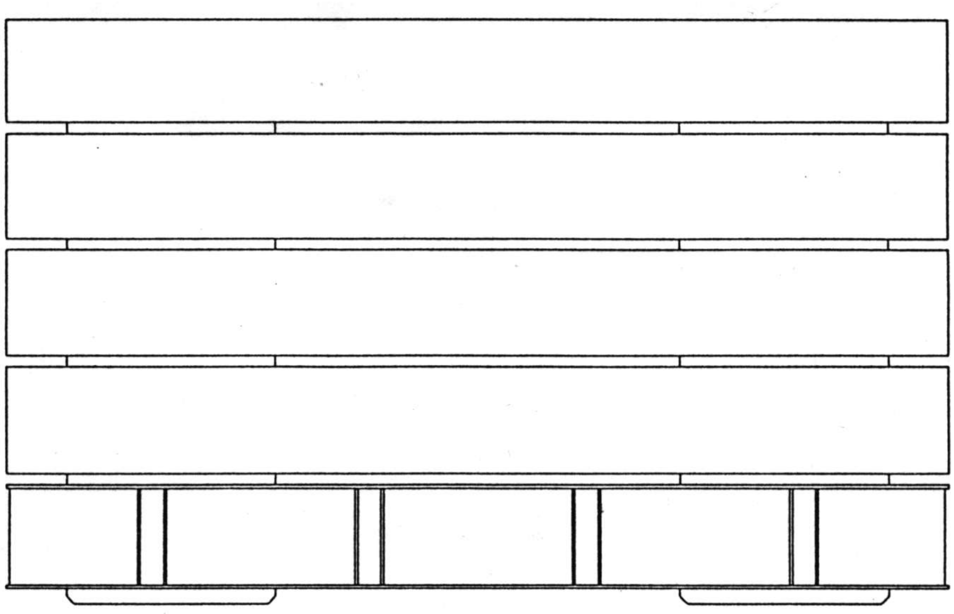

Figure 2-12 Stacking Arrangement

2.7. HYPOTHETICAL ACCIDENT CONDITIONS

The TN-B1 package, when subjected to the sequence of Hypothetical Accident Condition (HAC) tests specified in 10 CFR 71.73 is shown to meet the performance requirements specified in Subpart E of 10 CFR 71. The primary proof of performance for the HAC tests is via the use of full-scale testing. A certification test unit (CTU) was free dropped, and puncture tested to confirm that both the inner and outer containers protected the fuel and allowed containment to be maintained after a worst-case HAC sequence. Another CTU was free dropped from 9 meters on its end with the fuel maintaining containment after the drop. Observations from CTU testing confirm the conservative nature of the deformed geometry assumptions used in the criticality assessment provided in Chapter 6.0. Immersion is addressed by comparison to the design basis for the fuel.

Test results are summarized in Section 2.7.8, with details provided in Appendix 2.12.1.

2.7.1. *Free Drop*

Subpart F of 10 CFR 71 requires performing a free drop test in accordance with the requirements of 10 CFR 71.73(c)(1). The free drop test involves performing a 30-foot, HAC free drop onto a flat, essentially unyielding, horizontal surface, with the package striking the surface in a position (orientation) for which maximum damage is expected. The ability of the TN-B1 package to adequately withstand this specified free drop condition is demonstrated via testing of four full- scale, certification test units (CTUs).

To properly select a worst-case package orientation for the 30-foot free drop event, items that could potentially compromise containment integrity, shielding integrity, and/or criticality safety of the TN-B1 package must be clearly identified. For the TN-B1 packaging design, there are two primary considerations 1) protect the fuel so that containment is maintained and 2) ensure sufficient structure is around the package to maintain the geometry used in the criticality safety evaluation. Shielding integrity is not a controlling case for the reasons described in Section 5.0. Criticality safety is conservatively evaluated based on measured physical damage to the outer container from certification testing, as described in Section 6.0.

Since the containment is welded closed, the leak-tight capability of the containment may be compromised by two methods: 1) as a result of excessive deformation leading to rupture of the containment boundary, and/or 2) as a result of thermal degradation of the containment material itself in a subsequent fire event and rupture of the weld or the cladding tube by over-pressurization. Importantly, these methods require significant impact damage to the surrounding outer and inner container so that the fuel is either loaded externally or the fuel is directly exposed to the fire.

Additional items for consideration include the possibility of separating the OC lid from the OC body and buckling or deforming of the Outer Container (OC) and/or Inner Container (IC) from an end drop or horizontal drop.

For the above reasons, testing must include impact orientations that affect the lid and stability of the walls of the containers. In general, the energy absorbing capabilities of the TN-B1 are governed by the deformation of the stainless steel and impregnated paper honeycomb that is not significantly affected by temperature.

Appendices 2.12.1 and 2.12.2 provide a comprehensive report of the certification test process and results. Discussions specific to CTU test orientations for free drop and puncture, including initial test conditions, are also provided.

The TN-B1 package has undergone extensive testing during its development. Testing has included 1.2-meter (4-foot) drops on the end in the vertical orientation and the lid in the horizontal orientation. The package has been also dropped from 9 meters in the same orientation demonstrating that the damage from the 1.2-meter (4-foot) drops has little consequence on the performance of the package in 9-meter (30-foot) drop. Based on these preliminary tests it was determined that the worst-case orientation for the 9-meter (30-foot) drop test would be slap-down on the lid. The lid down drop demonstrated that the vibration isolation frame bolts would fail allowing the inner container to come in contact with the paper honeycomb in the lid and partially crush the honeycomb. It was expected that the slap-down orientation would maximize the crush of this material minimizing the separation distance between the fuel assemblies in the post accident condition.

A single “worst-case” 9-meter (30-foot) free drop is required by 10 CFR 71.73(c)(1). Based on the above discussion and experience with other long slender packages similar to the TN-B1, a 15 degree slap-down on the lid was chosen for the 9-meter (30-foot) drop. Following that drop, a 25 degree oblique puncture drop on the damaged lid was performed. See Figure 2-13, Figure 2-14 and Appendix 2.12.1.

Other free drop orientations that were tested include vertical end and bottom corner. These tests demonstrated that the TN-B1 package contains the fuel assemblies without breaching the fuel cladding (containment boundary).

2.7.1.1. **End Drop**

9-meter (30-foot) end free drops were performed on GNF-J CTU 1J and GNF-A CTU 2. The orientation was selected with the lower end of the fuel down to maximize the damage since the expansion springs in the fuel rods are located in the upper end. This orientation maximized the damage to the energy absorbing wood in the end of the TN-B1 and maximized the axial loading on the fuel assembly. Both tests resulted in deformations of the fuel but were within the limits evaluated in the criticality evaluation in Section 6.0. Following the GNF-A tests, the fuel rods were demonstrated to maintain containment after the free and puncture drops, thus maintaining its containment boundary integrity. Although this orientation caused the most severe damage to the fuel, the damage was well within the structural limits for the fuel and package.

2.7.1.2. **Side Drop**

No side drop testing was performed in this certification sequence. A side drop test was done in previous testing of the package. That testing resulted in the inner container holding frame top bolts failing and allowing the inner container to come in contact with the outer lid. The inner package showed little damage and the fuel was not deformed. It was judged that the slapdown and the horizontal drop tests bounded the side drop orientation.

2.7.1.3. **Corner Drop**

A 9-meter (30-foot) free drop on the OC body bottom corner was performed on GNF-J CTU 1J. The impact point previously sustained damage due to 0.3-meter (1-foot) and 1.2-meter (4-foot) free drops. The resultant cumulative deformation was approximately 163 mm (6 inches). There was no loss of contents or significant structural damage to the OC as a result of this free drop. The maximum recorded impact acceleration was 203g. Refer to Appendix 2.12.2 for complete details of the corner free drop.

2.7.1.4. **Oblique Drops**

An orientation of 15 degrees from horizontal was tested with GNF-A CTU 1. The IC holding frame was plastically deformed and only a portion of the bolts failed. Neither the fuel nor the IC were not significantly damaged. The damage sustained was bounded by the assumptions utilized in the criticality and thermal evaluations. The fuel was leak tested after the test and was demonstrated to have maintained containment boundary. Refer to Appendix 2.12.1 for complete details of the 15-degree oblique free drop.

2.7.1.5. **Horizontal Drop**

A 9-meter (30-foot) horizontal free drop on the OC lid was performed on GNF-J CTU 2J. The impact results in a maximum deformation of 19 mm (0.8 inch), which occurred in the OC lid. The side wall of the OC body bulged approximately 19 mm (0.8 inches). Some localized weld failure of OC lid flange/OC lid interface occurred where the bolster angles attach to the lid. None of the OC lid bolts failed as a result of the impact. There was no loss of contents as a result of the free drop. The maximum recorded impact acceleration was 146g. Refer to Appendix 2.12.2 for complete details of the horizontal free drop.

2.7.1.6. **Summary of Results**

Successful HAC free drop testing of the test units indicates that the various TN-B1 packaging design features are adequately designed to withstand the HAC 30-foot free drop event. The most important result of the testing program was the demonstrated ability of the fuel to remain undamaged and hence maintain its containment capability as defined by ANSI N14.5.

The TN-B1 also maintained its basic geometry required for nuclear criticality safety. Observed permanent deformations of the TN-B1 packaging were less than those assumed for the criticality evaluation.

The GNF-A mock-up fuel assembly rods were leakage rate tested after the conclusion of the testing and were demonstrated to be leaktight, as defined in ANSI N14.5.

A comprehensive summary of free drop test results are provided in Appendices 2.12.1 and 2.12.2.

2.7.2. *Crush*

Subpart F of 10 CFR 71 requires performing a dynamic crush test in accordance with the requirements of 10 CFR 71.73(c)(2). Since the TN-B1 package weight exceeds 500 kg (1,100 pounds), the dynamic crush test is not required.

2.7.3. *Puncture*

Subpart F of 10 CFR 71 requires performing a puncture test in accordance with the requirements of 10 CFR 71.73(c)(3). The puncture test involves a 1-meter (40-inch) free drop of a package onto the upper end of a solid, vertical, cylindrical, mild steel bar mounted on an essentially unyielding, horizontal surface. The bar must be 150 mm (6 inches) in diameter, with the top surface horizontal and its edge rounded to a radius of not more than 6 millimeter (0.25 inch). The package is to be oriented in a position for which maximum damage will occur. The length of the bar used was approximately 1.5 meters (60 inches). The ability of the TN-B1 package to adequately withstand this specified puncture drop condition is demonstrated via testing of the full-scale RAJ-II CTUs.

To properly select a worst-case package orientation for the puncture drop event, items that could potentially compromise containment integrity and/or criticality safety of the TN-B1 package must be clearly identified. For the TN-B1 package design, the foremost item to be addressed is the ability of the containment to remain leak-tight. Shielding integrity is not a controlling case for the reasons described in Chapter 5.0. Criticality safety is conservatively evaluated based on measured physical damage to the outer container walls as described in Section 6.0.

Previous testing has shown that the 1-meter drop onto the puncture bar did not penetrate the outer wall or damage the fuel. Based on this previous testing and other experience, an oblique and horizontal puncture drop orientations centered over the fuel were chosen as the most damaging.

Appendices 2.12.1 and 2.12.2 provide a comprehensive report of the certification test process and results. Discussions specific to the configuration and orientation of the test unit are provided.

The “worst-case” puncture drop as required by 10 CFR 71.73(c)(3) was performed on the package with the lid down and 25 degrees from horizontal. The angle was chosen based on experience with other packages and the TN-B1. The puncture bar was aimed at the CG of package to maximize the energy imparted to the package.

The puncture pin did not penetrate the outer container. It deformed the lid inward and it contacted the inner container lid and deformed it a small amount. The outer lid total deformation was less than 12 cm (4.7 inches) and the inner container lid deformed less than 5 cm (2.0 inches).

2.7.4. *Thermal*

Thermal testing of the GNF-J CTU 2J was performed following the free drop and puncture drop tests (refer to Appendix 2.12.2). Although there was no failure of the containment boundary due to the thermal testing, the thermal evaluation of the TN-B1 package for the HAC heat condition as presented in Section 3.0, demonstrates the regulatory compliance to 10 CFR 71.73(c)(4). Because the TN-B1 package does not contain pressure-tight seals, the HAC pressure for the OC and the IC is zero. The fuel assembly exhibits negligible decay heat.

2.7.4.1. **Summary of Pressures and Temperatures**

The maximum predicted HAC temperature for the fuel assembly is 921 K (1,198°F) during the fire event. The fuel rods are designed to withstand a minimum temperature of 1,073 K (1,475°F) without bursting. This has been demonstrated by heating representative fuel rods to this temperature for over 30 minutes. This heating resulted in rupture pressures in the excess of 3.6MPa (520 psi). The pressure due to the accident conditions does not exceed 3.5 MPa (508 psia). Summary of pressures and related stresses are provided in Section 3.0.

2.7.4.2. **Differential Thermal Expansion**

The fuel cladding is not restricted by the packaging and hence can not develop any significant differential thermal expansion stresses. The packaging itself is made of the same metal (austenitic stainless steel) eliminating any significant stresses due to differential thermal expansion.

2.7.4.3. **Stress Calculations**

Stress calculations for the controlling hoop stress for the fuel cladding that provides containment is provided in Section 3.0.

2.7.4.4. **Comparison with Allowable Stresses**

The allowable stress used in the analysis in Section 3.0 is based on empirical data from burst tests performed on fuel rods when heated to 800 °C and above. The allowed fuel cladding configurations for the TN-B1 have a positive margin of safety based on stresses required to fail the fuel in the test.

2.7.5. *Immersion – Fissile Material*

Subpart F of 10 CFR 71 requires performing an immersion test for fissile material packages in accordance with the requirements of 10 CFR 71.73(c)(5). The criticality evaluation presented in Chapter 6.0 assumes optimum hydrogenous moderation of the contents, thereby conservatively addressing the effects and consequences of water in-leakage.

2.7.6. *Immersion – All Packages*

Subpart F of 10 CFR 71 requires performing an immersion test for packages in accordance with the requirements of 10 CFR 71.73(c)(6). Since the TN-B1 package is not sealed against pressure, there will not be any differential pressure with the water immersion loads defined in 10 CFR 71.73(c)(6). The water immersion will have a negligible effect on the container and the payload, consisting of the fuel assemblies that provide the containment. The fuel rods are designed to withstand differential pressures greater than 1,000 psi. Submergence is a normal design condition for the fuel assemblies and the evaluations are performed on that condition.

2.7.7. *Deep Water Immersion Test (for Type B Packages Containing More than 10^5 A_2)*

Not applicable. The TN-B1 does not contain more than 10^5 A_2.

2.7.8. *Summary of Damage*

As discussed in the previous sections, the cumulative damaging effects of the free drops and a puncture drop were satisfactorily withstood by the RAJ-II packaging during certification testing. Subsequent helium leak testing confirmed that containment integrity was maintained throughout the test series. The package was also successfully evaluated for maintaining containment during and after the fire event. The deformation of the package in the worst-case HAC did not exceed that which is evaluated for in Chapter 6.0. Therefore, the requirements of 10 CFR 71.73 have been satisfied.

Table 2-9 Summary of Tests for RAJ-II

Test No.	Test Description	Test Unit Angular Orientation		CTU Temperature	Remarks
		Axial[1]	Rotational		
1	9 - meter (30-foot) slap down	15°	Lid down	Ambient	Top of package impacted first. Lid crushed over 11 cm (4.3 in).
2	Puncture	25°	Lid down	Ambient	Puncture pin crushed the outer lid down to the inner container lid. It did not rupture the outer lid or significantly deform the inner container lid or fuel.
3	9 - meter (30- foot) end drop	90°	Bottom down	Ambient	Crushed end wood impact absorber. Deformed the fuel assembly but did little damage to the rods

Notes:

1 Axial angle, θ, is relative to horizontal (i.e., side drop orientation)

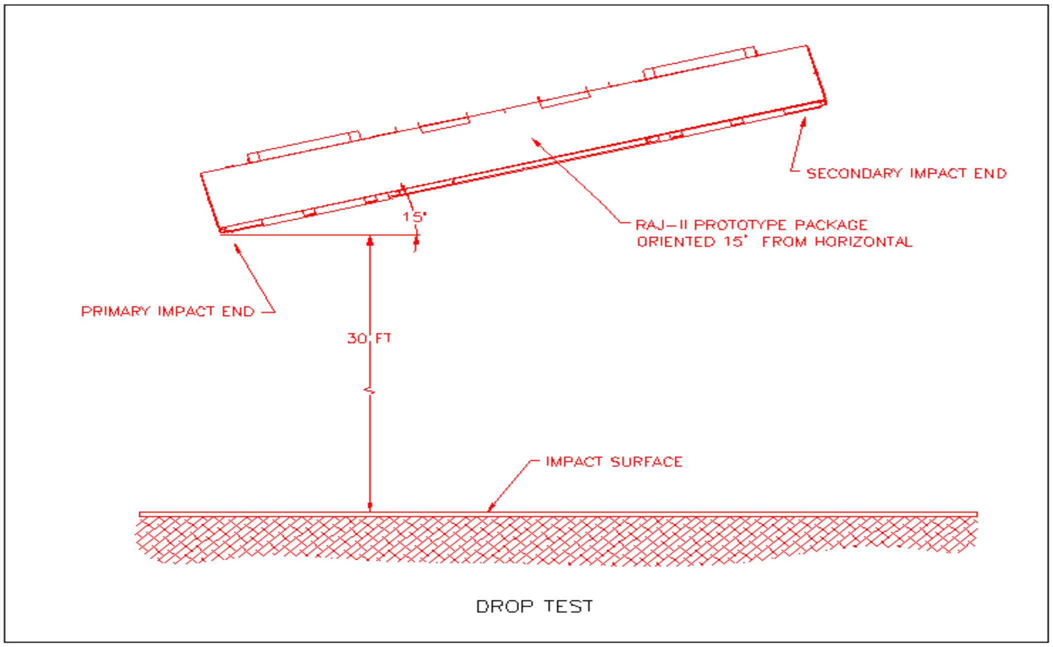

Figure 2-13 Slap-down Orientation

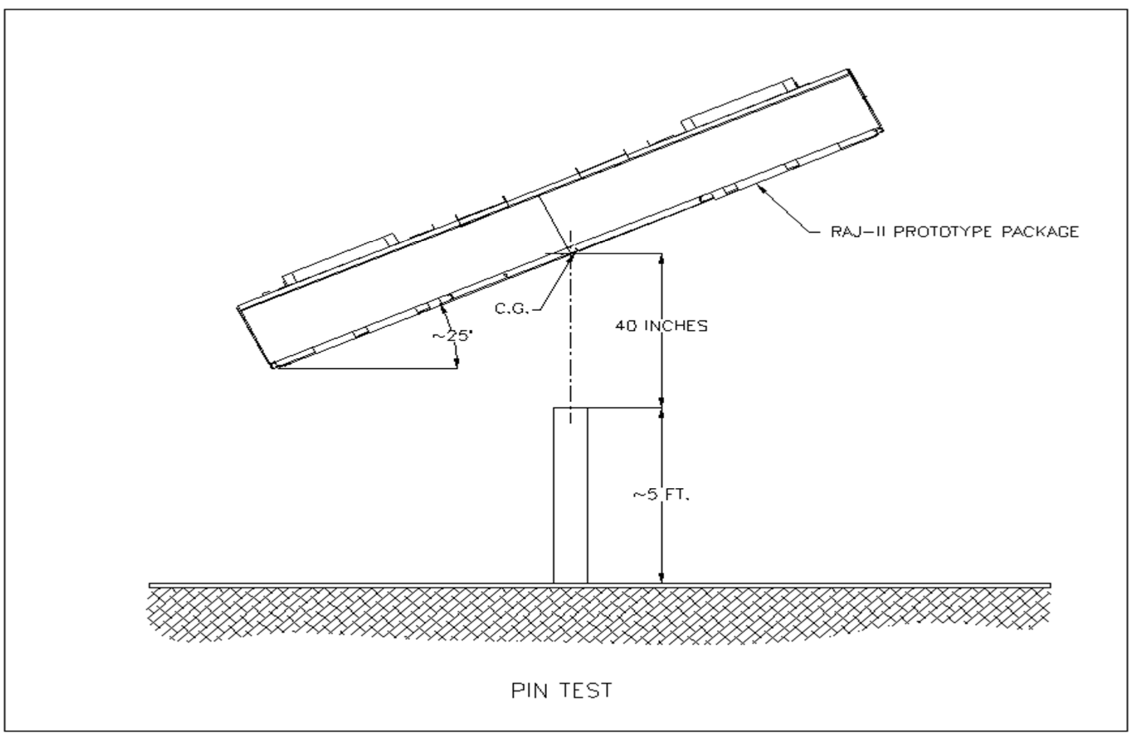

Figure 2-14 Puncture Pin Orientation

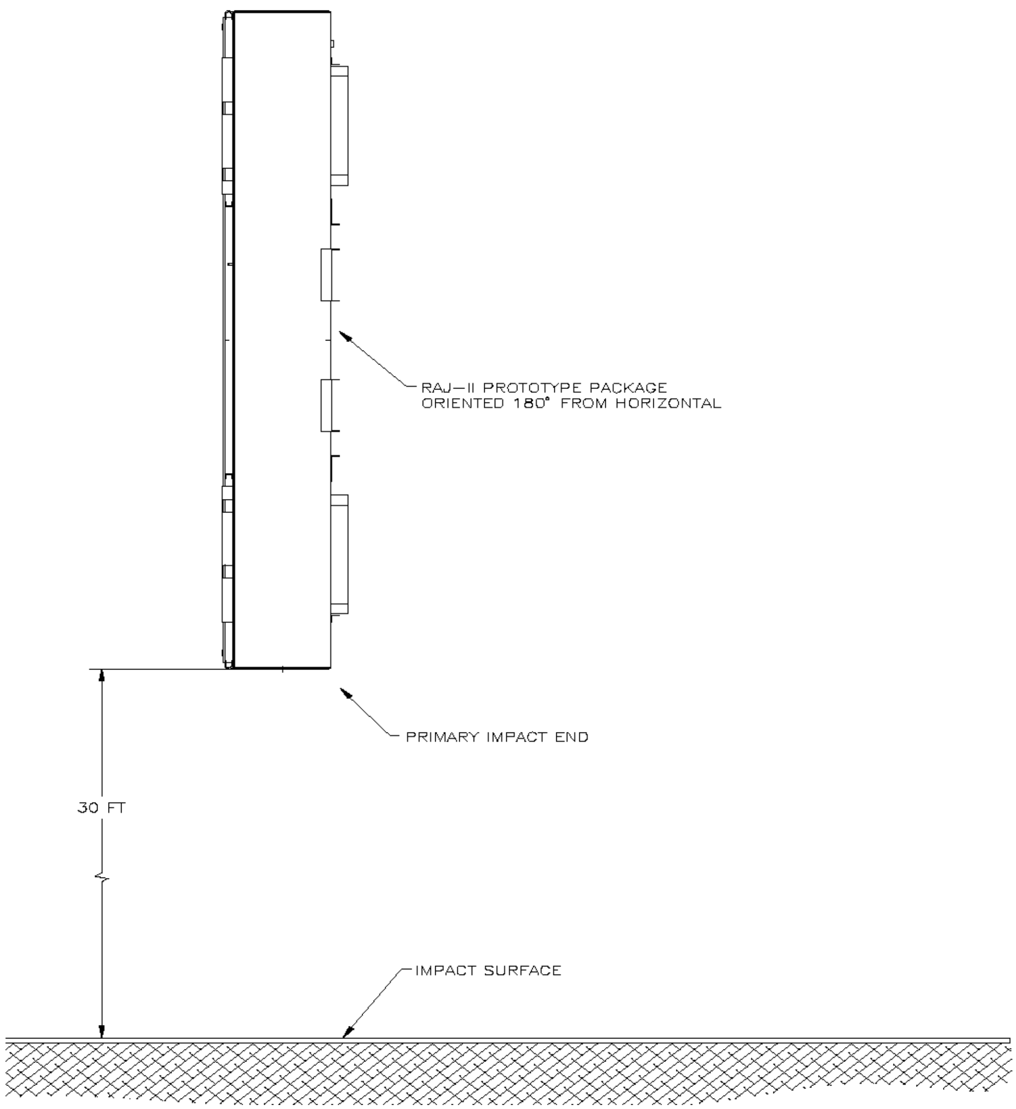

Figure 2-15 End Drop Orientation

2.8. ACCIDENT CONDITIONS FOR AIR TRANSPORT OF PLUTONIUM

Not Applicable. This package will not be used for the air transport of plutonium.

2.9. ACCIDENT CONDITIONS FOR FISSILE MATERIAL PACKAGES FOR AIR TRANSPORT

Not applicable. This package will not be used for the air transport of fissile material.

2.10. SPECIAL FORM

This section does not apply for the TN-B1 package, since special form is not claimed.

2.11. FUEL RODS

In each event evaluated above either by analysis or by test, the unirradiated fuel rods were protected by the TN-B1 package so that they sustained no significant damage. Fuel rod cladding is considered to provide containment of radioactive material under both normal and accident test conditions. Discussion of this cladding and its ability to maintain sufficient mechanical integrity to provide such containment is described in Section 1.2.3 and Chapter 4.0.

The expanded enrichment value up to 8.0 wt.% ^{235}U described in Tables 1-4, 1-5, and 1-6 does not cause a fuel design configuration that is beyond the previous RAJ-II/TN-B1 package structural evaluations and test conditions. Related to the fuel rods, there is no changes to the weights or materials of fabrication. Critical characteristics of the 17x17 Type 3 PWR fuel rods are equal to or bound by previously approved fuel rod design configurations including density, cladding diameter, and minimum fuel rod wall thickness as detailed in Table 6-131.

2.12. APPENDIX

2.12.1. *Certification Test*

2.12.1.1. Certification Test Unit

The TN-B1 test packages were fabricated identically to the configuration depicted in the Packaging General Arrangement Drawing found in Appendix 1.4.1. The certification test unit is identical to the production TN-B1 packages except for some minor differences.

1. For ease in documentation/evaluation, tape and marker were used for reference markings during testing.
2. Minor amounts of the internal foam cushioning material were cut out to accommodate added weight in the fuel cavity.
3. Weight was added to the exterior of the package to allow the test units to be at the maximum allowed package weight.

The fuel assemblies were represented by a mock up fuel assembly (an ATRIUM-10 design). Lead rods inside the cladding replaced the fuel pellets. The fuel rods were seal welded using the same techniques used on the production fuel rods. A composite fuel assembly was used to represent the second fuel assembly. Steel tubes represented the ends with added steel for correct weight. The center section was made up of a mock up fuel assembly similar to the full size mock up fuel assembly. The mock up of the fuel approximated the stiffness of the fuel and added no extra strength to the center section of the package that would potentially be damaged by the puncture test. See Figure 2-16 through Figure 2-22 for container and mock up fuel preparation. Weight was added to the fuel assembly cavity by placing lead sheeting on the side of the fuel where normally there is foam. The lead weighing 143 pounds represented the weight of the water channels that could be shipped with some fuel assemblies. The lead plate was cut into strips that were not over half the height of the fuel assemblies to ensure that there was no support or protection added to the fuel during any of the tests. The total weight of the CTUs is provided in Table 2-10. The added weight in the contents represents the maximum payload weight including the fuel, fuel assembly fittings and packing material that could be required in the future.

For CTU 1 that was dropped lid down for a 30-foot slap down event and a 1-meter oblique puncture event, the weight was added between the bolster boards at each end. The added weight representing the difference between the actual tare weights of the package and the maximum allowed tare weight consisted of two ½ inch carbon steel plates. For CTU 1, these were held in place by the bolster and brackets attached to the bolster with lag bolts. See Figure 2-23. These plates were taken off CTU 1 and placed on the opposite end of CTU 2 for the end drop. See Figure 2-24.

Table 2-10 Test Unit Weights

Property	CTU 1		CTU 2	
As fabricated weight	849 kg	1,872 lb	848 kg	1,869 lb
Max. fabricated weight	930 kg	2,050 lb	930 kg	2,050 lb
Added weight	81.7 kg	180 lb	81.7 kg	180 lb
Content weight	684 kg	1,508 lb	685 kg	1,510 lb
Measured drop weight	1,614 kg	3,558 lb	1,611 kg	3,552 lb
Approximate weight of attaching frame	2.3 kg	5.1 lb	11.3 kg	24.9 lb
Approximate drop weight	1,616 kg	3,562 lb	1,622 kg	3,576 lb

2.12.1.2. Test Orientations

Three certification tests were performed. Two tests were performed on CTU 1, a 9-meter (30-foot) slap-down on the lid and a 1-meter (40-inch) oblique puncture test on the lid. A 9-meter (30-foot) end drop was performed on CTU 2.

The 9-meter (30-foot) drop on the lid was designed to provide maximum acceleration to the end of the fuel as well as maximize the crush of the package for criticality evaluation purposes. The top down orientation was chosen since the lid contains the least material. The lid down orientation was also chosen since on previous tests horizontal lid down tests had maximized the crush and had resulted in the failure of the retaining bolts on the frame holding the inner container. As discussed in Section 2.7.1.1, the drop orientation was at 15 degrees with the horizontal. See Figure 2-25.

The 1-meter (40-inch) puncture test was performed on CTU 1 with the lid down after the 9-meter (30-foot) slap-down test. The package was oriented at a 25-degree angle to maximize the possibility of the corner of the puncture bar penetrating the outer container and maximizing the damage to the inner container and fuel. The puncture bar was aligned over the center of gravity of the package. See Figure 2-26 and Figure 2-27.

CTU 2 was dropped 9-meters (30-feet) with its bottom end down. The purpose of this orientation was to maximize the damage to the fuel. The bottom end was chosen since it is the most rigid end of the fuel assembly. The expansion springs inside the cladding tubes are on the upper end. See Figure 2-28.

2.12.1.3. Test Performance

Testing was performed at the National Transportation Research Center in Oak Ridge, Tennessee. The CTUs were shipped to the facility fully assembled. Only the additional tare weight as described in Section 2.12.1.1 was added at the test facility. Tests were performed on the packages prior to them being transported to the Framatome-ANP facility at Lynchburg, Virginia. At Lynchburg the packages were disassembled and examined and the fuel rods were helium leak tested.

The slapdown test at 15 degrees to horizontal demonstrated the ability of the outer package to protect the fuel and the inner container. The energy absorbing capabilities of the package allowed the package to deform and limited the secondary impact to less than the primary impact. See Figure 2-29 and Figure 2-30. This test resulted in deformation inside the package. See Figure 2-36 and Figure 2-37. The crush of the paper honeycomb was limited by the stiffening plates in the lid. See Figure 2-38. The inner container lid was deformed as well. Neither the lid bolts on either container nor the bolts on the inner container clamping device failed. The frame did bend over 3 cm. The fuel rods, although slightly deformed due to the test and the added weight in the fuel cavity, were not damaged. See Figure 2-39. The added weight placed between the bolster timbers caused a slight deformation of the bottom wall of the outer package in the local area of the weights.

The puncture test was performed with the lid down at a 25 degree angle from horizontal. See Figure 2-25. The puncture pin was bolted with three bolts to the drop pad. The puncture pin struck the lid over the CG of the package after the package had undergone the slapdown test. See Figure 2-26. The pin did not penetrate the outer lid. The outer lid was deformed inward until it came in contact with the inner container. This was confirmed by a slight mark on the inner container lid. The pin appears to have bounced since there are two indentations very close together which could have been caused by the outer lid bottoming out against the inner container lid. See Figure 2-31 and Figure 2-32. No significant internal package or fuel damage appeared to be attributable to the pin puncture test.

The 9-meter (30-foot) end drop test was performed on CTU 2 with the bottom end down. There was little exterior damage to the outer container. See Figure 2-33, Figure 2-34, and Figure 2-35. Extensive damage occurred to the inside of the inner container as the fuel assemblies and the added weight impacted the interior of the inner container. The rigid end fitting of the assembly crushed the wood located at the end of the package. Although some welds broke, the bottom end of the package remained in place. The fuel rods partially came out of the end fitting. The fuel assemblies bent to the side. See Figure 2-40, Figure 2-41, and, Figure 2-42.

The mock up fuel assemblies from both CTU 1 and CTU 2 were helium leak tested. The Assembly form CTU 1 was found to meet the leak tight requirements of having a leak rate less than 1 $x10^{-7}$ atm-cc/s. The assembly from CTU 2 was found to have a He leak rate of $5.5x10^{-6}$ atm-cc/s. This is within the allowable leakage for the fuel as shown in Section 4.0.

2.12.1.4. Test Summaries

Two 9-meter (30-foot) drops and one oblique puncture pin test were performed on two certification test units. The packages retained the fuel assemblies and protected the fuel. Mockup fuel assemblies from both certification units were leak tested after the drop tests and were determined to have maintained containment. The tests are summarized below.

Table 2-11 Testing Summary

Test	CTU	Orientation with horizontal	Exterior damage	Interior damage	Fuel
9-meter (30-foot) lid down	1	15º	Minor deformation on both ends.	No bolts broken on the frame or the lids. Significant deformation to inner container and internal clamp frame. Reduction of spacing between outside of package and fuel to about 4 inches.	Minimal damage to the fuel assemblies. Some twist to the assembly. No real damage to the fuel rods. The fuel was demonstrated to have a leak rate of less than 1×10^{-7} atm-cc/s after the testing.
1-meter (40 in) lid down over cg	1	25º	Did not penetrate outer wall	Outer wall contacted inner container. Section 2.12 Figure 2-39 through 2-42 show some damage to the inner container, however, this damage is conservatively modeled in the HAC criticality analyses in Section 6.0 and is not sufficient to allow fuel to leak from the container.	The fuel appeared not to be affected by this test. Passed helium leak test.
9-meter (30-foot) lower end	2	90º	Localized damage on impact end.	Major crushing of the wood at the end of the inner package and breaking of the inner wall of the inner container on the impacted end. The outer wall was damaged but did not fail completely.	Fuel was bent and separated from end fittings. Fuel spacers were damaged. Fuel rods had no significant damage. Fuel bending was influenced by the movement of the weight added to the fuel cavity. Post drop leak test giving a He leak rate of 5.5×10^{-6} atm-cc/s demonstrated that containment had been maintained.

Figure 2-16 Inner Container Being Prepared to Receive Mockup Fuel and Added Weight

Figure 2-17 Partial Fuel Assemblies in CTU 1

Figure 2-18 Top End Fittings on Fuel in CTU 1

Figure 2-19 Contents of CTU 2

Figure 2-20 Outer Container without Inner Container

Figure 2-21 Inner Container Secured in Outer Container

Figure 2-22 CTU 2 Prior to Testing

Figure 2-23 Addition of Tare Weight to CTU 1

Figure 2-24 Addition of Tare Weight to CTU 2

Figure 2-25 CTU 1 Positioned for 15° 9-m (30-foot) Slap-down Drop

Figure 2-26 Alignment for Oblique Puncture

Figure 2-27 Position for Puncture Test

Figure 2-28 Position for End Drop

Figure 2-29 Primary Impact End Slap-down Damage

Figure 2-30 Secondary Impact End Damage

Figure 2-31 Puncture Damage

Figure 2-32 Close Up of Puncture Damage

Figure 2-33 End Impact

Figure 2-34 Damage from End Impact (Bottom and Side)

Figure 2-35 End Impact Damage (Top and Side)

Figure 2-36 Damage Inside Outer Container to CTU 1

Figure 2-37 Internal Damage to Outer Container CTU 1

Figure 2-38 Lid Crush on CTU 1

Figure 2-39 Damage to Fuel in CTU 1

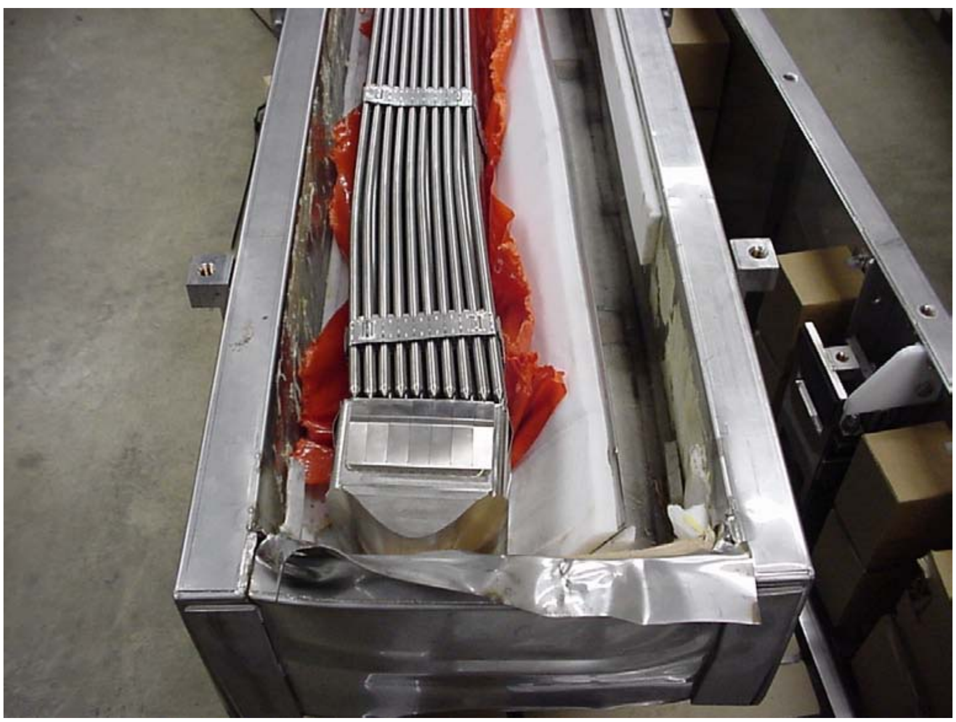

Figure 2-40 Internal Damage to CTU 2

Figure 2-41 Fuel Damage CTU 2

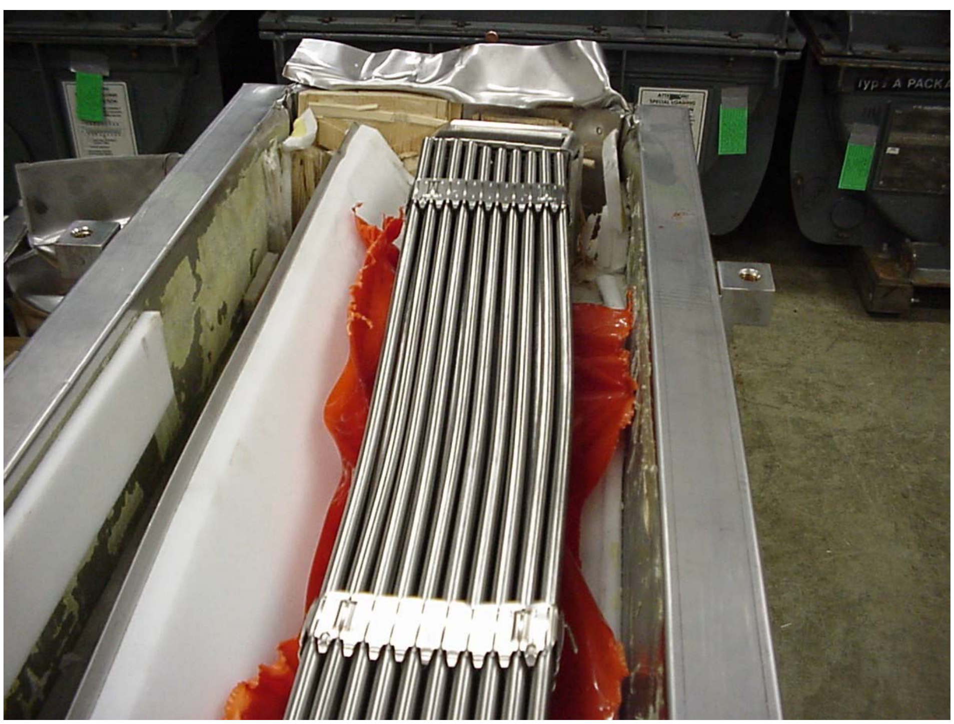

Figure 2-42 Fuel Prior to Leak Testing CTU 2

2.12.2. *GNF-J Certification Tests*

Normal conditions of transport (NCT) and hypothetical accident conditions (HAC) certification testing of the RAJ-II package was also performed by GNF-J as part of obtaining a Type AF certificate of compliance* in Japan. For the U.S. testing, the GNF-J certification tests were utilized to determine the worst-case test orientations for the certification tests identified in Appendix 2.12.1. This appendix summarizes the GNF-J RAJ-II certification tests.

2.12.2.1. Certification Test Units

Two certification test units (CTUs) were utilized for the GNF-J RAJ-II tests. Each CTU was fabricated in accordance with the Packaging General Arrangement Drawings found in Appendix 1.4.1, with the following exceptions:

1. The lateral wood bolsters on each end were not installed. Elimination of these wood bolsters is conservative for the free drops.
2. Maximum content weight was 560 kg (1,235 lbs), which results in a maximum package weight of 1,490 kg (3,285 lbs). This weight reduction is less than 8% lower than the maximum gross weight of the RAJ-II package, and will result in higher impact forces. The small difference in weight will have an insignificant effect on the free drop response of the package and/or fuel assembly.

One simulated fuel assembly and one dummy weight were utilized in each CTU to simulate the payload contents. Accelerometers were installed on the CTUs to measure and record each free drop impact. No accelerometers were used for the puncture drop tests.

2.12.2.2. Test Orientations

Since the RAJ-II package relies on the fuel cladding as the containment boundary, free drop and puncture drop orientations that could damage the fuel cladding and potentially breach the containment boundary should be included in the test series. In addition, orientations that could damage the package and/or the fuel assemblies such that an unsafe criticality geometry would exist should be included in the test series.

Free drop orientations that could result in this type of damage include:

1. Vertical drop on the package end – maximizes axial impact acceleration to a fuel assembly, potentially buckling and failing the fuel cladding (containment boundary).
2. Horizontal drop of the package – maximizes lateral impact acceleration on a fuel assembly, potentially bending and failing the fuel cladding (containment boundary).
3. CG-over-corner of the package – maximizes deformation of outer container (OC).

---

* Global Nuclear Fuel - Japan (fka Japan Nuclear Fuel Co., Ltd), Application for Approval of Packaging, Type RAJ-II, STO-M00-034, dated September 26, 2000.

All of these orientations were included in the free drop test series of the package. Puncture drop orientations that could potentially breach the containment boundary (cladding) include:

1. Horizontal puncture drop on the center of the package – maximizes puncture impact onto fuel pins and potentially shearing and failure of the fuel cladding (containment boundary).
2. Vertical puncture drop on the end of the package – maximizes puncture impact onto the fuel assembly

Because of the end internal structure and wood dunnage in the outer container, the puncture drop on the end will not result in any significant deformation of the fuel assembly or the inner container. Therefore, this puncture drop orientation is bounded by the horizontal puncture drop on the center of the package.

The free drop tests included NCT drops of 0.3 meters (1 foot) and 1.2 meters (4 feet) prior to performing the 9-meter (30-foot) HAC free drop on each CTU. The horizontal puncture drop test was only performed on CTU 2J.

Two certification test series were performed. Three free drop tests were performed on CTU 1J, and three free drop and one puncture drop tests were performed on CTU 2J. The test series for each CTU is summarized in Table 2-10. All drop tests were performed at ambient temperature.

2.12.2.3. **Test Performance**

Free drop and puncture testing was performed at two test facilities in Japan. At one facility, the drop pad consisted of a 32-mm (1.26-inch) thick steel plate that was embedded in a 1-meter (40-inch) thick concrete and steel support structure, with an overall length of 8 meters (26 feet). The other drop pad consisted of a 50-mm (1.97-inch) thick × 5-meter (16.4-feet) × 5-meter (16.4-feet) steel plate that was embedded in a 450-mm (12-inch) thick × 8.5-meter (27.9-feet) wide concrete and steel structure. The mass of each drop pad constituted an essentially unyielding surface for the CTUs, which weighed approximately 1,490 kg (3,285 lb).

2.12.2.3.1. ***CTU 1J***

CTU 1J was tested for a total of six free drop tests at heights of 0.3 meters (1 foot), 1.2 meters (4 feet), and 9 meters (30 feet). Figures 2-43 through 2-48 sequentially photo-document the CTU 1J tests.

The maximum resultant accumulated deformation, ~163 mm (~6 inches) occurred in the OC body corner. This orientation resulted in the maximum impact acceleration of 203g. No failure of the cladding (containment boundary) occurred from this test series.

2.12.2.3.2. *CTU 2J*

The testing of CTU 2J focused on free drop orientations not addressed by the CTU 1J tests. In addition, a HAC puncture drop test and HAC thermal test were performed. A total of three free drop tests at heights of 0.3 meters (1 foot), 1.2 meters (4 feet), and 9 meters (30 feet) were performed. Figures 2-49 and 2-50 sequentially photo-document the CTU 2J tests. The maximum resultant accumulated deformation, ~163 mm (~6 inches) occurred in the OC body corner. This orientation resulted in the maximum impact acceleration of 146g. No failure of the cladding (containment boundary) occurred from this test series.

2.12.2.4. **Test Summaries**

Two 0.3-meter (1-foot), four 1.2-meter (4-foot), three 9-meter (30-foot) free drops, one 1-meter (40-inch) puncture drop, and one HAC thermal test were performed on two CTUs. The packages retained the fuel assemblies and protected the fuel. There was no visual damage or loss of fuel pellets from the simulated fuel assemblies from both CTUs. A summary of the test results is provided in Table 2-11.

Table 2-12 GNF-J CTU Test Series Summary

CTU	Drop Height, m (ft)	Test Description	Purpose
1J	0.3 (1)	Free drop, CG-over-bottom end lower corner	Normal operation impact on OC body corner.
	1.2 (4)	NCT free drop, CG-over-bottom end lower corner	Impart initial deformation in same orientation as subsequent HAC free drop
		NCT free drop, horizontal on OC lid	Impart initial deformation in same orientation as planned HAC free drop
		NCT free drop, vertical, bottom end	Impart initial deformation in same orientation as subsequent HAC free drop
	9 (30)	HAC free drop, CG-over-bottom end lower corner	Maximize OC body deformation; potentially fail fuel rod and breach cladding.
		HAC free drop, vertical, bottom end	Maximize axial impact loads on fuel assemblies, potentially buckle fuel rod and
2J	0.3 (1)	Free drop, CG-over-lid corner	Normal operation impact on OC lid/body corner
	1.2 (4)	NCT free drop, horizontal on lid	Impart initial deformation in same orientation as subsequent HAC free drop
	9 (30)	HAC free drop, horizontal on lid	Maximize lateral impact loads on fuel assemblies, potentially breaching cladding.
	1 (3.3)	HAC puncture drop, horizontal on OC lid	Impact directly on HAC free drop damage; attempt to rupture fuel cladding.
	N/A	HAC thermal test	Demonstrate thermal performance of package.

Table 2-13 GNF-J CTU Test Series Results

CTU	Drop Height, m (ft)	Test Description	Result
1J	0.3 (1)	Free drop, CG-over-bottom end lower corner	Combined deformation of ~40 mm (~1.6 inches) of bottom corner.
	1.2 (4)	NCT free drop, CG-over-bottom end lower corner	
		NCT free drop, horizontal on OC lid	No significant deformation.
		NCT free drop, vertical, bottom end	Impacted end deformed ~3.9 mm (~0.2 inches)
	9 (30)	HAC free drop, CG-over-bottom end lower corner	Impacted OC bottom corner deformed ~163 mm (~6 inches), OC lid corner ~101 mm (~4 inches). Maximum acceleration of 203g.
		HAC free drop, vertical, bottom end	IC body/lid deformed ~2 - 81 mm (~0.08 - 3 inches) in length, U-shaped lifting bar on fuel assembly bent due to contact with wood end dunnage. Maximum acceleration of 58g.
2J	0.3 (1)	Free drop, CG-over-lid corner	Combined deformation of ~2.9 mm (~0.1 inches) of lid corner.
	1.2 (4)	NCT free drop, horizontal on lid	
	9 (30)	HAC free drop, horizontal on lid	Impacted side deformed ~2 - 19 mm (~0.08 -0.8 inches), localized weld failure of OC lid flange/OC lid sheet interface, no failure of OC lid bolts. Maximum acceleration of 146g.
	1 (3.3)	HAC puncture drop, horizontal on OC lid	~100 mm deep × ~2,000 mm (~4 inches × ~79 inches) wide indention in OC lid, no breach of OC lid sheet.
	N/A	HAC thermal test	No failure of simulated fuel assembly cladding.

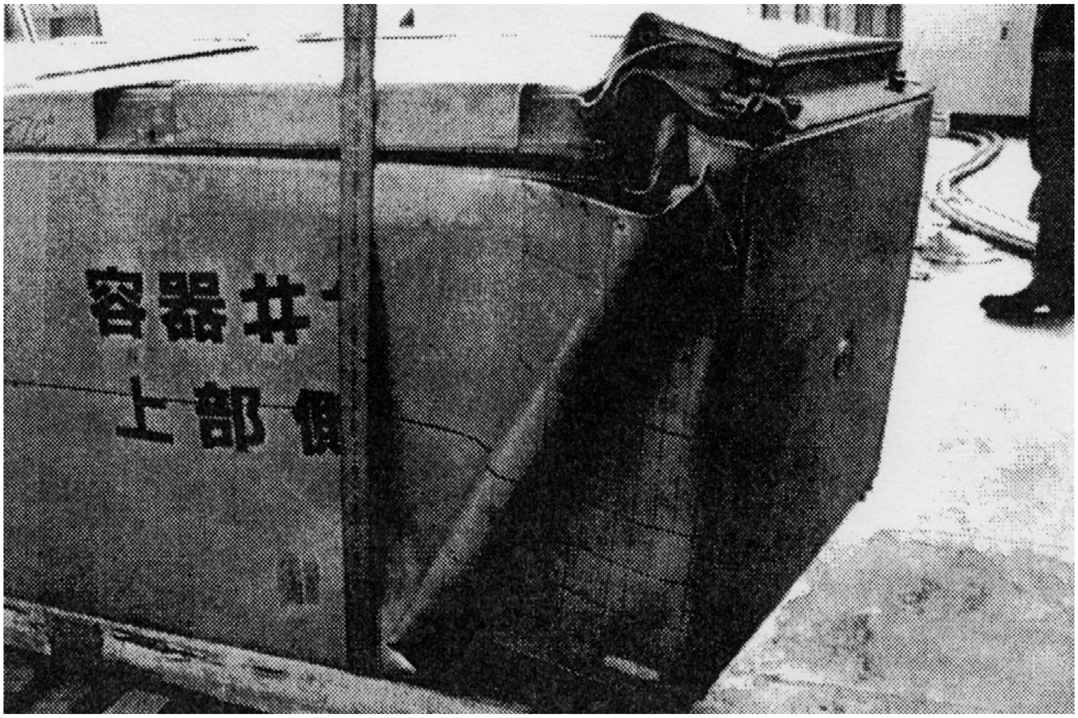

Figure 2-43 CTU 1J 9 m CG-Over-Bottom Corner Free Drop: View of Impacted Corner

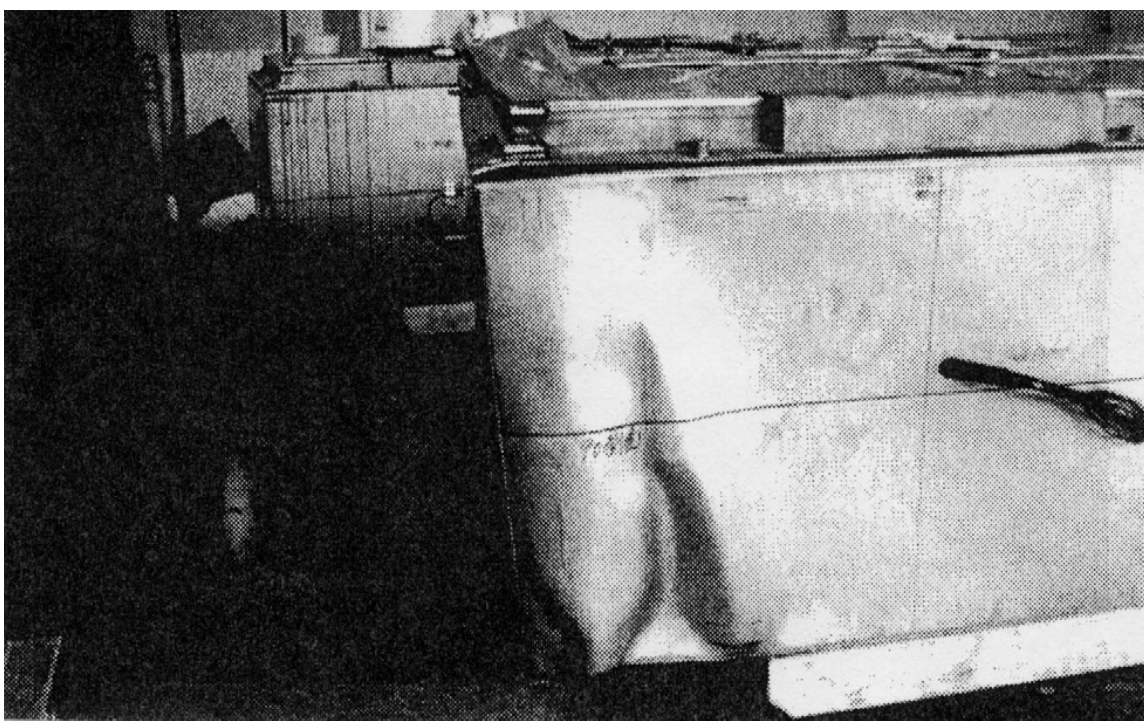

Figure 2-44 CTU 1J 9 m CG-Over-Bottom Corner Free Drop: View of Opposite Corner

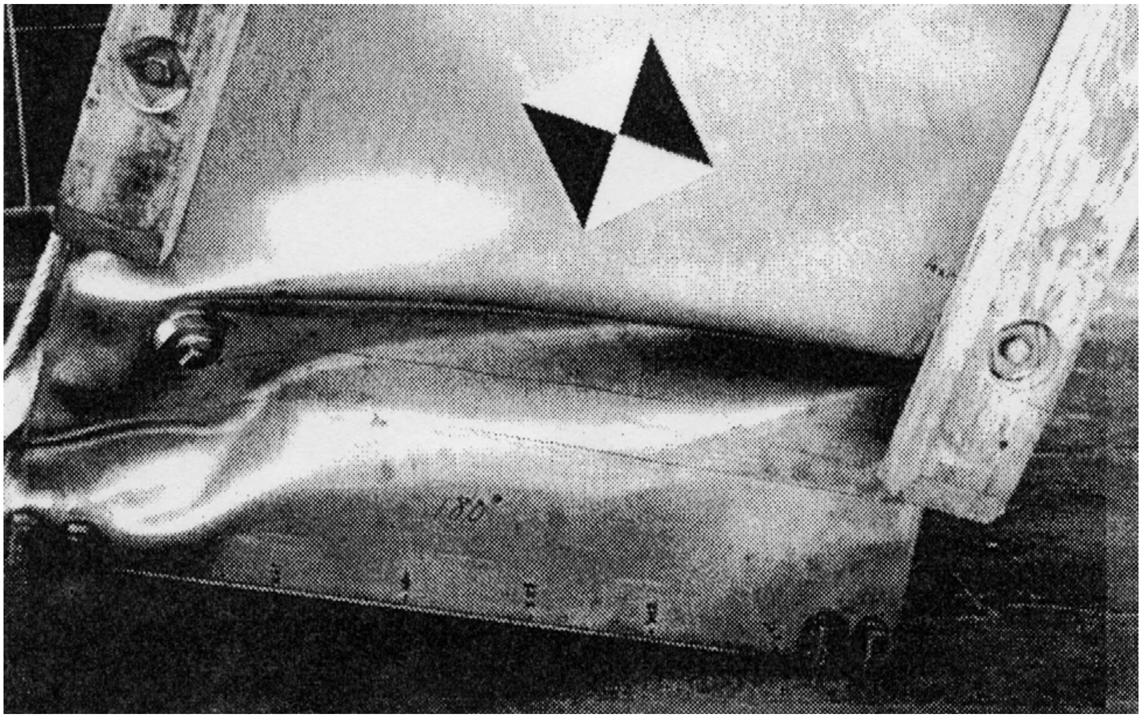

Figure 2-45 CTU 1J 9 m CG-Over-Bottom Corner Free Drop: View of Bottom

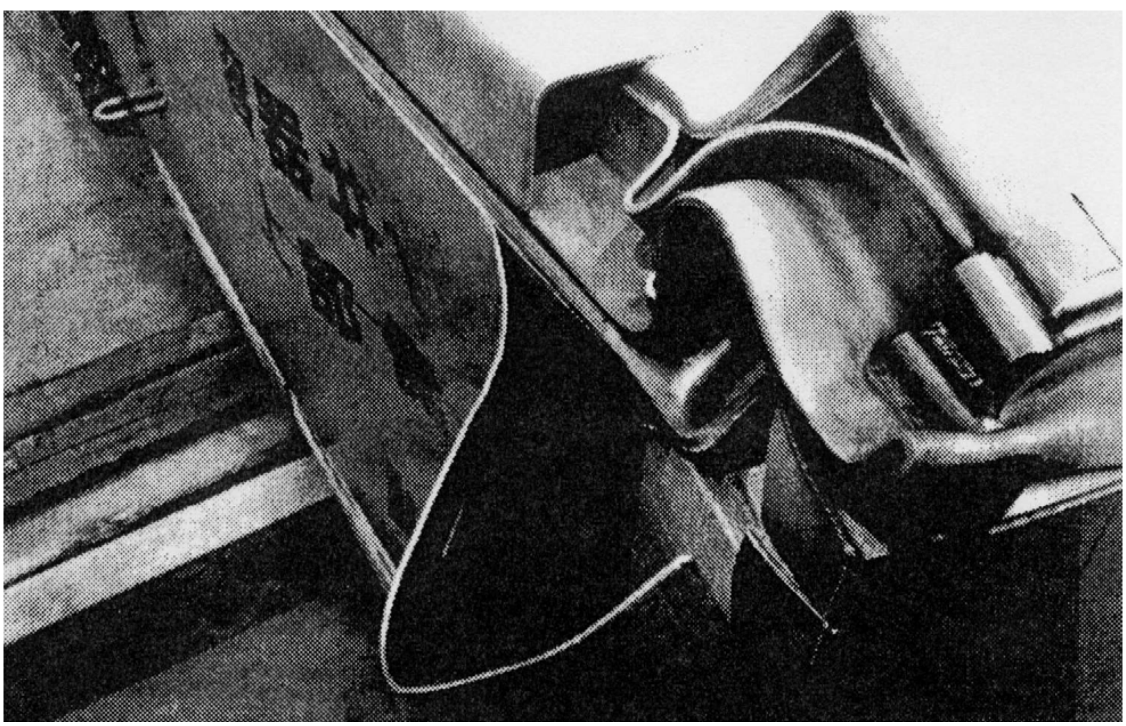

Figure 2-46 CTU 1J 9 m CG-Over-Bottom Corner Free Drop: Close-up View of Top Corner

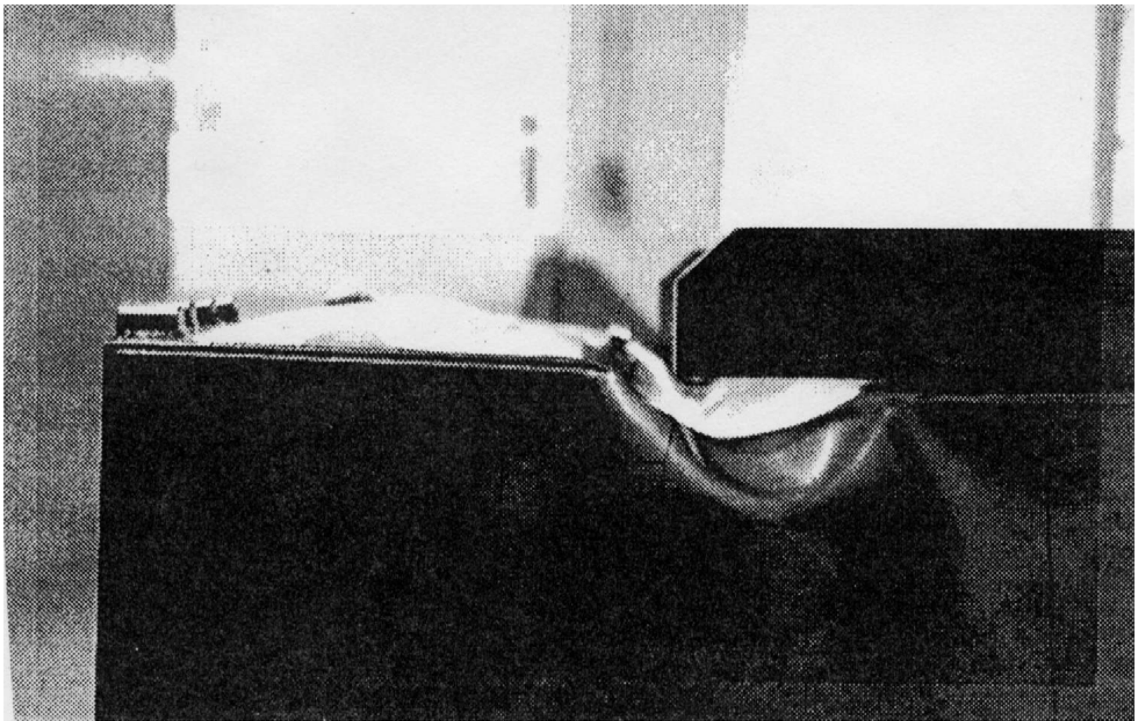

Figure 2-47 CTU 1J 9-m Vertical End Drop: Close-up Side View of Bottom Damage

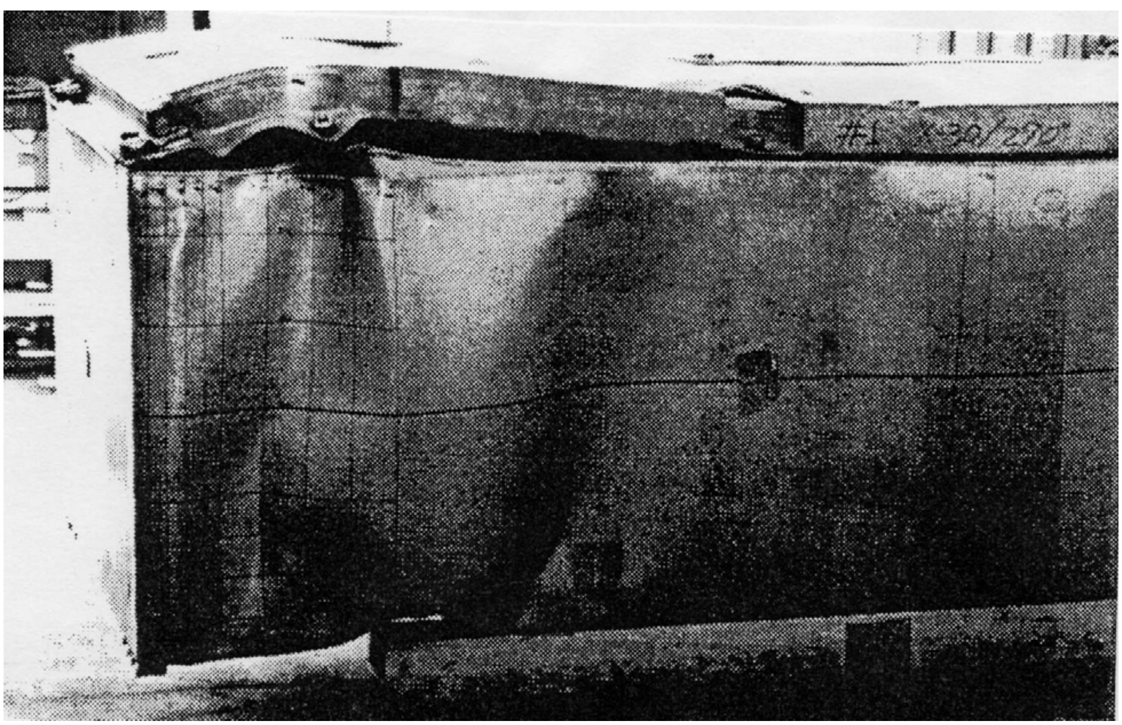

Figure 2-48 CTU 1J 9-m Vertical End Drop: Overall View of Damage

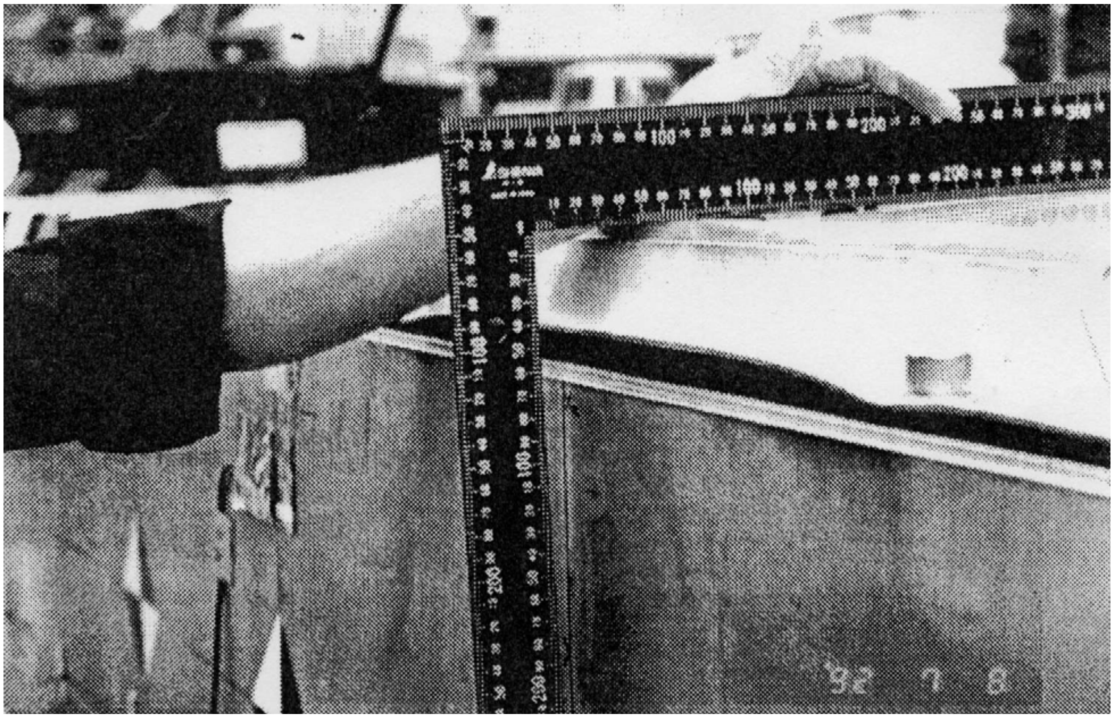

Figure 2-49 CTU 2J 9-m Horizontal Free Drop: Close-up Side View of Damage

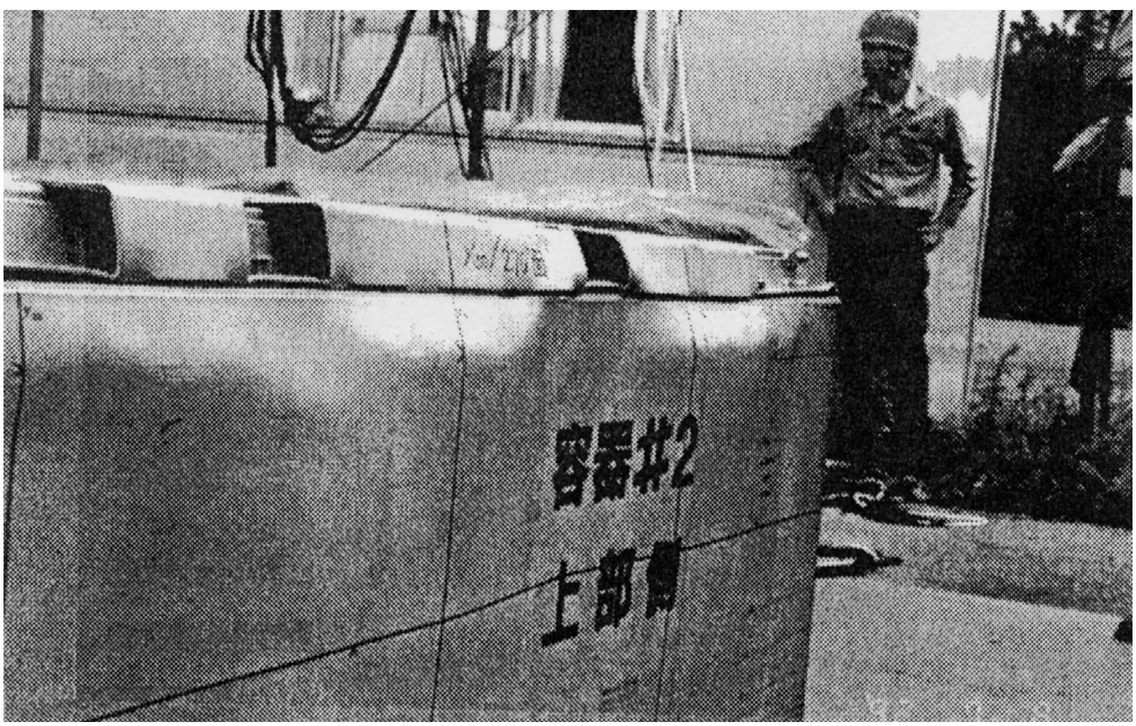

Figure 2-50 CTU 2J 9-m Horizontal Free Drop: Overall Side View of Damage

2.12.3. *Outer Container Gasket Sealing Capability*

The outer container for the TN-B1 packaging utilizes a 5 mm thick × 40 mm wide × 11,360 mm long, 50 shore durometer, solid natural rubber gasket. As shown in Appendix 1.4.1, Packaging General Arrangement Drawings, the gasket is attached to the flange of the outer container lid. The outer container lid is secured to the outer container body by twenty-four (24) M14 × 2, Type 304 stainless steel bolts, which are tightened to "wrench tight or as defined in user procedures". Since a specific tightening torque s not specified, the maximum bolt tension will be based on the minimum yield strength of the stainless steel.

The maximum force, F_b, in each lid bolt will be:

$$F_b = S_y (A_t)$$

where: S_y = Minimum yield strength = 206.8 MPa (30.0 ksi) (Ref. Table 2-2)
A_t = Tensile area for M14 × 2 bolt = 115 mm^2 (0.1783 in^2)

Substituting these values into the above equation yields a bolt force of 23,782 N (5,349 lb_f). The total compressive force applied to the gasket, F_{gasket}, is then:

$$F_{gasket} = (24)F_b = (24)(23{,}782) = 570{,}768 \text{ N } (128{,}376 \text{ lb}_f)$$

For the applied bolt force, the gasket compressive area, A_{gasket}, is 40 × 11,360 = 454,400 mm^2 (704.3 in^2). Conservatively neglecting any deflection of the 4-mm thick lid flange between the lid bolts, the resultant compressive stress on the gasket is then:

$$\sigma_{gasket} = \frac{570{,}768}{454{,}400} = 1.256\ MPa\ (182\ psi)$$

The shape factor, s, for the 5 × 40 gasket is:

$$s = \frac{One\ Load\ Area}{Total\ Free\ Area} = \frac{Width}{2(Thickness)} = \frac{40}{10} = 4.0$$

From Figure 5-12 of Handbook of Molded and Extruded Rubber,* the percent compressive deflection of the 50-durometer gasket with s = 4.0 at 182 psi compressive stress is approximately 3%, or 0.15 mm (0.006 in), which is minimal.

---

* *Handbook of Molded and Extruded Rubber, Third Edition*, Goodyear Tire & Rubber Company.

To determine whether the gasket is compressed with the applied bolt force, the compression modulus and the linear spring rate for the gasket is computed. Equation 3-7 of Handbook of Molded and Extruded Rubber, the linear spring rate, K_L, for the rubber gasket is:

$$K_L = \frac{E_c\,(A)}{h}$$

where: E_c = Compression modulus

A = Compression area of gasket = 454,400 mm^2 (704.3 in^2)

h = height of gasket = 5 mm (0.197 in)

The compression modulus is extracted from Figure 5-20 of the Handbook of Molded and Extruded Rubber for a shape factor "s" of 4.0 and an approximate compression of 3% for the 50 durometer gasket. From this figure, the compression modulus is interpolated to be 6,912 psi (47.7 MPa). The linear spring rate of the gasket is then:

$$K_L = \frac{6{,}912(704)}{0.197} = 24.7\ x\ 10^6 lb_f\ /in\ \ (4.33\ x\ 10^6\ Nmm)$$

To compress the gasket 0.15 mm (0.006 in), the required force in the bolts is:

$$24F_{bolt} = K_L\Delta = 24.7\times10^6\ (0.006) = 148{,}200\ lb_f\ \ (659{,}266\ N)$$

$$\Rightarrow F_{bolt} = 6{,}175\ lb_f\ \ (27{,}648\ N)$$

Since the resultant bolt force required to compress the gasket 3% is greater than the yield strength of the lid bolts, the gasket will not be compressed to the estimated 3% compression. To determine the estimated gasket compression with the maximum lid bolt force at yield strength (23,782 N [5,349 lb_f]), the linear spring rate will be computed for zero compression and then compared to the applied maximum force. From Figure 5-20 of the Handbook of Molded and Extruded Rubber for a shape factor "s" of 4.0, the compression modulus at zero compression will be:

$$E_c = 9{,}000(0.75) = 6{,}750\ psi\ (46.5\ MPa)$$

For zero compression and this compression modulus, the linear spring rate is:

$$K_L = \frac{6{,}750(704)}{0.197} = 24.1\ x\ 10^6 lb_f\ /in\ \ (4.23\ x\ 10^6\ Nmm)$$

The resultant deformation of the gasket for this spring rate with the maximum bolt force is:

$$\Delta_{gasket} = \frac{24(F_{bolt})}{K_L} = \frac{24(23{,}782)}{4.23\ x\ 10^6} = 0.135\ mm\ (0.005\ in)$$

This deformation is approximately 2.7% compression of the gasket. Prototypic seal testing in support of the TRUPACT-II package* has demonstrated that a pressure seal requires a minimum of 10% – 12% compression. Section 3.6, *Squeeze*, of the Parker O-ring Handbook† states that "*The minimum squeeze for all seals, regardless of cross-section should be about 0.2 mm (0.007 inches). The reason is that with a very light squeeze almost all elastomers quickly take 100% compression set.* " Based on these test results and the recommendations of Parker, the outer lid gasket will not form a pressure retaining seal.

Based on the results of this section, the optional use of synthetic rubber gasket material such as neoprene will not change the sealing of the package.

---

* U. S. Department of Energy (DOE), *Safety Analysis Report for the TRUPACT-II Shipping Package*, USNRC Certificate of Compliance 71-9218, U.S Department of Energy, Carlsbad Field Office, Carlsbad, New Mexico.

† ORD 5700A/US, *Parker O-ring Handbook*, 2001, Parker Hannifin Corporation, Lexington, KY.

3. THERMAL EVALUATION

Provides an evaluation of the package to protect the fuel during varying thermal conditions.

3.1. DESCRIPTION OF THERMAL DESIGN

The TN-B1 package is designed to provide thermal protection as described in Subpart F of 10 CFR 71 for transport of two BWR fuel assemblies with negligible decay heat. Compliance is demonstrated with 10 CFR 71 subpart F in the following subsections. The TN-B1 protects the fuel through the use of an inner and outer container that restricts the exposure of the fuel to external heat loads. The insulated inner container further restricts the heat input to the fuel through its insulation. The fuel requires very little thermal protection since similar fuel has been tested to the 800ºC temperature without rupture.

Given negligible decay heat, the thermal loads on the package come solely from the environment in the form of solar radiation for Normal Conditions of Transport (NCT), as described in Section 3.4 or a half-hour, 800ºC (1,475°F) fire for Hypothetical Accident Conditions (HAC), described in Section 3.5.

Specific ambient temperatures and solar heat loads are considered in the package thermal evaluations. Ambient temperatures ranging from -40ºC to 38ºC (-40ºF to 100ºF) are considered for NCT. The HAC fire event considers an ambient temperature of 38ºC (100 F), with solar heat loading (insulation) before and after the HAC half-hour fire event.

Details and assumptions used in the analytical thermal models are described with the thermal evaluations.

3.1.1. *Design Features*

The primary features that affect the thermal performance of the package are 1) the materials of construction, 2) the inner and outer containers and 3) the thermal insulation of the inner container. The stainless sheet metal construction of the structural components of the inner and outer containers influences the maximum temperatures under normal conditions. The material also ensures structural stability under the hypothetical accident conditions as well as provides some protection to the fuel. Likewise the zirconium alloy cladding has also been proven to be stable at the high temperatures potentially seen during the Hypothetical Accident Conditions (HAC).

The multi walled construction of the single walled outer container and the double walled inner container reduces the heat transfer as well as provides additional stability. The multi walled construction also reduces the opportunity for the fire in the accident conditions to impinge directly on the fuel.

The thermal insulation also greatly reduces the heat transfer to the fuel from external sources. The insulation consists of alumina silicate around most of the package plus the use of wood on the ends that both provide some insulation as well as shock absorbing capabilities.

3.1.2. *Content's Decay Heat*

Since the contents are unirradiated fuel, the decay heat is insignificant. A sum of the heat generated from the maximum allowable contents of each isotope from Table 1-5 (worst case) concludes the maximum decay heat remains less than 1 Watt.

Table 3-1 Decay Heat Generation

Isotope	Activity, Ci	Heat Generation, Watts/Ci	Heat Generation, Watts
U-232	1.20E+00	3.1553E-02	3.79E-02
U-234	2.35E+01	2.8311E-02	6.65E-01
U-235	8.73E-02	2.7115E-02	2.37E-03
U-236	8.06E-01	2.6697E-02	2.15E-02
U-238	1.50E-01	2.4920E-02	3.74E-03
Np-237	5.85E-04	2.8779E-02	1.68E-05
Pu-238	5.23E-04	3.2587E-02	1.70E-05
Pu-239	9.35E-05	3.0551E-02	2.86E-06
Pu-240	3.47E-04	3.0614E-02	1.06E-05
Total			**.73**

3.1.3. *Summary Tables of Temperatures*

Since the decay heat load is negligible, the maximum NCT temperature of 171ºF (77ºC, 350 K) occurs on the package exterior, and the maximum HAC temperature of 1198ºF (648ºC, 921 K) occurs at the inner surface of the inner container at the end of the fire. These analyses demonstrate that the TN-B1 package provides adequate thermal protection for the fuel assembly and will maintain the maximum fuel rod temperature well below the fuel rod rupture temperature of 800+°C under all transportation conditions.

3.1.4. *Summary Tables of Maximum Pressures*

The maximum pressure within the containment, the fuel rods during normal conditions of transport is 1.33 MPa (192.9 psia) when the fuel rods are pressurized with helium to a maximum pressure of 1.1145 MPa (absolute pressure) (161.7 psia) at ambient temperature.

The maximum pressure during the hypothetical accident conditions for these rods is 3.50 MPa (508 psia). This pressure was used to conservatively derive a limiting allowable clad stress of 10.18 MPa at room temperature. For compliance to HAC, fuel rod designs must have a product of the maximum internal pressure to the maximum inside radius to thickness ratio of 10.18 MPa or less. For fuel rod clad with a liner, the thickness of the liner shall be excluded in the when determining the maximum radius and thickness ratio.

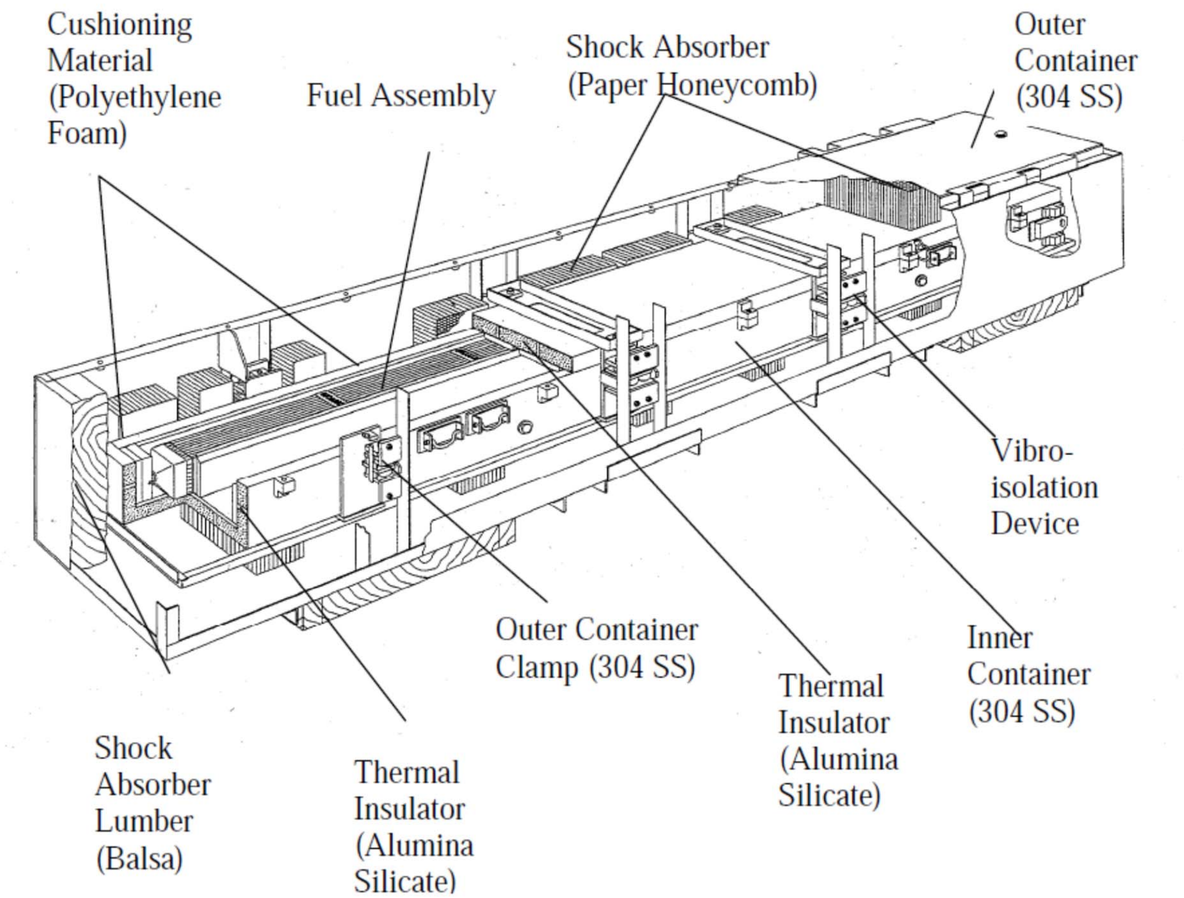

Figure 3-1 Overall View of TN-B1 Package

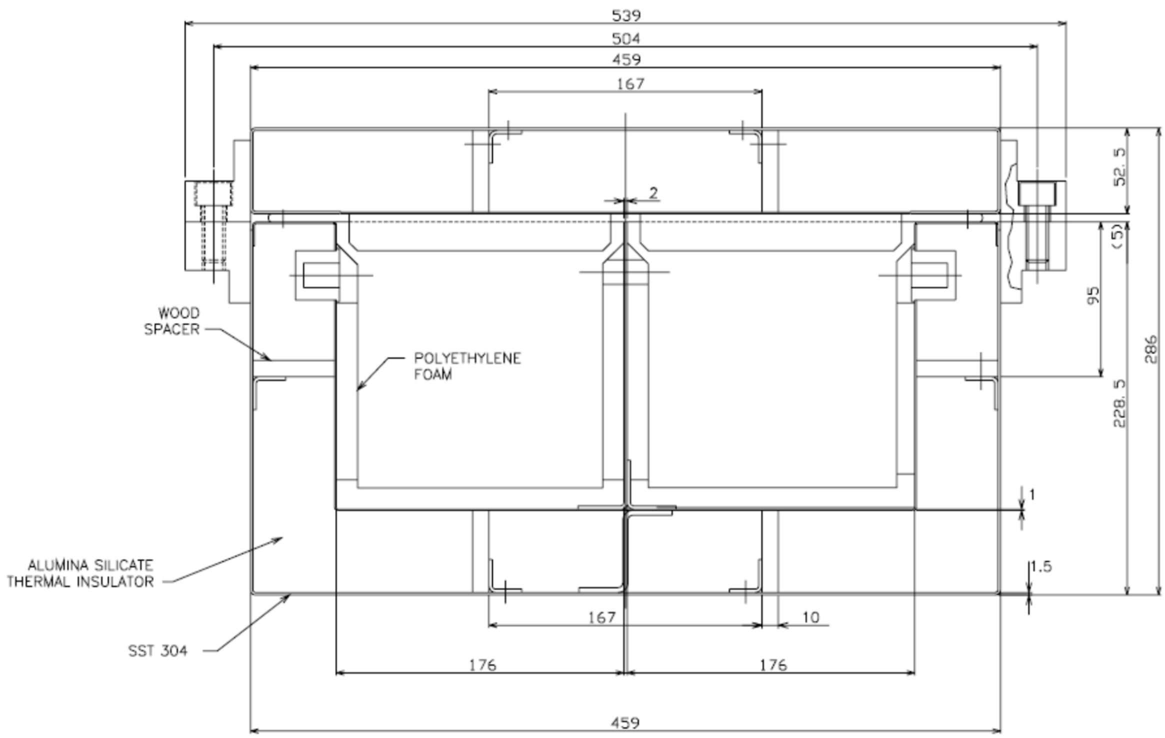

Figure 3-2 Transverse Cross-Sectional View of the Inner Container

3.2. MATERIAL PROPERTIES AND COMPONENT SPECIFICATIONS

3.2.1. *Material Properties*

The TN-B1 inner container is constructed primarily of Series 300 stainless steel, wood, and alumina silicate insulation. The void spaces within the inner container are filled with air at atmospheric pressure. The outer container is constructed of series 300 stainless steel, wood, and resin impregnated paper honeycomb. The thermal properties of the principal materials used in the thermal evaluations are presented in Table 3-2 and Table 3-3. Where necessary, the properties are presented as functions of temperature. Note that only properties for materials that constitute a significant heat transfer path are defined. A general view of the package is depicted in Figure 3-1. A sketch of the inner container transversal cross-section with the dimensions used in the calculation is presented in Figure 3-2.

For the Alumina Silicate, maximum values are specified because the maximum conductivity is the controlling parameter. This is because there is no decay heat in the payload and the only consideration is the material's ability to block of heat transfer to the fuel during the fire event.

Table 3-2 Material Properties for Principal Structural/Thermal Components

Material	Temperature, K	Thermal Conductivity, W/m-K	Specific Heat, J/kg-K	Density, kg/m³	Notes
Wood	300	0.240	2,800	500	1
Series 300 Stainless Steel	300	15	477	7,900	2
	400	17	515		
	500	18	539		
	600	20	557		
	800	23	582		
	1,000	25	611		
Alumina Silicate Insulation	673	≤0.105	1,046 (Nominal)	250 (Nominal)	3
	873	≤0.151			
	1,073	≤0.198			4
	1,273	≤0.267			4

Notes:

1 The material specified for the wood spacers. The properties have been placed with typical values for generic softwood.

2 [Reference. 3.6.1.2. p.809, 811, 812, and 820]

3 The values shown are based on published data for Unifrax Duraboard LD [Reference 3.6.1.11] and include compensation for the possible variation in test data (see discussion in Section 3.2.1).

4 Values at higher temperatures than 1,000 K are linearly extrapolated.

Table 3-3 Material Properties for Air

Temperature (K)	Thermal Conductivity (W/m·K)	Density (kg/m^3)	Specific Heat (J/kg·K)	Coefficient of Kinematic Viscosity ν (m^2/s)	Prandtl Pr
300	0.0267	1.177	1005	15.66 E-06	0.69
310	0.0274	1.141	1005	16.54 E-06	0.69
320	0.0281	1.106	1006	17.44 E-06	0.69
330	0.0287	1.073	1006	18.37 E-06	0.69
340	0.0294	1.042	1007	19.32 E-06	0.69
350	0.030	1.012	1007	20.30 E-06	0.69
360	0.0306	0.983	1007	21.30 E-06	0.69
370	0.0313	0.956	1008	22.32 E-06	0.69
380	0.0319	0.931	1008	23.36 E-06	0.69
390	0.0325	0.906	1009	24.42 E-06	0.69
400	0.0331	0.883	1009	25.50 E-06	0.69
500	0.0389	0.706	1017	37.30 E-06	0.69
600	0.0447	0.589	1038	50.50 E-06	0.69
700	0.0503	0.507	1065	65.15 E-06	0.70
800	0.0559	0.442	1089	81.20 E-06	0.70
900	0.0616	0.392	1111	98.60 E-06	0.70
1000	0.0672	0.354	1130	117.3 E-06	0.70

Source: Reference 3.6.1.2, p.824

3.2.2. *Component Specifications*

None of the materials used in the construction of TN-B1 package, such as series 300 stainless steel and alumina silicate insulation, are sensitive to temperatures within the range of -40ºC to 800ºC (-40°F to 1,475°F) that spans the NCT and HAC environment. Stainless steel has a melting point above 1,400°C (2,550°F), and maximum service temperature of 427°C (800°F). Similarly, the ceramic fiber insulation has a maximum operating temperature of 1,300°C (2,372°F). Wood is used as dunnage and as part of the inner package wall in the TN-B1 package. Before being consumed in the HAC fire, the wood would insulate portions of the inner container from exposure to the flames. However, the HAC transient thermal analyses presented herein conservatively neglects the wood's insulating effect, and assumes that all of the wood is consumed in the fire generating heat for all of its total mass.

The temperature limit for the fuel assembly's rods is greater than 800°C (1,472°F), based on the pressure evaluation provided in Section 3.5.3.2.

3.3. GENERAL CONSIDERATIONS

3.3.1. *Evaluation by Analysis*

The normal conditions of transport thermal conditions are evaluated by closed form calculations. The details of this analysis and supporting assumptions are found in that evaluation. The evaluation finds the maximum temperature for the outside of the package due to the insulation and uses that temperature for the contents of the package.

The transient hypothetical accident conditions are evaluated using an ANSYS finite element model. The model does not take credit for the outer container or the wood used in the inner container. Details of the model and the supporting assumptions maybe found in Section 3.5.

3.3.2. *Evaluation by Test*

Thermal testing was performed on fuel rods to determine the ability of the cladding (primary containment) to withstand temperatures greater than 800°C. The testing was performed for a range of fuel rods of different diameters, clad thickness and internal pressure. Since some of the current fuel designs for use in the TN-B1 are outside the range of parameters tested, additional thermal analyses have been performed to demonstrate the fuel rod's ability to withstand the HAC fire. In these tests, the fuel rods were heated to various temperatures from 700°C to 900°C for periods over one hour to determine the rupture temperature and pressure of the fuel. It was found that the fuel cladding did not fail at 800°C the temperature of the hypothetical accident conditions. This temperature associated pressure and resulting stress were used to provide the allowable conditions of the fuel which is used for containment.

3.3.3. *Margins of Safety*

For the normal condition evaluation the margins of safety are qualitative, based on comparisons to the much higher temperatures the fuel is designed for when it is in service in the reactors. There is no thermal deterioration of the packaging components at normal condition temperatures therefore no margins for the package components are calculated.

The margins of safety for the accident conditions are evaluated in Section 3.5 and are based on the testing discussed in Section 3.3.2.

3.4. THERMAL EVALUATION UNDER NORMAL CONDITIONS OF TRANSPORT

This section presents the results of thermal analysis of the TN-B1 package for the Normal Conditions of Transport (NCT) specified in 10 CFR 71.71. The maximum temperature for the normal conditions of transport is used as input (initial conditions) in the Hypothetical Accident Condition (fire event) analysis.

3.4.1. *Heat and Cold*

Per 10 CFR 71.71(c)(1), the maximum environmental temperature is 100°F (311 K), and per 10 CFR 71.71(c)(2), the minimum environmental temperature is -40°F (233 K).

Given the negligible decay heat of the fuel assembly, the thermal loads on the TN-B1 package come solely from the environment in the form of solar radiation for NCT as prescribed by 10 CFR 71.71(c)(1). As such, the solar heat input into the package is 800 g·cal/cm^2 for horizontal surfaces and 200 g·cal/cm^2 for vertical surfaces for a varying insolation over a 24-hour period).

3.4.1.1. **Maximum Temperatures**

For the analysis, the applied insolation is modeled transiently as sinusoidal over a 24-hour period, except when the sine function is negative (the insolation level is set to zero). The timing of the sine wave is set to achieve its peak at 12:00 PM and peak value of the curve is adjusted to ensure that the total energy delivered matched the regulatory values (800 g·cal/cm^2 for horizontal surfaces, 200 g·cal/cm^2 for vertical surfaces). As such, the total energy delivered in one day by the sine wave model is given by:

$$\int_{6-hr}^{18-hr} Q_{peak} \cdot \sin\left(\frac{\pi t}{12 \cdot hr} - \frac{\pi}{2}\right) dt = \left(\frac{24 \cdot hr}{\pi}\right) x\, Q_{Peak}$$

Using the expression above for the peak rate of insolation, the peak rates for top and side insolation may be calculated as follows:

Based on these inputs, the maximum NCT temperature on the inside surface of the inner container, as calculated in Appendix 3.6.3, is 350 K (77ºC, 171ºF).

Given negligible decay heat, the maximum accessible surface temperature of the TN-B1 package in the shade is the maximum environment temperature of 38°C (100°F), which is less than the 50°C (122°F) limit established in 10 CFR 71.43(g) for a non-exclusive use shipment.

3.4.1.2. **Minimum Temperatures**

The minimum environmental temperature that the TN-B1 package will be subjected to is -40°F, per 10 CFR 71.71(c)(2). Given the negligible decay heat load, the minimum temperature of the TN-B1 package is -40°F.

3.4.2. ***Maximum Normal Operating Pressure***

For fuel rods that are pressurized with helium to a maximum pressure of 1.1145 MPa (absolute pressure) (161.7 psia) helium at ambient temperature prior to sealing, the Maximum Normal Operating Pressure (MNOP) at the maximum normal temperature is:

$$MNOP = P_1 \frac{T_{max}}{T_{ambient}} = 1.1145\ x\ \frac{350}{293} = 1.33\ MPa = 192.9\ psia$$

Since there is no significant decay heat and the fuel composition is stable, MNOP calculated above would not be expected to change over a one year time period.

3.4.3. ***Maximum Thermal Stresses***

Due to the construction of the TN-B1, light sheet metal constructed primarily of the same material, 304 SS, there are no significant thermal stresses. The package is constructed so that there is no significant constraint on any component as it heats up and cools down. The fuel cladding which provides containment is likewise designed for thermal transients, greater than what is found in the normal conditions of transport. The fuel rod is allowed to expand in the package. The fuel within the cladding is also designed to expand without interfering with the cladding.

3.5. <u>THERMAL EVALUATION UNDER HYPOTHETICAL ACCIDENT CONDITIONS</u>

This section presents the results of the thermal analysis of the TN-B1 package for the Hypothetical Accident Condition (HAC) specified in 10 CFR 71.73(c) (4).

For the purposes of the Hypothetical Accident Conditions fire analysis, the outer container of the TN-B1 package is conservatively assumed to be not present during the fire. This allows the outer surface of the inner container to be fully exposed to the fire event. The wood used in the inner container is conservatively assumed to combust completely. By ignoring the outer container and applying the fire environment directly to the inner container, the predicted temperature of the fuel rods is bounded. To provide a conservative estimate of the worst-case fuel rod temperature, the fuel assembly and its corresponding thermal mass are not explicitly modeled as well as the polyethylene foam/rubber vibration absorber. The maximum fuel rod temperature is conservatively derived from the maximum temperature of the inside surface of the inner stainless steel wall. The analysis considering the insulation and multi-layers of packaging is very conservative because as discussed in Section 3.3.2 the bare fuel has been demonstrated to maintain integrity when exposed to temperatures that equal those found in the hypothetical accident conditions.

Thermal performance of the TN-B1 package is evaluated analytically using a 2-D model that represents a transversal cross-section of the inner container (Figure 3-2) in the region containing the metallic and wood spacers. The 2-D inner container finite element model was developed using the ANSYS computer code [Reference 3.6.1.3]. ANSYS is a comprehensive thermal, structural and fluid flow analysis package. It is a finite element analysis code capable of solving steady state and transient thermal analysis problems in one, two or three dimensions. Heat transfer via a combination of conduction, radiation and convection can be modeled.

The solid entities were modeled in the present analysis with PLANE55 two-dimensional elements and the radiation was modeled using the AUX12 Radiation Matrix method. The developed ANSYS input file is included as Appendix 3.6.2.

The initial temperature distribution in the inner container prior to the HAC fire event is a uniform 375 K conservatively corresponding to the outer surface temperature of the inner container per the normal condition calculations presented in Appendix 3.6.3.

3.5.1. *Initial Conditions*

The environmental conditions preceding and succeeding the fire consist of an ambient temperature of 38 ºC (311 K) and insulation per the normal condition thermal analysis. The solar absorptivity coefficient of the outer surface has been increased for the post-fire period to 1 to include changes due to charring of the surfaces during the fire event.

3.5.2. *Fire Test Conditions*

The Hypothetical Accident Condition fire event is specified per 10 CFR 71.73(c) (4) as a half-hour, 800ºC (1,073 K) fire with forced convection. For the purpose of calculation, the value of the package surface absorptivity coefficient (0.8) is selected as the highest value between the actual value of the surface (0.42) and a value of 0.8 as specified in 10 CFR 71.73(c) (4).

A value of 1.0 for the emissivity of the flame for the fire condition is used in the calculation. The rationale for this is that 1.0 maximizes the heating of the package. This value exceeds the minimum value of 0.9 specified in 10 CFR 71.73(c) (4). The Hypothetical Accident Condition (HAC) fire event is specified per 10 CFR 71.73(c)(3) as a half-hour, 800°C (1,475°F) fire with forced convection and an emissivity of 0.9. The environmental conditions preceding and succeeding the fire consist of an ambient temperature of 100 °F and insulation per the NCT thermal analyses.

To model the combustion of the wood, the wood elements of the model are given a heat generation rate based on the high heat value of Western Hemlock of 3630 Btu/lb (8.442×10^6 J/kg) from Reference 3.6.1.8, Section 7, Table 9. It is conservatively assumed that the entire mass of the wood will burn. Moreover, the wood will burn across its thinnest section from opposite faces. Using data burn rate data for redwood which has approximately the same density as hemlock [3.6.1.8], each face will burn 5 mm at a minimum rate of 0.543 mm/min [Reference 3.6.1.10] resulting in a 9.2 minute time of combustion. This conservatively results in the longest burn time for the hemlock, and the greatest effect on temperature. The resulting heat generation rate in the wood spacers is equal to:

$$\dot{Q} = (8.42 \times 10^6) \times (500 \text{ kg / m}^3) / (9.2 \text{ s} \times 60) = 7.63 \times 10^6 \text{ W/m}^3\text{/s}$$

3.5.2.1. Heat Transfer Coefficient during the Fire Event

During a HAC hydrocarbon fire, the heating gases surrounding the package will achieve velocities sufficient to induce forced convection on the surface of the package. Peak velocities measured in the vicinity of the surfaces were under 10 m/s [Reference 3.6.1.4].

The heat transfer coefficient takes the form [Reference 3.6.1.4, p. 369]:

$$h = k/D \cdot C \cdot (u \cdot D/\upsilon)^m \cdot Pr^{1/3}$$

Where:

- D: average width of the cross-section of the inner container (0.373 m)
- k: thermal conductivity of the fluid
- υ: kinematic viscosity of the fluid
- u: free stream velocity
- C, m: constants that depend on the Reynolds number ($Re = u \cdot D/\upsilon$)
- Pr: Prandtl number for the fluid

The property values of k, υ and Pr are evaluated at the film temperature, which is defined as the mean of the wall and free stream fluid temperatures. At the start of the fire the wall temperature is 375 K (101.7ºC, 215ºF) and the stream fluid temperature is 1,073 K (1,475ºF). The film temperature is therefore 710.5 K, and the property values for air at this temperature (interpolated from Table 3-3) are k=0.0509 W/m·K, υ=66.84E-06 m^2/s and Pr= 0.70. Assuming a maximum stream velocity of 10 m/s this yields a Reynolds number of 55.8E03. At this value of Re, the constants C and n are 0.102 and 0.675 respectively [Reference 3.6.1.4, Table 7.3].

$$h = \frac{0.0509 \cdot 0.102 \cdot \left(10 \cdot \frac{0.373}{66.84x10^{-6}}\right)^{0.675} \cdot (0.70)^{1/3}}{0.373}$$

h = 19.8 W/m^2 K

A value of 19.8 W/m^2·K was conservatively used in the analysis of the regulatory fire.

3.5.2.2. **Heat Transfer Coefficient during Post-Fire Period**

During the post-fire period of the HAC, it is conservatively assumed that there is negligible wind and that heat is transferred from the inner container to the environment via natural convection. Natural heat transfer coefficients from the outer surface of the square inner container are calculated as follows.

Reference 3.6.1.4 recommends the following correlations for the Nusselt number (Nu) describing natural convection heat transfer to air from heated vertical and horizontal surfaces:

Vertical heated surfaces [Reference 3.6.1.4, p. 493]:

$$N_u = (0.825 + \frac{0.387\ x\ (G_r x\ P_r)^{\frac{1}{6}}}{(1 + \left(0.492/_{P_r}\right)^{9/_{16}})^{\frac{8}{27}}})^2$$

For entire range of Ra=Gr x Pr (9)

Where:

- Nu: Nusselt number
- Gr: Grashof number
- Pr: Prandtl number

Horizontal heated surfaces facing upward [Reference 3.6.1.4, p.498]:

$$Nu = 0.54 \times (Gr \times Pr)^{1/4} \text{ for } (10^4 < Gr \times Pr < 10^7) \quad (10)$$

$$Nu = 0.15 \times (Gr \times Pr)^{1/3} \text{ for } (10^7 < Gr \times Pr < 10^{11}) \quad (11)$$

and, for horizontal heated surfaces facing downward:

$$Nu = 0.27 \times (Gr \times Pr)^{1/4} \text{ for } (10^5 < Gr \cdot Pr < 10^{10}) \quad (12)$$

The correlations for the horizontal surfaces are calculated using a characteristic length defined by the relation L=A/P, where A is the horizontal surface area and P is the perimeter [Reference 3.6.1.4, p. 498]. The calculated characteristic length for the horizontal surfaces of the inner container is L=0.209 m (A=2.14812 m^2 and P=10.278 m).

The following convective heat transfer coefficients (Table 3-2) have been calculated using Eq. (5), (6), (9), (10), (11) and (12). The corresponding characteristic length used in calculating the Nusselt number for each surface is also used in Eq. 5 for calculating the heat transfer coefficient. The thermal properties of air have been evaluated at the mean film temperature (=(T_s+$T_{ambient}$)/2).

The effects of solar radiation are included during the post-fire period by specifying the equivalent heat flow for each node f the surfaces exposed to fire for an additional 3.5 hours, i.e. the fire starts at the time of the peak temperature in the inner container (8 hours after sunrise) and is 0.5 hours in duration. This results in an additional 3.5 hours of solar insolation. Using the peak rates calculated in section 3.4.1.1, the nodal heat flows at 2:30 PM are equal to:

$$\dot{q}_{top} = \frac{1{,}218 \frac{W}{m^2}\left(Sin\left(\frac{\pi\ x\ (6+8.5)}{12} - \frac{\pi}{2}\right)\right)(0.459\ m)}{(155-1)} = 2.88\ W/m$$

$$\dot{q}_{side} = \frac{305 \frac{W}{m^2}\left(Sin\left(\frac{\pi\ x\ 14.5}{12} - \frac{\pi}{2}\right)\right)(0.281\ m)}{(99-1)} = 0.69\ W/m$$

Where 0.459 m is the width of the inner container, 0.281 m is its height, and the model is 155 nodes in width by 99 nodes in height. For the remaining 3.5 hours of solar insolation, these heat fluxes are conservatively applied as bounding constant values rather than varying with time.

The solar absorptivity coefficient of the outer surface is conservatively assumed to be 1. The duration of the post-fire period has been extended to 12.5 hr to investigate the cool-down of the inner container.

3.5.3. *Maximum Temperatures and Pressure*

3.5.3.1. Maximum Temperatures

The peak fuel rod temperature, which is conservatively assumed to be the same as the inner wall temperature of the package, response over the course of the HAC fire scenario is illustrated in Figure 3-3. The temperature reaches its maximum point of 921 K or 648°C (1198°F) at the end of the fire or 1,800 seconds after the start of the fire. This peak temperature occurs at top corners of the inner wall.

The maximum temperature even when applied to the fuel directly is well below the maximum temperature the fuel can withstand. Similar fuel with no thermal protection has been tested in fire conditions at over 800°C (1,475°F) for more than 60 minutes without failures.

3.5.3.2. **Maximum Internal Pressure**

The maximum pressure for the fuel can be determined by considering that the fuel is pressurized initially with helium. As the fuel is heated, the internal pressure in the cladding increases. By applying the ideal gas law the pressure can be determined and the resulting stresses in the cladding can be determined. Since the temperatures can be well above the normal operating range of the fuel the cladding performance can best be determined by comparison to test data.

Similar fuel with similar initial pressures has been heated in an oven to over 800ºC for over an hour without failures (Reference 3.6.1.6). The fuel that was tested in the oven was pressurized with 10 atmospheres of helium. When heated to the 800°C it had an equivalent pressure of:

$$P_{max} = (P_1)\frac{T_{max}}{T_{ambient}} = 1.1145MPa\ x\ \frac{1{,}073}{293} = 4.08\ MPa = 592\ psia$$

This results in an applied load to the cladding of 3.98 MPa or 577.3 psig. The fuel that was tested had an outer diameter of 0.4054 inch (10.30 mm). Since the fuel when tested to 850°C had some ruptures but did not rupture at 800°C when held at those temperatures for 1 hour, the stresses at 800°C are used as the conservative allowable stress. Both the tested fuel and the fuels to be shipped in the TN-B1 have similar zirconium cladding. The stress generated in the cladding of the test fuel is:

$$\rho = \frac{pr}{t} = \frac{3.98MPa\ x\ 4.56mm}{0.584mm} = 31.1MPa = 4{,}510\ psi$$

Recognizing that the properties of the fuel cladding degrade as the temperature increases the above calculated stress is conservatively used as the allowable stress for the fuel cladding for the various fuels to be shipped. The fuel is evaluated at the maximum temperature the inner wall of the inner container sees during the Hypothetical Accident Condition thermal event evaluated above. Table 3-6 shows the maximum pressure for each type of fuel and the resulting stress and margin. The limiting design properties of the fuel, maximum cladding internal diameter, minimum cladding wall thickness and initial pressurization for each type of fuel are considered in determining the margin of safety. Positive margins are conservatively determined for each type of fuel demonstrating that containment would be maintained during the Hypothetical Accident events. The minimum cladding thickness does not include the thickness of the liner if used.

The results of the transient analysis are summarized in Table 3-5. The temperature evolution during the transient in three representative locations on the inner wall and one on the outer wall is included. The maximum temperature on the inner wall is 921 K (648°C, 1198°F) and is reached at the upper inner corners of the container, 1,800 seconds after the beginning of the fire. The graphic evolution of the temperatures listed in Table 3-5 is represented in Figure 3-3. Representative plots of the isotherms at various points in time are depicted in Figure 3-4 through Figure 3-7.

The temperatures and resulting pressures are within the capabilities of the fuel cladding as shown by test. Therefore the fuel cladding and closure welds maintain containment during the Hypothetical Accident Conditions.

The temperatures and resulting pressures are within the capabilities of the fuel cladding as shown by test. Therefore the fuel cladding and closure welds maintain containment during the Hypothetical Accident Conditions.

3.5.4. *Accident Conditions for Fissile Material Packages for Air Transport*

Approval for air transport is not requested for the TN-B1.

Table 3-4 Convection Coefficients for Post-fire Analysis

T_S (surface temperature)		$T_{ambient}$		H (vertical surface)	h (horizontal surface facing upward)	h (horizontal surface facing downward)
ºF	K	ºF	K	(W/m^2·K)	(W/m^2·K)	(W/m^2·K)
150	338.71	100	311	4.68	5.19	2.34
200	366.48	100	311	5.61	6.34	2.74
250	394.26	100	311	6.18	7.05	2.99
300	422.04	100	311	6.60	7.55	3.17
350	449.82	100	311	6.90	7.92	3.30
400	477.59	100	311	7.13	8.18	3.41
600	588.71	100	311	7.64	8.74	3.67
900	755.37	100	311	8.00	9.07	3.89
1,375	1,019.26	100	311	8.25	9.17	4.09

Table 3-5 Calculated Temperatures for Different Positions on the Walls of the Inner Container Walls

Time (s)	Inner Wall Temperature (top right corner) (K)	Inner Wall Temperature (bottom) (K)	Inner Wall Temperature (top) (K)	Outer Wall Temperature (K)
0.1	375	375	375	377
911	750	667	546	1,062
1,800	921	821	696	1,067
1,900	918	823	710	807
2,000	905	817	723	686
2,200	868	797	742	583
2,600	803	761	760	509
3,268	723	715	758	463
4,280	639	662	727	437
27,973	354	335	369	378
45,000	349	324	358	377

Table 3-6 Maximum Pressure

Parameter	Units	8 x 8 Fuel	9 x 9 Fuel	10 X 10 Fuel	11 X 11 Fuel
Initial Pressure	MPa absolute	0.608	1.1145	1.1145	1.1145
Fill temperature	°C	20	20	20	20
Temperature during HAC	°C	648	648	648	648
Outside Diameter Maximum	mm	12.5	11.46	10.52	10.14
	inches	0.492	.4512	.4142	0.399
Minimum Allowable Cladding Thickness	mm	0.68	0.570	0.520	0.500
	inches	0.0268	0.0224	0.0205	0.0197
Cladding Inside Diameter Maximum	mm	11.14	10.32	9.48	9.14
	inches	0.439	.406	.373	0.360
Pressure @ HAc	MPa absolute	1.91	3.50	3.50	3.50
	psia	277	508	508	508
Applied Pressure @ HAC	MPa	1.81	3.40	3.40	3.40
	psig	262	493	493	493
Stress Pr/t	MPa	14.82	30.8	31.0	31.1
	psi	2149	4,467	4,498	4510
Margin, (allowed stress / actual stress) - 1	None	1.10	0.01	0.003	0.000
Max Allowed Cladding Inside Radius / Thickness	None	16.75	9.14	9.14	9.14

Note: Table values for cladding thickness and diameters bound current fuel designs and are for example purposes only. However, all fuel to be shipped must have a maximum pre-pressure times the maximum Inside Radius/Thickness product of 9.14 x 1.1145 MPa = 10.18653 MPa or less. The thickness of the liner in liner cladding shall be excluded when determining radius and thickness. Thus, all products must meet the maximum product of allowed pressure multiplied by Inside Radius/Thickness of 10.18653 MPa.

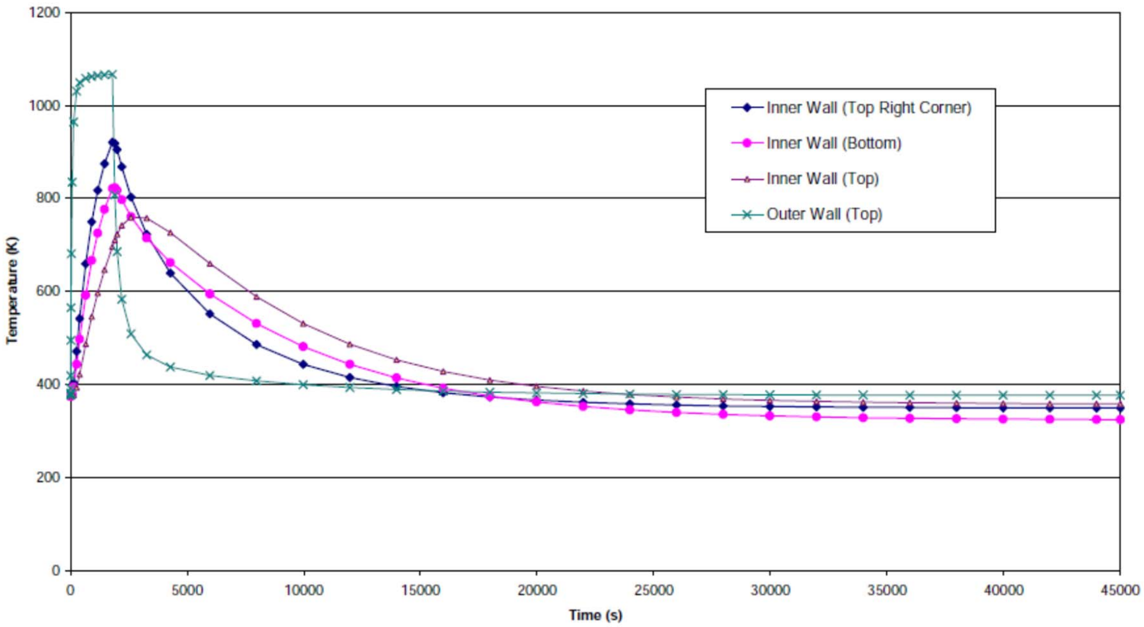

Figure 3-3 Calculated Temperature Evolution During Transient

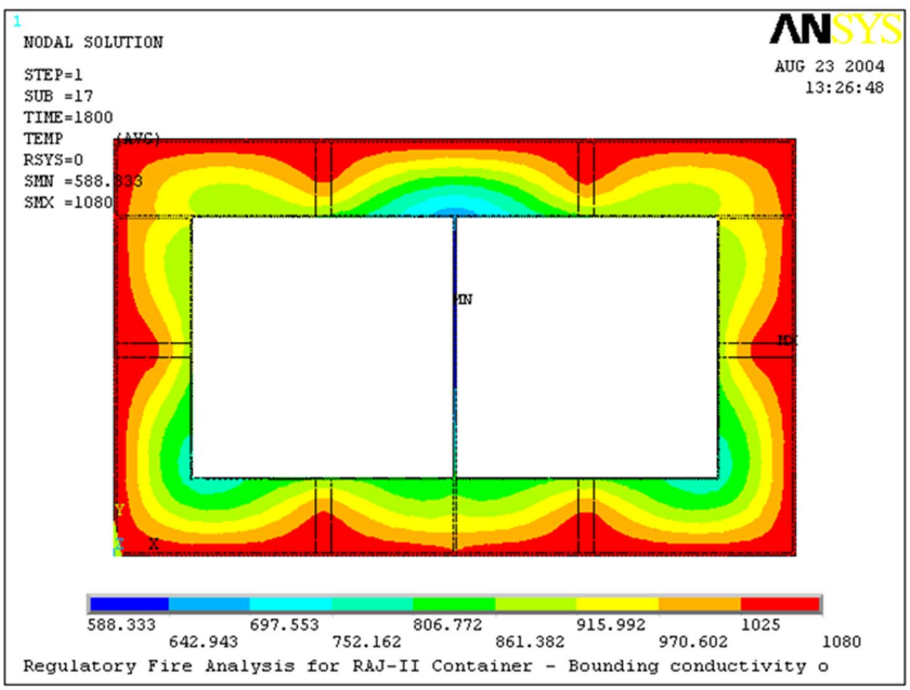

Figure 3-4 Calculated Isotherms at the End of Fire Phase (1,800 s)

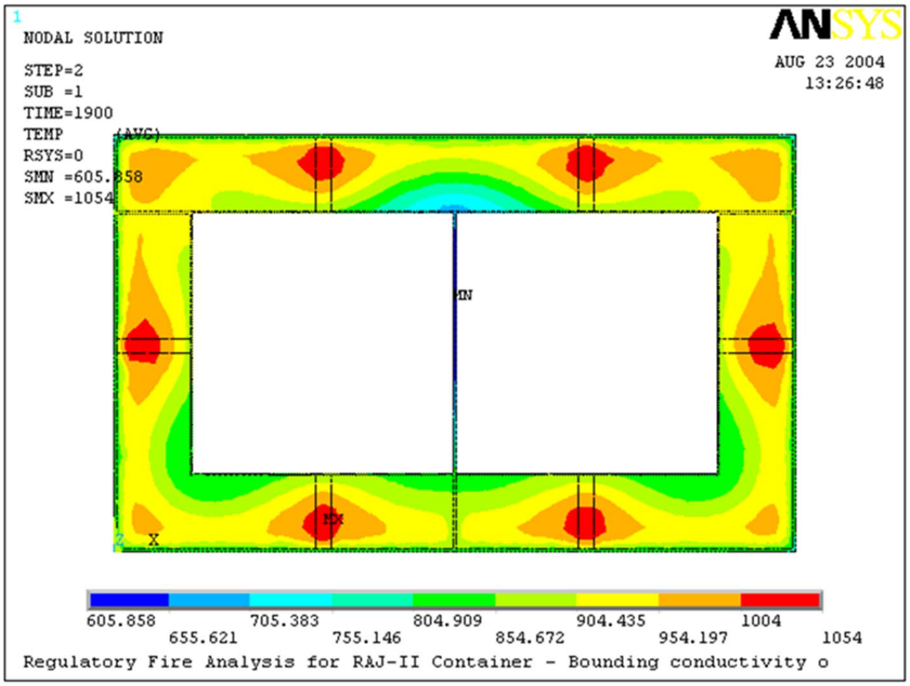

Figure 3-5 Calculated Isotherms at 100s After the End of Fire

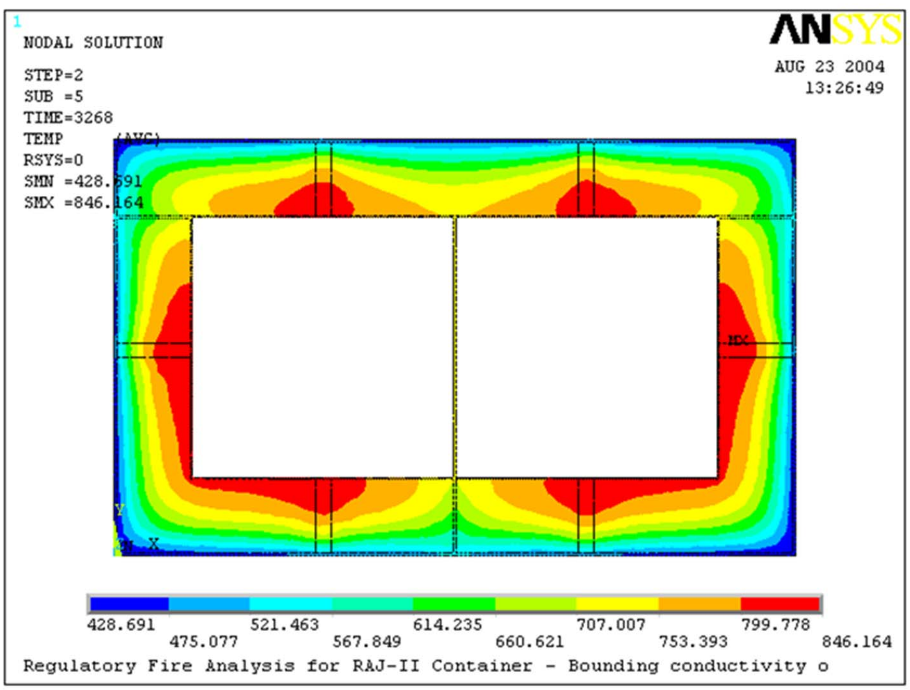

Figure 3-6 Calculated Isotherms at 1,468 s After the End of Fire

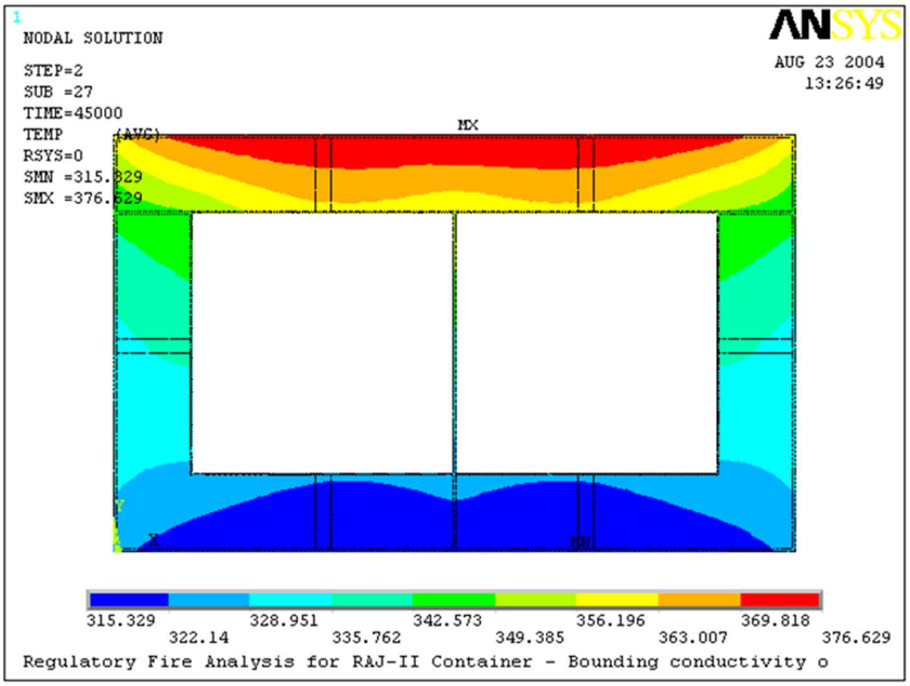

Figure 3-7 Calculated Isotherms at 12 hr After the End of Fire

3.6. APPENDIX

3.6.1. *References*

3.6.1.1. **10 CFR 71, Packaging and Transportation of Radioactive Material**

3.6.1.2. **Mills, A.F., Heat Transfer, Irwin, Inc., Homewood, Illinois, 1992**

3.6.1.3. **ANSYS Finite Element Computer Code, Version 5.6, ANSYS, Inc., 2000**

3.6.1.4. **McCaffery, B.J., Purely Buoyant Diffusion Flames – Some Experimental Results, Report PB80-112113, U.S. National Bureau of Standards, Washington, D.C., 1979**

3.6.1.5. **Incropera, F.P., Dewitt, D.P., Fundamentals of Heat and Mass Transfer, John Wiley and Sons, Inc., New York, New York, 1996**

3.6.1.6. **GNF-2 Fuel Rod Response to An Abnormal Transportation Event (proprietary)(30 Minute Fire)**

3.6.1.7. **Handbook of Heat Transfer, Warren M. Rohsenow, James P. Hartnett, McGraw Hill book company.**

3.6.1.8. **Standard Handbook for Mechanical Engineers, Baumeister , Marks, McGraw Hill book company, Seventh edition.**

3.6.1.9. **Thermal Properties of Paper, PTN149, Charles Green, Webster New York, 2002 (http://www.frontiernet.net/~charmar/).**

3.6.1.10. **Tran, H.C., and White, R. H., Burning Rate of Solid Wood Measured in a Heat Release Calrimeter, Fire and Materials, Vol. 16, pp 197-206, 1992.**

3.6.1.11. **"Pactec Specification: Regarding Global Nuclear Fuel Specification for Alumina Silicate for use in the RAJ-II Shipping container," Unifrax Corporation, 6/3/04.**

3.6.2. *ANSYS Input File Listing*

Listing of the ANSYS input file (file: model_fl_heat.inp)

```
fini
/clear
/filnam,model_f1_heat,
/outp,model_f1_heatout,out
/PREP7
/TITLE, Regulatory Fire Analysis for RAJ-II Container -
Bounding conductivity of Alumina
/UNITS,SI
/SHOW,JPEG
!*
!*set element types
!*
ET,1,PLANE55,1
ET,2,LINK32
ET,3,MATRIX50,1
!*
!*  define keypoints
!* K,1,0,0,0,
K,2,0.459,0,0,
K,3,0,0.0015,0,
K,4,0.0015,0.0015,0,
K,5,0.136,0.0015,0,
K,6,0.146,0.0015,0,
K,7,0.2285,0.0015,0,
K,8,0.2305,0.0015,0,
K,9,0.313,0.0015,0,
K,10,0.323,0.0015,0,
K,11,0.4575,0.0015,0,
K,12,0.459,0.0015,0,
K,13,0.0015,0.0515,0,
K,14,0.0515,0.0515,0,
K,15,0.136,0.0515,0,
K,16,0.146,0.0515,0,
K,17,0.2285,0.0515,0,
K,18,0.2305,0.0515,0,
K,19,0.313,0.0515,0,
K,20,0.323,0.0515,0,
K,21,0.4075,0.0515,0,
K,22,0.4575,0.0515,0,
K,23,0.0515,0.0525,0,
K,24,0.0525,0.0525,0,
```

```
K,73,0.2285,0.2285,0,
K,74,0.2305,0.2285,0,
K,75,0.2355,0.2285,0,
K,76,0.399,0.2285,0,
K,77,0.4065,0.2285,0,
K,78,0.459,0.2285,0,
K,79,0.,0.2295,0,
K,80,0.0015,0.2295,0,
K,81,0.136,0.2295,0,
K,82,0.146,0.2295,0,
K,83,0.313,0.2295,0,
K,84,0.323,0.2295,0,
K,85,0.4575,0.2295,0,
K,86,0.459,0.2295,0,
K,87,0.,0.2795,0,
K,88,0.0015,0.2795,0,
K,89,0.136,0.2795,0,
K,90,0.146,0.2795,0,
K,91,0.313,0.2795,0,
K,92,0.323,0.2795,0,
K,93,0.4575,0.2795,0,
K,94,0.459,0.2795,0,
K,95,0.,0.281,0,
K,96,0.459,0.281,0,
```

```
SAVE
!*
!* define material properties
!*
!*
!* STAINLESS STEEL (SS304)
!*
MP,DENS,1,7900
MPTEMP,1,300,400,500,600,800,1000
MPDATA,kxx,1,1,15,17,18,20,23,25
MPDATA,c,1,1,477,515,539,557,582,611
!*
!* THERMAL INSULATOR
!*
MP,DENS,2,260
MP,C,2,1046
MPTEMP
MPTEMP,1,673,873,1073,1273
MPDATA,KXX,2,1,0.105,0.151,0.198,0.267 !MAX
VALUES
!*
!*
!*  WOOD (generic softwood)
!*
```

```
K,73,0.2285,0.2285,0,
K,74,0.2305,0.2285,0,
K,75,0.2355,0.2285,0,
K,76,0.399,0.2285,0,
K,77,0.4065,0.2285,0,
K,78,0.459,0.2285,0,
K,79,0.,0.2295,0,
K,80,0.0015,0.2295,0,
K,81,0.136,0.2295,0,
K,82,0.146,0.2295,0,
K,83,0.313,0.2295,0,
K,84,0.323,0.2295,0,
K,85,0.4575,0.2295,0,
K,86,0.459,0.2295,0,
K,87,0.,0.2795,0,
K,88,0.0015,0.2795,0,
K,89,0.136,0.2795,0,
K,90,0.146,0.2795,0,
K,91,0.313,0.2795,0,
K,92,0.323,0.2795,0,
K,93,0.4575,0.2795,0,
K,94,0.459,0.2795,0,
K,95,0.,0.281,0,
K,96,0.459,0.281,0,
SAVE
!*
!* define material properties
!*
!*
!* STAINLESS STEEL (SS304)
!*
MP,DENS,1,7900
MPTEMP,1,300,400,500,600,800,1000
MPDATA,kxx,1,1,15,17,18,20,23,25
MPDATA,c,1,1,477,515,539,557,582,611
!*
!* THERMAL INSULATOR
!*
MP,DENS,2,260
MP,C,2,1046
MPTEMP
MPTEMP,1,673,873,1073,1273
MPDATA,KXX,2,1,0.105,0.151,0.198,0.267 !MAX
VALUES
!*
!*
!*  WOOD (generic softwood)
!*
```

```
UIMP,3,NUXY, , , ,
UIMP,3,ALPX, , , ,
UIMP,3,REFT, , , ,
UIMP,3,MU, , , ,
UIMP,3,DAMP, , , ,
UIMP,3,DENS, , ,500,
UIMP,3,KXX, , ,0.24,
UIMP,3,C, , ,2800,
UIMP,3,ENTH, , , ,
UIMP,3,HF, , , ,
UIMP,3,EMIS, , , ,
UIMP,3,QRATE, , , ,
UIMP,3,VISC, , , ,
UIMP,3,SONC, , , ,
UIMP,3,MURX, , , ,
UIMP,3,MGXX, , , ,
UIMP,3,RSVX, , , ,
UIMP,3,PERX, , , ,
!*
!* define areas
!*
FLST,2,12,3
FITEM,2,1
FITEM,2,12
FITEM,2,11
FITEM,2,10
FITEM,2,9
FITEM,2,8
FITEM,2,7
FITEM,2,6
FITEM,2,5
FITEM,2,4
FITEM,2,3
A,P51X
FLST,2,7,3
FITEM,2,3
FITEM,2,4
FITEM,2,13
FITEM,2,37
FITEM,2,41
FITEM,2,62
FITEM,2,61
A,P51X
FLST,2,5,3
FITEM,2,4
FITEM,2,5
```

FITEM,2,14
FITEM,2,13
A,P51X
FLST,2,4,3
FITEM,2,5
FITEM,2,6
FITEM,2,16
FITEM,2,15
A,P51X
FLST,2,4,3
FITEM,2,6
FITEM,2,7
FITEM,2,17
FITEM,2,16
A,P51X
FLST,2,4,3
FITEM,2,7
FITEM,2,8
FITEM,2,18
FITEM,2,17
A,P51X
FLST,2,4,3
FITEM,2,8

FITEM,2,19
FITEM,2,18
A,P51X
FLST,2,4,3
FITEM,2,9
FITEM,2,10
FITEM,2,20
FITEM,2,19
A,P51X
FLST,2,5,3
FITEM,2,10
FITEM,2,11
FITEM,2,22
FITEM,2,21
FITEM,2,20
A,P51X
FLST,2,7,3
FITEM,2,11
FITEM,2,12
FITEM,2,68
FITEM,2,67
FITEM,2,44
FITEM,2,40

```
A,P51X
FLST,2,5,3
FITEM,2,13
FITEM,2,14
FITEM,2,23
FITEM,2,38
FITEM,2,37
A,P51X
FLST,2,8,3
FITEM,2,23
FITEM,2,24
FITEM,2,29
FITEM,2,49
FITEM,2,64
FITEM,2,63
FITEM,2,42
FITEM,2,38
A,P51X
FLST,2,14,3
FITEM,2,14
FITEM,2,15
FITEM,2,16
FITEM,2,17
FITEM,2,19
FITEM,2,20
FITEM,2,21
FITEM,2,28
FITEM,2,27
FITEM,2,26
FITEM,2,25
FITEM,2,24
FITEM,2,23
A,P51X
FLST,2,8,3
FITEM,2,25
FITEM,2,26
FITEM,2,33
FITEM,2,55
FITEM,2,74
FITEM,2,73
FITEM,2,54
FITEM,2,32
A,P51X
FLST,2,8,3
FITEM,2,27
FITEM,2,28
```

```
FITEM,2,43
FITEM,2,66
FITEM,2,65
FITEM,2,60
FITEM,2,36
A,P51X
FLST,2,5,3
FITEM,2,21
FITEM,2,22
FITEM,2,40
FITEM,2,39
FITEM,2,28
A,P51X
FLST,2,4,3
FITEM,2,37
FITEM,2,38
FITEM,2,42
FITEM,2,41
A,P51X
FLST,2,4,3
FITEM,2,39
FITEM,2,40
FITEM,2,44
A,P51X
FLST,2,4,3
FITEM,2,41
FITEM,2,42
FITEM,2,63
FITEM,2,62
A,P51X
FLST,2,4,3
FITEM,2,43
FITEM,2,44
FITEM,2,67
FITEM,2,66
A,P51X
SAVE
FLST,2,6,3
FITEM,2,61
FITEM,2,62
FITEM,2,63
FITEM,2,64
FITEM,2,70
FITEM,2,69
A,P51X
FLST,2,6,3
```

```
FITEM,2,66
FITEM,2,67
FITEM,2,68
FITEM,2,78
FITEM,2,77
A,P51X
FLST,2,18,3
FITEM,2,69
FITEM,2,70
FITEM,2,71
FITEM,2,72
FITEM,2,73
FITEM,2,74
FITEM,2,75
FITEM,2,76
FITEM,2,77
FITEM,2,78
FITEM,2,86
FITEM,2,85
FITEM,2,84
FITEM,2,83
FITEM,2,82
FITEM,2,81
FITEM,2,79
A,P51X
FLST,2,4,3
FITEM,2,79
FITEM,2,80
FITEM,2,88
FITEM,2,87
A,P51X
FLST,2,4,3
FITEM,2,80
FITEM,2,81
FITEM,2,89
FITEM,2,88
A,P51X
FLST,2,4,3
FITEM,2,81
FITEM,2,82
FITEM,2,90
FITEM,2,89
A,P51X
FLST,2,4,3
FITEM,2,82
FITEM,2,83
```

```
FITEM,2,90
A,P51X
FLST,2,4,3
FITEM,2,83
FITEM,2,84
FITEM,2,92
FITEM,2,91
A,P51X
FLST,2,4,3
FITEM,2,84
FITEM,2,85
FITEM,2,93
FITEM,2,92
A,P51X
FLST,2,4,3
FITEM,2,85
FITEM,2,86
FITEM,2,94
FITEM,2,93
A,P51X
SAVE
FLST,2,10,3
FITEM,2,87
FITEM,2,89
FITEM,2,90
FITEM,2,91
FITEM,2,92
FITEM,2,93
FITEM,2,94
FITEM,2,96
FITEM,2,95
A,P51X
SAVE
!*
!* glue all areas
!*
FLST,2,31,5,ORDE,2
FITEM,2,1
FITEM,2,-31
AGLUE,P51X
!*
/PNUM,KP,0
/PNUM,LINE,0
/PNUM,AREA,1
/PNUM,VOLU,0
/PNUM,NODE,0
```

```
/PNUM,SVAL,0
/NUMBER,0
!*
/PNUM,ELEM,0
/REPLOT
!* APLOT
FLST,5,14,5,ORDE,10
FITEM,5,1
FITEM,5,-2
FITEM,5,6
FITEM,5,10
FITEM,5,12
FITEM,5,-15
FITEM,5,21
FITEM,5,-24
FITEM,5,30
FITEM,5,-31
ASEL,S, , ,P51X
/REPLOT
FLST,5,14,5,ORDE,10
FITEM,5,1
FITEM,5,-2
FITEM,5,6
FITEM,5,10
FITEM,5,12
FITEM,5,-15
FITEM,5,21
FITEM,5,-24
FITEM,5,30
FITEM,5,-31
CM,_Y,AREA
ASEL, , , ,P51X
CM,_Y1,AREA
CMSEL,S,_Y
!*
CMSEL,S,_Y1
AATT,       1, ,   1,       0
CMSEL,S,_Y
CMDELE,_Y
CMDELE,_Y1
!* ALLSEL,ALL
FLST,5,11,5,ORDE,11
FITEM,5,3
FITEM,5,5
FITEM,5,7
FITEM,5,9
```

```
FITEM,5,11
FITEM,5,16
FITEM,5,19
FITEM,5,-20
FITEM,5,25
FITEM,5,27
FITEM,5,29
ASEL,S, , ,P51X
FLST,5,11,5,ORDE,11
FITEM,5,3
FITEM,5,5
FITEM,5,7
FITEM,5,9
FITEM,5,11
FITEM,5,16
FITEM,5,19
FITEM,5,-20
FITEM,5,25
FITEM,5,27
FITEM,5,29
CM,_Y,AREA
ASEL, , , ,P51X
CM,_Y1,AREA
!*
CMSEL,S,_Y1
AATT,       2, ,    1,       0
CMSEL,S,_Y
CMDELE,_Y
CMDELE,_Y1
!* ALLSEL,ALL
FLST,5,6,5,ORDE,6
FITEM,5,4
FITEM,5,8
FITEM,5,17
FITEM,5,-18
FITEM,5,26
FITEM,5,28
ASEL,S, , ,P51X
FLST,5,6,5,ORDE,6
FITEM,5,4
FITEM,5,8
FITEM,5,17
FITEM,5,-18
FITEM,5,26
FITEM,5,28
CM,_Y,AREA
```

```
ASEL, , , ,P51X
CM,_Y1,AREA
CMSEL,S,_Y
!*
CMSEL,S,_Y1
AATT,      3, ,   1,       0
CMSEL,S,_Y
CMDELE,_Y
CMDELE,_Y1
!*
ALLSEL,ALL
SAVE
!*
!* mesh the areas
!*
ALLSEL,ALL
APLOT
SMRT,10
FLST,5,31,5,ORDE,2
FITEM,5,1
FITEM,5,-31
CM,_Y,AREA
ASEL, , , ,P51X
CHKMSH,'AREA'
CMSEL,S,_Y
!*
AMESH,_Y1
!*
CMDELE,_Y
CMDELE,_Y1
CMDELE,_Y2
!*
/PNUM,KP,0
/PNUM,LINE,0
/PNUM,AREA,0
/PNUM,VOLU,0
/PNUM,NODE,0
/PNUM,TABN,0
/PNUM,SVAL,0
/NUMBER,0
!*
/PNUM,MAT,1
/REPLOT
ALLSEL,ALL
!* select nodes on the outer sufaces
NSEL,S,LOC,X,0.,0.0001
```

```
NSEL,A,LOC,Y,0.,0.0001
NSEL,A,LOC,Y,0.2809,0.281
!* define element for outer surface
!*
TYPE,   2
MAT,       1
NPLOT
esurf
!*
!* create space node
N,50000,0.3,0.5,0,,,,
!* select the nodes and elements that
!* make up the radiation surfaces
ESEL,S,TYPE,,2
NSLE,R
NSEL,S,LOC,X,0.,0.0001
NSEL,A,LOC,X,0.4589,0.459
NSEL,A,LOC,Y,0.,0.0001
NSEL,A,LOC,Y,0.2809,0.281
ESLN,R
NSEL,a,node,,50000
FINISH
!* define radiation matrix
EMIS,1,0.8,
STEF,5.67e-08,
GEOM,1,0,
SPACE,50000,
!*
VTYPE,0,20,
MPRINT,0
WRITE,rad
!*
ALLSEL,ALL
FINISH
/PREP7
!*
!*
TYPE,   3
MAT,       1
REAL,
ESYS,       0
SECNUM,
TSHAP,LINE
!*
SE,rad, , ,0.0001,
ESEL,S,TYPE,,2
```

```
SAVE

!* Define effective heat transfer coeficients for

!*  post-fire (vert-20,horiz-up-25, horiz-down-35) MPTEMP

MPTEMP,1,338.71,366.48,394.26,422.04,449.82,477.59,

MPTEMP,7,588.71,755.37,1019.26,

MPDATA,HF,20,1,4.68,5.61,6.18,6.60,6.90,7.13,

MPDATA,HF,20,7,7.64,8.00,8.25,

MPDATA,HF,25,1,5.19,6.34,7.05,7.55,7.92,8.18,

MPDATA,HF,25,7,8.74,9.07,9.17,

MPDATA,HF,35,1,2.34,2.74,2.99,3.17,3.30,3.41,

MPDATA,HF,35,7,3.67,3.89,4.09,

MPLIST

SAVE

FINISH

/SOLU

!* setup convection coefficients for fire case

ALLSEL,ALL

NSEL,S,LOC,X,0.,0.0001

NSEL,A,LOC,X,0.4589,0.459

NSEL,A,LOC,Y,0.,0.0001

NSEL,A,LOC,Y,0.2809,0.281

SF,ALL,CONV,19.8,1073

NSEL,ALL

!*****************************************************************
******

!* Test Heat Generation modelling wood burning

ASEL,S,MAT,,3

ESLA,S

/GO

!*

*DIM,burning,TABLE,5,1,0,TIME

!*

BFE,ALL,HGEN, , %burning%

!*

!*********BFA,ALL,HGEN, %burning%

*SET,BURNING(1,0,1) , 0.0

*SET,BURNING(2,0,1) , 0.1

*SET,BURNING(3,0,1) , 0.2

*SET,BURNING(4,0,1) , 552.2

*SET,BURNING(5,0,1) , 552.3

*SET,BURNING(1,1,1) , 0.0

*SET,BURNING(2,1,1) , 0.0

*SET,BURNING(3,1,1) , 7.63e6

*SET,BURNING(4,1,1) , 7.63e6

*SET,BURNING(5,1,1) , 0.0

ALLSEL,ALL

SAVE
```

```
!**********************************************************************
D,50000,TEMP, 1073
!**********************************************************************
TUNIF,375,                    !REVISED FOR NEW NCT NUMBER (IC OUTER SHELL)
!**********************************************************************
SAVE
!*
!* set up run parameters for fire case
!*
ANTYPE,4
!*
TRNOPT,FULL
LUMPM,0
!*
TIME,1800
AUTOTS,-1
DELTIM,0.1,0.1,600,1
KBC,1
!*
TSRES,ERASE
!*
!*
LSWRITE,2,
!*
!* change boundary conditions for post fire case
!* ALLSEL,ALL
NSEL,S,LOC,X,0.000,0.0001
NSEL,A,LOC,X,0.4589,0.459
SF,ALL,CONV,-20, 311
ALLSEL,ALL
NSEL,S,LOC,Y,0.0,0.0001
SF,ALL,CONV,-35, 311
ALLSEL,ALL
NSEL,S,LOC,Y,0.2809,0.281
SF,ALL,CONV,-25, 311
ALLSEL,ALL
D,50000,TEMP,311
!*
!* apply solar heat flux
!*
ALLSEL,ALL
!* select vertical lines and nodes on the left side
nsel,s,loc,x,0
!FLST,5,4,4,ORDE,4
```

```
!FITEM,5,18
!FITEM,5,76
!FITEM,5,94
!FITEM,5,97
!LSEL,S, , ,P51X
!NSLL,S,1
!FLST,2,97,1,ORDE,9
!FITEM,2,12
!FITEM,2,17
!FITEM,2,56
!FITEM,2,70
!FITEM,2,72
!FITEM,2,447
!FITEM,2,-521
!FITEM,2,2039
!FITEM,2,-2055
/GO
!*
F,all,HEAT,0.69

ALLSEL,ALL
!* select lines and nodes on the right side
nsel,s,loc,x,.459,.460
```

```
!FITEM,5,35
!FITEM,5,77
!FITEM,5,86
!FITEM,5,108
!LSEL,S, , ,P51X
!NSLL,S,1
!FLST,2,97,1,ORDE,9
!FITEM,2,3
!FITEM,2,27
!FITEM,2,57
!FITEM,2,63
!FITEM,2,78
!FITEM,2,795
!FITEM,2,-869
!FITEM,2,2240
!FITEM,2,-2256
!/GO
!*
F,all,HEAT,0.69

!* select nodes on upper surface
ALLSEL,ALL
NSEL,S,LOC,Y,0.2809,0.281
```

```
!FITEM,2,79
!FITEM,2,-80
!FITEM,2,2257
!FITEM,2,-2409
!/GO
!*
F,all,HEAT,2.88
ALLSEL,ALL
!* set up run parameters for post fire
TIME,14400   !was 9000
AUTOTS,-1
DELTIM,0.5,0.1,2000,1
KBC,1
!*
TSRE S,ERASE
!*
TINTP,0.005, , ,-1,0.5,-1
!*
OUTRES,ALL,ALL,
TIME,45000
DELTIM,100,10,2000,1
LSWRITE,3,
SAVE
/SOLU
/STATUS,SOLU
LSSOLVE,2,3,1
FINISH
SAVE
/POST26
!*
!* plot temperature evolution at specified nodes
!*
!*
!* inner wall, top right corner
NSOL,2,58,TEMP, ,inn_wtr
!*
!*
!*  inner wall, bottom mid position
NSOL,3,1185,TEMP, ,inn_wbm
!*
!*
!*  inner wall, top mid position
NSOL,4,1720,TEMP, ,inn_wtm
!*
!*
!*  outer wall, top mid position
```

```
!*
!*
PLVAR,2,3,4,5,,, , , , ,
PRVAR,2,3,4,5,,,
FINISH
!* plot isothermes at certain moments in time
/POST1
SET,LIST,2
SET, , ,1, , , ,17,
/EFACE,1
!*
PLNSOL,TEMP, ,0,
FINISH
/POST1
SET, , ,1, , , ,18,
/EFACE,1
!*
PLNSOL,TEMP, ,0,
SET, , ,1, , , ,20,
/EFACE,1
!*
PLNSOL,TEMP, ,0,
SET, , ,1, , , ,22,
!*
PLNSOL,TEMP, ,0,
SET, , ,1, , , ,30,
/EFACE,1
!*
PLNSOL,TEMP, ,0,
SET, , ,1, , , ,43,
/EFACE,1
!*
PLNSOL,TEMP, ,0,
SET,PREVIOUS
FINISH

!*********************************NEW
allsel
/post1

Tmax=0
TimeMAX=0
nmax=0

nsel,s,loc,x,0.0525,.4065,
nsel,r,loc,y,0.0525,.2285,
```

```
nplot
*GET, ncount, NODE, 0, count
cm,icnodes,node

set,1,1

*do,t,1,46
tmaxn=0
cmsel,s,icnodes

*do,i,1,ncount
nodei=node(0,0,0)
*get,tempi,node,nodei,temp
*if,tempi,gt,tmaxn,then
tmaxn=tempi
nmaxn=nodei
*endif
nsel,u,,,nodei
*enddo
*if,tmaxn,gt,tmax,then
tmax=tmaxn
nmax=nmaxn
*endif
set,next
*enddo

tmax=tmax
nmax=nmax
timemax=timemax

allsel

/show,term
/post1,
! Reverse Video
/rgb,index,100,100,100,0
/rgb,index,80,80,80,13
/rgb,index,60,60,60,14
/rgb,index,0,0,0,15
set,1,17
plnsol,temp
/image,save,fig3-4(1800),wmf
set,2,1
/replot
/image,save,fig3-5(1900),wmf
```

```
/replot

/image,save,fig3-6(3268),wmf

set,last

/replot

/image,save,fig3-7(45000),wmf

!*********************************NEW

! /EXIT,ALL
```

3.6.3. *NCT Transient Analysis*

The transient analysis uses a one dimensional model of the vertical face of the packaging (thinner part of the packaging) as described in the figure below:

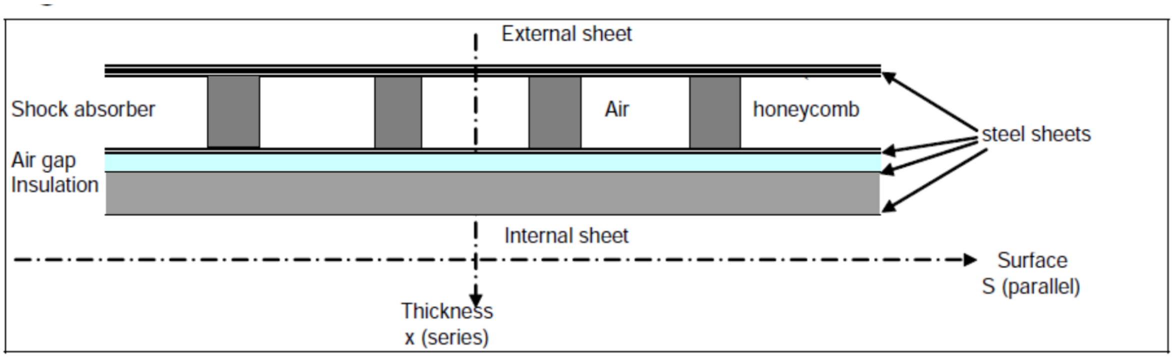

Figure 3-8 Vertical Face Model

The heat flux is set as a sine wave function:

$Q = \pi/2 \times 800 \sin(\omega\,\theta)$ $\quad 0 < (\omega\,\theta) < \pi$

$Q = 0$ $\quad \pi < (\omega\,\theta) < 2\pi$

With: Q = heat energy in g-cal/cm^2

$\omega = 2\pi / 24$ pulsation

θ = time in hour

Note that the peak value of ($\pi/2 \times 800$) complies with 10CFR 71.71(c)(1), conservatively assuming the highest value of 800 g-cal/cm^2 for the insolation.

$$\int_0^{24\,hr} Q\,d\theta = 800 \text{ g-cal}/\text{cm}^2$$

Assuming that at each time step, the external surface of the package achieves steady state conditions, the energy balance between the solar heat load, and the convection and radiation exchanges (see section 3.4.1.1), results time dependant solution for the external surface temperature.

The result is plotted on the Figure 3.6.3-1 (blue curve) and is close to a sine wave function. Indeed, when calculating the energy balance equation, it appears that the convention term represents 65% of the exchange, and the radiation term 35%. As the convection term is linearly proportional to the external temperature, this curve is nearly proportional to the solar heat load.

Assume that the external temperature is a sine function with respect to time as follows (and as plotted on Figure 3.6.3-1):

$Ts = T_{avg} + T^{+} \sin(\omega\,\theta)$

With: $T_{avg} = 420$ K (maximum value of the blue curve)

$T^{+} = (420\text{-}311) = 109$ K

The system is thus modeled as a one dimensional model of conduction, with a sinusoidal wave temperature on the external surface as a boundary condition.

Using equation 4-22 of the "Handbook of Heat Transfer", Reference 3.6.1.7, the heat equation through a layer of material leads to a temperature of:

$$T(x,\theta) = T_{avg} + T^{+} \exp(-L\ x/d) \sin[L(2\ L\ Fo - x/d)]$$

Using the reference's notation, it becomes:

$$T(x,\theta) = T_{avg} + T^{+} \exp[-(\omega/2\alpha)^{1/2}\ x] \sin[\omega\ \theta - (\omega/2\alpha)^{1/2} x]$$

With: $\alpha = K / \rho\ C$ = thermal diffusivity,

K = conductivity if material,

ρ = density of material,

C = specific heat of the material,

x = thickness thru the material.

Through each layer of material "i" in the TN-B1 packaging, the temperature of the external surface is so decreased by a factor η and lagged by a factor φ:

$$\eta_i = \exp[-(\omega/2\alpha_i)^{1/2}\ x_i]$$

$$\varphi_i = (\omega/2\alpha_i)^{1/2} x_i$$

Table 3.6.3-1 summarizes the material properties for each component layer through the thickness of the model.

Equivalent properties of material

The thermal properties (K, ρ, C) of a material equivalent to materials of a system are following the rules:

$$Material\ in\ series\ K = \frac{e_T}{\sum_i \frac{e_i}{K_i}}$$

$$Material\ in\ parallel\ K = \frac{1}{S_T} \sum_i S_i K_i$$

$$Material\ in\ series\ \rho\ C = \frac{\sum_i \rho_i C_i e_i}{e_T}$$

$$Materials\ in\ parallel\ \rho\ C = \frac{\sum_i \rho_i C_i S_i}{S_T}$$

The maximum temperature of the cavity surface of the packaging resulting from solving the one dimensional model occurs at ten hours into the cycle and is equal to 350 K. The maximum temperature on the outer surface of the inner container occurs at 8 hours and is equal to 375K. Temperatures are summarized on Table 3.6.3-2.

Table 3-7 Material properties

Component	Material	Thickness x (m)	Surface S (m)	Conductivity K (W/m-K)	Density r (kg/m3)	Specific heat C (J/kg-K)	Diffusivity a (m2/s)
OC outer sheet	steel	0.004	-	15	7900	477	3.981E-06
Honeycomb [1]	paper	-	0.084 [1]	0.13595	700 [1]	1531 [1]	3.932E-07
	air	-	0.916 [1]	0.0267	1.177	1005	
Shock absorbers	honeycomb	0.108	0.64	0.0359	60	1522	1.737E-06
	air		3.186	0.0267	1.177	1005	
OC inner sheet	steel	0.001	-	15	7900	477	3.981E-06
Air gap	air	0.01	-	0.0267	1.177	1005	2.257E-05
IC outer sheet	steel	0.0015	-	15	7900	477	3.981E-06
IC insulation	Alumina	0.048	-	0.09	250	1046	3.442E-07
IC inner sheet	steel	0.001	-	15	7900	477	3.981E-06

1 The honeycomb is assumed to be a combination of paper and air in a parallel system (see below). The proportion of paper and air is determined by the ratio of the densities:

Honeycomb density = 60 kg/m^3

Paper density = 700 kg/m^3 8.4%

Air density = 1.177 kg/m^3 91.6%

Thermal properties of resin impregnated kraft paper (density, conductivity, specific heat) are conservatively assumed to correspond to that of ordinary paper according to Reference 3.6.1.9.

Table 3-8 NCT Temperatures Through the Package Thickness

Time (hour)	Surface temp sin wave Ts	T thru OC Outer	T thru Honeycomb and	T thru OC Inner	T thru Air Gap	T thru IC Inner Shell	T thru Alumina Slilicate
0	311	311	311	311	311	311	311
0.5	325	324	311	311	311	311	311
1	339	338	311	311	311	311	311
1.5	353	351	311	311	311	311	311
2	366	364	312	312	311	311	311
2.5	377	376	321	320	320	319	311
3	388	386	329	329	328	327	311
3.5	397	396	337	337	336	335	311
4	405	404	345	345	343	343	312
4.5	412	410	352	352	350	350	317
5	416	415	358	358	357	356	322
5.5	419	418	364	364	362	362	327
6	420	419	368	368	367	367	332
6.5	419	418	372	372	371	370	336
7	416	415	375	375	373	373	340
7.5	412	411	376	376	375	375	343
8	405	405	377	376	376	**375**	346
8.5	397	397	376	376	375	375	348
9	388	388	374	374	373	373	349
9.5	377	378	371	371	371	371	**350**
10	366	366	367	367	367	367	350
10.5	353	353	362	362	362	362	350
11	339	340	357	357	357	357	349
11.5	325	326	350	350	350	350	347
12	311	312	343	343	343	343	344
12.5	311	311	335	335	336	336	342
13	311	311	327	327	328	328	338
13.5	311	311	318	319	319	320	334
14	311	311	311	311	311	311	330
14.5	311	311	311	311	311	311	325
15	311	311	311	311	311	311	320
15.5	311	311	311	311	311	311	315
16	311	311	311	311	311	311	311
16.5	311	311	311	311	311	311	311

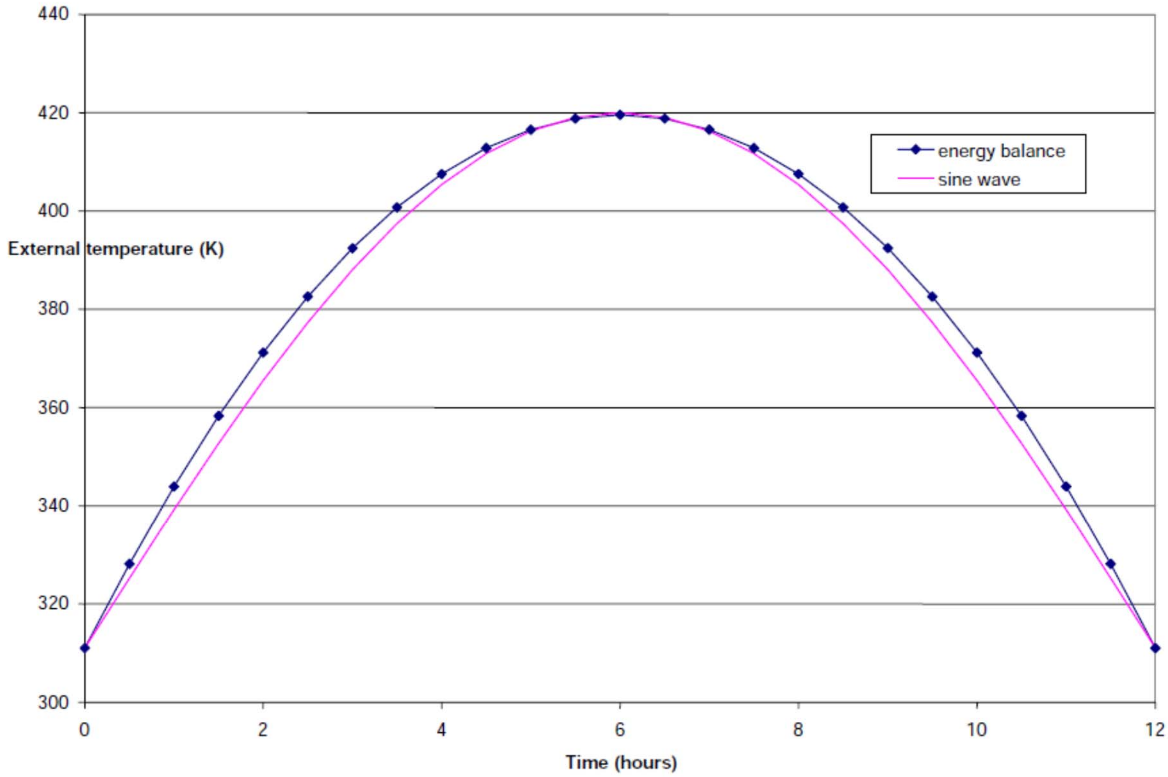

Figure 3-9 Comparison Between Energy Equation Solution with a Sine Wave Equation

4. CONTAINMENT

4.1. DESCRIPTION OF THE CONTAINMENT SYSTEM

4.1.1. *Containment Boundary*

TN-B1 container is limited to use for transporting low enriched uranium, nuclear reactor fuel assemblies and rods. The radioactive material is bound in sintered ceramic pellets having very limited solubility and has minimal propensity to suspend in air. The pellets are sintered at temperatures greater than 1,600°C. These pellets are further sealed into zirconium alloy cladding to form the fuel rod portion of each assembly. The containment boundary for the TN-B1 package is the fuel rod. The components of the fuel rod which constitutes the containment boundary are the zirconium cladding and end caps. The fuel cladding is sealed on each end by end caps which are welded to the cladding. Figure 1-6 Example Fuel Rod (Primary Containment), shows the containment system. The containment system includes the ceramic sintered pellet, clad in sealed zirconium fuel rods which are contained in a stainless steel box which is contained in another stainless steel box.

The fuel rods are manufactured under a Quality Assurance program meeting the requirements of 10 CFR 71 Subpart H. Welds of the fuel rod end caps to the cladding are conducted under a qualified process and verified for integrity using approved inspection procedures performed by qualified inspection personnel. There are no penetrations in the fuel cladding when shipped. The fuel cladding, after loading with the pellets, is pressurized with helium and the end plugs are welded on to close the rod. These welds are designed to withstand the rigorous operating environment of a nuclear reactor.

For 11x11 fuel rods, the closure weld process qualification includes the following: (1) transverse metallographic samples of the welds, upon examination of the samples a single discontinuity >0.005 inch is not permitted along the solid state bond line in the plane of polish and the sum of all discontinuities along the solid state bond line shall be ≤0.010 inch along the solid state bond line in the plane of the polish; and (2) meet the in-process inspections listed below. The critical parameters for welding; current, cladding tube extension, and electrode force are established during the weld qualification process.

For 11x11 fuel rods, the following in-process inspections are performed: (1) visual inspection of each completed weld to verify that the surface is free of folds, holes, cracks, porosity, and inclusions at a minimum of 1X magnification; (2) burst testing, per Framatome's proprietary burst testing procedure of representative welds on cladding samples shall be conducted at room temperature during initial weld parameter qualification and on in process samples during production. The burst strength shall be ≥ 17,400 psi (≥ 1,200 bar) and failure shall not occur along the solid state bond line at the original interface between the cladding and end cap. The failure location will be determined by visual inspection of the burst tested sample. Visual standards may be used to determine the failure location. Rod inspection requirements specified in the Product Specification (Reference 1) applicable to the containment boundary include 100% dimensional inspections to the applicable drawing (example, Reference 2), 100% helium leak check and initial fill pressure.

Burst test frequency for each welder will be as follows:

- Five consecutive at the beginning of the contract
- One after each repair or change of the welding machine that may impact the process
- One after interruption for more than twenty-four (24) hours
- One for every approximately 350 rods during the contract (367 rods maximum between tests).
- One at the end of the contract.

The critical parameters for welding; current, cladding tube extension, and electrode force are monitored and recorded for each weld.

Each completed fuel rod (of any design) is helium leak tested after fabrication to demonstrate that it is leak tight (<1x10^{-7} atm-cc/s).

4.1.2. *Special Requirements for Plutonium*

This section is not applicable since the package is not being used for plutonium shipments.

4.2. GENERAL CONSIDERATIONS

4.2.1. *Type A Fissile Packages*

The Type A fissile package is constructed, and prepared for shipment so that there is no loss or dispersal of the radioactive contents and no significant increase in external surface radiation levels and no substantial reduction in the effectiveness of the packaging during normal conditions of transport. The fissile material is bound as a ceramic pellet and contained in a zirconium fuel rod. These rods are leak tested prior to shipment to assure their integrity. Chapter 6.0 demonstrates that the package remains subcritical under normal and hypothetical accident conditions.

4.2.2. *Type B Packages*

The Type B fissile package is constructed, and prepared for shipment so that there is no loss or dispersal of the radioactive contents and no significant increase in external surface radiation levels and no substantial reduction in the effectiveness of the packaging during normal conditions of transport.

The package satisfies the quantified release rate of 10 CFR 71.51 by having a release rate less than 10^{-6} A_2/hr as demonstrated below.

A_2 = 0.18 Ci (maximum from Table 1-5), therefore$10^{-6}A_2 = 1.8 \times 10^{-7}$ Ci/hr

The mass density of UO_2 in an aerosol from NUREG/CR-6487, page 17 is 9×10^{-6} g/cm^3. Specific Activity of fuel material is 4.7×10^{-5} Ci/g UO_2 (26.5 Ci/562kg UO_2).

Leak rate at 1×10^{-7} atm-cm^3/s (3.6×10^{-4} cm^3/hr) is equal to 1×10^{-6} atm-cm^3/s (3.6×10^{-3} cm^3/h) when pressurized to 10 atm. Assuming that the pressure is further increased due to temperature the leak rate is assumed to increase by an additional factor of 10 so that it is equal to 3.6×10^{-2} cm^3/h.

$$\text{Release rate} = 3.6 \times 10^{-2}\ \text{cm}^3/\text{hr} \times 4.7 \times 10^{-5}\ \text{Ci/g } UO_2 \times 9 \times 10^{-6}\ \text{g/cm}^3$$

$$= 1.5 \times 10^{-11}\ \text{Ci/h}$$

Much less than the 1.7×10^{-7} Ci/hr limit.

4.3. CONTAINMENT UNDER NORMAL CONDITIONS OF TRANSPORT (TYPE B PACKAGES)

The nature of the contained radioactive material and the structural integrity of the fuel rod cladding including the closure welds are such that there will be no release of radioactivity under normal conditions of transport. The welded close containment boundary is not affected by any of the normal conditions of transport as demonstrated in the previous chapters. The pressurization that could be seen by the containment boundary is far below the normal conditions the fuel experiences while in service.

4.4. CONTAINMENT UNDER HYPOTHETICAL ACCIDENT CONDITIONS (TYPE B PACKAGES)

The sintered pellet form of the radioactive material and the integrity of the fuel rod cladding are such that there will be no substantial release of radioactivity under the Hypothetical Accident Conditions. Before and after the accident condition testing the rods were helium leak tested demonstrating leak tightness. Similar fuel rods have been tested at temperatures and resulting pressures that will be seen by fuel shipped in the TN-B1.

10 CFR 71.51 requires that no escape of other radioactive material exceeding a total amount A_2 in 1 week, and no external radiation dose rate exceeding 10 mSv/h (1 rem/h) at 1 m (40 in) from the external surface of the package. The following qualitative assessment demonstrates that the performance requirement of 10 CFR 71.51(a)(2) will be satisfied.

Table 1-5 shows the calculated A_2 for the mixture of the maximum radionuclide content in the package is 0.18 Ci. The total radioactivity in the package using the maximum isotopic values is 26.5 Ci from Table 1-4. The mass of UO_2 equivalent to an activity of 26.5 Ci is 562 kg (281 kg UO_2/assembly x 2 assemblies) which yields a mass to activity ratio of 21.2 kg UO_2/Ci. The conservatively applied mass equivalent A_2 is therefore 3.8 kg UO_2.

Following the drop test, fuel rods were leak tested and shown to have a very low leak rate of He at a rate of 5.5 x 10^{-6} cm^3/s. Over one week this is equal to 3.3 cm^3 (5.5E-6 cm^3/s x 6.05E5 s/wk = 3.3 cm^3/wk). The tested assembly had 91 fuel rods while the 11x11 has 112 fuel rods. As a result a conservative assumption was made that the amount released would increase proportionately to the number of fuel rods. This was determined to be 4.1 cm^3/wk (3.3 cm^3/wk x 112 rods/91 rods). Conservatively assuming that the density of the radioactive material is 10g/cm^3 and using the A_2 mass above of 3.8 kg of UO_2, the UO_2 would have a volume of 380 cm^3/wk. This is much greater than the volume leaked. This calculation is extremely conservative since the UO_2 would predominantly stay in a ceramic form and not be available for dispersion.

Test fuel rods as described in Section 2.0 have been baked at 800°C for over 30 minutes and did not leak.

Additionally, the large mass, 3.8 kg, of material required to exceed the A_2 would require a catastrophic failure of the rod, significant leak of the inner and outer container.

Dose rates are less than the 10 mSv/hr under any condition because of the low specific activity and low abundance of gamma emitters in the fuel.

Based on this evaluation, it is demonstrated that the package meets the containment requirements of 10 CFR 71.51

4.5. LEAKAGE RATE TESTS FOR TYPE B PACKAGES

During manufacturing each fuel rod is He leak tested to demonstrate that it is leak tight (<1x 10^{-7}atm-cc/s). There are no leak rate requirements for the inner and outer packaging.

4.6. APPENDIX

None

4.7. REFERENCES

1. FS1-0019890 Revision 1.0, “Upset Shape Welded BWR Fuel Rod Assemblies” AREVA, February 2015.
2. FS1-0011596 Revision 2.0, “3-Segment Fuel Rod Assembly” AREVA, March 2014.

5. SHIELDING EVALUATION

The contents of the TN-B1 require no shielding since unirradiated fuel gives off no significant radiation either gamma or neutron. Hence the TN-B1 provides no shielding. The minimal shielding provided by the stainless steel sheet is not required. The dose rate limits established by 10 CFR 71.47(a) for normal conditions of transport (NCT) are verified prior to shipping by direct measurement.

Since there is no shielding provided by the package, there is no shielding change during the Hypothetical Accident Conditions (HAC). Therefore, the higher dose rate allowed by 10 CFR 71.51(a)(2) will be met.

Prior to transport, the TN-B1 package shall be surveyed for radiation dose rate to demonstrate compliance with 10 CFR 71.47. Under conditions normally incident to transportation (non-exclusive use), the radiation level does not exceed 2 mSv/hour (200 mrem/hour) at any point on the external surface of the package and less than 0.1 mSv/hour (10 mrem/hour) at a distance of 1 meter from the surface of the package. The transport index, as defined in 10 CFR 71.4, will be determined by measuring the dose rate a distance of one meter from the package surface per the requirements of 49 CFR 173.441.

A conservative dose estimate of the Table 1-4 contents results in an external surface exposure rate of 0.1 mSv/hr (10 mrem/hr). As expected, this is greater than, but consistent with, actual experience measuring the ≤ 5.0 wt.% ^{235}U (Table 1-3) contents and remains significantly below the non-exclusive use transport limits identified above.

6. CRITICALITY EVALUATION

Through multiple updates to the allowable contents, the criticality evaluations are separated into multiple sections. Sections 6.1 and 6.2 include updated information for all fuel assembly configurations. Sections 6.3 through 6.11 address the ≤ 5.0 wt.% ^{235}U enrichment contents for the 8x8, 9x9, FANP 10x10, and GNF 10x10 arrays. A second evaluation is attached in Section 6.12 (Appendix B) to cover the ≤ 5.0 wt.% ^{235}U enrichment contents limited to the ATRIUM 11 (11x11) array design. The third evaluation attached in Section 6.13 (Appendix C) covers the ≤ 8.0 wt.% ^{235}U enrichment contents limited to the ATRIUM 11 (11x11) array design and individual 11x11 (BWR) or 17x17 Type 3 (PWR) fuel rods.

6.1. DESCRIPTION OF CRITICALITY DESIGN

A criticality safety analysis is performed to demonstrate the TN-B1 shipping container safety. The TN-B1 meets applicable IAEA and 10 CFR 71 requirements for a Type B fissile material-shipping container, transporting heterogeneous UO_2 enriched to a maximum of 8.0 wt. percent U-235 or a maximum of 5.0 wt. percent U-235 depending on fuel assembly type; see Tables 6-1 and 6-2.

The TN-B1 shipping container design features a stainless steel inner container positioned inside an outer stainless steel container by four evenly spaced stainless steel fixture assemblies. The fixture assemblies cradle the inner container and prevent horizontal or vertical movement. The inner container has two fuel assembly transport compartments, aligned side-by-side and separated by a stainless steel divider. Each transport compartment is lined with polyethylene foam and/or rubber in which the fuel assemblies rest. Additional container details are described in Section 1.2, Package Description. Material manufacturing tolerances are presented in the general arrangement drawings in Section 1.4.1.

The uranium transported in the TN-B1 container is UO2 pellets enclosed in zirconium alloy cladding. The fuel rods are arranged in 8x8, 9x9, 10x10, or 11x11 square lattice arrays at fixed center-to-center spacing. Fuel rods may also be transported loose with no fixed center-to-center spacing, bundled together in a close packed configuration, or inside a 5-inch diameter stainless steel pipe or protective case.

Water exclusion from the inner container is not required for this package design. The inner container is analyzed in both undamaged and damaged package arrays under optimal moderation conditions and is demonstrated to be safe under Normal Conditions of Transport (NCT) and Hypothetical Accident Condition (HAC) testing.

The criticality analysis for the TN-B1 container is performed for UO2 or Uranium-Carbide fuel pellets contained in zirconium alloy or stainless steel clad cylindrical rods. The cylindrical fuel rods are arranged in 8x8, 9x9, 10x10, or 11x11 square lattice arrays at fixed center-to-center spacing. Sensitivity analyses are performed by varying fuel parameters (rod pitch, clad ID, clad OD, pellet OD, fuel orientation, polyethylene spacer quantity, and moderator density) to obtain the most reactive configuration. The most reactive configuration is modeled for each authorized payload to demonstrate safety and to validate the fuel parameter ranges specified as loading criteria.

Table 6-1 TN-B1 Fuel Assembly Loading Criteria summarizes the fuel loading criteria for the TN-B1 shipping container.

Table 6-1 TN-B1 Fuel Assembly Loading Criteria

Parameter	Units	Type	Type	Type	Type
Fuel Assembly Type	Rods	8x8	9x9	FANP 10x10	GNF 10x10
UO_2 Density[a2]	g/cm^3	≤ 10.74	≤ 10.74	≤ 10.74	≤ 10.74
Number of water rods	#	0, 2x2	0, 2-2x2 off-center diagonal, 3x3	0, 2-2x2 off-center diagonal, 3x3	0, 2-2x2 off-center diagonal, 3x3
Number of fuel rods	#	60 - 64	72 - 81	91 - 100	91 - 100
Fuel Rod OD	cm	≥ 1.176	≥ 1.093	≥ 1.000	≥ 1.010
Fuel Pellet OD	cm	≤ 1.05	≤ 0.96	≤ 0.895	≤ 0.895
Cladding Type		Zirconium Alloy	Zirconium Alloy	Zirconium Alloy	Zirconium Alloy
Cladding ID	cm	≤ 1.10	≤ 1.02	≤ 0.933	≤ 0.934
Cladding Thickness	cm	≥ 0.038	≥ 0.036	≥ 0.033	≥ 0.038
Active fuel length	cm	≤ 381	≤ 381	≤ 385	≤ 385
Fuel Rod Pitch	cm	≤ 1.692	≤ 1.51	≤ 1.350	≤ 1.350
U-235 Pellet Enrichment	wt%	≤ 5.0	≤ 5.0	≤ 5.0	≤ 5.0
Maximum Lattice Average Enrichment	wt%	≤ 5.0	≤ 5.0	≤ 5.0	≤ 5.0
Channel Thickness[a1]	cm	0.17 – 0.3048	0.17 – 0.3048	0.17 – 0.3048	0.17 – 0.3048
Part Length Fuel Rods (1/3 through 2/3 normal length)	Max #	None	12	14	14

a1. Transport with or without channels is acceptable
a2. Density based on a pellet modeled as a right cylinder.

Table 6-1 TN-B1 Fuel Assembly Loading Criteria (continued)

Parameter	Units	Value
Fuel Assembly Type		11x11
UO_2 Density[b3]	g/cm^3	≤ 10.763
Number of water rods	#	3x3 center
Number of fuel rods	#	112
Fuel Rod OD	cm	≥ 0.930
Fuel Pellet OD	cm	≤ 0.820
Cladding Type		Zirconium Alloy
Cladding ID	cm	≤ 0.840
Cladding Thickness	cm	≥ 0.045
Fuel Rod Pitch[b1]	cm	≤ 1.195
U-235 Pellet Enrichment	wt%	≤ 8.0
Maximum Lattice Average Enrichment	wt%	≤ 8.0
Fuel Channel Side Thickness[b2]	cm	≤ 0.320
Full Length Fuel Rods Quantity Active length	 # cm	 92 ≤ 385
Short Part Length Fuel Rods Quantity Active length	 # cm	 12 ≤ 155.1
Long Part Length Fuel Rods Quantity Active length	 # cm	 8 ≤ 236.8

b1. Equivalent nominal pitch per Section 6.12.3.1.1.
b2. Transport with or without channels is acceptable.
b3. Density based on a pellet modeled as a right cylinder.

Table 6-1 TN-B1 Fuel Assembly Loading Criteria (continued)

Parameter	Units	Type	Type	Type	Type
Fuel Assembly Type	Rods	8x8	9x9	FANP 10x10	GNF 10x10
Gadolinia Requirements Lattice Average Enrichment[c1]					
≤ 5.0 wt % U-235	#	7 @ 2 wt %	10 @ 2 wt %	12 @ 2 wt %	12 @ 2 wt %
≤ 4.7 wt % U-235	@ wt% Gd_2O_3	6 @ 2 wt %	8 @ 2 wt %	12 @ 2 wt %	12 @ 2 wt %
≤ 4.6 wt % U-235		6 @ 2 wt %	8 @ 2 wt %	10 @ 2 wt %	10 @ 2 wt %
≤ 4.3 wt % U-235		6 @ 2 wt %	8 @ 2 wt %	9 @ 2 wt %	9 @ 2 wt %
≤ 4.2 wt % U-235		6 @ 2 wt %	6 @ 2 wt %	8 @ 2 wt %	8 @ 2 wt %
≤ 4.1 wt % U-235		4 @ 2 wt %	6 @ 2 wt %	8 @ 2 wt %	8 @ 2 wt %
≤ 3.9 wt % U-235		4 @ 2 wt %	6 @ 2 wt %	6 @ 2 wt %	6 @ 2 wt %
≤ 3.8 wt % U-235		4 @ 2 wt %	4 @ 2 wt %	6 @ 2 wt %	6 @ 2 wt %
≤ 3.7 wt % U-235		2 @ 2 wt %	4 @ 2 wt %	6 @ 2 wt %	6 @ 2 wt %
≤ 3.6 wt % U-235		2 @ 2 wt %	4 @ 2 wt %	4 @ 2 wt %	4 @ 2 wt %
≤ 3.5 wt % U-235		2 @ 2 wt %	2 @ 2 wt %	4 @ 2 wt %	4 @ 2 wt %
≤ 3.3 wt % U-235		2 @ 2 wt %	2 @ 2 wt %	2 @ 2 wt %	2 @ 2 wt %
≤ 3.1 wt % U-235		None	2 @ 2 wt %	2 @ 2 wt %	2 @ 2 wt %
≤ 3.0 wt % U-235		None	None	2 @ 2 wt %	2 @ 2 wt %
≤ 2.9 wt % U-235		None	None	None	None
Polyethylene Equivalent Mass (Maximum per Assembly)[c2]	kg	11	11	10.2	10.2

c1. Required gadolinia rods must be distributed symmetrically about the major diagonal
c2. Polyethylene equivalent mass (refer to 6.3.2.2)

Table 6-1 TN-B1 Fuel Assembly Loading Criteria (continued)

Parameter	Units	Type
Fuel Assembly Type	Rods	11x11
Gadolinia Requirements Lattice Average Enrichment[d1]		
≤ 8.0 wt % U-235	#	21 @ 4 wt %
≤ 7.5 wt % U-235	@ wt%	19 @ 4 wt %
≤ 7.0 wt % U-235	Gd_2O_3	17 @ 4 wt %
≤ 6.5 wt % U-235		15 @ 4 wt %
≤ 6.1 wt % U-235		13 @ 4 wt %
≤ 5.8 wt % U-235		13 @ 2 wt %
≤ 5.0 wt % U-235		13 @ 2 wt %
≤ 4.8 wt % U-235		12 @ 2 wt %
≤ 4.6 wt % U-235		11 @ 2 wt %
≤ 4.4 wt % U-235		10 @ 2 wt %
≤ 4.2 wt % U-235		9 @ 2 wt %
≤ 4.1 wt % U-235		8 @ 2 wt %
≤ 3.9 wt % U-235		7 @ 2 wt %
≤ 3.8 wt % U-235		6 @ 2 wt %
≤ 3.6 wt % U-235		5 @ 2 wt %
≤ 3.5 wt % U-235		4 @ 2 wt %
≤ 3.3 wt % U-235		3 @ 2 wt %
≤ 3.2 wt % U-235		2 @ 2 wt %
≤ 2.9 wt % U-235		None
Polyethylene Equivalent Mass (Maximum per Assembly)[d2]	kg	10.2

d1. Required gadolinia-urania rods shall be distributed symmetrically about the major diagonal and shall not be placed on the periphery.

d2. Polyethylene equivalent mass (refer to 6.3.2.2)

Cylindrical fuel rods containing UO_2, enriched up to 8.0 wt. percent U-235, are analyzed within the TN-B1 inner container in a 5-inch stainless steel pipe, loose, in a protective case, or bundled together. The fuel rod loading criteria, determined from the criticality evaluation for the TN-B1 shipping container, are shown in *Table 6-2 TN-B1 Fuel Rod Loading Criteria*.

Table 6-2 TN-B1 Fuel Rod Loading Criteria

Parameter	Units	Type							
Fuel Assembly Type		8x8 (UO_2)	9x9 (UO_2)	10x10 (UO_2)	11x11 (UO_2)	CANDU-14 (UC)	CANDU-25 (UC)	Generic PWR (UO_2)	PWR 17x17 Type 3 (UO_2)
UO_2 or UC Fuel Density[a]	g/cm^3	≤10.74	≤10.74	≤10.74	≤10.763	≤13.36	≤13.36	≤10.74	≤10.763
Fuel rod OD	cm	≥1.10	≥1.02	≥1.00	≥0.930	≥1.340	≥0.996	≥1.118	≥0.9449
Fuel Pellet OD	cm	≤1.05	≤0.96	≤0.90	≤0.820	≤1.254	≤0.950	≤0.98	≤0.8265
Cladding Type		Zirc. Alloy	Zirc. Alloy	Zirc. Alloy	Zirc. Alloy	Zirc. Alloy or SS	Zirc. Alloy or SS	Zirc. Alloy or SS	Zirc. Alloy
Cladding ID	cm	≤1.10	≤1.02	≤1.00	≤0.930	≤1.267	≤0.951	≤1.004	≤0.8407
Cladding Thickness	cm	≥0.00	≥0.00	≥0.00	≥0.00	≥0.00	≥0.00	≥0.00	≥0.00
Active fuel Length	cm	≤381	≤381	≤385	≤385	≤47.752	≤40.013	≤450	≤381
Maximum U-235 Pellet Enrichment	wt.%	≤5.0	≤5.0	≤5.0	≤8.0	≤5.0	≤5.0	≤5.0	≤8.0
Maximum Average fuel rod Enrichment	wt.%	≤5.0	≤5.0	≤5.0	≤8.0	≤5.0	≤5.0	≤5.0	≤8.0
Loose Rod Configuration									
Freely Loose or Strapped Together	#	≤25	≤25	≤25	≤25	N/A	N/A	N/A	≤25
Packed in 5” SS Pipe or Protective Case	#	≤22	≤26	≤30	≤30	≤74	≤130	≤105	≤30

a. Density based on a pellet modeled as a right cylinder.

6.1.1. *Design Features*

6.1.1.1. Packaging

A general discussion of the TN-B1 container design is provided in Section 1.2, Package Description. A detailed set of licensing drawings for the TN-B1 container is provided in Appendix 1.4.1 TN-B1 General Arrangement Drawings. Components important to criticality safety are described below.

The TN-B1 is comprised of two primary components: 1) an inner stainless steel container, and 2) an outer stainless steel container.

The inner stainless steel container is 468.6 cm (184.49 in) in length, 45.9 cm (18.07 in) in width, and 28.6 cm (11.26 in) in height, and provides containment for the uranium inside the cylindrical zirconium alloy tubes. The fuel rods are located inside one of two compartments within the inner container. The compartments are fabricated from 18-gauge (0.122 cm thick) stainless steel, 456.7 cm (179.8 in) in length, 17.6 cm (6.93in) in width and height. Each compartment is lined with 1.8 cm (0.71 in) thick polyethylene foam and separated from each other by the compartment walls. A 5 cm (1.97 in) thick Alumina Silicate fiber surrounds the compartments to provide thermal insulation, and a 16-gauge (0.15 cm thick) stainless steel sheet surrounds the insulator. The inner container lid consists of an Alumina Silicate layer encased in a 16-gauge (0.15 cm thick) stainless steel sheet. The lid width and length are consistent with the inner container and the overall height is 5.25 cm (2.07 in).

The nominal density of the polyethylene foam is 4 pounds per cubic feet (pcf). Optionally, when transporting FANP 10x10 and 11x11 fuel assemblies, strips of 9 pcf foam may be used under the grid spacers to provide additional support to the fuel assemblies.

The outer container is 506.8 cm (199.53 in) in length, 72.0 cm (28.35 in) in width, and 64.2 cm (25.28 in) in height (with the skids attached the height is 74.2 cm (29.21 in)). The inner container is held rigidly within the outer stainless steel container by four evenly spaced stainless steel fixture assemblies. Shock absorbers, fabricated from a phenol impregnated cardboard material, are placed at six locations above and below the inner container, and twelve locations on either side of the inner container. The wall for the outer container is fabricated from 14 gauge (0.2 cm thick) stainless steel.

6.1.2. *Summary Table of Criticality Evaluation*

Table 6-3 Criticality Evaluation Summary, lists the bounding cases evaluated for a given set of conditions. The cases include: fuel assembly transport single package normal and Hypothetical Accident Conditions (HAC), fuel assembly transport package array normal conditions of transport, fuel assembly transport package array HAC, fuel rod transport single package normal and hypothetical accident conditions, fuel rod transport package array normal conditions of transport, and fuel rod transport package array HAC.

The criticality analysis for 8x8, 9x9, and 10x10 fuel assemblies (and the corresponding rods) is performed using the KENO V.a module of SCALE 4.4a. The SCALE 4.4a analysis comprises the main body of Chapter 6, as documented in Sections 6.3 through 6.11. The benchmarking analysis for the SCALE 4.4a analysis is documented in Section 6.10, Benchmark Evaluations. The USL for the SCALE 4.4a evaluation is 0.94254.

The criticality analysis for the 11x11 fuel assembly (and the corresponding 11x11 fuel rods) is performed using the KENO V.a module of SCALE 6.1.3. The 11x11 fuel assembly criticality analysis is documented in Appendix B (Section 6.12). The benchmarking analysis for the SCALE 6.1.3 analysis is documented in Section 6.12.9, Benchmark Evaluation for SCALE 6.1.3. A USL of 0.94094 is justified for the 11x11 fuel assembly analysis, and a USL of 0.94047 is justified for the 11x11 fuel rod analysis.

The benchmark USL results for SCALE 4.4a and SCALE 6.1.3 are quite similar, indicating that both programs are acceptable for TN-B1 criticality analysis.

Table 6-3 Criticality Evaluation Summary

Bounding Results for 8x8, 9x9, and 10x10 Fuel (SCALE 4.4a)					
Case	**Bounding Fuel Type**	k_{eff}	σ	$k_{eff} + 2\sigma$	**USL**
Fuel Assembly Single Package Normal	GNF 10x10 with worst-case fuel parameters, 12, 2.0 wt % Gd_2O_3 fuel rods, and 12 part-length fuel rods	0.6673	0.0008	0.6689	0.94254
Fuel Assembly Single Package HAC	GNF 10x10 with worst-case fuel parameters, 12, 2.0 wt % Gd_2O_3 fuel rods, and 12 part-length fuel rods	0.6931	0.0010	0.6951	0.94254
Fuel Assembly Package Array Normal	GNF 10x10 with worst-case fuel parameters, 12, 2.0 wt % Gd_2O_3 fuel rods, and 12 part-length fuel rods	0.8519	0.0008	0.8535	0.94254
Fuel Assembly Package Array HAC	GNF 10x10 with worst-case fuel parameters, 12, 2.0 wt % Gd_2O_3 fuel rods, and 12 part-length fuel rods	0.9378	0.0009	0.9396	0.94254
Fuel Rod Single Package Normal	25 GNF 8x8 fuel rods per container with worst-case fuel parameters	0.6365	0.0008	0.6381	0.94254
Fuel Rod Single Package HAC	25 GNF 8x8 fuel rods per container with worst-case fuel parameters	0.6532	0.0008	0.6548	0.94254
Fuel Rod Package Array Normal	25 GNF 8x8 fuel rods per container with worst-case fuel parameters	0.6365	0.0008	0.6381	0.94254
Fuel Rod Package Array HAC	25 GNF 8x8 fuel rods per container with worst-case fuel parameters	0.8731	0.0007	0.8745	0.94254

Table 6-3 Criticality Evaluation Summary (continued)

Bounding Results for 11x11 Fuel (SCALE 6.1.3)					
Case	**Bounding Fuel Type**	**k_{eff}**	**σ**	**k_{eff} + 2σ**	**USL**
Fuel Assembly Single Package NCT	11x11 with worst-case fuel parameters, 13-2.0 wt% Gd_2O_3 fuel rods	0.64510	0.00046	0.65302	0.94094
Fuel Assembly Single Package HAC	11x11 with worst-case fuel parameters, 13/13/3-2.0 wt% Gd_2O_3 fuel rods [a]	0.79328	0.00047	0.80122	0.94094
Fuel Assembly Package Array NCT	11x11 with worst-case fuel parameters, 13/13/3-2.0 wt% Gd_2O_3 fuel rods [a]	0.92829	0.00044	0.93417	0.94094
Fuel Assembly Package Array HAC	11x11 with worst-case fuel parameters, 13-2.0 wt% Gd_2O_3 fuel rods	0.93155	0.00032	0.93819	0.94094
Fuel Rod Single Package NCT	30 fuel rods in stainless steel pipe (2 per container) with worst-case fuel parameters [b]	0.59145	0.00045	0.59735	0.94047
Fuel Rod Single Package HAC	30 fuel rods in stainless steel pipe (2 per container) with worst-case fuel parameters [b]	0.66316	0.00042	0.67000	0.94047
Fuel Rod Package Array NCT	30 fuel rods in stainless steel pipe (2 per container) with worst-case fuel parameters [b]	0.80006	0.00046	0.80598	0.94047
Fuel Rod Package Array HAC	30 fuel rods in stainless steel pipe (2 per container) with worst-case fuel parameters[,b]	0.81947	0.00044	0.82635	0.94047

a. This configuration contains 13-2.0 wt% Gd_2O_3 fuel rods in the bottom and middle axial regions and 3-2.0 wt% Gd_2O_3 fuel rods in the top axial region.
b. This configuration bounds the 25 loose fuel rod configuration.

Table 6-3 Criticality Evaluation Summary (continued)

Fuel Load	Normal Conditions of Transport			Hypothetical Accident Conditions		
	Single	Array		Single	Array	
	k_{eff}+2σ*	No. Packages	k_{eff}+2σ*	k_{eff}+2σ*	No. Packages	k_{eff}+2σ*
ATRIUM 11 assemblies enrichment (# UO_2+Gd_2O_3 rods, wt% Gd_2O_3)						
≤ 8.0 (13, 2.0)**	0.7514	1	--	0.8513	1	--
≤ 8.0 wt% ^{235}U (21, 4.0)		81	0.9252		32	--
≤ 8.0 (19, 4.0)		81	--		32	0.9255
≤ 7.6 (17, 4.0)		81	--		32	0.9307
≤ 7.5 (19, 4.0)		81	0.9292		32	--
≤ 7.0 (17, 4.0)		81	0.9299		32	--
≤ 7.0 (15, 4.0)		81	--		32	0.9289
≤ 6.6 (13, 4.0)		81	--		32	0.9304
≤ 6.7 (15, 2.0)		81	--		32	0.9301
≤ 6.5 (15, 4.0)		81	0.9308		32	--
≤ 6.3 (13, 2.0)		81	--		32	0.9300
≤ 6.1 (13, 4.0)		81	0.9311		32	--
≤ 5.8 (13, 2.0)		81	0.9295		32	--
ATRIUM 11 rods, ≤ 8.0 wt% ^{235}U						
25 loose rods	0.6647	256	0.8904	0.6832	100	0.8652
30 rods in 5-inch ss-pipe	0.7014	110	0.9285	0.7630	81	0.9240
ATRIUM 10 rods, ≤ 5.0 wt% ^{235}U						
25 loose rods	0.6181	256	0.8255	0.6328	100	0.8024
30 rods in 5-inch ss-pipe	0.6531	264	0.8978	0.7114	100	0.8690
PWR 17x17, type 3 rods, ≤ 8.0 wt% ^{235}U						
25 loose rods	0.6656	256	0.8937	0.6838	100	0.8681
30 rods in 5-inch ss-pipe	0.7043	100	0.9241	0.7655	81	0.9266

* Also includes polyethylene cross-section error penalty (see Section 6.13.5)

** Used maximum enrichment with minimum Gd rod loading to bound single package evaluations

A comparison between the nominal fuel parameters and the worst-case fuel parameters used in the criticality evaluation is shown in Table 6-4 Nominal vs. Worst Case Fuel Parameters for the TN-B1 Criticality Analysis.

Table 6-4 Nominal vs. Worst Case Fuel Parameters for the TN-B1 Criticality Analysis

Case	Fuel Rod Pitch (cm)	Clad Outer Diameter (cm)	Clad Inner Diameter (cm)	Pellet Outer Diameter (cm)	Pellet Density (g/cm^3)
11x11					
Nominal	1.195[a]	**Reference 20**	**Reference 20**	**Reference 20**	< 10.74
Worst Case Modeled for Fuel Assembly Transport	1.2548	0.930	0.840	0.820	10.763
Worst Case Modeled for Fuel Rod Transport	3.52	0.930	0.930	0.820	10.763
FANP 10x10					
Nominal	1.284, 1.2954	1.010, 1.033	0.9020, 0.9217	0.8682, 0.8882	< 10.74
Worst Case Modeled for Fuel Assembly Transport	1.350	1.000	0.9330	0.895	10.74
Worst Case Modeled for Fuel Rod Transport	1.350	1.000	1.000	0.900	10.74
GNF 10x10					
Nominal	1.2954	1.019	0.9322	0.8941	< 10.74
Worst Case Modeled for Fuel Assembly Transport	1.350	1.010	0.9338	0.895	10.74
Worst Case Modeled for Fuel Rod Transport	1.350	1.000	1.000	0.900	10.74
FANP 9x9					
Nominal	1.4478	1.095, 1.0998	0.968, 0.9601	0.94, 0.9398	< 10.74
Worst Case Modeled for Fuel Assembly Transport	1.510	1.093	1.020	0.960	10.74
Worst Case Modeled for Fuel Rod Transport	1.510	1.020	1.020	0.960	10.74
GNF 9x9					
Nominal	1.438	1.110	0.983	0.955	< 10.74
Worst Case Modeled for Fuel Assembly Transport	1.510	1.093	1.020	0.960	10.74
Worst Case Modeled for Fuel Rod Transport	1.510	1.020	1.020	0.960	10.74
GNF 8x8					
Nominal	1.6256	1.2192	1.072	1.044	< 10.74
Worst Case Modeled for Fuel Assembly Transport	1.6923	1.176	1.100	1.050	10.74
Worst Case Modeled for Fuel Rod Transport	1.6923	1.100	1.100	1.050	10.74

a. Equivalent nominal pitch per Section 6.12.3.1.1.

6.1.3. ***Criticality Safety Index***

8x8, 9x9, and 10x10 fuel assemblies; BWR uranium oxide fuel rods

For the TN-B1 for 8x8, 9x9, and 10x10 fuel assemblies, undamaged packages have been analyzed in 21x3x24 arrays and damaged packages have been analyzed in 10x1x10 arrays. Pursuant to 10 CFR 71.59, the number of packages "N" in a 2N array that are subjected to the tests specified in 10 CFR 71.73, or in a 5N array for undamaged packages is used to determine the Criticality Safety Index (CSI). The CSI is determined by dividing the number 50 by the most limiting value of "N" as specified in 10 CFR 71.59.

The TN-B1 criticality analysis demonstrates safety for 5N=1,512 (undamaged) and 2N=100 (damaged) packages. The corresponding Criticality Safety Index (CSI) for criticality control is given by CSI = 50/N. Since 5N=1,512 and 2N = 100, it follows that the more restrictive N = 50 and CSI = 50/50 = 1.0. Therefore the maximum allowable number of packages per shipment is 50/1.0 = 50.

11x11 fuel assemblies and corresponding BWR uranium oxide fuel rods

For the TN-B1 with 11x11 fuel assemblies containing ≤ 5.0 wt.% ^{235}U enrichment, undamaged packages have been analyzed in 12x2x10 arrays and damaged packages have been analyzed in 10x1x7 arrays. Pursuant to 10 CFR 71.59, the number of packages "N" in a 2N array that are subjected to the tests specified in 10 CFR 71.73, or in a 5N array for undamaged packages is used to determine the Criticality Safety Index (CSI). The CSI is determined by dividing the number 50 by the most limiting value of "N" as specified in 10 CFR 71.59.

The TN-B1 criticality analysis demonstrates safety for 5N=240 (undamaged) and 2N=70 (damaged) packages. The corresponding Criticality Safety Index (CSI) for criticality control is given by CSI = 50/N. Since 5N=240 and 2N = 70, it follows that the more restrictive N = 35 and CSI = 50/35 = 1.5. Therefore, the maximum allowable number of packages per shipment is 50/1.5 = 33.

For the TN-B1 with 11x11 fuel assemblies containing ≤ 8.0 wt.% ^{235}U enrichment, undamaged packages have been analyzed in 9x1x9 arrays and damaged packages have been analyzed in 4x1x8 arrays. Pursuant to 10 CFR 71.59, the number of packages "N" in a 2N array that are subjected to the tests specified in 10 CFR 71.73, or in a 5N array for undamaged packages is used to determine the Criticality Safety Index (CSI). The CSI is determined by dividing the number 50 by the most limiting value of "N" as specified in 10 CFR 71.59.

The TN-B1 criticality analysis demonstrates safety for 5N=81 (undamaged) and 2N=32 (damaged) packages. The corresponding Criticality Safety Index (CSI) for criticality control is given by CSI = 50/N. Since 5N=81 and 2N = 32, it follows that the more restrictive N = 16 and CSI = 50/16 = 3.2. Therefore, the maximum allowable number of packages per shipment is 50/3.2 = 15.

Uranium carbide and generic PWR uranium oxide fuel rods, ≤ 5.0 wt.% ^{235}U

Under hypothetical accident conditions, the contents of 2N=64 (8x1x8 array), 48 (4x1x6 array) TN-B1 damaged packages are demonstrated to remain subcritical. Therefore, the CSI for criticality control purposes is 1.6 for an 8x1x8 array and 2.1 for a 4x2x6 array (Ref. 13).

11x11 fuel rods, ≤ 8.0 wt.% ^{235}U

For loose rods, the TN-B1 criticality analysis demonstrates safety for 5N=256 (16x1x16 array) and 2N=100 (10x1x10 array) of packages. The corresponding CSI for criticality control is CSI=50/N. Since 5N=256 and 2N=100, it is more restrictive for N = 50 and CSI = 50/50 = 1.0.

For 11x11 rods in a 5-inch stainless steel pipe, the criticality analysis demonstrates safety for 5N=110 (8x1x8 array) and 2N=81 (9x1x9) array of packages. The corresponding CSI for criticality control is CSI=50/N. Since 5N=110 and 2N=81, it is more restrictive for N = 22 and CSI = 50/22 = 2.3.

PWR 17x17 Type 3 fuel rods, ≤ 8.0 wt.% ^{235}U

For PWR 17x17 Type 3 rods in a 5-inch stainless steel pipe, the criticality analysis demonstrates safety for 5N=100 (10x1x10 array) and 2N=81 (9x1x9) array of packages. The corresponding CSI for criticality control is CSI=50/N. Since 5N=100 and 2N=81, it is more restrictive for N = 20 and CSI = 50/20 = 2.5.

6.2. FISSILE MATERIAL CONTENTS

The TN-B1 shall be used to transport UO_2 conforming to the requirements stated in Section 6.1, Table 6-1 and Table 6-3. The uranium isotopic distribution considered in the models used for the criticality safety demonstration is shown in Table 6-5 Uranium Isotopic Distribution.

Table 6-5 Uranium Isotopic Distribution

Isotope	Modeled wt. % ≤ 5.0 wt.% ^{235}U	Modeled wt. % ≤ 8.0 wt.% ^{235}U
U-235	5.00	8.00
U-238	95.00	92.00

The criticality analysis conservatively demonstrates safety for UO_2 pellets within cylindrical zirconium alloy tubes, arranged in 8x8, 9x9, 10x10, or 11x11 square assembly lattices. Cylindrical fuel rods containing UO_2, enriched up to either 5 wt. percent or 8 wt. percent U-235, are also conservatively demonstrated safe within the TN-B1 container in a 5-inch stainless steel pipe, loose, in a protective case, or bundled together. The fuel loadings demonstrated safe in the TN-B1 are specified in Table 6-1 and Table 6-3.

6.3. GENERAL CONSIDERATIONS

Models are generated for single package and package arrays under normal conditions and Hypothetical Accident Conditions (HAC).

6.3.1. *Model Configuration*

6.3.1.1. TN-B1 Shipping Container Single Package Model

The TN-B1 single package models are constructed for both normal conditions of transport and hypothetical accident conditions. The single package models are enveloped with a 30.48 cm layer of full density water for reflection.

6.3.1.1.1. *Single Package Normal Conditions of Transport Model*

The TN-B1 is comprised of an inner and outer container fabricated from Stainless Steel. The inner container dimensions are shown in Figure 6-4 TN-B1 Inner Container Normal Conditions of Transport Model and Figure 6-5 TN-B1 Container Cross-Section Normal Conditions of Transport Model. It is lined with polyethylene foam having a density of up to 0.080 g/cm3. The fuel assemblies rest against the polyethylene foam in a fixed position, and the inner container is positioned within the outer container as shown in Figure 6-5. The inner container has Alumina Silicate thermal insulation between the inner and outer walls. The Alumina Silicate density is approximately 0.25 g/cm3. The outer container dimensions are contained in Figure 6-3 and Figure 6-5. The outer container provides protection for the inner container and additional separation between fuel assemblies in adjacent containers. No credit is taken for any of the structural steel between the inner and outer containers. The honeycomb shock absorbers, located between the inner and outer containers, are not explicitly modeled. Instead, water is placed in the space between the inner and outer containers, and its density is varied from 0.0 – 1.0 g/cm3. The honeycomb shock absorbers have a density between 0.04 and 0.08 g/cm3. The hydrogen number densities for water (1.0 g/cm3) and for the honeycomb shock absorber (0.08 g/cm3) are 6.677x10-2 and 2.973x10-3 atoms/b*cm, respectively. As a result, water is more effective at thermalizing neutrons than the honeycomb shock absorbers. Therefore, the use of water at 1.0 g/cm3 between the inner and outer containers is considered a conservative replacement for the honeycomb shock absorbers.

The fuel assemblies are modeled inside the inner container, flush with the polyethylene foam. No fuel assembly structures outside the active length of the rod are represented in the models, with the exception of the fuel assembly channel. The fuel assembly structures outside the active fuel length, other than the fuel assembly channel, are composed of materials that absorb neutrons by radiative capture, therefore, neglecting them is conservative. In addition, no grids within the rod active length are represented. The internal grid structure displaces water from between the fuel rods, decreasing the H/X ratio. Since the fuel assemblies are undermoderated, decreasing the H/X ratio decreases system reactivity. Therefore, it is conservative to neglect the internal grid structure in modeling the TN-B1 container. The maximum pellet enrichment and maximum fuel lattice average enrichment is 5.0 wt% U-235. Only 75% credit is taken for gadolinia present in the fuel rods.

Calculations performed with the package array HAC model determine the fuel assembly modeling for the single package Normal Conditions of Transport (NCT) model. A fuel parameter sensitivity study is conducted and a worst-case fuel assembly is developed for each fuel design. The sensitivity study results determine the fuel parameter ranges for the fuel assembly loading criteria shown in Table 6-1 and Table 6-2. The ranges are broad enough to accommodate future fuel assembly design changes. The fuel rod pitch, fuel pellet outer diameter, fuel rod clad inner and outer diameters, fuel rod number, and part length fuel rod number are varied independently in the package array HAC calculations. Reactivity effects are investigated, and the worst-case is identified for each parameter perturbation. To validate the ranges for worst-case fuel parameter combinations (e.g., worst-case pellet OD, clad OD, clad ID, etc.) within the same assembly, a worst-case fuel assembly is created for each fuel design considered for transport in the TN-B1 container, by choosing each parameter value that provides the highest system reactivity. Calculations performed with the worst-case fuel assemblies validate the parameter ranges to be used as fuel acceptance criteria. Both un-channeled (Figure 6-9 through Figure 6-15) and channeled fuel assemblies, Figure 6-16, are considered in the worst-case orientation, subjected to the worst-case fuel damage, and the most reactive configuration is chosen for subsequent calculations.

The GNF 10x10 worst-case fuel assembly is used for the TN-B1 single package NCT model since it is determined to be the most reactive assembly type in the package array HAC fuel parameter studies. The worst-case fuel parameters for the GNF 10x10 assembly are presented in Table 6-11.

Polyethylene inserts or cluster separators are positioned between fuel rods at various locations along the axis of the fuel assembly to avoid stressing the axial grids during transportation. Two types of inserts, shown in Figure 6-1 and Figure 6-2, are considered for use with the TN-B1 container. Since the polyethylene cluster separators provide a higher volume average density polyethylene inventory, they are chosen for the TN-B1 criticality analysis. Other types of inserts are acceptable provided that their polyethylene inventory is within the limits established using the cluster separators.

The normal condition model utilizes the maximum allowable polyethylene mass and applies it over the full axial length of the fuel. The polyethylene is smeared into the water region surrounding the fuel rods as well as the water region surrounding the fuel assembly normally occupied by the cluster holder.

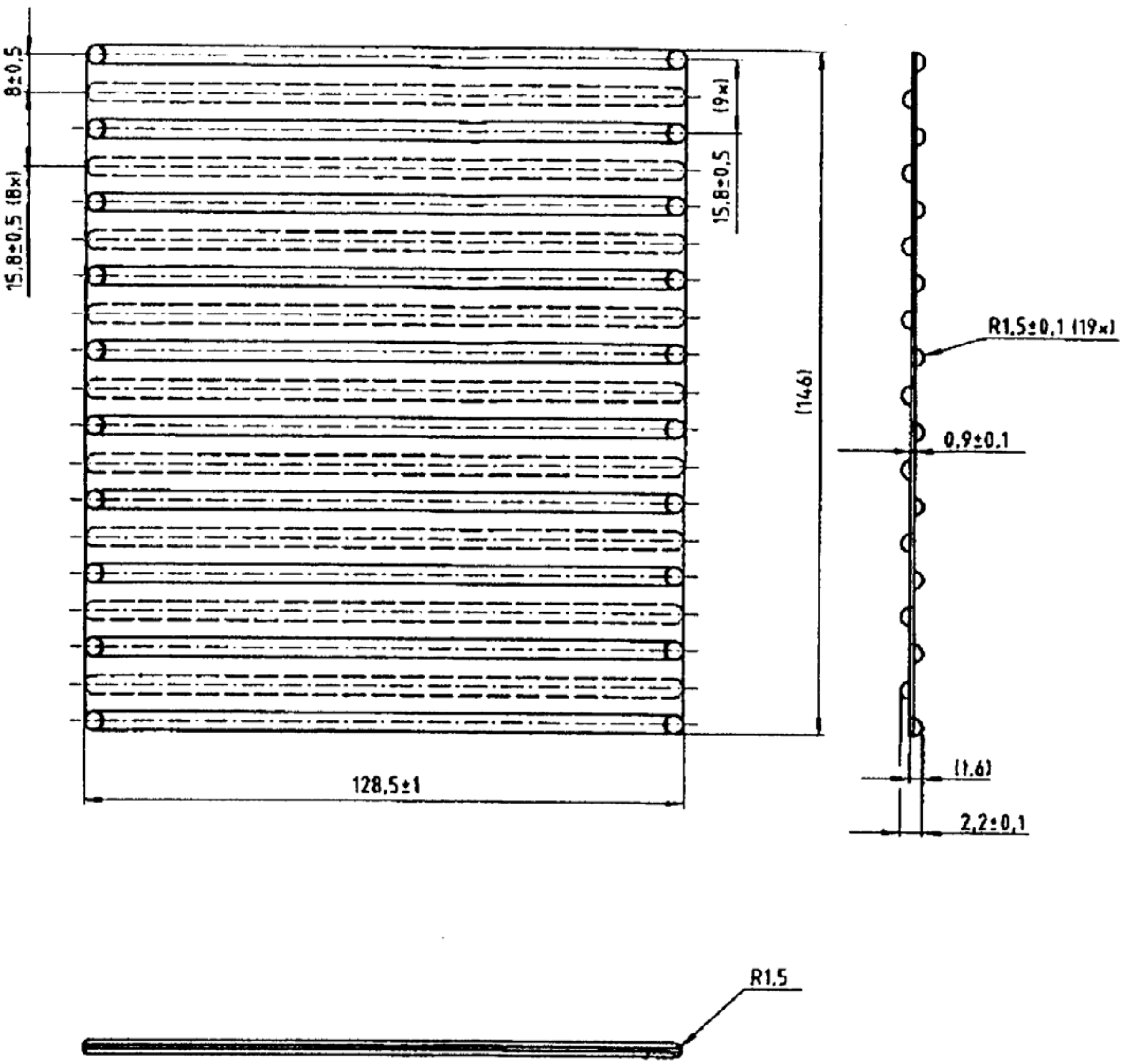

Figure 6-1 Polyethylene Insert (FANP Design)

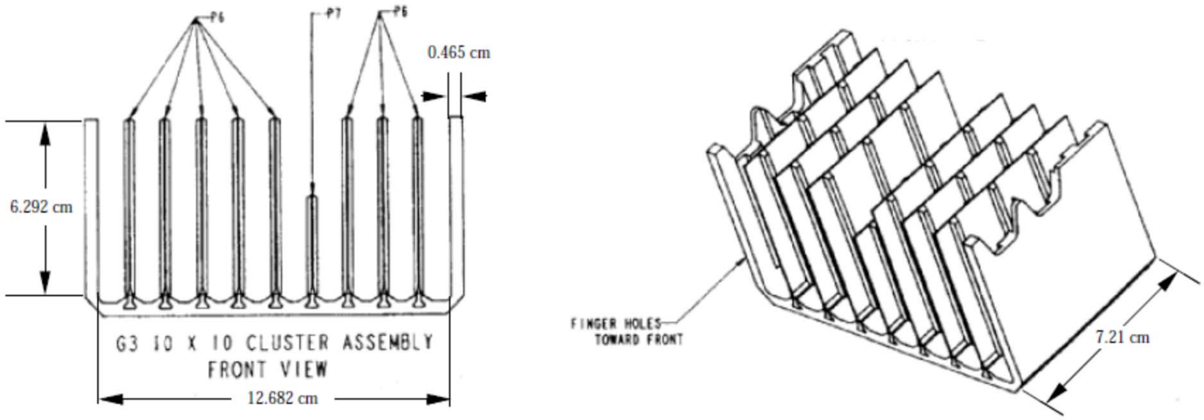

Figure 6-2 Polyethylene Cluster Separator Assembly (GNF Design)

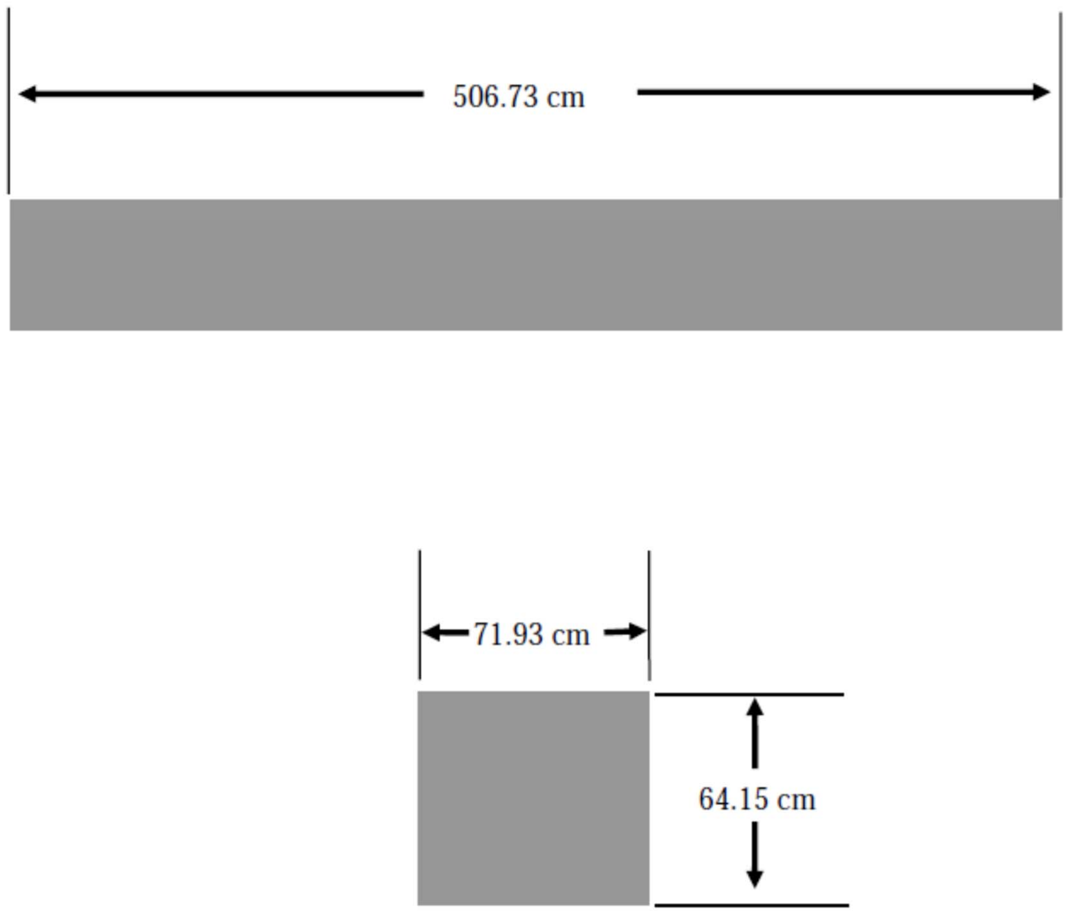

Figure 6-3 TN-B1 Outer Container Normal Conditions of Transport Model

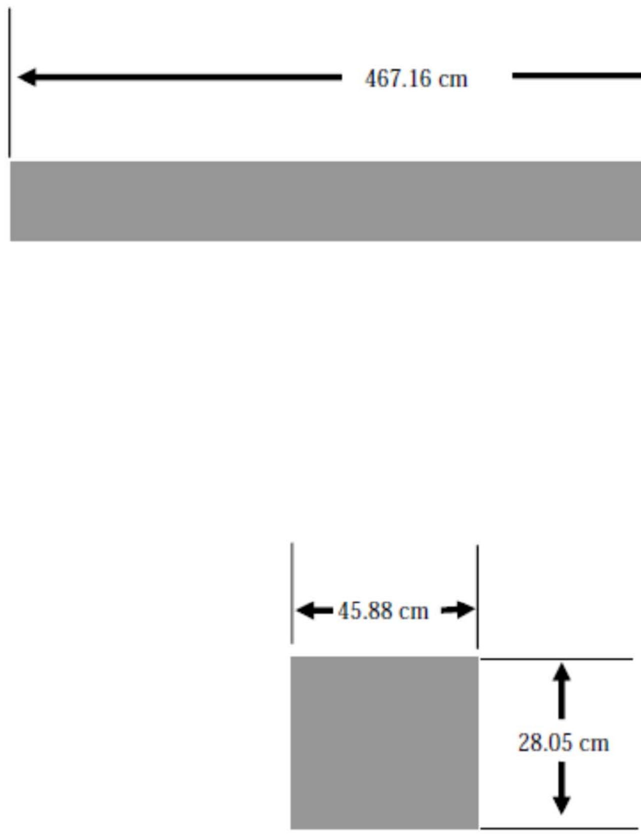

Figure 6-4 TN-B1 Inner Container Normal Conditions of Transport Model

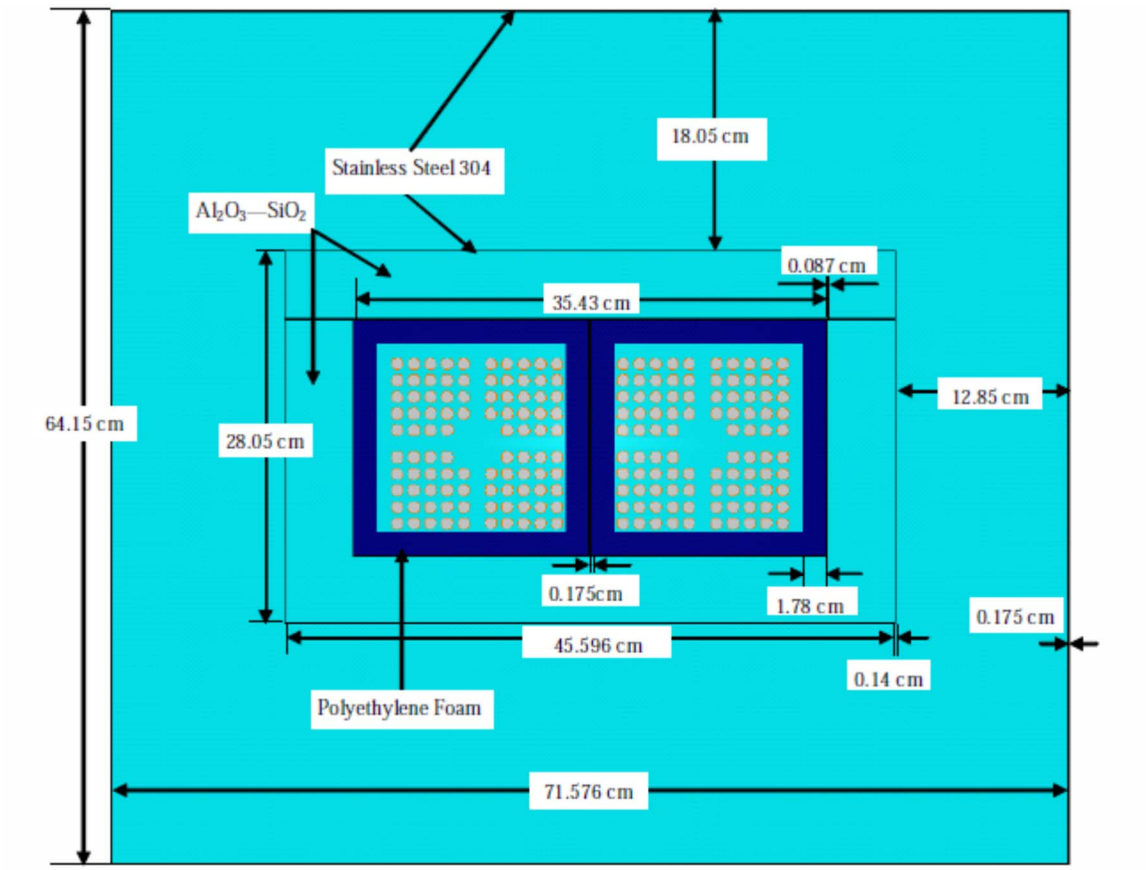

Figure 6-5 TN-B1 Container Cross-Section Normal Conditions of Transport Model

6.3.1.1.2. *Single Package Hypothetical Accident Condition Model*

The TN-B1 HAC model inner container dimensions are shown in Figure 6-7 and Figure 6-8. The container deformation modeled for the TN-B1 HAC model includes the damage incurred from the 9-meter drop onto an unyielding surface as well as conservative factors. The TN-B1 inner container length is conservatively reduced by 8.1 cm to bound the damage incurred from the 9-meter drop onto an unyielding surface. The polyethylene foam is assumed to burn away for the HAC single package model. Full density water that provides more reflection capability is assumed to flood the TN-B1 inner container fuel compartment. The Alumina Silicate insulation is assumed to remain in place, since scoping calculations proved it to provide a more reactive configuration. The fuel assemblies are assumed to freely move within the respective compartment resulting in a worst-case orientation. The rubber vibro-isolating devices are also assumed to melt when exposed to an external fire, allowing the inner container to shift downward about 2.54 cm. However, scoping calculations reveal no increase in reactivity by moving the inner container; therefore, the inner container is positioned within the outer container as shown in Figure 6-8. The inner container horizontal position within the outer container remains the same as the normal condition model, since the stainless steel fixture assemblies remained intact following the 9-meter drop. The outer container dimensions are shown in Figure 6-6 TN-B1 Outer Container Hypothetical Accident Condition Model and Figure 6-8. The outer container length is reduced by 4.7 cm to bound the damage sustained from a 9-meter drop onto an unyielding surface. In addition, the outer container height is reduced by 2.4 cm to bound the damage sustained during the 9-meter drop (Reference 1). No credit is taken for the structural steel between the inner and outer containers. The honeycomb shock absorbers, located between the inner and outer containers, are not explicitly modeled. Instead, water is placed in the space between the inner and outer containers, and its density is varied from 0.0 – 1.0 g/cm3. The honeycomb shock absorbers have a density between 0.04 and 0.08 g/cm3. The hydrogen number densities for water (1.0 g/cm3) and for the honeycomb shock absorber (0.08 g/cm3) are 6.677x10-2 and 2.973x10-3 atoms/b*cm, respectively. As a result, water is more effective at thermalizing neutrons than the honeycomb shock absorbers. Therefore, the use of water at 1.0 g/cm3 between the inner and outer containers is considered a conservative replacement for the honeycomb shock absorbers. The reduction in length for the inner and outer containers, the reduction in height for the outer container, the absence of polyethylene foam, the presence of the insulation, and the fuel assembly freedom of movement are consistent with the physical condition of the TN-B1 shipping container after being subjected to the tests specified in 10 CFR Part 71.

Calculations performed with the package array HAC model determine the fuel assembly modeling for the single package HAC model. No fuel assembly structures outside the active length of the rod are represented in the models, with the exception of the fuel assembly channel. The fuel assembly structures outside the active fuel length, other than the fuel assembly channel, are composed of materials that absorb neutrons by radiative capture, therefore, neglecting them is conservative. In addition, no grids within the rod active length are represented. The internal grid structure displaces water from between the fuel rods, decreasing the H/X ratio. Since the fuel assemblies are undermoderated, decreasing the H/X ratio decreases system reactivity. Therefore, it is conservative to neglect the internal grid structure in modeling the TN-B1 container. The maximum pellet enrichment and maximum fuel lattice average enrichment is 5.0 wt% U-235. The gadolinia content of any gadolinia-urania fuel rods is taken to be 75% of the minimum value specified in Table 6-1. The fuel assemblies are modeled inside the inner container, in one of seven orientations shown in Figure 6-9 TN-B1 Hypothetical Accident Condition Model with Fuel Assembly Orientation 1 through Figure 6-15 TN-B1 Hypothetical Accident Condition Model with Fuel Assembly Orientation 7. The worst-case orientation is chosen for each fuel assembly design considered for transport and used in subsequent calculations. Fuel damage sustained during the 9-meter (30 foot) drop test is simulated as a change in fuel rod pitch along the full axial length of each fuel assembly considered for transport. Based on the fuel damage sustained in the TN-B1 shipping container drop test (Reference 1), a 10% reduction in fuel rod pitch over the full length of each fuel assembly, or a 4.1% increase in fuel rod pitch over the full length of each fuel assembly, is determined to be conservative. Both un-channeled (Figure 6-9 through Figure 6-15) and channeled fuel assemblies (Figure 6-16) are considered in the worst-case orientation, subjected to the worst-case fuel damage, and the most reactive configuration is chosen for subsequent calculations.

The fuel damage sustained during the 9-meter drop test is bounded by performing a fuel parameter sensitivity study and creating a worst-case fuel assembly for each fuel design. The sensitivity study results determine the fuel parameter ranges for the fuel assembly loading criteria shown in Table 6-1. The ranges are broad enough to accommodate future fuel assembly design changes. The fuel rod pitch, fuel pellet outer diameter, fuel rod clad inner and outer diameters, fuel rod number, and part length fuel rod number are varied independently in the package array HAC calculations. Reactivity effects are investigated, and the worst-case is identified for each parameter perturbation. To validate the ranges for worst-case fuel parameter combinations (e.g. worst-case pellet OD, clad OD, clad ID, etc.) within the same assembly, a worst-case fuel assembly is created for each fuel design considered for transport in the TN-B1 container, by choosing each parameter value that provides the highest system reactivity. Calculations performed with the worst-case fuel assemblies validate the parameter ranges to be used as fuel acceptance criteria.

The GNF 10x10 worst-case fuel assembly at a 5.0 wt% U-235 enrichment, containing twelve 2 wt % gadolinia-urania fuel rods, and twelve part length fuel rods is used for the TN-B1 single package HAC model since it is determined to be the most reactive assembly in the package array HAC fuel parameter studies. The worst-case fuel parameters for the 10x10 assembly are presented in Table 6-11.

Polyethylene inserts (cluster separators) are positioned between fuel rods at various locations along the axis of the fuel assembly to avoid stressing the axial grids during transportation. Two types of inserts, shown in Figure 6-1 and Figure 6-2, are considered for use with the TN-B1 container. Since the polyethylene cluster separators provide a higher volume averaged density polyethylene inventory, they are chosen for the TN-B1 criticality analysis. Other types of inserts are acceptable provided that their polyethylene inventory is within the limits established using the cluster separators.

In the hypothetical accident condition model, the polyethylene inserts are assumed to melt when subjected to the tests specified in 10 CFR Part 71. The polyethylene is assumed to uniformly coat the fuel rods in each fuel assembly forming a cylindrical layer of polyethylene around each fuel rod. Different coating thicknesses are investigated in the package array HAC calculations, and a polyethylene mass limit is developed for each fuel assembly type considered for transport. The TN-B1 single package model contains 10x10 worst-case fuel assemblies with 10.2 kg of polyethylene per assembly. The polyethylene is smeared into the fuel rod cladding to accommodate the limitations in the lattice cell modeling for cross-section processing in SCALE. A visual representation of the smeared clad/polyethylene mixture compared to a discrete treatment is shown in Figure 6-21 Visual Representation of the Clad/Polyethylene Smeared Mixture versus Discrete Modeling. The polyethylene mass and the volume fractions of polyethylene and zirconium clad for each fuel assembly analyzed are shown in Table 6-13 Polyethylene Mass and Volume Fraction Calculations. The volume fractions in Table 6-13 are entered into the model input standard composition specification area. Mixtures representing the polyethylene inserts between fuel rods are created using the compositions specified, and used in the KENO V.a calculation. The mixtures are also used in the lattice cell description to provide the lump shape and dimensions for resonance cross-section processing, the lattice corrections for cross-section processing, and the information necessary to create flux-weighted cross-sections based on the lattice cell geometry.

6.3.1.2. **Package Array Models**

6.3.1.2.1. *Package Array Normal Condition Model*

The TN-B1 container package array normal condition model consists of a 21x3x24 array of containers, surrounded by a 30.48 cm layer of full density water for reflection. The container array is fully flooded with water at a density sufficient for optimum moderation. The container and fuel model in the array are those discussed in Section 6.3.1.1.1.

6.3.1.2.2. *Package Array Hypothetical Accident Condition (HAC) Model*

The TN-B1 package array HAC model consists of either a 14x2x16 or 10x1x10 array of containers, surrounded by a 30.48 cm layer of full density water for reflection. The 14x2x16 array (Sections 6.4.1 – 6.4.10) is initially used under the assumption that the polyethylene foam, on which the fuel assemblies rest, completely burns away during a fire. The 10x1x10 array (Sections 6.4.11 – 6.4.13) assumes the polyethylene foam remains intact following a fire. The container array has no interspersed water between packages in the array and no water in the outer container. These moderator conditions optimize the interaction between packages in the array. Unlike the HAC single package model, the HAC package array model assumes the polyethylene foam remains in place following the tests specified in 10 CFR 71. The presence of polyethylene foam allows increased neutron leakage from the inner container fuel compartment and promotes increased neutron interaction among containers in the array. The inner container fuel compartment space not occupied by the polyethylene foam is fully flooded with water at a density sufficient for optimum moderation. The remaining HAC model container and fuel details are those discussed in Section 6.3.1.1.2.

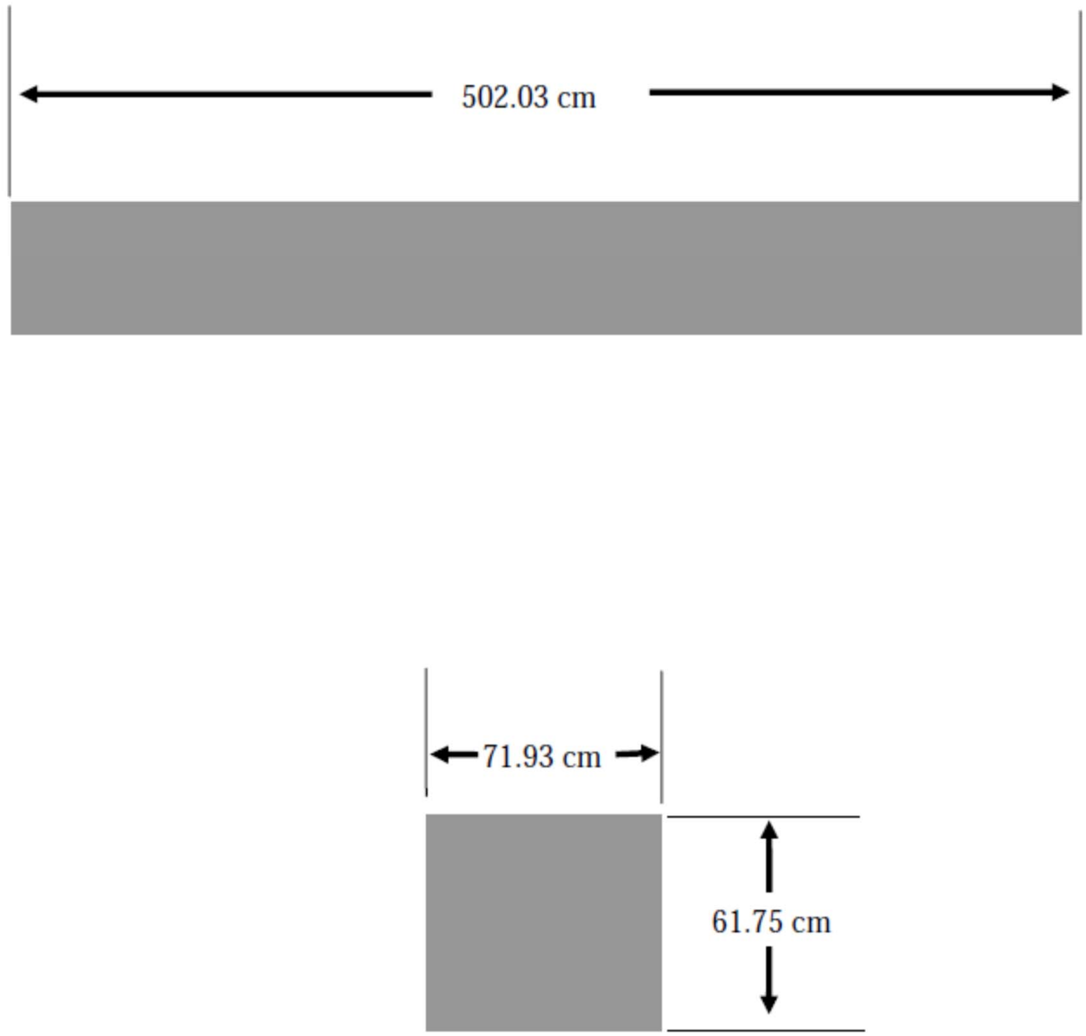

Figure 6-6 TN-B1 Outer Container Hypothetical Accident Condition Model

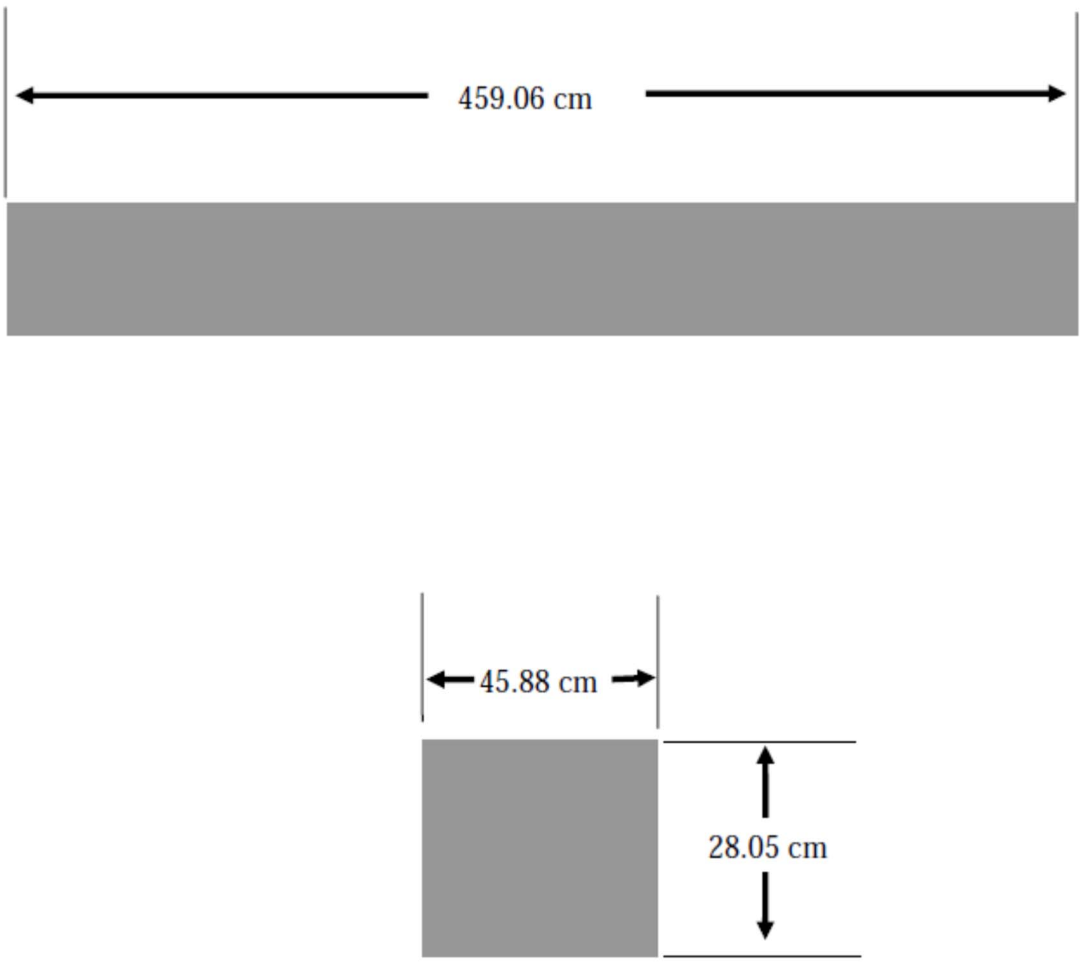

Figure 6-7 TN-B1 Inner Container Hypothetical Accident Condition Model

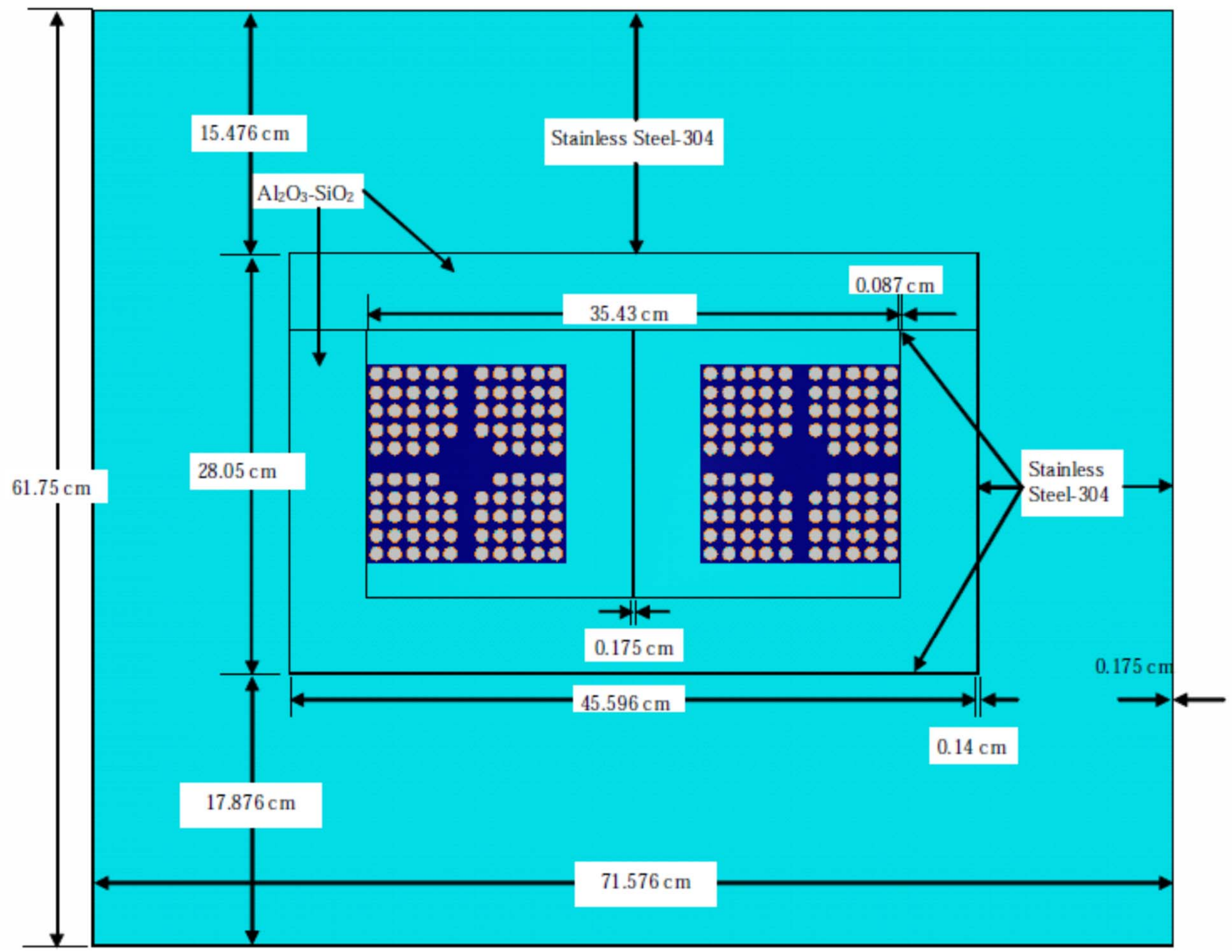

Figure 6-8 TN-B1 Cross-Section Hypothetical Accident Condition Model

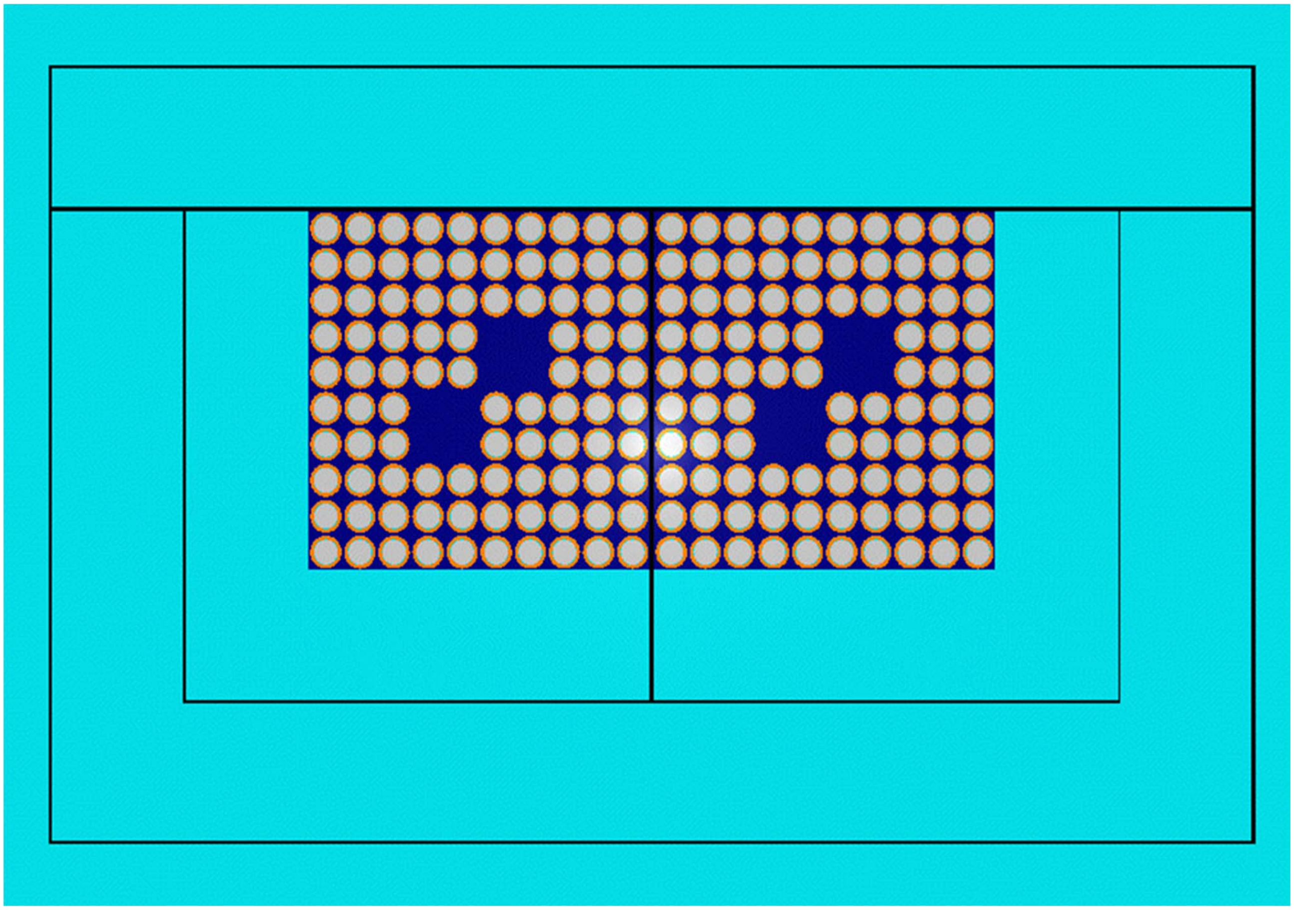

Figure 6-9 TN-B1 Hypothetical Accident Condition Model with Fuel Assembly Orientation 1

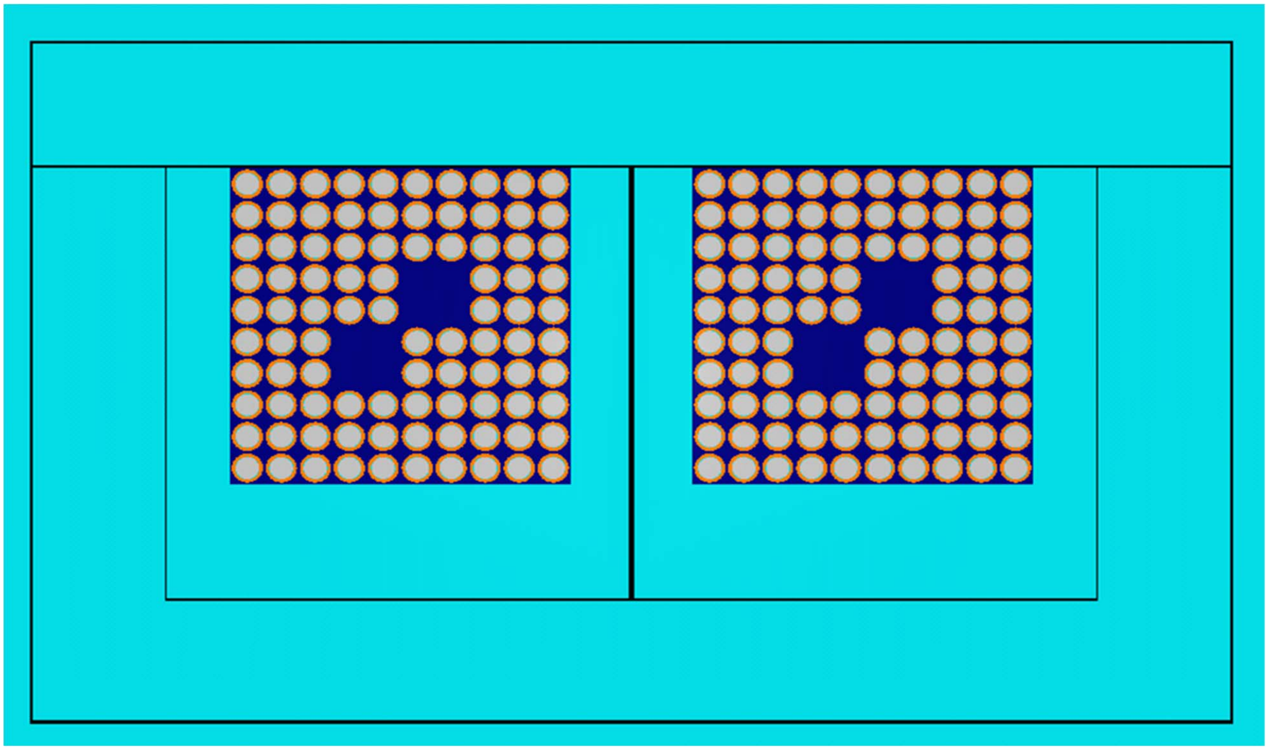

Figure 6-10 TN-B1 Hypothetical Accident Condition Model with Fuel Assembly Orientation 2

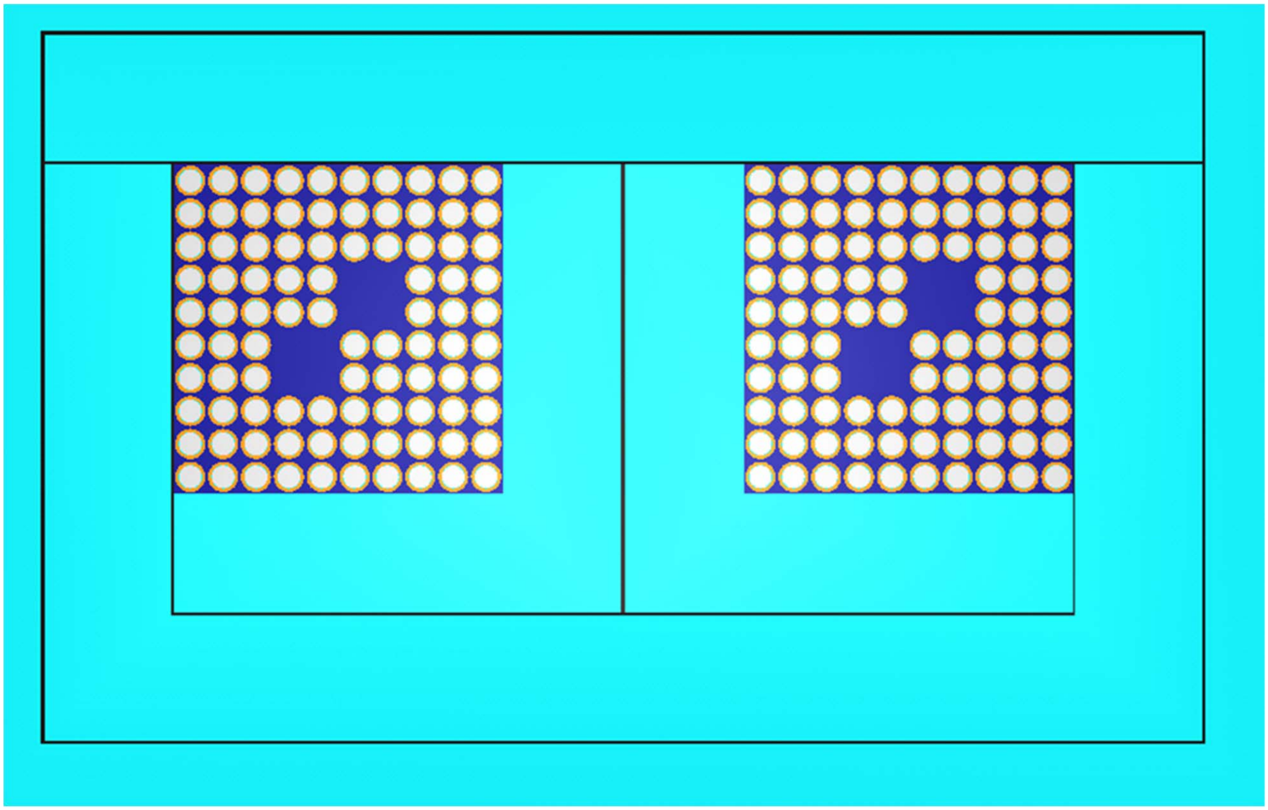

Figure 6-11 TN-B1 Hypothetical Accident Condition Model with Fuel Assembly Orientation 3

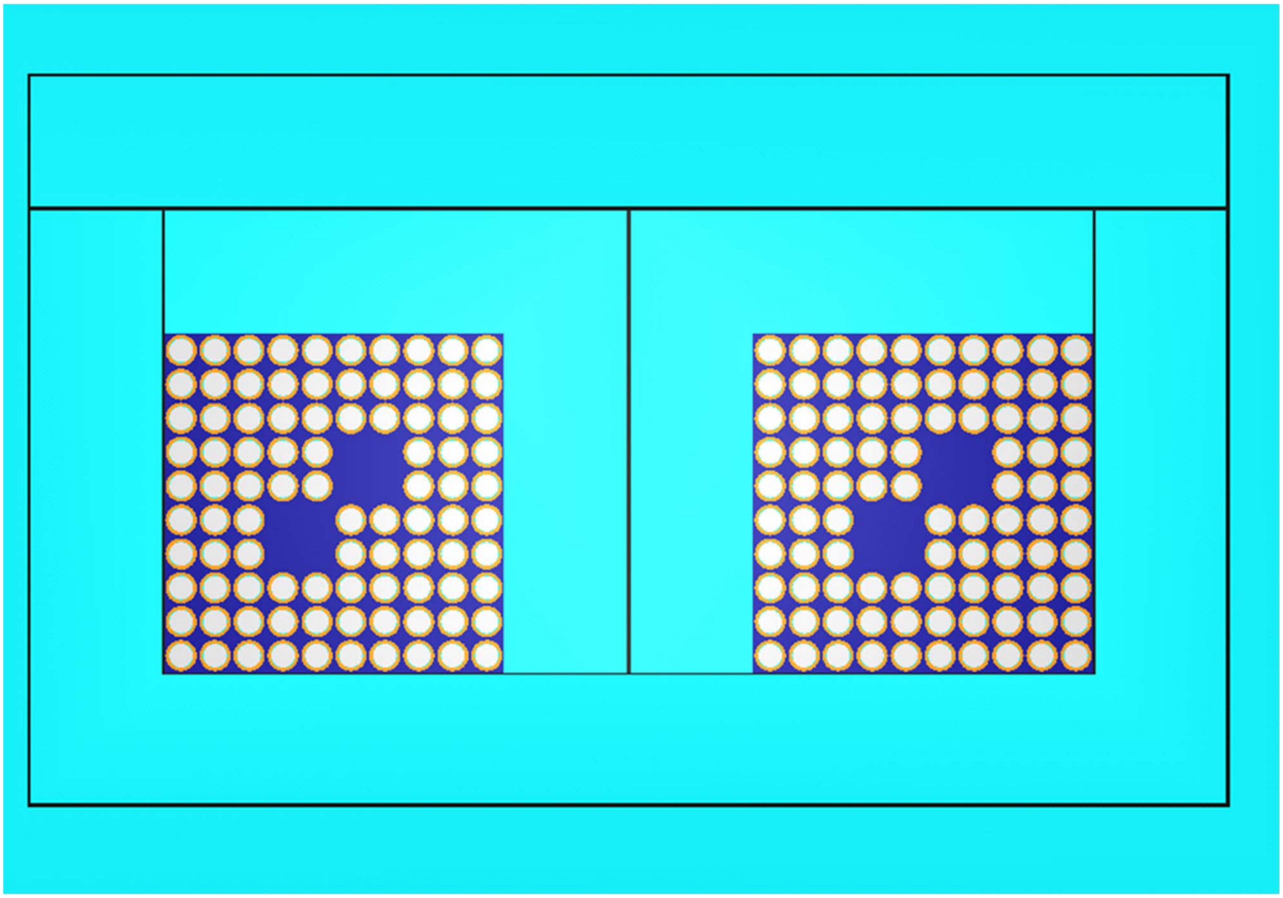

Figure 6-12 TN-B1 Hypothetical Accident Condition Model with Fuel Assembly Orientation 4

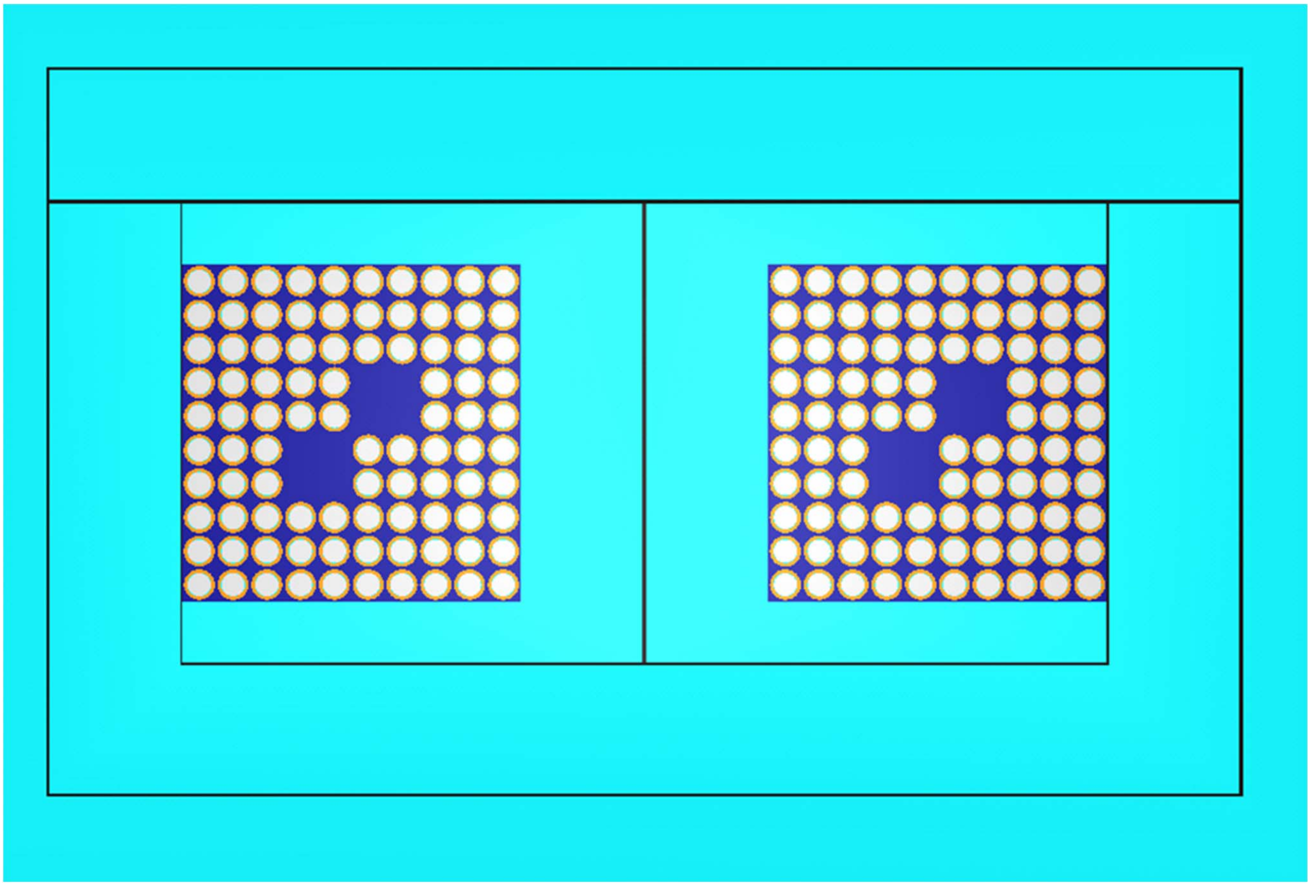

Figure 6-13 TN-B1 Hypothetical Accident Condition Model with Fuel Assembly Orientation 5

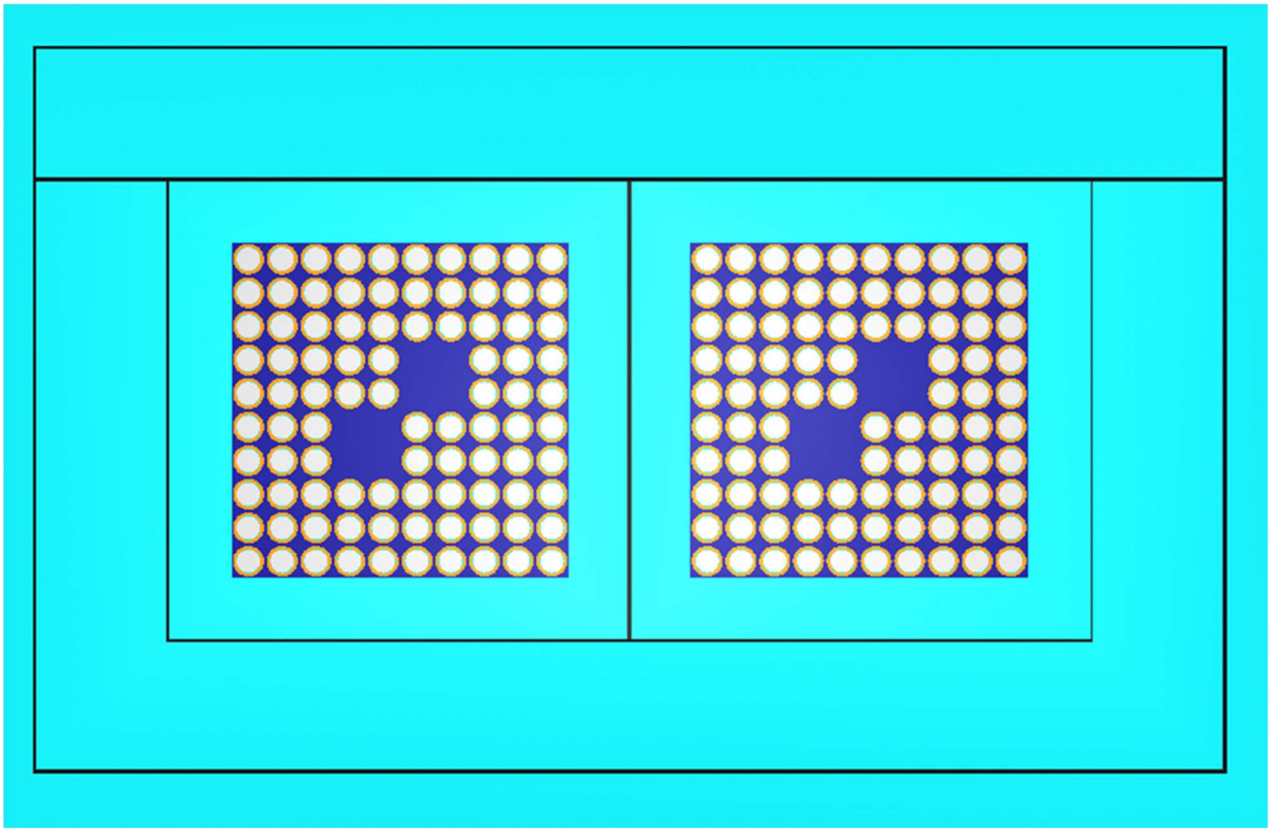

Figure 6-14 TN-B1 Hypothetical Accident Condition Model with Fuel Assembly Orientation 6

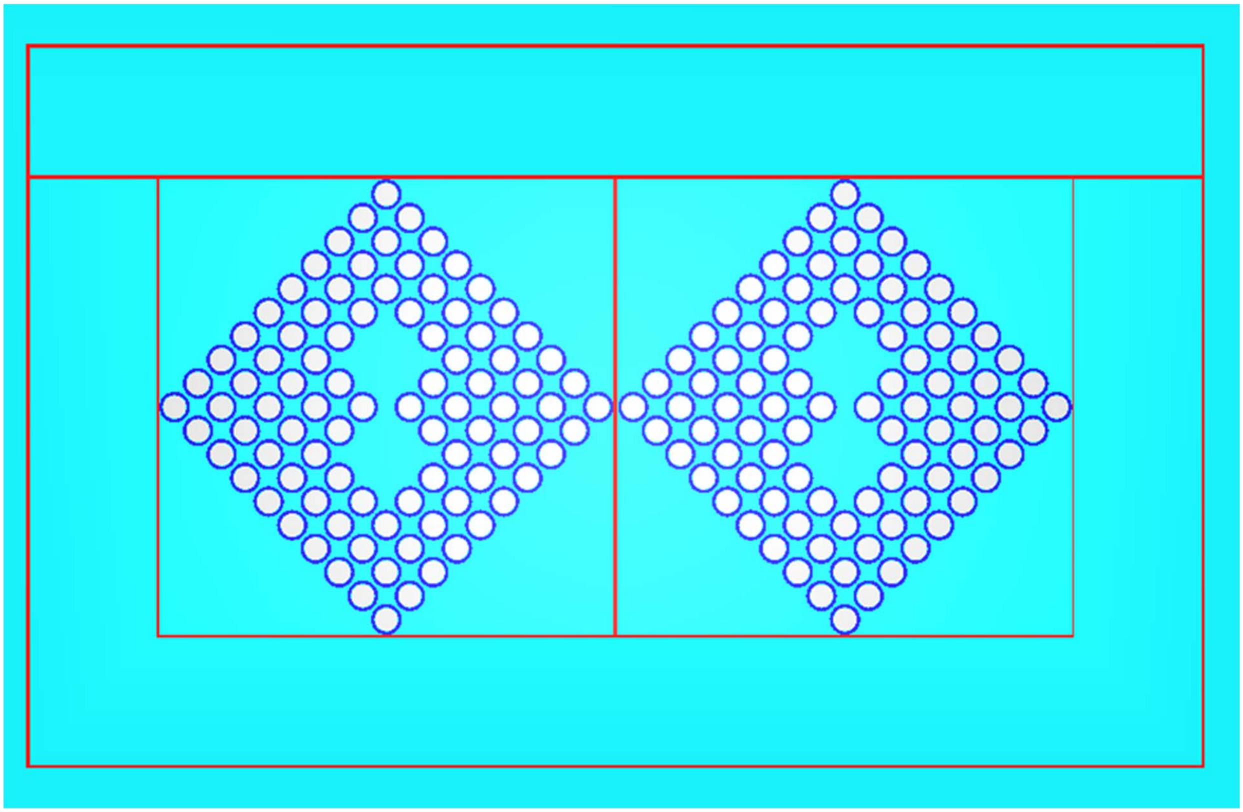

Figure 6-15 TN-B1 Hypothetical Accident Condition Model with Fuel Assembly Orientation 7

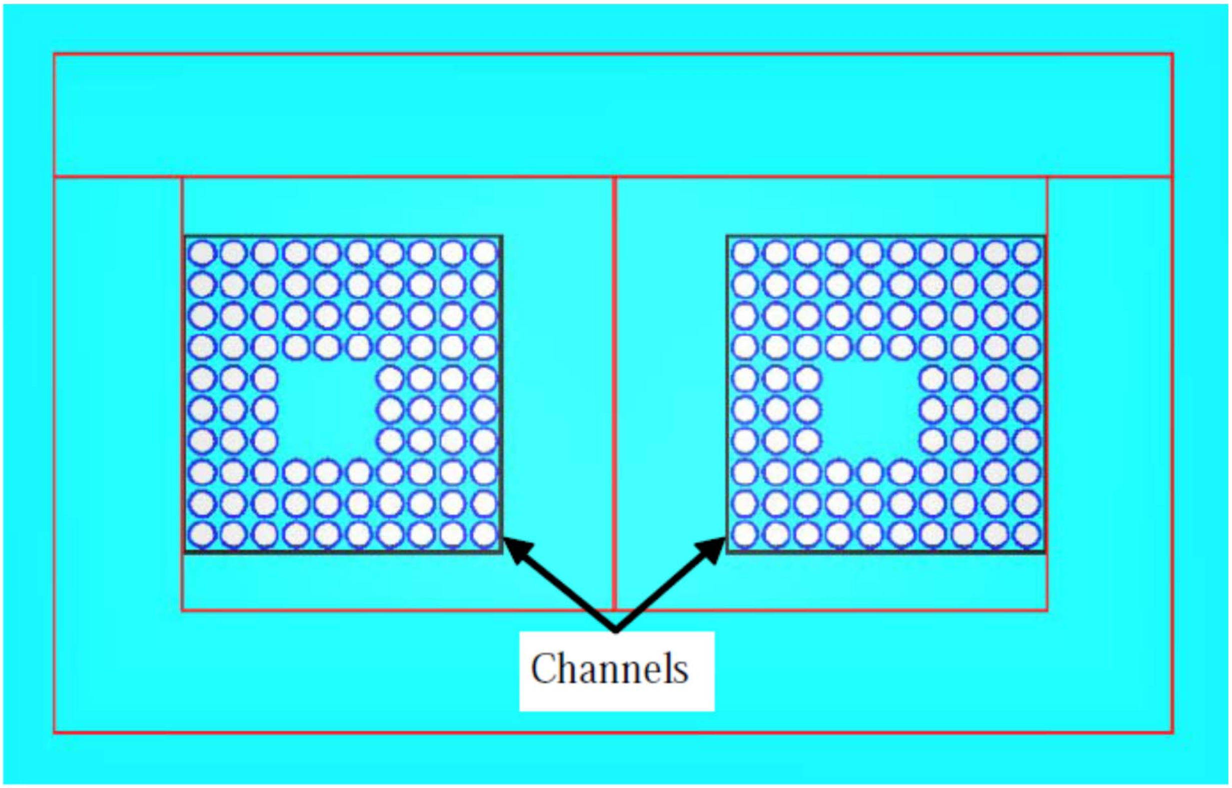

Figure 6-16 TN-B1 Hypothetical Accident Condition Model with Channels

6.3.1.3. **TN-B1 Fuel Rod Transport Model**

The TN-B1 fuel rod transport models are developed for single packages and package arrays under normal transport and hypothetical accident conditions. Cylindrical fuel rods containing UO_2, enriched to 5 wt. percent U-235, are modeled loose, bundled together, or in the TN-B1 inner container in 5-inch stainless steel pipe or protective case.

6.3.1.3.1. *TN-B1 Single Package Fuel Rod Transport NCT Model*

The TN-B1 single package normal conditions of transport described in Section 6.3.1.1.1 are used for the single package fuel rod transport models.

The fuel rods are modeled inside the inner container, flush with the polyethylene foam. A 0.0152 cm thick polyethylene layer is modeled around each fuel rod to simulate any protective material present. The worst-case fuel rod parameters are shown in Table 6-6 TN-B1 Fuel Rod Transport Model Fuel Parameters.

Table 6-6 TN-B1 Fuel Rod Transport Model Fuel Parameters

Fuel Rod Type	Pellet OD (cm)	Fuel Rod ID (cm)	Fuel Rod OD (cm)	Fuel Rod Length (cm)
10x10	0.9	1.000	1.000	385
9 x 9	0.9600	1.0200	1.0200	381
8 x 8	1.05	1.1000	1.1000	381

Calculations performed with the fuel rod transport, package array, HAC model determine the fuel assembly modeling for the fuel rod transport, single package, Normal Conditions of Transport (NCT) model. The calculations investigate transporting loose fuel rods, bundled fuel rods, and fuel rods in 5-inch stainless steel pipe within each TN-B1 shipping compartment. A fuel rod pitch sensitivity study is conducted for each fuel rod type to determine the number of fuel rods that can be transported in a loose configuration within the TN-B1 fuel assembly compartment. A square pitch fuel rod array is used for the sensitivity study since scoping calculations showed no statistically significant difference in system reactivity between fuel rods in a square pitch array and those in a triangular pitch array within the container geometry. The pitch sensitivity study results in the minimum and maximum allowable fuel rod quantity for shipping in a loose configuration. The loose rod analysis is used to bound a fuel rod shipment in which fuel rods are strapped or bundled together. A fuel rod pitch sensitivity analysis is also performed to determine the fuel rod quantity that may be transported inside a 5-inch stainless steel pipe. A triangular pitch fuel rod array is used for the sensitivity study since scoping calculations showed it to result in a higher system reactivity than a square pitch rod array inside a 5-inch stainless steel pipe. The stainless steel material is conservatively neglected when performing the calculations, therefore, any container with a volume equivalent to or less than the 5-inch stainless steel pipe is acceptable for fuel rod transport, as long as the fuel rod quantity is limited to that for the pipe.

The 8x8 worst-case fuel rod is used for the TN-B1 fuel rod transport, single package, NCT model since it is determined to be the most reactive rod in the fuel rod transport, package array, HAC pitch sensitivity studies. The TN-B1 fuel rod transport, single package NCT model is shown in Figure 6-17 TN-B1 Fuel Rod Transport Single Package NCT Model. The worst-case fuel parameters for the 8x8 rod are presented in Table 6-6. As shown in Table 6-6, the fuel rod cladding is not modeled for the 8x8 fuel rod. Although the cladding material is removed, the fuel rod external boundary is maintained (i.e. pellet clad gap to fuel rod OD is maintained, polyethylene coating applied to fuel rod OD region).

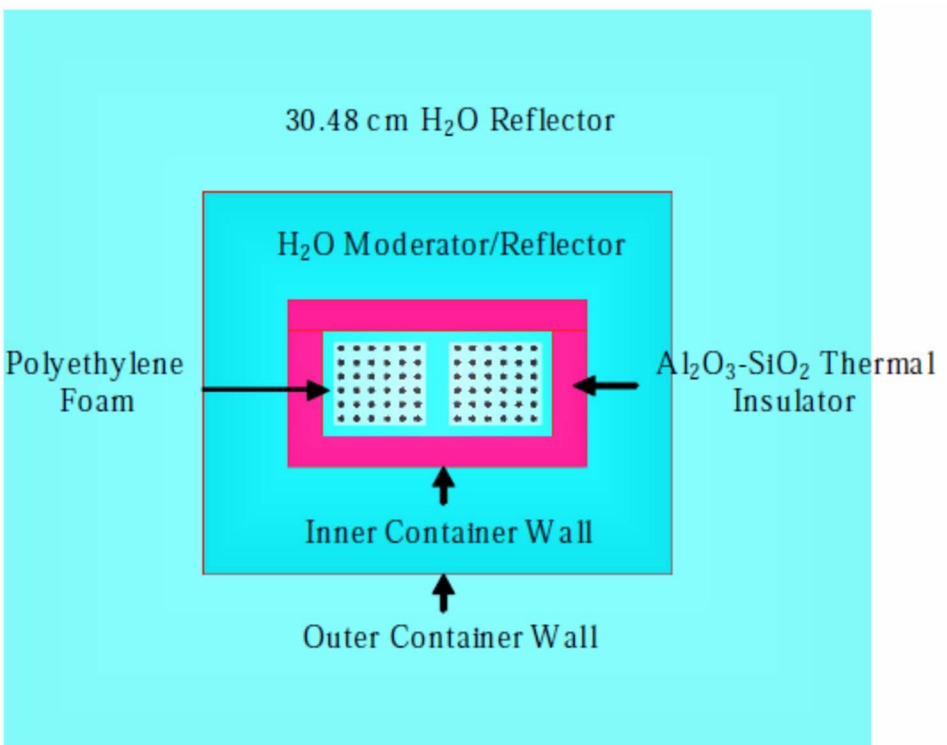

Figure 6-17 TN-B1 Fuel Rod Transport Single Package NCT Model

6.3.1.3.2. *TN-B1 Single Package Fuel Rod Transport HAC Model*

The TN-B1 single package hypothetical accident conditions described in Section 6.3.1.1.2 are used for the single package fuel rod transport models.

The fuel rods are modeled as filling the inner container fuel assembly compartment, since the polyethylene foam is removed due to the HAC. A 0.0152 cm thick polyethylene layer is modeled around each fuel rod to simulate any protective material present. Worst-case fuel rod parameters determined from the package array HAC parameter sensitivity analyses (Section 6.3.1.1.2), are used for the fuel rod transport models. The worst-case fuel rod parameters are shown in Table 6-6 TN-B1 Fuel Rod Transport Model Fuel Parameters.

Calculations performed with the fuel rod transport, package array, HAC model determine the fuel assembly modeling for the fuel rod transport, single package, HAC model. The calculations investigate transporting loose fuel rods, bundled fuel rods, fuel rods in a 5-inch stainless steel pipe and protective case within each TN-B1 shipping compartment. A fuel rod pitch sensitivity study is conducted for each fuel rod type to determine the number of fuel rods that can be transported in a loose configuration within the TN-B1 fuel assembly compartment. A square pitch fuel rod array is used for the sensitivity study since scoping calculations showed no statistically significant difference in system reactivity between fuel rods in a square pitch array and those in a triangular pitch array within the container geometry. The pitch sensitivity study results in the minimum and maximum allowable fuel rod quantity for shipping in a loose configuration. The loose rod analysis is used to bound a fuel rod shipment in which fuel rods are strapped together. A fuel rod pitch sensitivity analysis is also performed to determine the fuel rod quantity that may be transported inside a 5-inch stainless steel, Type 304 pipe. A triangular pitch fuel rod array is used for the sensitivity study since scoping calculations showed it to result in a higher system reactivity than a square pitch rod array inside a 5-inch stainless steel pipe. The stainless steel material is conservatively neglected when performing the calculations, therefore, any container with a volume equivalent to or less than the 5-inch stainless steel pipe is acceptable for fuel rod transport, as long as the fuel rod quantity is limited to that for the pipe.

The 8x8 worst-case fuel rod is used for the TN-B1 fuel rod transport, single package, HAC model since it is determined to be the most reactive rod in the fuel rod transport, package array, HAC pitch sensitivity studies. The TN-B1 fuel rod transport, single package HAC model is shown in Figure 6-18 TN-B1 Fuel Rod Transport Single Package HAC Model. The worst-case fuel parameters for the 8x8 rod are presented in Table 6-6. As shown in Table 6-6, the fuel rod cladding is not modeled for the 8x8 fuel rod. Although the cladding material is removed, the fuel rod external boundary is maintained (i.e., pellet clad gap to fuel rod OD is maintained, polyethylene coating applied to fuel rod OD region).

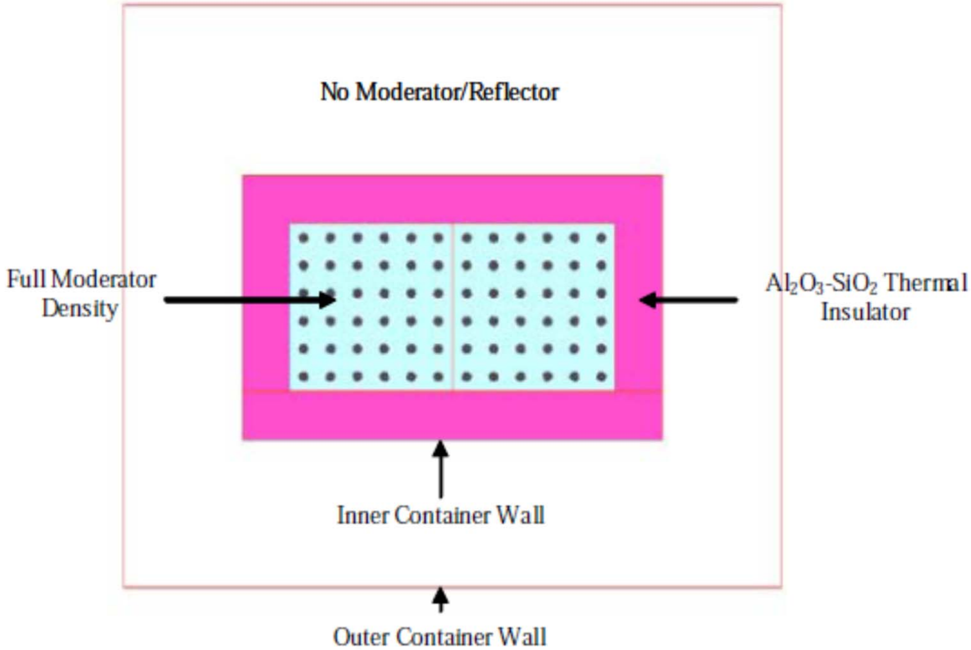

Figure 6-18 TN-B1 Fuel Rod Transport Single Package HAC Model

6.3.1.3.3. *TN-B1 Package Array Fuel Rod Transport NCT Model*

The TN-B1 package array normal conditions of transport described in Section 6.3.1.2.1 are used for the package array, normal conditions of transport, fuel rod transport models.

The fuel rods are modeled inside the inner container, flush with the polyethylene foam. A 0.0152 cm thick polyethylene layer is modeled around each fuel rod to simulate any protective material present. Worst-case fuel rod parameters determined from the package array HAC parameter sensitivity analyses (Section 6.3.1.2.2), are used for the fuel rod transport models. The worst-case fuel rod parameters are shown in Table 6-6.

Calculations performed with the fuel rod transport, package array, HAC model determine the fuel assembly modeling for the fuel rod transport, package array, Normal Conditions of Transport (NCT) model. The calculations investigate transporting loose fuel rods, bundled fuel rods, and fuel rods in 5-inch stainless steel pipe within each TN-B1 shipping compartment. A fuel rod pitch sensitivity study is conducted for each fuel rod type to determine the number of fuel rods that can be transported in a loose configuration within the TN-B1 fuel assembly compartment. A square pitch fuel rod array is used for the sensitivity study since scoping calculations showed no statistically significant difference in system reactivity between fuel rods in a square pitch array and those in a triangular pitch array within the container geometry. The pitch sensitivity study results in the minimum and maximum allowable fuel rod quantity for shipping in a loose configuration. The loose rod analysis is used to bound a fuel rod shipment in which fuel rods are strapped or bundled together.

A fuel rod pitch sensitivity analysis is also performed to determine the fuel rod quantity that may be transported inside a 5-inch stainless steel pipe. A triangular pitch fuel rod array is used for the sensitivity study since scoping calculations showed it to result in a higher system reactivity than a square pitch rod array inside a 5-inch stainless steel pipe. The stainless steel material is conservatively neglected when performing the calculations, therefore, any container with a volume equivalent to or less than the 5-inch stainless steel pipe is acceptable for fuel rod transport, as long as the fuel rod quantity is limited to that for the pipe.

The 8x8 worst-case fuel rod is used for the TN-B1 fuel rod transport, package array, NCT model since it is determined to be the most reactive rod in the fuel rod transport, package array, HAC pitch sensitivity studies. A portion of the TN-B1 fuel rod transport, 21x3x24 package array, NCT model is shown in Figure 6-19. The worst-case fuel parameters for the 8x8 rod are presented in Table 6-6. As shown in Table 6-6, the fuel rod cladding is not modeled for the 8x8 fuel rod. Although the cladding material is removed, the fuel rod external boundary is maintained (i.e., pellet clad gap to fuel rod OD is maintained, polyethylene coating applied to fuel rod OD region).

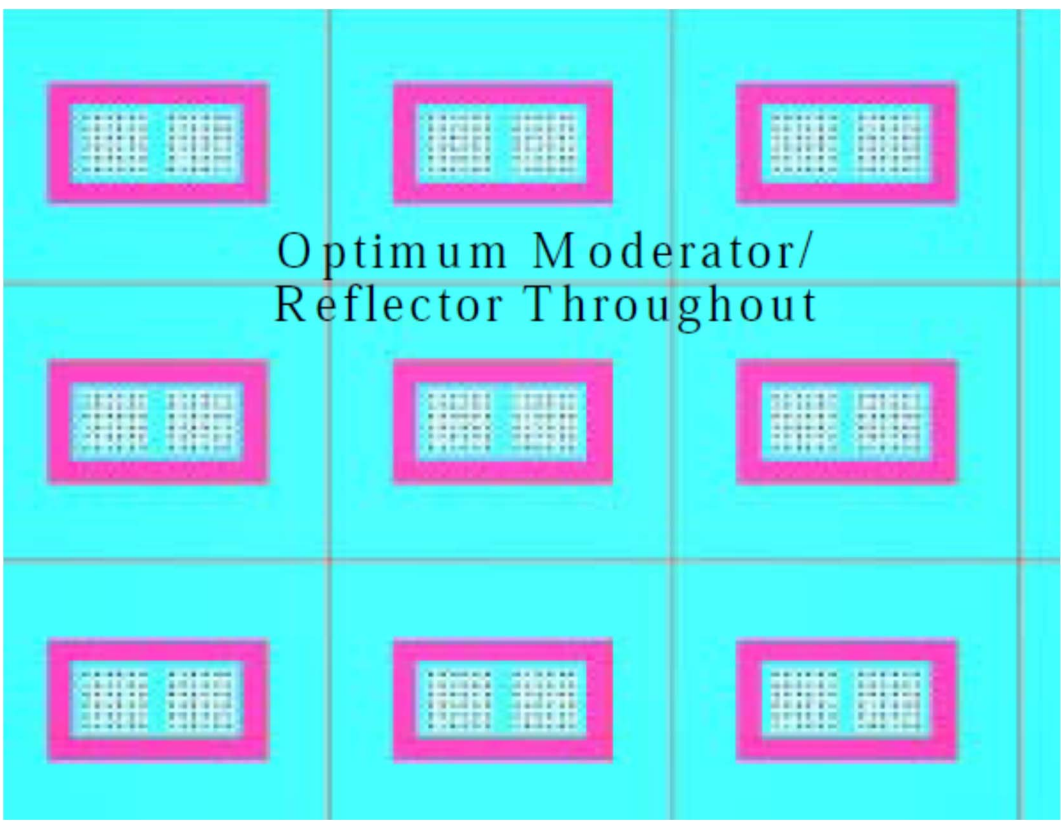

Figure 6-19 TN-B1 Fuel Rod Transport Package Array NCT Model

6.3.1.3.4. *TN-B1 Package Array Fuel Rod Transport HAC Model*

The TN-B1 package array hypothetical accident conditions described in Section 6.3.1.2.2 are used for the package array, HAC, fuel rod transport models.

The fuel rods are modeled filling the inner container for the hypothetical accident conditions. A 0.0152 cm thick polyethylene layer is modeled around each fuel rod to simulate any protective material present. Worst-case fuel rod parameters determined from the package array HAC parameter sensitivity analyses (Section 6.3.1.2.2), are used for the fuel rod transport models. The worst-case fuel rod parameters are shown in Table 6-6.

Calculations are conducted to investigate transporting loose fuel rods, bundled fuel rods, and fuel rods in 5-inch stainless steel pipe within each TN-B1 shipping compartment. A fuel rod pitch sensitivity study is conducted for each fuel rod type, to determine the number of fuel rods that can be transported in a loose configuration within the TN-B1 fuel assembly compartment. For convenience, a square pitch array is used to conduct the sensitivity study, since scoping calculations revealed little difference in the reactivity between square and triangular pitch arrays. The pitch sensitivity study results in the minimum and maximum allowable fuel rod quantity for shipping rods in a loose configuration. The loose rod analysis is used to bound a fuel rod shipment in which fuel rods are strapped or bundled together.

A fuel rod pitch sensitivity analysis is also performed to determine the fuel rod quantity that may be transported inside a 5-inch stainless steel pipe. Triangular pitch fuel rod arrays are used to find the maximum allowable quantity. The stainless steel material is conservatively neglected when performing the calculations, therefore, any container with a volume equivalent to or less than the 5-inch stainless steel pipe is acceptable for fuel rod transport, as long as the fuel rod quantity is limited to that for the pipe.

The fuel rod type with the most reactive configuration is chosen for the TN-B1 fuel rod transport, package array, HAC model. A portion of the TN-B1 fuel rod transport package array HAC model is shown in Figure 6-20.

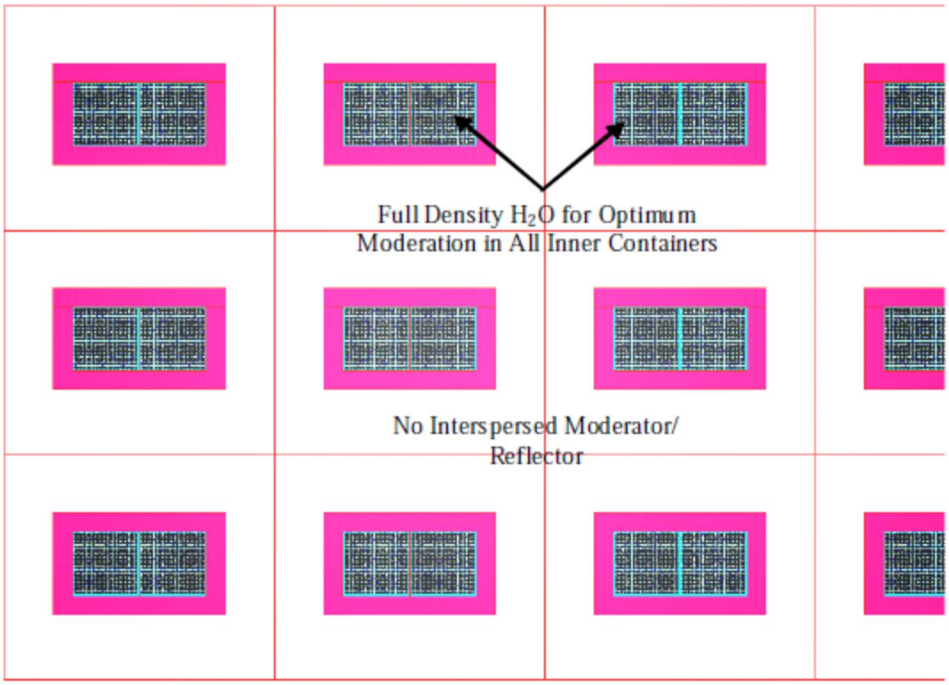

Figure 6-20 TN-B1 Fuel Rod Transport Package Array HAC Model

6.3.2. *Material Properties*

6.3.2.1. Material Tolerances

Table 6-7 Dimensional Tolerances provides sheet metal thickness dimensional tolerance from ASTM A240 and ASTM A480 (the former refers to the latter for specific tolerances). The table also provides the thicknesses used in the damaged and undamaged container models.

Table 6-7 Dimensional Tolerances

Stainless Steel Sheet Gauge	Nominal Thickness (mm)	Permissible Variations* (mm)	Model Thickness Used (in.) [cm] (description)
2 mm.	2.00 mm	± 0.18	0.0689 [0.175] (outer container wall)
1.5 mm	1.50 mm	± 0.15	0.0535 [0.136] (inner container wall)
1.0 mm.	1.00 mm	± 0.13	0.0344 [0.0875] (inner container fuel assembly compartments)

* ASTM-A240/A240M- 97b, Table A1.2, *Standard Specification for Heat Resisting Chromium and Chromium-Nickel Stainless Steel Plate, Sheet, and Strip for Pressure Vessels*, August 1997.

6.3.2.2. MATERIAL SPECIFICATIONS

Table 6-8 Material Specifications for the TN-B1 contains the material compositions for the TN-B1 shipping container. The UO_2 stack density is taken as 98% of theoretical. The presence of Gd_2O_3 in the UO_2-Gd_2O_3 pellet reduces the density from 10.74 to 10.67 g/cm^3.

Table 6-8 Material Specifications for the TN-B1

Material	Density (g/cm^3)	Constituent	Atomic Density (atoms/b-cm)
$U(5.0)O_2$ 98% Theoretical Density	10.74	U-235 U-238 O	$1.2128x10^{-3}$ $2.2753x10^{-2}$ $4.7931x10^{-2}$
$U(5.0)O_2$-Gd_2O_3 98% Theoretical Density 2 wt% Gd_2O_3 (75% credit for Gd)	10.67	U-235 U-238 O Gd-152 Gd-154 Gd-155 Gd-156 Gd-157 Gd-158 Gd-160	$1.18663x10^{-03}$ $2.22611x10^{-02}$ $4.76929x10^{-02}$ $1.06320x10^{-6}$ $1.15892x10^{-5}$ $7.86790x10^{-5}$ $1.08822x10^{-4}$ $8.31978x10^{-5}$ $1.32053x10^{-4}$ $1.16211x10^{-4}$
Zirconium	6.49	Zr	$4.2846x10^{-2}$
Stainless Steel 304	7.94	Fe Cr Ni Mn Si C P	$5.8545x10^{-2}$ $1.7473x10^{-2}$ $7.7402x10^{-3}$ $1.7407x10^{-3}$ $1.7025x10^{-3}$ $3.1877x10^{-4}$ $6.9468x10^{-5}$
Polyethylene Foam	≤ 0.05 – 0.075	C H	$3.4374x10^{-3}$ $6.8748x10^{-3}$
Low Density Polyethylene (LDPE) Insert	0.925	C H	$3.9745x10^{-2}$ $7.9490x10^{-2}$
Polyethylene Cluster Assembly	0.949	C H	$4.0776x10^{-2}$ $8.1552x10^{-2}$
Alumina Silicate [Al_2O_3(49%)-Si_{O2}(51%)]	0.25	Al Si O	$1.4474x10^{-3}$ $1.2783x10^{-3}$ $4.7277x10^{-3}$
Paper Honeycomb $C_6H_{10}O_5$	0.04 – 0.08	C H O	$1.7840x10^{-3}$ $2.9733x10^{-3}$ $1.4867x10^{-3}$
Full Density Water	1.0	H O	$6.6769x10^{-2}$ $3.3385x10^{-2}$

Polyethylene inserts or polyethylene cluster separators are positioned between fuel rods at various locations along the axis of the fuel assembly to avoid stressing the axial grids during transportation. The inserts are shown in Figure 6-1 while the separators are shown in Figure 6-2. The Low Density Polyethylene (LDPE) insert has a 0.925 g/cm^3 density and an approximate volume of 25 cm^3. Therefore, a 10x10 assembly with 9 polyethylene inserts has a 225 cm^3 total LDPE volume required for one location along the fuel assembly.

The cluster separator is composed of LDPE (0.925 g/cm^3) fingers and a High Density Polyethylene (HDPE, 0.959 g/cm^3) holder (The LDPE and HDPE densities are based on accepted industry definitions). The LDPE fingers (10x10) occupy an approximate volume of 38 cm^3 while the HDPE holder has an approximate volume of 85 cm^3. A volume average density of 0.949 g/cm^3 is calculated for the polyethylene cluster assembly, i.e.

$$\left[\frac{\{38cm^3 x\ 0.925g/cm^3\} + \{85cm^3 x\ 0.959g/cm^3\}}{123cm^3}\right]$$

For a 10x10 assembly, two cluster separators, shown in Figure 6-2, are placed at numerous locations along the fuel assembly. A total polyethylene volume of 246 cm^3 is calculated for each location in which the cluster separators are placed. The TN-B1 criticality calculations use the 10x10 cluster separator characteristics for the fuel types investigated. However, the polyethylene characteristics are only used to establish a polyethylene mass limit so that an accurate measurement of polyethylene characteristics by the user is unnecessary. Other plastics with equivalent hydrogen mass limits are acceptable. The following equation can be used to determine plastic equivalence (e.g., ABS plastic).

$$M_{eq,i} = M_{poly}\, x \frac{0.137}{\rho_{mix,i}\, x\, wf_{H,i}}$$

The formula for polyethylene mass equivalence is:

$M_{eq,i} = M_{poly}$ x [(rho$_{mix, poly}$)(wf$_{H, poly}$)]/[(rho$_{mix,i}$)(wf$_{H,i}$)]

= M_{poly} x [(0.949 g/cm^3)(0.144)]/[(rho$_{mix,i}$)(wf$_{H,i}$)]

= M_{poly} x (0.137 g/cm^3)/[(rho$_{mix,i}$)(wf$_{H,i}$)]

The fuel parameters used to calculate volume fractions for the water and polyethylene mixture in the TN-B1 normal condition model are shown in Table 6-9 TN-B1 Normal Condition Model Fuel Parameters. The volume fractions of polyethylene and water for the worst-case fuel assembly type analyzed are shown in Table 6-10 TN-B1 Normal Condition Model Polyethylene and Water Volume Fractions and Table 6-11 Single Package Normal and HAC Model Fuel Parameters. The volume fractions in Table 6-10 are entered into the model input standard composition specification area. Mixtures representing the polyethylene inserts between fuel rods are created using the compositions specified, and used in the KENO V.a calculation. The mixtures are also used in the lattice cell description to provide the lump shape and dimensions for resonance cross-section processing, the lattice corrections for cross-section processing, and the information necessary to create cell-weighted cross-sections.

Table 6-9 TN-B1 Normal Condition Model Fuel Parameters

Fuel Assembly	Fuel Rod OR (cm)	Number of Fuel Rods	Fuel Rod Pitch (cm)	Fuel Rod Length (cm)	Cluster Separator Volume Surrounding Fuel (cm^3)	Number of Part Length Fuel Rods
GNF 10x10	0.505	92	1.350	385	10,200	12

Table 6-10 TN-B1 Normal Condition Model Polyethylene and Water Volume Fractions

Fuel Assembly	Assembly Volume (cm^3)	Fuel Rod Volume (cm^3)	Interstitial Volume (cm^3)	Polyethylene Volume (cm^3)	Vf_{poly}	Vf_{H2O}
GNF 10x10	66,676.46	26,527.22	40,149.24	10,200	0.25405	0.74595

Table 6-11 Single Package Normal and HAC Model Fuel Parameters

Fuel Assembly	Partial Fuel Rods (#)	Pitch (cm)	Pellet Diameter (cm)	Clad Inner Diameter (cm)	Clad Outer Diameter (cm)
GNF 10X10	12	1.350	0.895	0.9338	1.010

In the hypothetical accident condition model, the polyethylene inserts are assumed to melt when subjected to the tests specified in 10 CFR Part 71. The polyethylene is assumed to uniformly coat the fuel rods in each fuel assembly forming a cylindrical layer of polyethylene around each fuel rod. Different coating thicknesses are investigated, and a maximum thickness is determined to set a polyethylene mass limit for each fuel assembly type considered for transport. The fuel assembly parameters used to calculate the polyethylene mass limits are shown in Table 6-12 Fuel Assembly Parameters for Polyethylene Mass Calculations. For the fuel parameter sensitivity study and the worst-case fuel assembly models, the polyethylene is smeared into the fuel rod cladding to accommodate the limitations in the lattice cell modeling for cross-section processing in SCALE. A visual representation of the smeared clad/polyethylene mixture compared to a discrete treatment is shown in Figure 6-21 Visual Representation of the Clad/Polyethylene Smeared Mixture versus Discrete Modeling. The polyethylene mass and the volume fractions of polyethylene and zirconium clad for each fuel assembly analyzed are shown in Table 6-13 Polyethylene Mass and Volume Fraction Calculations. The volume fractions in Table 6-13 are entered into the model input standard composition specification area. Mixtures representing the polyethylene inserts between fuel rods are created using the compositions specified, and used in the KENO V.a calculation. The mixtures are also used in the lattice cell description to provide the lump shape and dimensions for resonance cross-section processing, the lattice corrections for cross-section processing, and the information necessary to create cell-weighted cross-sections.

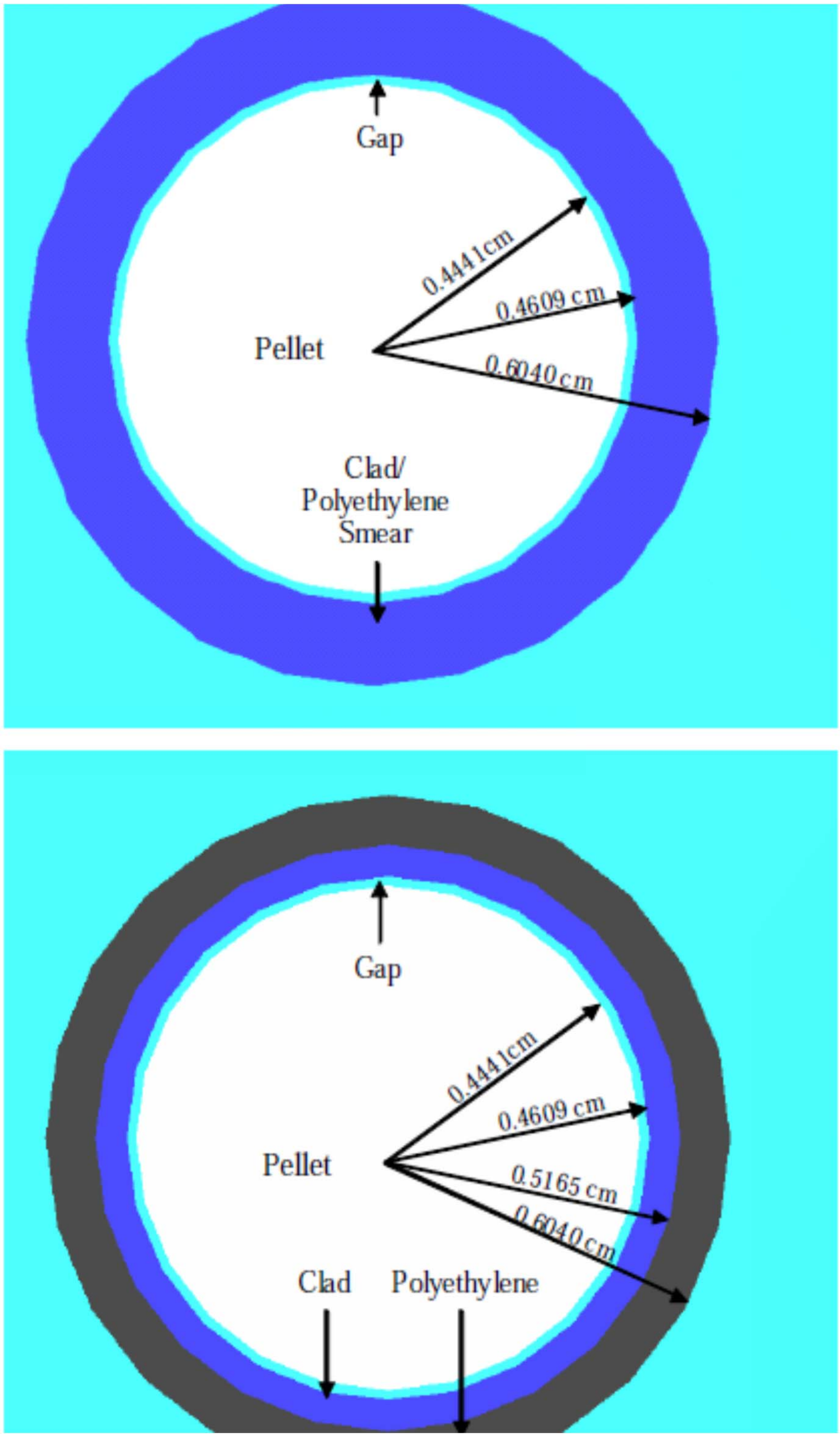

Figure 6-21 Visual Representation of the Clad/Polyethylene Smeared Mixture versus Discrete Modeling

Table 6-12 Fuel Assembly Parameters for Polyethylene Mass Calculations

Fuel Assembly Design	Fuel Rod OR (cm)	Number of Fuel Rods	Fuel Rod Pitch (cm)	Fuel Rod Length (cm)	Fuel Rod IR (cm)
ATRIUM 10x10	0.5165	91	1.284	383.54	0.4609
GNF 10x10	0.50927	92	1.2954	381	0.46609
Framatome 9x9	0.54991	72	1.4478	381	0.48006
GNF 9x9	0.55499	74	1.43764	381	0.49149
GNF 8x8	0.6096	60	1.6256	381	0.53594

Table 6-13 Polyethylene Mass and Volume Fraction Calculations

Radius (cm)	Thickness (cm)	Total Poly Volume[a] (cm^3)	Total Poly Mass[b] (g)	$Volume_{poly}$ Per Fuel Rod[c] (cm^3)	$Volume_{clad}$ Per Fuel Rod[d] (cm^3)	Vf_{clad}[e]	Vf_{poly}[f]
Two ATRIUM 10x10 Fuel Assemblies							
0.51650	0.00000	0	0	0.00	65.47985	1.00000	0.00000
0.56504	0.04854	11512.03	10924.92	63.25	65.47985	0.50865	0.49135
0.59071	0.07421	18019.18	17100.20	99.01	65.47985	0.39809	0.60191
0.60395	0.08745	21487	20391.16	118.06	65.47985	0.35676	0.64324
0.61369	0.08000	24087.04	22858.60	132.35	65.47985	0.33100	0.66900
0.62343	0.10693	26729.6	25366.39	146.87	65.47985	0.30836	0.69164
0.63317	0.11667	29414.68	27914.53	161.62	65.47985	0.28833	0.71167
Two GNF 10x10 Fuel							
0.50927	0.00000	0	0	0.00	50.41067	1.00000	0.00000
0.55824	0.04897	11512.03	10924.92	62.57	50.41067	0.44621	0.55379
0.59086	0.08159	19768.04	18759.87	107.43	50.41067	0.31937	0.68063
0.59743	0.08816	21487	20391.16	116.78	50.41067	0.30152	0.69848
0.60723	0.09796	24087.04	22858.6	130.91	50.41067	0.27802	0.72198
0.61703	0.10776	26729.6	25366.39	145.27	50.41067	0.25762	0.74238
0.62683	0.11756	29414.68	27914.53	159.86	50.41067	0.23974	0.76026
Two Framatome 9x9 Fuel Assemblies							
0.5499	0.0000	0	0	0.00	86.11243	1.00000	0.00000
0.6470	0.0971	20021.07	19000	139.04	86.11243	0.38247	0.61753
0.6610	0.1111	23182.3	22000	160.99	86.11243	0.34849	0.65151
0.6702	0.1203	25289.78	24000	175.62	86.11243	0.32901	0.67099
0.6792	0.1293	27397.26	26000	190.26	86.11243	0.31158	0.68842
0.6882	0.1383	29504.74	28000	204.89	86.11243	0.29591	0.70409
0.6970	0.1471	31612.22	30000	219.53	86.11243	0.28174	0.71826

Table 6-13 Polyethylene Mass and Volume Fraction Calculations (continued)

Radius (cm)	Thickness (cm)	Total Poly Volume[a] (cm^3)	Total Poly Mass[b] (g)	$Volume_{poly}$ Per Fuel Rod[c] (cm^3)	$Volume_{clad}$ Per Fuel Rod[d] (cm^3)	Vf_{clad}[e]	Vf_{poly}[f]
Two GNF 9x9 Fuel							
0.55499	0.00000	0	0	0.00	79.53889	1.00000	0.00000
0.65344	0.09845	21074.82	20000	142.40	79.53889	0.35839	0.64161
0.66248	0.10749	23182.3	22000	156.64	79.53889	0.33678	0.66322
0.67140	0.11641	25289.78	24000	170.88	79.53889	0.31763	0.68237
0.68020	0.12521	27397.26	26000	185.12	79.53889	0.30054	0.69946
0.68889	0.13390	29504.74	28000	199.36	79.53889	0.28519	0.71481
0.69747	0.14248	31612.22	30000	213.60	79.53889	0.27134	0.72866
Two GNF 8x8 Fuel							
0.60960	0.00000	0	0	0.00	100.9989	1.00000	0.00000
0.71484	0.10524	20021.07	19000	166.84	100.9989	0.37709	0.62291
0.73008	0.12048	23182.3	22000	193.19	100.9989	0.34332	0.65668
0.74006	0.13046	25289.78	24000	210.75	100.9989	0.32398	0.67602
0.74990	0.14030	27397.26	26000	228.31	100.9989	0.30670	0.69330
0.75962	0.15002	29504.74	28000	245.87	100.9989	0.29117	0.70883
0.76922	0.15962	31612.22	30000	263.44	100.9989	0.27714	0.72286

The following example calculations are for two Atrium 10x10 assemblies with a total 21,487 cm^3 polyethylene volume:

a. Total Polyethylene Volume = (Total Fuel Rod Number)x(2 Fuel Assemblies)x(Polyethylene Area)x(Fuel Rod Length)

$$Volume = (91\,fuelrods)(2\,fuelassemblies)\left\{(\pi)\left[(0.60395cm)^2 - (0.5165cm)^2\right]\right\}(383.54cm) = 21487cm^3$$

b. Total Polyethylene Mass = (Total Polyethylene Volume)x(Polyethylene Density)

$$Mass = \left(21487cm^3\right)\left(0.949\frac{g}{cm^3}\right) = 20391.16g$$

c. Polyethylene Volume per Fuel Rod = Total Polyethylene Volume/Total Fuel Rod Number

$$\frac{Volume_{Poly}}{FuelRod} = \frac{21487cm^3}{(91\,fuelrods)(2\,fuelassemblies)} = 118.06cm^3$$

d. Clad Volume per Fuel Rod = [(Fuel Rod Area to Outer Clad)-(Fuel Rod Area to Inner Clad)]x Fuel Rod Length

$$\frac{Volume_{clad}}{FuelRod} = (\pi)\left[(0.5165cm)^2 - (0.4609cm)^2\right](383.54cm) = 65.48cm^3$$

e. Clad Volume Fraction = Clad Volume/Total Clad and Polyethylene Volumes

$$VF_{clad} = 65.48cm^3 \Big/ \left[(118.06cm^3)(65.48cm^3)\right] = 0.35676$$

f. Polyethylene Volume Fraction = Polyethylene Volume/ Total Clad and Polyethylene Volumes

$$VF_{Poly} = 118.06cm^3 \Big/ \left[(118.06cm^3)(65.48cm^3)\right] = 0.64323$$

6.3.3. *Computer Codes and Cross-Section Libraries*

The calculational methodology employed in the analyses is based on that embodied in SCALE -PC (version 4.4a), as documented in Reference 8. The neutron cross-section library employed in the analyses and the supporting validation analyses was the 44 group ENDF/B-V library distributed with version 4.4a of the SCALE package. Each case was run using the CSAS25 sequence of codes, i.e., BONAMI, NITAWL, and KENO V.a. For each case, 400 generations with 2,500 neutrons per generation were run to ensure proper behavior about the mean value. The methodology and results of the validation of SCALE 4.4a on the PC is outlined in Section 6.10, and results in an Upper Safety Limit (USL) that is the basis for comparison to ensure subcriticality.

For the performance of the Uranium-Carbide and PWR loose rod provision analysis, the GEMER Monte Carlo code was used. GEMER is a Monte Carlo neutron transport code developed by combining geometry and Monte Carlo features from the KENO IV and MERIT Monte Carlo codes and be adding enhance geometry, picture geometry checking and editing features (Ref. 4). Hence, GEMER is the evolution of Geometry Enhanced MERIT. The MERIT code is premised on the Battelle Northwest Laboratory's BMC code and is characterized by its explicit treatment of resolved resonance in material cross section set. Functionally, the GEMER Monte Carlo code is similar in analytic capability to other industry recognized codes such as KENO Va. or MCNP.

Cross sections in GEMER are currently processed from the ENDF/B-IV library in multigroup and resonance parameter formats. Cross-sections are prepared in the 190 energy group format and those in the resonance energy range have the form of resonance parameters. The resonance parameters describe the cross sections in the resonance range and Monte Carlo sampling in this range is done from resonance kernels rather than from broad group cross sections (i.e., explicit treatment of resolved resonance's using a single level Breit-Wigner equation at each collision in the resonance energy range). Thus there is a single unique cross section set associated with each available isotope and dependence is not placed on Dancoff (flux shadowing) correction factors or effective scattering cross sections. This treatment of cross-sections with explicit resonance parameters is especially suited to the analysis of uranium compounds in the form of heterogeneous accumulations, lattices, or systems containing nuclear poisons.

Thermal scattering of hydrogen is represented by the Hayward Kernel $S(\alpha,\beta)$ data in the ENDF/B-IV library. The types of reactions considered in the GEMER Monte Carlo calculation are fission, capture, elastic, inelastic, and (n, 2n) reactions; absorption is implicitly treated by applying the non-absorption probability to neutron weights on each collision. As part of the solutions, GEMER produces eigenvalue, micro- and macro-group fluxes, reaction rates, cross sections, and neutron balance by isotopes.

6.3.4. *Demonstration of Maximum Reactivity*

The objectives for the TN-B1 shipping container analysis are to demonstrate package criticality safety and determine fuel loading criteria. To accomplish these objectives, calculations are performed to determine the most reactive fuel configuration inside the TN-B1 assembly compartments. Once the fuel configuration is determined, moderator and reflector conditions are investigated. Finally, package orientation (for arrays) is examined. When the worst-case fuel configuration, moderator/reflector conditions, and package orientation are found, the single package and package array calculations under both normal and hypothetical accident conditions are performed.

6.3.4.1. **Fuel Assembly Orientation Study (2N=448)**

The package array dimensions for the fuel assembly orientation are 14x2x16 (width x depth x height). Initial calculations are performed to find the worst-case fuel assembly orientation inside each TN-B1 fuel compartment. Nominal fuel assembly dimensions are used for these initial calculations (Table 6-4). Note that in all cases with cladding, zirconium is used to conservatively represent any zirconium alloy. The package array HAC model described in Section 6.3.1.2.2 is used and the fuel assembly orientations depicted in Figure 6-9 through Figure 6-15 are applied. In addition, a polyethylene coating covers each fuel rod in the assembly, the fuel assembly is un-channeled, and the moderator density is 1.0 g/cm^3 in the TN-B1 inner container fuel region. The polyethylene foam is assumed to burn away, Alumina Silicate thermal insulator envelopes the inner container, and no water is in either the outer container or between packages in the array. The results of the calculations are shown in Table 6-14 TN-B1 Array HAC Fuel Assembly Orientation. Based on the results in Table 6-14, assembly orientation 6, is bounding for all designs. Therefore, orientation 6 with the assembly centered in each fuel compartment is used in the remaining design calculations. It is also noted that most results in Table 6-14 exceed the 0.94254 USL. For this reason, gadolinia-urania fuel rods are added to the fuel assemblies to provide reactivity hold-down.

Table 6-14 TN-B1 Array HAC Fuel Assembly Orientation

Fuel Assembly	Interspersed Moderator Density (g/cm^3)	Polyethylene Mass Per Assembly (kg)	Assembly Orientation	k_{eff}	σ	$k_{eff} + 2\sigma$
FANP 10x10	0.0	10.2	1	0.9375	0.0010	0.9395
FANP 10x10	0.0	10.2	2	0.9529	0.0008	0.9545
FANP 10x10	0.0	10.2	3	0.8973	0.0008	0.8989
FANP 10x10	0.0	10.2	4	0.8965	0.0010	0.8985
FANP 10x10	0.0	10.2	5	0.9248	0.0010	0.9268
FANP 10x10	0.0	10.2	6	0.9741	0.0009	**0.9759** [b]
FANP 10x10	0.0	10.2	7	0.9486	0.0009	0.9504
GNF 10x10	0.0	10.2	1	0.9586	0.0010	0.9606
GNF 10x10	0.0	10.2	2	0.9721	0.0009	0.9739
GNF 10x10	0.0	10.2	3	0.9184	0.0008	0.9200
GNF 10x10	0.0	10.2	4	0.9183	0.0009	0.9201
GNF 10x10	0.0	10.2	5	0.9431	0.0008	0.9447
GNF 10x10	0.0	10.2	6	0.9909	0.0010	**0.9929** [b]
GNF 10x10	0.0	10.2	7	0.9652	0.0008	0.9668
FANP 9x9[a]	0.0	11	1	0.9486	0.0009	0.9504
FANP 9x9	0.0	11	2	0.9559	0.0009	0.9577
FANP 9x9	0.0	11	3	0.9052	0.0008	0.9068
FANP 9x9	0.0	11	4	0.9056	0.0008	0.9072
FANP 9x9	0.0	11	5	0.9293	0.0010	0.9313
FANP 9x9	0.0	11	6	0.9791	0.0008	**0.9807** [b]
FANP 9x9	0.0	11	7	0.9362	0.0009	0.9380
GNF 9x9	0.0	11	1	0.9491	0.0008	0.9507
GNF 9x9	0.0	11	2	0.9577	0.0008	0.9593
GNF 9x9	0.0	11	3	0.9051	0.0008	0.9067
GNF 9x9	0.0	11	4	0.9042	0.0009	0.9060
GNF 9x9	0.0	11	5	0.9287	0.0009	0.9305
GNF 9x9	0.0	11	6	0.9787	0.0008	**0.9803** [b]
GNF 9x9	0.0	11	7	0.9556	0.0008	0.9572
GNF 8x8	0.0	11	1	0.9506	0.0009	0.9524
GNF 8x8	0.0	11	2	0.9563	0.0008	0.9579

a. The Framatome D-lattice 9x9 assembly was modeled. However, the results presented here are applicable to the C-lattice as well

b. Limiting case shown in bold

Table 6-14 TN-B1 Array HAC Fuel Assembly Orientation (continued)

Fuel Assembly	Interspersed Moderator Density (g/cm^3)	Polyethylene Mass Per Assembly (kg)	Assembly Orientation	k_{eff}	σ	k_{eff} + 2σ
GNF 8x8	0.0	11	3	0.9048	0.0008	0.9064
GNF 8x8	0.0	11	4	0.9052	0.0009	0.9070
GNF 8x8	0.0	11	5	0.9299	0.0009	0.9317
GNF 8x8	0.0	11	6	0.9764	0.0008	**0.9780**[b]
GNF 8x8	0.0	11	7	0.9554	0.0009	0.9572

b. Limiting case shown in bold

6.3.4.2. **Fuel Assembly Gadolinia Rod Study (2N=448)**

Fuel assemblies with lattice average U-235 enrichments of 5.0 wt% are qualified for transport in the TN-B1 shipping container by crediting the gadolinia-urania fuel rods present in the assembly. The gadolinia-urania fuel rods decrease system reactivity such that the k_{eff} + 2σ remains below the 0.94254 USL. The gadolinia content of each gadolinia-urania fuel rod is limited to 75% of the value specified in Table 6-1. Scoping studies are performed using numerous gadolinia-urania fuel rod placement patterns in the orientation 6 models, from the fuel assembly orientation study, to find the pattern that yields the highest reactivity for each fuel assembly type. Of the patterns investigated, three patterns that produce the highest reactivity for each fuel assembly type are shown in Figure 6-22 - Figure 6-24. The calculations are performed using optimum moderator conditions. The results for the 14x2x16 TN-B1 container array transporting 10x10, 9x9, or 8x8 fuel assembies with gadolinia-urania fuel rods arranged in the patterns displayed in Figure 6-22 - Figure 6-24 are listed in Table 6-15. As shown in Table 6-15, the gadolinia-urania fuel rods hold the system reactivity below the 0.94254 USL. Based on the gadolinia-urania fuel rod pattern optimization calculations:

- Gadolinia-urania fuel rod Pattern G is selected for future FANP 10x10 fuel assembly sensitivity calculations;
- Gadolinia-urania fuel rod Pattern B is selected for future GNF 10x10 fuel assembly sensitivity calculations;
- Gadolinia-urania fuel rod Pattern A is selected for future FANP and GNF 9x9 fuel assembly sensitivity calculations; and
- Gadolinia-urania fuel rod Pattern I is selected for future GNF 8x8 fuel assembly sensitivity calculations.

Table 6-15 TN-B1 Shipping Container 14x2x16 Array with Gadolinia- Urania Fuel Rods

Assembly Type	Pattern Designation	U-235 Enrich (wt%)	Gad Rod #	Pitch (cm)	Pellet Diameter (cm)	Clad ID (cm)	Clad OD (cm)	k_{eff}	σ	k_{eff} + 2σ
FANP 10x10	B	5.0	12	1.284	0.8882	0.9218	1.033	0.8716	0.0008	0.8732
FANP 10x10	F	5.0	12	1.284	0.8882	0.9218	1.033	0.8699	0.0008	0.8715
FANP 10x10	G	5.0	12	1.284	0.8882	0.9218	1.033	0.8732	0.0008	**0.8748**
GNF 10x10	B	5.0	12	1.2954	0.8941	0.9322	1.019	0.8886	0.0008	**0.8902**
GNF 10x10	G	5.0	12	1.2954	0.8941	0.9322	1.019	0.8871	0.0008	0.8887
GNF 10x10	H	5.0	12	1.2954	0.8941	0.9322	1.019	0.8880	0.0009	0.8898
FANP 9x9	A	5.0	10	1.4478	0.9398	0.9601	1.099	0.8644	0.0007	**0.8658**
FANP 9x9	B	5.0	10	1.4478	0.9398	0.9601	1.099	0.8605	0.0008	0.8621
FANP 9x9	E	5.0	10	1.4478	0.9398	0.9601	1.099	0.8354	0.0009	0.8372
GNF 9x9	A	5.0	10	1.4376	0.9550	0.9830	1.110	0.8579	0.0008	**0.8596**
GNF 9x9	B	5.0	10	1.4376	0.9550	0.9830	1.110	0.8572	0.0008	0.8588
GNF 9x9	F	5.0	10	1.4376	0.9550	0.9830	1.110	0.8524	0.0009	0.8540
GNF 8x8	E	5.0	7	1.6256	1.0439	1.0719	1.219	0.8779	0.0009	0.8797
GNF 8x8	G	5.0	7	1.6256	1.0439	1.0719	1.219	0.8726	0.0008	0.8742
GNF 8x8	I	5.0	7	1.6256	1.0439	1.0719	1.219	0.8800	0.0009	**0.8818**

a. Limiting case(s) shown in bold

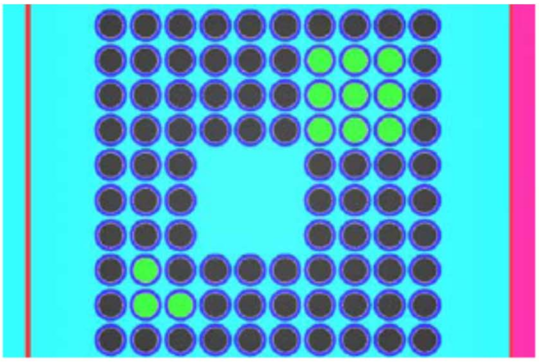

FANP 10x10 5.0 wt% ^{235}U, Pattern B

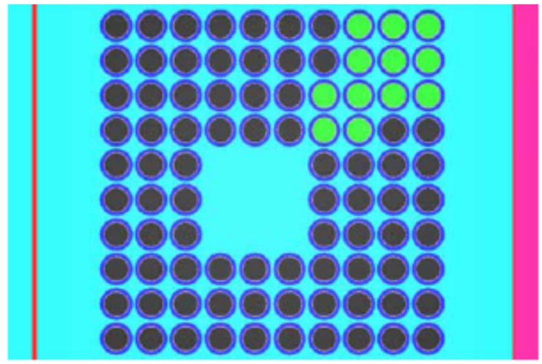

FANP 10x10 5.0 wt% ^{235}U, Pattern F

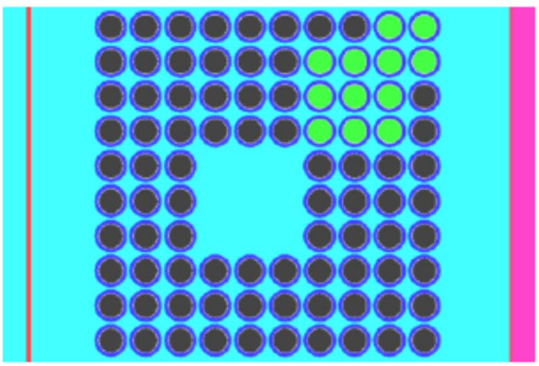

FANP 10x10 5.0 wt% ^{235}U, Pattern G

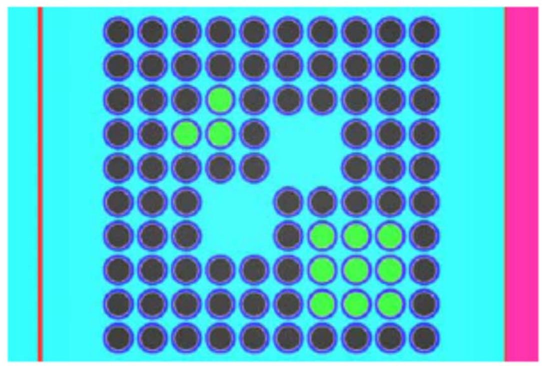

GNF 10x10 5.0 wt% ^{235}U, Pattern B

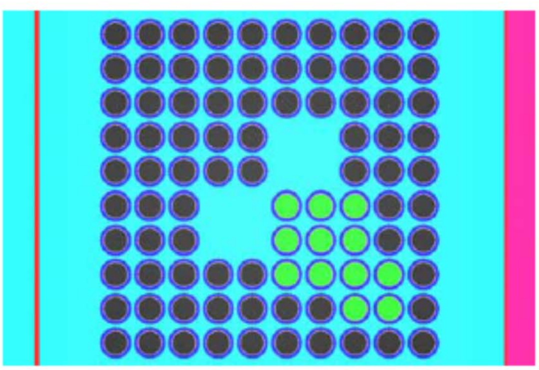

GNF 10x10 5.0 wt% ^{235}U, Pattern G

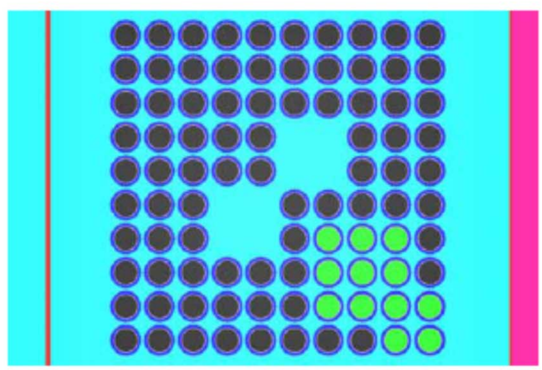

GNF 10x10 5.0 wt% ^{235}U, Pattern H

Figure 6-22 Gadolinia-Urania Fuel Rod Placement Pattern for 10x10 Fuel Assemblies at 5.0 wt% 235U

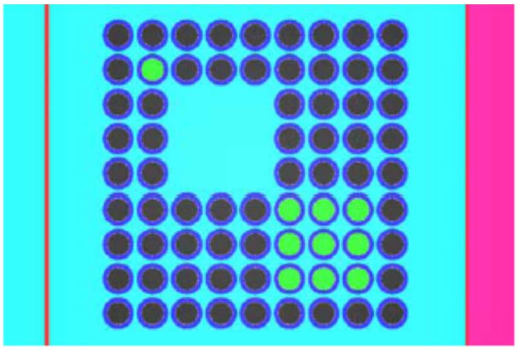

FANP 9x9 5.0 wt% ^{235}U, Pattern A

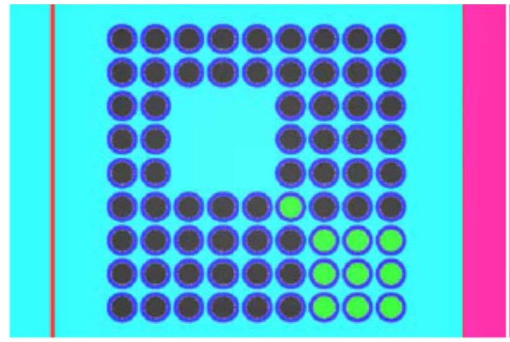

FANP 9x9 5.0 wt% ^{235}U, Pattern B

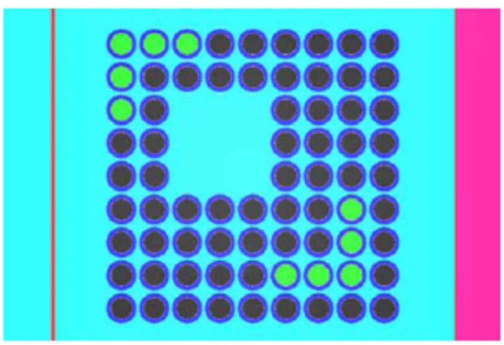

FANP 9x9 5.0 wt% ^{235}U, Pattern E

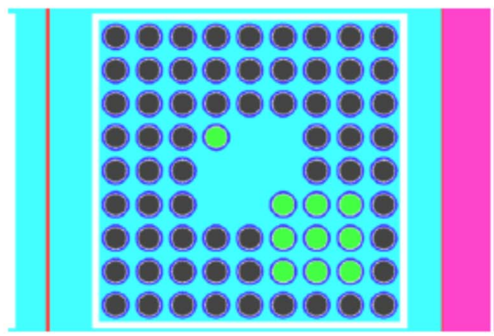

GNF 9x9 5.0 wt% ^{235}U, Pattern A

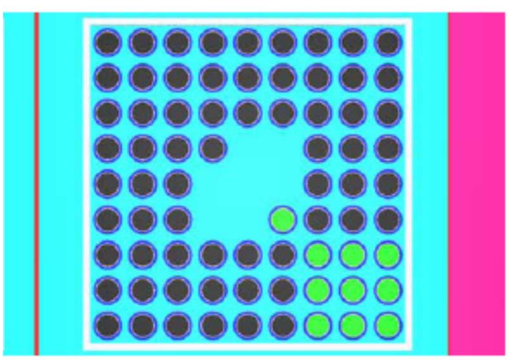

GNF 9x9 5.0 wt% ^{235}U, Pattern B

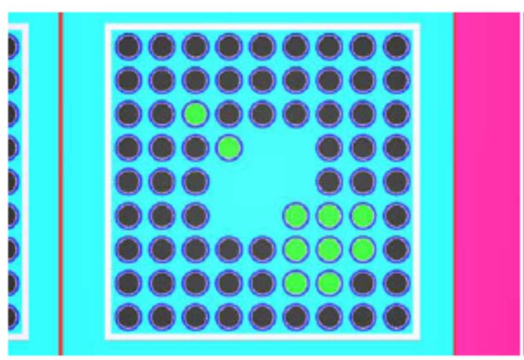

GNF 9x9 5.0 wt% ^{235}U, Pattern F

Figure 6-23 Gadolinia-Urania Fuel Rod Placement Pattern for 9x9 Fuel Assemblies at 5.0 wt% 235U

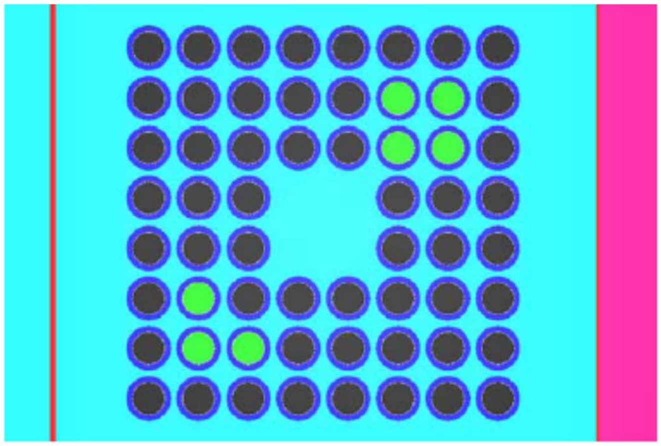

GNF 8x8 5.0 wt% ^{235}U, Pattern E

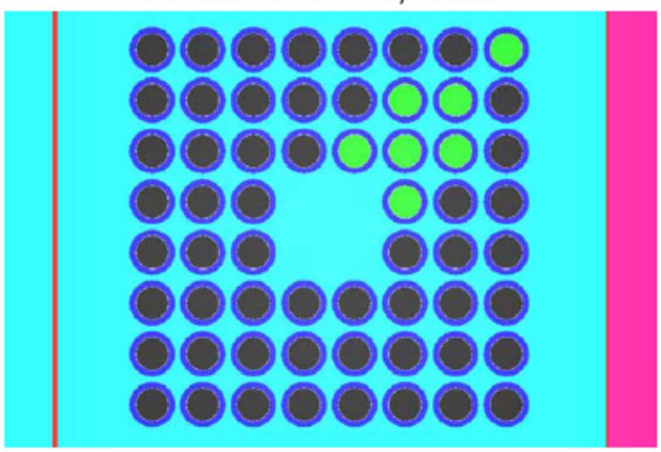

GNF 8x8 5.0 wt% ^{235}U, Pattern G

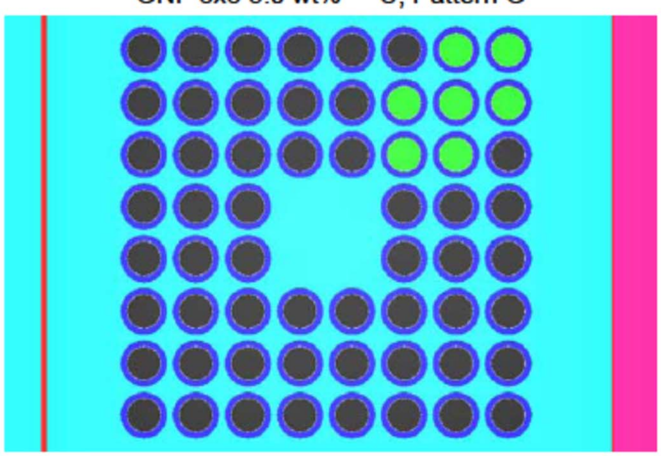

GNF 8x8 5.0 wt% ^{235}U, Pattern I

Figure 6-24 Gadolinia-Urania Fuel Rod Placement Pattern for 8x8 Fuel Assemblies at 5.0 wt% 235U

6.3.4.3. **Fuel Assembly Channel Study (2N=448)**

A calculation is performed to determine if the presence of channels around the fuel assembly increases system reactivity. The orientation 6 models with the gadolina-urania fuel rod patterns that produced the highest system reactivity from the previous studies are used and a zirconium channel is placed around each assembly as shown in Figure 6-16 TN-B1 Hypothetical Accident Condition Model with Channels. The channel thickness is varied from 0.17 cm to 0.3048 cm and the impact on reactivity is assessed. The fuel assembly channel is located in the reflector region for each fuel assembly. It has no effect on the assembly H/X ratio since it is not located within the fuel envelope. Therefore, removing it would not have the same impact on system reactivity as removing the internal grid structure. The results are shown in Table 6-16. Comparing the results in Table 6-16 and Table 6-15 indicates reactivity increases with the presence of channels due to increased neutron leakage from the inner fuel compartment, resulting in increased neutron interaction among containers in the array. Therefore, channels will be included in subsequent calculations.

Table 6-16 TN-B1 Sensitivity Analysis for Channeled Fuel Assemblies

Assembly Type	Channel Thickness (cm)	Poly Mass per Assembly (kg)	Pitch (cm)	Pellet Diameter (cm)	Clad ID (cm)	Clad OD (cm)	k_{eff}	σ	k_{eff} + 2σ
FANP 10x10	0.1700	10.2	1.284	0.8882	0.9218	1.033	0.8801	0.0008	0.8817
FANP 10x10	0.2032	10.2	1.284	0.8882	0.9218	1.033	0.8786	0.0008	0.8802
FANP 10x10	0.2540	10.2	1.284	0.8882	0.9218	1.033	0.8815	0.0009	**0.8833**
FANP 10x10	0.3048	10.2	1.284	0.8882	0.9218	1.033	0.8810	0.0008	0.8826
GNF 10x10	0.1700	10.2	1.2954	0.8941	0.9322	1.019	0.8922	0.0009	0.8940
GNF 10x10	0.2032	10.2	1.2954	0.8941	0.9322	1.019	0.8948	0.0008	0.8964
GNF 10x10	0.2540	10.2	1.2954	0.8941	0.9322	1.019	0.8947	0.0008	0.8963
GNF 10x10	0.3048	10.2	1.2954	0.8941	0.9322	1.019	0.8953	0.0008	**0.8969**
FANP 9x9	0.1700	11	1.4478	0.9398	0.9601	1.0998	0.8719	0.0009	0.8737
FANP 9x9	0.2032	11	1.4478	0.9398	0.9601	1.0998	0.8724	0.0009	0.8742
FANP 9x9	0.2540	11	1.4478	0.9398	0.9601	1.0998	0.8739	0.0008	0.8756
FANP 9x9	0.3048	11	1.4478	0.9398	0.9601	1.0998	0.8755	0.0009	**0.8773**

a. Limiting case(s) shown in bold

Table 6-16 TN-B1 Sensitivity Analysis for Channeled Fuel Assemblies (continued)

Assembly Type	Channel Thickness (cm)	Poly Mass per Assembly (kg)	Pitch (cm)	Pellet Diameter (cm)	Clad ID (cm)	Clad OD (cm)	k_{eff}	σ	k_{eff} + 2σ
GNF 9x9	0.1700	11	1.4376	0.9550	0.9830	1.11	0.8626	0.0009	0.8644
GNF 9x9	0.2032	11	1.4376	0.9550	0.9830	1.11	0.8651	0.0009	0.8669
GNF 9x9	0.2540	11	1.4376	0.9550	0.9830	1.11	0.8654	0.0010	**0.8674**
GNF 9x9	0.3048	11	1.4376	0.9550	0.9830	1.11	0.8659	0.0008	0.8676
GNF 8x8	0.1700	11	1.6256	1.0439	1.0719	1.2192	0.8834	0.0010	0.8854
GNF 8x8	0.2032	11	1.6256	1.0439	1.0719	1.2192	0.8857	0.0008	0.8873
GNF 8x8	0.2540	11	1.6256	1.0439	1.0719	1.2192	0.8884	0.0009	0.8902
GNF 8x8	0.3048	11	1.6256	1.0439	1.0719	1.2192	0.8900	0.0009	**0.8918**

a. Limiting case(s) shown in bold

6.3.4.4. **Polyethylene Mass Study (2N=448)**

The effect that polyethylene mass has on reactivity for each fuel assembly design is considered for transport in the TN-B1 shipping container. The results of the previous sensitivity studies are taken into consideration for the polyethylene mass study. The worst-case channeled (0.3048 cm thick channels) models, used in the previous study, are used for the polyethylene mass study.

The polyethylene and clad volume fractions, shown in Table 6-13, are used in the model material description to represent the polyethylene and clad mixture. They are also used in the lattice cell description for resonance cross-section processing. The polyethylene coating thickness around the fuel rods is varied, and the effect on reactivity is determined. The results of the calculations, Table 6-26, are displayed in Figure 6-25 TN-B1 Array HAC Polyethylene Sensitivity. Although the polyethylene addition increases reactivity, the increase is gradual and the resulting system k_{eff} remains subcritical. Based on the results in Figure 6-25:

- a polyethylene mass of 10.2 kg/assembly (20.4 kg/container) is chosen for further FANP and GNF 10x10 calculations; and
- an 11 kg/assembly (22 kg/container) polyethylene mass is selected for subsequent FANP 9x9, GNF 9x9, and GNF 8x8 fuel assembly calculations.

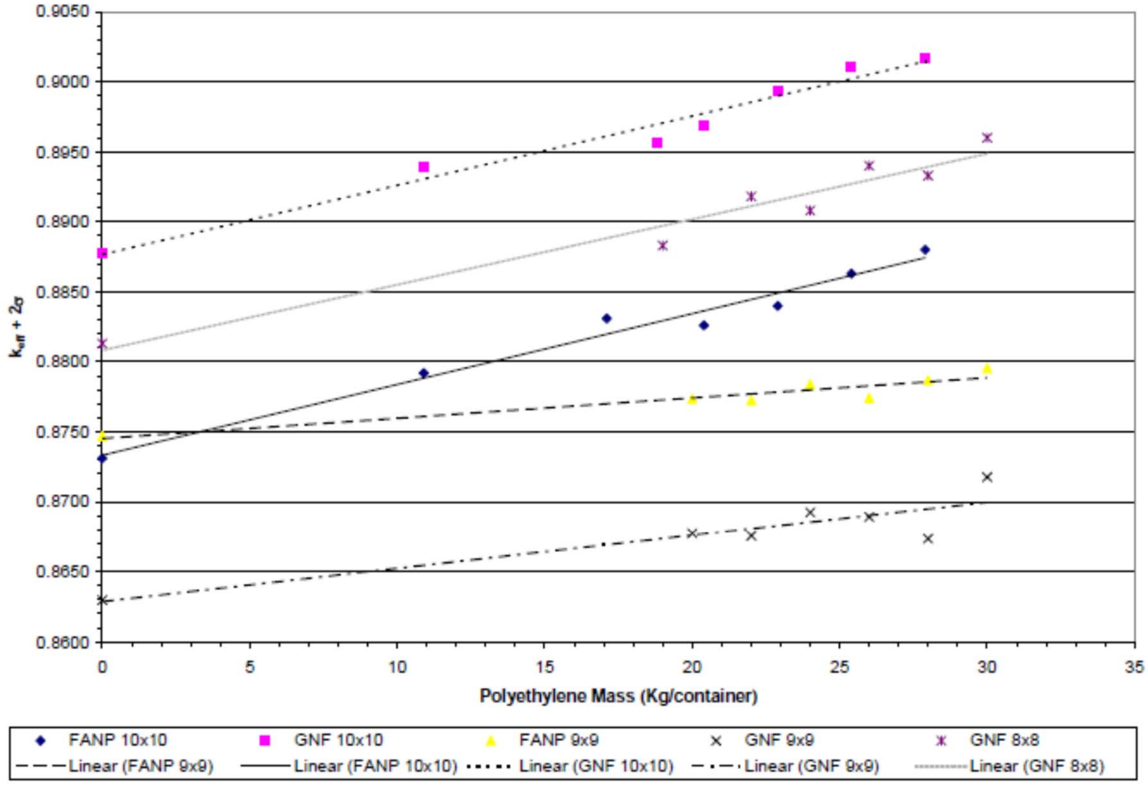

Figure 6-25 TN-B1 Array HAC Polyethylene Sensitivity

6.3.4.5. **Fuel Rod Pitch Sensitivity Study (2N=448)**

A fuel rod pitch sensitivity study is conducted using the worst-case models from the polyethylene sensitivity study. The minimum fuel rod pitch is chosen to be at the point that the polyethylene coating on adjacent fuel rods contact. The maximum fuel rod pitch is chosen to be 4.1% greater than the reference fuel designs to bound the damage sustained during the 9 meter drop. The results are shown in Figure 6-26 TN-B1 Fuel Rod Pitch Sensitivity Study. Based on the results in Figure 6-26, the fuel assemblies are under-moderated such that increasing the pitch increases system reactivity. Based on the pitch sensitivity calculations (Table 6-27):

- a 1.350 cm fuel rod pitch is selected as the upper limit for FANP and GNF 10x10 pitch range;
- a 1.510 cm fuel rod pitch is selected as the upper limit for FANP and GNF 9x9 pitch range; and
- a 1.6923 cm fuel rod pitch is selected as the upper limit for GNF 8x8 pitch range.

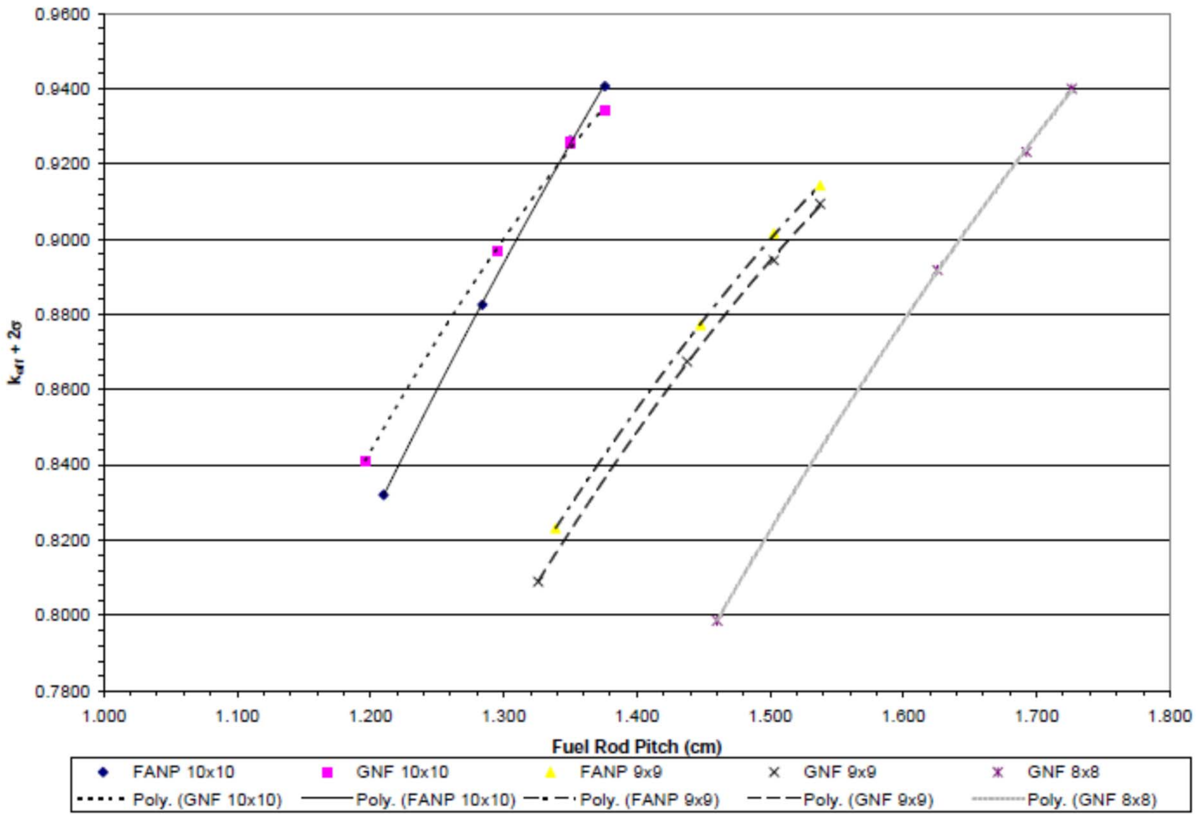

Figure 6-26 TN-B1 Fuel Rod Pitch Sensitivity Study

6.3.4.6. **Fuel Pellet Diameter Sensitivity Study (2N=448)**

With a polyethylene quantity chosen, the worst-case orientation known, the channeled fuel effect assessed, and the worst-case gadolinia-urania fuel rod patterns identified, a fuel pellet diameter sensitivity study is conducted. For the pellet diameter sensitivity study, the package array HAC model described in Section 6.3.1.2.2 is used for the study, fuel assembly orientation 6 is selected based on the results in Table 6-14, the maximum polyethylene amount for each fuel assembly design is chosen, the worst-case gadolinia-urania rod pattern is selected, the inner container fuel compartment is maintained at optimum density water, an Alumina Silicate thermal insulator envelopes the inner container fuel compartment, and water is removed from the outer container and between packages in the array. The results are shown in Figure 6-27 TN-B1 Array HAC Pellet Diameter Sensitivity Study. The results in Figure 6-27, demonstrate that reactivity increases as pellet diameter is increased. Pellet diameters of 0.895 cm for the FANP and GNF 10x10 designs, 0.96 cm for the Framatome and GNF 9x9 designs, and 1.05 cm for the GNF 8x8 design are found acceptable as the upper bounds for the fuel assembly design pellet ranges (Table 6-28).

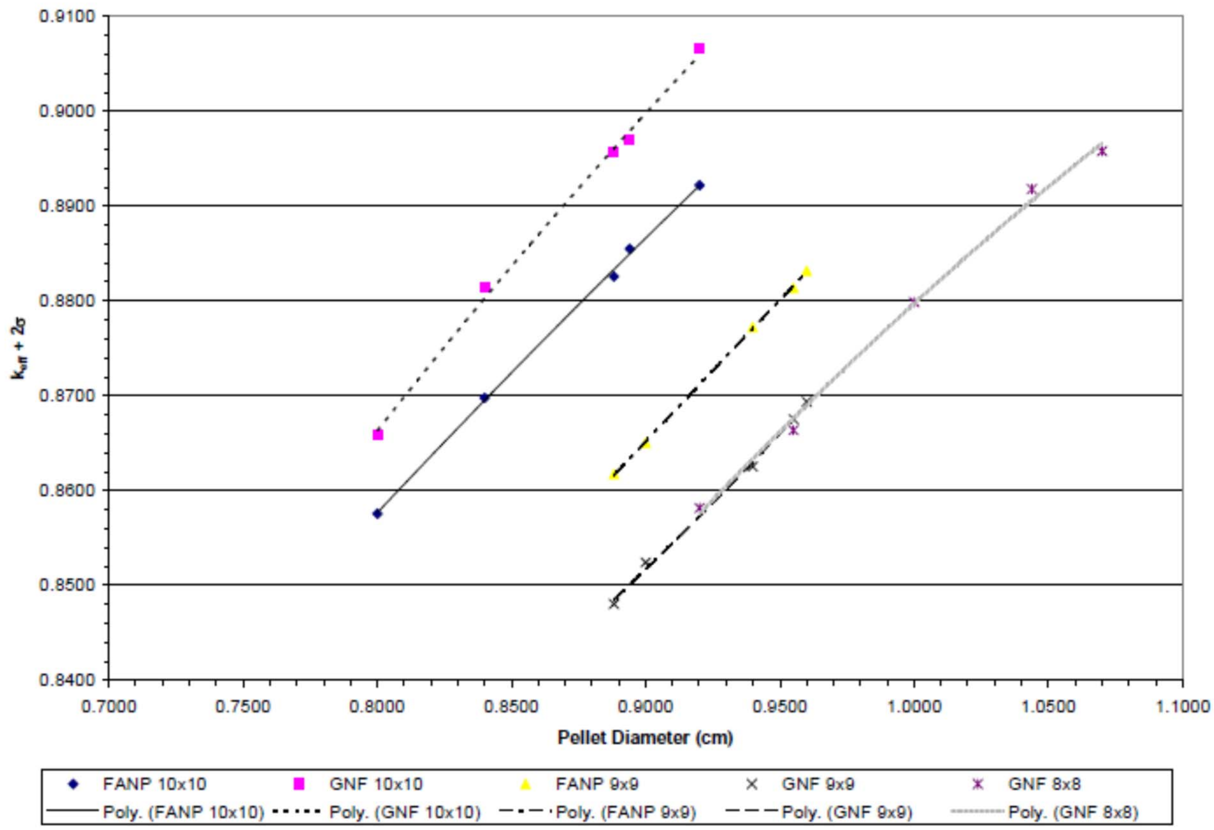

Figure 6-27 TN-B1 Array HAC Pellet Diameter Sensitivity Study

6.3.4.7. **Fuel Rod Clad Thickness Sensitivity Study (2N=448)**

Two sets of calculations are performed to assess the reactivity sensitivity to changes in cladding thickness. For the clad thickness sensitivity studies, the package array HAC model described in Section 6.3.1.2.2 is used for the study, fuel assembly orientation 6 is selected based on the results in Table 6-14, the maximum polyethylene amount for each fuel assembly design is chosen, the worst-case gadolinia-urania rod pattern is selected, the inner container fuel compartment is maintained at optimum density moderation, an Alumina Silicate thermal insulator envelopes the inner container fuel compartment, and water is removed from the outer container and between packages in the array. For the first set of calculations, the inner clad diameter is adjusted to determine the effect on reactivity while the outer clad diameter is fixed at its nominal value shown in Table 6-4. The minimum value for the parameter search range is the pellet OD, while the maximum value for the range is the clad OD. The second set of calculations involves adjustments to the outer clad diameter while the inner clad diameter is held at its nominal value Table 6-4. Figure 6-28 TN-B1 Array HAC Fuel Rod Clad ID Sensitivity Study displays the results for the inner clad diameter sensitivity calculations, and Figure 6-29 TN-B1 Array HAC

Fuel Rod Clad OD Sensitivity Study shows the results for the outer clad diameter sensitivity study. Both sets of results demonstrate that a decrease in the clad thickness results in an increase in system reactivity. The results also indicate that reactivity increases as the clad OD is decreased and increases as the clad ID is increased. Based on these results and fabrication constraints (Table 6-30 and Table 6-31):

- a 0.933 cm upper bound clad ID, and a 1.00 cm lower bound clad OD are selected for the FANP and GNF 10x10 parameter ranges;
- a 1.02 cm upper bound clad ID, and a 1.09 cm lower bound clad OD are selected for the FANP and GNF 9x9 parameter ranges; and
- a 1.10 cm upper bound clad ID, and a 1.17 cm lower bound clad OD are selected for the GNF 8x8 parameter range.

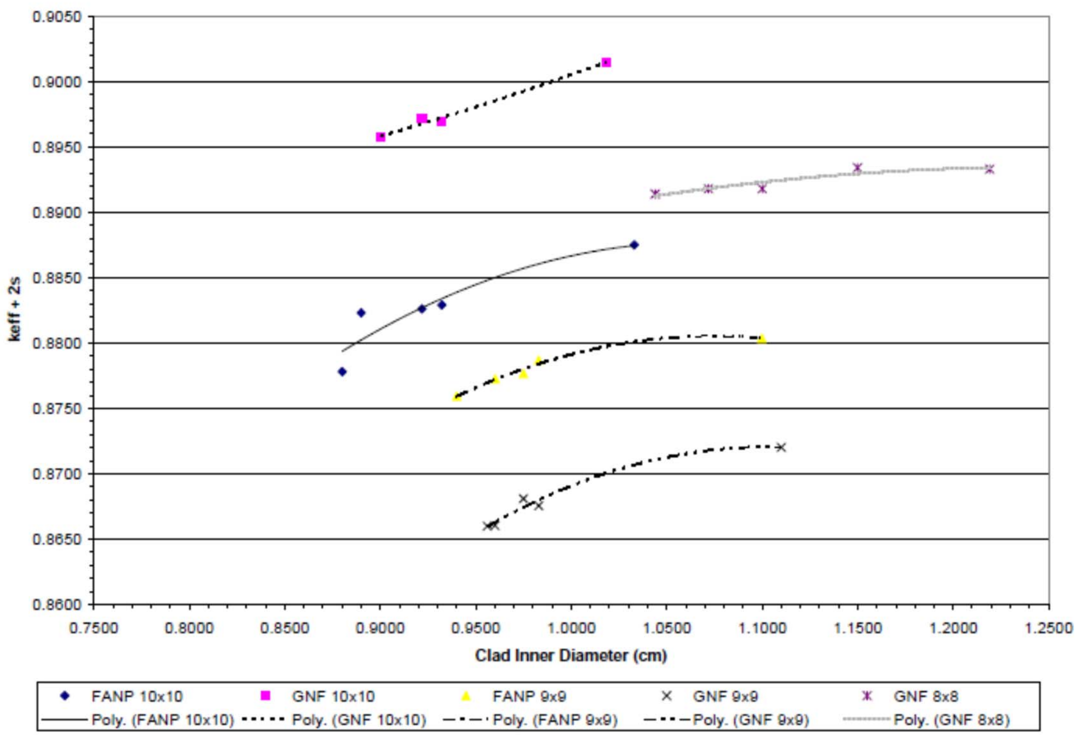

Figure 6-28 TN-B1 Array HAC Fuel Rod Clad ID Sensitivity Study

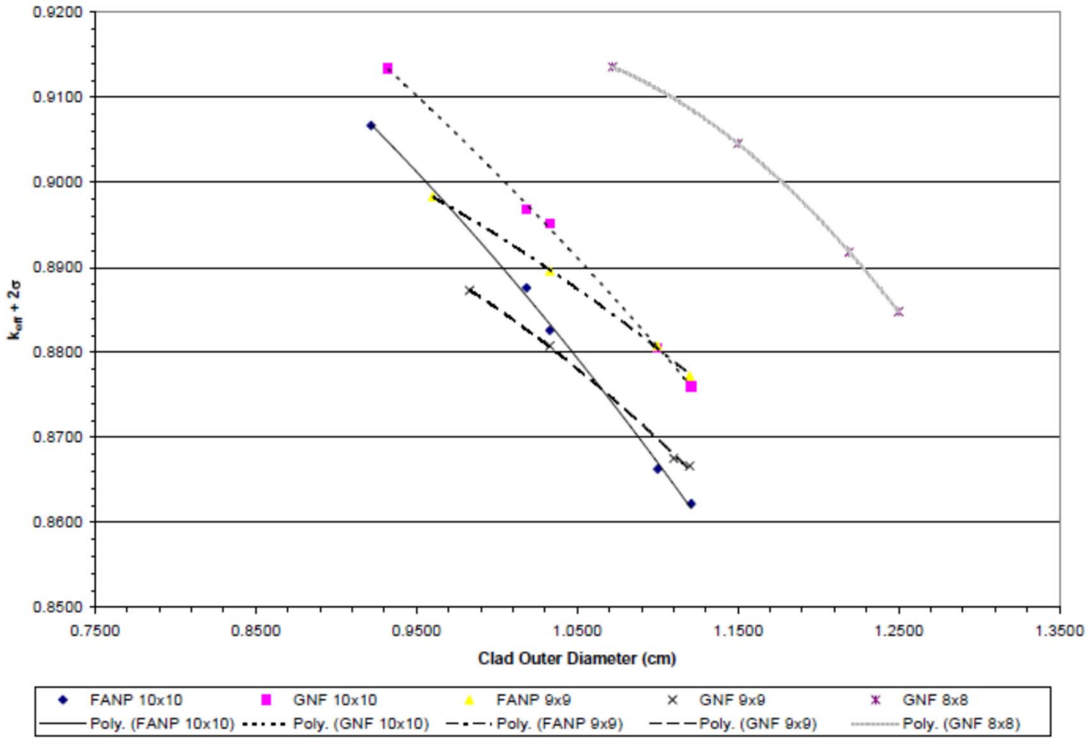

Figure 6-29 TN-B1 Array HAC Fuel Rod Clad OD Sensitivity Study

6.3.4.8. Worst-case Parameter Fuel Designs (2N=448)

The previous calculations have varied single parameters and assessed the impact on reactivity. Since the ranges investigated are to be a part of the fuel loading criteria, an assessment must be made for more than one parameter change at a time. To validate the parameter ranges selected to appear in the fuel loading criteria, a fuel design is developed by assembling the worst-case parameters for each design considered for transport in the TN-B1 container. Table 6-17 TN-B1 Array HAC Worst Case Parameter Fuel Designs contains the worst-case parameters for each design. The worst-case models from the clad ID and OD sensitivity study are used to conduct the worst-case fuel parameter study. The polyethylene is smeared into the fuel rod cladding to accommodate the limitations in the lattice cell modeling for cross-section processing in SCALE. A search for the worst-case gadolinia-urania fuel rod pattern is also conducted to validate the worst-case fuel design. Numerous patterns were investigated for each fuel assembly with the worst-case fuel parameters determined from the sensitivity studies. Of the patterns investigated, three patterns that produce the highest reactivity for each fuel assembly type are shown in Figure 6-22 - Figure 6-24. Additional calculations are performed to investigate the number of gadolinia-urania fuel rods needed based on fuel assembly U-235 enrichment. For each fuel assembly U-235 enrichment, a gadolinia-urania fuel rod pattern optimization study is conducted. The three patterns that produce the highest reactivity for each fuel assembly based on U-235 enrichment are shown in Figure 6-30 - Figure 6-32. All results are listed in Table 6-17 and are below the USL of 0.94254. Based on the results listed in Table 6-17, all worst-case fuel assembly designs result in maximum system reactivities that are within the statistical uncertainty of one another.

Table 6-17 TN-B1 Array HAC Worst Case Parameter Fuel Designs

Assembly Type	Gadolinia -Urania Fuel Rod Number	^{235}U Enrichment (wt%)	Poly Mass per Assembly (kg)	Pitch (cm)	Pellet Diameter (cm)	Clad ID (cm)	Clad OD (cm)	k_{eff}	σ	k_{eff} + 2σ
FANP 10x10	12	5.0	10.2	1.350	0.895	0.933	1.00	0.9368	0.0008	0.9384
FANP 10x10	10	4.6	10.2	1.350	0.895	0.933	1.00	0.9360	0.0009	0.9378
FANP 10x10	9	4.3	10.2	1.350	0.895	0.933	1.00	0.9325	0.0010	0.9345
FANP 10x10	8	4.2	10.2	1.350	0.895	0.933	1.00	0.9366	0.0009	**0.9384**
FANP 10x10	6	3.9	10.2	1.350	0.895	0.933	1.00	0.9353	0.0007	0.9367
FANP 10x10	4	3.6	10.2	1.350	0.895	0.933	1.00	0.9341	0.0009	0.9359
FANP 10x10	2	3.3	10.2	1.350	0.895	0.933	1.00	0.9305	0.0009	0.9323
FANP 10x10	0	2.9	10.2	1.350	0.895	0.933	1.00	0.9274	0.0008	0.9290
GNF 10x10	12	5.0	10.2	1.350	0.895	0.933	1.00	0.9393	0.0008	0.9409
GNF 10x10	10	4.6	10.2	1.350	0.895	0.933	1.00	0.9349	0.0010	0.9369
GNF 10x10	9	4.3	10.2	1.350	0.895	0.933	1.00	0.9346	0.0008	0.9362
GNF 10x10	8	4.2	10.2	1.350	0.895	0.933	1.00	0.9395	0.0009	**0.9413**
GNF 10x10	6	3.9	10.2	1.350	0.895	0.933	1.00	0.9377	0.0009	0.9395
GNF 10x10	4	3.6	10.2	1.350	0.895	0.933	1.00	0.9370	0.0008	0.9386
GNF 10x10	2	3.3	10.2	1.350	0.895	0.933	1.00	0.9344	0.0009	0.9362
GNF 10x10	0	2.9	10.2	1.350	0.895	0.933	1.00	0.9317	0.0007	0.9331
FANP 9x9	10	5.0	11	1.510	0.96	1.02	1.09	0.9191	0.0008	0.9207
FANP 9x9	8	4.7	11	1.510	0.96	1.02	1.09	0.9294	0.0008	**0.9310**
FANP 9x9	6	4.2	11	1.510	0.96	1.02	1.09	0.9242	0.0010	0.9262
FANP 9x9	4	3.8	11	1.510	0.96	1.02	1.09	0.9264	0.0007	0.9278
FANP 9x9	2	3.5	11	1.510	0.96	1.02	1.09	0.9257	0.0007	0.9271
FANP 9x9	0	3.0	11	1.510	0.96	1.02	1.09	0.9214	0.0008	0.9230
GNF 9x9	10	5.0	11	1.510	0.96	1.02	1.09	0.9151	0.0008	0.9167
GNF 9x9	8	4.8	11	1.510	0.96	1.02	1.09	0.9368	0.0009	**0.9386**
GNF 9x9	6	4.2	11	1.510	0.96	1.02	1.09	0.9294	0.0009	0.9312
GNF 9x9	4	3.8	11	1.510	0.96	1.02	1.09	0.9333	0.0007	0.9347
GNF 9x9	2	3.5	11	1.510	0.96	1.02	1.09	0.9311	0.0008	0.9327
GNF 9x9	0	3.0	11	1.510	0.96	1.02	1.09	0.9290	0.0008	0.9306
GNF 8x8	7	5.0	11	1.6923	1.05	1.10	1.17	0.9356	0.0008	**0.9372**
GNF 8x8	6	4.7	11	1.6923	1.05	1.10	1.17	0.9323	0.0009	0.9341
GNF 8x8	4	4.1	11	1.6923	1.05	1.10	1.17	0.9305	0.0008	0.9321
GNF 8x8	2	3.7	11	1.6923	1.05	1.10	1.17	0.9321	0.0008	0.9337
GNF 8x8	0	3.1	11	1.6923	1.05	1.10	1.17	0.9311	0.0008	0.9327

a. Limiting case(s) shown in bold

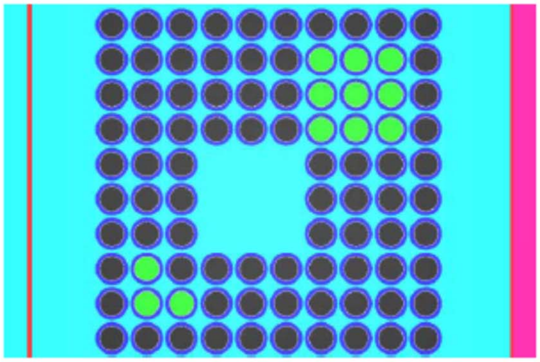

FANP 10x10 5.0 wt% ^{235}U, Pattern B

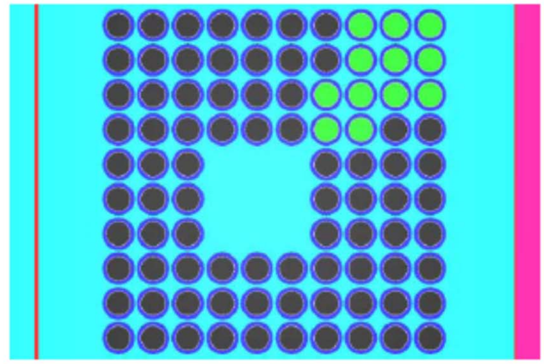

FANP 10x10 5.0 wt% ^{235}U, Pattern F

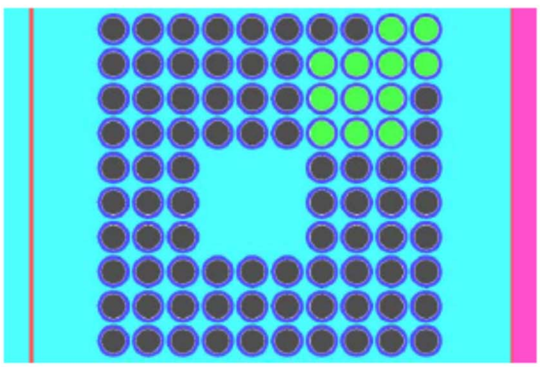

FANP 10x10 5.0 wt% ^{235}U, Pattern G

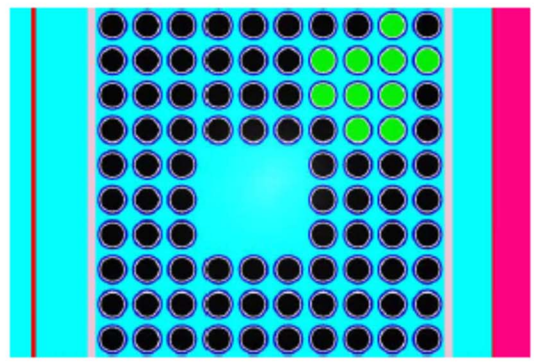

FANP 10x10 4.6 wt% ^{235}U, Pattern E

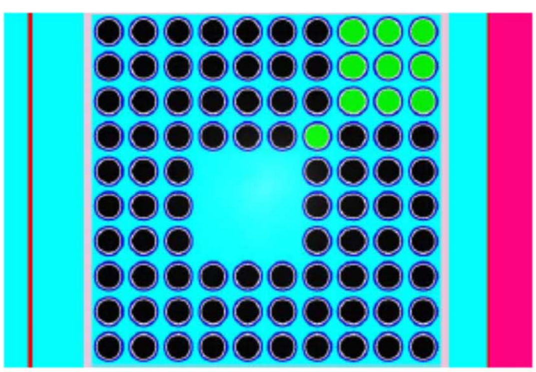

FANP 10x10 4.6 wt% ^{235}U, Pattern F

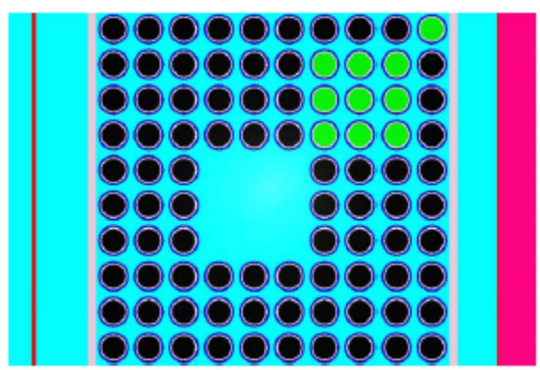

FANP 10x10 4.6 wt% ^{235}U, Pattern G

Figure 6-30 Gadolinia-Urania Fuel Rod Placement Pattern for 10x10 Fuel Assemblies

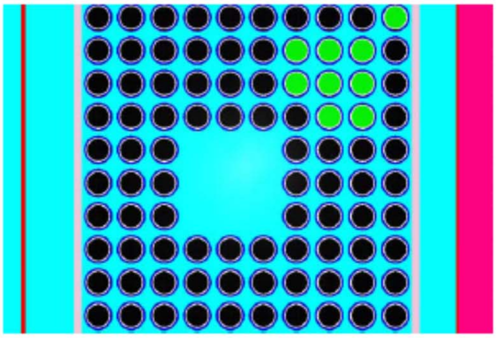

FANP 10x10 4.3 wt% ^{235}U, Pattern E

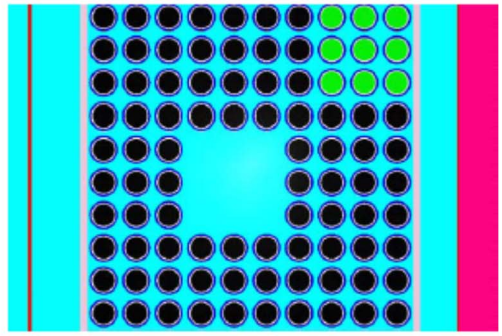

FANP 10x10 4.3 wt% ^{235}U, Pattern F

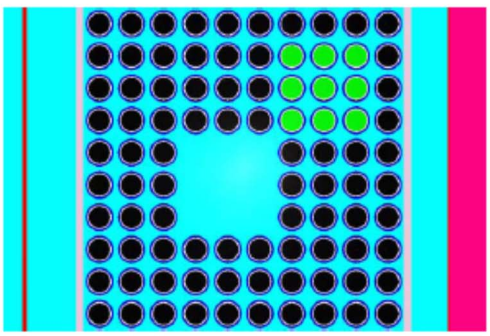

FANP 10x10 4.3 wt% ^{235}U, Pattern G

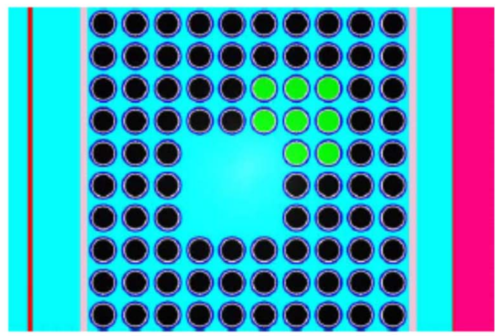

FANP 10x10 4.2 wt% ^{235}U, Pattern D

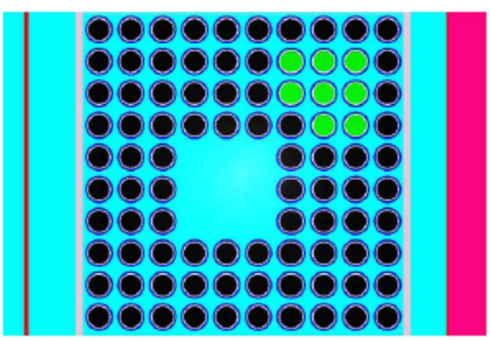

FANP 10x10 4.2 wt% ^{235}U, Pattern E

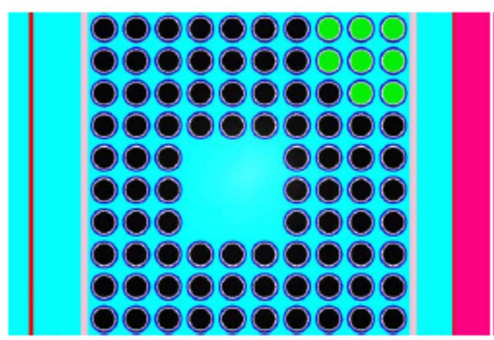

FANP 10x10 4.2 wt% ^{235}U, Pattern F

Figure 6 30 Gadolinia-Urania Fuel Rod Placement Pattern for 10x10 Fuel Assemblies (Continued)

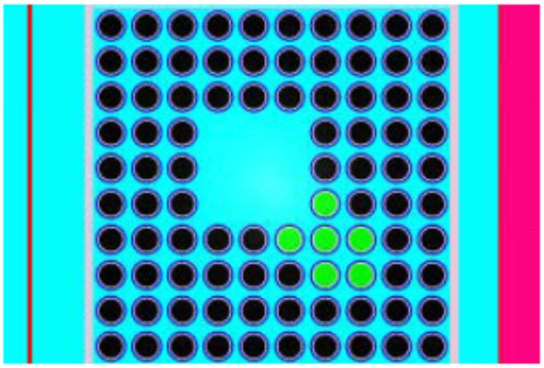

FANP 10x10 3.9 wt% ^{235}U, Pattern E

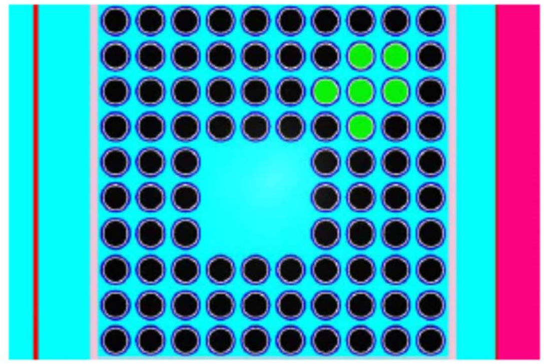

FANP 10x10 3.9 wt% ^{235}U, Pattern F

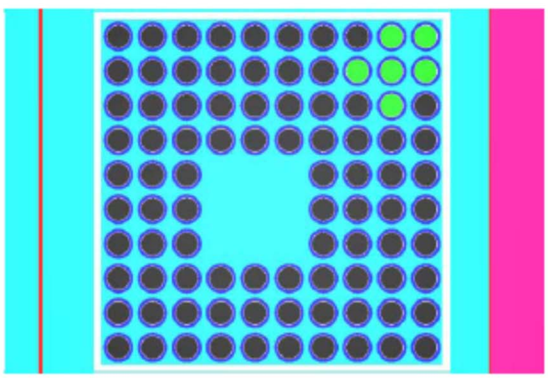

FANP 10x10 3.9 wt% ^{235}U, Pattern G

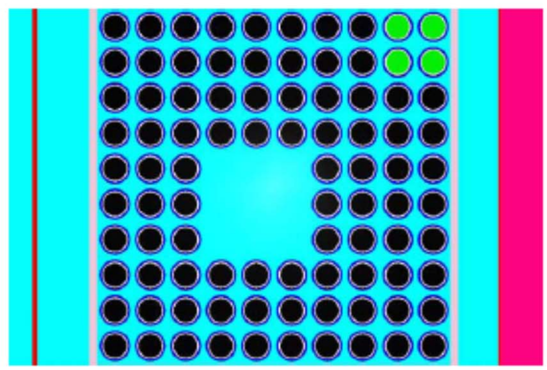

FANP 10x10 3.6 wt% ^{235}U, Pattern H

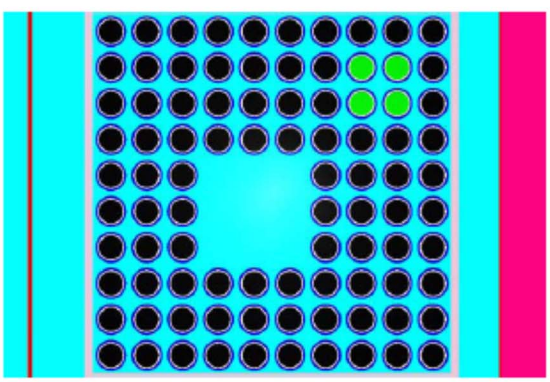

FANP 10x10 3.6 wt% ^{235}U, Pattern I

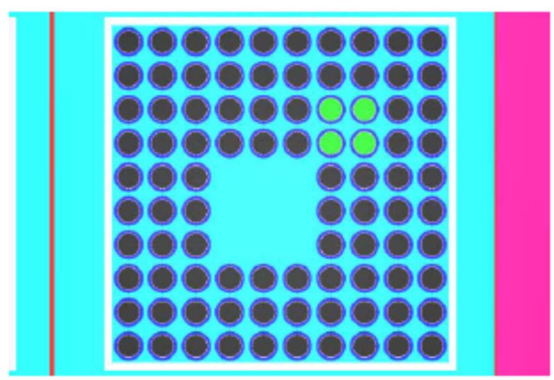

FANP 10x10 3.6 wt% ^{235}U, Pattern J

Figure 6 30 Gadolinia-Urania Fuel Rod Placement Pattern for 10x10 Fuel Assemblies (Continued)

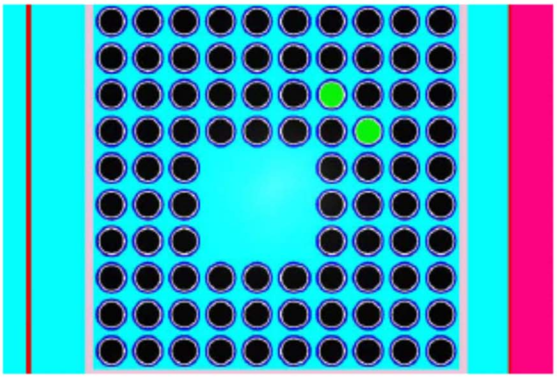

FANP 10x10 3.3 wt% ^{235}U, Pattern F

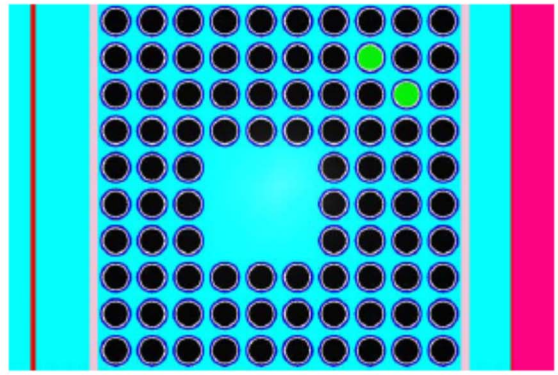

FANP 10x10 3.3 wt% ^{235}U, Pattern G

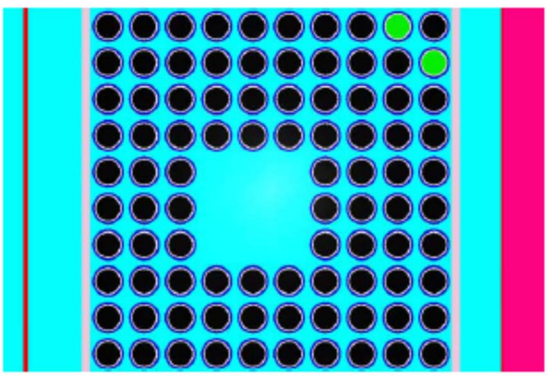

FANP 10x10 3.3 wt% ^{235}U, Pattern H

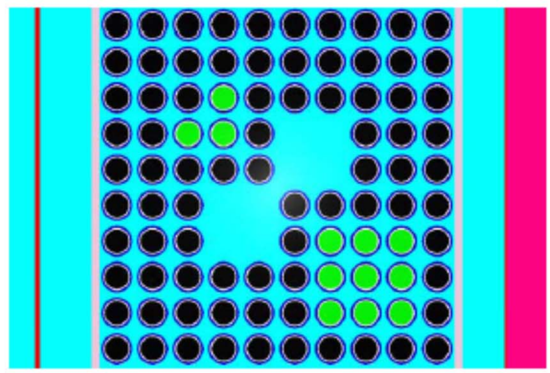

GNF 10x10 5.0 wt% ^{235}U, Pattern B

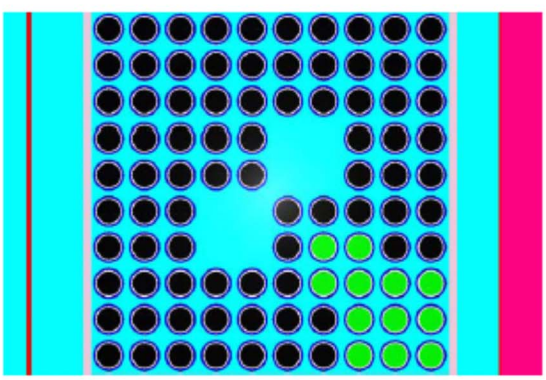

GNF 10x10 5.0 wt% ^{235}U, Pattern F

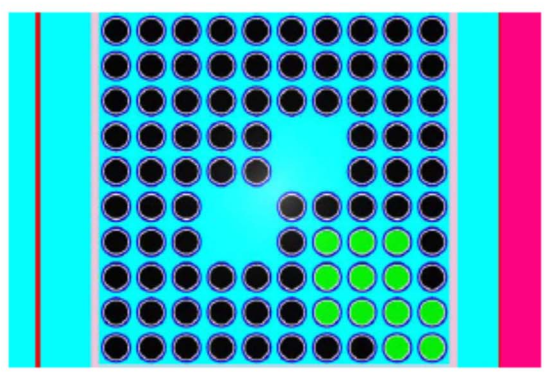

GNF 10x10 5.0 wt% ^{235}U, Pattern H

Figure 6 30 Gadolinia-Urania Fuel Rod Placement Pattern for 10x10 Fuel Assemblies (Continued)

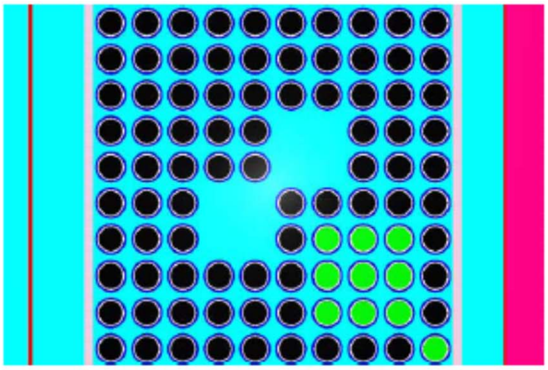

GNF 10x10 4.6 wt% ^{235}U, Pattern F

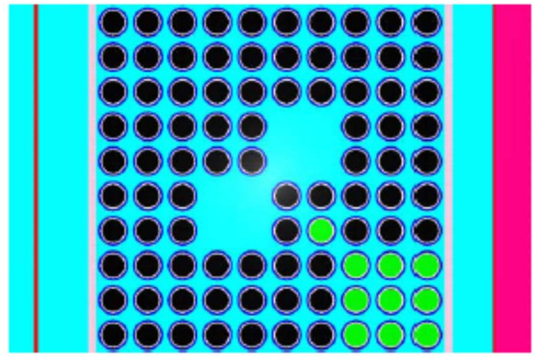

GNF 10x10 4.6 wt% ^{235}U, Pattern G

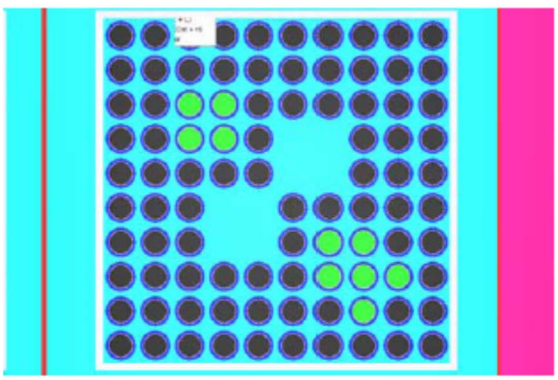

GNF 10x10 4.6 wt% ^{235}U, Pattern I

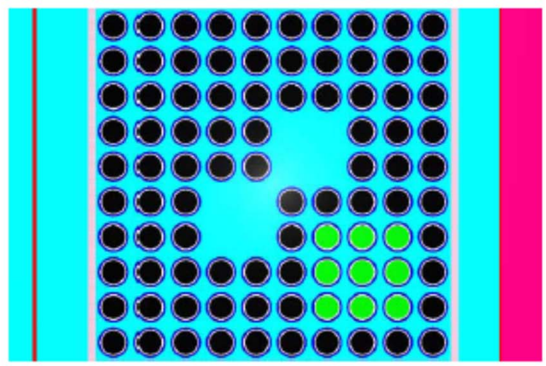

GNF 10x10 4.3 wt% ^{235}U, Pattern F

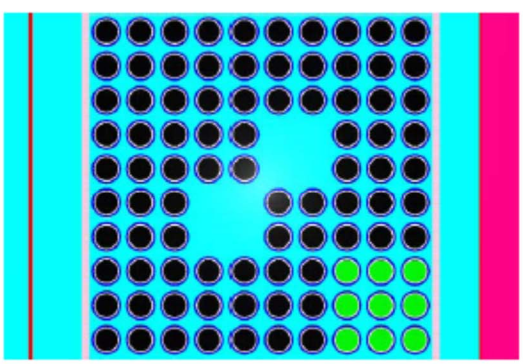

GNF 10x10 4.3 wt% ^{235}U, Pattern G

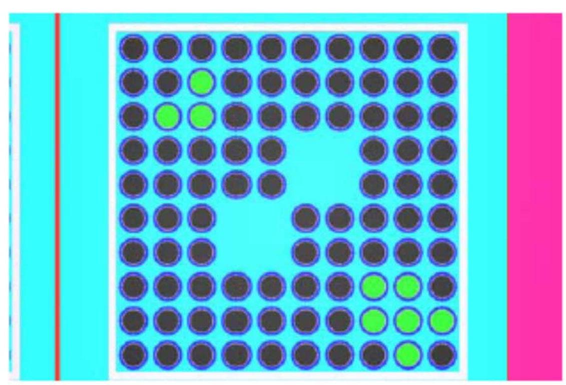

GNF 10x10 4.3 wt% ^{235}U, Pattern J

Figure 6 30 Gadolinia-Urania Fuel Rod Placement Pattern for 10x10 Fuel Assemblies (Continued)

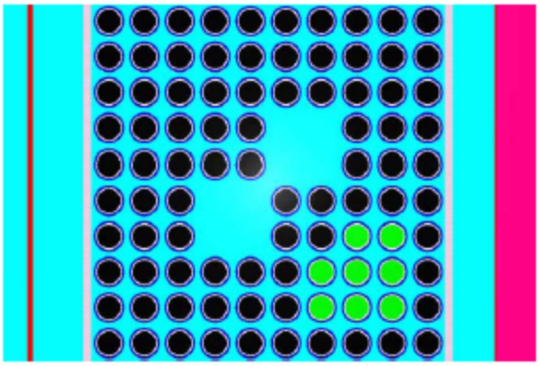

GNF 10x10 4.2 wt%^{235}U, Pattern F

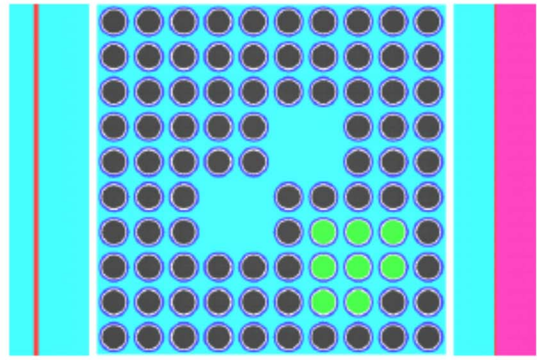

GNF 10x10 4.2 wt%^{235}U, Pattern I

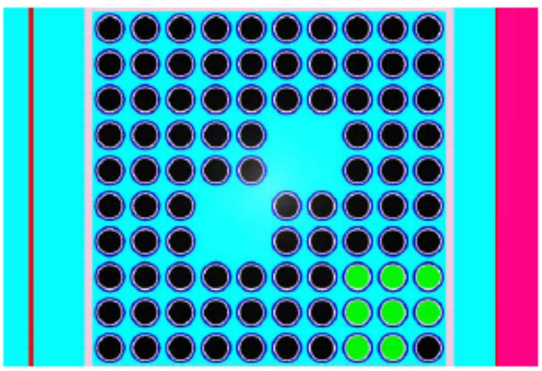

GNF 10x10 4.2 wt%^{235}U, Pattern J

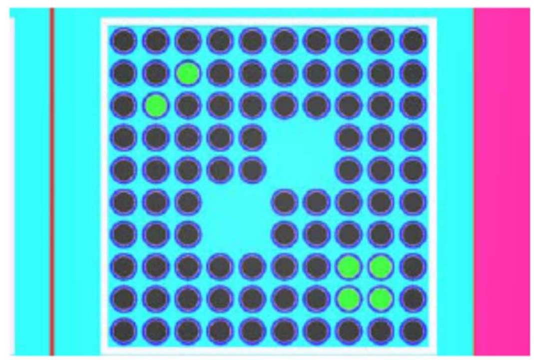

GNF 10x10 3.9 wt%^{235}U, Pattern G

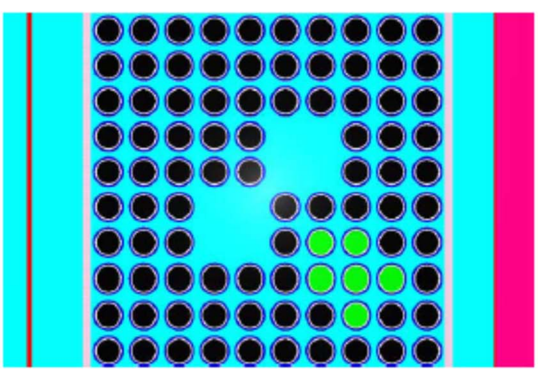

GNF 10x10 3.9 wt%^{235}U, Pattern J

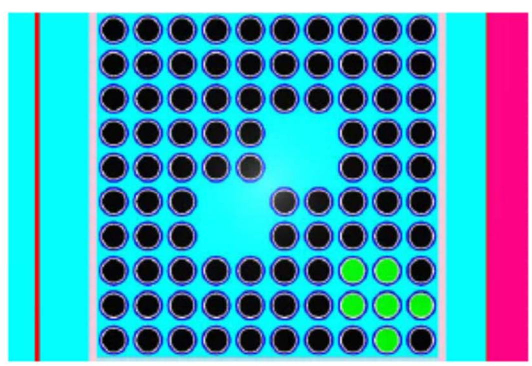

GNF 10x10 3.9 wt%^{235}U, Pattern K

Figure 6 30 Gadolinia-Urania Fuel Rod Placement Pattern for 10x10 Fuel Assemblies (Continued)

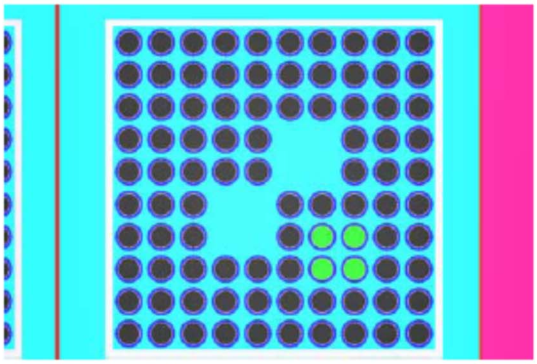

GNF 10x10 3.6 wt% ^{235}U, Pattern F

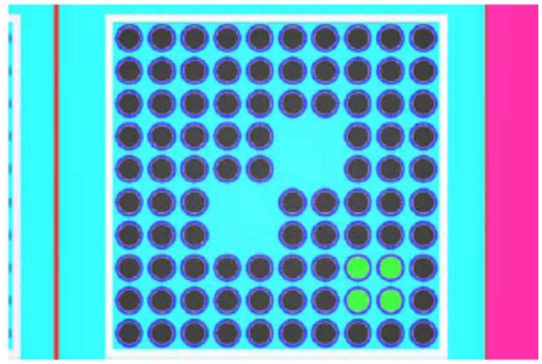

GNF 10x10 3.6 wt% ^{235}U, Pattern G

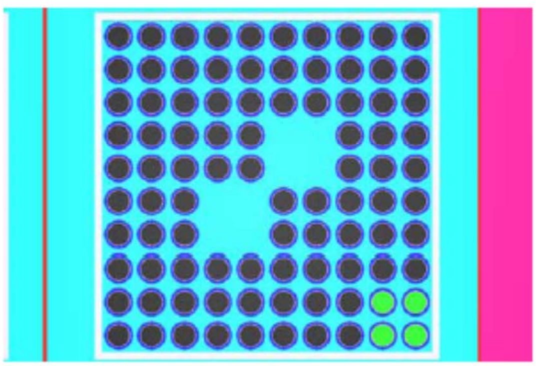

GNF 10x10 3.6 wt% ^{235}U, Pattern H

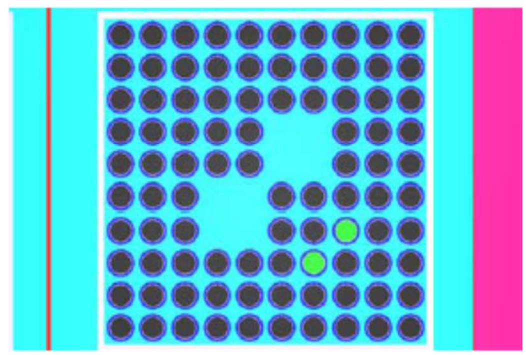

GNF 10x10 3.3 wt% ^{235}U, Pattern A

Figure 6 30 Gadolinia-Urania Fuel Rod Placement Pattern for 10x10 Fuel Assemblies (Continued)

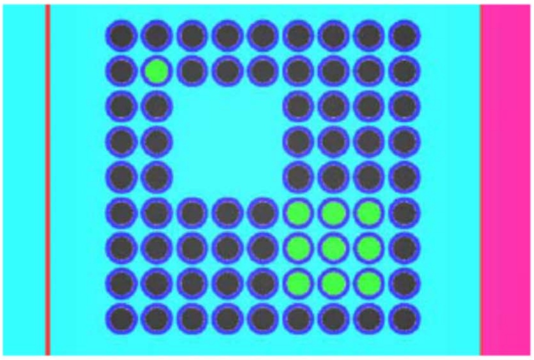

FANP 9x9 5.0 wt% ^{235}U, Pattern A

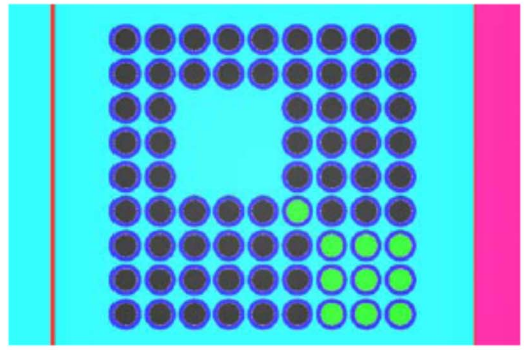

FANP 9x9 5.0 wt% ^{235}U, Pattern B

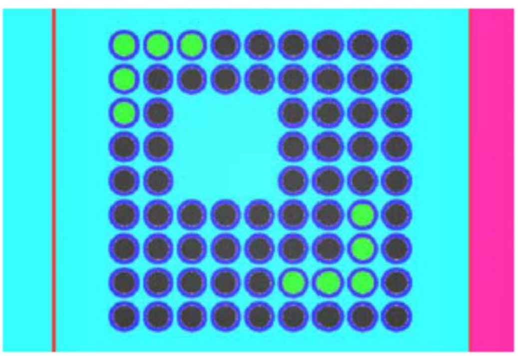

FANP 9x9 5.0 wt% ^{235}U, Pattern E

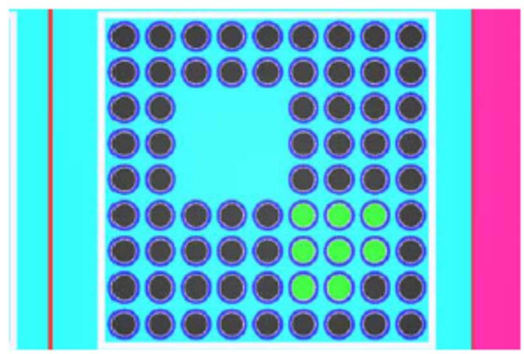

FANP 9x9 4.7 wt% ^{235}U, Pattern A

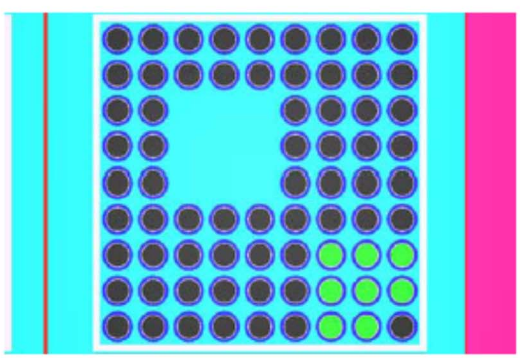

FANP 9x9 4.7 wt% ^{235}U, Pattern B

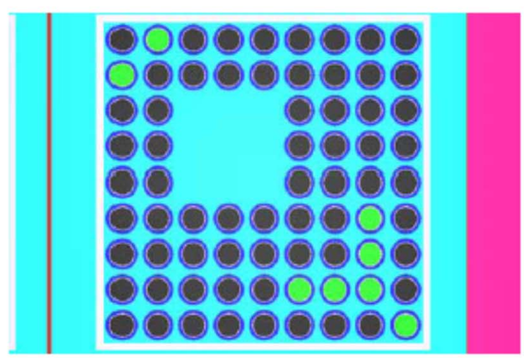

FANP 9x9 4.7 wt% ^{235}U, Pattern E

Figure 6-31 Gadolinia-Urania Fuel Rod Placement Pattern for 9x9 Fuel Assemblies

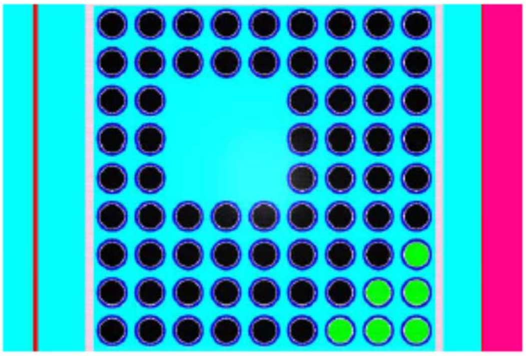

FANP 9x9 4.2 wt% U-235, Pattern A

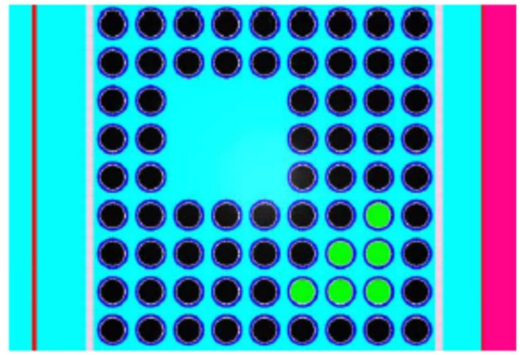

FANP 9x9 4.2 wt% U-235, Pattern B

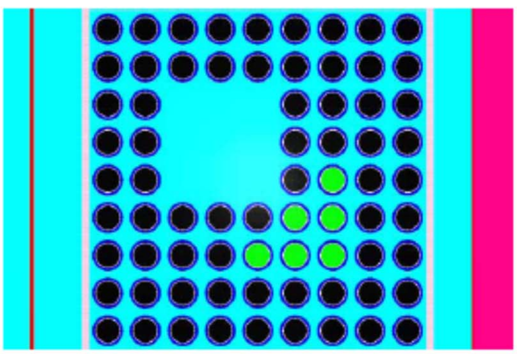

FANP 9x9 4.2 wt% U-235, Pattern C

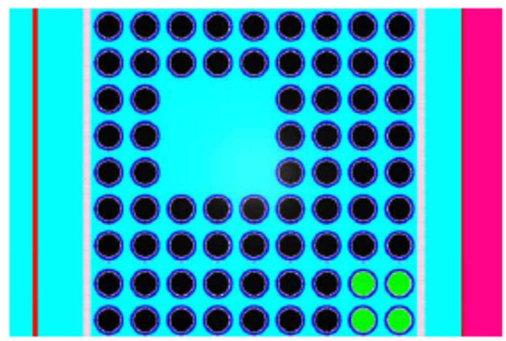

FANP 9x9 3.8 wt% U-235, Pattern A

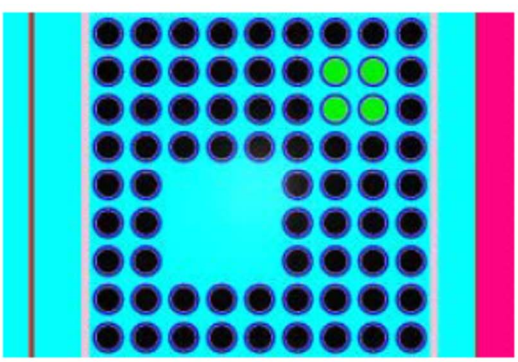

FANP 9x9 3.8 wt% U-235, Pattern B

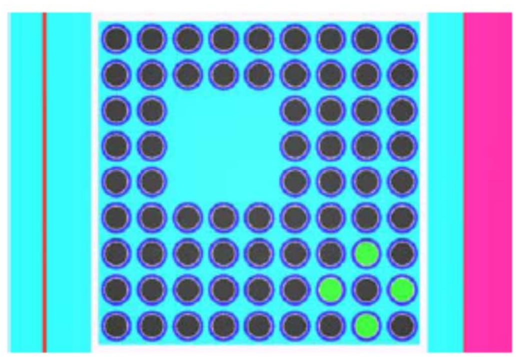

FANP 9x9 3.8 wt% U-235, Pattern F

Figure 6 31 Gadolinia-Urania Fuel Rod Placement Pattern for 9x9 Fuel Assemblies (Continued)

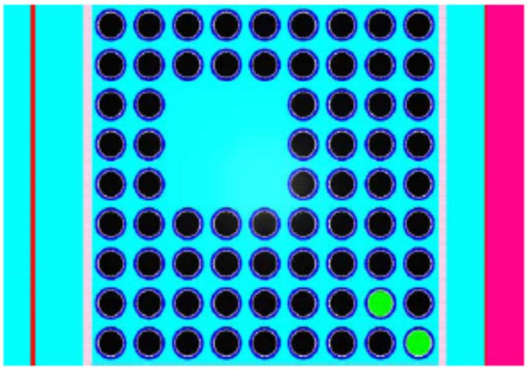

FANP 9x9 3.5 wt% U-235, Pattern B

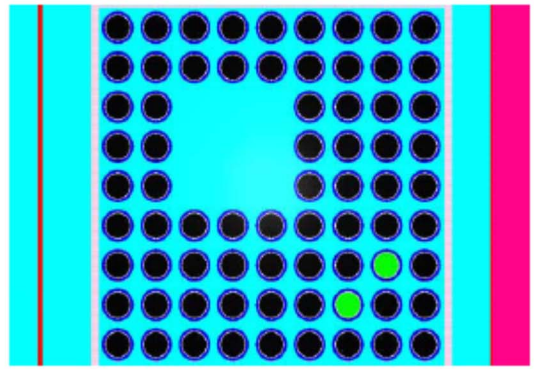

FANP 9x9 3.5 wt% U-235, Pattern C

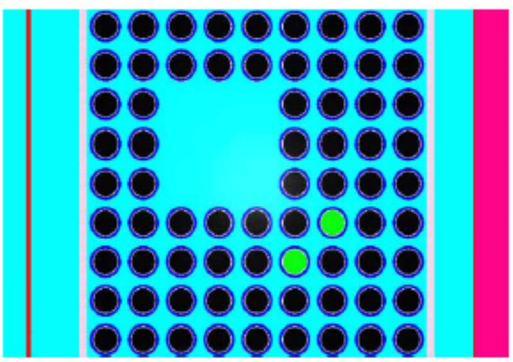

FANP 9x9 3.5 wt% U-235, Pattern D

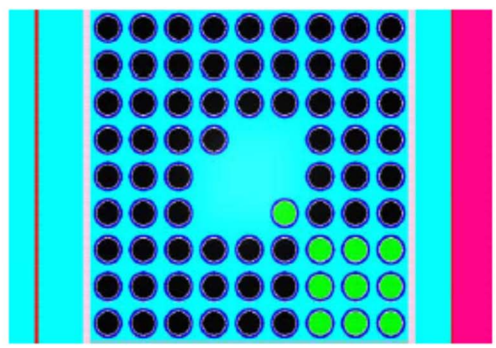

GNF 9x9 5.0 wt% U-235, Pattern B

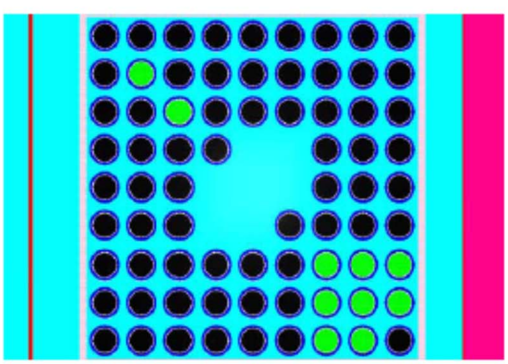

GNF 9x9 5.0 wt% U-235, Pattern G

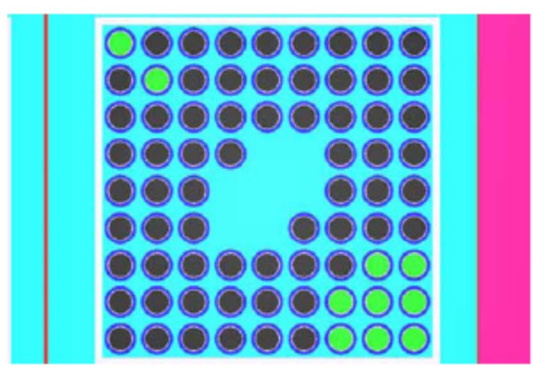

GNF 9x9 5.0 wt% U-235, Pattern H

Figure 6 31 Gadolinia-Urania Fuel Rod Placement Pattern for 9x9 Fuel Assemblies (Continued)

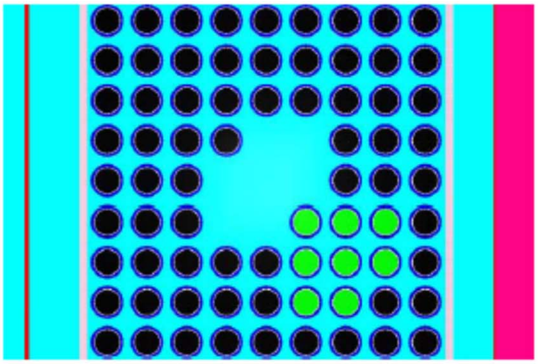

GNF 9x9 4.8 wt% U-235, Pattern A

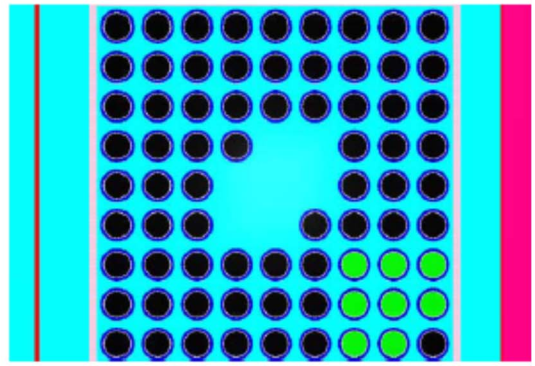

GNF 9x9 4.8 wt% U-235, Pattern B

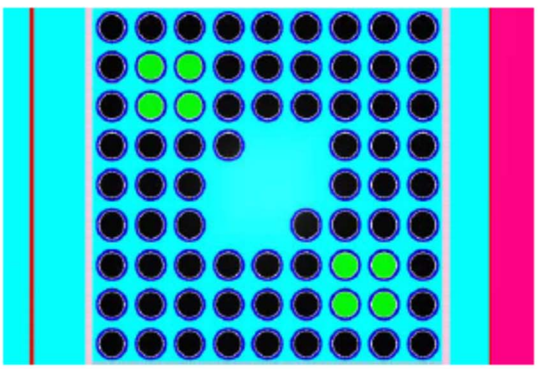

GNF 9x9 4.8 wt% U-235, Pattern H

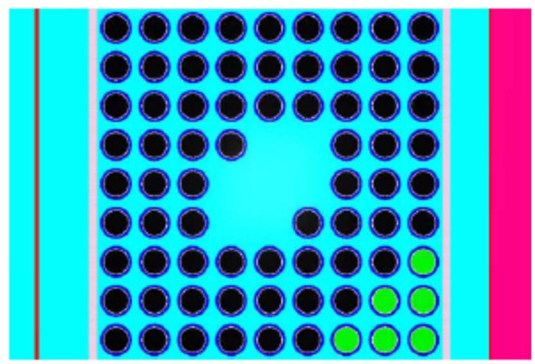

GNF 9x9 4.2 wt% U-235, Pattern A

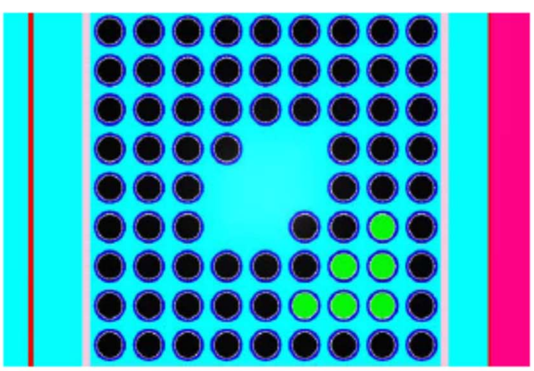

GNF 9x9 4.2 wt% U-235, Pattern B

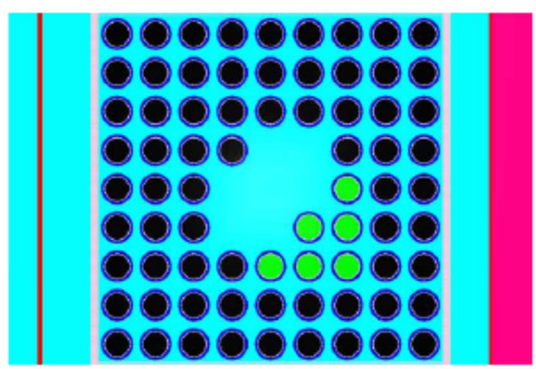

GNF 9x9 4.2 wt% U-235, Pattern C

Figure 6 31 Gadolinia-Urania Fuel Rod Placement Pattern for 9x9 Fuel Assemblies (Continued)

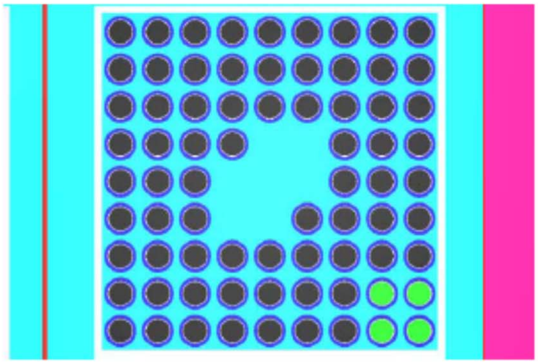

GNF 9x9 3.8 wt% ^{235}U, Pattern A

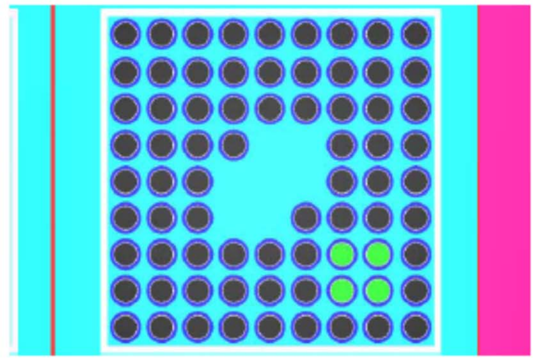

GNF 9x9 3.8 wt% ^{235}U, Pattern B

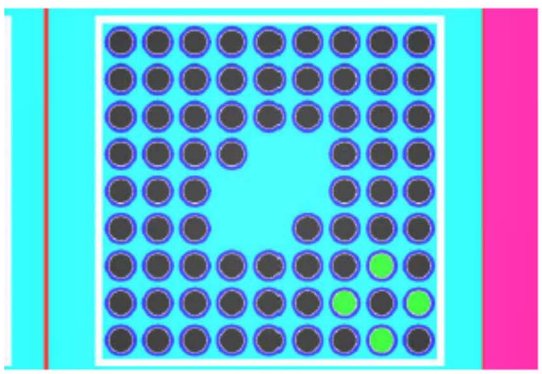

GNF 9x9 3.8 wt% ^{235}U, Pattern F

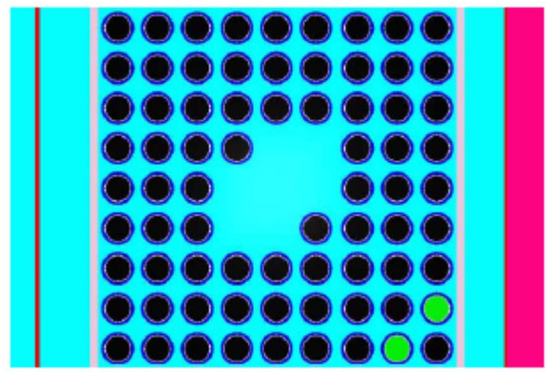

GNF 9x9 3.5 wt% ^{235}U, Pattern A

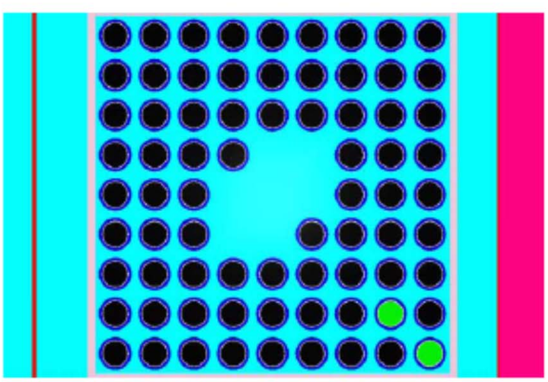

GNF 9x9 3.5 wt% ^{235}U, Pattern B

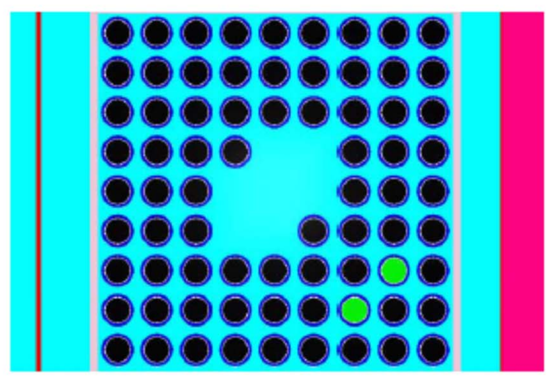

GNF 3.5 wt% ^{235}U, Pattern C

Figure 6 31 Gadolinia-Urania Fuel Rod Placement Pattern for 9x9 Fuel Assemblies (Continued)

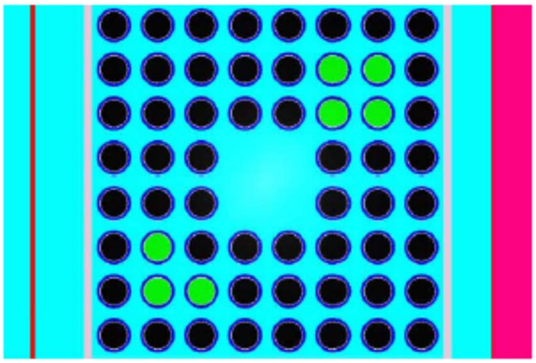

GNF 8x8 5.0 wt% ^{235}U, Pattern E

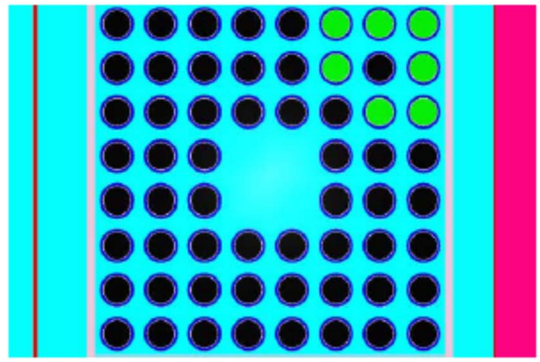

GNF 8x8 5.0 wt% ^{235}U, Pattern H

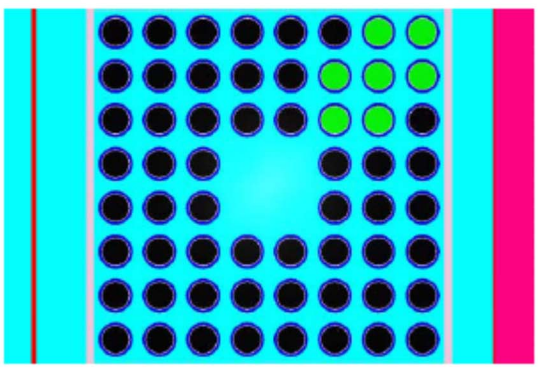

GNF 8x8 5.0 wt% ^{235}U, Pattern I

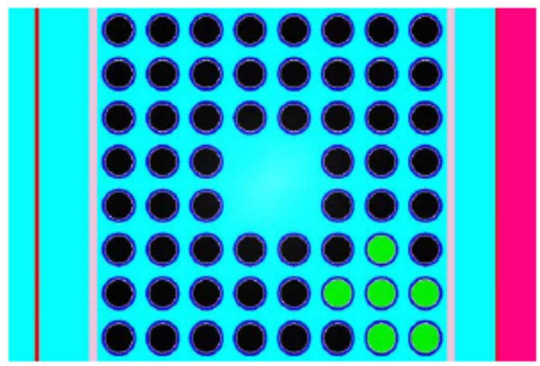

GNF 8x8 4.7 wt% ^{235}U, Pattern B

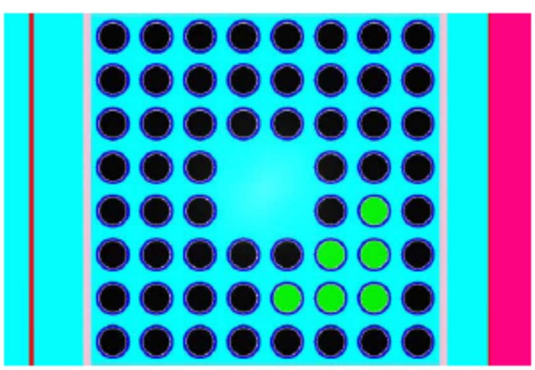

GNF 8x8 4.7 wt% ^{235}U, Pattern C

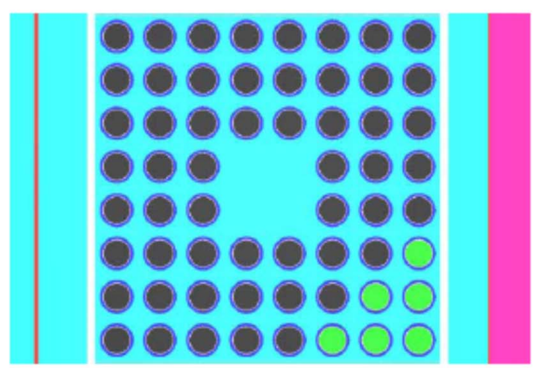

GNF 8x8 4.7 wt% ^{235}U, Pattern D

Figure 6-32 Gadolinia-Urania Fuel Rod Placement Pattern for 8x8 Fuel Assemblies

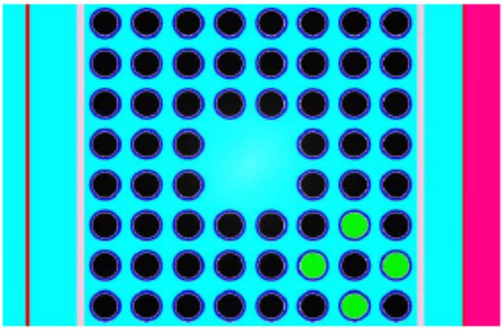

GNF 8x8 4.1 wt% ^{235}U, Pattern B

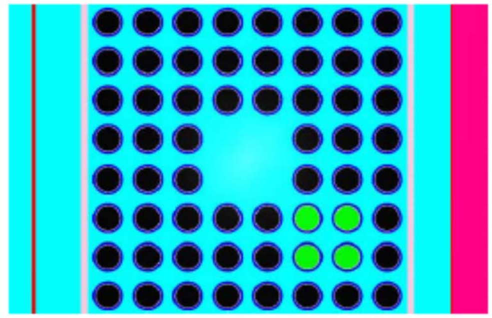

GNF 8x8 4.1 wt% ^{235}U, Pattern C

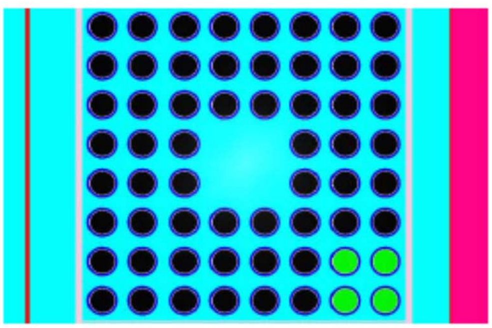

GNF 8x8 4.1 wt% ^{235}U, Pattern D

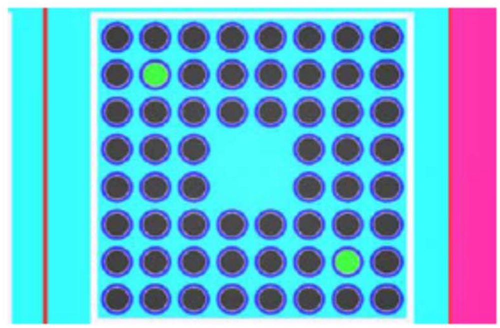

GNF 8x8 3.7 wt% ^{235}U, Pattern A

Figure 6 32 Gadolinia-Urania Fuel Rod Placement Pattern for 8x8 Fuel Assemblies (Continued)

6.3.4.9. **Part Length Fuel Rod Study (2N=448)**

The FANP 10x10, FANP 9x9, GNF 10x10, and GNF 9x9 worst-case designs are used to investigate the impact that part length fuel rods have on system reactivity. The worst-case part length fuel rod patterns identified by performing scoping studies for the 10x10 designs are shown in Figure 6-33 and Figure 6-34. The worst-case part length fuel rod patterns identified by performing scoping studies for the 9x9 designs are shown in Figure 6-35 and Figure 6-36. The fuel rod lengths for the part length rods are half that of the normal rod, and calculations showed that reducing the length further decreases system reactivity. To maintain the same amount of polyethylene when the part length rods are inserted, the polyethylene is redistributed to all rodsin the assembly. The worst-case models from the moderator density sensitivity study are used to conduct the part length fuel rod study, and the worst-case fuel parameters listed in Table 6-17 are utilized. The part length fuel rod study results are contained in Table 6-18. All results for the FANP 9x9, the FANP 10x10, and the GNF 9x9 are below the USL of 0.94254. Several cases for the GNF 10x10 fuel design are above the USL of 0.94254. Therefore, an increased clad thickness is investigated for the 10x10 designs to reduce the system reactivity; these cases are included at the end of Table 6-18. The increased clad thickness for the 10x10 designs reduce system reactivity and all 10x10 results are below the USL of 0.94254. Comparing the results in Table 6-18 with those in Table 6-17 reveals the system reactivity remains about the same for the 9x9 fuel assembly designs with part length fuel rods. The FANP 10x10 and GNF 10x10 fuel designs are more reactive with the part length fuel rod configuration. Based on the results in Table 6-17 and Table 6-18:

- The maximum system reactivity with FANP 10x10 fuel assemblies having part length fuel rods and gadolinia-urania fuel is statistically greater than the maximum system reactivity with FANP 10x10 fuel assemblies having gadolinia-urania fuel and no part length fuel rods. The configuration that yields the highest $k_{eff} + 2\sigma$ consists of fuel assemblies with a lattice average enrichment of 5.0 wt% U-235, 12 gadolinia-urania fuel rods enriched to 2.0 wt% gadolinia arranged in Pattern G, and 10 part length fuel rods. With the clad thickness for the fuel assemblies increased from 0.0335 cm to 0.0381 cm, the $k_{eff} + 2\sigma$ for this configuration is 0.9394.

- The maximum system reactivity with GNF 10x10 fuel assemblies having part length fuel rods and gadolinia-urania fuel is statistically greater than the maximum system reactivity with GNF 10x10 fuel assemblies having gadolinia-urania fuel and no part length fuel rods. The configuration that yields the highest $k_{eff} + 2\sigma$ consists of fuel assemblies with a lattice average enrichment of 5.0 wt% U-235, 12 gadolinia-urania fuel rods enriched to 2.0 wt% gadolinia arranged in Pattern H, and 12 part-length fuel rods. With the clad thickness for the fuel assemblies increased from 0.0335 cm to 0.0381 cm, the $k_{eff} + 2\sigma$ for this configuration is 0.9418.

- Based on fuel parameter changes made to the 10x10 designs to lower reactivity, a 0.9338 cm upper bound clad ID, and a 1.01 cm lower bound clad OD are established for theGNF 10x10 parameter ranges. The 0.9330 cm upper bound clad ID and 1.00 cm lower bound clad OD may still be used for the FANP 10x10 design since the fuel assembly with this configuration remained below the USL of 0.94254.
  - The most reactive FANP 9x9 configuration consists of fuel assemblies with a lattice average enrichment of 4.7 wt% U-235 and 8 gadolinia-urania fuel rods enriched to 2.0 wt% gadolinia arranged in Pattern A and 8 part length rods. The k_{eff} + 2σ for this configuration is 0.9303.
  - The most reactive GNF 9x9 configuration consists of fuel assemblies with a lattice average enrichment of 4.7 wt% U-235 and 8 gadolinia-urania fuel rods enriched to 2.0 wt% gadolinia arranged in Pattern B and 8 part length fuel rods. The k_{eff} + 2σ for this configuration is 0.9407.
  - The most reactive GNF 8x8 configuration consists of fuel assemblies with a lattice average enrichment of 5.0 wt% U-235, 7 gadolinia-urania fuel rods enriched to 2.0 wt% gadolinia arranged in Pattern I, and no part length fuel rods. The k_{eff} + 2σ for this configuration is 0.9372 (Table 6-17). The GNF 8x8 fuel assembly is not evaluated for part length fuel rods.

The GNF 10x10 assembly is chosen as the overall bounding fuel type since the k_{eff} + 2σ is among the largest numerical values, however, the system reactivity of the 10x10, and 9x9 worst-case fuel assembly designs in the 14x2x16 TN-B1 container array are statistically indistinguishable.

Table 6-18 TN-B1 Array HAC Part Length Fuel Rod Calculations

Assembly Type	Number of Part Length Rods	Gadolinia -Urania Fuel Rod Number	^{235}U Enrich-ment (wt%)	Pitch (cm)	Pellet Diameter (cm)	Clad ID (cm)	Clad OD (cm)	k_{eff}	σ	k_{eff} + 2σ
FANP 10x10	8	0	2.9	1.350	0.895	0.933	1.00	0.9228	0.0008	0.9244
FANP 10x10	8	2	3.3	1.350	0.895	0.933	1.00	0.9282	0.0008	0.9298
FANP 10x10	8	4	3.6	1.350	0.895	0.933	1.00	0.9332	0.0008	0.9348
FANP 10x10	8	6	3.9	1.350	0.895	0.933	1.00	0.9327	0.0008	0.9343
FANP 10x10	8	8	4.2	1.350	0.895	0.933	1.00	0.9367	0.0008	0.9383
FANP 10x10	8	9	4.3	1.350	0.895	0.933	1.00	0.9282	0.0008	0.9298
FANP 10x10	8	10	4.6	1.350	0.895	0.933	1.00	0.9363	0.0009	0.9381
FANP 10x10	8	12	5.0	1.350	0.895	0.933	1.00	0.9403	0.0008	**0.9419**
FANP 10x10	10	0	2.9	1.350	0.895	0.933	1.00	0.9224	0.0008	0.9240
FANP 10x10	10	2	3.3	1.350	0.895	0.933	1.00	0.9283	0.0008	0.9299
FANP 10x10	10	4	3.6	1.350	0.895	0.933	1.00	0.9330	0.0007	0.9344
FANP 10x10	10	6	3.9	1.350	0.895	0.933	1.00	0.9333	0.0008	0.9349
FANP 10x10	10	8	4.2	1.350	0.895	0.933	1.00	0.9367	0.0008	0.9383
FANP 10x10	10	9	4.3	1.350	0.895	0.933	1.00	0.9301	0.0008	0.9317
FANP 10x10	10	10	4.6	1.350	0.895	0.933	1.00	0.9379	0.0009	0.9397
FANP 10x10	10	12	5.0	1.350	0.895	0.933	1.00	0.9399	0.0008	**0.9415**
FANP 10x10	12	0	2.9	1.350	0.895	0.933	1.00	0.9234	0.0008	0.9250
FANP 10x10	12	2	3.3	1.350	0.895	0.933	1.00	0.9281	0.0008	0.9297
FANP 10x10	12	4	3.6	1.350	0.895	0.933	1.00	0.9329	0.0008	0.9345
FANP 10x10	12	6	3.9	1.350	0.895	0.933	1.00	0.9319	0.0008	0.9335
FANP 10x10	12	8	4.2	1.350	0.895	0.933	1.00	0.9356	0.0008	0.9372
FANP 10x10	12	9	4.3	1.350	0.895	0.933	1.00	0.9294	0.0007	0.9308
FANP 10x10	12	10	4.6	1.350	0.895	0.933	1.00	0.9371	0.0008	0.9387
FANP 10x10	12	12	5.0	1.350	0.895	0.933	1.00	0.9404	0.0009	**0.9422**
FANP 10x10	14	0	2.9	1.350	0.895	0.933	1.00	0.9225	0.0008	0.9241
FANP 10x10	14	2	3.3	1.350	0.895	0.933	1.00	0.9274	0.0008	0.9290
FANP 10x10	14	4	3.6	1.350	0.895	0.933	1.00	0.9326	0.0009	0.9344
FANP 10x10	14	6	3.9	1.350	0.895	0.933	1.00	0.9313	0.0008	0.9329
FANP 10x10	14	8	4.2	1.350	0.895	0.933	1.00	0.9348	0.0010	0.9368
FANP 10x10	14	9	4.3	1.350	0.895	0.933	1.00	0.9310	0.0008	0.9326
FANP 10x10	14	10	4.6	1.350	0.895	0.933	1.00	0.9371	0.0008	0.9387
FANP 10x10	14	12	5.0	1.350	0.895	0.933	1.00	0.9393	0.0009	**0.9411**

a. Limiting case(s) shown in bold

Table 6-18 TN-B1 Array HAC Part Length Fuel Rod Calculations (continued)

Assembly Type	Number of Part Length Rods	Gadolinia -Urania Fuel Rod Number	^{235}U Enrich-ment (wt%)	Pitch (cm)	Pellet Diameter (cm)	Clad ID (cm)	Clad OD (cm)	k_{eff}	σ	k_{eff} + 2σ
GNF 10x10	8	0	2.9	1.350	0.895	0.933	1.00	0.9321	0.0007	0.9335
GNF 10x10	8	2	3.3	1.350	0.895	0.933	1.00	0.9327	0.0007	0.9341
GNF 10x10	8	4	3.6	1.350	0.895	0.933	1.00	0.9395	0.0010	0.9415
GNF 10x10	8	6	3.9	1.350	0.895	0.933	1.00	0.9367	0.0008	0.9383
GNF 10x10	8	8	4.2	1.350	0.895	0.933	1.00	0.9402	0.0008	**0.9418**
GNF 10x10	8	9	4.3	1.350	0.895	0.933	1.00	0.9369	0.0009	0.9387
GNF 10x10	8	10	4.6	1.350	0.895	0.933	1.00	0.9376	0.0009	0.9394
GNF 10x10	8	12	5.0	1.350	0.895	0.933	1.00	0.9386	0.0010	0.9406
GNF 10x10	10	0	2.9	1.350	0.895	0.933	1.00	0.9300	0.0008	0.9316
GNF 10x10	10	2	3.3	1.350	0.895	0.933	1.00	0.9319	0.0008	0.9335
GNF 10x10	10	4	3.6	1.350	0.895	0.933	1.00	0.9380	0.0009	0.9398
GNF 10x10	10	6	3.9	1.350	0.895	0.933	1.00	0.9347	0.0008	0.9363
GNF 10x10	10	8	4.2	1.350	0.895	0.933	1.00	0.9419	0.0010	**0.9439**
GNF 10x10	10	9	4.3	1.350	0.895	0.933	1.00	0.9374	0.0008	0.9390
GNF 10x10	10	10	4.6	1.350	0.895	0.933	1.00	0.9385	0.0009	0.9403
GNF 10x10	10	12	5.0	1.350	0.895	0.933	1.00	0.9412	0.0008	0.9428
GNF 10x10	12	0	2.9	1.350	0.895	0.933	1.00	0.9300	0.0007	0.9314
GNF 10x10	12	2	3.3	1.350	0.895	0.933	1.00	0.9316	0.0007	0.9330
GNF 10x10	12	4	3.6	1.350	0.895	0.933	1.00	0.9377	0.0009	0.9395
GNF 10x10	12	6	3.9	1.350	0.895	0.933	1.00	0.9352	0.0008	0.9368
GNF 10x10	12	8	4.2	1.350	0.895	0.933	1.00	0.9408	0.0009	0.9426
GNF 10x10	12	9	4.3	1.350	0.895	0.933	1.00	0.9374	0.0008	0.9390
GNF 10x10	12	10	4.6	1.350	0.895	0.933	1.00	0.9406	0.0009	0.9424
GNF 10x10	12	12	5.0	1.350	0.895	0.933	1.00	0.9415	0.0008	**0.9431**
GNF 10x10	14	0	2.9	1.350	0.895	0.933	1.00	0.9277	0.0008	0.9293
GNF 10x10	14	2	3.3	1.350	0.895	0.933	1.00	0.9305	0.0008	0.9321
GNF 10x10	14	4	3.6	1.350	0.895	0.933	1.00	0.9374	0.0009	0.9392
GNF 10x10	14	6	3.9	1.350	0.895	0.933	1.00	0.9347	0.0008	0.9363
GNF 10x10	14	8	4.2	1.350	0.895	0.933	1.00	0.9401	0.0009	**0.9419**
GNF 10x10	14	9	4.3	1.350	0.895	0.933	1.00	0.9370	0.0009	0.9388
GNF 10x10	14	10	4.6	1.350	0.895	0.933	1.00	0.9381	0.0009	0.9399
GNF 10x10	14	12	5.0	1.350	0.895	0.933	1.00	0.9401	0.0008	0.9417

a. Limiting case(s) shown in bold

Table 6-18 TN-B1 Array HAC Part Length Fuel Rod Calculations (continued)

Assembly Type	Number of Part Length Rods	Gadolinia -Urania Fuel Rod Number	^{235}U Enrich-ment (wt%)	Pitch (cm)	Pellet Diameter (cm)	Clad ID (cm)	Clad OD (cm)	k_{eff}	σ	keff + 2σ
FANP 9x9	8	0	3.0	1.510	0.96	1.02	1.09	0.9168	0.0008	0.9184
FANP 9x9	8	2	3.5	1.510	0.96	1.02	1.09	0.9219	0.0008	0.9235
FANP 9x9	8	4	3.8	1.510	0.96	1.02	1.09	0.9234	0.0009	0.9252
FANP 9x9	8	6	4.2	1.510	0.96	1.02	1.09	0.9227	0.0007	0.9241
FANP 9x9	8	8	4.7	1.510	0.96	1.02	1.09	0.9287	0.0008	**0.9303**
FANP 9x9	8	10	5.0	1.510	0.96	1.02	1.09	0.9165	0.0008	0.9181
FANP 9x9	10	0	3.0	1.510	0.96	1.02	1.09	0.9139	0.0008	0.9155
FANP 9x9	10	2	3.5	1.510	0.96	1.02	1.09	0.9195	0.0008	0.9211
FANP 9x9	10	4	3.8	1.510	0.96	1.02	1.09	0.9189	0.0008	0.9205
FANP 9x9	10	6	4.2	1.510	0.96	1.02	1.09	0.9208	0.0008	0.9224
FANP 9x9	10	8	4.7	1.510	0.96	1.02	1.09	0.9256	0.0009	**0.9274**
FANP 9x9	10	10	5.0	1.510	0.96	1.02	1.09	0.9135	0.0009	0.9153
FANP 9x9	12	0	3.0	1.510	0.96	1.02	1.09	0.9100	0.0007	0.9114
FANP 9x9	12	2	3.5	1.510	0.96	1.02	1.09	0.9155	0.0007	0.9169
FANP 9x9	12	4	3.8	1.510	0.96	1.02	1.09	0.9168	0.0008	0.9184
FANP 9x9	12	6	4.2	1.510	0.96	1.02	1.09	0.9147	0.0007	0.9161
FANP 9x9	12	8	4.7	1.510	0.96	1.02	1.09	0.9208	0.0008	**0.9224**
FANP 9x9	12	10	5.0	1.510	0.96	1.02	1.09	0.9087	0.0009	0.9105
GNF 9x9	8	0	3.0	1.510	0.96	1.02	1.09	0.9261	0.0008	0.9277
GNF 9x9	8	2	3.5	1.510	0.96	1.02	1.09	0.9311	0.0008	0.9327
GNF 9x9	8	4	3.8	1.510	0.96	1.02	1.09	0.9303	0.0008	0.9319
GNF 9x9	8	6	4.2	1.510	0.96	1.02	1.09	0.9293	0.0008	0.9309
GNF 9x9	8	8	4.7	1.510	0.96	1.02	1.09	0.9391	0.0008	**0.9407**
GNF 9x9	8	10	5.0	1.510	0.96	1.02	1.09	0.9140	0.0008	0.9156
GNF 9x9	10	0	3.0	1.510	0.96	1.02	1.09	0.9249	0.0009	0.9267
GNF 9x9	10	2	3.5	1.510	0.96	1.02	1.09	0.9315	0.0008	0.9331
GNF 9x9	10	4	3.8	1.510	0.96	1.02	1.09	0.9287	0.0008	0.9303
GNF 9x9	10	6	4.2	1.510	0.96	1.02	1.09	0.9297	0.0009	0.9315
GNF 9x9	10	8	4.7	1.510	0.96	1.02	1.09	0.9377	0.0008	**0.9393**
GNF 9x9	10	10	5.0	1.510	0.96	1.02	1.09	0.9048	0.0008	0.9064
GNF 9x9	12	0	3.0	1.510	0.96	1.02	1.09	0.9235	0.0008	0.9251

a. Limiting case(s) shown in bold

Table 6-18 TN-B1 Array HAC Part Length Fuel Rod Calculations (continued)

Assembly Type	Number of Part Length Rods	Gadolinia -Urania Fuel Rod Number	235U Enrich-ment (wt%)	Pitch (cm)	Pellet Diameter (cm)	Clad ID (cm)	Clad OD (cm)	keff	σ	keff + 2σ
GNF 9x9	12	2	3.5	1.510	0.96	1.02	1.09	0.9294	0.0009	0.9312
GNF 9x9	12	4	3.8	1.510	0.96	1.02	1.09	0.9288	0.0009	0.9306
GNF 9x9	12	6	4.2	1.510	0.96	1.02	1.09	0.9263	0.0008	0.9279
GNF 9x9	12	8	4.7	1.510	0.96	1.02	1.09	0.9370	0.0009	**0.9388**
GNF 9x9	12	10	5.0	1.510	0.96	1.02	1.09	0.9056	0.0008	0.9072
FANP 10x10	8	0	2.9	1.350	0.895	0.9338	1.01	0.9203	0.0008	0.9219
FANP 10x10	8	2	3.3	1.350	0.895	0.9338	1.01	0.9150	0.0008	0.9166
FANP 10x10	8	4	3.6	1.350	0.895	0.9338	1.01	0.9290	0.0008	0.9306
FANP 10x10	8	6	3.9	1.350	0.895	0.9338	1.01	0.9303	0.0008	0.9319
FANP 10x10	8	8	4.2	1.350	0.895	0.9338	1.01	0.9292	0.0008	0.9308
FANP 10x10	8	9	4.3	1.350	0.895	0.9338	1.01	0.9293	0.0008	0.9309
FANP 10x10	8	10	4.6	1.350	0.895	0.9338	1.01	0.9335	0.0008	0.9351
FANP 10x10	8	12	5.0	1.350	0.895	0.9338	1.01	0.9353	0.0009	**0.9371**
FANP 10x10	10	0	2.9	1.350	0.895	0.9338	1.01	0.9218	0.0008	0.9234
FANP 10x10	10	2	3.3	1.350	0.895	0.9338	1.01	0.9265	0.0008	0.9281
FANP 10x10	10	4	3.6	1.350	0.895	0.9338	1.01	0.9320	0.0008	0.9336
FANP 10x10	10	6	3.9	1.350	0.895	0.9338	1.01	0.9311	0.0008	0.9327
FANP 10x10	10	8	4.2	1.350	0.895	0.9338	1.01	0.9345	0.0008	0.9361
FANP 10x10	10	9	4.3	1.350	0.895	0.9338	1.01	0.9296	0.0009	0.9314
FANP 10x10	10	10	4.6	1.350	0.895	0.9338	1.01	0.9369	0.0009	0.9387
FANP 10x10	10	12	5.0	1.350	0.895	0.9338	1.01	0.9376	0.0009	**0.9394**
FANP 10x10	12	0	2.9	1.350	0.895	0.9338	1.01	0.9216	0.0008	0.9232
FANP 10x10	12	2	3.3	1.350	0.895	0.9338	1.01	0.9256	0.0008	0.9272
FANP 10x10	12	4	3.6	1.350	0.895	0.9338	1.01	0.9314	0.0009	0.9332
FANP 10x10	12	6	3.9	1.350	0.895	0.9338	1.01	0.9319	0.0007	0.9333
FANP 10x10	12	8	4.2	1.350	0.895	0.9338	1.01	0.9345	0.0008	0.9361
FANP 10x10	12	9	4.3	1.350	0.895	0.9338	1.01	0.9277	0.0008	0.9293
FANP 10x10	12	10	4.6	1.350	0.895	0.9338	1.01	0.9347	0.0009	0.9365
FANP 10x10	12	12	5.0	1.350	0.895	0.9338	1.01	0.9370	0.0009	**0.9388**
FANP 10x10	14	0	2.9	1.350	0.895	0.9338	1.01	0.9207	0.0008	0.9223
FANP 10x10	14	2	3.3	1.350	0.895	0.9338	1.01	0.9247	0.0009	0.9265
FANP 10x10	14	4	3.6	1.350	0.895	0.9338	1.01	0.9291	0.0008	0.9307

a. Limiting case(s) shown in bold

Table 6-18 TN-B1 Array HAC Part Length Fuel Rod Calculations (continued)

Assembly Type	Number of Part Length Rods	Gadolinia -Urania Fuel Rod Number	^{235}U Enrich-ment (wt%)	Pitch (cm)	Pellet Diameter (cm)	Clad ID (cm)	Clad OD (cm)	k_{eff}	σ	keff + 2σ
FANP 10x10	14	6	3.9	1.350	0.895	0.9338	1.01	0.9301	0.0009	0.9319
FANP 10x10	14	8	4.2	1.350	0.895	0.9338	1.01	0.9324	0.0008	0.9340
FANP 10x10	14	9	4.3	1.350	0.895	0.9338	1.01	0.9293	0.0008	0.9309
FANP 10x10	14	10	4.6	1.350	0.895	0.9338	1.01	0.9352	0.0008	0.9368
FANP 10x10	14	12	5.0	1.350	0.895	0.9338	1.01	0.9370	0.0009	**0.9388**
GNF 10x10	8	0	2.9	1.350	0.895	0.9338	1.01	0.9292	0.0008	0.9308
GNF 10x10	8	2	3.3	1.350	0.895	0.9338	1.01	0.9296	0.0009	0.9314
GNF 10x10	8	4	3.6	1.350	0.895	0.9338	1.01	0.9357	0.0010	0.9377
GNF 10x10	8	6	3.9	1.350	0.895	0.9338	1.01	0.9354	0.0009	0.9372
GNF 10x10	8	8	4.2	1.350	0.895	0.9338	1.01	0.9399	0.0008	**0.9415**
GNF 10x10	8	9	4.3	1.350	0.895	0.9338	1.01	0.9346	0.0010	0.9366
GNF 10x10	8	10	4.6	1.350	0.895	0.9338	1.01	0.9376	0.0009	0.9394
GNF 10x10	8	12	5.0	1.350	0.895	0.9338	1.01	0.9375	0.0008	0.9391
GNF 10x10	10	0	2.9	1.350	0.895	0.9338	1.01	0.9292	0.0008	0.9308
GNF 10x10	10	2	3.3	1.350	0.895	0.9338	1.01	0.9296	0.0008	0.9312
GNF 10x10	10	4	3.6	1.350	0.895	0.9338	1.01	0.9371	0.0008	0.9387
GNF 10x10	10	6	3.9	1.350	0.895	0.9338	1.01	0.9370	0.0008	0.9386
GNF 10x10	10	8	4.2	1.350	0.895	0.9338	1.01	0.9372	0.0008	0.9388
GNF 10x10	10	9	4.3	1.350	0.895	0.9338	1.01	0.9363	0.0009	0.9381
GNF 10x10	10	10	4.6	1.350	0.895	0.9338	1.01	0.9345	0.0009	0.9363
GNF 10x10	10	12	5.0	1.350	0.895	0.9338	1.01	0.9375	0.0008	**0.9391**
GNF 10x10	12	0	2.9	1.350	0.895	0.9338	1.01	0.9276	0.0008	0.9292
GNF 10x10	12	2	3.3	1.350	0.895	0.9338	1.01	0.9309	0.0008	0.9325
GNF 10x10	12	4	3.6	1.350	0.895	0.9338	1.01	0.9373	0.0009	0.9391
GNF 10x10	12	6	3.9	1.350	0.895	0.9338	1.01	0.9347	0.0009	0.9365
GNF 10x10	12	8	4.2	1.350	0.895	0.9338	1.01	0.9374	0.0009	0.9392
GNF 10x10	12	9	4.3	1.350	0.895	0.9338	1.01	0.9333	0.0009	0.9351
GNF 10x10	12	10	4.6	1.350	0.895	0.9338	1.01	0.9378	0.0008	0.9394
GNF 10x10	12	12	5.0	1.350	0.895	0.9338	1.01	0.9404	0.0007	**0.9418**
GNF 10x10	14	0	2.9	1.350	0.895	0.9338	1.01	0.9261	0.0008	0.9277
GNF 10x10	14	2	3.3	1.350	0.895	0.9338	1.01	0.9299	0.0008	0.9315

a. Limiting case(s) shown in bold

Table 6-18 TN-B1 Array HAC Part Length Fuel Rod Calculations (continued)

Assembly Type	Number of Part Length Rods	Gadolinia -Urania Fuel Rod Number	^{235}U Enrich- ment (wt%)	Pitch (cm)	Pellet Diameter (cm)	Clad ID (cm)	Clad OD (cm)	k_{eff}	σ	keff + 2σ
GNF 10x10	14	4	3.6	1.350	0.895	0.9338	1.01	0.9345	0.0008	0.9361
GNF 10x10	14	6	3.9	1.350	0.895	0.9338	1.01	0.9351	0.0009	0.9369
GNF 10x10	14	8	4.2	1.350	0.895	0.9338	1.01	0.9376	0.0009	0.9394
GNF 10x10	14	9	4.3	1.350	0.895	0.9338	1.01	0.9353	0.0008	0.9369
GNF 10x10	14	10	4.6	1.350	0.895	0.9338	1.01	0.9368	0.0009	0.9386
GNF 10x10	14	12	5.0	1.350	0.895	0.9338	1.01	0.9398	0.0008	**0.9414**

a. Limiting case(s) shown in bold

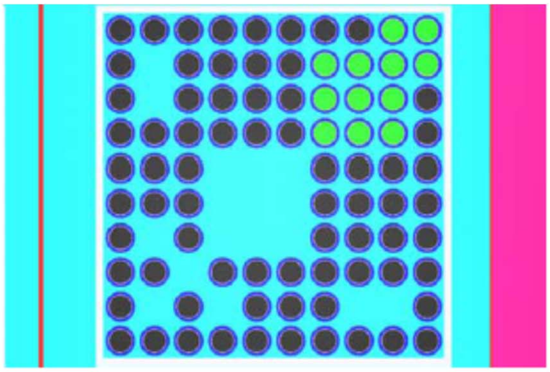

FANP 10x10 5.0 wt% ^{235}U, 8 Part Length Rods

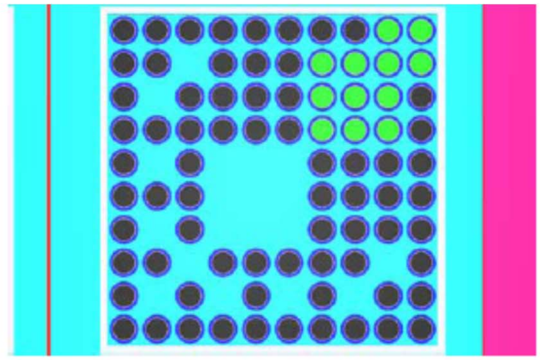

FANP 10x10 5.0 wt% ^{235}U, 10 Part Length Rods

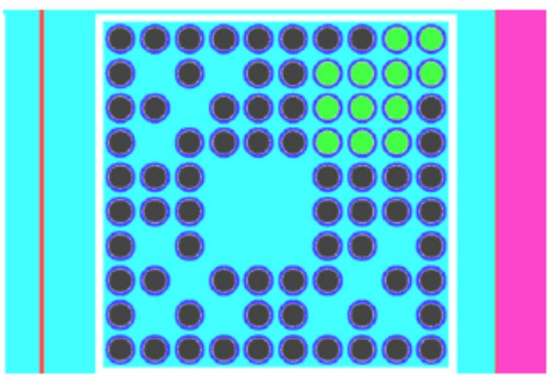

FANP 10x10 5.0 wt% ^{235}U, 12 Part Length Rods

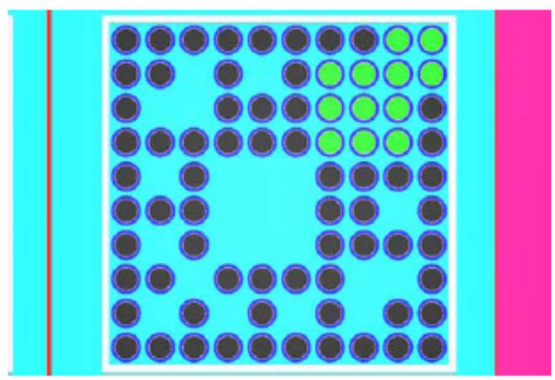

FANP 10x10 5.0 wt% ^{235}U, 14 Part Length Rods

Figure 6-33 FANP 10x10 Worst Case Fuel Parameters Model with Part Length Fuel Rods

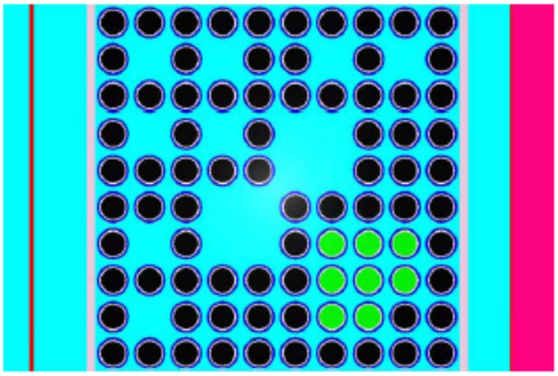

GNF 10x10 4.2 wt% ^{235}U, 8 Part Length Rods

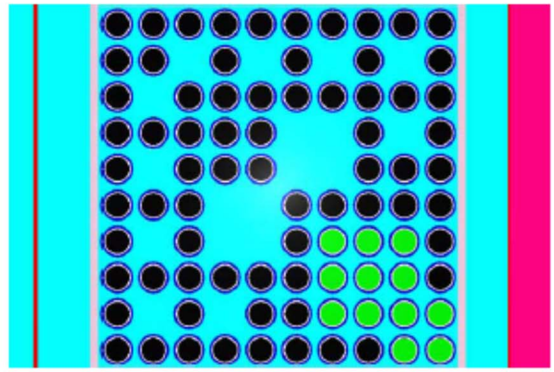

GNF 10x10 5.0 wt% ^{235}U, 10 Part Length Rods

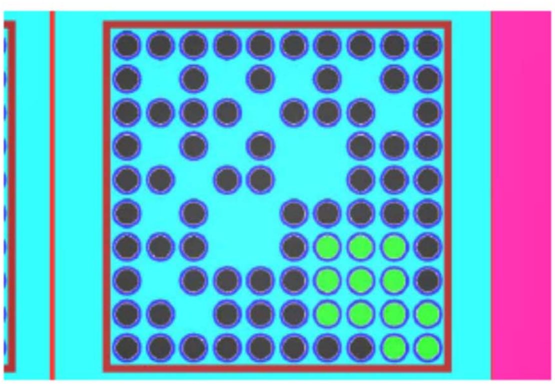

GNF 10x10 5.0 wt% ^{235}U, 12 Part Length Rods

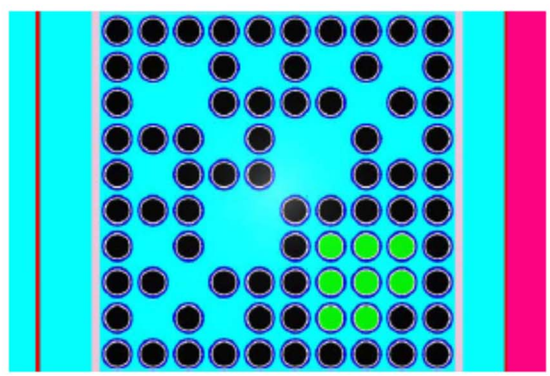

GNF 10x10 4.2 wt% ^{235}U, 14Part Length Rods

Figure 6-34 GNF 10x10 Worst Case Fuel Parameters Model with Part Length Fuel Rods

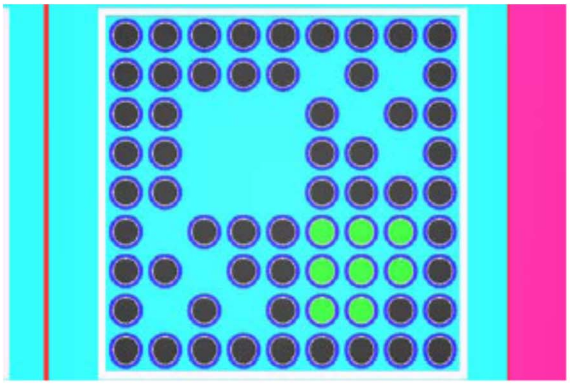

FANP 9x9 4.7 wt% ^{235}U, 8 Part Length Rods

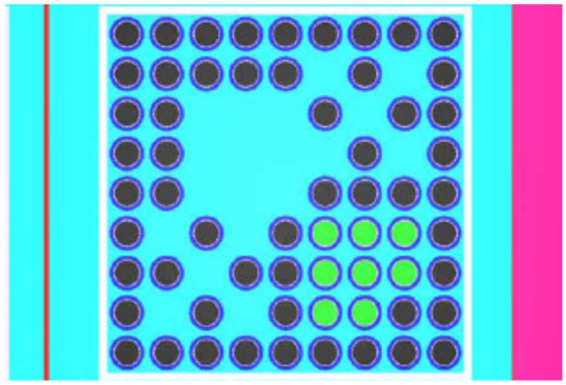

FANP 9x9 4.7 wt% ^{235}U, 10 Part Length Rods

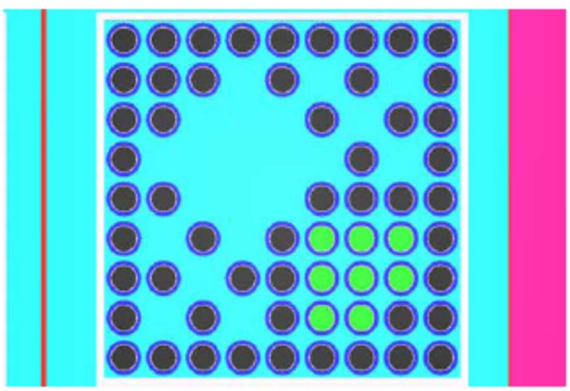

FANP 9x9 4.7 wt% ^{235}U, 12 Part Length Rods

Figure 6-35 FANP 9x9 Worst Case Fuel Parameters Model with Part Length Fuel Rods

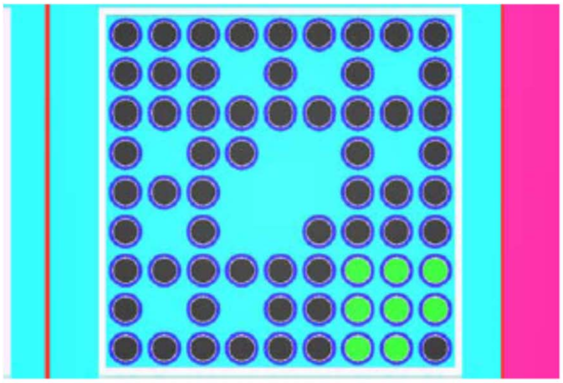

GNF 9x9 4.8 wt% ^{235}U, 8 Part Length Rods

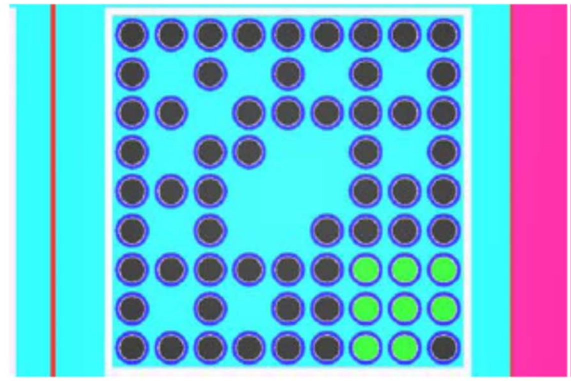

GNF 9x9 4.8 wt% ^{235}U, 10 Part Length Rods

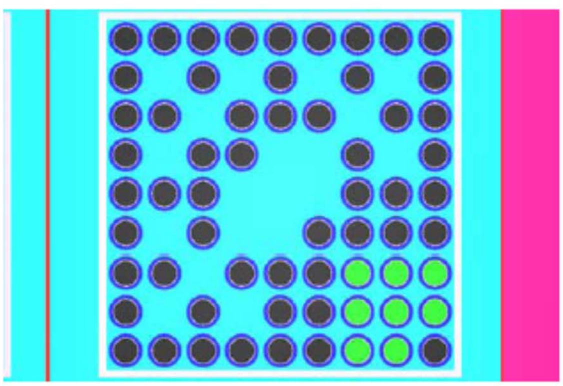

GNF 9x9 4.8 wt% ^{235}U, 12 Part Length Rods

Figure 6-36 GNF 9x9 Worst Case Fuel Parameters Model with Part Length Fuel Rods

6.3.4.10. Moderator Density Study (2N=448)

The worst-case design from Table 6-18 TN-B1 Array HAC Part Length Fuel Rod Calculations is used to conduct a moderator density sensitivity analysis. The GNF 10x10 fuel bundle is chosen for the study since it resulted in the highest reactivity in Table 6-18. Previous calculations demonstrated the worst-case condition for maximum reactivity is a configuration in which there is no moderator between the TN-B1 shipping packages. The moderator density study is conducted by varying the moderator density inside the inner container fuel compartment. The outer region of the inner container is filled with the Alumina Silicate thermal insulating material. The results of the moderator density study, Table 6-31, are shown in Figure 6-37. As shown in Figure 6-37, all cases peak at full moderator density. Therefore, a moderator density of 1.0 g/cm^3 is chosen as the worst-case moderator condition for the TN-B1 inner container fuel compartment.

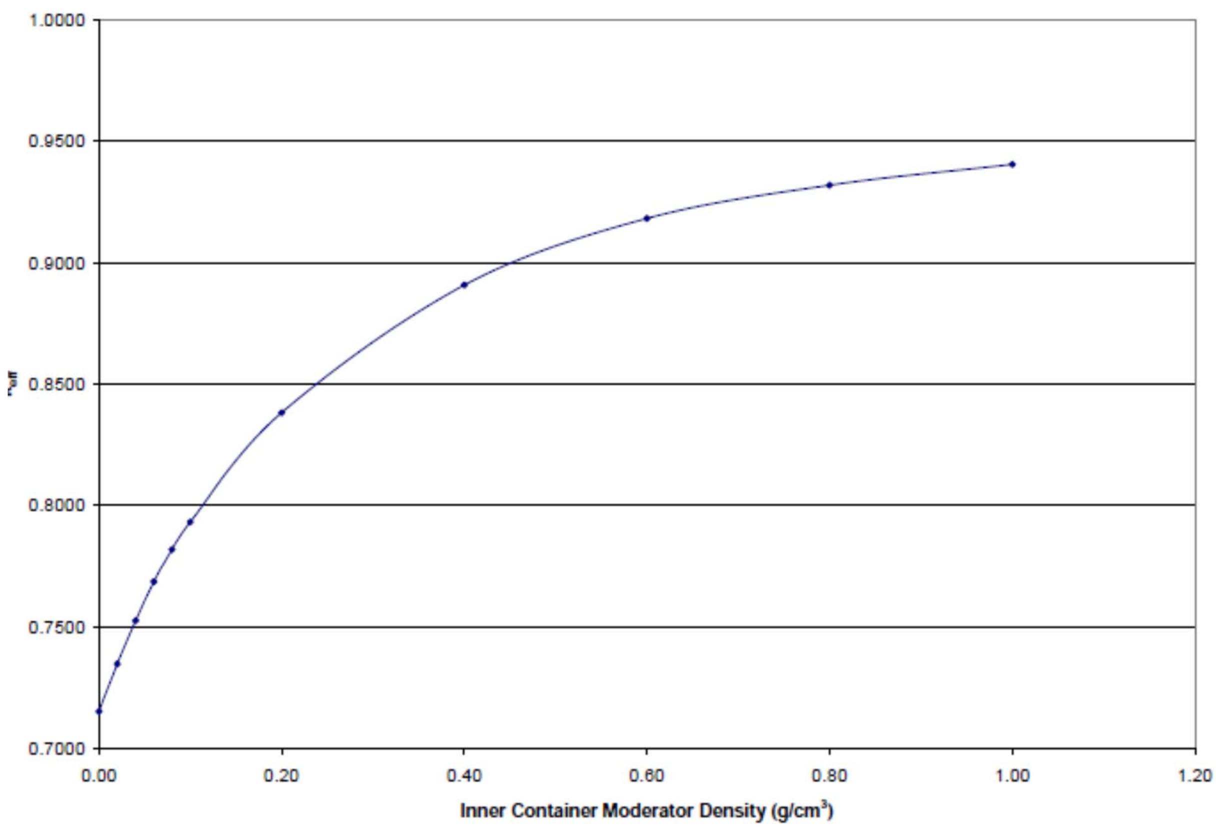

Figure 6-37 Moderator Density Sensitivity Study for the TN-B1 HAC Worst-case Parameter Fuel Design

6.3.4.11. Material Distribution Reactivity Study (2N=448, 2N=100)

A study is performed to determine the worst packing material distribution within the TN-B1 inner container. The material normally present around the inner container fuel compartment is a thermal insulator consisting of Alumina Silicate. The material normally lining the inner container fuel compartment is a polyethylene foam material which has a density in the range 0.05 – 0.075 g/cm^3.

The first part of the material distribution study investigates replacing the Alumina Silicate alternately with full density water and void while the inner container fuel compartment is filled with full density water. The GNF 10x10 fuel bundle is chosen for the study since it resulted in the highest reactivity in Table 6-18. In addition, the worst-case TN-B1 model is used in a 14x2x16 array (2N=448). The results are shown in Table 6-19. The first three cases in Table 6-19 show the most reactive condition is achieved with the Alumina Silicate thermal insulator in place. Therefore, the Alumina Silicate thermal insulator will remain a part of the worst-case TN-B1 model.

The second part of the material distribution study investigates placing the polyethylene foam material in its proper location within the TN-B1 fuel assembly compartment. Until this point, the polyethylene foam was assumed to burn away in the fire that also melted the polyethylene spacers. It should be noted that it is extremely unlikely that this configuration would exist post thermal excursion. The polyethylene foam would be as susceptible to the fire as the polyethylene spacers. However, the incomplete foam burn is considered in this study for conservatism. The GNF 10x10 fuel bundle is chosen for the study since it resulted in the highest reactivity in Table 6-18. In addition, the worst-case TN-B1 model is used in a 14x2x16 array (2N=448). The results are shown in Table 6-19. As shown in Table 6-19, the most reactive condition is achieved with the full thickness of ethafoam in place. Since the k_{eff} values exceed the 0.94254 USL with the polyethylene foam in place, the package array size is reduced to 10x1x10 (2N=100) to meet the acceptance criterion (last row in Table 6-19). The full thickness of ethafoam will be maintained for the remaining TN-B1 calculations since that configuration resulted in the highest k_{eff} value.

Table 6-19 TN-B1 Inner Container Thermal Insulator Region and Polyethylene Foam Material Study

Fuel Type	Array Size	Inner Container Foam Space	Insulator Space Fill	k_{eff}	σ	$k_{eff} + 2\sigma$
GNF 10x10	14x2x16 (2N=448)	Water	Thermal Ins.	0.9404	0.0007	0.9418
GNF 10x10	14x2x16 (2N=448)	Water	Water	0.7938	0.0009	0.7956
GNF 10x10	14x2x16 (2N=448)	Water	None	0.9362	0.0008	0.9378
GNF 10x10	14x2x16 (2N=448)	¼ Foam Thickness-Water	Thermal Ins.	0.9618	0.0009	0.9636
GNF 10x10	14x2x16 (2N=448)	½ Foam Thickness-Water	Thermal Ins.	0.9808	0.0009	0.9826
GNF 10x10	14x2x16 (2N=448)	5/8 Foam Thickness-Water	Thermal Ins.	0.9902	0.0008	0.9918

Fuel Type	Array Size	Inner Container Foam Space	Insulator Space Fill	k_{eff}	σ	$k_{eff} + 2\sigma$
GNF 10x10	14x2x16 (2N=448)	¾ Foam Thickness-Water	Thermal Ins.	0.9943	0.0008	0.9959
GNF 10x10	14x2x16 (2N=448)	7/8 Foam Thickness-Water	Thermal Ins.	0.9965	0.0008	0.9981
GNF 10x10	14x2x16 (2N=448)	Full Foam Thickness	Thermal Ins.	0.9971	0.0010	**0.9991**
GNF 10x10	10x1x10 (2N=100)	Full Foam Thickness	Thermal Ins.	0.9378	0.0009	0.9396

6.3.4.12. Inner Container Partial Flooding Study (2N=100)

Calculations are run in which the fuel bundle rows are partially filled within the TN-B1 inner fuel compartment as shown in Figure 6-39. The GNF 10x10 fuel bundle is chosen for the analysis since it produced the highest reactivity in Figure 6-37. The TN-B1 HAC model from the polyethylene foam study is used with an array size of 10x1x10 (2N=100). The results are shown in Table 6-20. As shown in Table 6-20, the most reactive condition exists when water fully covers each fuel bundle. Therefore, the inner container fuel compartment will be fully flooded with water in the worst-case TN-B1 model.

Table 6-20 TN-B1 Inner Container Partially Filled with Moderator

Fuel Type	Fuel Rows Filled	Moderator Density (g/cm^3)	k_{eff}	σ	$k_{eff} + 2\sigma$
GNF 10x10	1	1.00	0.6643	0.0007	0.6657
GNF 10x10	3	1.00	0.7678	0.0009	0.7696
GNF 10x10	5	1.00	0.8653	0.0008	0.8669
GNF 10x10	7	1.00	0.9212	0.0008	0.9228
GNF 10x10	9	1.00	0.9355	0.0009	0.9373
GNF 10x10	10	1.00	0.9378	0.0009	**0.9396**

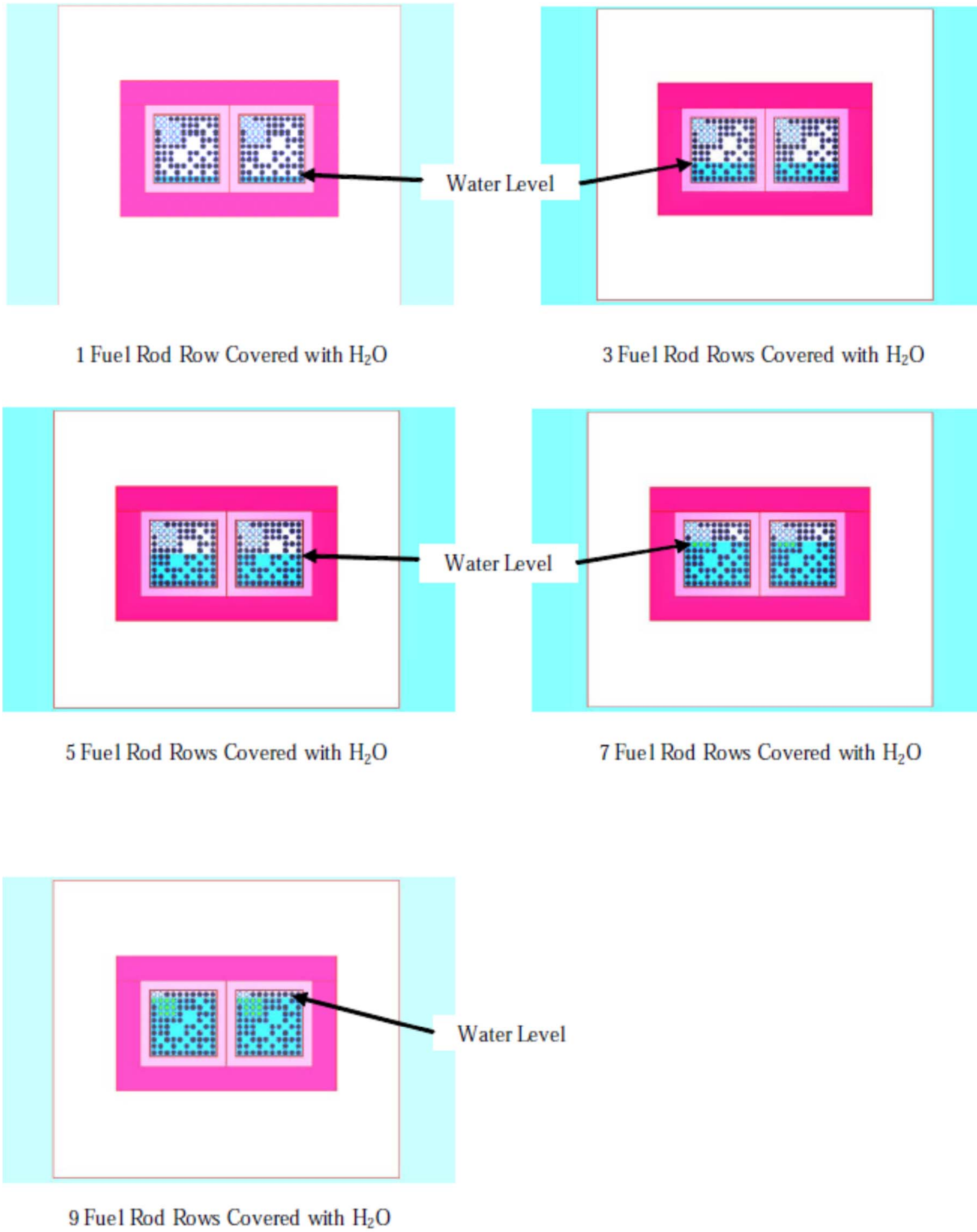

Figure 6-38 TN-B1 Inner Container Fuel Compartment Flooding Cases

6.3.4.13. TN-B1 Container Spacing Study (2N=100)

Calculations performed previously assume the TN-B1 shipping containers are resting next to one another with no spacing between them. A container pitch sensitivity study is conducted to determine if reactivity increases as containers are moved away from one another. The HAC model used in the inner container partial flooding study is used for the pitch sensitivity study with an array size of 10x1x10 (2N=100). The GNF 10x10 fuel assemblies with an average lattice enrichment of 5.0 wt% U-235, 12 gadolinia-urania fuel rods enriched to 2.0 wt % gadolinia, and 12 part-length fuel rods is used. The worst-case fuel parameters listed in Table 6-18 for the GNF 10x10 fuel design are utilized. The edge-to-edge separation is increased from 0 to 10 cm and the reactivity impact is observed. The results shown in Table 6-21 show a decrease in reactivity with increased spacing between containers. Therefore, the most reactive container configuration occurs when there is minimum spacing between containers.

Table 6-21 TN-B1 Array Spacing Sensitivity Study

Assembly Type	Interspersed Moderator Density (g/cm^3)	Container Pitch (cm)	Pitch (cm)	Pellet Diameter (cm)	Clad ID (cm)	Clad OD (cm)	k_{eff}	σ	$k_{eff} + 2\sigma$
GNF 10x10	0.0	71.926	1.350	0.895	0.9338	1.01	0.9378	0.0009	**0.9396**
GNF 10x10	0.0	74.426	1.350	0.895	0.9338	1.01	0.9259	0.0009	0.9277
GNF 10x10	0.0	76.926	1.350	0.895	0.9338	1.01	0.9122	0.0008	0.9138
GNF 10x10	0.0	81.926	1.350	0.895	0.9338	1.01	0.8865	0.0008	0.8881

6.4. SINGLE PACKAGE EVALUATION

Based on the sensitivity studies performed in this section, the single package and package array normal transport condition and HAC calculations are performed using the GNF 10x10 at an average lattice enrichment of 5.0 wt % U-235, twelve 2.0 wt% gadolinia fuel rods, and 12 part-ength fuel rods.

6.4.1. *Configuration*

The single package model described in Section 6.3.1.1 is used to demonstrate criticality safety of the TN-B1 shipping container using the worst-case fuel design. The GNF 10x10 at an average lattice enrichment of 5.0 wt % U-235, twelve 2.0 wt% gadolinia fuel rods, and 12 part-length fuel rods is used for the NTC and HAC evaluations. A moderator density study is conducted under both hypothetical accident and normal conditions. In the HAC study, the water density in the inner package is varied while the void in the outer container is maintained. For the normal conditions of transport, the moderator density is uniformly varied.

6.4.2. *Single Package Results*

The results for the single package normal conditions of transport evaluation are displayed in Figure 6-39. The results for the single package HAC evaluation are shown in Figure 6-40. The results in the figures indicate reactivity for the single package increases with increasing moderator density. The highest k_{eff} is achieved for both cases at full density moderation in the inner container. The polyethylene foam remains in place for the NTC single package configuration, but the polyethylene foam is removed from the HAC single package configuration. Removing the polyethylene foam in the HAC single package model, decreases neutron leakage which increases reactivity for a single container. In addition, full density moderation is included in the outer container for the single package NTC configuration. In both cases, the k_{eff} remains far below the USL of 0.94254. The maximum $k_{eff} + 2\sigma$ for the single package normal conditions of transport case is 0.6689 (Table 6-32), and the maximum $k_{eff} + 2\sigma$ for the single package HAC case is 0.6951 (Table 6-33). Therefore, criticality safety is established for the single package TN-B1 container.

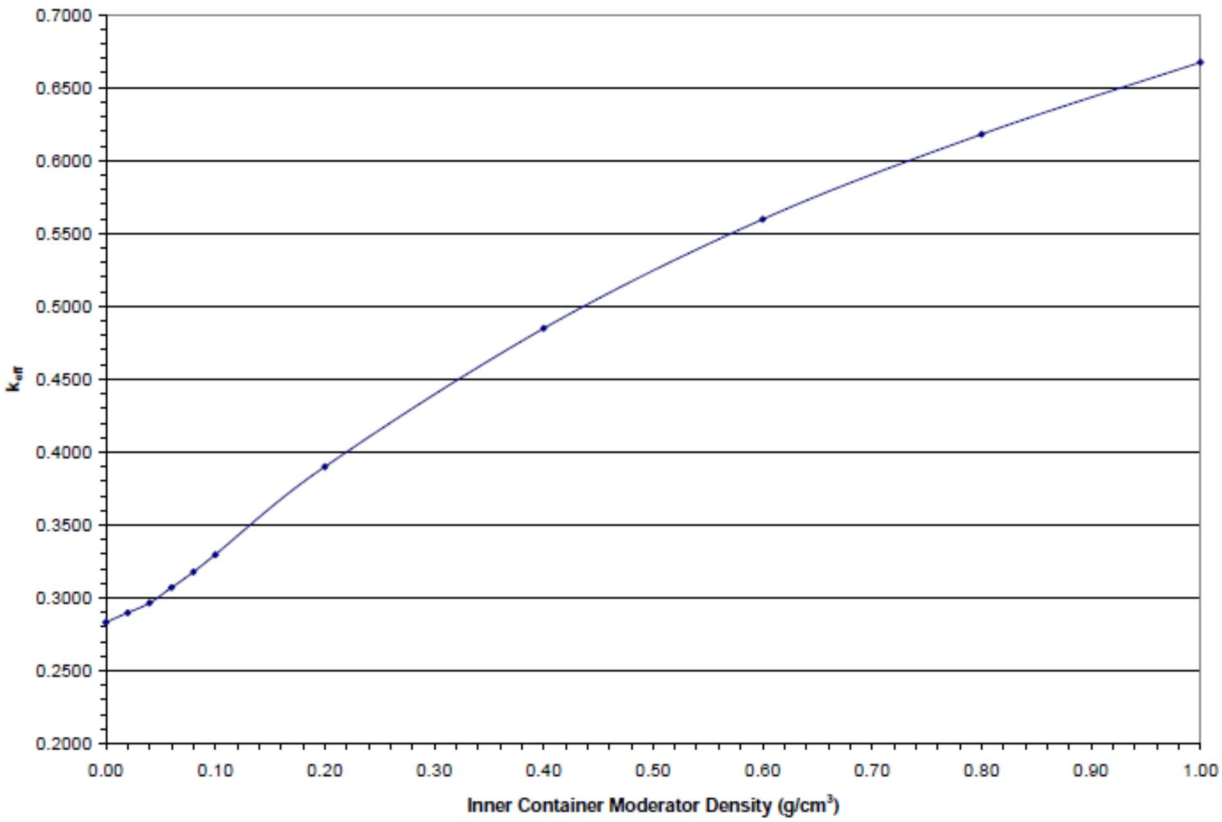

Figure 6-39 TN-B1 Single Package Normal Conditions of Transport Results

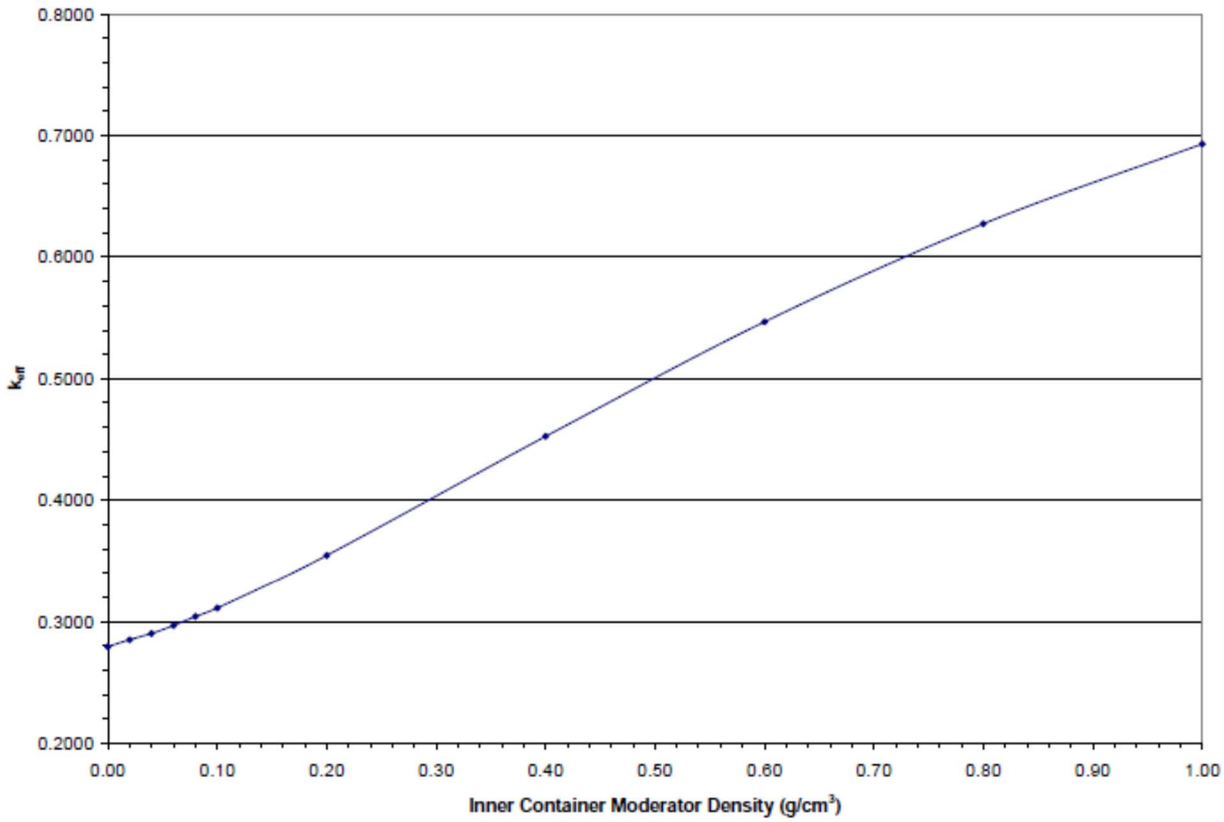

Figure 6-40 TN-B1 Single Package HAC Results

6.5. EVALUATION OF PACKAGE ARRAYS UNDER NORMAL CONDITIONS OF TRANSPORT

6.5.1. *Configuration*

The package array normal condition model described in Section 6.3.1.2.1 is used to demonstrate criticality safety of the TN-B1 shipping container using the GNF 10x10 worst-case fuel design at an average lattice enrichment of 5.0 wt % U-235, twelve 2.0 wt% gadolinia fuel rods, and 12 part-length fuel rods. The calculation using the normal conditions of transport model involves a moderator density sensitivity study. In the model, the moderator density is uniformly varied and the system reactivity is observed.

6.5.2. *Package Array NCT Results*

The results of the package array normal condition model calculations are shown in Figure 6-41. The reactivity peaks with no moderator present. A decreasing trend continues until the moderator density reaches 0.4 g/cm^3 at which point reactivity increases almost linearly to full water density. The maximum k_{eff} + 2σ obtained is 0.8535 (Table 6-34) which is below the USL of 0.94254. Therefore, criticality safety of the TN-B1 shipping container is demonstrated under normal conditions of transport.

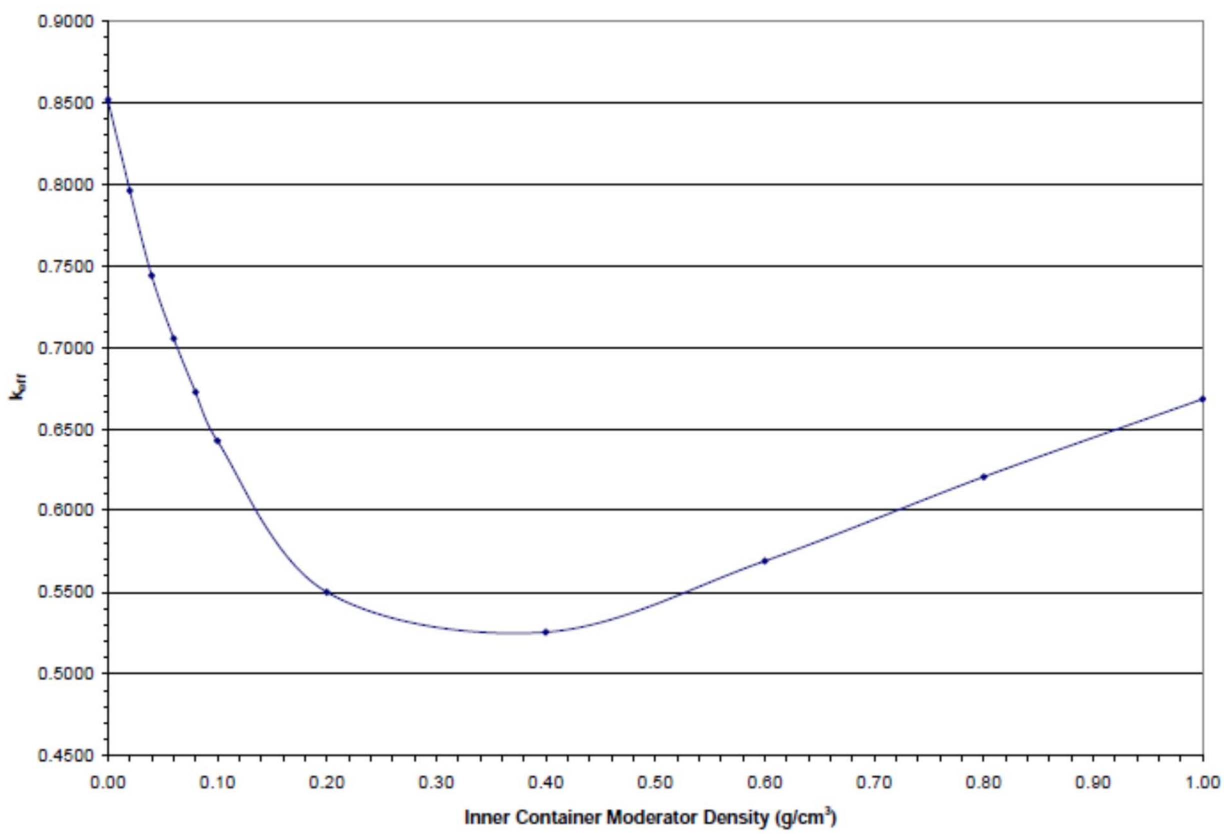

Figure 6-41 TN-B1 Package Array Under Normal Conditions of Transport Results

6.6. PACKAGE ARRAYS UNDER HYPOTHETICAL ACCIDENT CONDITIONS

6.6.1. *Configuration*

The package array hypothetical accident condition model described in Section 6.3.1.2.2 is used to demonstrate criticality safety of a 10x1x10 array (2N=100) of TN-B1 shipping containers using the GNF 10x10 worst-case fuel design at an average lattice enrichment of 5.0 wt % U-235, twelve 2.0 wt% gadolinia fuel rods, and 12 part-length fuel rods. The calculation using the HAC model involves a moderator density sensitivity study. In the study, no moderator is present in the outer container while the moderator density inside the inner container is varied. The polyethylene foam inside the inner container fuel compartment is modeled because previous calculations demonstrated this configuration to be the most reactive.

6.6.2. *Package Array HAC Results*

The results of the package array (2N=10x1x10=100 array) HAC model calculations are shown in Figure 6-42. The system reactivity begins at its lowest value and increases with increasing interspersed moderator density. This trend highlights the neutronics of the problem. Initially, no moderator, other than the polyethylene surrounding the fuel rods, is present to thermalize neutrons that enter the inner container. As the inner container moderator density increases, higher energy neutrons pass into adjacent containers and thermalize in the vicinity of the fuel creating a more reactive situation. The maximum $k_{eff} + 2\sigma$ for the package array HAC case is 0.9396 (Table 6-35) which is below the USL of 0.94254. Therefore, criticality safety of the TN-B1 shipping container is demonstrated for the package array under hypothetical accident conditions.

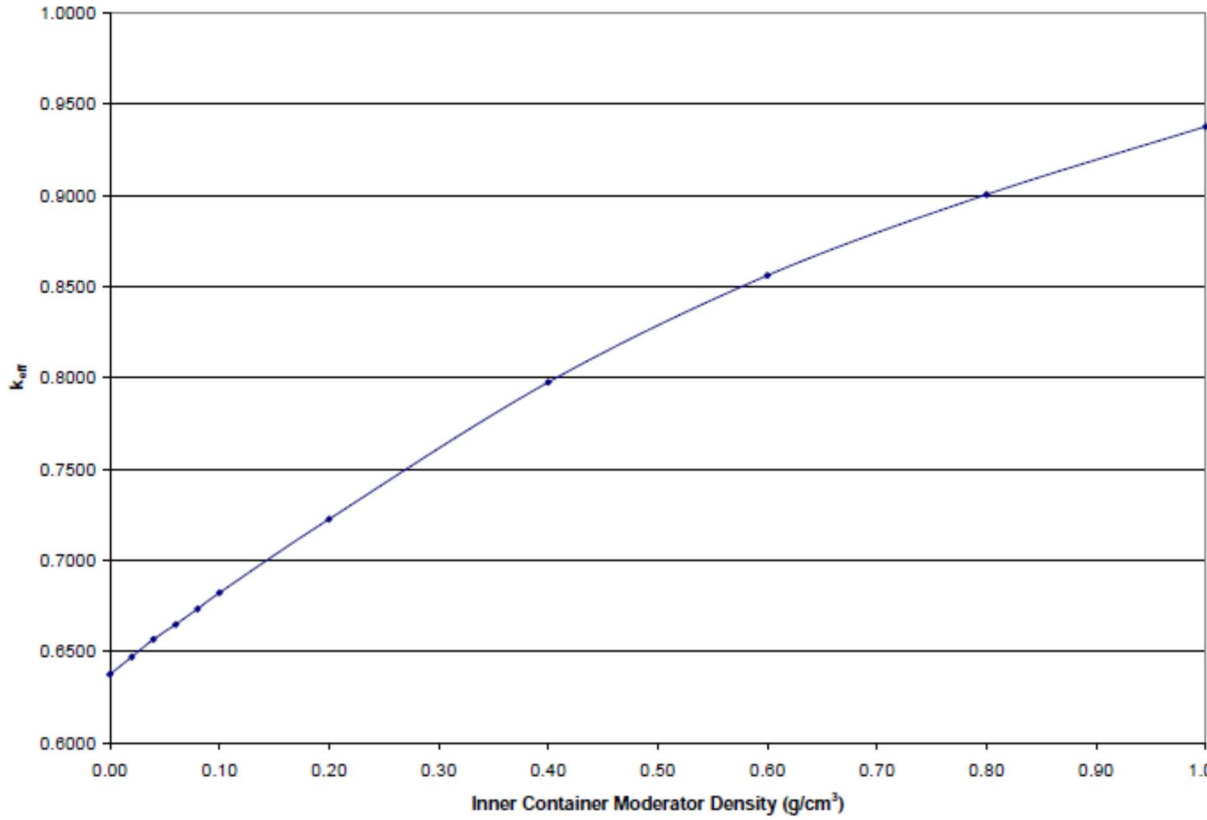

Figure 6-42 TN-B1 Package Array Hypothetical Accident Condition Results

6.6.2.1. Pu-239 Effect on Reactivity for the TN-B1 Package Array Hypothetical Accident Condition

Because the fuel scheduled for transport in the TN-B1 could have a small Pu-239 content, the effect on the TN-B1 Package HAC reactivity is investigated. The maximum plutonium concentration (3.04×10^{-9} gPu-239/gU) listed in Table 1-3 of the SAR is added to the worst-case package array HAC model (10x1x10 array), determined in the previous sections, and the k_{eff} is calculated. The results showed no statistically significant difference between the cases with and without plutonium. The $k_{eff} \pm 2\sigma$ for the worst-case with plutonium is 0.9406. The $k_{eff} + 2\sigma$ for the worst-case without plutonium, calculated in Section 6.6.2, is 0.9396. Both results remain below the USL of 0.94254. Therefore, the plutonium is justifiably neglected in the TN-B1 evaluation.

6.7. FUEL ROD TRANSPORT IN THE TN-B1

Studies are conducted to allow transport of UO2 fuel rods in the TN-B1 container. Several configurations are investigated including: loose fuel rods, fuel rods bundled together, and fuel rods contained in 5-inch stainless steel pipe/protective case. The model uses the 10x10, 9x9, or 8x8 worst-case fuel rod designs developed in Section 6.3.4. A 6-mil layer of polyethylene encircles each fuel rod in the model to bound protective packing material that may be used for fuel rod transport.

6.7.1. *Loose Fuel Rod Study*

The package array model under hypothetical accident conditions is used for fuel rod calculations in the TN-B1, since it was demonstrated to be more reactive than the normal conditions of transport, package array model. The worst-case fuel rods are arranged in a square pitch array inside each TN-B1 transport compartment. Scoping studies indicated little difference between the square and triangular pitch array, therefore the square pitch array is chosen for convenience. The inner container is filled with full density water and the outer container has no water, which facilitates leakage of neutrons into neighboring containers. The fuel rod pitch is varied, and the results are illustrated with curves. The curves are shown Figure 6-43 Fuel Rod Pitch Sensitivity Study and corresponding calculational data listed in Table 6-22 Fuel Rod Pitch Sensitivity Study Results. The results demonstrate that a fully loaded inner compartment in which the rods are all in contact with each other is a supercritical configuration. As a result, a minimum number of fuel rods to ensure subcriticality cannot be established for the TN-B1 shipping container. A maximum fuel rod quantity to ensure subcriticality can be established for the loose configuration. For all three fuel designs, a maximum of 25 fuel rods may be safely transported in each RAJ- II fuel assembly compartment. The 8x8 rod design is limiting as shown in Figure 6-43 and Table 6-22 Fuel Rod Pitch Sensitivity Study Results.

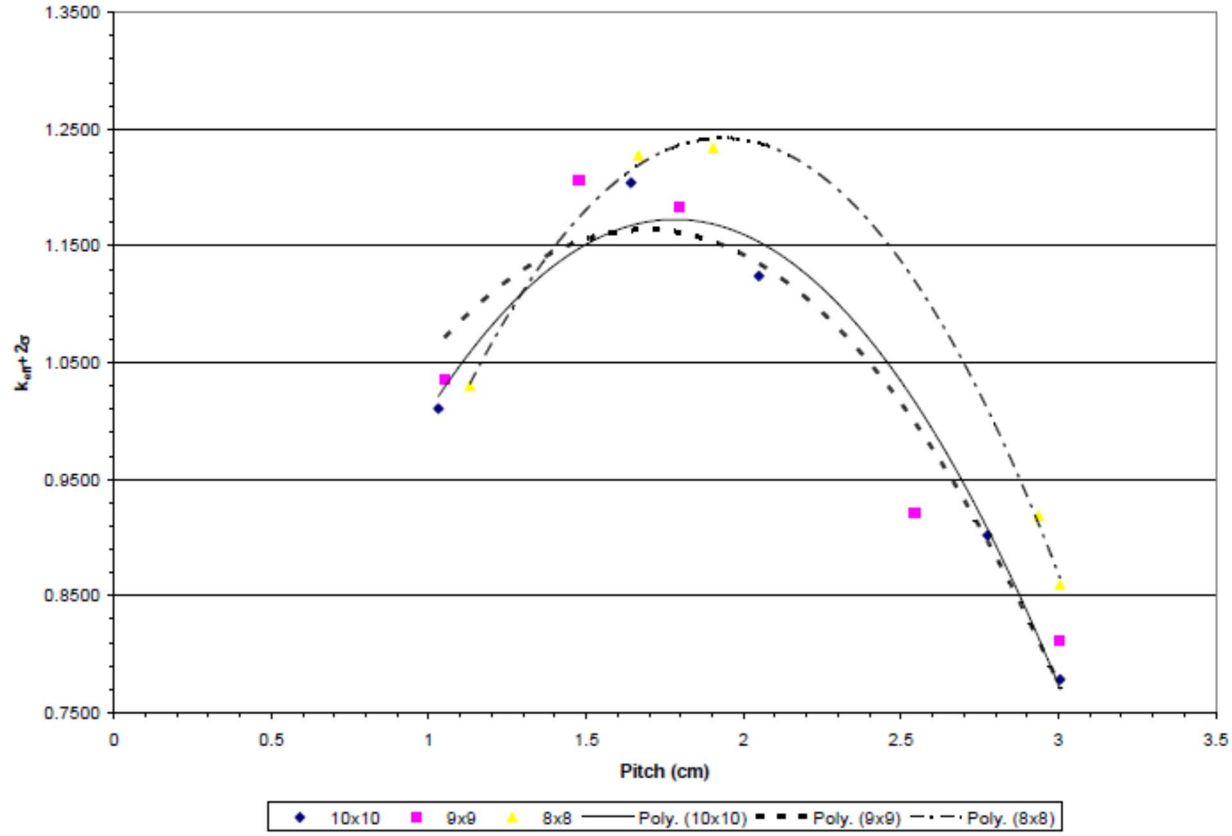

Figure 6-43 Fuel Rod Pitch Sensitivity Study

Table 6-22 Fuel Rod Pitch Sensitivity Study Results

Fuel Rod Type	Fuel Rod Pitch (cm)	Fuel Rod Number	Fuel Pellet OD (cm)	Clad Inner Diameter (cm)	Clad Outer Diameter (cm)	k_{eff}	σ	$k_{eff} + 2\sigma$
10x10	1.0305	289	0.9	1.000	1.000	1.0092	0.0007	1.0106
10x10	1.6416	100	0.9	1.000	1.000	1.2024	0.0009	1.2042
10x10	2.0484	64	0.9	1.000	1.000	1.1224	0.0009	1.1242
10x10	2.7754	34	0.9	1.000	1.000	0.9005	0.0008	0.9021
10x10	3.0056	25	0.9	1.000	1.000	0.7769	0.0007	0.7783
9x9	1.0505	256	0.9600	1.0200	1.0200	1.0341	0.0007	1.0355
9x9	1.4770	121	0.9600	1.0200	1.0200	1.2045	0.0008	1.2061
9x9	1.7972	81	0.9600	1.0200	1.0200	1.1816	0.0008	1.1832
9x9	2.5432	34	0.9600	1.0200	1.0200	0.9196	0.0008	0.9212
9x9	3.0056	25	0.9600	1.0200	1.0200	0.8096	0.0007	0.8110
8x8	1.1305	225	1.05	1.1000	1.1000	1.0288	0.0007	1.0302
8x8	1.6662	100	1.05	1.1000	1.1000	1.2259	0.0008	1.2275
8x8	1.9035	81	1.05	1.1000	1.1000	1.2328	0.0007	1.2342
8x8	2.9370	30	1.05	1.1000	1.1000	0.9172	0.0008	0.9188
8x8	3.0056	25	1.05	1.1000	1.1000	0.8577	0.0008	0.8593

The results in Table 6-22 Fuel Rod Pitch Sensitivity Study Results are based on calculations performed with full water density inside the inner container. It appears the maximum fuel rod quantity allowable for the 10x10 and 9x9 fuel rods should be 34, while that for the 8x8 fuel rods should be 30. However, the rod configurations at full moderator densities represent an overmoderated condition in which reactivity peaks at a reduced moderator density. Therefore, calculations are performed with 25 fuel rods in each transport compartment for each fuel rod type, and the moderator density inside the inner container is varied from 0.4 g/cm^3 to 1.00 g/cm^3 to investigate the possibility that reactivity peaks at a lower moderator density. The results of these calculations are shown in Table 6-23. The peak reactivity for all the fuel rod types occurs at a moderator density of 0.6 g/cm^3 and are all below the USL of 0.94254. Therefore, criticality safety for loose fuel rod transport with a maximum of 25 rods in each transport compartment is demonstrated.

Table 6-23 Fuel Rod Maximum Quantity at Reduced Moderator Densities

Fuel Rod Type	Fuel Rod Pitch (cm)	Fuel Rod Number	Inner Container Moderator Density (g/cm^3)	Fuel Pellet OD (cm)	Clad Inner Diameter (cm)	Clad Outer Diameter (cm)	k_{eff}	σ	$k_{eff} + 2\sigma$
10x10	3.0056	25	0.40	0.9	1.000	1.000	0.7875	0.0009	0.7893
10x10	3.0056	25	0.60	0.9	1.000	1.000	0.8113	0.0008	**0.8129**
10x10	3.0056	25	0.80	0.9	1.000	1.000	0.8012	0.0007	0.8026
10x10	3.0056	25	1.00	0.9	1.000	1.000	0.7769	0.0007	0.7783
9x9	3.0056	25	0.40	0.9600	1.0200	1.0200	0.8128	0.0008	0.8144
9x9	3.0056	25	0.60	0.9600	1.0200	1.0200	0.8404	0.0008	**0.8420**
9x9	3.0056	25	0.80	0.9600	1.0200	1.0200	0.8321	0.0008	0.8337
9x9	3.0056	25	1.00	0.9600	1.0200	1.0200	0.8096	0.0007	0.8110
8x8	3.0056	25	0.40	1.05	1.1000	1.1000	0.8529	0.0008	0.8545
8x8	3.0056	25	0.60	1.05	1.1000	1.1000	0.8832	0.0008	**0.8848**
8x8	3.0056	25	0.80	1.05	1.1000	1.1000	0.8799	0.0009	0.8817
8x8	3.0056	25	1.00	1.05	1.1000	1.1000	0.8577	0.0008	0.8593

a. Limiting case(s) shown in bold

6.7.2. *Fuel Rods Bundled Together*

Based on the results in the previous calculation, there is no advantage to bundling fuel rods together since close packed rods do not guarantee subcriticality. Besides, the straps holding the fuel rods together in the bundle may fail during an accident, and the rods could move about the transport compartment without restraint. Therefore, the maximum number of fuel rods allowable in each TN-B1 fuel compartment when fuel rods are transported in bundles is 25 for all types.

6.7.3. *Fuel Rods Transported in 5-Inch Stainless Steel Pipe*

A fuel rod pitch sensitivity study is conducted for the transport of fuel rods inside 5-inch stainless steel pipe, residing in the TN-B1 fuel compartment. The package array model under hypothetical accident conditions is used for fuel rod calculations in the TN-B1 container, since it was demonstrated to be more reactive than the normal conditions of transport, package array model. The GNF 10x10, the GNF 9x9, and the GNF 8x8, the UC and PWR worst-case fuel rod designs are used for the study. Since the 5-inch stainless steel pipe presents a more difficult volume to accommodate rods in a square pitch, a triangular pitch array is used for the rod configuration. The pipe's stainless steel wall is also neglected for conservatism. The fuel rod configuration inside the pipe is shown in Figure 6-44 for the GNF 8x8 fuel rods. The volume inside the pipe is filled with water at a density sufficient for optimum moderation. The inner fuel compartment volume outside the pipe is modeled with no material present to maximize neutron interaction among packages in the array.

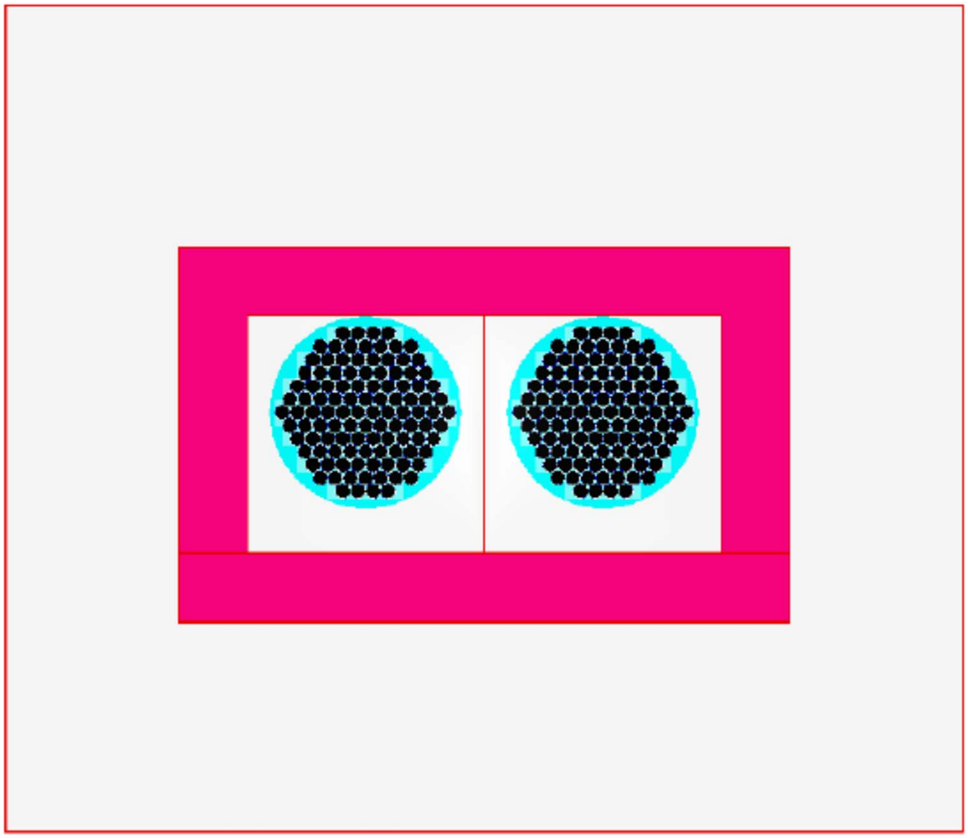

Figure 6-44 TN-B1 with Fuel Rods in 5-Inch Stainless Steel Pipes for Transport

The results for fuel rod transport in a SS pipe within the TN-B1 container for the all rod designs are displayed in Figure 6-45. As shown in Figure 6-45, optimum peaks are formed above the USL of 0.94254. Therefore, the stainless steel pipe may be used to ship a limited number of fuel rods. The maximum number of 10x10 fuel rods that may be transported in the stainless steel pipe is 30. The maximum number of 9x9 fuel rods that may be transported in the stainless steel pipe is 26. The maximum number of 8x8 fuel rods that may be transported in the stainless steel pipe is 22. The $k_{eff} + 2\sigma$ values (Table 6-36) for all fuel rod types with the appropriate fuel rod quantity are below the USL of 0.94254. Therefore, criticality safety is demonstrated for fuel rod transport inside a SS pipe within the TN-B1 container.

The optimum peak for the 10x10 fuel rods is greater than that for the 9x9 or 8x8 fuel rods in the SS pipe. Since the reactivity peak for the 8x8 fuel rod in the loose rod study is greater than that for the 10x10 fuel rods in the SS pipe, it is chosen as the bounding fuel assembly type.

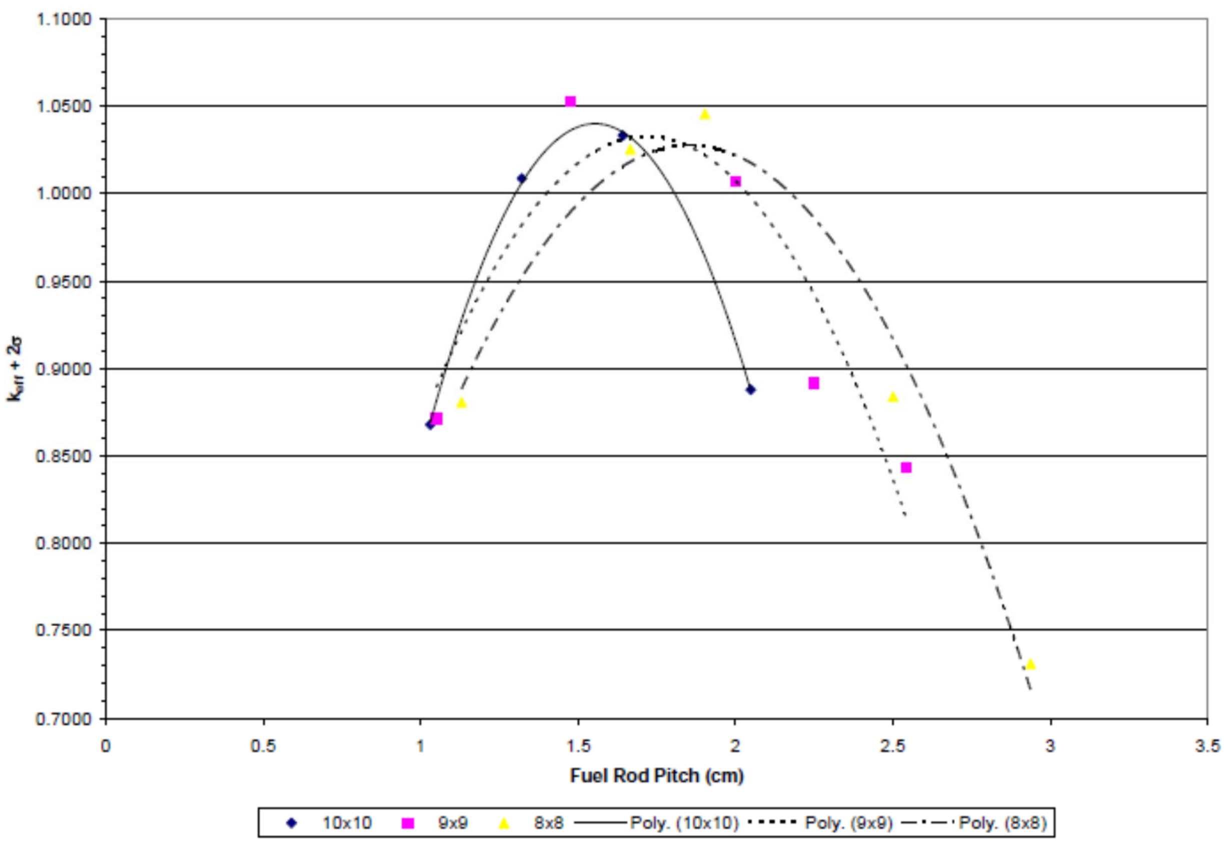

Figure 6-45 TN-B1 Fuel Rod Transport in Stainless Steel Pipe

This addendum to the TN-B1 SAR includes analysis of Uranium-Carbide and UO2 PWR rods inside the 5” stainless steel pipe. Loose rods in the product container are evaluated in this analysis ACEL’s CANDU Uranium-Carbide (UC) or generic Uranium-Dioxide (UO_2) fuel rods with a maximum U-235 (pellet) enrichment of 5.0%. The analysis is also applicable to UC or UO_2 fuel rods with GdO_2 or boron, provided that the maximum enrichment and dimensional limits are met since the presence of GdO_2 or boron in the fuel rods will result in a reduction in the applicable neutron multiplication factors. The same applies to fuel rods clad with stainless steel since stainless steel (with the same or greater clad thickness) is a better neutron absorber than zircaloy.

Three different fuel rods have been considered in this analysis, as designated by the labels “CANDU-14”, “CANDU-25” and “PWR”. The CANDU-14 and CANDU-25 types are those corresponding to the fuel rods in typical CANDU 14 element and 25 element fuel bundle assemblies (Table 6-2). The PWR type is that corresponding to generic PWR fuel rods.

The optimum condition for interspersed water in 8x1x8 and 4x2x6 arrays of damaged containers has been determined as in the case for the infinite arrays of undamaged containers by scoping calculations independently varying the W/F ratios inside the product containers and the interspersed water outside. The results of the scoping calculations are that the optimum interspersed water is again the 0.0 case, presumably because the fuel region inside the Product Containers is already fully moderated by the water and plastic sleeving surrounding the fuel rods.

Based on the results of the horizontally infinite arrays of damaged packages, calculations have been made for the 8x1x8 arrays of damaged TN-B1 containers for most reactive water-to-fuel ratios inside the product containers without interspersed water outside the product containers. Tables 6-24 and 6-25 show the results for three types of rods. The maximum $k_{eff} + 2\sigma$ for 8x1x8 arrays of TN-B1 containers is 0.9131 which occurs for loose CANDU-14 UC fuel rods at a W/F ratio of 2.68. As in the case for the horizontally infinite arrays of undamaged TN-B1, this result also bounds the k_{eff} values of the CANDU-25 UC fuel rod and generic PWR UO_2 designs.

Table 6-24 Results for 8x1x8 Array of Containers with Loose Fuel Rods

Type of Rods	W/F Ratio	k_{eff}	σ	k_{eff} + 2σ
CANDU-14 (UC)	2.12	0.90794	0.00076	0.90946
CANDU-25 (UC)	2.68	0.91162	0.00074	**0.91310**
PWR (UO_2)	2.24	0.85480	0.00074	0.85628

Table 6-25 Results for 4x2x6 Array of Containers with Loose Fuel Rods

Type of Rods	W/F Ratio	k_{eff}	σ	k_{eff} + 2σ
CANDU-14 (UC)	2.12	0.82820	0.00073	0.82966
CANDU-25 (UC)	2.68	0.83361	0.00072	**0.83505**
PWR (UO_2)	2.24	0.77301	0.00075	0.77451

6.7.4. *Fuel Rods Transported in Stainless Steel Protective Case*

The fuel rod pitch sensitivity study conducted for the transport of fuel rods inside the 5-inch stainless steel pipe described in Section 6.7.3 bounds the transport of fuel rods in the protective case. The protective case cross-section is 89 mm (3.50 inches) by 80 mm (3.15 inches). Based on this small cross-sectional area, the total number of fuel rods that will fit in the protective case is less than the total for the 5-inch pipe. Based on the calculations for the stainless steel pipe, the maximum number of 10x10 fuel rods that may be transported in the protective case is 30, the maximum number of 9x9 fuel rods that may be transported in in the protective case is 26, the maximum number of 8x8 fuel rods that may be transported in in the protective case is 22.

6.7.5. *Single Package Fuel Rod Transport Evaluation*

6.7.5.1. **Configuration**

The single package model described in Section 6.3.1.1 is used to demonstrate criticality safety of the TN-B1 shipping container using the worst-case fuel design. The single package is evaluated under both normal conditions of transport and hypothetical accident conditions. The evaluation consists of a moderator density sensitivity study. For the normal conditions of transport model, the moderator density is uniformly varied. In contrast, the moderator density is fixed in the inner container for the hypothetical accident condition model, and the moderator in the outer container is varied. Based on the results in Table 6-22, the GNF 8x8 worst-case fuel rod design is used for the study since it produced the highest reactivity peak among all fuel rods considered.

6.7.5.2. Single Package Fuel Rod Transport Result

The results for the single package, loose fuel rod, normal conditions of transport evaluation are displayed in Figure 6-46. The results for the single package, loose fuel rod, HAC evaluation are shown in Figure 6-47. The results in the figures indicate reactivity for the single package increases with increasing moderator density. The highest k_{eff} is achieved for both cases at fulldensity moderation. In both cases, the k_{eff} remains far below the USL of 0.94254. The maximum k_{eff} + 2σ for the single package normal conditions of transport case is 0.6381 (Table 6-37), and the maximum k_{eff} + 2σ for the single package HAC case is 0.6548 (Table 6-38). Therefore, criticality safety is established for the single package TN-B1 container transporting up to 25 loose fuel rods.

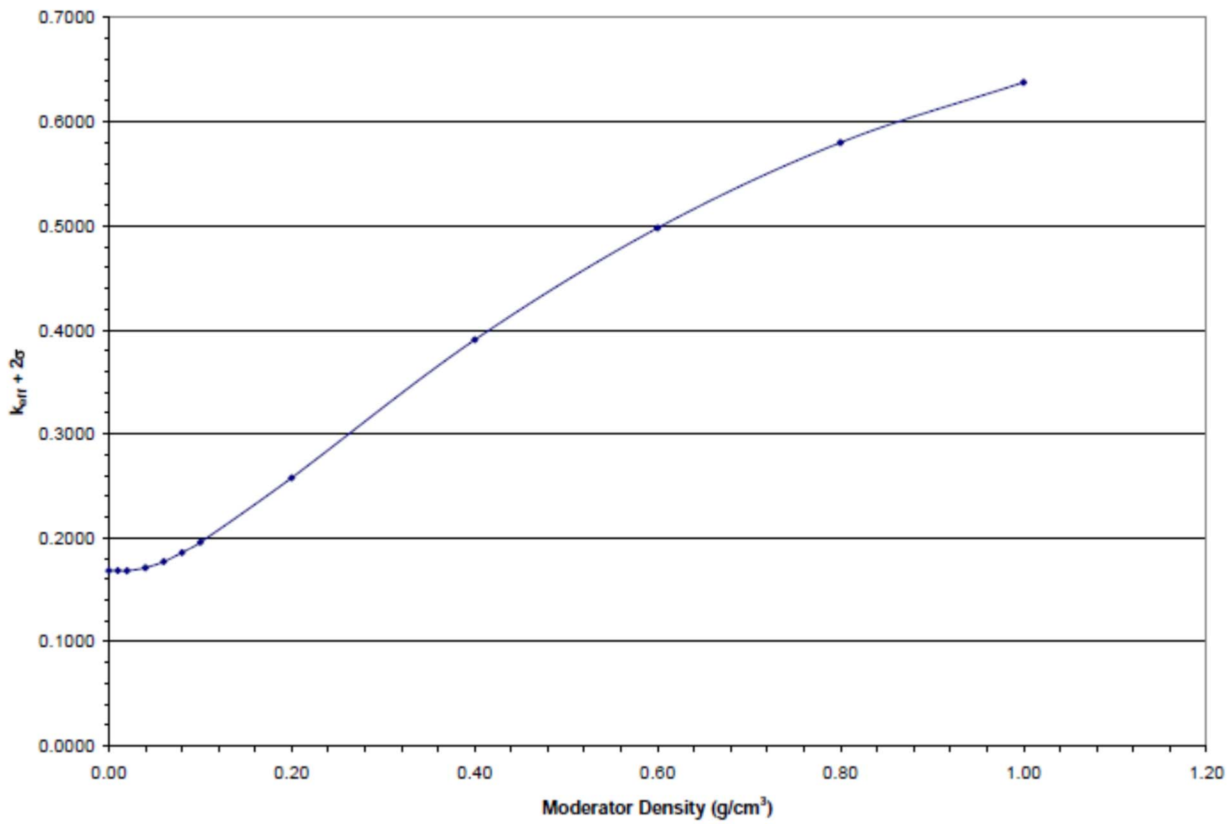

Figure 6-46 TN-B1 Fuel Rod Single Package Under Normal Conditions of Transport

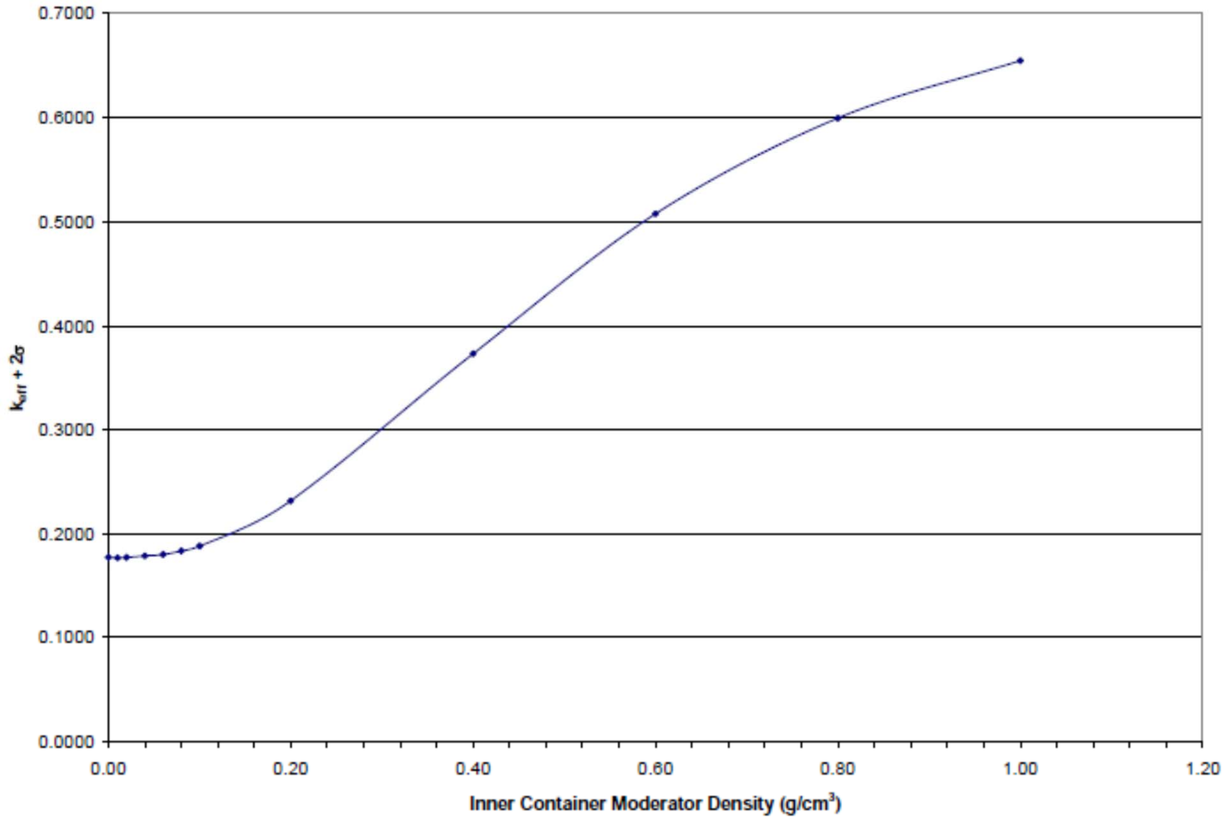

Figure 6-47 TN-B1 Fuel Rod Transport Single Package HAC

6.7.6. *Evaluation of Package Arrays with Fuel Rods Under Normal Conditions of Transport*

The package array normal condition model described in Section 6.3.1.2.1 is used to demonstrate criticality safety of the TN-B1 shipping container when transporting fuel rods. Based on the results in Table 6-22, the GNF 8x8 worst-case fuel rod design is used for the study since it produced the highest reactivity peak among all fuel rod designs considered. The calculation using the package array normal conditions of transport model for fuel rod transport involves a moderator density sensitivity study. In the model, the moderator density is uniformly varied and the system reactivity is observed.

6.7.6.1. **Package Array NCT Fuel Rod Transport Results**

The results of the package array fuel rod transport normal condition model calculations are shown in Figure 6-48. As shown, the reactivity initially increases then decreases as the moderator density increases until a density of 0.4 g/cm3 is reached, then it increases essentially linearly until full density is reached. The maximum keff + 2σ obtained is 0.6381 (Table 6-39) which is below the USL of 0.94254. Therefore, criticality safety of the TN-B1 shipping container with fuel rods is demonstrated under normal conditions of transport.

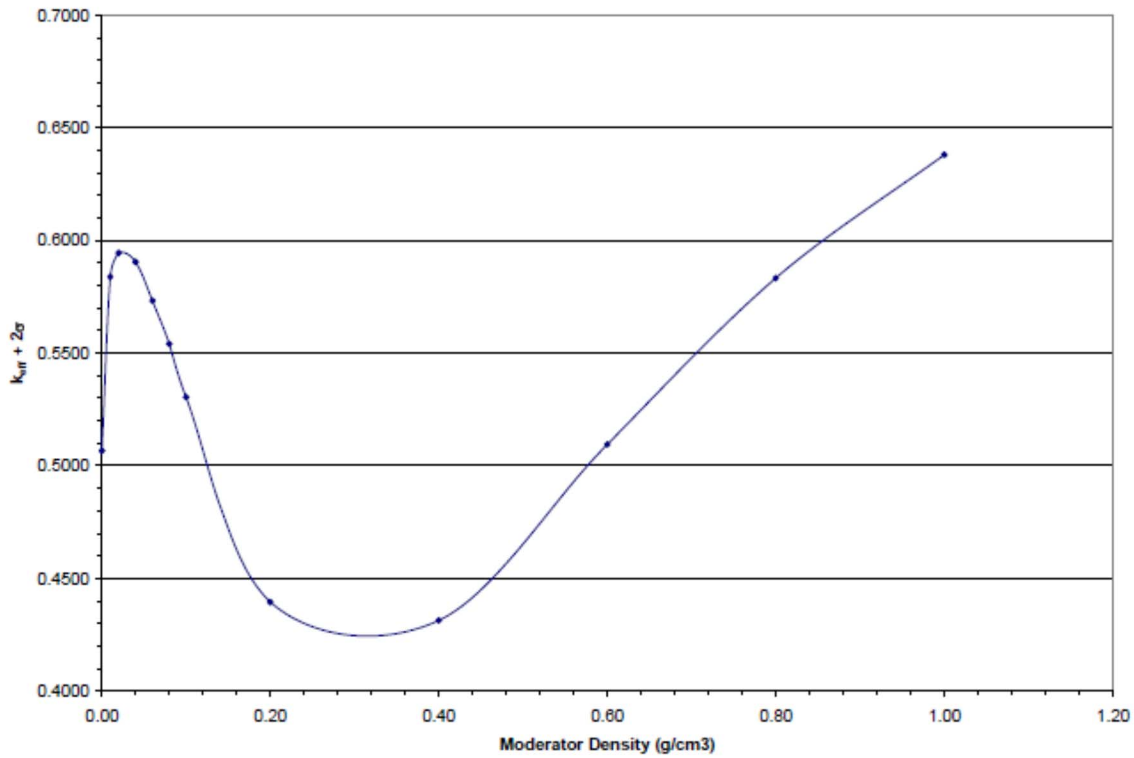

Figure 6-48 TN-B1 Package Array Under Normal Conditions of Transport with Loose Fuel Rods

6.7.7. *Fuel Rod Transport Package Arrays Under Hypothetical Accident Conditions*

The package array hypothetical accident condition model described in Section 6.3.1.2.2 is used to demonstrate criticality safety of a 10x1x10 array (2N=100) of TN-B1 shipping containers when transporting loose fuel rods. Based on the results in Table 6-22, the GNF 8x8 worst-case fuel rod design is used for the study since it produced the highest reactivity peak among the fuel rod designs considered. The calculation using the HAC model involves a moderator density sensitivity study. In the study, there is no interspersed moderator, and the moderator density inside the inner container is varied. The polyethylene foam lines the inner container fuel compartment since the configuration resulted in the most reactive conditions.

6.7.7.1. **Package Array HAC Fuel Rod Transport Results**

The results of the package array HAC model calculations are shown in Figure 6-49. The reactivity begins at its lowest value and increases with increasing internal moderator density until a peak is reached at a density of 0.6 g/cm^3. The maximum $k_{eff} + 2\sigma$ for the package array fuel rod transport HAC case is 0.8745 (Table 6-40), which is below the USL of 0.94254. Therefore, criticality safety of the TN-B1 shipping container is demonstrated for the package array under hypothetical accident conditions when fuel rods are being transported

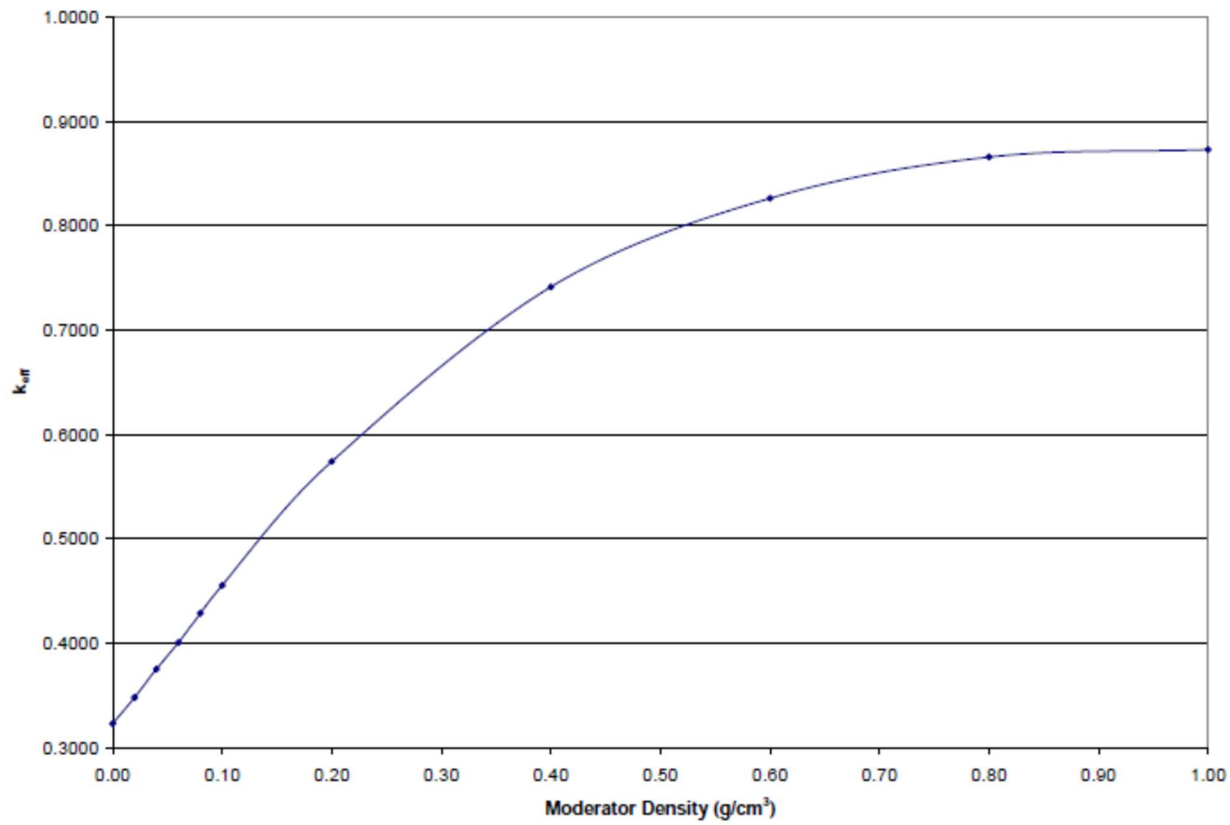

Figure 6-49 TN-B1 Fuel Rod Transport Under HAC

6.8. FISSILE MATERIAL PACKAGES FOR AIR TRANSPORT

This package is not intended for the air transport of fissile material.

6.9. CONCLUSION

Based on the calculations that have been documented, the TN-B1 shipping container is qualified to transport UO_2 fuel assemblies, including 10x10, 9x9, and 8x8 BWR designs, in accordance with the criticality safety requirements of the IAEA and 10 CFR 71. The fuel assemblies may be channeled or un-channeled.

The calculations documented in Chapter 6.0 also demonstrate a finite 10x1x10 array of damaged, or a 21x3x24 array of un-damaged packages remains below a k_{eff} of 0.95 with optimum interspersed moderation. Therefore, the calculations support a CSI of 1.0.

In addition, the calculations demonstrate UO_2 fuel rods may be packaged within the TN-B1 inner container in 5-inch stainless steel pipe/protective case, loose, or bundled together. The UO_2 fuel rods may consist of 10x10, 9x9, or 8x8 fuel rod designs.

The calculations documented in Chapter 6.0 also demonstrate the 10x10 fuel assemblies may be transported with 8, 10, 12, or 14 part length fuel rods, and 9x9 fuel assemblies may be transported with 8, 10 and 12 part-length fuel rods.

6.10. BENCHMARK EVALUATIONS

6.10.1. *Applicability of Benchmark Experiments*

The criticality calculation method is verified by comparison with critical experiment data which is sufficiently diverse to establish that the method bias and uncertainty will apply to conditions considered in the TN-B1 shipping container criticality analysis. A set of 27 critical experiments are analyzed using SCALE-PC to demonstrate its applicability to criticality analysis and to establish a set of Upper Subcritical Limits (USLs) that define acceptance criteria. Benchmark experiments are selected with compositions, configurations, and nuclear characteristics that are comparable to those encountered in the TN-B1 shipping container loaded with fuel as described in Table 6-1. The critical experiments are described in detail in References 2-5 and 9-12 and summarized in Section 6.11.10.

The critical experiments consisted of water moderated, oxide fuel arrays in square lattices. Fourteen experiments were 15x8 fuel rod lattices, with 4.31 weight percent (w/o) U-235 enrichment, and different absorber plates in the water gaps between rods. The absorber plates include aluminum, Type 304L stainless steel, Type 304L stainless steel with various boron enrichments, zircaloy-4, and Boral™. Thirteen experiments were 15x15 fuel rod lattices using multiple enrichments, no absorbers between rod clusters, and gadonium absorber integral to the fuel in most cases (9 cases). The lattice arrays in these experiments had enrichments of 2.46, 2.73, 2.74, 2.75, 2.76, 2.77, or 2.78 w/o U-235. Comparison with these experiments demonstrates the applicability of the criticality calculation method.

6.10.2. *Bias Determination*

A set of Upper Subcritical Limits is determined using the results from the 27 critical experiments and USL Method 1, Confidence Band with Administrative Margin, described in Section 4.0 of NUREG/CR-6361 (Reference 7). The USL Method 1 applies a statistical calculation of the method bias and its uncertainty plus an administrative margin (0.05 Δk) to a linear fit of the critical experiment benchmark data. The USLs are determined as a function of the critical experiment system parameters; enrichment, water-to-fuel ratio, hydrogen-to- U-235 ratio, pin pitch, average energy of the lethargy causing fission, and the average energy group causing fission.

- The following equation is determined for the USL as a function of enrichment:
  $USL = 0.9388 + (8.6824 \times 10^{-4})\ x$ for all x
  The variance of the equation fit is 3.6827x10^{-6}. The applicable range for enrichment is 2.46 $\leq x \leq$ 4.31.

- The following equation is determined for the USL as a function of water-to-fuel ratio:
  $USL = 0.9398 + (6.6864 \times 10^{-4})\ x$ for all x
  The variance of the equation fit is 3.8188x10^{-6}. The applicable range for water-to-fuel ratio is 1.8714 $\leq x \leq$ 3.8832.

- The following equation is determined for the USL as a function of hydrogen-to-U-235:
  $USL = 0.9380 + (1.4976 \times 10^{-5})\ x$ for all x
  The variance of the equation fit is 4.1692x10^{-6}. The applicable range for hydrogen-to-U-235 ratio is 200.56 $\leq$ 255.92.

- The following equation is determined for the USL as a function of pin pitch:
  $USL = 0.9387 + (1.4894 \times 10^{-3})\ x$ for all x
  The variance of the equation fit is 3.7993x10^{-6}. The applicable range for pin pitch is 1.6358 $\leq x \leq$ 2.54.

- The following equation is determined for the USL as a function of average energy of the lethargy causing fission:
  $USL = 0.9423 - (3.8725 \times 10^{-3})\ x$ for all x
  The variance of the equation fit is 4.1339x10^{-6}. The applicable range for average energy of the lethargy causing fission is 0.1127 $\leq x \leq$ 0.3645.

- The following equation is determined for the USL as a function of the average energy group causing fission:

USL = $0.9281 + (3.9834 \times 10^{-4})x$ for all x

The variance of the equation fit is 4.0641×10^{-6}. The applicable range for the average energy group causing fission is $32.89 \leq x \leq 35.77$.

Of the preceding equations, the USL as a function of enrichment is the best correlated to the data since the variance of the equation fit is the smallest. Therefore, the USL as a function of enrichment is used to determine a minimum USL for each fuel assembly type considered for use with the TN-B1 shipping container (Table 6-1). Figure 6-50 shows the USL as a function of enrichment. USL values are calculated as a function of enrichment for each candidate fuel design. All candidate fuel designs have the same maximum enrichment of 5.0 wt. percent U-235. Although the 5.0 wt. percent U-235 enrichment falls outside the range of applicability, ANSI/ANS-8.1 (Reference 6) allows the range of applicability to be extended beyond the range of conditions represented by the benchmarks, as long as that extrapolation is not large. As outlined in Reference 7, k(x)-w(x) is used to extend the USL curve beyond the range of applicability. Figure 6-50 displays the USL curve extrapolation using k(x)-w(x); the extrapolated USL value corresponding to the 5.0 wt. percent U-235 enrichment is 0.94323. Since the extrapolated value results in a higher USL than the maximum enrichment within the range of applicability would produce, the USL corresponding to the 4.31 wt. percent U-235 enrichment is conservatively selected. Therefore, the USL for the TN-B1 shipping container is 0.94254.

The following equation is used to develop the k_{eff} for the transportation of fuel in the TN-B1 shipping container:

$$K_{eff} = k_{case} + 2\sigma$$

where:

k_{case} = KENO V.a k_{eff} for a particular case of interest

σ = uncertainty in calculated KENO V.a k_{eff} for a particular case of interest

The k_{eff} for each container configuration analyzed in the TN-B1 shipping container criticality analysis is compared to the minimum USL (0.94254) to ensure subcriticality.

The GEMER program has been validated against experiments that have uranium form, chemical composition and moderation/reflection conditions similar to those of this application. For low-enriched UO_2 lattice systems without poison, the calculational bias and bias uncertainty of GEMER is given by (Ref. 13):

$$b^* = 0.017$$

A minimum margin of subcriticality is applied as:

$$\Delta k_m = 0.05$$

Since the GEMER validation benchmarks for heterogeneous UO_2 systems do not include uranium-carbide (UC) fuel types in the Area of Applicability (AOA), an additional margin D.k_{AOA} = 0.01 will be applied for loose UC rods since no UC critical benchmarks are currently available. Therefore,

For UO_2 Rods: $USL = 1 + b^* - \Delta k_m = 1 + (-0.017) - 0.05 = 0.933$

For UC Rods: $USL = 1 + b^* - \Delta k_m - \Delta k_{AOA} = 1 + (-0.017) - 0.05 - 0.01 = 0.923$

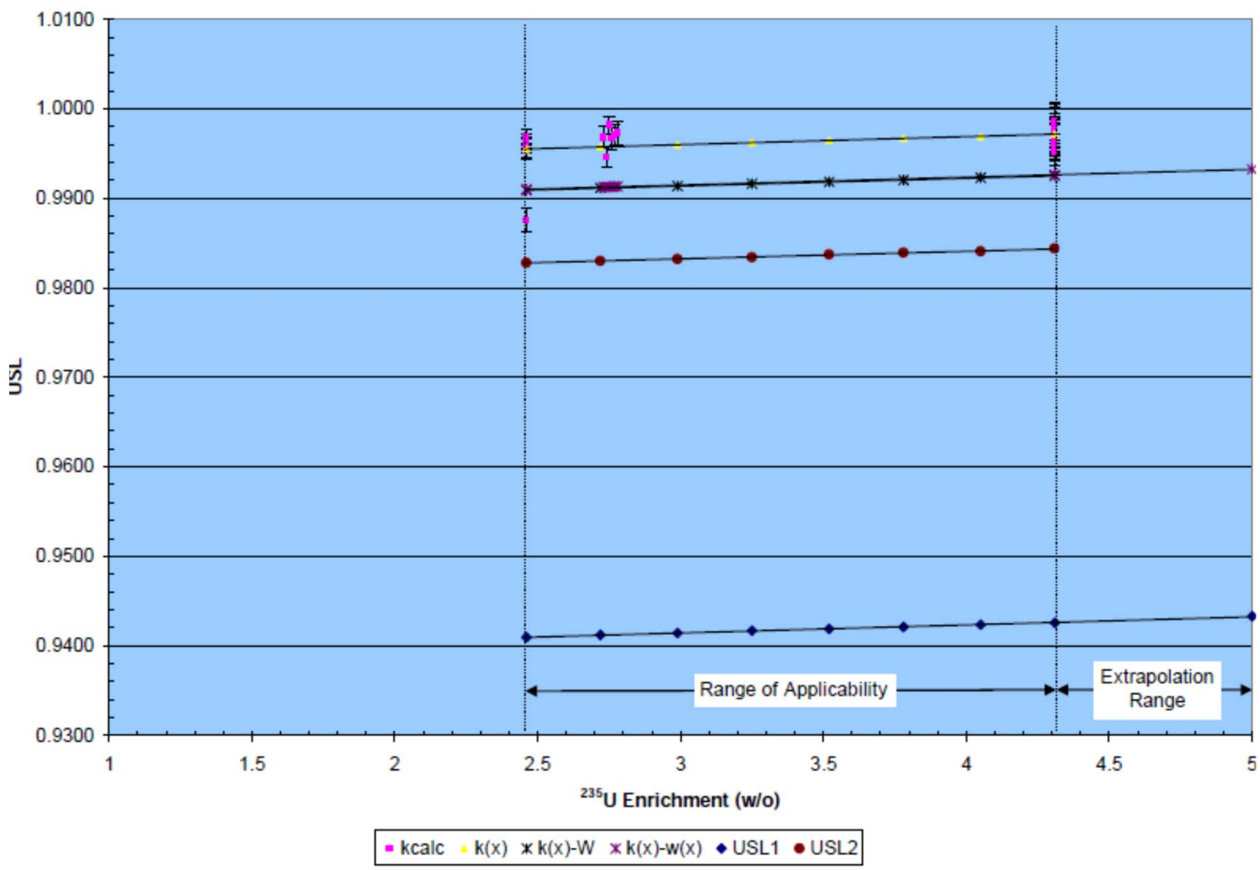

Figure 6-50 USL as a Function of Enrichment

6.11. APPENDIX A

6.11.1. *Single Package Normal Conditions of Transport Input*

```
=CSAS25             PARM=SIZE=500000
TN-B1 CONTAINER, HAC, NO INTERSPERSED H2O, 100% INNER H2O DENSITY, 5.0 W/O
235U, 12 GAD RODS, SINGLE PACKAGE
44GROUPNDF5                 LATTICECELL
UO2            1  DEN=10.74    1.0  293 92235 5.0 92238 95.0  END
ZR             2  1.00              293                       END H2O
3  1.00              293                   END ARBMUO2        10.74
2 1 1 1 92000 1
                             8016 2 4 0.97840 293 92235   5.0
                                                  92238 95.0  END
ARBMGD2O3      7.407 2 0 1 1 64000 2
                              8016 3 4 0.02160 293            END
H2O            5  1.00              293                       END
SS304          6  1.00              293                       END
POLYETHYLENE   7  DEN=0.080000 1.0  293                       END
POLYETHYLENE   8  DEN=0.949 0.25405 293                       END
H2O            8  DEN=1.00  0.74595 293                       END
H2O            9  1.00              293                       END
ARBMAL2O3      0.25 2 0 1 0 13027 2 8016 3 10  0.49           END
ARBMSIO2       0.25 2 0 1 0 14000 1 8016 2 10  0.51           END
ZR             11 1.00              293                       END
END COMP
SQUAREPITCH 1.3500 0.8950 1 8 1.01000 2 0.9338 0              END MORE
DATA
RES=4 CYLINDER 0.4475  DAN(4)=2.3197146E-01
END MORE DATA
TN-B1 CONTAINER, HAC, NO INTERSPERSED H2O, 100% INNER H2O DENSITY, 5.0 W/O
235U, 12 GAD RODS, SINGLE PACKAGE
READ PARM TME=400 GEN=400 NPG=2500 NSK=50 NUB=YES RUN=YES END PARM READ GEOM

UNIT 1
COM=!CONTAINER INNER BOX!
'DEFINE GEOMETRY FOR SEPARATOR PLATE BETWEEN ASSEMBLY COMPARTMENTS
CUBOID     6  1  2P0.0875   2P228.34  2P8.829
'DEFINE REGION FOR ASSEMBLY COMPARTMENTS WITHIN INNER BOX
CUBOID     9  1  2P17.713   2P228.34  2P8.829
'INSERT FOAM POLYETHYLENE
HOLE       4      -8.9003       0.00    0.00
HOLE       5       8.9003       0.00    0.00
'DEFINE WALLS FOR ASSEMBLY COMPARTMENTS WITHIN INNER BOX
CUBOID     6  1  2P17.800   2P228.34    8.829  -8.9165
```

```
'DEFINE REGION OUTSIDE THE WALLS OF THE ASSEMBLY COMPARTMENTS CUBOID
          10  1  2P22.798   2P228.34    8.829  -13.839
'DEFINE THE INNER WALLS OF THE BOX ENDS
CUBOID     6  1  2P22.798   2P228.48    8.829  -13.979
'DEFINE INNER CORE OF BOX ENDS
CUBOID    10  1  2P22.798   2P233.44    8.829  -13.979
'DEFINE OUTER WALLS OF THE INNER BOX

CUBOID     6  1  2P22.938   2P233.58    8.829  -13.979

UNIT 2
COM=!INNER BOX LID!
'DEFINE INNER CORE OF INNER BOX LID
CUBOID    10 1  2P22.798    2P233.44   2P2.48
'DEFINE WALLS FOR INNER BOX LID
CUBOID    6  1  2P22.938    2P233.58   2P2.62

UNIT 3
COM=!INNER BOX WITH ENDS AND LID! ARRAY
1 3*0

UNIT 4
COM=!FOAM POLYETHYLENE FOR LEFT ASSEMBLY COMPARTMENT!
CUBOID     9  1  2P7.055   2P228.34  2P7.055
HOLE      70      -6.7500  -192.50  -6.750
'FOAM POLYETHYLENE FOR ASSEMBLY COMPARTMENTS CUBOID  7
           1  2P8.8126      2P228.34  2P8.829

UNIT 5
COM=!FOAM POLYETHYLENE FOR RIGHT ASSEMBLY COMPARTMENT!
CUBOID     9  1  2P7.055   2P228.34  2P7.055
HOLE      70      -6.7500  -192.50  -6.750
'FOAM POLYETHYLENE FOR ASSEMBLY COMPARTMENT CUBOID
           7  1  2P8.8126   2P228.34  2P8.829

UNIT 10
COM=!5 W/O FUEL PINS W/O GAD!
'DEFINE THE FUEL PELLET
YCYLINDER 1  1    0.4475   192.5  0
'DEFINE THE PELLET-CLAD GAP YCYLINDER
0            1    0.4669   192.5
             0
'DEFINE THE FUEL ROD CLADDING/POLY
YCYLINDER 2  1    0.5050   192.5  0
'DEFINE THE FUEL ROD PITCH FILLED WITH POLYETHYLENE
CUBOID    8  1  2P0.6750    192.5  0  2P0.6750
```

```
UNIT 20
COM=!SPACE WITHIN FUEL ASSEMBLY LATTICE! CUBOID
          8  1  2P0.6750   192.5  0  2P0.6750

UNIT 40
COM=!5 W/O FUEL PINS W (2.0 WT % X 0.75) GAD!
'DEFINE THE FUEL PELLET
YCYLINDER 4  1    0.4475   192.5   0
'DEFINE THE PELLET-CLAD GAP YCYLINDER 0
             1    0.4669   192.5   0
'DEFINE THE FUEL ROD CLADDING/POLY
YCYLINDER 2  1    0.5050   192.5   0
'DEFINE THE FUEL ROD PITCH FILLED WITH POLYETHYLENE
CUBOID    8  1  2P0.6750    192.5  0  2P0.6750

UNIT 50
COM=!LOWER HALF FUEL ASSEMBLY WITH CLUSTER SEPARATOR!
ARRAY 2 3*0

UNIT 60
COM=!UPPER HALF FUEL ASSEMBLY WITH CLUSTER SEPARATOR!
ARRAY 3 3*0

UNIT 70
COM=!COMPLETE FUEL ASSEMBLY!
ARRAY 4 3*0
REFLECTOR 11 1  2R0.3048 2R0.0  2R0.3048  1

GLOBAL
UNIT 400
COM=!OUTER CONTAINER BODY AND LID!
'DEFINE INNER REGION OF THE OUTER CONTAINER
CUBOID   3  1   2P35.788    2P253.188  2P31.900
'INNER CONTAINER PLACEMENT WITHIN OUTER CONTAINER HOLE 3
               -22.938      -233.58    -14.024
'DEFINE WALLS OF THE OUTER CONTAINER AND LID
CUBOID   6  1   2P35.963    2P253.363  2P32.075

'GLOBAL
'UNIT 500
'ARRAY 10 3*0
REFLECTOR  5  1  6R30.48  1
END GEOM
```

```
READ ARRAY
ARA=1 NUX=1 NUY=1 NUZ=2
FILL 1 2
END FILL
ARA=2 NUX=10 NUY=1 NUZ=10
FILL 10 10 10 10 10 10 10 10 40 40
     10 10 20 10 10 10 40 40 40 40
     10 20 10 10 10 10 40 40 40 10
     10 10 10 20 20 10 40 40 40 10
     10 20 10 20 20 10 10 10 10 10
     10 10 20 10 10 20 20 10 10 10
     10 20 10 20 10 20 20 10 10 10
     10 10 10 10 20 10 10 10 20 10
     10 20 10 20 10 20 10 20 10 10
     10 10 10 10 10 10 10 10 10 10
END FILL
ARA=3 NUX=10 NUY=1 NUZ=10
FILL 10 10 10 10 10 10 10 10 40 40
     10 10 10 10 10 10 40 40 40 40
     10 10 10 10 10 10 40 40 40 10
     10 10 10 20 20 10 40 40 40 10
     10 10 10 20 20 10 10 10 10 10
     10 10 10 10 10 20 20 10 10 10
     10 10 10 10 10 20 20 10 10 10
     10 10 10 10 10 10 10 10 10 10
     10 10 10 10 10 10 10 10 10 10
     10 10 10 10 10 10 10 10 10 10
END FILL
ARA=4  NUX=1  NUY=2  NUZ=1
FILL 50 60
END FILL
ARA=10 NUX=21 NUY=3 NUZ=24


FILL F400
END FILL END
ARRAY

READ BNDS ALL VACUUM END
BNDS
END DATA END
```

6.11.2. *Single Package Hypothetical Accident Conditions Input*

```
=CSAS25            PARM=SIZE=500000
TN-B1 CONTAINER, HAC, 12 PART LENGTH RODS, 12 GAD RODS, 1.350 CM PITCH, PATTERN
H, SINGLE PACKAGE
44GROUPNDF5                 LATTICECELL
UO2           1  DEN=10.74 1.0 293 92235 5.0 92238 95.0      END
ZR              2               0.26380  293                        END
POLYETHYLENE  2  DEN=0.949  0.73620  293                        END H2O
3  0.01 293                                  END ARBMUO2       10.74 2
1 1 1 92000 1
                           8016 2 4 0.97840 293 92235   5.0
                                                 92238 95.0 END
ARBMGD2O3      7.407 2 0 1 1 64000 2
                           8016  3  4  0.02160  293             END  H2O
5  1.00 293                                 END SS304          6  1.00
293                                     END H2O           7  1.00 293
END H2O            8  1.00 293                                    END
ZR                9  1.00 293                                     END
ARBMAL2O3      0.25 2 0 1 0 13027 2 8016 3 10  0.49         END ARBMSIO2
0.25 2 0 1 0 14000 1 8016 2 10  0.51          END END COMP
SQUAREPITCH 1.3500 0.8950 1 7 1.19720 2 0.9338 0             END MORE DATA
RES=4 CYLINDER 0.4475  DAN(4)=2.2023524E-01
END MORE DATA
TN-B1 CONTAINER, HAC, 12 PART LENGTH RODS, 12 GAD RODS, 1.350 CM PITCH, PATTERN
H, SINGLE PACKAGE
READ PARM TME=400 GEN=400 NPG=2500 NSK=50 NUB=YES RUN=YES END PARM READ
GEOM

UNIT  1
COM=!CONTAINER INNER BOX!
'DEFINE GEOMETRY FOR SEPARATOR PLATE BETWEEN ASSEMBLY COMPARTMENTS CUBOID
           6  1  2P0.0875   225.20  -228.34  2P8.829
'DEFINE REGION FOR ASSEMBLY COMPARTMENTS WITHIN INNER BOX
CUBOID     7  1  2P17.713   225.20  -228.34  2P8.829
'PLACE THE FUEL ASSEMBLIES INSIDE INNER BOX HOLE
           70     -15.290  -192.50  -6.477
HOLE       70       2.336  -192.50  -6.477
'DEFINE WALLS FOR ASSEMBLY COMPARTMENTS WITHIN INNER BOX
CUBOID     6  1  2P17.800   225.20  -228.34  8.829  -8.9165
'DEFINE REGION OUTSIDE THE WALLS OF THE ASSEMBLY COMPARTMENTS CUBOID
           10 1  2P22.798   225.20  -228.34  8.829  -13.839
'DEFINE THE INNER WALLS OF THE BOX ENDS
CUBOID     6  1  2P22.798   225.34  -228.48  8.829  -13.979
'DEFINE INNER CORE OF BOX ENDS -8.1CM IN Y FOR TOTAL DEFORMATION CUBOID
           10 1  2P22.798   225.34  -233.44  8.829  -13.979
```

```
'DEFINE OUTER WALLS OF THE INNER BOX -8.1CM IN Y FOR TOTAL DEFORMATION
CUBOID     6  1  2P22.938   225.48  -233.58  8.829  -13.979

UNIT 2
COM=!INNER BOX LID!
'DEFINE INNER CORE OF INNER BOX LID -8.1CM IN Y FOR TOTAL DEFORMATION

CUBOID    10 1  2P22.798    2P229.39   2P2.48
'DEFINE WALLS FOR INNER BOX LID -8.1CM IN Y FOR TOTAL DEFORMATION
CUBOID    6  1  2P22.938    2P229.53   2P2.62

UNIT 3
COM=!INNER BOX WITH ENDS AND LID! ARRAY
1 3*0

UNIT 10
COM=!5 W/O FUEL PINS W/O GAD!
'DEFINE THE FUEL PELLET
YCYLINDER 1  1    0.4475   192.5  0
'DEFINE THE PELLET-CLAD GAP YCYLINDER
0            1    0.4669   192.5    0
'DEFINE THE FUEL ROD CLADDING/POLY
YCYLINDER 2  1    0.5986   192.5     0
'DEFINE THE FUEL ROD PITCH FILLED WITH POLYETHYLENE
CUBOID    7  1  2P0.6750    192.5  0  2P0.6750

UNIT 20
COM=!SPACE WITHIN FUEL ASSEMBLY LATTICE!
CUBOID    7  1  2P0.6750   192.5  0  2P0.6750

UNIT 30
COM=!ARRAY FOR COMPLETE FUEL ASSEMBLY!
ARRAY 2 3*0
REFLECTOR 9  1  2R0.3048 2R0.0  2R0.3048  1

UNIT 40
COM=!5 W/O FUEL PINS W (2.0 WT % X 0.75) GAD!
'DEFINE THE FUEL PELLET
YCYLINDER 4  1    0.4475   192.5  0
'DEFINE THE PELLET-CLAD GAP YCYLINDER
0            1    0.4669   192.5     0
'DEFINE THE FUEL ROD CLADDING/POLY
YCYLINDER 2  1    0.5986   192.5       0
'DEFINE THE FUEL ROD PITCH FILLED WITH POLYETHYLENE
CUBOID    7  1  2P0.6750    192.5  0  2P0.6750

UNIT 50
```

```
COM=!LOWER HALF FUEL ASSEMBLY WITH CLUSTER SEPARATOR!
ARRAY 2 3*0

UNIT 60
COM=!UPPER HALF FUEL ASSEMBLY WITH CLUSTER SEPARATOR! ARRAY
3 3*0

UNIT 70
COM=!COMPLETE FUEL ASSEMBLY! ARRAY
4 3*0
REFLECTOR 9  1  2R0.3048 2R0.0  2R0.3048  1

GLOBAL UNIT 400
COM=!OUTER CONTAINER BODY AND LID!
'DEFINE INNER REGION OF THE OUTER CONTAINER
'MINUS 4.7CM IN Y AND -2.4CM IN Z FOR TOTAL DEFORMATION

CUBOID    0  1   2P35.788  247.960  -253.190  29.500  -31.900
'INNER CONTAINER PLACEMENT WITHIN OUTER CONTAINER HOLE
3               -22.938      -229.53    -14.024
'DEFINE WALLS OF THE OUTER CONTAINER AND LID
CUBOID    6  1   2P35.963  248.135  -253.365  29.675  -32.075

'GLOBAL
'UNIT 500
'ARRAY 10 3*0
REFLECTOR  5  1  6R30.48  1
END GEOM

READ ARRAY
ARA=1 NUX=1 NUY=1 NUZ=2
FILL 1 2
END FILL
ARA=2 NUX=10 NUY=1 NUZ=10
FILL 10 10 10 10 10 10 10 10 40 40
     10 10 20 10 10 10 40 40 40 40
     10 20 10 10 10 10 40 40 40 10
     10 10 10 20 20 10 40 40 40 10
     10 20 10 20 20 10 10 10 10 10
     10 10 20 10 10 20 20 10 10 10
     10 20 10 20 10 20 20 10 10 10
     10 10 10 10 20 10 10 10 20 10
     10 20 10 20 10 20 10 20 10 10
     10 10 10 10 10 10 10 10 10 10
END FILL
```

```
ARA=3 NUX=10 NUY=1 NUZ=10
FILL 10 10 10 10 10 10 10 10 40 40
     10 10 10 10 10 10 40 40 40 40
     10 10 10 10 10 10 40 40 40 10
     10 10 10 20 20 10 40 40 40 10
     10 10 10 20 20 10 10 10 10 10
     10 10 10 10 10 20 20 10 10 10
     10 10 10 10 10 20 20 10 10 10
     10 10 10 10 10 10 10 10 10 10
     10 10 10 10 10 10 10 10 10 10
     10 10 10 10 10 10 10 10 10 10
END FILL
ARA=4  NUX=1  NUY=2  NUZ=1
FILL 50 60
END FILL END ARRAY

READ BNDS ALL=VACUUM
END BNDS
END DATA END
```

6.11.3. *Package Array Normal Conditions of Transport Input*

```
=CSAS25            PARM=SIZE=500000
TN-B1 CONTAINER, HAC, NO INTERSPERSED H2O, 100% INNER H2O DENSITY, 5.0 W/O
235U, 12 GAD RODS, 21 X 3 X 24 ARRAY
44GROUPNDF5                LATTICECELL
UO2           1  DEN=10.74    1.0  293 92235 5.0 92238 95.0   END
ZR            2  1.00              293                        END
H2O           3  1.00              293                        END
ARBMUO2       10.74 2 1 1 1 92000 1
                           8016 2 4 0.97840 293 92235  5.0
                                                92238 95.0  END
ARBMGD2O3      7.407 2 0 1 1 64000 2
                           8016 3 4 0.02160 293           END
H2O           5  1.00              293                        END
SS304         6  1.00              293                        END
POLYETHYLENE  7  DEN=0.080000 1.0  293                        END
POLYETHYLENE  8  DEN=0.949 0.25405 293                        END
H2O           8  DEN=1.00  0.74595 293                        END
H2O           9  1.00              293                        END
ARBMAL2O3     0.25 2 0 1 0 13027 2 8016 3 10  0.49            END
ARBMSIO2      0.25 2 0 1 0 14000 1 8016 2 10  0.51            END
ZR            11 1.00              293                        END
END COMP
```

```
SQUAREPITCH 1.3500 0.8950 1 8 1.01000 2 0.9338 0              END
MORE DATA
RES=4 CYLINDER 0.4475  DAN(4)=2.3197146E-01
END MORE DATA
TN-B1 CONTAINER, HAC, NO INTERSPERSED H2O, 100% INNER H2O DENSITY, 5.0 W/O
235U, 12 GAD RODS, 21 X 3 X 24 ARRAY
READ PARM TME=400 GEN=400 NPG=2500 NSK=50 NUB=YES RUN=YES END PARM READ
GEOM

UNIT  1
COM=!CONTAINER INNER BOX!
'DEFINE GEOMETRY FOR SEPARATOR PLATE BETWEEN ASSEMBLY COMPARTMENTS
CUBOID     6  1  2P0.0875   2P228.34  2P8.829
'DEFINE REGION FOR ASSEMBLY COMPARTMENTS WITHIN INNER BOX
CUBOID     9  1  2P17.713   2P228.34  2P8.829
'INSERT FOAM POLYETHYLENE
HOLE       4      -8.9003       0.00    0.00
HOLE       5       8.9003       0.00    0.00
'DEFINE WALLS FOR ASSEMBLY COMPARTMENTS WITHIN INNER BOX
CUBOID     6  1  2P17.800   2P228.34    8.829  -8.9165
'DEFINE REGION OUTSIDE THE WALLS OF THE ASSEMBLY COMPARTMENTS
CUBOID    10  1  2P22.798   2P228.34    8.829  -13.839
'DEFINE THE INNER WALLS OF THE BOX ENDS
CUBOID     6  1  2P22.798   2P228.48    8.829  -13.979
'DEFINE INNER CORE OF BOX ENDS
CUBOID    10  1  2P22.798   2P233.44    8.829  -13.979
'DEFINE OUTER WALLS OF THE INNER BOX
CUBOID     6  1  2P22.938   2P233.58    8.829  -13.979

UNIT 2

COM=!INNER BOX LID!
'DEFINE INNER CORE OF INNER BOX LID
CUBOID    10 1  2P22.798    2P233.44   2P2.48
'DEFINE WALLS FOR INNER BOX LID
CUBOID    6  1  2P22.938    2P233.58   2P2.62

UNIT 3
COM=!INNER BOX WITH ENDS AND LID!
ARRAY 1 3*0

UNIT 4
COM=!FOAM POLYETHYLENE FOR LEFT ASSEMBLY COMPARTMENT!
CUBOID     9  1  2P7.055   2P228.34  2P7.055
HOLE      70      -6.7500  -192.50  -6.750
'FOAM POLYETHYLENE FOR ASSEMBLY COMPARTMENTS
CUBOID     7  1  2P8.8126   2P228.34  2P8.829
```

```
UNIT 5
COM=!FOAM POLYETHYLENE FOR RIGHT ASSEMBLY COMPARTMENT!
CUBOID     9  1  2P7.055   2P228.34  2P7.055
HOLE      70      -6.7500  -192.50  -6.750
'FOAM POLYETHYLENE FOR ASSEMBLY COMPARTMENT
CUBOID     7  1  2P8.8126   2P228.34  2P8.829

UNIT 10
COM=!5 W/O FUEL PINS W/O GAD!
'DEFINE THE FUEL PELLET
YCYLINDER 1  1    0.4475   192.5  0
'DEFINE THE PELLET-CLAD GAP
YCYLINDER 0  1    0.4669   192.5  0
'DEFINE THE FUEL ROD CLADDING/POLY
YCYLINDER 2  1    0.5050   192.5    0
'DEFINE THE FUEL ROD PITCH FILLED WITH POLYETHYLENE
CUBOID    8  1  2P0.6750    192.5  0  2P0.6750

UNIT 20
COM=!SPACE WITHIN FUEL ASSEMBLY LATTICE!
CUBOID    8  1  2P0.6750   192.5  0  2P0.6750

UNIT 40
COM=!5 W/O FUEL PINS W (2.0 WT % X 0.75) GAD!
'DEFINE THE FUEL PELLET
YCYLINDER 4  1    0.4475   192.5  0
'DEFINE THE PELLET-CLAD GAP
YCYLINDER 0  1    0.4669   192.5  0
'DEFINE THE FUEL ROD CLADDING/POLY
YCYLINDER 2  1    0.5050   192.5      0
'DEFINE THE FUEL ROD PITCH FILLED WITH POLYETHYLENE
CUBOID    8  1  2P0.6750    192.5  0  2P0.6750

UNIT 50
COM=!LOWER HALF FUEL ASSEMBLY WITH CLUSTER SEPARATOR!
ARRAY 2 3*0

UNIT 60
COM=!UPPER HALF FUEL ASSEMBLY WITH CLUSTER SEPARATOR!
ARRAY 3 3*0
```

```
UNIT 70
COM=!COMPLETE FUEL ASSEMBLY! ARRAY
4 3*0
REFLECTOR 11 1  2R0.3048 2R0.0  2R0.3048  1

UNIT 400
COM=!OUTER CONTAINER BODY AND LID!
'DEFINE INNER REGION OF THE OUTER CONTAINER
CUBOID   3  1   2P35.788    2P253.188  2P31.900
'INNER CONTAINER PLACEMENT WITHIN OUTER CONTAINER
HOLE 3         -22.938      -233.58    -14.024
'DEFINE WALLS OF THE OUTER CONTAINER AND LID
CUBOID   6  1   2P35.963    2P253.363  2P32.075

GLOBAL UNIT
500
ARRAY 10 3*0
REFLECTOR  5  1  6R30.48  1
END GEOM

READ ARRAY
ARA=1 NUX=1 NUY=1 NUZ=2
FILL 1 2
END FILL
ARA=2 NUX=10 NUY=1 NUZ=10
FILL 10 10 10 10 10 10 10 10 40 40
     10 10 20 10 10 10 40 40 40 40
     10 20 10 10 10 10 40 40 40 10
     10 10 10 20 20 10 40 40 40 10
     10 20 10 20 20 10 10 10 10 10
     10 10 20 10 10 20 20 10 10 10
     10 20 10 20 10 20 20 10 10 10
     10 10 10 10 20 10 10 10 20 10
     10 20 10 20 10 20 10 20 10 10
     10 10 10 10 10 10 10 10 10 10
END FILL
ARA=3 NUX=10 NUY=1 NUZ=10
FILL 10 10 10 10 10 10 10 10 40 40
     10 10 10 10 10 10 40 40 40 40
     10 10 10 10 10 10 40 40 40 10
     10 10 10 20 20 10 40 40 40 10
     10 10 10 20 20 10 10 10 10 10
     10 10 10 10 10 20 20 10 10 10
     10 10 10 10 10 20 20 10 10 10
     10 10 10 10 10 10 10 10 10 10
```

```
     10 10 10 10 10 10 10 10 10 10
     10 10 10 10 10 10 10 10 10 10
END FILL
ARA=4  NUX=1  NUY=2  NUZ=1
FILL 50 60
END FILL
ARA=10 NUX=21 NUY=3 NUZ=24
FILL F400
END FILL
END ARRAY


READ BNDS ALL = VACUUM END
BNDS
END DATA END
```

6.11.4. *Package Array Hypothetical Accident Conditions Input*

6.11.4.1. GNF 10x10

```
=CSAS25            PARM=SIZE=500000
TN-B1 CONTAINER, HAC, 100% H2O DENSITY, WORSTCASE, GNF 10x10, 10 X 1 X 10
ARRAY
44GROUPNDF5                LATTICECELL
UO2            1  DEN=10.74 1.0 293 92235 5.0 92238 95.0     END
ZR             2            0.26380  293                     END
POLYETHYLENE   2  DEN=0.949  0.73620  293                    END
H2O            3  0.01 293                                   END
ARBMUO2        10.74 2 1 1 1 92000 1
                             8016 2 4 0.97840 293 92235  5.0
                                                  92238 95.0 END
ARBMGD2O3      7.407 2 0 1 1 64000 2
                             8016 3 4 0.02160 293            END
H2O            5  1.00 293                                   END
SS304          6  1.00 293                                   END
H2O            7  1.00 293                                   END
POLYETHYLENE   8  DEN=0.080000 1.0  293                      END
ZR             9  1.00 293                                   END
ARBMAL2O3      0.25 2 0 1 0 13027 2 8016 3 10  0.49          END
ARBMSIO2       0.25 2 0 1 0 14000 1 8016 2 10  0.51          END
END COMP
SQUAREPITCH 1.3500 0.8950 1 7 1.19720 2 0.9338 0             END
MORE DATA
RES=4 CYLINDER 0.4475  DAN(4)=2.2023524E-01
END MORE DATA
TN-B1 CONTAINER, HAC, 100% H2O DENSITY, WORSTCASE, GNF 10x10, 10 X 1 X 10
```

```
ARRAY
READ PARM TME=400 GEN=400 NPG=2500 NSK=50 NUB=YES RUN=YES END PARM READ
GEOM

UNIT  1
COM=!CONTAINER INNER BOX!
'DEFINE GEOMETRY FOR SEPARATOR PLATE BETWEEN ASSEMBLY COMPARTMENTS CUBOID
           6  1  2P0.0875   225.20  -228.34  2P8.829
'DEFINE REGION FOR ASSEMBLY COMPARTMENTS WITHIN INNER BOX
CUBOID     7  1  2P17.713   225.20  -228.34  2P8.829
'INSERT FOAM POLYETHYLENE AND FUEL
HOLE       4      -8.9001     0.00      0.00
HOLE       5       8.9001     0.00      0.00
'DEFINE WALLS FOR ASSEMBLY COMPARTMENTS WITHIN INNER BOX
CUBOID     6  1  2P17.800   225.20  -228.34  8.829  -8.9165
'DEFINE REGION OUTSIDE THE WALLS OF THE ASSEMBLY COMPARTMENTS
CUBOID     10 1  2P22.798   225.20  -228.34  8.829  -13.839
'DEFINE THE INNER WALLS OF THE BOX ENDS
CUBOID     6  1  2P22.798   225.34  -228.48  8.829  -13.979
'DEFINE INNER CORE OF BOX ENDS -8.1CM IN Y FOR TOTAL DEFORMATION
CUBOID     10 1  2P22.798   225.34  -233.44  8.829  -13.979
'DEFINE OUTER WALLS OF THE INNER BOX -8.1CM IN Y FOR TOTAL DEFORMATION
CUBOID     6  1  2P22.938   225.48  -233.58  8.829  -13.979


UNIT 2
COM=!INNER BOX LID!
'DEFINE INNER CORE OF INNER BOX LID -8.1CM IN Y FOR TOTAL DEFORMATION
CUBOID    10 1  2P22.798    2P229.39   2P2.48
'DEFINE WALLS FOR INNER BOX LID -8.1CM IN Y FOR TOTAL DEFORMATION
CUBOID    6  1  2P22.938    2P229.53   2P2.62

UNIT 3
COM=!INNER BOX WITH ENDS AND LID!
ARRAY 1 3*0

UNIT 4
COM=!FOAM POLYETHYLENE FOR LEFT ASSEMBLY COMPARTMENT!
CUBOID     7  1  2P7.055   225.20  -228.34  2P7.055
HOLE      70      -6.7500 -192.50   -6.750
'FOAM POLYETHYLENE FOR ASSEMBLY COMPARTMENTS
CUBOID     8  1  2P8.8126  225.20  -228.34  2P8.829

UNIT 5
COM=!FOAM POLYETHYLENE FOR RIGHT ASSEMBLY COMPARTMENT!
CUBOID     7  1  2P7.055   225.20  -228.34  2P7.055
HOLE      70      -6.7500 -192.50   -6.750
'FOAM POLYETHYLENE FOR ASSEMBLY COMPARTMENT
```

```
CUBOID     8  1  2P8.8126  225.20  -228.34  2P8.829

UNIT 10
COM=!5 W/O FUEL PINS W/O GAD!
'DEFINE THE FUEL PELLET
YCYLINDER 1  1    0.4475   192.5  0
'DEFINE THE PELLET-CLAD GAP YCYLINDER 0  1
             0.4669        192.5   0
'DEFINE THE FUEL ROD CLADDING/POLY
YCYLINDER 2  1    0.5986   192.5   0
'DEFINE THE FUEL ROD PITCH FILLED WITH POLYETHYLENE
CUBOID    7  1  2P0.6750    192.5  0  2P0.6750

UNIT 20
COM=!SPACE WITHIN FUEL ASSEMBLY LATTICE!
CUBOID    7  1  2P0.6750   192.5  0  2P0.6750

UNIT 30
COM=!ARRAY FOR COMPLETE FUEL ASSEMBLY! ARRAY
2 3*0
REFLECTOR 9  1  2R0.3048 2R0.0  2R0.3048  1

UNIT 40
COM=!5 W/O FUEL PINS W (2.0 WT % X 0.75) GAD!
'DEFINE THE FUEL PELLET
YCYLINDER 4  1    0.4475   192.5  0
'DEFINE THE PELLET-CLAD GAP
YCYLINDER 0  1    0.4669   192.5  0
'DEFINE THE FUEL ROD CLADDING/POLY
YCYLINDER 2  1    0.5986   192.5      0
'DEFINE THE FUEL ROD PITCH FILLED WITH POLYETHYLENE
CUBOID    7  1  2P0.6750    192.5  0  2P0.6750

UNIT 50

COM=!LOWER HALF FUEL ASSEMBLY WITH CLUSTER SEPARATOR!
ARRAY 2 3*0

UNIT 60
COM=!UPPER HALF FUEL ASSEMBLY WITH CLUSTER SEPARATOR!
ARRAY 3 3*0
```

```
UNIT 70
COM=!COMPLETE FUEL ASSEMBLY!
ARRAY 4 3*0
REFLECTOR 9  1  2R0.3048 2R0.0  2R0.3048  1

UNIT 400
COM=!OUTER CONTAINER BODY AND LID!
'DEFINE INNER REGION OF THE OUTER CONTAINER
'MINUS 4.7CM IN Y AND -2.4CM IN Z FOR TOTAL DEFORMATION
CUBOID    0  1   2P35.788  247.960  -253.190  29.500  -31.900
'INNER CONTAINER PLACEMENT WITHIN OUTER CONTAINER
HOLE 3          -22.938      -229.53    -14.024
'DEFINE WALLS OF THE OUTER CONTAINER AND LID
CUBOID    6  1   2P35.963  248.135  -253.365  29.675  -32.075

GLOBAL
UNIT 500
ARRAY 10 3*0
REFLECTOR  5  1  6R30.48  1
END GEOM

READ ARRAY
ARA=1 NUX=1 NUY=1 NUZ=2
FILL 1 2
END FILL
ARA=2 NUX=10 NUY=1 NUZ=10
FILL 10 10 10 10 10 10 10 10 40 40
     10 10 20 10 10 10 40 40 40 40
     10 20 10 10 10 10 40 40 40 10
     10 10 10 20 20 10 40 40 40 10
     10 20 10 20 20 10 10 10 10 10
     10 10 20 10 10 20 20 10 10 10
     10 20 10 20 10 20 20 10 10 10
     10 10 10 10 20 10 10 10 20 10
     10 20 10 20 10 20 10 20 10 10
     10 10 10 10 10 10 10 10 10 10
END FILL
ARA=3 NUX=10 NUY=1 NUZ=10
FILL 10 10 10 10 10 10 10 10 40 40
     10 10 10 10 10 10 40 40 40 40
     10 10 10 10 10 10 40 40 40 10
     10 10 10 20 20 10 40 40 40 10
     10 10 10 20 20 10 10 10 10 10
     10 10 10 10 10 20 20 10 10 10
```

```
     10 10 10 10 10 20 20 10 10 10
     10 10 10 10 10 10 10 10 10 10
     10 10 10 10 10 10 10 10 10 10
     10 10 10 10 10 10 10 10 10 10
END FILL
ARA=4  NUX=1  NUY=2  NUZ=1


FILL 50 60
END FILL
ARA=10 NUX=10 NUY=1 NUZ=10
FILL F400
END FILL END
ARRAY

READ BNDS ALL=VACUUM END
BNDS
END DATA END
```

6.11.5. *Single Package Loose Rods Normal Conditions of Transport Input*

```
=CSAS25            PARM=SIZE=500000
TN-B1 CONTAINER, 8, NTC, 100% H20, 2.8150 CM PITCH, LOOSE FUEL RODS, SINGLE
PACKAGE
44GROUPNDF5                LATTICECELL
UO2            1  DEN=10.74    1.0  293 92235 5.0 92238 95.0  END
POLYETHYLENE   2  DEN=0.925    1.0  293                       END
H2O            3  1.00              293                       END
UO2            4  DEN=10.4799 1.0  293 92235 3.25 92238 96.75 END
GD             4  DEN=0.17374  1.0  293                       END
O              4  DEN=0.026514 1.0  293                       END
H2O            5  1.00              293                       END
SS304          6  1.00              293                       END
H2O            8  1.00              293                       END
H2O            9  1.00              293                       END
ARBMAL2O3      0.25 2 0 1 0 13027 2 8016 3 10  0.49           END
ARBMSIO2       0.25 2 0 1 0 14000 1 8016 2 10  0.51           END
ZR             11 1.00              293                       END
END COMP
SQUAREPITCH 2.8150 1.0500 1 8 1.13048 2 1.100 0             END
TN-B1 CONTAINER, 8, NTC, 100% H20, 2.8150 CM PITCH, LOOSE FUEL RODS, SINGLE
PACKAGE
READ PARM TME=400 GEN=400 NPG=2500 NSK=50 NUB=YES END PARM READ GEOM
```

```
UNIT  1
COM=!CONTAINER INNER BOX!
'DEFINE GEOMETRY FOR SEPARATOR PLATE BETWEEN ASSEMBLY COMPARTMENTS
CUBOID     6  1  2P0.0875   2P228.34  2P8.829
'DEFINE REGION FOR ASSEMBLY COMPARTMENTS WITHIN INNER BOX
CUBOID     3  1  2P17.713   2P228.34  2P8.829
'INSERT FOAM POLYETHYLENE
HOLE      4      -8.9003       0.00    0.00
HOLE      5       8.9003       0.00    0.00
'DEFINE WALLS FOR ASSEMBLY COMPARTMENTS WITHIN INNER BOX
CUBOID     6  1  2P17.800   2P228.34    8.829  -8.9165
'DEFINE REGION OUTSIDE THE WALLS OF THE ASSEMBLY COMPARTMENTS
CUBOID   10  1  2P22.798   2P228.34    8.829  -13.839
'DEFINE THE INNER WALLS OF THE BOX ENDS
CUBOID    6  1  2P22.798   2P228.48    8.829  -13.979
'DEFINE INNER CORE OF BOX ENDS
CUBOID   10  1  2P22.798   2P233.44    8.829  -13.979
'DEFINE OUTER WALLS OF THE INNER BOX
CUBOID    6  1  2P22.938   2P233.58    8.829  -13.979

UNIT 2
COM=!INNER BOX LID!
'DEFINE INNER CORE OF INNER BOX LID
CUBOID   10 1  2P22.798    2P233.44   2P2.48
'DEFINE WALLS FOR INNER BOX LID
CUBOID   6  1  2P22.938    2P233.58   2P2.62

UNIT 3
COM=!INNER BOX WITH ENDS AND LID! ARRAY
1 3*0

UNIT 4
COM=!FOAM POLYETHYLENE FOR LEFT ASSEMBLY COMPARTMENT!
CUBOID     3  1  2P7.0378   2P228.34  2P7.054
HOLE      30      -7.0376  -191.77   -7.0376
'FOAM POLYETHYLENE FOR ASSEMBLY COMPARTMENTS
CUBOID     7  1  2P8.8126   2P228.34  2P8.829

UNIT 5
COM=!FOAM POLYETHYLENE FOR RIGHT ASSEMBLY COMPARTMENT!
CUBOID     3  1  2P7.0378   2P228.34  2P7.054
HOLE      30      -7.0376  -191.77   -7.0376
'FOAM POLYETHYLENE FOR ASSEMBLY COMPARTMENT
CUBOID     7  1  2P8.8126   2P228.34  2P8.829
```

```
UNIT 10
COM=!5 W/O FUEL PINS W/O GAD!
'DEFINE THE FUEL PELLET
YCYLINDER 1  1    0.52500  381  0
'DEFINE THE PELLET-CLAD GAP YCYLINDER 0  1
             0.55000       381  0
'DEFINE THE FUEL ROD CLADDING YCYLINDER
2            1    0.56524  381    0
'DEFINE THE FUEL ROD PITCH FILLED WITH WATER
CUBOID    8  1  2P1.40750  381  0  2P1.40750

UNIT 20
COM=!SPACE WITHIN FUEL ASSEMBLY LATTICE!
CUBOID    8  1  2P1.40750  381  0  2P1.40750

UNIT 30
COM=!ARRAY FOR COMPLETE FUEL ASSEMBLY!
ARRAY 2 3*0

UNIT 400
COM=!OUTER CONTAINER BODY AND LID!
'DEFINE INNER REGION OF THE OUTER CONTAINER
CUBOID   3  1   2P35.788    2P253.188  2P31.900
'INNER CONTAINER PLACEMENT WITHIN OUTER CONTAINER
HOLE 3         -22.938      -233.58    -14.024
'DEFINE WALLS OF THE OUTER CONTAINER AND LID
CUBOID   6  1   2P35.963    2P253.363  2P32.075

GLOBAL
UNIT 500
ARRAY 10 3*0
REFLECTOR  5  1  6R30.48  1
END GEOM

READ ARRAY
ARA=1 NUX=1 NUY=1 NUZ=2
FILL 1 2
END FILL
ARA=2 NUX=5  NUY=1 NUZ=5

FILL 10 10 10 10 10
     10 10 10 10 10
     10 10 10 10 10
     10 10 10 10 10
     10 10 10 10 10
END FILL
```

```
ARA=10 NUX=21 NUY=3  NUZ=24
FILL F400
END FILL
END ARRAY

READ BNDS ALL=VACUUM END
BNDS
END DATA
END
```

6.11.6. *Single Package Loose Fuel Rods Hypothetical Accident Conditions Input*

```
=CSAS25            PARM=SIZE=500000
TN-B1 CONTAINER, 8, HAC, 100% H2O, WORST CASE MODEL, 3.0056 CM PITCH, LOOSE FUEL
RODS, SINGLE PACKAGE
44GROUPNDF5                LATTICECELL
UO2            1  DEN=10.74 1.0 293 92235 5.0 92238 95.0     END
POLYETHYLENE   2  DEN=0.925    1.0    293                    END
H2O            3  1.00                293                    END
UO2            4  DEN=10.4799  1.0 293 92235 3.25 92238 96.75END
GD             4  DEN=0.17374  1.0 293                       END
O              4  DEN=0.026514 1.0 293                       END
H2O            5  1.00 293                                   END
SS304          6  1.00 293                                   END
H2O            7  DEN=1.00  1.0 293                          END
H2O            8  DEN=1.00     1.0    293                    END
ZR             9  1.00 293                                   END
ARBMAL2O3      0.25 2 0 1 0 13027 2 8016 3 10  0.49          END
ARBMSIO2       0.25 2 0 1 0 14000 1 8016 2 10  0.51          END
END COMP
SQUAREPITCH 3.0056 1.0500 1 8 1.13048 2 1.100 0              END
TN-B1 CONTAINER, 8, HAC, 100% H2O, WORST CASE MODEL, 3.0056 CM PITCH, LOOSE FUEL
RODS, SINGLE PACKAGE
READ PARM TME=400 GEN=400 NPG=2500 NSK=50 NUB=YES ENDPARM READ
GEOM

UNIT 1
COM=!CONTAINER INNER BOX!
'DEFINE GEOMETRY FOR SEPARATOR PLATE BETWEEN ASSEMBLY COMPARTMENTS
CUBOID     6  1  2P0.0875   225.20  -228.34  2P8.829
'DEFINE REGION FOR ASSEMBLY COMPARTMENTS WITHIN INNER BOX
CUBOID     7  1  2P17.713   225.20  -228.34  2P8.829
'PLACE THE FUEL ASSEMBLIES INSIDE INNER BOX
HOLE       30     -16.413  -190.50  -7.514
HOLE       30       1.386  -190.50  -7.514
'DEFINE WALLS FOR ASSEMBLY COMPARTMENTS WITHIN INNER BOX
CUBOID     6  1  2P17.800   225.20  -228.34  8.829  -8.9165
```

```
'DEFINE REGION OUTSIDE THE WALLS OF THE ASSEMBLY COMPARTMENTS
CUBOID     10 1  2P22.798   225.20  -228.34  8.829  -13.839
'DEFINE THE INNER WALLS OF THE BOX ENDS
CUBOID     6  1  2P22.798   225.34  -228.48  8.829  -13.979
'DEFINE INNER CORE OF BOX ENDS -8.1CM IN Y FOR TOTAL DEFORMATION
CUBOID     10 1  2P22.798   225.34  -233.44  8.829  -13.979
'DEFINE OUTER WALLS OF THE INNER BOX -8.1CM IN Y FOR TOTAL DEFORMATION
CUBOID     6  1  2P22.938   225.48  -233.58  8.829  -13.979

UNIT 2
COM=!INNER BOX LID!
'DEFINE INNER CORE OF INNER BOX LID -8.1CM IN Y FOR TOTAL DEFORMATION
CUBOID    10 1  2P22.798    2P229.39   2P2.48
'DEFINE WALLS FOR INNER BOX LID -8.1CM IN Y FOR TOTAL DEFORMATION
CUBOID    6  1  2P22.938    2P229.53   2P2.62

UNIT 3

COM=!INNER BOX WITH ENDS AND LID! ARRAY
1 3*0

UNIT 10
COM=!5 W/O FUEL PINS W/O GAD!
'DEFINE THE FUEL PELLET
YCYLINDER 1  1    0.52500  381  0
'DEFINE THE PELLET-CLAD GAP YCYLINDER
0            1    0.55000  381     0
'DEFINE THE FUEL ROD CLADDING
YCYLINDER 2  1    0.56524  381  0
'DEFINE THE FUEL ROD PITCH FILLED WITH WATER
CUBOID    8  1  2P1.50280  381  0  2P1.50280

UNIT 20
COM=!SPACE WITHIN FUEL ASSEMBLY LATTICE!
CUBOID    8  1  2P1.50280  381  0  2P1.50280

UNIT 30
COM=!ARRAY FOR COMPLETE FUEL ASSEMBLY!
ARRAY 2 3*0

GLOBAL UNIT 400
COM=!OUTER CONTAINER BODY AND LID!
'DEFINE INNER REGION OF THE OUTER CONTAINER
'MINUS 4.7CM IN Y AND -2.4CM IN Z FOR TOTAL DEFORMATION
CUBOID    0  1   2P35.788  247.960  -253.190  29.500  -31.900
'INNER CONTAINER PLACEMENT WITHIN OUTER CONTAINER
HOLE 3          -22.938      -229.53    -14.024
```

```
'DEFINE WALLS OF THE OUTER CONTAINER AND LID
CUBOID    6  1   2P35.963  248.135  -253.365  29.675  -32.075

'GLOBAL
'UNIT 500
'ARRAY 10 3*0
REFLECTOR  5  1  6R30.48  1
END GEOM

READ ARRAY
ARA=1 NUX=1 NUY=1 NUZ=2
FILL 1 2
END FILL
ARA=2 NUX=5  NUY=1 NUZ=5
FILL 10 10 10 10 10
     10 10 10 10 10
     10 10 10 10 10
     10 10 10 10 10
     10 10 10 10 10
END FILL
ARA=10 NUX=14 NUY=2 NUZ=16
FILL F400
END FILL END
ARRAY

READ BNDS ALL=VACUUM END
BNDS
END DATA
```

6.11.7. *Package Array Loose Fuel Rods Normal Conditions of Transport Input*

```
=CSAS25             PARM=SIZE=500000
TN-B1 CONTAINER, 8, NTC, 100% H20, 2.8150 CM PITCH, LOOSE FUEL RODS, 21 x 3x 24
44GROUPNDF5            LATTICECELL
UO2             1  DEN=10.74    1.0  293 92235 5.0 92238 95.0 END
POLYETHYLENE    2  DEN=0.925    1.0  293                      END
H2O             3  1.00              293                      END
UO2             4  DEN=10.4799  1.0  293 92235 3.25 92238 96.75
END GD             4  DEN=0.17374  1.0  293
END
O             4  DEN=0.026514 1.0  293
END H2O            5  1.00              293
END SS304          6  1.00              293
END POLYETHYLENE   7  DEN=0.067967 1.0  293
END H2O            8  1.00              293
END H2O            9  1.00              293
END ARBMAL2O3      0.25 2 0 1 0 13027 2 8016 3 10  0.49
```

```
END ARBMSIO2       0.25 2 0 1 0 14000 1 8016 2 10  0.51
END ZR             11 1.00              293
END END COMP
SQUAREPITCH 2.8150 1.0500 1 8 1.13048 2 1.100 0                END
TN-B1 CONTAINER, 8, NTC, 100% H20, 2.8150 CM PITCH, LOOSE FUEL RODS, 21 x 3 x 24
READ PARM TME=400 GEN=400 NPG=2500 NSK=50 NUB=YES END PARM READ GEOM

UNIT  1
COM=!CONTAINER INNER BOX!
'DEFINE GEOMETRY FOR SEPARATOR PLATE BETWEEN ASSEMBLY COMPARTMENTS
CUBOID     6     1     2P0.0875    2P228.34    2P8.829
'DEFINE REGION FOR ASSEMBLY COMPARTMENTS WITHIN INNER BOX
CUBOID     3     1     2P17.713    2P228.34    2P8.829
'INSERT FOAM POLYETHYLENE
HOLE       4      -8.9003       0.00    0.00
HOLE       5       8.9003       0.00    0.00
'DEFINE WALLS FOR ASSEMBLY COMPARTMENTS WITHIN INNER BOX
CUBOID     6     1     2P17.800    2P228.34    8.829 -8.9165
'DEFINE REGION OUTSIDE THE WALLS OF THE ASSEMBLY COMPARTMENTS
CUBOID    10  1  2P22.798   2P228.34    8.829  -13.839
'DEFINE THE INNER WALLS OF THE BOX ENDS
CUBOID     6  1  2P22.798   2P228.48    8.829  -13.979
'DEFINE INNER CORE OF BOX ENDS
CUBOID    10  1  2P22.798   2P233.44    8.829  -13.979
'DEFINE OUTER WALLS OF THE INNER BOX
CUBOID     6  1  2P22.938   2P233.58    8.829  -13.979

UNIT 2
COM=!INNER BOX LID!
'DEFINE INNER CORE OF INNER BOX LID
CUBOID    10 1  2P22.798    2P233.44   2P2.48
'DEFINE WALLS FOR INNER BOX LID
CUBOID    6  1  2P22.938    2P233.58   2P2.62

UNIT 3
COM=!INNER BOX WITH ENDS AND LID! ARRAY 1 3*0

UNIT 4
COM=!FOAM POLYETHYLENE FOR LEFT ASSEMBLY COMPARTMENT!
CUBOID     3     1     2P7.0378    2P228.34    2P7.054
HOLE 30    -7.0376     -191.77     -7.0376
'FOAM POLYETHYLENE FOR ASSEMBLY COMPARTMENTS
CUBOID     7     1     2P8.8126    2P228.34    2P8.829
```

```
UNIT 5
COM=!FOAM POLYETHYLENE FOR RIGHT ASSEMBLY COMPARTMENT!
CUBOID     3     1     2P7.0378    2P228.34    2P7.054
HOLE 30    -7.0376     -191.77     -7.0376
'FOAM POLYETHYLENE FOR ASSEMBLY COMPARTMENT
CUBOID     7     1     2P8.8126    2P228.34
     2P8.829

UNIT 10
COM=!5 W/O FUEL PINS W/O GAD!
'DEFINE THE FUEL PELLET
YCYLINDER 1      1     0.52500     381         0
'DEFINE THE PELLET-CLAD GAP YCYLINDER 0  1     0.55000     381   0
'DEFINE THE FUEL ROD CLADDING YCYLINDER 2      1     0.56524     381   0
'DEFINE THE FUEL ROD PITCH FILLED WITH WATER
CUBOID     8     1     2P1.40750   381   0
     2P1.40750

UNIT 20
COM=!SPACE WITHIN FUEL ASSEMBLY LATTICE!
CUBOID     8     1     2P1.40750   381   0
     2P1.40750

UNIT 30
COM=!ARRAY FOR COMPLETE FUEL ASSEMBLY! ARRAY 2 3*0

UNIT 400
COM=!OUTER CONTAINER BODY AND LID!
'DEFINE INNER REGION OF THE OUTER CONTAINER
CUBOID     3     1     2P35.788    2P253.188
     2P31.900
'INNER CONTAINER PLACEMENT WITHIN OUTER CONTAINER
HOLE 3     -22.938     -233.58     -14.024
'DEFINE WALLS OF THE OUTER CONTAINER AND LID
CUBOID     6     1     2P35.963    2P253.363   2P32.075

GLOBAL UNIT 500
ARRAY 10 3*0
REFLECTOR  5     1     6R30.48     1
END GEOM

READ ARRAY
ARA=1 NUX=1 NUY=1 NUZ=2
FILL 1 2
END FILL
ARA=2 NUX=5      NUY=1 NUZ=5
```

```
FILL 10 10 10 10 10
10 10 10 10 10
10 10 10 10 10
10 10 10 10 10
10 10 10 10 10
END FILL
ARA=10 NUX=21 NUY=3    NUZ=24
FILL F400
END FILL
END ARRAY

READ BNDS ALL=VACUUM END BNDS
END DATA
END
```

6.11.8. *Package Array Loose Fuel Rods Hypothetical Accident Conditions Input*

```
=CSAS25              PARM=SIZE=500000
TN-B1 CONTAINER, 8, HAC, 100% H2O, WORST CASE MODEL, 3.0056 CM PITCH, LOOSE
FUEL RODS, 10 X 1 X 10 ARRAY
44GROUPNDF5                    LATTICECELL
UO2             1  DEN=10.74 1.0 293 92235 5.0 92238 95.0     END
POLYETHYLENE    2  DEN=0.925    1.0    293                    END
H2O             3  1.00                293                    END
H2O             5  1.00 293                                   END
SS304           6  1.00 293                                   END
POLYETHYLENE    7  DEN=0.08000  1.0  293                      END
H2O             8  DEN=1.00     1.0    293                    END
ZR              9  1.00 293                                   END
ARBMAL2O3       0.25 2 0 1 0 13027 2 8016 3 10  0.49          END
ARBMSIO2        0.25 2 0 1 0 14000 1 8016 2 10  0.51          END
END COMP
SQUAREPITCH 3.0056 1.0500 1 8 1.13048 2 1.100 0               END
TN-B1 CONTAINER, 8, HAC, 100% H2O, WORST CASE MODEL, 3.0056 CM PITCH, LOOSE
FUEL RODS, 10 X 1 X 10 ARRAY
READ PARM TME=400 GEN=400 NPG=2500 NSK=50 NUB=YES END PARM READ GEOM
```

```
UNIT  1
COM=!CONTAINER INNER BOX!
'DEFINE GEOMETRY FOR SEPARATOR PLATE BETWEEN ASSEMBLY COMPARTMENTS
CUBOID     6     1     2P0.0875    225.20      -228.34     2P8.829
'DEFINE REGION FOR ASSEMBLY COMPARTMENTS WITHIN INNER BOX
CUBOID     7     1     2P17.713    225.20      -228.34
     2P8.829
'PLACE THE FUEL ASSEMBLIES INSIDE INNER BOX
HOLE 30    -15.913     -190.50     -7.014
HOLE       30      1.886  -190.50  -7.014
'DEFINE WALLS FOR ASSEMBLY COMPARTMENTS WITHIN INNER BOX
CUBOID     6     1     2P17.800    225.20      -228.34
     8.829 -8.9165
'DEFINE REGION OUTSIDE THE WALLS OF THE ASSEMBLY COMPARTMENTS
CUBOID     10 1  2P22.798    225.20      -228.34     8.829 -
13.839
'DEFINE THE INNER WALLS OF THE BOX ENDS
CUBOID     6  1  2P22.798   225.34  -228.48  8.829  -13.979
'DEFINE INNER CORE OF BOX ENDS -8.1CM IN Y FOR TOTAL DEFORMATION
CUBOID     10 1  2P22.798   225.34  -233.44  8.829  -13.979
'DEFINE OUTER WALLS OF THE INNER BOX -8.1CM IN Y FOR TOTAL DEFORMATION
CUBOID     6     1     2P22.938    225.48      -233.58     8.829 -13.979

UNIT 2
COM=!INNER BOX LID!
'DEFINE INNER CORE OF INNER BOX LID -8.1CM IN Y FOR TOTAL DEFORMATION
CUBOID     10 1  2P22.798    2P229.39    2P2.48
'DEFINE WALLS FOR INNER BOX LID -8.1CM IN Y FOR TOTAL DEFORMATION
CUBOID     6     1     2P22.938    2P229.53    2P2.62

UNIT 3
COM=!INNER BOX WITH ENDS AND LID! ARRAY 1 3*0

UNIT 10
COM=!5 W/O FUEL PINS W/O GAD!
'DEFINE THE FUEL PELLET
YCYLINDER 1      1     0.52500     381   0
'DEFINE THE PELLET-CLAD GAP
YCYLINDER 0      1     0.55000     381   0
'DEFINE THE FUEL ROD CLADDING
YCYLINDER 2      1     0.56524     381   0
'DEFINE THE FUEL ROD PITCH FILLED WITH WATER
CUBOID     8     1     2P1.50280   381   0     2P1.50280

UNIT 20
COM=!SPACE WITHIN FUEL ASSEMBLY LATTICE!
CUBOID     8     1     2P1.50280   381   0     2P1.50280
```

```
UNIT 30
COM=!ARRAY FOR COMPLETE FUEL ASSEMBLY! ARRAY 2 3*0

UNIT 40
COM=!5 W/O FUEL PINS W/O GAD LEFT SIDE FOAM!
'DEFINE THE FUEL PELLET
YCYLINDER 1      1     0.52500     381   0
'DEFINE THE PELLET-CLAD GAP
YCYLINDER 0      1     0.55000     381   0
'DEFINE THE FUEL ROD CLADDING
YCYLINDER 2      1     0.56524     381   0
'DEFINE THE FUEL ROD PITCH FILLED WITH WATER
CUBOID     8     1     1.50280     -1.00280 381      0     2P1.50280

UNIT 46
COM=!5 W/O FUEL PINS W/O GAD LEFT SIDE TOP FOAM!
'DEFINE THE FUEL PELLET
YCYLINDER 1      1     0.52500     381   0
'DEFINE THE PELLET-CLAD GAP
YCYLINDER 0      1     0.55000     381   0
'DEFINE THE FUEL ROD CLADDING
YCYLINDER 2      1     0.56524     381   0
'DEFINE THE FUEL ROD PITCH FILLED WITH WATER
CUBOID     8     1     1.50280     -1.00280 381      0     1.00280     -1.50280

UNIT 47
COM=!5 W/O FUEL PINS W/O GAD LEFT SIDE BOTTOM FOAM!
'DEFINE THE FUEL PELLET
YCYLINDER 1      1     0.52500     381   0
'DEFINE THE PELLET-CLAD GAP YCYLINDER 0  1     0.55000     381   0
'DEFINE THE FUEL ROD CLADDING YCYLINDER 2      1     0.56524     381   0
'DEFINE THE FUEL ROD PITCH FILLED WITH WATER
CUBOID     8     1     1.50280     -1.00280 381      0     1.50280     -1.00280

UNIT 50
COM=!5 W/O FUEL PINS W/O GAD RIGHT SIDE FOAM!
'DEFINE THE FUEL PELLET
YCYLINDER 1      1     0.52500     381   0
'DEFINE THE PELLET-CLAD GAP

YCYLINDER 0      1     0.55000     381   0
'DEFINE THE FUEL ROD CLADDING YCYLINDER 2      1     0.56524     381   0
'DEFINE THE FUEL ROD PITCH FILLED WITH WATER
CUBOID     8     1     1.00280     -1.50280 381      0     2P1.50280
```

```
UNIT 56
COM=!5 W/O FUEL PINS W/O GAD RIGHT SIDE TOP FOAM!
'DEFINE THE FUEL PELLET
YCYLINDER 1      1     0.52500     381   0
'DEFINE THE PELLET-CLAD GAP
YCYLINDER 0      1     0.55000     381   0
'DEFINE THE FUEL ROD CLADDING
YCYLINDER 2      1     0.56524     381   0
'DEFINE THE FUEL ROD PITCH FILLED WITH WATER
CUBOID     8     1     1.00280     -1.50280 381      0     1.00280     -1.50280

UNIT 57
COM=!5 W/O FUEL PINS W/O GAD RIGHT BOTTOM SIDE FOAM!
'DEFINE THE FUEL PELLET
YCYLINDER 1      1     0.52500     381   0
'DEFINE THE PELLET-CLAD GAP
YCYLINDER 0      1     0.55000     381   0
'DEFINE THE FUEL ROD CLADDING
YCYLINDER 2      1     0.56524     381   0
'DEFINE THE FUEL ROD PITCH FILLED WITH WATER
CUBOID     8     1     1.00280     -1.50280 381      0     1.50280     -1.00280

UNIT 60
COM=!5 W/O FUEL PINS W/O GAD TOP SIDE FOAM!
'DEFINE THE FUEL PELLET
YCYLINDER 1      1     0.52500     381   0
'DEFINE THE PELLET-CLAD GAP
YCYLINDER 0      1     0.55000     381   0
'DEFINE THE FUEL ROD CLADDING
YCYLINDER 2      1     0.56524     381   0
'DEFINE THE FUEL ROD PITCH FILLED WITH WATER
CUBOID     8     1     2P1.50280   381   0     1.00280     -1.50280

UNIT 70
COM=!5 W/O FUEL PINS W/O GAD BOTTOM SIDE FOAM!
'DEFINE THE FUEL PELLET
YCYLINDER 1      1     0.52500     381   0
'DEFINE THE PELLET-CLAD GAP
YCYLINDER 0      1     0.55000     381   0
'DEFINE THE FUEL ROD CLADDING
YCYLINDER 2      1     0.56524     381   0
'DEFINE THE FUEL ROD PITCH FILLED WITH WATER
CUBOID     8     1     2P1.50280   381   0     1.50280     -1.00280
```

```
UNIT 400
COM=!OUTER CONTAINER BODY AND LID!
'DEFINE INNER REGION OF THE OUTER CONTAINER
'MINUS 4.7CM IN Y AND -2.4CM IN Z FOR TOTAL DEFORMATION
CUBOID     0     1     2P35.788    247.960     -253.190    29.500      -31.900
'INNER CONTAINER PLACEMENT WITHIN OUTER CONTAINER
HOLE 3     -22.938     -229.53     -14.024

'DEFINE WALLS OF THE OUTER CONTAINER AND LID
CUBOID     6     1     2P35.963    248.135     -253.365    29.675      -32.075

GLOBAL UNIT 500
ARRAY 10 3*0
REFLECTOR  5     1     6R30.48     1
END GEOM

READ ARRAY
ARA=1 NUX=1 NUY=1 NUZ=2
FILL 1 2
END FILL
ARA=2 NUX=5      NUY=1 NUZ=5
FILL 47 70 70 70 57
40 10 10 10 50
40 10 10 10 50
40 10 10 10 50
46 60 60 60 56
END FILL
ARA=10 NUX=10 NUY=1 NUZ=10
FILL F400
END FILL END ARRAY

READ BNDS ALL=VACUUM
END BNDS
END DATA END
```

6.11.9. *Data Tables for Figures in TN-B1 CSE*

Table 6-26 Data for Figure 6-25 TN-B1 Array HAC Polyethylene Sensitivity

Output File Name	Case Description	Interspersed Moderator Density (g/cm^3)	Polyethylene Mass (kg)	k_{eff}	σ	$k_{eff} + 2σ$
rajII_hac_a10_nointerspersedh2o_polyethylenesensitivity_1.284cmpitch_14X2X16	Atrium 10XP+	0.00	0	0.8715	0.0008	0.8731
"	Atrium 10XP+	0.00	10.9	0.8774	0.0009	0.8792
"	Atrium 10XP+	0.00	17.1	0.8813	0.0009	0.8831
"	Atrium 10XP+	0.00	20.4	0.8810	0.0008	0.8826
"	Atrium 10XP+	0.00	22.9	0.8822	0.0009	0.8840
"	Atrium 10XP+	0.00	25.4	0.8847	0.0008	0.8863
"	Atrium 10XP+	0.00	27.9	0.8860	0.001	0.8880
rajII_hac_g10_nointerspersedh2o_polyethylenesensitivity_pitch1.2954cm_14X2X16	GNF 10 x 10	0.00	0	0.8863	0.0007	0.8877
"	GNF 10 x 10	0.00	10.9	0.8923	0.0008	0.8939
"	GNF 10 x 10	0.00	17.1	0.8940	0.0008	0.8956
"	GNF 10 x 10	0.00	20.4	0.8955	0.0007	0.8969
"	GNF 10 x 10	0.00	22.9	0.8975	0.0009	0.8993
"	GNF 10 x 10	0.00	25.4	0.8994	0.0008	0.9010
"	GNF 10 x 10	0.00	27.9	0.9001	0.0008	0.9017

Table 6-26 Data for Figure 6-25 TN-B1 Array HAC Polyethylene Sensitivity (continued)

Output File Name	Case Description	Interspersed Moderator Density (g/cm^3)	Polyethylene Mass (kg)	k_{eff}	σ	$k_{eff} + 2\sigma$
rajII_hac_f9_10g adrods_refassy_ 14x2x16_polysen s	FANP 9x9	0.00	0	0.8728	0.0009	0.8746
rajII_hac_f9_10g adrods_refassy_ 14x2x16_polysen s	FANP 9x9	0.00	20	0.8756	0.0009	0.8774
rajII_hac_f9_10g adrods_refassy_ 14x2x16_channel s	FANP 9x9	0.00	22	0.8755	0.0009	0.8773
rajII_hac_f9_10g adrods_refassy_ 14x2x16_polysen s	FANP 9x9	0.00	24	0.8769	0.0007	0.8783
rajII_hac_f9_10g adrods_refassy_ 14x2x16_polysen s	FANP 9x9	0.00	26	0.8758	0.0008	0.8774
rajII_hac_f9_10g adrods_refassy_ 14x2x16_polysen s	FANP 9x9	0.00	28	0.8766	0.0008	0.8782
rajII_hac_f9_10g adrods_refassy_ 14x2x16_polysen s	FANP 9x9	0.00	30	0.8776	0.0009	0.8794
rajII_hac_g9_10g adrods_refassy_ 14X2X16_polyse ns	GNF 9x9	0.00	0	0.8612	0.0008	0.8628
rajII_hac_g9_10g adrods_refassy_ 14X2X16_polyse ns	GNF 9x9	0.00	20	0.8661	0.0009	0.8679
rajII_hac_g9_10g adrods_refassy_ 14X2X16_chann els	GNF 9x9	0.00	22	0.8659	0.0008	0.8676
rajII_hac_g9_10g adrods_refassy_ 14X2X16_polyse ns	GNF 9x9	0.00	24	0.8676	0.0007	0.8690
rajII_hac_g9_10g adrods_refassy_ 14X2X16_polyse ns	GNF 9x9	0.00	26	0.8670	0.0009	0.8688
rajII_hac_g9_10g adrods_refassy_ 14X2X16_polyse ns	GNF 9x9	0.00	28	0.8656	0.0009	0.8674
rajII_hac_g9_10g adrods_refassy_ 14X2X16_polyse ns	GNF 9x9	0.00	30	0.8702	0.0008	0.8718

Table 6-26 Data for Figure 6-25 TN-B1 Array HAC Polyethylene Sensitivity (continued)

Output File Name	Case Description	Interspersed Moderator Density (g/cm^3)	Polyethylene Mass (kg)	k_{eff}	σ	$k_{eff} + 2\sigma$
rajII_hac_g8_noi nterspersedh2o_ polyethylenesens itivity_1.6256cm_ 14X2X16	GNF 8x8	0.00	0	0.8795	0.0009	0.8813
“	GNF 8x8	0.00	19	0.8865	0.0009	0.8883
“	GNF 8x8	0.00	22	0.8900	0.0009	0.8918
“	GNF 8x8	0.00	24	0.8892	0.0008	0.8908
“	GNF 8x8	0.00	26	0.8924	0.0008	0.8940
“	GNF 8x8	0.00	28	0.8915	0.0009	0.8933
“	GNF 8x8	0.00	30	0.8942	0.0009	0.8960

Table 6-27 Data for Figure 6-26 TN-B1 Fuel Rod Pitch Sensitivity Study

Output File Name	Interspersed Moderator Density (g/cm³)	Polyethylene Mass (kg)	Pitch (cm)	keff	σ	keff + 2σ
rajII_hac_a10_nointerspersedh2o_pitchsensitivity_14X2X16	0.00	20.4	1.210	0.8301	0.0010	0.8321
“	0.00	20.4	1.284	0.8810	0.0008	0.8826
“	0.00	20.4	1.350	0.9245	0.0009	0.9263
“	0.00	20.4	1.376	0.9391	0.0008	0.9407
rajII_hac_g10_nointerspersedh2o_pitchsensitivity_14X2X16	0.00	20.4	1.1960	0.8394	0.0009	0.8412
“	0.00	20.4	1.2954	0.8955	0.0007	0.8969
“	0.00	20.4	1.350	0.9241	0.0008	0.9257
“	0.00	20.4	1.3760	0.9328	0.0008	0.9344
rajII_hac_f9_10gadrods_refassy_14x2x16_pitch	0.00	22	1.3389	0.8219	0.0008	0.8235
“	0.00	22	1.4478	0.8755	0.0009	0.8773
“	0.00	22	1.5028	0.8998	0.0008	0.9014
rajII_hac_f9_10gadrods_refassy_14x2x16_channels	0.00	22	1.5376	0.9126	0.0009	0.9144
rajII_hac_g9_10gadrods_refassy_14X2X16_pitchsens	0.00	22	1.3260	0.8073	0.0008	0.8089
“	0.00	22	1.4376	0.8659	0.0008	0.8676
“	0.00	22	1.5028	0.8929	0.0008	0.8944
rajII_hac_g9_10gadrods_refassy_14X2X16_channels	0.00	22	1.5376	0.9076	0.0009	0.9095
rajII_hac_g8_nointerspersedh2o_pitchsensitivity_14X2X16	0.00	22	1.4603	0.7968	0.0009	0.7986
“	0.00	22	1.6256	0.8900	0.0009	0.8918
“	0.00	22	1.6923	0.9216	0.0008	0.9232
“	0.00	22	1.7264	0.9384	0.0008	0.9400

Table 6-28 Data for Figure 6-27 TN-B1 Array HAC Pellet Diameter Sensitivity Study

Output File Name	Interspersed Moderator Density (g/cm^3)	Pellet Diameter (cm)	k_{eff}	σ	k_{eff} + 2σ
rajII_hac_a10_nointerspersedh2o_pelletodsensitivity_14X2X16	0	0.8000	0.8560	0.0008	0.8576
"	0	0.8400	0.8680	0.0009	0.8698
"	0	0.8882	0.8810	0.0008	0.8826
"	0	0.8941	0.8839	0.0008	0.8855
"	0	0.9200	0.8906	0.0008	0.8922
rajII_hac_g10_nointerspersedh2o_pelletodsensitivity_14X2X16	0	0.8000	0.8641	0.0009	0.8659
"	0	0.8400	0.8796	0.0009	0.8814
"	0	0.8882	0.8941	0.0008	0.8957
"	0	0.8941	0.8955	0.0007	0.8969
"	0	0.9200	0.9050	0.0008	0.9066
rajII_hac_f9_10gadrods_refassy_14x2x16_pelletod	0	0.8882	0.8600	0.0008	0.8616
"	0	0.9000	0.8633	0.0009	0.8651
rajII_hac_f9_10gadrods_refassy_14x2x16_channels	0	0.9398	0.8755	0.0009	0.8773
rajII_hac_f9_10gadrods_refassy_14x2x16_pelletod	0	0.9550	0.8799	0.0008	0.8815
"	0	0.9600	0.8817	0.0007	0.8831
rajII_hac_g9_10gadrods_refassy_14X2X16_pelletodsens	0	0.8882	0.8462	0.0008	0.8478
"	0	0.9000	0.8509	0.0009	0.8527
"	0	0.9398	0.8609	0.0008	0.8625
rajII_hac_g9_10gadrods_refassy_14X2X16_channels	0	0.9550	0.8659	0.0008	0.8676
rajII_hac_g9_10gadrods_refassy_14X2X16_pelletodsens	0	0.9600	0.8678	0.0008	0.8694
rajII_hac_g8_nointerspersedh2o_pelletodsensitivity_14X2X16	0	0.9200	0.8566	0.0008	0.8582
"	0	0.9550	0.8648	0.0008	0.8664
"	0	1.0000	0.8783	0.0008	0.8799
"	0	1.0439	0.8900	0.0009	0.8918
"	0	1.0700	0.8940	0.0009	0.8958

Table 6-29 Data for Figure 6-28 TN-B1 Array HAC Fuel Rod Clad ID Sensitivity Study

Output File Name	Moderator Density (g/cm^3)	Clad Inner Diameter (cm)	k_{eff}	σ	$k_{eff} + 2\sigma$
rajII_hac_a10_nointerspersedh2o_cladidsensitivity_14X2X16	0	0.8800	0.8760	0.0009	0.8778
“	0	0.8900	0.8805	0.0009	0.8823
“	0	0.9218	0.8810	0.0008	0.8826
“	0	0.9322	0.8813	0.0008	0.8829
“	0	1.0330	0.8855	0.0010	0.8875
rajII_hac_g10_nointerspersedh2o_cladidsensitivity_14X2X16	0	0.9000	0.8937	0.0010	0.8957
“	0	0.9218	0.8956	0.0008	0.8972
“	0	0.9322	0.8955	0.0007	0.8969
“	0	1.0185	0.8999	0.0008	0.9015
rajII_hac_f9_10gadrods_refassy_14x2x16_cladid	0	0.9400	0.8742	0.0009	0.8759
rajII_hac_f9_10gadrods_refassy_14x2x16_channels	0	0.9601	0.8755	0.0009	0.8773
rajII_hac_f9_10gadrods_refassy_14x2x16_cladid	0	0.9750	0.8760	0.0009	0.8777
“	0	0.9830	0.8768	0.0009	0.8786
“	0	1.0998	0.8789	0.0008	0.8804
rajII_hac_g9_10gadrods_refassy_14X2X16_cladid	0	0.9560	0.8641	0.0008	0.8657
“	0	0.9600	0.8643	0.0008	0.8659
“	0	0.9750	0.8660	0.0009	0.8678
rajII_hac_g9_10gadrods_refassy_14X2X16_channels	0	0.9830	0.8659	0.0008	0.8676
rajII_hac_g9_10gadrods_refassy_14X2X16_cladid	0	1.1100	0.8702	0.0008	0.8718
rajII_hac_g8_nointerspersedh2o_cladidsensitivity_14X2X16	0	1.0440	0.8894	0.001	0.8914
“	0	1.0719	0.8900	0.0009	0.8918
“	0	1.1000	0.8900	0.0009	0.8918
“	0	1.1500	0.8918	0.0008	0.8934
“	0	1.2192	0.8917	0.0008	0.8933

Table 6-30 Data for Figure 6-29 TN-B1 Array HAC Fuel Rod Clad OD Sensitivity Study

Output File Name	Moderator Density (g/cm^3)	Clad Outer Diameter (cm)	k_{eff}	σ	k_{eff} + 2σ
rajII_hac_a10_nointerspersedh2o_cladodsensitivity_14X2X16	0	0.9218	0.9051	0.0008	0.9067
"	0	1.0185	0.8858	0.0009	0.8876
"	0	1.0330	0.8810	0.0008	0.8826
"	0	1.1000	0.8647	0.0008	0.8663
"	0	1.1210	0.8604	0.0009	0.8622
rajII_hac_g10_nointerspersedh2o_cladodsensitivity_14X2X16	0	0.9322	0.9118	0.0008	0.9134
"	0	1.0185	0.8955	0.0007	0.8969
"	0	1.0330	0.8935	0.0008	0.8951
"	0	1.1000	0.8790	0.0008	0.8806
"	0	1.1210	0.8742	0.0009	0.8760
rajII_hac_f9_10gadrods_refassy_14x2x16_cladod	0	0.9601	0.8967	0.0008	0.8984
"	0	1.0330	0.8876	0.0008	0.8892
"	0	1.0998	0.8792	0.0008	0.8808
rajII_hac_f9_10gadrods_refassy_14x2x16_channels	0	1.1200	0.8755	0.0009	0.8773
rajII_hac_g9_10gadrods_refassy_14X2X16_cladod	0	0.9830	0.8857	0.0008	0.8873
"	0	1.0330	0.8791	0.0009	0.8809
rajII_hac_g9_10gadrods_refassy_14X2X16_channels	0	1.1100	0.8659	0.0008	0.8676
rajII_hac_g9_10gadrods_refassy_14X2X16_cladod	0	1.1200	0.8644	0.0010	0.8664
rajII_hac_g8_nointerspersedh2o_cladodsensitivity_14X2X16	0	1.0719	0.9120	0.0008	0.9136
"	0	1.1500	0.9030	0.0008	0.9046
"	0	1.2192	0.8900	0.0009	0.8918
"	0	1.2500	0.8832	0.0008	0.8848

Table 6-31 Data For Figure 6-37 Moderator Density Sensitivity Study for the TN-B1 HAC Worst Case Parameter Fuel Design

Output File Name	Moderator Density (g/cm^3)	Clad Inner Diameter (cm)	Clad Outer Diameter (cm)	k_{eff}	σ	$k_{eff} + 2\sigma$
rajII_hac_g10_ worst case_ moderatordensity_14 X2X16	0.00	0.9338	1.010	0.7154	0.0006	0.7166
“	0.02	0.9338	1.010	0.7349	0.0007	0.7363
“	0.04	0.9338	1.010	0.7526	0.0007	0.7540
“	0.06	0.9338	1.010	0.7686	0.0006	0.7698
“	0.08	0.9338	1.010	0.7820	0.0007	0.7834
“	0.10	0.9338	1.010	0.7933	0.0008	0.7949
“	0.20	0.9338	1.010	0.8383	0.0007	0.8397
“	0.40	0.9338	1.010	0.8908	0.0007	0.8922
“	0.60	0.9338	1.010	0.9182	0.0009	0.9200
“	0.80	0.9338	1.010	0.9319	0.0008	0.9335
“	1.00	0.9338	1.010	0.9404	0.0007	0.9418

Table 6-32 Data for Figure 6-39 TN-B1 Single Package Normal Conditions of Transport Results

Output File Name	Fuel Assembly Type	Moderator Density (g/cm^3)	Gadolinia Rod (#)	Pitch (cm)	Pellet OD (cm)	Clad Inner Diameter (cm)	Clad Outer Diameter (cm)	k_{eff}	σ	k_{eff} + 2σ
rajII_normal_g10_5.0wtpct235u_h2odensitysensitivity_12gadrods_singlepackage	GNF 10 x 10	0.00	12	1.35	0.895	0.9338	1.010	0.2833	0.0005	0.2843
"	GNF 10 x 10	0.02	12	1.35	0.895	0.9338	1.010	0.2899	0.0005	0.2909
"	GNF 10 x 10	0.04	12	1.35	0.895	0.9338	1.010	0.2966	0.0006	0.2978
"	GNF 10 x 10	0.06	12	1.35	0.895	0.9338	1.010	0.3071	0.0006	0.3083
"	GNF 10 x 10	0.08	12	1.35	0.895	0.9338	1.010	0.3178	0.0006	0.3190
"	GNF 10 x 10	0.10	12	1.35	0.895	0.9338	1.010	0.3297	0.0005	0.3307
"	GNF 10 x 10	0.20	12	1.35	0.895	0.9338	1.010	0.3899	0.0006	0.3911
"	GNF 10 x 10	0.40	12	1.35	0.895	0.9338	1.010	0.4848	0.0008	0.4864
"	GNF 10 x 10	0.60	12	1.35	0.895	0.9338	1.010	0.5597	0.0008	0.5613
"	GNF 10 x 10	0.80	12	1.35	0.895	0.9338	1.010	0.6180	0.0007	0.6194
"	GNF 10 x 10	1.00	12	1.35	0.895	0.9338	1.010	0.6673	0.0008	0.6689

Table 6-33 Data for Figure 6-40 TN-B1 Single Package HAC Results

Output File Name	Fuel Assembly Type	Inner Container Moderator Density (g/cm^3)	Gadolinia Fuel Rods (#)	Pitch (cm)	Pellet OD (cm)	Clad Inner Diameter (cm)	Clad Outer Diameter (cm)	k_{eff}	σ	k_{eff} + 2σ
rajII_hac_g10__wor stcase_moderatord ensity_singlepacka ge	GNF 10 x 10	0.00	12	1.35	0.895	0.9338	1.010	0.2794	0.0005	0.2804
“	GNF 10 x 10	0.02	12	1.35	0.895	0.9338	1.010	0.2850	0.0005	0.2860
“	GNF 10 x 10	0.04	12	1.35	0.895	0.9338	1.010	0.2902	0.0005	0.2912
“	GNF 10 x 10	0.06	12	1.35	0.895	0.9338	1.010	0.2967	0.0006	0.2979
“	GNF 10 x 10	0.08	12	1.35	0.895	0.9338	1.010	0.3041	0.0006	0.3053
“	GNF 10 x 10	0.10	12	1.35	0.895	0.9338	1.010	0.3111	0.0005	0.3121
“	GNF 10 x 10	0.20	12	1.35	0.895	0.9338	1.010	0.3546	0.0006	0.3558
“	GNF 10 x 10	0.40	12	1.35	0.895	0.9338	1.010	0.4526	0.0007	0.4540
“	GNF 10 x 10	0.60	12	1.35	0.895	0.9338	1.010	0.5468	0.0008	0.5484
“	GNF 10 x 10	0.80	12	1.35	0.895	0.9338	1.010	0.6274	0.0008	0.6290
rajII_hac_g10_100 pcth20density_wor stcase_singlepacka ge	GNF 10 x 10	1.00	12	1.35	0.895	0.9338	1.010	0.6931	0.0010	0.6951

Table 6-34 Data for Figure 6-41 TN-B1 Package Array Under Normal Conditions of Transport Results

Output File Name	Fuel Assembly Type	Interspersed Moderator Density (g/cm^3)	Part Length Fuel Rods (#)	Pitch (cm)	Pellet OD (cm)	Clad Inner Diameter (cm)	Clad Outer Diameter (cm)	k_{eff}	σ	k_{eff} + 2σ
rajII_normal_g10_5.0wtpct235u_h2odensitysensitivity_12gadrods_21X3X24	GNF 10 x 10	0.00	12	1.35	0.895	0.9338	1.010	0.8519	0.0008	0.8535
“	GNF 10 x 10	0.02	12	1.35	0.895	0.9338	1.010	0.7962	0.0007	0.7976
“	GNF 10 x 10	0.04	12	1.35	0.895	0.9338	1.010	0.7441	0.0007	0.7455
“	GNF 10 x 10	0.06	12	1.35	0.895	0.9338	1.010	0.7054	0.0008	0.7070
“	GNF 10 x 10	0.08	12	1.35	0.895	0.9338	1.010	0.6726	0.0008	0.6742
“	GNF 10 x 10	0.10	12	1.35	0.895	0.9338	1.010	0.6427	0.0008	0.6443
“	GNF 10 x 10	0.20	12	1.35	0.895	0.9338	1.010	0.5500	0.0008	0.5516
“	GNF 10 x 10	0.40	12	1.35	0.895	0.9338	1.010	0.5254	0.0007	0.5268
“	GNF 10 x 10	0.60	12	1.35	0.895	0.9338	1.010	0.5690	0.0007	0.5704
“	GNF 10 x 10	0.80	12	1.35	0.895	0.9338	1.010	0.6206	0.0007	0.6220
“	GNF 10 x 10	1.00	12	1.35	0.895	0.9338	1.010	0.6683	0.0008	0.6699

Table 6-35 Data for Figure 6-42 TN-B1 Package Array Hypothetical Accident Condition Results

Output File Name	Fuel Assembly Type	Inner Container Moderator Density (g/cm^3)	Gadolinia-urania Fuel Rods (#)	Pitch (cm)	Pellet OD (cm)	Clad Inner Diameter (cm)	Clad Outer Diameter (cm)	k_{eff}	σ	k_{eff} + 2σ
rajII_hac_g10_12partlengthrods_worstcase_moderatordensity_10X1X10	GNF 10 x 10	0.00	12	1.35	0.895	0.9338	1.010	0.6375	0.0007	0.6389
"	GNF 10 x 10	0.02	12	1.35	0.895	0.9338	1.010	0.6470	0.0007	0.6484
"	GNF 10 x 10	0.04	12	1.35	0.895	0.9338	1.010	0.6567	0.0007	0.6581
"	GNF 10 x 10	0.06	12	1.35	0.895	0.9338	1.010	0.6648	0.0007	0.6662
"	GNF 10 x 10	0.08	12	1.35	0.895	0.9338	1.010	0.6734	0.0007	0.6748
"	GNF 10 x 10	0.10	12	1.35	0.895	0.9338	1.010	0.6822	0.0007	0.6836
"	GNF 10 x 10	0.20	12	1.35	0.895	0.9338	1.010	0.7226	0.0007	0.7240
"	GNF 10 x 10	0.40	12	1.35	0.895	0.9338	1.010	0.7976	0.0007	0.7990
"	GNF 10 x 10	0.60	12	1.35	0.895	0.9338	1.010	0.8561	0.0009	0.8579
"	GNF 10 x 10	0.80	12	1.35	0.895	0.9338	1.010	0.9005	0.0008	0.9021
"	GNF 10 x 10	1.00	12	1.35	0.895	0.9338	1.010	0.9378	0.0009	0.9396

Table 6-36 Data for Figure 6-45 TN-B1 Fuel Rod Transport in Stainless Steel Pipe

Output File Name	Fuel Assembly Type	Interspersed Moderator Density (g/cm^3)	Pitch (cm)	Fuel Rod (#)	Pellet OD (cm)	Clad Inner Diameter (cm)	Clad Outer Diameter (cm)	k_{eff}	σ	k_{eff} + 2σ
rajII_hac_8_ worstcase_ssp ipe_14x2x16	8x8	1.000	1.1305	110	1.05	1.1000	1.1000	0.8793	0.0007	0.8807
"	8x8	1.000	1.6662	52	1.05	1.1000	1.1000	1.0235	0.0009	1.0253
"	8x8	1.000	1.9035	43	1.05	1.1000	1.1000	1.0440	0.0008	1.0456
rajII_hac_8_ worstcase_ssp ipe_22fuelrod s_14x2x16	8x8	1.000	2.5	22	1.05	1.1000	1.1000	0.8823	0.0008	0.8839
rajII_hac_8_ worstcase_ssp ipe_14x2x16	8x8	1.000	2.937	14	1.05	1.1000	1.1000	0.7294	0.0008	0.7310
rajII_hac_9_ worstcase_ssp ipe_14x2x16	9x9	1.000	1.0505	140	0.9600	1.0200	1.0200	0.8701	0.0006	0.8713
"	9x9	1.000	1.4770	72	0.9600	1.0200	1.0200	1.0515	0.0008	1.0531
"	9x9	1.000	2	38	0.9600	1.0200	1.0200	1.0056	0.0009	1.0074
rajII_hac_9_ worstcase_ssp ipe_26fuelrod s_14x2x16	9x9	1.000	2.25	26	0.9600	1.0200	1.0200	0.8900	0.0008	0.8916
rajII_hac_9_ worstcase_ssp ipe_14x2x16	9x9	1.000	2.5432	22	0.9600	1.0200	1.0200	0.8416	0.0010	0.8436

Table 6-36 Data for Figure 6-45 TN-B1 Fuel Rod Transport in Stainless Steel Pipe(continued)

Output File Name	Fuel Assembly Type	Interspersed Moderator Density (g/cm^3)	Pitch (cm)	Fuel Rod (#)	Pellet OD (cm)	Clad Inner Diameter (cm)	Clad Outer Diameter (cm)	k_{eff}	σ	k_{eff} + 2σ
rajII_hac_10_ worstcase_sspipe_14x2x16	10x10	1.000	1.0305	144	0.9	1.000	1.000	0.8666	0.0007	0.8680
“	10x10	1.000	1.3213	84	0.9	1.000	1.000	1.0070	0.0008	1.0086
“	10x10	1.000	1.6416	56	0.9	1.000	1.000	1.0310	0.0011	1.0332
“	10x10	1.000	2.0484	30	0.9	1.000	1.000	0.8863	0.0008	0.8879

Table 6-37 Data for Figure 6-46 TN-B1 Fuel Rod Single Package Under Normal Conditions of Transport

Output File Name	Fuel Assembly Type	Interspersed Moderator Density (g/cm^3)	Pitch (cm)	Fuel Rod Number (#)	Pellet OD (cm)	Clad Inner Diameter (cm)	Clad Outer Diameter (cm)	k_{eff}	σ	$k_{eff} + 2\sigma$
rajII_normal_8_worstcasefuel_fuelrodtransport_moderatordensitysensitivity_singlep ackage	8x8	0.00	2.815	25	1.05	1.1000	1.1000	0.1675	0.0004	0.1683
"	8x8	0.01	2.815	25	1.05	1.1000	1.1000	0.1675	0.0004	0.1683
"	8x8	0.02	2.815	25	1.05	1.1000	1.1000	0.1672	0.0004	0.1680
"	8x8	0.04	2.815	25	1.05	1.1000	1.1000	0.1702	0.0004	0.1710
"	8x8	0.06	2.815	25	1.05	1.1000	1.1000	0.1757	0.0005	0.1767
"	8x8	0.08	2.815	25	1.05	1.1000	1.1000	0.1845	0.0005	0.1855
"	8x8	0.10	2.815	25	1.05	1.1000	1.1000	0.1949	0.0004	0.1957
"	8x8	0.20	2.815	25	1.05	1.1000	1.1000	0.2567	0.0005	0.2577
"	8x8	0.40	2.815	25	1.05	1.1000	1.1000	0.3890	0.0007	0.3904
"	8x8	0.60	2.815	25	1.05	1.1000	1.1000	0.4967	0.0007	0.4981
"	8x8	0.80	2.815	25	1.05	1.1000	1.1000	0.5783	0.0009	0.5801
"	8x8	1.00	2.815	25	1.05	1.1000	1.1000	0.6365	0.0008	0.6381

Table 6-38 Data for Figure 6-47 TN-B1 Fuel Rod Transport Single Package HAC

Output File Name	Fuel Assembly Type	Interspersed Moderator Density (g/cm^3)	Pitch (cm)	Fuel Rod Number (#)	Pellet OD (cm)	Clad Inner Diameter (cm)	Clad Outer Diameter (cm)	k_{eff}	σ	k_{eff} + 2σ
rajII_hac_8_worstcase_fuelrodtransport_moderatordensitysensitivity_singlepa ckage	8x8	0.00	3.0056	**25**	1.05	1.1000	1.1000	0.1769	0.0004	0.1777
"	8x8	0.01	3.0056	25	1.05	1.1000	1.1000	0.1761	0.0004	0.1769
"	8x8	0.02	3.0056	25	1.05	1.1000	1.1000	0.1767	0.0004	0.1775
"	8x8	0.04	3.0056	25	1.05	1.1000	1.1000	0.1778	0.0005	0.1788
"	8x8	0.06	3.0056	25	1.05	1.1000	1.1000	0.1794	0.0004	0.1802
"	8x8	0.08	3.0056	25	1.05	1.1000	1.1000	0.1829	0.0004	0.1837
"	8x8	0.10	3.0056	25	1.05	1.1000	1.1000	0.1876	0.0004	0.1884
"	8x8	0.20	3.0056	25	1.05	1.1000	1.1000	0.2306	0.0005	0.2316
"	8x8	0.40	3.0056	25	1.05	1.1000	1.1000	0.3718	0.0007	0.3732
"	8x8	0.60	3.0056	25	1.05	1.1000	1.1000	0.5062	0.0007	0.5076
"	8x8	0.80	3.0056	25	1.05	1.1000	1.1000	0.5980	0.0008	0.5996
"	8x8	1.00	3.0056	25	1.05	1.1000	1.1000	0.6532	0.0008	0.6548

Table 6-39 Data for Figure 6-48 TN-B1 Package Array Under Normal Conditions of Transport with Loose Fuel Rods

Output File Name	Fuel Assembly Type	Interspersed Moderator Density (g/cm^3)	Pitch (cm)	Fuel Rod Number (#)	Pellet OD (cm)	Clad Inner Diameter (cm)	Clad Outer Diameter (cm)	k_{eff}	σ	k_{eff} + 2σ
rajII_normal_8_worstcasefuel_fuelrodtransport_moderatordensitysensitivity_21X3X24	8x8	0.00	2.815	25	1.05	1.1000	1.1000	0.5055	0.0006	0.5067
“	8x8	0.01	2.815	25	1.05	1.1000	1.1000	0.5827	0.0006	0.5839
“	8x8	0.02	2.815	25	1.05	1.1000	1.1000	0.5931	0.0007	0.5945
“	8x8	0.04	2.815	25	1.05	1.1000	1.1000	0.5891	0.0007	0.5905
“	8x8	0.06	2.815	25	1.05	1.1000	1.1000	0.5719	0.0007	0.5733
“	8x8	0.08	2.815	25	1.05	1.1000	1.1000	0.5523	0.0009	0.5541
“	8x8	0.10	2.815	25	1.05	1.1000	1.1000	0.5291	0.0007	0.5305
“	8x8	0.20	2.815	25	1.05	1.1000	1.1000	0.4383	0.0006	0.4395
“	8x8	0.40	2.815	25	1.05	1.1000	1.1000	0.4300	0.0007	0.4314
“	8x8	0.60	2.815	25	1.05	1.1000	1.1000	0.5079	0.0008	0.5095
“	8x8	0.80	2.815	25	1.05	1.1000	1.1000	0.5817	0.0008	0.5833
“	8x8	1.00	2.815	25	1.05	1.1000	1.1000	0.6365	0.0008	0.6381

Table 6-40 Data for Figure 6-49 TN-B1 Fuel Rod Transport Under HAC

Output File Name	Fuel Assembly Type	Interspersed Moderator Density (g/cm^3)	Pitch (cm)	Fuel Rod Number (#)	Pellet OD (cm)	Clad Inner Diameter (cm)	Clad Outer Diameter (cm)	keff	σ	keff + 2σ
rajII_hac_8_worstcase_fuelrodtransport_100pcth2odensity_10x1x10	8x8	0.00	3.0056	25	1.05	1.1000	1.1000	0.3230	0.0005	0.3240
“	8x8	0.01	3.0056	25	1.05	1.1000	1.1000	0.3479	0.0005	0.3489
“	8x8	0.02	3.0056	25	1.05	1.1000	1.1000	0.3752	0.0007	0.3766
“	8x8	0.04	3.0056	25	1.05	1.1000	1.1000	0.4007	0.0006	0.4019
“	8x8	0.06	3.0056	25	1.05	1.1000	1.1000	0.4287	0.0006	0.4299
“	8x8	0.08	3.0056	25	1.05	1.1000	1.1000	0.4556	0.0006	0.4568
“	8x8	0.10	3.0056	25	1.05	1.1000	1.1000	0.5743	0.0009	0.5761
“	8x8	0.20	3.0056	25	1.05	1.1000	1.1000	0.7416	0.0009	0.7434
“	8x8	0.40	3.0056	25	1.05	1.1000	1.1000	0.8264	0.0008	0.8280
“	8x8	0.60	3.0056	25	1.05	1.1000	1.1000	0.8660	0.0008	0.8676
“	8x8	0.80	3.0056	25	1.05	1.1000	1.1000	0.8731	0.0007	0.8745
“	8x8	1.00	3.0056	25	1.05	1.1000	1.1000	0.3752	0.0007	0.3766

6.11.10. *Summary of Experiments*

This document provides a summary of the experiments used in Reference 3 to determine the SCALE 4.4a bias. Trending data is either from the original experiments or calculated herein, i.e., H/U values, have been added to the data. Note that in most cases the experimental $k_{eff} \pm \sigma$ from Reference 3 do not have a reference. If data from the original experiment and/or data from the International Handbook of Evaluated Criticality Safety Benchmark Experiments (see Reference 4) provided these values, it was so noted or additional values provided.

The USL method of NUREG/CR-6361 (Reference 7) has the tacit assumption that the experimental k is 1.0000. Likewise, it does not account for the uncertainty in the experimental values. It is recommended that the procedure discussed in NUREG/CR-6698, “Guide for Validation of Nuclear Criticality Safety Calculational Methodology,**”** be considered. The document has the following definitions for the calculated’ values used for the bias evaluation:

$$k_{norm} = k_{calc}/k_{exp} \text{ and}$$

$$\sigma_{norm} = [(\sigma_{calc})^2 + (\sigma_{exp})^2]^{1/2}$$

This will normalize the calculated to experimental to account for uncertainties in the experimental values.

Note: The reference numbers quoted in the following sections are references listed in each section, rather than those listed in Section 6.11.

6.11.10.1. Critical Configurations

6.11.10.1.1. *Water-Moderated U(4.31)O2 Fuel Rods in 2.54-cm Square-Pitched Arrays*

References:

1. “Critical Separation Between Subcritical Clusters of 4.29 Wt% U-235 Enriched UO_2 Rods in Water With Fixed Neutron Poisons,” S.R. Bierman, B. M. Durst, E.D. Clayton, Battelle Pacific Northwest Laboratories, NUREG/CR-0073(PNL-2695).

2. “Water-Moderated U(4.31)O_2 Fuel Rods in 2.54-cm Square-Pitched Arrays,” V.F.Dean, Evaluator, International Handbook of Evaluated Criticality Safety Benchmark Experiments,” NEA/NSC/DOC(95)03, Sept 2001, Nuclear Energy Agency.

3. “Software Validation Document, EMF-2670, PC-SCALE 4.4a V&V”, C.D. Manning, EMF-2670, Rev. 1, 11/26/2002, Framatome ANP.

Reference 3 uses the data from this set of experiments as part of a heterogeneous uranium oxide set of benchmark calculations. Table 6 of that reference provides some information on the experimental configuration and Tables 7 and 9 provide results for the 238 and 44 group Scale 4.4a cross-sections, respectively. Table 6-41 Summary of Information for Experiment below provides a summary of the benchmark information from References 1 and 2. The rod and oxide dimensional and material information came from Reference 1. The enrichment quoted in Reference 1 was changed in Reference 2 due to a later chemical analysis of the fuel rods used in the experiment. Thus, the table uses the 4.31 value from Reference 2 rather than 4.29 quoted in Reference 1. The temperatures of the experiments were not included in Reference 1 and were not explicitly noted at the time of the experiment. The authors of Reference 2 obtained logbooks from similar experiments at PNL that showed temperatures ranging from ~18^{o}C to ~25^{o}C. From these data Reference 2 inferred an average value of ~22^{o}C which is listed here. The value used in the calculations of Reference 3 is not currently known. The temperature value is used to calculate the hydrogen atom density and a deviation of a few degrees will not significantly change the results. The U and H atom densities used a value of Avogadro's number of 0.6022142E-24. The H/U value applies only to the fuel cluster.

Table 6-44 Urania Gadolinia Experiment Summary[a] contains cases using cell-weighted models, 'x' added to case ID. These are included for completeness and should not be included in the normal benchmarking trending.

Table 6-41 Summary of Information for Experiment

Pellet OD, cm	1.2649	Enrichment, wt%	4.31[a]	V_{H2O}/V_{oxide}	3.883228
Rod ID, cm	1.2827	Oxide Density, g/cm^3	94.9	U-235 Atom Density	1.0125E-03
Rod OD, cm	1.4147	Temperature, ^{o}C	22[b]	H Atom Density	0.066724
Rod Pitch, cm	2.54	Water Density, g/cm^3	0.9978	H/U	255.92
Clad Material	Aluminum	Boron, ppm	0.0		

a) Redefined from 4.29 in Reference 2 due to fuel evaluation after publication of Reference 1.

b) Not defined in Reference 1, assumed in Reference 2 based upon inference from data notebooks of experiments.

Table 6-42 Parameters for Benchmark Cases for SCALE 4.4a 44 Group Cross-Section Set

Case ID[C]	Lattice[a]	Spacing[a] between clusters, cm		Experimental k_{eff} and σ				SCALE 4.4a 44 Group Cross-Section Calculated k_{eff} and σ				Absorber Plates in Water Gap
		Rod-rod	Cell-cell	k_{eff}[b]	σ[b]	k_{eff}[c]	σ[c]	k_{eff}[d]	σ[d]	AFG[d]	EALF[d] (ev)	
c004.out	15x8	11.72	10.62	1.0000	0.0020	0.9997	0.0020	0.9971	0.0008	35.772	0.112667	None
c005b.out	15x8	10.77	9.64	1.0000	0.0180	0.9997	0.0020	0.9960	0.0008	35.763	0.112942	0.625 cm Al plates
c006b.out	15x8	10.72	9.59	1.0000	0.0019	0.9997	0.0020	0.9960	0.0008	35.768	0.112841	0.625 cm Al plates
c007a.out	15x8	9.76	8.63	1.0000	0.0021	0.9997	0.0020	0.9966	0.0008	35.768	0.112705	0.302 cm SS 304L plates
c008b.out	15x8	9.22	8.09	1.0000	0.0021	0.9997	0.0020	0.9948	0.0008	35.755	0.113485	0.302 cm SS 304L plates
c009b.out	15x8	8.08	6.95	1.0000	0.0021	0.9997	0.0020	0.9963	0.0008	35.748	0.113698	0.298 cm 304L plates with 1.05 wt% B
c010b.out	15x8	6.60	5.47	1.0000	0.0021	0.9997	0.0020	0.9980	0.0008	35.728	0.114519	0.298 cm 304L plates with 1.05 wt% B
c011b.out	15x8	7.90	6.77	1.0000	0.0021	0.9997	0.0020	0.9983	0.0009	35.750	0.113450	0.298 cm 304L plates with 1.62 wt% B
c012b.out	15x8	5.76	4.63	1.0000	0.0021	0.9997	0.0020	0.9975	0.0007	35.729	0.114508	0.298 cm 304L plates with 1.62 wt% B
c013b.out	15x8	9.65	8.52	1.0000	0.0021	0.9997	0.0020	0.9956	0.001	35.768	0.112832	0.485 cm, SS 304L plates
c014b.out	15x8	8.58	7.45	1.0000	0.0021	0.9997	0.0020	0.9970	0.0009	35.745	0.113819	0.485 cm, SS 304L plates
c029b.out	15x8	10.90	9.77	1.0000	0.0021	0.9997	0.0020	0.9967	0.0008	35.770	0.112874	0.652 cm, Zircaloy-4 plates
c030b.out	15x8	10.86	9.73	1.0000	0.0021	0.9997	0.0020	0.9977	0.0009	35.767	0.112860	0.652 cm, Zircaloy-4 plates
c031b.out	15x8	7.672	6.55	1.0000	0.0021	0.9997	0.0020	0.9975	0.0008	35.727	0.114536	0.723 cm, Boral plates, 28.7 wt% B

a) From Reference 1. The ‘rod surface-to-rod’ surface spacing is reported in Reference 1. Reference 2 (p. 9) provides the cell-to-cell spacing for selected experiments from Reference 1 as: (rod-rod) – (pitch) + (rod diameter). This formula was applied to all above values even though some ‘rod-rod’ may be ‘array plate-to-plate’.

b) Values from Reference 3, Table 6, p. 42. Source of σ values is not listed in this reference.

c) Values from Reference 2, p. 23 based upon calculational uncertainties in parameters and assumptions in the benchmark models of the reference. Note that Reference 2 only includes 4 of the cases from Reference 1 listed above. Here it is assumed that the values listed above apply to all cases.

d) From Reference 3, Table 9, p. 61 for 44 group cross-sections. Table 7 in this reference has values for 238 group cross-sections

Table 6-43 Parameters for Benchmark Cases for SCALE 4.4a 238 Group Cross-Section Set

Case ID[C]	Lattice[a]	Cluster Spacing[a], cm		Experimental k_{eff} and σ				SCALE 4.4a 238 Group Cross-Section Calculated k_{eff} and σ				Absorber Plates in Water Gap
		Rod-rod	Cell-cell	k_{eff}[b]	σ[b]	k_{eff}[c]	σ[c]	k_{eff}[d]	σ[d]	AFG[d]	EALF[d] (ev)	
c001x.out[e]	10x11.51	0.0	0.0	1.0000	0.0021	0.9997	0.0020	0.9987	0.0008	208.112	0.108721	--
c002x.out	8x16.37	0.0	0.0	1.0000	0.0021	0.9997	0.0020	0.9993	0.0008	208.157	0.108277	--
c003x.out	9x13.35	0.0	0.0	1.0000	0.0021	0.9997	0.0020	1.0015	0.0010	208.136	0.108496	--
c004.out	15x8	11.72	10.62	1.0000	0.0020	0.9997	0.0020	0.9930	0.0010	207.568	0.114058	None
c005b.out	15x8	10.77	9.64	1.0000	0.0180	0.9997	0.0020	0.9931	0.0008	207.550	0.114504	0.625 cm Al plates
c006b.out	15x8	10.72	9.59	1.0000	0.0019	0.9997	0.0020	0.9941	0.0009	207.508	0.114748	0.625 cm Al plates
c007a.out	15x8	9.76	8.63	1.0000	0.0021	0.9997	0.0020	0.9944	0.0008	207.547	0.114468	0.302 cm SS 304L plates
c007x.out	15x8	9.76	8.63	1.0000	0.0021	0.9997	0.0020	1.0010	0.0008	208.273	0.107285	0.302 cm SS 304L plates
c008b.out	15x8	9.22	8.09	1.0000	0.0021	0.9997	0.0020	0.9931	0.0007	207.487	0.114939	0.302 cm SS 304L plates
c008x.out	15x8	9.22	8.09	1.0000	0.0021	0.9997	0.0020	0.9981	0.0008	208.220	0.107758	0.302 cm SS 304L plates
c009b.out	15x8	8.08	6.95	1.0000	0.0021	0.9997	0.0020	0.9928	0.0008	207.472	0.114907	0.298 cm 304L plates with 1.05 wt% B
c010b.out	15x8	6.60	5.47	1.0000	0.0021	0.9997	0.0020	0.9952	0.0009	207.373	0.115896	0.298 cm 304L plates with 1.05 wt% B
c011b.out	15x8	7.90	6.77	1.0000	0.0021	0.9997	0.0020	0.9964	0.0008	207.507	0.114703	0.298 cm 304L plates with 1.62 wt% B
c012b.out	15x8	5.76	4.63	1.0000	0.0021	0.9997	0.0020	0.9938	0.0009	207.364	0.116224	0.298 cm 304L plates with 1.62 wt% B
c013b.out	15x8	9.65	8.52	1.0000	0.0021	0.9997	0.0020	0.9953	0.0008	207.495	0.114944	0.485 cm, SS 304L plates
c013x.out	15x8	9.65	8.52	1.0000	0.0021	0.9997	0.0020	1.0002	0.0009	208.270	0.107272	0.485 cm, SS 304L plates
c014b.out	15x8	8.58	7.45	1.0000	0.0021	0.9997	0.0020	0.9942	0.0009	207.484	0.115038	0.485 cm, SS 304L plates
c014x.out	15x8	8.580	7.45	1.0000	0.0021	0.9997	0.0020	1.0018	0.0008	208.211	0.107849	0.485 cm, SS 304L plates
c029b.out	15x8	10.90	9.77	1.0000	0.0021	0.9997	0.0020	0.9942	0.0008	207.549	0.114428	0.652 cm, Zircaloy-4 plates
c030b.out	15x8	10.86	9.73	1.0000	0.0021	0.9997	0.0020	0.9946	0.0008	207.508	0.114783	0.652 cm, Zircaloy-4 plates
c031b.out	15x8	7.672	6.55	1.0000	0.0021	0.9997	0.0020	0.9951	0.0008	207.387	0.115885	0.723 cm, Boral plates, 28.7 wt% B

a) From Reference 1. The ‘rod surface-to-rod’ surface spacing is reported in Reference 1. Reference 2 (p. 9) provides the cell-to-cell spacing for selected experiments from Reference 1 as: (rod-rod) – (pitch) + (rod diameter). This formula was applied to all above values even though some ‘rod-rod’ may be ‘array plate-to-plate’.

b) Values from Reference 3, Table 6, p. 42. Source of σ values is not listed in this reference.

c) Values from Reference 2, p. 23 based upon calculational uncertainties in parameters and assumptions in the benchmark models of the reference. Note that Reference 2 only includes 4 of the cases from Reference 1 listed above. Here it is assumed that the values listed above apply to all cases.

d) From Reference 3, Table 9, p. 61 for 44 group cross-sections. Table 7 in this reference has values for 238 group cross-sections. e) From Reference 3, Table 6. The ‘x’ before ‘.out’ means the case is a cell weighted model.

e) From Reference 3, Table 6. The ‘x’ before ‘.out’ means the case is a cell weighted model.

6.11.10.1.2. *Urania Gadolinia Experiments*

References:

4. FANP Doc: 32-5012895-00, “Validation Report – SCALEPC-44A Urania-Gadolinia Experiments,” R.S. Harding.
5. “Urania Gadolinia: Nuclear Model Development and Critical Experiment Benchmark,” L.W. Newman, Babcock & Wilcox for DOE, DOE/ET/34212-41, BAW-1910, April 1984.
6. “Development and Demonstration of An Advanced Extended-Burnup Fuel Assembly Design Incorporating Urania-Gadolinia,” L.W. Newman, Babcock & Wilcox for DOE, DOE/ET/34212-41, BAW-1681-2, August 1982.

Reference 4 uses the experimental data from References 5 and 6 to construct benchmark cases for SCALE 4.4a. Table 6-44 Urania Gadolinia Experiment Summary[a] summarizes the experimental configuration data that form the basis for the KENO V.a models. Table 6-46 Urania Gadolinia Critical Experiment Trending Data provides trending parameters for this set of experiments. Table 6-45 Experimental Parameters for Calculating U-235 and H Atom Densities lists the basis for the H/U values tabulated in Table 6-46 Urania Gadolinia Critical Experiment Trending Data. Table 6-47 Urania Gadolinia Benchmark k_{eff} Data provides the experimental and calculated results for the 44 and 238 group SCALE 4.4a cross-section sets from Reference 3.

Table 6-44 Urania Gadolinia Experiment Summary[a]

Parameter	Rod 1	Rod 2	Rod 3
U-235 wt%	4.02	2.459	1.944
Gadolinia Wt%	-	-	4
Pellet density[b], g/cm^3	9.46	10.218	10.328
Pellet OD, cm	1.1265	1.03	1.0296
Rod ID, cm	1.1265	1.044	1.0439
Rod OD, cm	1.2078	1.206	1.2065
Rod Pitch, cm	1.6358	1.6358	1.6358
Clad Material	SS	Al	Al
$V_{fuel/cell}$	0.996654	0.833229	0.832582
$V_{H2O/cell}$	1.530044	1.533399	1.532452
Water boron factor[c]		0.99928	
Temperature[d], ^{o}C		22	
Water density, g/cm^3		0.99777	

a) From Reference 4.

b) Based upon rod mass and fuel volume in rod.

c) A factor to correct water density from 25 ^{o}C to 20 ^{o}C. Boron ppm is based upon 25 ^{o}C measurements. See Reference 4, p. 9.

d) Not specified explicitly for this set of experiments. This value is inferred from temperature data in Reference 7.

Table 6-45 Experimental Parameters for Calculating U-235 and H Atom Densities

Case ID	Number of Different Type Rods in each Critical Configuration(Reference 1 Table 1))						Core Volume[a]		Atom Density[a]	
	2.46 Wt%	4.02 Wt%	1.94 Wt% (Gd)	Water	Misc	Core Total	Fuel	Water	U-235	H
core01.out	4808	-	-	153	-	4961	4006.16	7765.83	5.67711E-04	0.066676
core03.out	4788	-	-	137	16	4941	3989.50	7692.42	5.67711E-04	0.066676
core05.out	4780	-	28	153	-	4961	4006.15	7765.90	5.67061E-04	0.066676
core5a.out	4776	-	32	153	-	4961	4006.14	7765.91	5.66968E-04	0.066676
core5b.out	4780	-	28	153	-	4961	4006.15	7765.90	5.67061E-04	0.066676
core08.out	4772	-	36	153	-	4961	4006.14	7765.92	5.66875E-04	0.066676
core10.out	4772	-	36	137	16	4961	4006.14	7723.11	5.66875E-04	0.066676
core12a.out	3920	888	-	153	-	4961	4151.29	7768.81	6.21492E-04	0.066676
core14.out	3920	860	28	153	-	4961	4146.69	7768.79	6.19146E-04	0.066676
core16.out	3920	852	36	153	-	4961	4145.38	7768.78	6.18475E-04	0.066676
core18.out	3676	944	-	180	-	4800	4003.79	7553.60	6.27210E-04	0.066676
core19.out	3676	928	16	180	-	4800	4001.17	7553.58	6.25815E-04	0.066676
core20.out	3676	912	32	180	-	4800	3998.54	7553.57	6.24420E-04	0.066676

a) Calculated values. Atom densities based upon Avogadro's number of 0.6022142E-24

Table 6-46 Urania Gadolinia Critical Experiment Trending Data

Case Name	Clad[a]	Lattice[a]	wt% 235[a]	Boron, ppm[a]	Vh2o/Vfuel[b]	H/U[b]	k_{eff}[c]	Sigma[c]	Rod Configurations[a]
core01.out	Al	15x15	2.46	1337.9	1.9385	227.67	1.0002	0.0005	0
core03.out	Al	15x15	2.46/1.94	1239.3	1.9282	226.46	1.0000	0.0006	20-4%Gd
core05.out	Al	15x15	2.46/1.94	1208.0	1.9385	227.93	0.9999	0.0006	28-4%Gd
core5a.out	Al	15x15	2.46/1.94	1191.3	1.9385	227.97	0.9999	0.0006	32-4%Gd
core5b.out	Al	15x15	2.46/1.94	1207.1	1.9385	227.93	0.9999	0.0006	28-4%Gd
core08.out	Al	15x15	2.46/1.94	1170.7	1.9385	228.01	1.0083	0.0012	36-4%Gd
core10.out	Al	15x15	2.46/1.94	1177.1	1.9278	226.75	1.0001	0.0009	36-4%Gd+3 void rods
core12a.out	SS/Al	15x15	4.02/2.46	1899.3	1.8714	200.77	1.0000	0.0007	4.02 inner/2.456 outer
core14.out	SS/Al	15x15	4.02/2.46/1.94	1653.8	1.8735	201.76	1.0030	0.0009	28-4%Gd
core16.out	SS/Al	15x15	4.02/2.46/1.94	1579.4	1.8741	202.04	1.0001	0.0010	36-4%Gd
core18.out	SS/Al	16x16	4.02/2.46	1776.8	1.8866	200.56	1.0002	0.0011	CE Large Guide Tubes
core19.out	SS/Al	16x16	4.02/2.46/1.94	1628.3	1.8878	201.14	1.0002	0.0010	16-4%Gd
core20.out	SS/Al	16x16	4.02/2.46/1.94	1499.0	1.8891	201.72	1.0002	0.0010	Zone + 32-4%

a) Reference 4.
b) Calculated values from Table 5.
c) Reference 3, Table 6. The source of these values is not documented in the reference.

Table 6-47 Urania Gadolinia Benchmark k_{eff} Data

Case ID	Experimental k_{eff} and σ		SCALE 4.4a 44 Group Cross-Section Calculated k_{eff} and σ				SCALE 4.4a 238 Group Cross-Section Calculated k_{eff} and σ			
	k_{eff}[a]	σ[a]	k_{eff}[b]	σ[b]	AFG[b]	EALF[b] (ev)	k_{eff}[b]	σ[b]	AFG[b]	EALF[b] (ev)
core01.out	1.0002	0.0005	0.9955	0.0006	33.8930	0.2530	0.9952	0.0007	197.6190	0.2567
core03.out	1.0000	0.0006	0.9963	0.0006	33.9190	0.2499	0.9943	0.0006	197.6810	0.2547
core05.out	0.9999	0.0006	0.9968	0.0006	33.9280	0.2493	0.9935	0.0006	197.6840	0.2543
core5a.out	0.9999	0.0006	0.9963	0.0005	33.9270	0.2494	0.9940	0.0006	197.6850	0.2547
core5b.out	0.9999	0.0006	0.9959	0.0006	33.9160	0.2504	0.9941	0.0007	197.6280	0.2558
core08.out	1.0083	0.0012	0.9958	0.0006	33.9200	0.2503	0.9928	0.0005	197.7470	0.2534
core10.out	1.0001	0.0009	0.9956	0.0006	33.9130	0.2512	0.9922	0.0007	197.6080	0.2562
core12a.out	1.0000	0.0007	0.9982	0.0006	32.8910	0.3644	0.9950	0.0006	193.1960	0.3697
core14.out	1.0030	0.0009	0.9976	0.0007	33.0670	0.3421	0.9942	0.0007	193.8910	0.3488
core16.out	1.0001	0.0010	0.9969	0.0007	33.1010	0.3376	0.9941	0.0007	194.1570	0.3412
core18.out	1.0002	0.0011	0.9975	0.0007	32.8960	0.3645	0.9950	0.0007	193.2390	0.3684
core19.out	1.0002	0.0010	0.9973	0.0006	33.0140	0.3489	0.9941	0.0007	193.6610	0.3553
core20.out	1.0002	0.0010	0.9969	0.0007	33.1050	0.3382	0.9950	0.0006	194.0850	0.3425

a) Values from Reference 3, Table 6, p. 42. Source of σ values is not documented in this reference.

b) From Reference 3, Table 9, p. 61 for 44 group cross-sections. Table 7 in this reference has values for 238 group cross-sections

6.11.10.1.3. *Critical Experiments Supporting Close Proximity Water Storage of Power Reactor Fuel*

References:

7. FANP Doc. 32-5012896-00, “Validation Report – SCALEPC-44A Close Proximity Experiments,” R.S. Harding.
8. “Critical Experiments Supporting Close Proximity Water Storage of Power Reactor Fuel,” M.N. Baldwin, et.al., BAW-1484-7, July 1979.

Reference 7 uses the experimental data from Reference 8 to construct benchmark cases for SCALE 4.4a. Table 6-48 Close Proximity Experiment Summary[a] summarizes the experimental configuration data that form the basis for the KENO V.a models. Table 6-49 Close Proximity Experiment Trending Data provides trending parameters for this set of experiments. Table 6-50 Close Proximity Experiment k_{eff} Data provides the experimental and calculated results for the 44 and 238 group SCALE 4.4a cross-section sets from Reference 3.

Table 6-48 Close Proximity Experiment Summary[a]

U-235 wt%	2.459	Fuel Lattice	14x14
Pellet Density[b], g/cm^3	10.218	Clad Material	Al
Pellet OD, cm	1.030	Vfuel/cell	0.8332
Rod ID, cm	1.044	Vh2o/cell	1.5342
Rod OD, cm	1.206	Vh2o/Vf	1.8413
Rod Pitch, cm	1.636		

a) From Reference 7.
b) Based upon rod mass and fuel volume in rod

Table 6-49 Close Proximity Experiment Trending Data

Case ID	Cluster Spacing[a], cm	Temp[a], °C	Boron[a], ppm	Boron Factors[b]	Water density[b], g/cm³	Atom Density[c]		H/U[c]	Absorbers[a]
						U-235	H		
aclp1.out	--	21	0	0.999788	0.99799	5.6991E-04	0.066725	215.57	--
aclp2.out	0.000	18.5	1037	1.000298	0.99850	5.6991E-04	0.066793	215.79	--
aclp3.out	1.636	18	764	1.000392	0.99860	5.6991E-04	0.066806	215.83	H2O
aclp4.out	1.636	17	0	1.000572	0.99878	5.6991E-04	0.066830	215.91	84 B4C pins/H2O
aclp5.out	3.272	17.5	0	1.000483	0.99869	5.6991E-04	0.066818	215.87	64 B4C pins/H2O
aclp6.out	3.272	17.5	0	1.000483	0.99869	5.6991E-04	0.066818	215.87	64 B4C pins/H2O
aclp7.out	4.908	17.5	0	1.000483	0.99869	5.6991E-04	0.066818	215.87	34 B4C pins/H2O
aclp8.out	4.908	17.5	0	1.000483	0.99869	5.6991E-04	0.066818	215.87	34 B4C pins/H2O
aclp9.out	6.544	17.5	0	1.000483	0.99869	5.6991E-04	0.066818	215.87	H2O
aclp10.out	6.544	24.5	143	0.998967	0.99718	5.6991E-04	0.066616	215.22	H2O
acp11a.out	1.636	25.5	510	0.999712	0.99692	5.6991E-04	0.066648	215.32	0.462 cm, SS 304/H2O
acp11b.out	1.636	26	514	0.998578	0.99992	5.6991E-04	0.066773	215.73	0.462 cm, SS 304/H2O
acp11c.out	1.636	25.5	501	0.999712	0.99692	5.6991E-04	0.066648	215.32	0.462 cm, SS 304/H2O
acp11d.out	1.636	25.5	493	0.998840	0.99692	5.6991E-04	0.066590	215.14	0.462 cm, SS 304/H2O
acp11e.out	1.636	25	474	0.999712	0.99404	5.6991E-04	0.066456	214.70	0.462 cm, SS 304/H2O
acp11f.out	1.636	25	462	0.998840	0.99404	5.6991E-04	0.066398	214.52	0.462 cm, SS 304/H2O
acp11g.out	1.636	25.5	432	0.999712	0.99992	5.6991E-04	0.066849	215.97	0.462 cm, SS 304/H2O
aclp12.out	3.272	26	217	0.998578	0.99679	5.6991E-04	0.066564	215.05	0.462 cm, SS 304/H2O
aclp13.out	1.636	20	15	1.000000	0.99821	5.6991E-04	0.066754	215.67	0.645 cm, BAl 1.614 wt% B/H2O
acp13a.out	1.636	17	28	1.000572	0.99878	5.6991E-04	0.066830	215.91	0.645 cm, BAl 1.614 wt% B/H2O
aclp14.out	1.636	18	92	1.000392	0.99860	5.6991E-04	0.066806	215.83	0.645 cm, BAl 1.614 wt% B/H2O
aclp15.out	1.636	18	395	1.000392	0.99860	5.6991E-04	0.066806	215.83	0.645 cm, BAl 1.614 wt% B/H2O

a) Reference 8.
b) Boron factors to correct water density from 25°C to 20°C. Boron ppm is based upon 25°C measurements. See Reference 7, Table 3.0-1, p. 46. Water density from standard tables.
c) Calculated values based upon Avogadro's number of 0.6022142E-24

Table 6-49 Close Proximity Experiment Trending Data (continued)

Case ID	Cluster Spacing[a], cm	Temp[a], °C	Boron[a], ppm	Boron Factors[b]	Water density[b], g/cm³	Atom Density[c]		H/U[c]	Absorbers[a]
						U-235	H		
aclp16.out	3.272	17.5	121	1.000483	0.99878	5.6991E-04	0.066824	215.89	0.645 cm, BAl 1.614 wt% B/H2O
aclp17.out	1.636	17.5	487	1.000483	0.99878	5.6991E-04	0.066824	215.89	0.645 cm, BAl 1.614 wt% B/H2O
aclp18.out	3.272	18	197	1.000392	0.99860	5.6991E-04	0.066806	215.83	0.645 cm, BAl 1.614 wt% B/H2O
aclp19.out	1.636	17.5	634	1.000483	0.99878	5.6991E-04	0.066824	215.89	0.645 cm, BAl 1.614 wt% B/H2O
aclp20.out	3.272	17.5	320	1.000483	0.99878	5.6991E-04	0.066824	215.89	0.645 cm, BAl 1.614 wt% B/H2O
aclp21.out	6.544	16.5	72	1.000740	0.99992	5.6991E-04	0.066918	216.19	0.645 cm, BAl 1.614 wt% B/H2O

a) Reference 8.
b) Boron factors to correct water density from 25°C to 20°C. Boron ppm is based upon 25°C measurements. See Reference 7, Table 3.0-1, p. 46. Water density from standard tables.
c) Calculated values based upon Avogadro's number of 0.6022142E-24

Table 6-50 Close Proximity Experiment k_{eff} Data

Case ID	Experimental k_{eff} and σ		SCALE 4.4a 44 Group Cross-Section Calculated k_{eff} and σ				SCALE 4.4a 238 Group Cross-Section Calculated k_{eff} and σ			
	k_{eff}[a]	σ[a]	k_{eff}[b]	σ[b]	AFG[b]	EALF[b] (ev)	k_{eff}[b]	σ[b]	AFG[b]	EALF[b] (ev)
aclp1.out	1.0002	0.0005	0.9931	0.0008	34.8710	0.1712	0.9889	0.0009	201.9510	0.1761
aclp2.out	1.0001	0.0005	0.9956	0.0008	33.9420	0.2484	0.9939	0.0008	197.6580	0.2540
aclp3.out	1.0000	0.0006	0.9963	0.0006	34.5210	0.1960	0.9934	0.0007	200.5280	0.2002
aclp4.out	0.9999	0.0006	0.9897	0.0008	34.6110	0.1910	0.9875	0.0008	200.7350	0.1946
aclp5.out	1.0000	0.0007	0.9883	0.0008	34.9500	0.1662	0.9873	0.0008	202.4670	0.1689
aclp6.out	1.0097	0.0012	0.9884	0.0007	34.8840	0.1716	0.9872	0.0007	201.9760	0.1760
aclp7.out	0.9998	0.0009	0.9900	0.0007	35.2100	0.1496	0.9867	0.0008	203.6900	0.1527
aclp8.out	1.0083	0.0012	0.9906	0.0008	35.1720	0.1526	0.9874	0.0007	203.3420	0.1573
aclp9.out	1.0030	0.0009	0.9906	0.0006	35.3620	0.1411	0.9879	0.0007	204.4120	0.1438
aclp10.out	1.0001	0.0009	0.9913	0.0007	35.2090	0.1494	0.9883	0.0008	203.7410	0.1528
acp11a.out	1.0000	0.0006	0.9955	0.0007	34.4600	0.2001	0.9919	0.0006	200.2820	0.2046
acp11b.out	1.0007	0.0007	0.9942	0.0007	34.4640	0.1997	0.9916	0.0009	200.2900	0.2043
acp11c.out	1.0007	0.0006	0.9943	0.0008	34.4550	0.2007	0.9915	0.0008	200.1800	0.2060
acp11d.out	1.0007	0.0006	0.9939	0.0006	34.4290	0.2035	0.9920	0.0009	200.1670	0.2063
acp11e.out	1.0007	0.0006	0.9952	0.0007	34.4350	0.2030	0.9918	0.0006	200.0830	0.2078
acp11f.out	1.0007	0.0006	0.9947	0.0008	34.4360	0.2033	0.9916	0.0006	200.0020	0.2089
acp11g.out	1.0007	0.0006	0.9941	0.0007	34.4200	0.2054	0.9908	0.0007	199.9760	0.2096
aclp12.out	1.0000	0.0007	0.9911	0.0007	34.8740	0.1702	0.9889	0.0008	202.2960	0.1727
aclp13.out	1.0000	0.0010	0.9922	0.0007	34.5220	0.1963	0.9906	0.0009	200.3490	0.2013
acp13a.out	1.0000	0.0010	0.9901	0.0008	34.5020	0.1979	0.9884	0.0007	200.2550	0.2031
aclp14.out	1.0001	0.0010	0.9905	0.0007	34.4720	0.2005	0.9891	0.0009	200.1840	0.2045
aclp15.out	0.9998	0.0016	0.9881	0.0008	34.4020	0.2057	0.9823	0.0007	199.8980	0.2102
aclp16.out	1.0001	0.0006	0.9860	0.0007	34.8250	0.1737	0.9841	0.0007	202.0010	0.1769
aclp17.out	1.0007	0.0019	0.9897	0.0007	34.3970	0.2061	0.9874	0.0007	199.9490	0.2097
aclp18.out	1.0002	0.0011	0.9869	0.0007	34.8410	0.1728	0.9859	0.0008	202.0310	0.1759
aclp19.out	1.0002	0.0010	0.9910	0.0007	34.4010	0.2052	0.9888	0.0006	199.9530	0.2096
aclp20.out	1.0003	0.0011	0.9889	0.0006	34.8410	0.1726	0.9869	0.0008	202.0440	0.1758
aclp21.out	0.9997	0.0013	0.9868	0.0008	35.1290	0.1544	0.9854	0.0007	203.3850	0.1570

a) Values from Reference 3, Table 6, p. 42. Generally obtained from Tables 8 and 9 of Reference 8; acp11 series of values not documented in Reference 3.

b) From Reference 3, Table 9, p. 61 for 44 group cross-sections. Table 7 in this reference has values for 238 group cross-sections.

6.11.10.1.4. *Critical Experiments Supporting Underwater Storage of Tightly Packed Configurations of Spent Fuel Pins*

References:

9. FANP Doc. 32-5012897-00, "Validation Report – SCALEPC-44A Consolidation Experiments," R.S. Harding
10. "Critical Experiments Supporting Underwater Storage of Tightly Packed Configurations of Spent Fuel Pins," G.S. Hoovler, et.al., BAW-1645-4, November, 1981.

Reference 9 uses the experimental data from Reference 10 to construct benchmark cases for SCALE 4.4a. Table 6-51 Tightly Packed Configuration Experiment Summary[a] summarizes the experimental configuration data that form the basis for the KENO V.a models. Table 6-52 Tightly Packed Configuration Experiment Trending Data provides trending parameters for this set of experiments. Table 6-53 Tightly Packed Configuration Experiment k_{eff} Data provides the experimental and calculated results for the 44 and 238 group SCALE 4.4a cross-section sets from Reference 3.

Table 6-51 Tightly Packed Configuration Experiment Summary[a]

U-235 wt%	2.459	Fuel Volume, cm^3	0.833229
Pellet Density[b], g/cm^3	10.233	Pitch, cm	Vh20/Ffuel
U-235 atom density[c]	5.7075E-04	1.2093	0.149022
Pellet OD, cm	1.0300	1.2090	0.383292
Rod ID, cm	1.0440	1.4097	1.014058
Rod OD, cm	1.2060		
Clad Material	Al		

a) From Reference 9.
b) Based upon rod mass and fuel volume in rod, note this is the same 2.459 wt% fuel used in the previous 2 benchmark cases. The difference in densities has not been discussed.
c) Calculated values based upon Avogadro's number of 0.6022142E-24.

Table 6-52 Tightly Packed Configuration Experiment Trending Data

Case ID	Rod Pitch[a], cm	Lattice[a]	Cluster Spacing[a], cm	Temp[a], °C	Boron[a], ppm	Boron Factor[b]	Water density[b]	V_{h2o}/V_{fuel}[c]	H atom density[c]	H/U[c]
rcon01.out	1.2093	15x17 tria[d]	1.778x1.945	22.5	435	0.999451	0.99767	0.1490	0.066681	17.41
rcon02.out	1.2093	15x17 tria	1.778x1.945	23.5	426	0.999214	0.99742	0.1490	0.066648	17.40
rcon03.out	1.2093	15x17 tria	1.778x1.945	24.0	406	0.999091	0.99730	0.1490	0.066632	17.40
rcon04.out	1.2093	15x17 tria	1.778x1.945	22.5	383	0.999451	0.99767	0.1490	0.066681	17.41
rcon05.out	1.2093	15x17 tria	1.778x1.945	23.0	354	0.999334	0.99754	0.1490	0.066665	17.41
rcon06.out	1.2093	15x17 tria	1.778x1.945	23.0	335	0.999334	0.99754	0.1490	0.066665	17.41
rcon07.out	1.2093	15x17 tria	2.539x2.709	20.0	361	1.000000	0.99821	0.1490	0.066754	17.43
rcon09.out	1.2090	15x15 sq	1.7780	21.0	886	0.999788	0.99799	0.3833	0.066725	44.81
rcon10.out	1.2090	15x15 sq	1.7780	21.0	871	0.999788	0.99799	0.3833	0.066725	44.81
rcon11.out	1.2090	15x15 sq	1.7780	22.0	852	0.999566	0.99777	0.3833	0.066695	44.79
rcon12.out	1.2090	15x15 sq	1.7780	21.0	834	0.999788	0.99799	0.3833	0.066725	44.81
rcon13.out	1.2090	15x15 sq	1.7780	21.0	815	0.999788	0.99799	0.3833	0.066725	44.81
rcon14.out	1.2090	15x15 sq	1.7780	22.0	781	0.999566	0.99777	0.3833	0.066695	44.79
rcon15.out	1.2090	15x15 sq	1.7780	22.0	746	0.999566	0.99777	0.3833	0.066695	44.79
rcon16.out	1.4097	13x13 sq	1.7920	22.5	1156	0.999451	0.99767	1.0141	0.066681	118.47
rcon17.out	1.4097	13x13 sq	1.7920	22.5	1141	0.999451	0.99767	1.0141	0.066681	118.47
rcon18.out	1.4097	13x13 sq	1.7920	23.0	1123	0.999334	0.99754	1.0141	0.066665	118.44
rcon19.out	1.4097	13x13 sq	1.7920	23.0	1107	0.999334	0.99754	1.0141	0.066665	118.44
rcon20.out	1.4097	13x13 sq	1.7920	23.0	1093	0.999334	0.99754	1.0141	0.066665	118.44
rcon21.out	1.4097	13x13 sq	1.7920	23.0	1068	0.999334	0.99754	1.0141	0.066665	118.44
rcon28.out	1.4097	15x17 tria	3.807x2.976	18.5	121	1.000298	0.99850	1.0141	0.066793	17.44

a) Reference 9.

b) Boron factors to correct water density from 25 °C to 20 °C. Boron ppm is based upon 25 °C measurements. See Reference 10, Table 3.0-1, p. 46. Water density from standard tables.

c) Calculated values based upon Avogadro's number of 0.6022142E-24.

d) Triangular pitch for array.

Table 6-53 Tightly Packed Configuration Experiment keff Data

Case ID	Experimental k_{eff} and σ		SCALE 4.4a 44 Group Cross-Section Calculated k_{eff} and σ				SCALE 4.4a 238 Group Cross-Section Calculated k_{eff} and σ			
	k_{eff}^{a}	$σ^{a}$	k_{eff}^{b}	$σ^{b}$	AFG^{b}	$EALF^{b}$ (ev)	k_{eff}^{b}	$σ^{b}$	AFG^{b}	$EALF^{b}$ (ev)
rcon01.out	1.0007	0.0006	0.9999	0.0008	28.9400	2.4011	0.9910	0.0007	170.1330	2.4368
rcon02.out	1.0007	0.0006	1.0009	0.0007	28.9020	2.4444	0.9909	0.0008	169.9770	2.4688
rcon03.out	1.0007	0.0006	0.9973	0.0008	28.8680	2.4872	0.9882	0.0007	169.6020	2.5454
rcon04.out	1.0007	0.0006	1.0008	0.0007	28.8990	2.4644	0.9899	0.0007	169.6960	2.5284
rcon05.out	1.0007	0.0006	0.9995	0.0008	28.8970	2.4706	0.9899	0.0008	169.6200	2.5435
rcon06.out	1.0007	0.0006	0.9980	0.0007	28.8900	2.4915	0.9906	0.0008	169.5520	2.5553
rcon07.out	1.0007	0.0006	0.9982	0.0008	29.8910	1.6259	0.9904	0.0008	175.2760	1.6431
rcon09.out	1.0007	0.0006	0.9977	0.0006	29.8930	1.4607	1.0092	0.0007	180.0400	1.1271
rcon10.out	1.0007	0.0006	0.9966	0.0008	29.8760	1.4759	0.9884	0.0006	176.1470	1.4891
rcon11.out	1.0007	0.0006	0.9959	0.0007	29.8450	1.4982	0.9909	0.0008	176.1150	1.4922
rcon12.out	1.0007	0.0006	0.9980	0.0008	29.8490	1.4979	0.9876	0.0007	175.8550	1.5240
rcon13.out	1.0007	0.0006	0.9969	0.0007	29.8430	1.5074	0.9897	0.0007	175.8220	1.5280
rcon14.out	1.0007	0.0006	0.9963	0.0007	29.8310	1.5207	0.9894	0.0007	175.7230	1.5402
rcon15.out	1.0007	0.0006	0.9975	0.0008	29.8450	1.5180	0.9915	0.0007	175.7200	1.5399
rcon16.out	1.0007	0.0006	0.9948	0.0007	32.7100	0.4216	0.9892	0.0007	175.7140	1.5415
rcon17.out	1.0007	0.0006	0.9952	0.0006	32.6820	0.4276	0.9894	0.0006	191.3680	0.4309
rcon18.out	1.0007	0.0006	0.9939	0.0006	32.6400	0.4370	0.9909	0.0007	191.2180	0.4360
rcon19.out	1.0007	0.0006	0.9965	0.0006	32.6540	0.4344	0.9897	0.0007	191.0430	0.4426
rcon20.out	1.0007	0.0006	0.9967	0.0007	32.6370	0.4391	0.9915	0.0007	190.9880	0.4447
rcon21.out	1.0007	0.0006	0.9959	0.0008	32.6220	0.4427	0.9903	0.0007	190.8780	0.4485
rcon28.out	1.0007	0.0006	0.9968	0.0008	31.0790	1.0062	0.9915	0.0008	190.7670	0.4529

a) Values from Reference 3, Table 6, p. 42. Source of value not documented in this reference.

b) From Reference 3, Table 9, p. 61 for 44 group cross-sections. Table 7 in this reference has values for 238 group cross-sections

6.11.10.1.5. *Reduced Density Moderation Between Fuel Clusters with 4.738 Wt% Fuel*

References:

11. FANP Doc. 32-5012894-00, “Validation Report – SCALEPC-44A Dissolution Experiments,” R.S. Harding.
12. “Dissolution and Storage Experimental Program with U[4.75]O_2 Rods,” Transactions of the American Nuclear Society, Vol. 33, pg. 362.

Reference 11 uses the experimental data from Reference 12 to construct benchmark cases for SCALE 4.4a. Table 6-54 Reduced Density Moderation Experiments Summary and Trending Parameters[a] summarizes the experimental configuration data that form the basis for the KENO V.a models and provides trending parameters that are constant for the series of experiments. Table 6-55 Reduced Density Moderation Experiments Trending Data and k_{eff} Data provides trending parameters for this set of experiments. It also provides the experimental and calculated results for the 44 and 238 group SCALE 4.4a cross-section sets from Reference 3.

Table 6-54 Reduced Density Moderation Experiments Summary and Trending Parameters[a]

U-235 wt%	4.738	Temperature, ^oC	22
Pellet Density, g/cm^3	10.38	Water density, g/cm^3	0.99777
Pellet OD, cm	0.7900	Fuel Volume, cm^3	0.49017
Rod ID, cm	0.8200	Water Volume, cm^3	1.12852
Rod OD, cm	0.9400	V_{h2o}/V_{fuel}	2.30232
Rod Pitch, cm	1.3500	U-235 atom density[b]	1.1155E-03
Clad Material	Al alloy	H atom density[b]	0.066676
Lattice	18x18	H/U	1.3761E+02

a) From Reference 11.

b) Calculated values based upon Avogadro’s number of 0.6022142E-24.

Table 6-55 Reduced Density Moderation Experiments Trending Data and k_{eff} Data

Case ID	Cluster Spacing[a], cm	Spacing Material[a] [Material (density)]	Experimental k_{eff} and σ		SCALE 4.4a 44 Group Cross-Section Calculated k_{eff} and σ				SCALE 4.4a 238 Group Cross-Section Calculated k_{eff} and σ			
			k_{eff}[b]	σ[b]	k_{eff}[c]	σ[c]	AFG[c]	EALF[c] (ev)	k_{eff}[c]	σ[c]	AFG[c]	EALF[c] (ev)
mdis01.out	0.0	-	1.0000	0.0014	0.9914	0.0008	33.5390	0.2824	0.9885	0.0010	195.994	0.2879
mdis02.out	2.5	H2O	1.0000	0.0014	0.9871	0.0009	33.6720	0.2644	0.9862	0.0008	196.836	0.2685
mdis03.out	2.5	Air/Box	1.0000	0.0014	0.9841	0.0011	33.6720	0.2647	0.9805	0.0008	196.750	0.2702
mdis04.out	2.5	Polystr(0.0323)/Box	1.0000	0.0014	0.9902	0.0008	33.8040	0.2514	0.9884	0.0008	197.439	0.2559
mdis05.out	2.5	Polyeth(0.2879)/Box	1.0000	0.0014	0.9908	0.0010	33.9160	0.2407	0.9891	0.0009	198.001	0.2442
mdis06.out	2.5	Polyeth(0.5540)/Box	1.0000	0.0014	1.0008	0.0010	34.0370	0.2295	0.9963	0.0008	198.539	0.2344
mdis07.out	2.5	H2O/Box	1.0000	0.0014	0.9917	0.0009	34.1100	0.2242	0.9886	0.0008	198.827	0.2288
mdis08.out	5.0	H2O	1.0000	0.0014	0.9873	0.0010	33.8000	0.2497	0.9840	0.0009	197.504	0.2545
mdis09.out	5.0	Air/Box	1.0000	0.0014	0.9869	0.0010	33.8110	0.2485	0.9861	0.0009	197.586	0.2524
mdis10.out	5.0	Polystr(0.0323)/Box	1.0000	0.0014	0.9938	0.0008	34.0940	0.2225	0.9912	0.0008	198.934	0.2267
mdis11.out	5.0	Polyeth(0.2879)/Box	1.0000	0.0014	1.0031	0.0010	34.3010	0.2048	0.9997	0.0008	200.018	0.2076
mdis12.out	5.0	Polyeth(0.0.5540)/Box	1.0000	0.0014	-	-	-	-	1.0027	0.0009	200.577	0.1984
mdis13.out	5.0	H2O/Box	1.0000	0.0014	0.9907	0.0008	34.4280	0.1951	0.9878	0.0008	200.547	0.1988
mdis14.out	10.0	H2O	1.0000	0.0014	0.9890	0.0008	33.9850	0.2294	0.9854	0.0009	198.552	0.2333
mdis15.out	10.0	Air/Box	1.0000	0.0014	0.9894	0.0009	34.0150	0.2266	0.9842	0.0008	198.647	0.2315
mdis16.out	10.0	Polystr(0.0323)/Box	1.0000	0.0014	1.0013	0.0008	34.4450	0.1907	0.9970	0.0009	200.792	0.1948
mdis17.out	10.0	Polyeth(0.2879)/Box	1.0000	0.0014	0.9985	0.0008	34.5970	0.1788	0.9951	0.0009	201.537	0.1831
mdis18.out	10.0	Polyeth(0.0.5540)/Box	1.0000	0.0014	0.9965	0.0008	34.6430	0.1740	0.9923	0.0009	201.894	0.1774
mdis19.out	10.0	H2O/Box	1.0000	0.0014	0.9931	0.0009	34.6530	0.1737	0.9888	0.0008	201.908	0.1772

a) References 11 and 12.

b) Values from Reference 3, Table 6, p. 42. Source of value not documented in this reference.

c) From Reference 3, Table 9, p. 61 for 44 group cross-sections. Table 7 in this reference has values for 238 group cross-sections

6.12. APPENDIX B: 11X11 FUEL ASSEMBLY CRITICALITY ANALYSIS (≤ 5.0 WT.% ^{235}U)

Appendix B documents the criticality analysis of the TN-B1 package with a payload of two 11x11 fuel assemblies at ≤ 5.0 wt.% ^{235}U enrichment. Appendix B also documents the criticality analysis for up to 25 11x11 loose rods or up to 30 11x11 rods in a 5-in stainless steel pipe. The format of Appendix B follows the same general outline of the main body of the report and references the main body of the report for information common to both analyses.

The 11x11 fuel assembly criticality analysis is performed using SCALE 6.1.3 (Reference 15), while the analysis for the 8x8, 9x9, and 10x10 was performed using SCALE 4.4a (Reference 8). SCALE 6.1.3 is used for the 11x11 fuel assembly analysis to take advantage of the ENDF/B-VII cross section data and resonance cross section processing using CENTRM. In addition, SCALE 6.1.3 allows fuel resonance parameters to be computed separately for fuel rods with and without gadolinia without the use of the MORE DATA card, which simplifies input preparation. Benchmarking for SCALE 6.1.3 is documented in Section 6.12.9, *Benchmark Evaluation for SCALE 6.1.3*. A USL of 0.94094 is justified for the 11x11 fuel assembly analysis, and a USL of 0.94047 is justified for the 11x11 fuel rod analysis.

The evaluation and discussion in Sections 6.12.3 through 6.12.6 consider a fuel channel thickness up to 0.254 cm for the 11x11 fuel assemblies and remains applicable for the conditions considered. Section 6.12.11 extends the criticality analysis for 11x11 fuel assemblies with a fuel channel thickness up to 0.320 cm. The full list of additional criteria evaluated for the 11x11 fuel assemblies is provided in Section 6.12.11.

6.12.1. *Description of the Criticality Design*

6.12.1.1. Design Features

Refer to Section 6.1.1, *Design Features*, for a description of the design features of the package.

A criticality safety analysis is performed to demonstrate the TN-B1 shipping container safety for the 11x11 fuel assembly and associated rods when detached from the fuel assembly. The TN-B1 meets applicable IAEA and 10 CFR 71 requirements for a Type B fissile material-shipping container, transporting heterogeneous UO_2 enriched to a maximum of 5.00 wt. percent U-235.

Water exclusion from the inner container is not required for this package design. The inner container is analyzed in both undamaged and damaged package arrays under optimal moderation conditions and is demonstrated to be safe under Normal Conditions of Transport (NCT) and Hypothetical Accident Condition (HAC) testing.

Sensitivity analyses are performed by varying fuel parameters (rod pitch, clad ID, clad OD, pellet OD, fuel orientation, polyethylene quantity, and moderator density) to obtain the most reactive configuration.

Table 6-56 TN-B1 11x11 Fuel Assembly General Loading Criteria summarizes the general fuel loading criteria for the TN-B1 shipping container for 11x11 fuel. Table 6-57 TN-B1 11x11 Fuel Assembly Gadolinia Loading Criteria summarizes the gadolinia loading requirements for 11x11 fuel assemblies. The gadolinia loading requirements are provided as a minimum number of 2.0 wt.% gadolinia-urania rods required per lattice. Required gadolinia-urania rods shall be distributed symmetrically about the major diagonal and shall not be placed on the periphery.

Plastic inserts may optionally be used between fuel rods at various locations along the axis of the fuel assembly to avoid stressing the axial grids during transportation. An example of a plastic insert is shown in Figure 6-1 Polyethylene Insert (FANP Design). The option for plastic inserts is bounded by allowing up to 10.2 kg of polyethylene equivalent mass per fuel assembly. In addition to the inserts, the polyethylene equivalent mass also includes all polyethylene/plastic components within the inner compartment, excluding the foam liner. Polyethylene equivalent mass is defined in Section 6.3.2.2.

Cylindrical fuel rods containing UO_2, enriched to 5 wt. percent U-235, are analyzed within the TN-B1 inner container in a 5-inch stainless steel pipe (which bounds fuel rods in a protective case), or loose within the cavity (which bounds fuel rods bundled together). No gadolinia credit is taken in the fuel rod analysis. Only bare pellet columns (i.e., no cladding) are conservatively modeled. The fuel rod loading criteria are provided in Table 6-58 TN-B1 11x11 Fuel Rod Loading Criteria.

Table 6-56 TN-B1 11x11 Fuel Assembly General Loading Criteria

Parameter	Units	Value
UO_2 Density[c]	g/cm^3	≤ 10.763
Number of water rods	#	3x3 center
Number of fuel rods	#	112
Fuel Rod OD	cm	≥ 0.930
Fuel Pellet OD	cm	≤ 0.820
Cladding Type		Zirconium Alloy
Cladding ID	cm	≤ 0.840
Cladding Thickness	cm	≥ 0.045
Fuel Rod Pitch[a]	cm	≤ 1.195
U-235 Pellet Enrichment	wt%	≤ 5.0
Maximum Lattice Average Enrichment	wt%	≤ 5.0
Fuel Channel Side Thickness[b]	cm	≤ 0.320
Full Length Fuel Rods Quantity Active length	 # cm	 92 ≤ 385
Short Part Length Fuel Rods Quantity Active length	 # cm	 12 ≤ 155.1
Long Part Length Fuel Rods Quantity Active length	 # cm	 8 ≤ 236.8

a. Equivalent nominal pitch per Section 6.12.3.1.1.
b. Transport with or without channels is acceptable.
c. Density based on a pellet modeled as a right cylinder.

Table 6-57 TN-B1 11x11 Fuel Assembly Gadolinia Loading Criteria

Parameter	Units	Type
Gadolinia Requirements		
Lattice Average Enrichment[a]		
≤ 5.0 wt % U-235	# @ wt% Gd_2O_3	13 @ 2 wt %
≤ 4.8 wt % U-235		12 @ 2 wt %
≤ 4.6 wt % U-235		11 @ 2 wt %
≤ 4.4 wt % U-235		10 @ 2 wt %
≤ 4.2 wt % U-235		9 @ 2 wt %
≤ 4.1 wt % U-235		8 @ 2 wt %
≤ 3.9 wt % U-235		7 @ 2 wt %
≤ 3.8 wt % U-235		6 @ 2 wt %
≤ 3.6 wt % U-235		5 @ 2 wt %
≤ 3.5 wt % U-235		4 @ 2 wt %
≤ 3.3 wt % U-235		3 @ 2 wt %
≤ 3.2 wt % U-235		2 @ 2 wt %
≤ 2.9 wt % U-235		None
Polyethylene Equivalent Mass (Maximum per Assembly)[b]	kg	10.2

a. Required gadolinia rods shall be distributed symmetrically about the major diagonal and shall not be placed on the periphery.

b. Polyethylene equivalent mass (refer to Section 6.3.2.2)

Table 6-58 TN-B1 11x11 Fuel Rod Loading Criteria

Parameter	Units	Type
UO_2 Density[a]	g/cm³	≤ 10.763
Fuel Rod OD	cm	≥ 0.930
Fuel Pellet OD	cm	≤ 0.820
Cladding Type		Zirc. Alloy
Cladding ID	cm	≤ 0.930
Cladding Thickness	cm	≥ 0.00
Active Fuel Length	cm	≤ 385
Maximum U-235 Pellet Enrichment	wt.%	≤ 5.0
Maximum Average Fuel Rod Enrichment	wt.%	≤ 5.0
Rods loose in cavity (or bundled)	#	≤ 25 (50 per package)
Rods in pipe component (or protective case)	#	≤ 30 (60 per package)

a. Density based on a pellet modeled as a right cylinder.

6.12.1.2. Summary Table of Criticality Evaluation

The following configurations are allowed for transport in the TN-B1:

- Up to two 11x11 fuel assemblies
- Up to 25 11x11 fuel rods loose within each package cavity (50 rods per package). This configuration bounds 25 fuel rods bundled together.
- Up to 30 11x11 fuel rods contained within a 5-in stainless steel pipe within each package cavity (up to 60 rods per package). This configuration bounds the stainless steel protective case, which has a smaller cross sectional area than the stainless steel pipe component.

Calculations are performed for the NCT and HAC single package, NCT array, and HAC array. Water moderation is allowed for both NCT and HAC cases. The limiting HAC array size is 10x1x7 (70 packages) and the limiting NCT array size is 12x2x10 (240 packages). The most reactive results are summarized in Table 6-59 Criticality Evaluation Summary for 11x11 Fuel Assemblies and Rods. Note that because the NCT single package case is flooded, it meets the requirements of 71.55(b).

Table 6-59 Criticality Evaluation Summary for 11x11 Fuel Assemblies and Rods

Case	Bounding Fuel Type	k_{eff}	σ	k_{eff} + 2σ	USL
Fuel Assembly Single Package NCT	11x11 with worst-case fuel parameters, 13-2.0 wt% Gd_2O_3 fuel rods	0.64510	0.00046	0.65302	0.94094
Fuel Assembly Single Package HAC	11x11 with worst-case fuel parameters, 13/13/3-2.0 wt% Gd_2O_3 fuel rods [a]	0.79328	0.00047	0.80122	0.94094
Fuel Assembly Package Array NCT	11x11 with worst-case fuel parameters, 13/13/3-2.0 wt% Gd_2O_3 fuel rods [a]	0.92829	0.00044	0.93417	0.94094
Fuel Assembly Package Array HAC	11x11 with worst-case fuel parameters, 13-2.0 wt% Gd_2O_3 fuel rods	0.93155	0.00032	0.93819	0.94094
Fuel Rod Single Package NCT	30 fuel rods in stainless steel pipe (2 per container) with worst-case fuel parameters [b]	0.59145	0.00045	0.59735	0.94047
Fuel Rod Single Package HAC	30 fuel rods in stainless steel pipe (2 per container) with worst-case fuel parameters [b]	0.66316	0.00042	0.67000	0.94047
Fuel Rod Package Array NCT	30 fuel rods in stainless steel pipe (2 per container) with worst-case fuel parameters [b]	0.80006	0.00046	0.80598	0.94047
Fuel Rod Package Array HAC	30 fuel rods in stainless steel pipe (2 per container) with worst-case fuel parameters [b]	0.81947	0.00044	0.82635	0.94047

a. This configuration contains 13-2.0wt% Gd_2O_3 fuel rods in the bottom and middle axial regions and 3-2.0 wt% Gd_2O_3 fuel rods in the top axial region.
b. This configuration bounds the 25 loose fuel rod configuration.

6.12.1.3. Criticality Safety Index

Undamaged packages have been analyzed in 12x2x10 arrays and damaged packages have been analyzed in 10x1x7 arrays. Pursuant to 10 CFR 71.59, the number of packages "N" in a 2N array that are subjected to the tests specified in 10 CFR 71.73, or in a 5N array for undamaged packages is used to determine the Criticality Safety Index (CSI). The CSI is determined by dividing the number 50 by the most limiting value of "N" as specified in 10 CFR 71.59.

The TN-B1 criticality analysis demonstrates safety for 5N=240 (undamaged) and 2N=70 (damaged) packages. The corresponding CSI for criticality control is given by CSI = 50/N. Since 5N=240 and 2N = 70, it follows that the more restrictive N = 35 and CSI = 50/35 = 1.5. Therefore, the maximum allowable number of packages per shipment is 50/1.5 = 33.

Note that the NCT array size is significantly larger than the array size needed to justify a CSI of 1.0 (5N = 250 minimum). The large NCT array size is selected to be consistent with the NCT array size utilized in the 8x8, 9x9, and 10x10 fuel assembly analysis.

6.12.2. *Fissile Material Contents*

The following fissile material contents are allowed for transport in the TN-B1:

- Up to two 11x11 fuel assemblies
- Up to 25 11x11 fuel rods loose within each package cavity (50 rods per package). This configuration bounds 25 fuel rods bundled together.
- Up to 30 11x11 fuel rods contained within a 5-in stainless steel pipe component within each package cavity (up to 60 rods per package). This configuration bounds the stainless steel protective case, which has a smaller cross sectional area than the stainless steel pipe component.

Details of the 11x11 fuel assembly and loose rods are defined in Table 6-56 TN-B1 11x11 Fuel Assembly General Loading Criteria, Table 6-57 TN-B1 11x11 Fuel Assembly Gadolinia Loading Criteria, and Table 6-58 TN-B1 11x11 Fuel Rod Loading Criteria.

6.12.3. *General Considerations*

6.12.3.1. Model Configuration

6.12.3.1.1. *Fuel Assembly Model*

Details of the development of the bounding fuel assembly model are provided in Section 6.12.3.5, *Parameter Selection for 11x11 Fuel Assembly Model*. Following is a summary of the bounding fuel assembly. The bounding fuel assembly has the following parameters:

- NCT: pitch = 1.195 cm, HAC: pitch = 1.2548 cm (5% pitch expansion)
- NCT: dry pellet/cladding gap, HAC: wet pellet/cladding gap
- NCT/HAC: pellet density = 10.763 g/cm^3
- NCT/HAC: pellet diameter = 0.820 cm
- NCT/HAC: cladding outer diameter = 0.930 cm
- NCT/HAC: cladding inner diameter = 0.840 cm
- NCT/HAC: 10.2 kg of polyethylene equivalent mass per fuel assembly. The polyethylene equivalent mass includes all polyethylene/plastic components within the inner compartment, excluding the foam liner.
- NCT/HAC (single package): 5% enrichment with 13 gadolinia-urania rods per lattice with the loading pattern as shown on Figure 6-52 Bounding Fuel Assembly Model.
- HAC (package array): 5% enrichment with 13 gadolinia-urania rods in the bottom and middle axial regions and 3.3% enrichment with 3 gadolinia-urania rods per lattice in the top region with the loading pattern as shown on Figure 6-52 Bounding Fuel Assembly Model.

- NCT/HAC: Zirconium water channel (i.e., the zirconium channel in the center of the fuel assembly) modeled as water
- NCT/HAC: Models developed with and without the zirconium fuel channel. A range of thicknesses is examined (0 to 0.254 cm).

The 11x11 fuel assembly has variable rod pitch, with the upper section of the assembly having a constant 1.195 cm nominal pitch and the lower section of the assembly having rods at varying pitches (see Reference 20). Both sections have the same total distance across the assembly. The variation from the nominal pitch in the lower region is very small, <1 mm. Since the overall envelope of the fuel region is unchanged, the H/U-235 ratio for this region is the same as a region which is fully rodded (i.e., no water spaces from partial length rods). As such, no reactivity change is anticipated for this region and the pitch throughout the entire assembly is modeled with an equivalent nominal pitch of 1.195 cm in the NCT models.

In the HAC models, the fuel assembly is modeled with a 5% expanded pitch. The average pitch expansion determined analytically using an LS-Dyna model is 2.6% (Reference 19). The expansion of the outside perimeter of the fuel assembly determined analytically using an LS-Dyna model is 3.4% (Reference 19). The pitch expansion modeled bounds the LS-Dyna computed pitch expansion. The 5% pitch expansion also bounds the 4.1% pitch expansion experimentally determined by drop testing an FANP 10x10 fuel assembly (Reference 1).

The 11x11 fuel assembly has three distinct axial regions (lattices) due to the presence of long and short partial-length rods. There are 92 full-length rods, 8 long partial-length rods, and 12 short partial-length rods. In the center of the fuel assembly is a 3x3 water hole. The bottom lattice has 92+8+12 = 112 rods, the middle lattice has 92+8 = 100 rods, and the top lattice has 92 rods. The loading pattern of the three rod types is depicted in Figure 6-51 Position of Fuel Rods in 11x11 Assembly.

The fuel rod lengths are modeled conservatively. The length of the partial length fuel rods is increased by 9.2 cm to account for upper and lower plenum regions and for additional conservatism. An additional 4 cm is conservatively added to the length of all fuel rods. This results in modeled lengths of 155.1 cm, 236.8 cm, and 385 cm for the short partial-length rods, long partial-length rods and full-length rods, respectively. All fuel is modeled such that the bottom of the fuel column for all rod types is even with each other.

No fuel assembly structures outside the active region of the assembly are represented in the models. The neglected structures are composed of materials that absorb neutrons by radiative capture; therefore, not considering these structures in the analysis is conservative. In addition, no grids are represented within the rod active length. The internal grid structure displaces water from between the fuel rods, decreasing moderation. Because the fuel assemblies are undermoderated, decreasing the moderation decreases system reactivity. Therefore, it is conservative to neglect the internal grid structure in the TN-B1 container analysis.

Some fuel rods contain gadolinia to hold-down the reactivity. The minimum allowed gadolinia loading is 2 wt.%. In the KENO models, only 75% credit is taken for the gadolinia. The number of gadolinia-urania rods required is a function of the lattice average enrichment. Gadolinium may be present in the full-length and/or partial-length rods. For any given fuel assembly, the number of gadolinia-urania rods in each lattice is a constant, although the pattern may vary from lattice to lattice. The most reactive gadolinia-urania rod pattern is independently determined for each lattice within a fuel assembly.

The gadolinia-urania rod patterns are developed using the following rules: (1) the gadolinia-urania rods shall be symmetric about the major diagonal, and (2) gadolinia-urania rods shall not be placed on the periphery. For the NCT models and for the HAC single package, the final gadolinia-urania loading pattern for each of the three lattices for the bounding fuel assembly (5 wt.% enrichment, 13 gadolinia-urania rods per lattice) is illustrated in Figure 6-52 Bounding Fuel Assembly Model. For the HAC package array, the final gadolinia-urania loading pattern for each of the three lattices for the bounding fuel assembly (5 wt.% enrichment, 13 gadolinia-urania rods in the bottom and middle lattices and 3.3 wt.% enrichment, 3 gadolinia-urania rods in the top lattice) is also illustrated in Figure 6-52 Bounding Fuel Assembly Model. The bounding enrichment and gadolinia-urania loading pattern is developed in Section 6.12.3.5, Parameter Selection for 11x11 Fuel Assembly Model.

Each fuel assembly may contain up to 10.2 kg of polyethylene equivalent mass, as defined in Section 6.3.2.2. In the NCT models, 10.2 kg of polyethylene is homogenized with the water inside the fuel assembly boundary. In the HAC models, the polyethylene is modeled in two configurations: (1) homogenized with the cladding (which approximates polyethylene melted onto the cladding), and (2) homogenized with the water inside the fuel assembly boundary. The 10.2 kg of polyethylene equivalent mass does not include the polyethylene liner foam, which is treated separately.

6.12.3.1.2. *Single Package NCT Model with 11x11 Fuel*

The geometrical parameters of the single package NCT models are the same as defined in Section 6.3.1.1.1, *Single Package Normal Conditions of Transport Model*. Refer to that section for detailed information about the packaging dimensions. Key dimensions of the NCT single package model are also illustrated on Figure 6-3 TN-B1 Outer Container Normal Conditions of Transport Model, Figure 6-4 TN-B1 Inner Container Normal Conditions of Transport Model, and Figure 6-5 TN-B1 Container Cross-Section Normal Conditions of Transport Model.

The fuel is modeled with or without fuel channels, which extend axially along the active fuel length. The polyethylene liner foam is modeled in close contact with the fuel assembly, and the fuel assembly is centered within each compartment. The foam has a nominal density of 4 pounds per cubic feet (pcf), although small strips of 9 pcf foam may be used under the grid spacers to provide extra support. The foam is conservatively modeled with a density of 5 pcf on the sides and top and 10 pcf on the bottom. Modeling 10 pcf foam across the entire bottom bounds the actual density.

In the NCT single package models, full-density water is modeled between the inner and outer containers to maximize reflection, and the entire package is reflected with 30.48 cm of water.

Note that the single package NCT case with full flooding meets the requirements of 71.55(b).

6.12.3.1.3. *Single Package HAC Model with 11x11 Fuel*

The geometrical parameters of the single package HAC models are the same as defined in Section *6.3.1.1.2*, *Single Package Hypothetical Accident Condition Model*. Refer to that section for detailed information about the packaging dimensions, which include damage from drop testing. Key dimensions of the HAC single package model are also illustrated on Figure 6-6 TN-B1 Outer Container Hypothetical Accident Condition Model, Figure 6-7 TN-B1 Inner Container Hypothetical Accident Condition Model, and Figure 6-8 TN-B1 Cross-Section Hypothetical Accident Condition Model.

The fuel is modeled with or without fuel channels, which extend axially along the active fuel length. The polyethylene foam liner is modeled as intact, partially burned, or totally burned to determine the most reactive condition. The burned foam is replaced with water. Fuel assemblies are also modeled in various orientations to determine the most reactive condition. Full-density water is modeled between the inner and outer containers to maximize reflection, and the entire package is reflected with 30.48 cm of water.

6.12.3.1.4. *NCT Array Model with 11x11 Fuel*

The NCT array model is similar to the NCT single package model. The NCT array size is selected to be 21x3x24 (1,512 packages) to be consistent with the original analysis documented in Section 6.3.1.2.1, *Package Array Normal Condition Model*. The minimum NCT array size needed to justify a CSI = 1.0 is only 250 packages, a significantly smaller number.

Per Regulatory Guide 7.9 (Reference 16), if a water spray test has demonstrated that water would not leak into the package, water inleakage need not be assumed for the NCT array analysis. While little or no water intrusion is expected as a result of the water spray test, because a water spray test has not been performed, water inleakage is assumed in the NCT array models. Consistent with the approach in Section 6.3.1.2.1, *Package Array Normal Condition Model*, in the NCT array cases, the water density is modeled at a constant value in all void spaces within the package. Cases are run in which the water density ranges from 0 to 1.0 g/cm^3. The entire package array is reflected with 30.48 cm of water.

6.12.3.1.5. *HAC Array Model with 11x11 Fuel*

The HAC array model is similar to the HAC single package model. The HAC array size is selected to be 10x1x10 (100 packages), consistent with a CSI = 1.0.

Potential burn scenarios of the polyethylene liner foam are investigated. As a result of a postulated fire, some or all of the foam may burn. In general, partial burn scenarios are the most reactive, and numerous partial burn scenarios are investigated. The most reactive assembly orientation is determined with and without the fuel channel.

In the HAC array analysis, the water density inside the inner container is allowed to vary independently from the water density between the inner and outer containers. The entire package array is reflected with 30.48 cm of water.

6.12.3.1.6. *11x11 Rod Models*

An analysis is also performed for 11x11 rods (i.e., rods that are not part of a fuel assembly). Two separate analyses are performed for 11x11 rods: (1) rods loose (or bundled) within the liner, and (2) rods contained within a 5-in stainless steel pipe or protective case.

Up to 25 loose rods are placed directly into each liner, or up to 50 loose rods per package. Loose rods may also be bundled together, as bundles of close-packed rods would be less reactive than rods that are allowed to achieve an optimum pitch. In this loose rod configuration, the pitch is varied until optimum moderation is achieved, see *Figure 6-53 Twenty-five 11x11 Fuel Rods in Liner*.

Up to 30 loose rods are placed in a 5-in schedule 40 stainless steel pipe (see General Arrangement Drawing 0028B98, *Shipping Container Loose Fuel Rods*). Two pipes may be placed in the package, for a total of 60 rods per package. The pipe itself is conservatively modeled as water. A pitch study is performed for rods in the pipe component, and a triangular pitch is used to better match the circular pipe boundary, see Figure 6-54 Thirty 11x11 Fuel Rods in Pipe Component. Studies are also performed for less than 30 rods in the pipe, and various moderation scenarios are investigated to determine the most reactive configuration.

The analysis of 30 rods in a pipe component bounds 30 rods in the protective case (see General Arrangement Drawing 105E3773, *RAJ-II Protective Case Licensing Drawing*). The pipe component has an inner diameter of 5.047-in, or an area of 20.0 in^2. The protective case has a cavity cross sectional area of 80 mm x 89 mm (3.15-in x 3.50-in), or an area of 11.0 in^2. Therefore, the pipe component has a significantly larger area than the protective case and allows greater pitch expansion and moderation. Therefore, the analysis of 30 rods in the pipe component bounds 30 rods in the protective case.

Each fuel rod is placed in a plastic sleeve 6-mil (0.006-in) thick, and this plastic sleeve is modeled explicitly around each fuel rod. In addition, the cladding is replaced with water to conservatively increase moderation. The pellet/cladding gap is also filled with water.

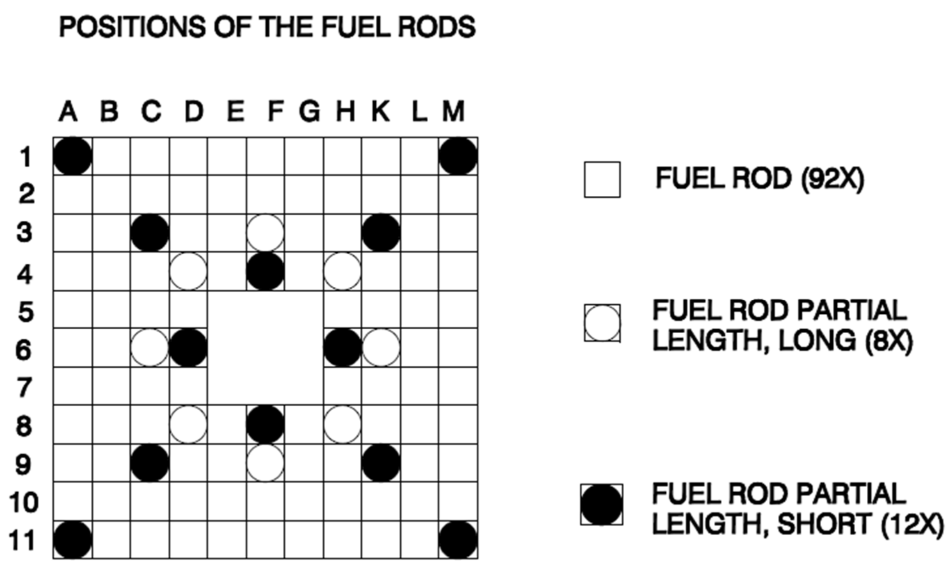

Figure 6-51 Position of Fuel Rods in 11x11 Assembly

Bottom Axial Layer (5 wt%, Full and Partial Length Rods)

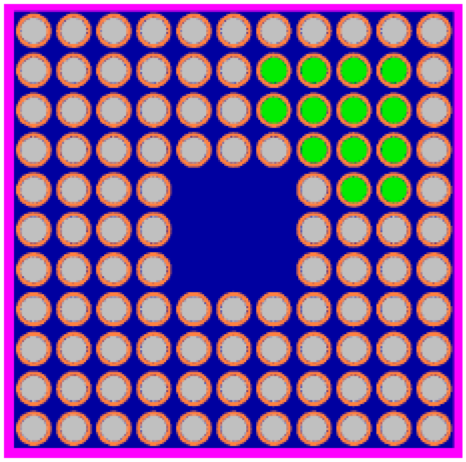

Middle Axial Layer (5 wt%, Full and Long Partial-Length Rods)

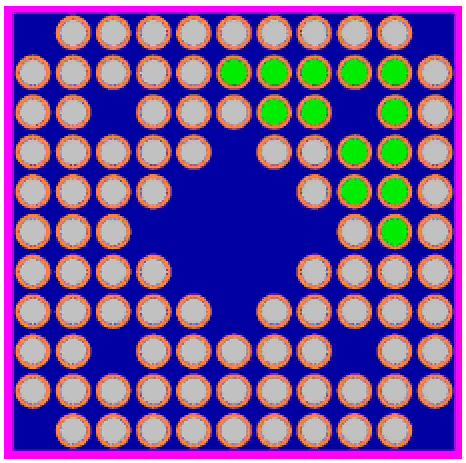

Top Axial Layer (Full-length Rods Only)

5 wt% (NCT, HAC single package)

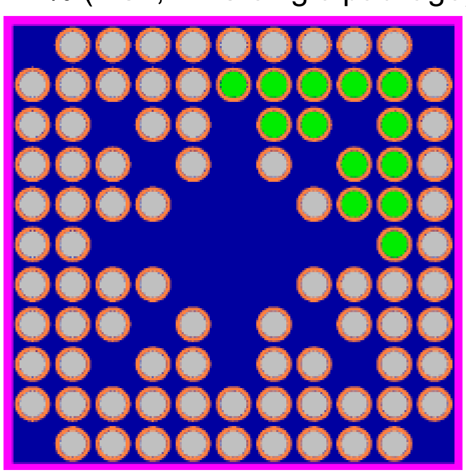

3.3 wt% (HAC package array)

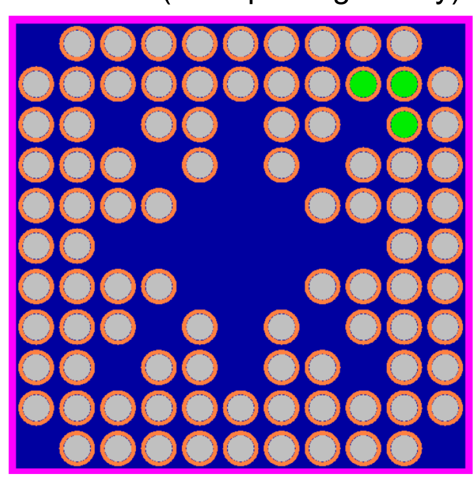

Figure 6-52 Bounding Fuel Assembly Model

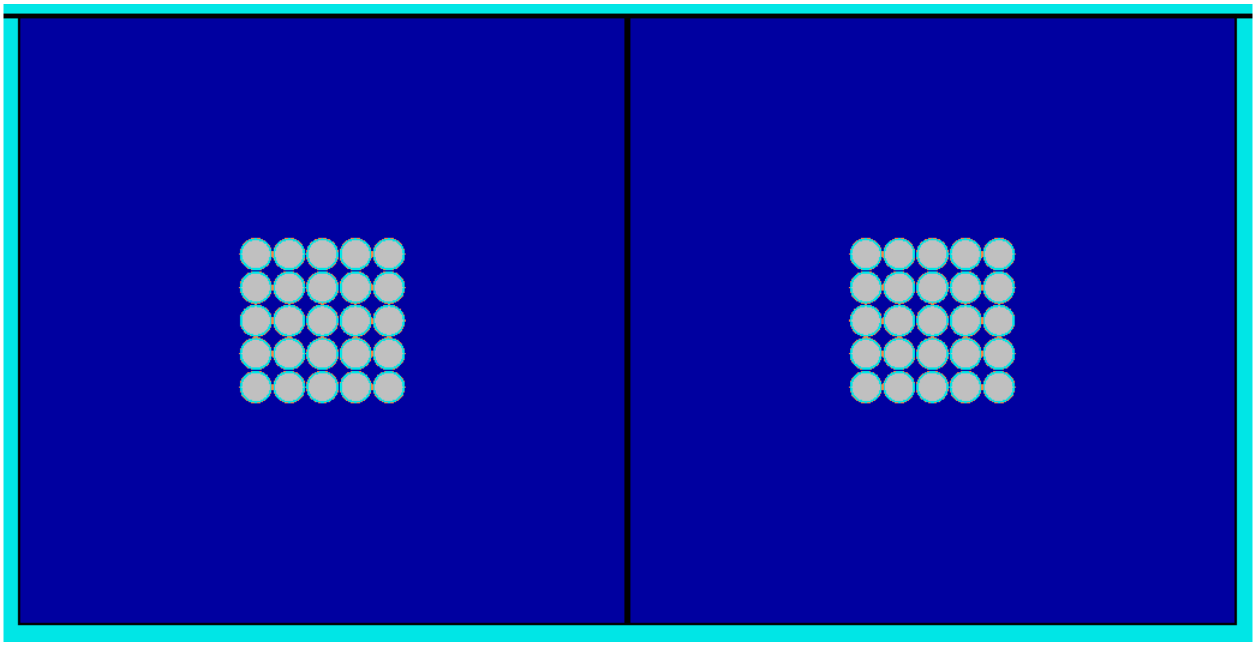

Close-packed loose fuel rods

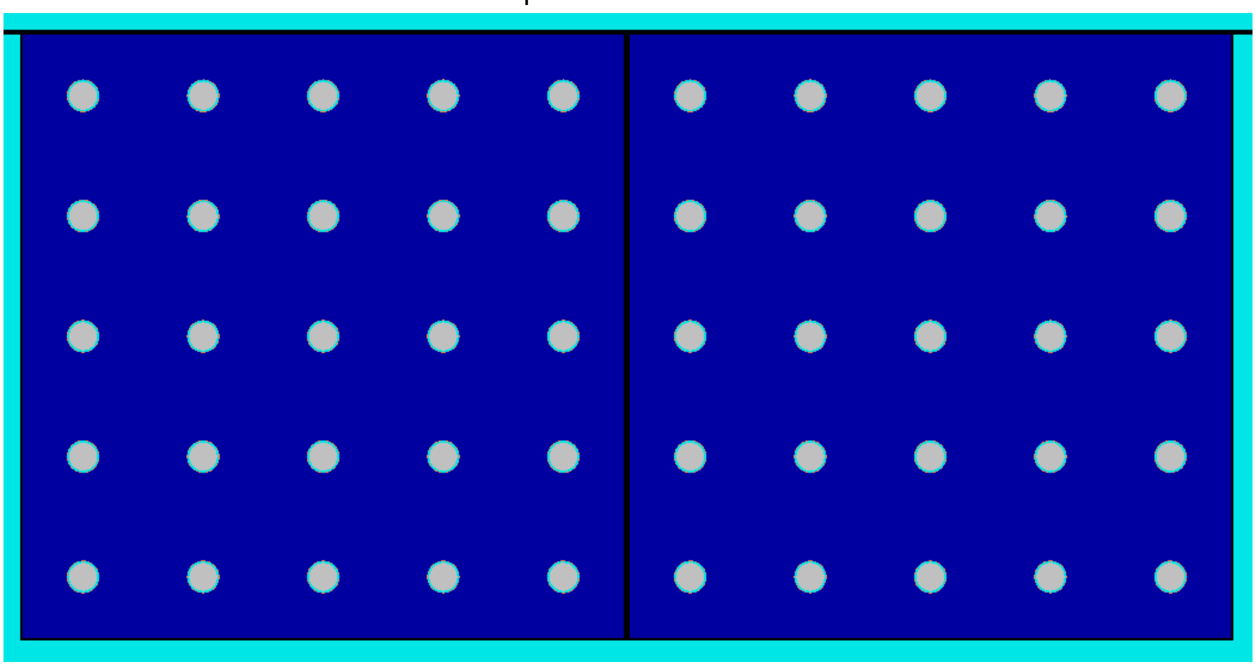

Maximum-pitch loose fuel rods

Figure 6-53 Twenty-five 11x11 Fuel Rods in Liner

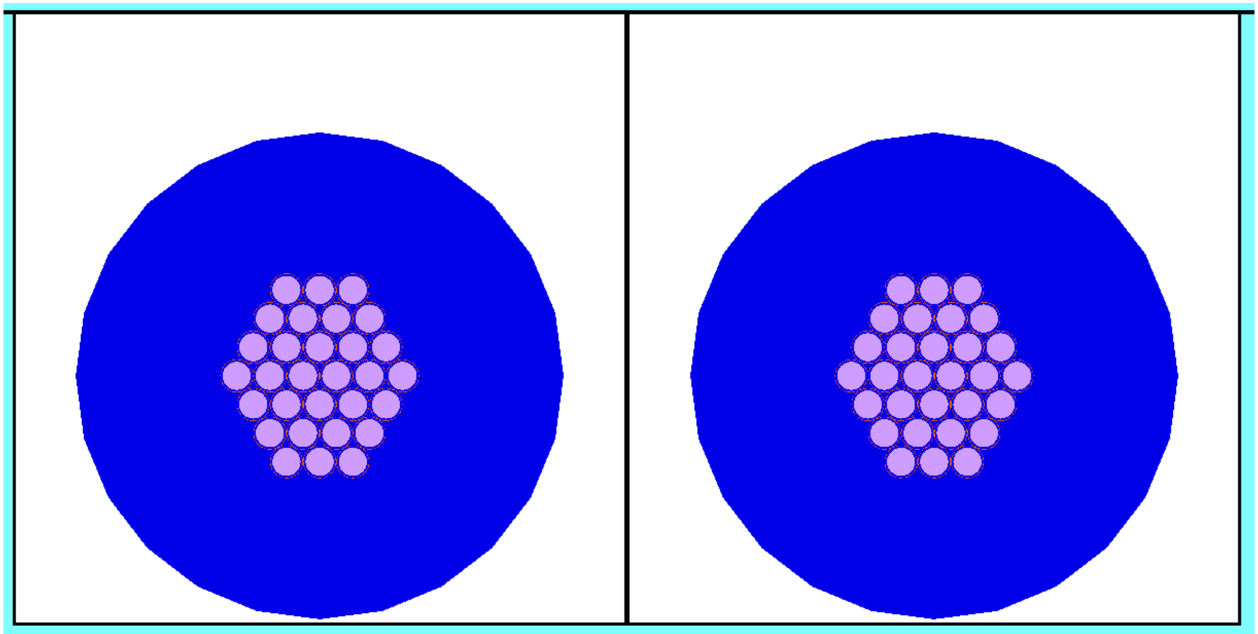

Close-packed fuel rods in pipe component

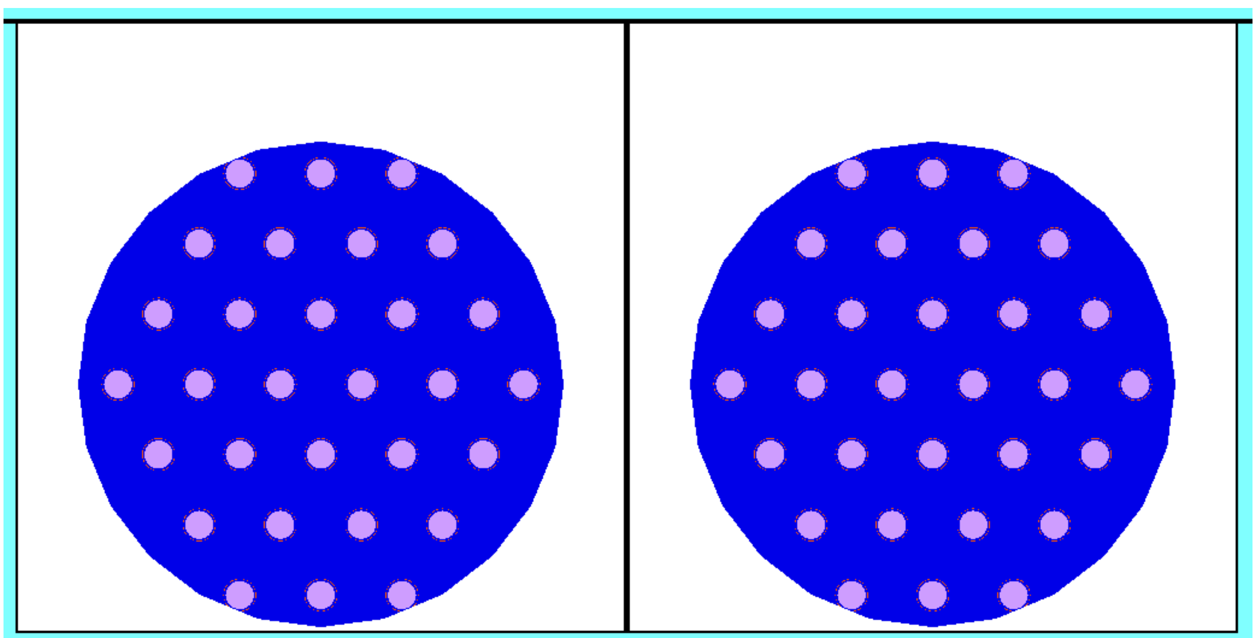

Maximum-pitch fuel rods in pipe component

Figure 6-54 Thirty 11x11 Fuel Rods in Pipe Component

6.12.3.2. Material Properties

The material specifications for the 11x11 analysis are summarized in Table 6-60 Material Specifications for the TN-B1 11x11 Analysis. The atomic densities are extracted directly from the SCALE 6.1.3/KENO V.a output files. Because ENFD/B-VII cross sections are used, elements are represented as individual isotopes.

The UO_2 stack density is modeled as 10.763 g/cm^3. The UO_2 material is included as material 1 in the sample problem inputs given in Section 6.12.10 *Sample Input Files*.

The 4 pcf polyethylene foam is conservatively modeled with a density of 5 pcf. Likewise, the 9 pcf polyethylene foam is conservatively modeled with a density of 10 pcf.

The presence of Gd_2O_3 in the UO_2-Gd_2O_3 pellet reduces the density from 10.763 to 10.691 g/cm^3. The UO_2-Gd_2O_3 is included as material 4 (see the sample problem input in Section 6.12.10.1). In the input, the UO_2- Gd_2O_3 is defined with two entries: UO_2 is defined as the first entry of material 4 with a density of 10.763 g/cm^3. Gd_2O_3 is defined as the second entry of material 4 with a density of 7.407 g/cm^3. Using these densities and the volume fractions calculated below, the density of the UO_2- Gd_2O_3 material is calculated by SCALE 6.1.3 to be 10.691 g/cm^3.

A 2 wt% gadolinia-urania rod is used in the analysis. However, only 75% of this is credited in the current analysis. Thus the gadolinium weight percent in the gadolinia-urania fuel is 1.5%. The fraction of the UO_2 and Gd_2O_3 of the gadolinia fuel material is determined using the following equation:

$$wf_{Gd} = \frac{\rho_{Gd} * VF_{Gd}}{\rho_{UO2} * VF_{UO2} + \rho_{Gd} * VF_{Gd}}$$

where wf_{Gd} = weight fraction of Gd_2O_3 in the gadolinia-urania fuel = 0.015
ρ_{Gd} = density of Gd_2O_3 = 7.407 g/cm^3
VF_{Gd} = volume fraction of Gd_2O_3
ρ_{UO2} = density of UO_2 = 10.96 g/cm^3 * 0.982 theoretical density = 10.763 g/cm^3
VF_{UO2} = volume fraction of UO_2 = 1 - VF_{Gd}

Substituting (1-VF_{Gd}) for VF_{UO2} into the above equation and solving for VF_{Gd} gives

$$VF_{Gd} = \frac{wf_{Gd} * \rho_{UO2}}{\rho_{Gd} + wf_{Gd} * \rho_{UO2} - wf_{Gd} * \rho_{Gd}} = 0.0216$$

$$VF_{UO2} = 0.9784$$

6.12.3.3. Computer Codes and Cross-Section Libraries

The KENO V.a module of SCALE 6.1.3 is used in the analysis (CSAS5 sequence). The 238 group ENDF/B-VII cross section set is used in all input files. CENTRM is used for resonance processing. This cross section set and resonance processing methodology is used in the benchmark set described in Section 6.12.9, *Benchmark Evaluation for SCALE 6.1.3*. For each case, a minimum of 3 million active histories are run to ensure proper behavior about the mean value (e.g, 1,550 generations, 2,000 neutrons per generation, skipping the first 50 generations).

Table 6-60 Material Specifications for the TN-B1 11x11 Analysis

Material	Density (g/cm^3)	Constituent	Atomic Density (atoms/b-cm)
$U(5.0)O_2$	10.763 [a]	O-16	4.80319E-02
		U-235	1.21538E-03
		U-238	2.28006E-02
$U(5.0)O_2$-Gd_2O_3 2 wt% Gd_2O_3 (75% credit for Gd)	10.691 [b]	O-16	4.77918E-02
		Gd-152	1.06321E-06
		Gd-154	1.15888E-05
		Gd-155	7.86763E-05
		Gd-156	1.08818E-04
		Gd-157	8.31949E-05
		Gd-158	1.32049E-04
		Gd-160	1.16207E-04
		U-235	1.18913E-03
		U-238	2.23081E-02
Zirconium	6.49	Zr-90	2.20431E-02
		Zr-91	4.80708E-03
		Zr-92	7.34772E-03
		Zr-94	7.44626E-03
		Zr-96	1.19963E-03
Polyethylene Foam (4 pcf)	≤ 0.08	H-1 (in poly)	6.86951E-03
		C	3.43476E-03
Polyethylene Foam (9 pcf)	≤ 0.16	H-1 (in poly)	1.37390E-02
		C	6.86951E-03
Polyethylene	0.949	H-1 (in poly)	8.14896E-02
		C	4.07448E-02
Alumina Silicate [Al_2O_3(49%)-SiO_2(51%)]	0.25	O-16	4.72705E-03
		Al-27	1.44724E-03
		Si-28	1.17870E-03
		Si-29	5.98790E-05
		Si-30	3.95189E-05
Full Density Water	1.0	H-1 (in water)	6.68734E-02
		O-16	3.34367E-02

---

a UO_2 is represented in the input file as material 1 with a density of 10.763 g/cm^3 (see sample input files in Section 6.12.10 *Sample Input Files*).

b UO_2-Gd_2O_3 is represented in the input file as material 4 with two entries. Entry 1 of material 4 is UO_2 with a density 10.763 g/cm^3 and volume fraction of 0.9784 as calculated in Section 6.12.3.2. Entry 2 of material 4 is Gd_2O_3 with a density of 7.407 g/cm^3 and a volume fraction of 0.0216. The density of the UO_2-Gd_2O_3 material is

Table 6-60 Material Specifications for the TN-B1 11x11 Analysis (continued)

Material	Density (g/cm^3)	Constituent	Atomic Density (atoms/b-cm)
Stainless Steel 304	7.94	C	3.18488E-04
		Si-28	1.57010E-03
		Si-29	7.97625E-05
		Si-30	5.26416E-05
		P-31	6.94688E-05
		Cr-50	7.59178E-04
		Cr-52	1.46402E-02
		Cr-53	1.65988E-03
		Cr-54	4.13224E-04
		Mn-55	1.74072E-03
		Fe-54	3.45419E-03
		Fe-56	5.36980E-02
		Fe-57	1.22946E-03
		Fe-58	1.63927E-04
		Ni-58	5.28417E-03
		Ni-60	2.02017E-03
		Ni-61	8.74631E-05
		Ni-62	2.77870E-04
		Ni-64	7.04349E-05

6.12.3.4. Demonstration of Maximum Reactivity

6.12.3.4.1. *11x11 Fuel Assembly Analysis*

The most reactive condition occurs for the HAC array. Therefore, the following discussion refers to the parameters of the HAC array analysis for the 11x11 fuel assembly. A parameter study is performed for the 11x11 fuel assembly to determine the most reactive fuel assembly parameters. The results are:

- The zirconium water channel (i.e., the zirconium channel in the center of the fuel assembly) is modeled as water, which increases moderation and hence increases reactivity.
- The zirconium fuel channel (i.e., the zirconium channel on the outside of the fuel assembly) is modeled at the maximum thickness of 0.254 cm. It is demonstrated that when the fuel channel is modeled at the maximum thickness the system reactivity peaks with a 1.2 cm thick polyethylene liner. If the zirconium fuel channel is modeled as water, maximum reactivity occurs with a 1.5 cm thick polyethylene liner. The two results are

calculated by SCALE 6.1.3 to be 10.691 g/cm^3 using the input densities and volume fractions (see the sample input file in Section 6.12.10.1).

statistically the same. Therefore, fuel may be shipped either with or without the fuel channel.

- The polyethylene equivalent mass for each fuel assembly is limited to 10.2 kg. This mass of polyethylene is smeared into the fuel cladding. Polyethylene is a superior moderator than water and increases the reactivity. For the final most reactive HAC configurations, a second modeling approach was considered in which the mass of polyethylene is smeared into the moderator.
- Pitch is increased 5% to 1.2548 cm. Increasing the pitch increases moderation and hence the reactivity. A structural analysis of the 11x11 fuel assembly has demonstrated that the average pitch expansion is a lower value of 2.6%, and the expansion of the fuel assembly outer perimeter is a lower value of 3.4% (Reference 19).
- Maximum pellet diameter of 0.820 cm. This is the largest allowed pellet diameter, as increasing the pellet diameter increases the reactivity.
- Maximum cladding inner diameter of 0.840 cm and minimum cladding outer diameter of 0.930 cm. These parameters control the thickness of the cladding, and reactivity increases as the cladding thickness decreases because replacing cladding with water increases moderation.
- While a range of enrichments and the number of gadolinia-urania rods are considered, the most reactive combination for uniform axial enrichment is 5.0% enriched fuel with 13 gadolinia-urania rods in each lattice in the pattern shown in Figure 6-52 Bounding Fuel Assembly Model. Numerous patterns are considered and the most reactive pattern is selected. Gadolinia-urania rods shall be placed symmetrically about the major diagonal and shall not be placed on the periphery. When axial variation of enrichment is considered, the reactivity of the HAC array configuration increases slightly if an enrichment of 5.0% with 13 gadolinia-urania rods is used in the bottom and middle lattices and an enrichment of 3.3% with 3 gadolinia-urania rods is used in the top lattice.
- The minimum Gd_2O_3 loading in a Gadolinia-urania rod is 2.0%, and only 75% credit is taken for the gadolinia.
- The density of UO_2 is modeled as 10.763 g/cm^3. Reactivity increases with increasing fuel loading.
- The lengths of the full-length, long partial-length, and short partial-length rods are conservatively increased by at least 4 cm to increase the fuel loading.
- Water is modeled in the pellet/cladding gap.

Other system parameters are also selected to maximize reactivity:

- Outer dimensions of the package reduced to account for HAC damage, which reduces the overall size of the array and increases reactivity.
- Inner container flooded with full-density water to maximize moderation.

- The region between the inner and outer containers is modeled as void to maximize neutron interactions between packages. Modeling water in this region reduces the reactivity.
- All rods of a fuel assembly are fully flooded to maximize moderation. Uncovering some fuel rods reduces the reactivity.
- Thermal insulator modeled as Alumina-Silica. This bounds modeling this region as either void or water.
- Polyethylene foam liner modeled as partially burned with a thickness of 1.2 cm. Modeling the foam liner as partially burned is more reactive than either complete foam burn or no foam burn scenarios. In general, modeling some polyethylene foam increases neutron interactions between arrays of packages because the mean free path for a neutron in low-density foam is much higher than neutrons in full-density water.
- A fuel assembly orientation study demonstrates that the system is most reactive in a partial foam burn scenario with the fuel assemblies centered within the compartments with the fuel channel present.
- Trace amounts of plutonium are shown to have a negligible effect on reactivity and thus is neglected.

With the conservative modeling choices noted above, $k_{eff} + 2\sigma$ is 0.94068, which is below the fuel assembly USL of 0.94094.

6.12.3.4.2. *11x11 Fuel Rod Analysis*

The most reactive condition occurs for the HAC array. Therefore, the following discussion refers to the parameters of the HAC array analysis for 11x11 fuel rods.

Two scenarios are considered:

1. 25 fuel rods loose within each liner cavity. This analysis bounds fuel rods that are bundled together, as bundled fuel rods would have significantly less moderation than loose rods, and credit could not be taken for the bundles remaining intact in an accident.
2. 30 fuel rods within a 5-in stainless steel pipe. This analysis bounds fuel rods transported in a protective case, as the protective case has a much smaller cross sectional area than the pipe and would allow significantly less moderation.

In both analyses, conservative fuel rod parameters are used:

- A 6-mil thick polyethylene sleeve is modeled around each fuel rod. Polyethylene is a superior moderator than water and increases the reactivity.
- Maximum pellet diameter of 0.820 cm. This is the largest allowed pellet diameter, as increasing the pellet diameter increases the reactivity.
- The cladding is modeled as water to conservatively increase moderation. The pellet-cladding gap is also modeled as water.

- No gadolinia is credited.
- The density of UO_2 is modeled as 10.763 g/cm^3. Reactivity increases with increasing fuel loading.
- The lengths of the rods are conservatively modeled as 385 cm, which increases the fuel loading compared to partial-length rods.

In the loose rod analysis, 25 loose rods are modeled per compartment (50 rods per package). The rods are arranged in a 5x5 square array within each compartment.

- A pitch study is performed and optimum moderation is achieved. Therefore, reactivity will decrease for less than 25 rods.
- A moderation study is performed and the system is most reactive with 0.6 g/cm^3 moderator.
- A foam liner partial burn study is performed and the system is most reactive with 0.4 cm liner thickness.
- The most reactive case has $k_{eff} + 2\sigma = 0.72725$, which is significantly less than the rod USL of 0.94047.

In the 5-in pipe analysis, 30 rods are modeled per pipe (60 rods per package). The rods are arranged in a triangular pitch within the pipe.

- The wall of the pipe is conservatively modeled as water. A pitch study is performed in which the pitch is allowed to expand until the rods extend to the outer diameter of the pipe. This geometry is not physically possible because the rods would contact the inner diameter of the pipe before this level of moderation is achieved. The case with the maximum pitch expansion is the most reactive, indicating the system is likely undermoderated.
- A moderator density study indicates that the system is most reactive with full-density water within the pipe to maximize moderation.
- Moderation is increased by removing rods for the same pitch and reactivity decreased compared to modeling 30 rods in the pipe. Moderation is also increased by removing rods and increasing the pitch and reactivity decreased compared to modeling 30 rods in the pipe. Therefore, less than 30 rods per pipe is bounded by 30 rods per pipe.
- Several different orientations of the pipes within the package are investigated, along with partial foam burn. It is demonstrated that complete foam burn with the pipes shifted to the center of the package is the most reactive condition.
- The insulation is modeled as Alumina-Silica consistent with the 11x11 fuel assembly HAC models.
- The outer region is modeled as void consistent with the 11x11 fuel assembly HAC array models.

- The region outside the pipes but inside the inner container is modeled with a density of 0.1 g/cm^3, which is slightly more reactive than modeling this region as void.
- The most reactive case has $k_{eff} + 2\sigma = 0.82035$, which is significantly less than the rod USL of 0.94047.

6.12.3.5. Parameter Selection for 11x11 Fuel Assembly Model

Prior to performing the criticality analysis for the 11x11 fuel assembly, the parameters of the fuel assembly are selected to determine the most reactive fuel assembly configuration. The following parameter studies are performed:

1. Fuel assembly orientation
2. Fuel assembly zirconium channel
3. Zirconium water channel
4. Polyethylene equivalent mass
5. Fuel rod pitch
6. Fuel pellet diameter
7. Fuel rod cladding thickness
8. Inner container partial flooding
9. Thermal insulator material
10. Polyethylene foam liner thickness (i.e., partial burn)
11. Number of gadolinia-urania rods as a function of enrichment.

The parameter selection model is based upon the 10x1x10 HAC array model because this model results in reactivities close to the USL. The single package and NCT array reactivities do not approach the USL. In the baseline HAC model used in this parameter study, the inner container is fully flooded while the region between the inner and outer containers is void. This moderation condition is used as the starting point of the analysis because it has been shown to be the most reactive moderation condition for 8x8, 9x9, and 10x10 fuel (see Section 6.6, *Package Arrays Under Hypothetic Accident Conditions*), and 11x11 fuel behaves in a similar manner.

The parameters listed above are optimized using an HAC array model and are applicable for NCT single package, HAC single package, and NCT array analyses with the exception of fuel assembly orientation, fuel assembly zirconium channel, and polyethylene foam liner thickness. These parameters are re-evaluated for NCT single package, HAC single package, and NCT array analyses because the system response for these parameters may be different than an HAC array.

Basic bounding data for the 11x11 fuel assembly is summarized in Table 6-61 11x11 Fuel Assembly Data. A simple diagram of the assembly showing the location of the fuel rods is shown in Figure 6-51 Position of Fuel Rods in 11x11 Assembly.

The maximum pellet enrichment and maximum fuel lattice average enrichment is 5 wt% U-235. A density of 10.763 g/cm^3 is used in the analysis.

6.12.3.5.1. *Fuel Assembly Orientation Study*

The 10x1x10 HAC array model described in Section 6.12.3.1.5, *HAC Array Model with 11x11 Fuel*, is used to perform initial calculations to find the worst-case fuel assembly orientation inside each TN-B1 fuel compartment. The base model features 5 wt.% UO_2 rods (no gadolinium), nominal fuel dimensions, and no fuel channel or water channel. 10.2 kg of polyethylene per fuel assembly is modeled as smeared into the fuel rod cladding to increase moderation. The nominal pitch of 1.195 cm is modeled. The polyethylene foam liner is assumed to have burned away in this initial model, which allows a greater degree of fuel orientation scenarios (the fuel must be centered in the compartment if the foam does not burn). All analyzed orientations are shown in Figure 6-55 Fuel Assembly Orientation 1 through Figure 6-66 Fuel Assembly Orientation 12.

The results of the calculations are provided in Table 6-62 11x11 Fuel Assembly Orientation Results. Based on these results, assembly orientation 7 is bounding. Orientation 7 has one assembly centered in the fuel compartment and one assembly shifted toward the center of the container. Orientation 7 is used in the subsequent studies in which the foam is assumed to have completely burned away. When partial foam is present (partial foam burn), it is later demonstrated that centered fuel assemblies are more reactive.

It is noted that many of the results in Table 6-62 11x11 Fuel Assembly Orientation Results exceed the 0.94094 USL because no gadolinia-urania rods are modeled. For this reason, 12 gadolinia-urania fuel rods are added to each lattice (i.e., bottom, middle, top) in a reasonably conservative pattern to provide reactivity hold-down in subsequent parametric models. This initial gadolinia-urania loading pattern is preliminary. The final gadolinia-urania loading pattern is explicitly derived at the end of the parametric study as a function of lattice enrichment.

6.12.3.5.2. *Fuel Assembly Zirconium Channel Study*

The 11x11 fuel assembly may have a zirconium channel around the outer boundary of the fuel assembly. The channel thickness is ≤ 0.254 cm. A range of channel thicknesses from 0 cm (no channel) to the maximum value of 0.254 cm are investigated to determine the most reactive condition.

The fuel assembly channel is located in the reflector region for each assembly. It has no effect on the assembly H/U-235 ratio since it is not located within the fuel envelope. Calculations are performed both with and without a water gap between the fuel rods and the channel.

Since the orientation used in the current analysis (Orientation 7) has the assembly in the right compartment shifted left to the center of the shipping container, it is necessary to shift the assembly further to the right to accommodate the presence of the channel (and water gap if present).

The results are shown in Table 6-63 11x11 Zirconium Channel Study Results. The results indicate that reactivity increases with the presence of channels due to increased leakage from the inner fuel compartment, resulting in increased neutron interaction among containers in the array. In addition, reactivity increases with increasing thickness of the channel. Furthermore, including a water gap between the fuel pin cells and the channel has no statistically significant effect on reactivity. Therefore, the model using the thickest channel of 0.254 cm with no gap between the pin cells and the channel is chosen for further study. Note that additional channel studies are performed when the polyethylene foam liner is considered.

6.12.3.5.3. ***Zirconium Water Channel Study***

The limiting channeled model discussed in the previous section is used to determine if the presence of the zirconium water channel within the fuel assembly increases system reactivity. A zirconium channel is placed within the center 3x3 water hole. The channel is modeled with an inner width and thickness as described in Reference 20. The result for including a water channel within the 11x11 assembly is listed in Table 6-64 11x11 Zirconium Water Channel Study Results. By including the zirconium water channel, system reactivity is decreased; therefore, it is conservative to neglect the zirconium water channel within the TN-B1 analysis.

6.12.3.5.4. ***Polyethylene Mass Study***

The effect that polyethylene mass has on reactivity is considered. Plastic inserts may be used during transportation, which are inserted into the fuel assembly. Other plastic materials may also be used, such as spacer straps. A polyethylene equivalent mass limit of 10.2 kg is set for the 11x11 fuel assembly. To verify that this limit is sufficiently conservative for the 11x11 assembly, a polyethylene mass study is performed in which the polyethylene mass is varied from 0 kg per assembly to 10.2 kg per assembly. This study uses the limiting channeled model discussed in Section 6.12.3.5.2, *Fuel Assembly Zirconium Channel* Study, as the base case. The polyethylene mass is smeared into the fuel cladding for all fuel rods, which simulates the polyethylene melted onto the fuel rods. The volume fractions as a function of polyethylene mass are provided in Table 6-65 11x11 Polyethylene Mass and Volume Fraction Calculations.

The results of the polyethylene mass study are provided in Table 6-66 11x11 Polyethylene Mass Sensitivity Analysis Results. This shows that the value of 10.2 kg/assembly bounds the results given for lower polyethylene mass values.

6.12.3.5.5. *Fuel Rod Pitch Study*

A fuel rod pitch sensitivity study is conducted using the limiting channeled model. The minimum fuel rod pitch is chosen to be at the point that the polyethylene coating on adjacent fuel rods contact. The maximum fuel rod pitch is chosen to be 5% greater than the nominal pitch. A structural analysis of the 11x11 fuel assembly has demonstrated that the average pitch expansion is a lower value of 2.6%, and the expansion of the fuel assembly outer perimeter is a lower value of 3.4% (Reference 19).

The results of the fuel rod pitch study are provided in Table 6-67 11x11 Fuel Rod Pitch Sensitivity Analysis Results. The results show that the fuel assemblies are under-moderated such that increasing the rod pitch increases system reactivity from minimum pitch to the maximum of 5% increase.

6.12.3.5.6. *Fuel Pellet Diameter Study*

A fuel pellet diameter sensitivity study is conducted. Using the limiting channeled model, the diameter of the fuel pellet is varied from 0.780 cm to 0.820 cm. The results are provided in Table 6-68 11x11 Pellet Diameter Sensitivity Analysis Results. The results show that reactivity increases as the pellet diameter is increased. A pellet diameter of 0.820 cm is selected as the upper bound for the 11x11 fuel assembly pellet range.

6.12.3.5.7. *Fuel Rod Cladding Thickness Study*

Two sets of calculations are performed to assess the reactivity sensitivity to changes in cladding thickness. For both sets of calculations the limiting channeled model is used.

For the first set of calculations, the inner cladding diameter is adjusted to determine the effect on reactivity while the outer cladding diameter is fixed at 0.940 cm. The minimum value for the parameter search range is the pellet outer diameter, while the maximum value for the range is the cladding outer diameter. The volume fractions of the zircaloy and polyethylene cladding material are calculated with the cladding/polyethylene outer diameter remaining fixed to correspond to the cladding thickness being considered. The volume fractions for the calculations varying the clad inner diameter are given in Table 6-69 11x11 Zirc and Polyethylene Volume Fractions, Varying Cladding ID. Results are provided in Table 6-70 11x11 Cladding ID Sensitivity Analysis Results.

The second set of calculations involves adjustments to the outer cladding diameter while the inner cladding diameter is held at 0.826 cm. The range of cladding outer diameters studied is between 0.826 cm (cladding inner diameter) and 1.0386 cm (maximum outer diameter for nominal rod pitch and a polyethylene limit of 10.2 kg/assembly). The cladding/polyethylene outer diameter and the volume fractions of the zircaloy and polyethylene cladding material are calculated with the cladding inner diameter remaining fixed to correspond to the cladding thickness being considered. The volume fractions for the calculations varying the clad outer diameter are given in Table 6-71 11x11 Zirc and Polyethylene Volume Fractions, Varying Cladding OD. Results are provided in Table 6-72 11x11 Cladding OD Sensitivity Analysis Results.

Both sets of results demonstrate that a decrease in the cladding thickness results in an increase in system reactivity as cladding is replaced by water. Based on these results and future design considerations, 0.840 cm (maximum) and 0.930 cm (minimum) are selected for the cladding inner diameter and cladding outer diameter, respectively, or a minimum cladding thickness of 0.045 cm. For these dimensions and 10.2 kg polyethylene, VF_{clad} = 0.31309 and VF_{poly} = 0.68691.

6.12.3.5.8. *Inner Container Partial Flooding Study*

The fuel assembly parameters utilized in the inner container partial flooding study (and subsequent studies) are consistent with the conclusions of the previous sections:

- Assembly orientation 7 (for full foam burn)
- 0.254 cm thick fuel assembly channel included
- Zirconium water channel not included
- 10.2 kg polyethylene per fuel assembly
- Pitch increased 5% to 1.2548 cm
- Pellet diameter of 0.820 cm
- Cladding inner diameter of 0.840 cm
- Cladding outer diameter of 0.930 cm

The fuel bundle rows are partially filled within the TN-B1 inner fuel compartment, as shown in Figure 6-67 Inner Container Partial Flooding. For this study, the polyethylene foam is modeled as water within the inner compartment (i.e, complete foam burn). The conclusions of the study remain valid if polyethylene material is used in this region.

The results of the partial flooding study are provided in Table 6-73 11x11 Sensitivity Analysis Results for Partially Flooded Inner Container. The results show that the most reactive conditions exist when water fully covers each fuel bundle. Therefore, the inner container fuel compartment will be fully flooded with water in the worst-case TN-B1 model.

6.12.3.5.9. *Thermal Insulator Material Study*

The most reactive case from Table 6-73 11x11 Sensitivity Analysis Results for Partially Flooded Inner Container is used to conduct a study to determine if the system is more reactive with or without the thermal insulating material. The material normally present around the inner container fuel compartment is a thermal insulator consisting of Alumina Silicate.

The Alumina Silicate insulator is replaced with full density water or void. The inner container fuel compartment for both scenarios is filled with full density water. Results for the thermal insulator sensitivity study are given in Table 6-74 11x11 Sensitivity Analysis Results for Thermal Insulator Material and show that the most reactive condition is achieved with the Alumina Silicate thermal insulator in place. Therefore, the Alumina Silicate thermal insulator will remain a part of the worst-case TN-B1 model. This is consistent with the physical condition of the TN-B1 shipping container after being subjected to the tests specified in 10 CFR Part 71 (see Sections 3.2.2 and 3.5.2)

6.12.3.5.10. ***Polyethylene Foam Liner Study***

In the previous cases in this section, the polyethylene foam liner is assumed to burn away in the fire. In this study, incomplete foam burn is modeled to determine the effect on the reactivity.

The material normally lining the inner container fuel compartment is a polyethylene foam material that has a density of 4 pcf on the top and sides. The 11x11 fuel assembly is supported at the grid spacers using small strips of 9 pcf foam, although the majority of the bottom foam is only 4 pcf. Because sensitivity studies show that reactivity increases slightly with increasing foam density, 5 pcf foam (0.08 g/cm^3) is modeled on the top and sides and 10 pcf foam (0.16 g/cm^3) is modeled on the bottom.

To determine the effect on reactivity from the liner, the thickness of the foam is varied within the container from no liner to a liner that fills the container from the walls to the fuel assembly. The presence of the liner affects the most reactive assembly orientation determined in Section 6.12.3.5.1, *Fuel Assembly Orientation Study*, because for a full liner thickness (i.e., no foam burn) the fuel assemblies must be centered. The presence or absence of the channel also affects the fuel assembly orientation, as well as the system response. For these reasons, four different scenarios are considered:

1. Fuel assemblies centered, fuel channel included
2. Fuel assemblies centered, no fuel channel
3. Fuel assembly in left compartment centered, fuel assembly in right compartment shifted to the left, fuel channel included.
4. Fuel assembly in left compartment centered, fuel assembly in right compartment shifted to the left, no fuel channel.

For the channeled fuel, the maximum thickness of the liner is from the container wall to the fuel assembly channel. For the unchanneled fuel, the maximum thickness of the liner is from the container wall to the fuel assembly envelope.

In the models with the fuel channel in the right compartment shifted to the left, the fuel assembly is placed directly next to the foam liner on the center wall between compartments. The assembly is shifted towards the center of the right compartment as the liner thickness is increased. Including the fuel channel also increases the distance between the fuel assemblies when the right fuel assembly is shifted to the left.

Results of the polyethylene liner sensitivity studies are given in Table 6-75 11x11 Sensitivity Analysis Results for Polyethylene Liner. Several observations may be made from these results:

1. Modeling partial foam burn is more reactive than either no foam burn or complete foam burn. In fact, the increase in reactivity is such that the USL is violated. The placement and number of gadolinia-urania rods is determined in the next section for a variety of U-235 enrichments such that reactivity will remain below the USL of 0.94094.
2. Reactivity increases as the thickness of the liner increases until the liner fills ~75% of the compartment.
3. For thinner polyethylene liners, the presence of the fuel channel results in a higher system reactivity than using unchanneled fuel. For thicker liners, the unchanneled fuel results in higher system reactivity.
4. In general, for partial foam burn scenarios, shifting the right fuel assembly toward the center of the container results in lower system reactivity than having both fuel assemblies centered within their respective compartments.

The highest system reactivity is observed for a centered, channeled configuration with a 1.2-cm-thick polyethylene liner. This configuration will be used for further calculations, including the gadolinia-urania rod analysis versus U-235 enrichment. It is noted that the maximum reactivity for unchanneled assemblies is observed in the centered orientation with a 1.5-cm-thick polyethylene liner. The reactivity of these systems is statistically the same.

Finally, as mentioned above, the 9 pcf foam is intended to be located in discrete locations only and not a continuous liner. Thus a calculation replacing the 9 pcf bottom foam liner with 4 pcf foam is performed to show that modeling 9 pcf foam is more reactive. This calculation is performed for the most limiting case in the above analyses:

9 pcf foam liner (poly_liner_120_cc.out): $k_{eff} + 2\sigma = 0.95276$

Replacing 9 pcf foam with 4 pcf foam (poly_liner_120_DENS.out): $k_{eff} + 2\sigma = 0.95170$

Modeling the bottom as 9 pcf foam is slightly more reactive than modeling the bottom as 4 pcf foam, although the effect is small and within the uncertainty of the Monte Carlo method. For this reason, using small 9 pcf foam strips with FANP 10x10 fuel assemblies is also acceptable.

6.12.3.5.11. *Gadolinia-Urania Fuel Rod Restriction Study*

The parameter studies described in the preceding sections are performed using a 12 gadolinia-urania rods in a preliminary loading pattern. As the results in the polyethylene foam liner study exceed the USL, the number of gadolinia-urania rods is increased and the loading pattern is modified to lower the system reactivity.

As a result of the parameter studies performed in Sections 6.12.3.5.1 through 6.12.3.5.10, the most reactive system parameters for the 10x1x10 HAC array are:

- Assembly orientation 6 (fuel assemblies centered for partial foam burn)
- 0.254 cm thick fuel assembly channel included
- Zirconium water channel not included
- 10.2 kg polyethylene per fuel assembly smeared into the cladding (note that for the final most reactive HAC configurations, a second modeling approach was considered in which the polyethylene per fuel assembly was smeared into the moderator)
- Pitch increased 5% to 1.2548 cm
- Pellet diameter of 0.820 cm
- Cladding inner diameter of 0.840 cm
- Cladding outer diameter of 0.930 cm
- Fuel assemblies fully flooded (i.e., no uncovered fuel rods)
- Thermal insulator modeled as Alumina-Silica
- Polyethylene foam liner modeled as partially burned with a thickness of 1.2 cm

A 2 wt% gadolinia rod is used in the analysis. However, only 75% of this is credited in the current analysis. Thus the gadolinia weight percent in the gadolinia-urania fuel is 1.5%. See Section 6.12.3.2, *Material Properties*.

The 11x11 assembly has three distinct axial layers, corresponding to the lengths of the different types of fuel rods. The three axial regions are defined as follows:

Bottom: This layer includes all full-length and all partial-length rods. No water holes from partial-length rods are present.

Middle: This layer includes the full-length rods and the long partial-length rods. 12 water holes are located in the short partial-length rod locations.

Top: This layer includes only full-length rods. 12 water holes are located in the short partial-length rod locations and 8 water holes are located in the long partial-length rod locations.

While the minimum required number of gadolinia-urania fuel rods is constant in each axial region, the gadolinia-urania fuel rod placement patterns may vary between each of the three axial regions. The approach is to initially model each of the axial regions as a full-length fuel assembly (i.e., 385 cm long) and vary the gadolinia-urania fuel rod placement in patterns expected to maximize reactivity. These initial models are referred to as “2-D” models because the geometry across each axial region of the fuel assembly is modeled over the full fuel assembly length. In general, reactivity is maximized when the gadolinia-urania fuel rods are clustered together, which reduces their worth due to self-shielding. In these initial "2-D" models, the reactivities should not be compared against the USL, as the intent is only to observe trends in the reactivities from the various loading patterns rather than absolute reactivities.

Two restrictions on the gadolinia-urania fuel rod placement patterns are stipulated:

1. Gadolinia-urania rods shall be distributed symmetrically about the major diagonal, and.
2. Gadolinia-urania rods shall not be placed on the periphery.

After the gadolinia-urania fuel rod placement patterns are independently determined for each of the three axial layers using the "2-D" models, final models are developed in which the 11x11 fuel assembly is modeled explicitly with each optimized axial layer to demonstrate the reactivity is below the USL.

The number of required gadolinia-urania rods and the loading pattern changes with enrichment. The following combinations of enrichment and number of gadolinia-urania rods are demonstrated to be acceptable:

1. 5.0 wt.%, 13 gadolinia-urania rods
2. 4.8 wt.%, 12 gadolinia-urania rods
3. 4.6 wt.%, 11 gadolinia-urania rods
4. 4.4 wt.%, 10 gadolinia-urania rods
5. 4.2 wt.%, 9 gadolinia-urania rods
6. 4.1 wt.%, 8 gadolinia-urania rods
7. 3.9 wt.%, 7 gadolinia-urania rods
8. 3.8 wt.%, 6 gadolinia-urania rods
9. 3.6 wt.%, 5 gadolinia-urania rods
10. 3.5 wt.%, 4 gadolinia-urania rods
11. 3.3 wt.%, 3 gadolinia-urania rods
12. 3.2 wt.%, 2 gadolinia-urania rods
13. 2.9 wt.%, 0 gadolinia-urania rods

Numerous gadolinia-urania rod loading patterns are investigated for each enrichment. The three most reactive loading patterns for each enrichment are illustrated on Figure 6-68 Most Reactive Gadolinia-Urania Fuel Rod Patterns: 5.0 wt% ^{235U,} 13 Gd Rods through Figure 6-79 Most Reactive Gadolinia-Urania Fuel Rod Patterns: 3.2 wt% ^{235U,} 2 Gd Rods. For brevity, all loading patterns considered are not provided.

The "2-D" results corresponding to the loading patterns described in the previous paragraph are provided for each enrichment in Table 6-76 11x11 Bottom Layer "2-D" Analysis Results, Table 6-77 11x11 Middle Layer "2-D" Analysis Results, and Table 6-78 11x11 Top Layer "2-D" Analysis Results.

The most reactive loading patterns determined using the "2-D" models are combined in a full 3-D model of the 11x11 fuel assembly with each axial layer modeled explicitly. The final results for each enrichment are provided in Table 6-79 11x11 Gadolinia-Urania Analysis Results. The most reactive case for each enrichment is highlighted in boldface.

Because the number of gadolinia-urania rods are selected for each enrichment for the reactivity to be close to the USL, the maximum reactivities for each enrichment are necessarily similar. The maximum $k + 2\sigma$ is 0.93810 and occurs for the 5.0% enrichment with 13 gadolinia-urania rods. The minimum $k + 2\sigma$ is 0.93404 and occurs for 3.2% enrichment and 2 gadolinia-urania rods. Although all of the enrichment/gadolinia-urania rod configurations have similar reactivities, the 5.0% enrichment assembly with 13 gadolinia-urania rods per lattice is used as the bounding fuel assembly configuration because it is slightly more reactive than the other configurations.

The most reactive results from Table 6-79 11x11 Gadolinia-Urania Analysis Results are also summarized in Table 6-1 TN-B1 Fuel Assembly Loading Criteria.

It is recognized that each axial region may contain a different U-235 enrichment. To address this in a bounding configuration, the most reactive "2-D" configuration for each axial region, regardless of enrichment, was combined to form a 3-D model. This model contained 5 wt% enrichment with 13 gadolinia-urania rods in the bottom and middle axial regions. The upper axial region contained 3.3 wt% enrichment with 3 gadolinia-urania rods. The result of this model is also provided in Table 6-79 11x11 Gadolinia-Urania Analysis Results.

Table 6-61 11x11 Fuel Assembly Data

Parameter	Units	Value
Fuel Assembly Type		11x11
UO_2 Density[b]	g/cm^3	≤ 10.763
Number of water rods	#	3x3 center
Number of fuel rods	#	112
Fuel Rod OD	cm	≥ 0.930
Fuel Pellet OD	cm	≤ 0.820
Cladding Type		Zirconium Alloy
Cladding ID	cm	≤ 0.840
Cladding Thickness	cm	≥ 0.045
Fuel Rod Pitch[a]	cm	≤ 1.195
U-235 Pellet Enrichment	wt%	≤ 5.0
Maximum Lattice Average Enrichment	wt%	≤ 5.0
Fuel Channel Side Thickness	cm	≤ 0.254
Full Length Fuel Rods Quantity Active length	 # cm	 92 ≤ 385
Short Part Length Fuel Rods Quantity Active length	 # cm	 12 ≤ 155.1
Long Part Length Fuel Rods Quantity Active length	 # cm	 8 ≤ 236.8

a. Equivalent nominal pitch per Section 6.12.3.1.1.
b. Density based on a pellet modeled as a right cylinder.

Table 6-62 11x11 Fuel Assembly Orientation Results

Filename	Assembly Orientation	k_{eff}	σ	$k_{eff} + 2\sigma$
atrium-11_orient01.out	1	0.94507	0.00052	0.94611
atrium-11_orient02.out	2	0.94906	0.00044	0.94994
atrium-11_orient03.out	3	0.89695	0.00054	0.89803
atrium-11_orient04.out	4	0.89730	0.00046	0.89822
atrium-11_orient05.out	5	0.91769	0.00045	0.91859
atrium-11_orient06.out	6	0.96649	0.00048	0.96745
atrium-11_orient07.out	**7**	**0.98108**	**0.00051**	**0.98210**
atrium-11_orient08.out	8	0.94141	0.00046	0.94233
atrium-11_orient09.out	9	0.93333	0.00046	0.93425
atrium-11_orient10.out	10	0.97212	0.00047	0.97306
atrium-11_orient11.out	11	0.95334	0.00047	0.95428
atrium-11_orient12.out	12	0.89655	0.00044	0.89743

Table 6-63 11x11 Zirconium Channel Study Results

Filename	Channel Thickness (cm)	Water gap between fuel cells and channel?	k_{eff}	σ	$k_{eff} + 2\sigma$
atrium-11_5wt_12gd.out	0	No	0.88494	0.00052	0.88598
channel_1100.out	0.110	No	0.88585	0.00052	0.88689
channel_1300.out	0.130	No	0.88759	0.00047	0.88853
channel_1600.out	0.160	No	0.88784	0.00048	0.88880
channel_1700.out	0.170	No	0.88769	0.00046	0.88861
channel_1800.out	0.180	No	0.88824	0.00048	0.88920
channel_2000.out	0.200	No	0.88741	0.00044	0.88829
channel_2540.out	**0.254**	**No**	**0.88852**	**0.00044**	**0.88940**
channel_1300_h2ogap.out	0.130	Yes	0.88756	0.00044	0.88844
channel_1800_h2ogap.out	0.180	Yes	0.88804	0.00047	0.88898
channel_2540_h2ogap.out	0.254	Yes	0.88845	0.00047	0.88939

Table 6-64 11x11 Zirconium Water Channel Study Results

Filename	Water channel included?	k_{eff}	σ	$k_{eff} + 2\sigma$
channel_2540.out	**No**	**0.88852**	**0.00044**	**0.88940**
water_channel.out	Yes	0.88691	0.00045	0.88781

Table 6-65 11x11 Polyethylene Mass and Volume Fraction Calculations

Clad IR, cm	0.4130	Clad OR, cm	0.4700
Number of full length fuel rods	92	Length, cm	385.0
Number of long partial length fuel rods	8	Length, cm	236.8
Number of short partial length fuel rods	12	Length, cm	155.1

Poly Mass (kg/assembly)	Clad/Poly Radius (cm)	Thickness (cm)	VF_{clad}	VF_{poly}
0	0.4700	0	1.00000	0.00000
2.5	0.4923	0.0223	0.70108	0.29892
5.0	0.5136	0.0436	0.53994	0.46006
6.0	0.5218	0.0518	0.49487	0.50513
7.0	0.5300	0.0600	0.45618	0.54382
8.0	0.5380	0.0680	0.42339	0.57661
8.5	0.5419	0.0719	0.40891	0.59109
9.0	0.5459	0.0759	0.39495	0.60505
10.2	0.5552	0.0852	0.36557	0.63443

The following example is for a total polyethylene mass of 10.2 kg/assembly.

Total Polyethylene Volume = [(Total Fuel Rod Number) * (Polyethylene Area) * (Fuel Rod Length)]

Full length: Volume = $(92\text{rods}*\{\pi[(0.5552\text{cm})^2 - (0.4700\text{cm})^2]\}*385\text{cm}) = 9719.6\ \text{cm}^3$

Long Partial length: Volume = $(8\text{rods}*\{\pi[(0.5552\text{cm})^2 - (0.4700\text{cm})^2]\}*236.8) = 519.8\ \text{cm}^3$

Short Partial length: Volume = $(12\text{rods}*\{\pi[(0.5552\text{cm})^2 - (0.4700\text{cm})^2]\}*155.1) = 510.7\ \text{cm}^3$

Total: Volume = $9719.6 + 519.8 + 510.7 = 10750.1\ \text{cm}^3$

Total Polyethylene Mass = (Total Polyethylene Volume) * (Polyethylene Density), where density of polyethylene equivalent = 0.949 g/cm^3.

Total: Mass = $(10750\ \text{cm}^3) * 0.949\ \text{g/cm}^3 = 10202\ \text{g}$

Total Cladding Volume = [(Total Fuel Rod Number) * (Cladding Area) * (Fuel Rod Length)]

Full length: $\text{Volume}_{clad} = 92\text{rods}*\{\pi[(0.4700\text{cm})^2 - (0.4130\text{cm})^2]\}*385\text{cm} = 5600.6\ \text{cm}^3$

Long Partial length: $\text{Volume}_{clad} = 8\text{rods}*\{\pi[(0.4700\text{cm})^2 - (0.4130\text{cm})^2]\}*236.8\text{cm} = 299.5\ \text{cm}^3$

Short Partial length: $\text{Volume}_{clad} = 12\text{rods}*\{\pi[(0.4700\text{cm})^2 - (0.4130\text{cm})^2]\}*155.1\text{cm} = 294.3\ \text{cm}^3$

Total: $\text{Volume}_{clad} = 5600.6\ \text{cm}^3 + 299.5\ \text{cm}^3 + 294.3\ \text{cm}^3 = 6194.4\ \text{cm}^3$

Cladding Volume Fraction = Cladding Volume/(Cladding Volume + Polyethylene Volume)

Total: $VF_{clad} = 6194.4\text{cm}^3 / (6194.4\text{cm}^3 + 10750.1\text{cm}^3) = 0.36557$

Polyethylene Volume Fraction = Polyethylene Volume/(Cladding Volume + Polyethylene Volume)

Total: $VF_{poly} = 10750.1\text{cm}^3 / (6194.4\text{cm}^3 + 10750.1\text{cm}^3) = 0.63443$

Table 6-66 11x11 Polyethylene Mass Sensitivity Analysis Results

Filename	Polyethylene Mass (kg/assy)	k_{eff}	σ	k_{eff} + 2σ
poly_mass_000.out	0	0.88276	0.00048	0.88372
poly_mass_025.out	2.5	0.88425	0.00044	0.88513
poly_mass_050.out	5.0	0.88581	0.00046	0.88673
poly_mass_055.out	5.5	0.88496	0.00045	0.88586
poly_mass_060.out	6.0	0.88630	0.00044	0.88718
poly_mass_070.out	7.0	0.88715	0.00047	0.88809
poly_mass_080.out	8.0	0.88731	0.00046	0.88823
poly_mass_085.out	8.5	0.88718	0.00045	0.88808
poly_mass_090.out	9.0	0.88790	0.00048	0.88886
channel_2540.out	**10.2**	**0.88852**	**0.00044**	**0.88940**

Table 6-67 11x11 Fuel Rod Pitch Sensitivity Analysis Results

Filename	Change in pin pitch (%)	Pin Pitch (cm)	k_{eff}	σ	k_{eff} + 2σ
ppitch_min.out	-6.9	1.1130	0.83959	0.00050	0.84059
channel_2540.out	0	1.1950	0.88852	0.00044	0.88940
ppitch_041%.out	4.1	1.2440	0.91450	0.00046	0.91542
ppitch_050%.out	**5.0**	**1.2548**	**0.91996**	**0.00043**	**0.92082**

Table 6-68 11x11 Pellet Diameter Sensitivity Analysis Results

Filename	Pellet diameter (cm)	k_{eff}	σ	k_{eff} + 2σ
prad_7800.out	0.7800	0.88441	0.00049	0.88539
prad_8000.out	0.8000	0.88746	0.00048	0.88842
prad_8098.out	0.8098	0.88859	0.00052	0.88963
channel_2540.out	0.8110	0.88852	0.00044	0.88940
prad_8122.out	0.8122	0.88934	0.00043	0.89020
prad_8160.out	0.8160	0.88828	0.00044	0.88916
prad_8180.out	0.8180	0.88917	0.00047	0.89011
prad_8200.out	**0.8200**	**0.88952**	**0.00048**	**0.89048**

Table 6-69 11x11 Zirc and Polyethylene Volume Fractions, Varying Cladding ID

Fuel assembly parameters					
Cladding/Polyethylene OD, cm	1.1104		Clad OD, cm	0.9400	
Number of full length fuel rods	92		Length, cm	385.0	
Number of long partial length fuel rods	8		Length, cm	236.8	
Number of short partial length fuel rods	12		Length, cm	155.1	

Volume Fraction Calculations			
Clad inner diameter (cm)	Clad thickness (cm)	VF_{clad}	VF_{poly}
0.8110	0.0645	0.39265	0.60735
0.8140	0.0630	0.38746	0.61254
0.8220	0.0590	0.37307	0.62693
0.8260	0.0570	0.36557	0.63443
0.8300	0.0550	0.35785	0.64215
0.8400	0.0500	0.33751	0.66249
0.8500	0.0450	0.31558	0.68442
0.8700	0.0350	0.26613	0.73387
0.9000	0.0200	0.17400	0.82600
0.9400	0.0000	0.00000	1.00000

Table 6-70 11x11 Cladding ID Sensitivity Analysis Results

Filename	Clad inner diameter (cm)	Clad thickness (cm)	k_{eff}	σ	k_{eff} + 2σ
clad_thick_ID_8110.out	0.8110	0.0645	0.88528	0.00050	0.88628
clad_thick_ID_8140.out	0.8140	0.0630	0.88633	0.00043	0.88719
clad_thick_ID_8220.out	0.8220	0.0590	0.88821	0.00046	0.88913
channel_2540.out	0.8260	0.0570	0.88852	0.00044	0.88940
clad_thick_ID_8300.out	0.8300	0.0550	0.88957	0.00049	0.89055
clad_thick_ID_8400.out	**0.8400**	**0.0500**	**0.89191**	**0.00044**	**0.89279**
clad_thick_ID_8500.out	0.8500	0.0450	0.89424	0.00043	0.89510
clad_thick_ID_8700.out	0.8700	0.0350	0.90020	0.00048	0.90116
clad_thick_ID_9000.out	0.9000	0.0200	0.90712	0.00049	0.90810
clad_thick_ID_9400.out	0.9400	0.0000	0.91706	0.00051	0.91808

Table 6-71 11x11 Zirc and Polyethylene Volume Fractions, Varying Cladding OD

Fuel assembly parameters					
Clad ID, cm	0.8260				
Number of full length fuel rods	92		Length, cm	385.0	
Number of long partial length fuel rods	8		Length, cm	236.8	
Number of short partial length fuel rods	12		Length, cm	155.1	

Volume Fraction Calculations				
Clad outer diameter (cm)	Clad/poly diameter (cm)	Clad thickness (cm)	VF_{clad}	VF_{poly}
0.8260	1.0158	0.0000	0.00000	1.00000
0.8400	1.0272	0.0070	0.06255	0.93745
0.8750	1.0560	0.0245	0.19255	0.80745
0.9100	1.0852	0.0420	0.29437	0.70563
0.9200	1.0936	0.0470	0.31950	0.68050
0.9300	1.1020	0.0520	0.34320	0.65680
0.9350	1.1062	0.0545	0.35454	0.64546
0.9400	1.1104	0.0570	0.36557	0.63443
0.9450	1.1146	0.0595	0.37630	0.62370
0.9650	1.1316	0.0695	0.41613	0.58387
0.9850	1.1488	0.0795	0.45171	0.54829
1.0050	1.1660	0.0895	0.48392	0.51608
1.0358	1.1926	0.1049	0.52783	0.47217
1.0386	1.1950	0.1063	0.53156	0.46844

Table 6-72 11x11 Cladding OD Sensitivity Analysis Results

Filename	Clad outer diameter (cm)	Clad thickness (cm)	k_{eff}	σ	$k_{eff} + 2σ$
clad_thick_OD_08260.out	0.8260	0.0000	0.91500	0.00049	0.91598
clad_thick_OD_08400.out	0.8400	0.0070	0.91269	0.00046	0.91361
clad_thick_OD_08750.out	0.8750	0.0245	0.90355	0.00045	0.90445
clad_thick_OD_09100.out	0.9100	0.0420	0.89627	0.00046	0.89719
clad_thick_OD_09200.out	0.9200	0.0470	0.89326	0.00049	0.89424
clad_thick_OD_09300.out	**0.9300**	**0.0520**	**0.89093**	**0.00045**	**0.89183**
clad_thick_OD_09350.out	0.9350	0.0545	0.89064	0.00048	0.89160
channel_2540.out	0.9400	0.0570	0.88852	0.00044	0.88940
clad_thick_OD_09450.out	0.9450	0.0595	0.88782	0.00045	0.88872
clad_thick_OD_09650.out	0.9650	0.0695	0.88298	0.00044	0.88386
clad_thick_OD_09850.out	0.9850	0.0795	0.87673	0.00049	0.87771
clad_thick_OD_10050.out	1.0050	0.0895	0.87196	0.00043	0.87282
clad_thick_OD_10358.out	1.0358	0.1049	0.86185	0.00045	0.86275
clad_thick_OD_10386.out	1.0386	0.1063	0.86097	0.00048	0.86193

Table 6-73 11x11 Sensitivity Analysis Results for Partially Flooded Inner Container

Filename	# of fuel rows filled	k_{eff}	σ	k_{eff} + 2σ
rows_filled_01.out	1	0.74005	0.00042	0.74089
rows_filled_03.out	3	0.79346	0.00049	0.79444
rows_filled_05.out	5	0.85444	0.00050	0.85544
rows_filled_07.out	7	0.90061	0.00051	0.90163
rows_filled_09.out	9	0.92082	0.00049	0.92180
rows_filled_10.out	10	0.92672	0.00046	0.92764
worst_param.out	**11 (all)**	**0.92675**	**0.00053**	**0.92781**

Table 6-74 11x11 Sensitivity Analysis Results for Thermal Insulator Material

Filename	Insulator material	k_{eff}	σ	k_{eff} + 2σ
worst_param.out	**Alumina Silicate**	**0.92675**	**0.00053**	**0.92781**
therm_ins_to_void.out	Void	0.92225	0.00050	0.92325
therm_ins_to_water.out	Full density water	0.81792	0.00047	0.81886

Table 6-75 11x11 Sensitivity Analysis Results for Polyethylene Liner

Filename	Assembly Orientation in Right Compartment [a]	Fuel Channel?	Polyethylene liner thickness (cm)	Fraction polyethylene-to-water	k_{eff}	σ	k_{eff} + 2σ
poly_liner_000_cc.out	centered	yes	0	0.00	0.92303	0.00048	0.92399
poly_liner_020_cc.out	centered	yes	0.2	0.12	0.93105	0.00044	0.93193
poly_liner_040_cc.out	centered	yes	0.4	0.24	0.93749	0.00044	0.93837
poly_liner_060_cc.out	centered	yes	0.6	0.36	0.94371	0.00048	0.94467
poly_liner_080_cc.out	centered	yes	0.8	0.48	0.94852	0.00045	0.94942
poly_liner_100_cc.out	centered	yes	1.0	0.60	0.95019	0.00048	0.95115
poly_liner_110_cc.out	centered	yes	1.1	0.66	0.95110	0.00043	0.95196
poly_liner_120_cc.out	**centered**	**yes**	**1.2**	**0.72**	**0.95170**	**0.00053**	**0.95276**
poly_liner_130_cc.out	centered	yes	1.3	0.78	0.95173	0.00046	0.95265
poly_liner_140_cc.out	centered	yes	1.4	0.84	0.95052	0.00052	0.95156
poly_liner_150_cc.out	centered	yes	1.5	0.91	0.94894	0.00049	0.94992
poly_liner_160_cc.out	centered	yes	1.6	0.97	0.94711	0.00046	0.94803
poly_liner_full_cc.out	centered	yes	1.657	1.00	0.94532	0.00047	0.94626
poly_liner_000_cn.out	centered	no	0	0.00	0.91624	0.00044	0.91712
poly_liner_020_cn.out	centered	no	0.2	0.10	0.92450	0.00046	0.92542
poly_liner_040_cn.out	centered	no	0.4	0.21	0.93153	0.00054	0.93261
poly_liner_060_cn.out	centered	no	0.6	0.31	0.93777	0.00047	0.93871
poly_liner_080_cn.out	centered	no	0.8	0.42	0.94333	0.00044	0.94421
poly_liner_100_cn.out	centered	no	1.0	0.52	0.94711	0.00047	0.94805
poly_liner_110_cn.out	centered	no	1.1	0.58	0.94890	0.00052	0.94994
poly_liner_120_cn.out	centered	no	1.2	0.63	0.94997	0.00048	0.95093
poly_liner_130_cn.out	centered	no	1.3	0.68	0.95090	0.00045	0.95180
poly_liner_140_cn.out	centered	no	1.4	0.73	0.95126	0.00046	0.95218
poly_liner_150_cn.out	centered	no	1.5	0.78	0.95131	0.00048	0.95227
poly_liner_160_cn.out	centered	no	1.6	0.84	0.95026	0.00046	0.95118
poly_liner_170_cn.out	centered	no	1.7	0.89	0.94880	0.00044	0.94968
poly_liner_180_cn.out	centered	no	1.8	0.94	0.94747	0.00049	0.94845
poly_liner_full_cn.out	centered	no	1.911	1.00	0.94407	0.00045	0.94497

Table 6-75 11x11 Sensitivity Analysis Results for Polyethylene Liner (continued)

Filename	Assembly Orientation in Right Compartment [a]	Fuel Channel?	Polyethylene liner thickness (cm)	Fraction polyethylene-to-water	k_{eff}	σ	$k_{eff} + 2σ$
poly_liner_000_sc.out	shifted	yes	0	0.00	0.92677	0.00046	0.92769
poly_liner_020_sc.out	shifted	yes	0.2	0.12	0.93087	0.00046	0.93179
poly_liner_040_sc.out	shifted	yes	0.4	0.24	0.93609	0.00048	0.93705
poly_liner_060_sc.out	shifted	yes	0.6	0.36	0.94036	0.00048	0.94132
poly_liner_080_sc.out	shifted	yes	0.8	0.48	0.94399	0.00043	0.94485
poly_liner_100_sc.out	shifted	yes	1.0	0.60	0.94757	0.00043	0.94843
poly_liner_110_sc.out	shifted	yes	1.1	0.66	0.94835	0.00049	0.94933
poly_liner_120_sc.out	shifted	yes	1.2	0.72	0.94879	0.00050	0.94979
poly_liner_130_sc.out	shifted	yes	1.3	0.78	0.94907	0.00046	0.94999
poly_liner_140_sc.out	shifted	yes	1.4	0.84	0.94794	0.00044	0.94882
poly_liner_150_sc.out	shifted	yes	1.5	0.91	0.94746	0.00047	0.94840
poly_liner_160_sc.out	shifted	yes	1.6	0.97	0.94647	0.00047	0.94741
poly_liner_full_sc.out	shifted	yes	1.657	1.00	0.94563	0.00049	0.94661
poly_liner_000_sn.out	shifted	no	0	0.00	0.92242	0.00046	0.92334
poly_liner_020_sn.out	shifted	no	0.2	0.10	0.92716	0.00046	0.92808
poly_liner_040_sn.out	shifted	no	0.4	0.21	0.93223	0.00047	0.93317
poly_liner_060_sn.out	shifted	no	0.6	0.31	0.93651	0.00046	0.93743
poly_liner_080_sn.out	shifted	no	0.8	0.42	0.94041	0.00052	0.94145
poly_liner_100_sn.out	shifted	no	1.0	0.52	0.94493	0.00044	0.94581
poly_liner_110_sn.out	shifted	no	1.1	0.58	0.94662	0.00045	0.94752
poly_liner_120_sn.out	shifted	no	1.2	0.63	0.94676	0.00051	0.94778
poly_liner_130_sn.out	shifted	no	1.3	0.68	0.94852	0.00046	0.94944
poly_liner_140_sn.out	shifted	no	1.4	0.73	0.94822	0.00053	0.94928
poly_liner_150_sn.out	shifted	no	1.5	0.78	0.94861	0.00050	0.94961
poly_liner_160_sn.out	shifted	no	1.6	0.84	0.94844	0.00047	0.94938
poly_liner_170_sn.out	shifted	no	1.7	0.89	0.94764	0.00046	0.94856
poly_liner_180_sn.out	shifted	no	1.8	0.94	0.94698	0.00043	0.94784
poly_liner_full_sn.out	shifted	no	1.911	1.00	0.94500	0.00045	0.94590

[a] Assembly in left compartment is centered.

Table 6-76 11x11 Bottom Layer “2-D” Analysis Results

Filename	^{235}U wt%	# Gd rods	Pattern	k_{eff}	σ	$k_{eff} + 2\sigma$
FandPLRs_02gd_A1.out	3.2	2	A1	0.94716	0.00040	0.94796
FandPLRs_02gd_A2.out	3.2	2	A2	0.94639	0.00050	0.94739
FandPLRs_02gd_A4.out	3.2	2	A4	0.94728	0.00048	0.94824
FandPLRs_03gd_A1.out	3.3	3	A1	0.94725	0.00050	0.94825
FandPLRs_03gd_A2.out	3.3	3	A2	0.94549	0.00048	0.94645
FandPLRs_03gd_B3.out	3.3	3	B3	0.94248	0.00044	0.94336
FandPLRs_04gd_A1.out	3.5	4	A1	0.94881	0.00045	0.94971
FandPLRs_04gd_A2.out	3.5	4	A2	0.95449	0.00045	0.95539
FandPLRs_04gd_B3.out	3.5	4	B3	0.95015	0.00047	0.95109
FandPLRs_05gd_A1.out	3.6	5	A1	0.94950	0.00050	0.95050
FandPLRs_05gd_A2.out	3.6	5	A2	0.94886	0.00047	0.94980
FandPLRs_05gd_B3.out	3.6	5	B3	0.94806	0.00045	0.94896
FandPLRs_06gd_A2.out	3.8	6	A2	0.95510	0.00043	0.95596
FandPLRs_06gd_A3.out	3.8	6	A3	0.95397	0.00049	0.95495
FandPLRs_06gd_E1.out	3.8	6	E1	0.94981	0.00051	0.95083
FandPLRs_07gd_A1.out	3.9	7	A1	0.94977	0.00048	0.95073
FandPLRs_07gd_A3.out	3.9	7	A3	0.95213	0.00046	0.95305
FandPLRs_07gd_E1.out	3.9	7	E1	0.95044	0.00043	0.95130
FandPLRs_08gd_A2.out	4.1	8	A2	0.95357	0.00048	0.95453
FandPLRs_08gd_B1.out	4.1	8	B1	0.95784	0.00048	0.95880
FandPLRs_08gd_E1.out	4.1	8	E1	0.95462	0.00046	0.95554
FandPLRs_09gd_A2.out	4.2	9	A2	0.95166	0.00043	0.95252
FandPLRs_09gd_B1.out	4.2	9	B1	0.95356	0.00049	0.95454
FandPLRs_09gd_B3.out	4.2	9	B3	0.95174	0.00051	0.95276
FandPLRs_10gd_A2.out	4.4	10	A2	0.95594	0.00044	0.95682
FandPLRs_10gd_C2.out	4.4	10	C2	0.95262	0.00041	0.95344
FandPLRs_10gd_C5.out	4.4	10	C5	0.95048	0.00057	0.95162
FandPLRs_11gd_B1.out	4.6	11	B1	0.95642	0.00044	0.95730
FandPLRs_11gd_B2.out	4.6	11	B2	0.95622	0.00044	0.95710
FandPLRs_11gd_B3.out	4.6	11	B3	0.95311	0.00046	0.95403
FandPLRs_12gd_A2.out	4.8	12	A2	0.95692	0.00051	0.95794
FandPLRs_12gd_B2.out	4.8	12	B2	0.95926	0.00043	0.96012
FandPLRs_12gd_D2.out	4.8	12	D2	0.95303	0.00044	0.95391
FandPLRs_13gd_A2.out	5.0	13	A2	0.95763	0.00051	0.95865
FandPLRs_13gd_C3.out	5.0	13	C3	0.96128	0.00047	0.96222
FandPLRs_13gd_F1.out	5.0	13	F1	0.95707	0.00048	0.95803

Table 6-77 11x11 Middle Layer “2-D” Analysis Results

Filename	^{235}U wt%	# Gd rods	Pattern	k_{eff}	σ	k_{eff} + 2σ
LPL_02gd_A1.out	3.2	2	A1	0.92677	0.00042	0.92761
LPL_02gd_A4.out	3.2	2	A4	0.92843	0.00044	0.92931
LPL_02gd_B2.out	3.2	2	B2	0.92546	0.00043	0.92632
LPL_03gd_A1.out	3.3	3	A1	0.92806	0.00054	0.92914
LPL_03gd_B1.out	3.3	3	B1	0.92046	0.00046	0.92138
LPL_03gd_B2.out	3.3	3	B2	0.92201	0.00047	0.92295
LPL_04gd_A1.out	3.5	4	A1	0.92787	0.00044	0.92875
LPL_04gd_A3.out	3.5	4	A3	0.92828	0.00044	0.92916
LPL_04gd_A4.out	3.5	4	A4	0.92391	0.00042	0.92475
LPL_05gd_A1.out	3.6	5	A1	0.92765	0.00046	0.92857
LPL_05gd_A2.out	3.6	5	A2	0.92282	0.00045	0.92372
LPL_05gd_C1.out	3.6	5	C1	0.92173	0.00048	0.92269
LPL_06gd_A1.out	3.8	6	A1	0.92793	0.00050	0.92893
LPL_06gd_B1.out	3.8	6	B1	0.92678	0.00049	0.92776
LPL_06gd_B3.out	3.8	6	B3	0.92691	0.00044	0.92779
LPL_07gd_A1.out	3.9	7	A1	0.92803	0.00050	0.92903
LPL_07gd_A2.out	3.9	7	A2	0.92316	0.00043	0.92402
LPL_07gd_B1.out	3.9	7	B1	0.92456	0.00045	0.92546
LPL_08gd_A1.out	4.1	8	A1	0.92721	0.00048	0.92817
LPL_08gd_A2.out	4.1	8	A2	0.92866	0.00046	0.92958
LPL_08gd_A3.out	4.1	8	A3	0.92578	0.00047	0.92672
LPL_09gd_A1.out	4.2	9	A1	0.92598	0.00047	0.92692
LPL_09gd_B1.out	4.2	9	B1	0.92178	0.00047	0.92272
LPL_09gd_C2.out	4.2	9	C2	0.92164	0.00048	0.92260
LPL_10gd_A1.out	4.4	10	A1	0.92439	0.00044	0.92527
LPL_10gd_A2.out	4.4	10	A2	0.92657	0.00051	0.92759
LPL_10gd_A4.out	4.4	10	A4	0.92394	0.00047	0.92488
LPL_11gd_A1.out	4.6	11	A1	0.92859	0.00043	0.92945
LPL_11gd_B2.out	4.6	11	B2	0.92733	0.00051	0.92835
LPL_11gd_D3.out	4.6	11	D3	0.92450	0.00050	0.92550
LPL_12gd_A2.out	4.8	12	A2	0.93001	0.00047	0.93095
LPL_12gd_B1.out	4.8	12	B1	0.92732	0.00041	0.92814
LPL_12gd_C4.out	4.8	12	C4	0.92629	0.00050	0.92729
LPL_13gd_A3.out	5.0	13	A3	0.92655	0.00048	0.92751
LPL_13gd_B1.out	5.0	13	B1	0.93041	0.00046	0.93133
LPL_13gd_B2.out	5.0	13	B2	0.92729	0.00045	0.92819

Table 6-78 11x11 Top Layer “2-D” Analysis Results

Filename	^{235}U wt%	# Gd rods	Pattern	k_{eff}	σ	k_{eff} + 2σ
FLRs_02gd_A1.out	3.2	2	A1	0.91924	0.00052	0.92028
FLRs_02gd_A3.out	3.2	2	A3	0.92021	0.00041	0.92103
FLRs_02gd_B1.out	3.2	2	B1	0.91673	0.00046	0.91765
FLRs_03gd_A1.out	3.3	3	A1	0.92143	0.00045	0.92233
FLRs_03gd_A3.out	3.3	3	A3	0.91417	0.00042	0.91501
FLRs_03gd_B1.out	3.3	3	B1	0.91395	0.00041	0.91477
FLRs_04gd_A1.out	3.5	4	A1	0.92048	0.00044	0.92136
FLRs_04gd_A3.out	3.5	4	A3	0.92087	0.00042	0.92171
FLRs_04gd_B1.out	3.5	4	B1	0.91466	0.00039	0.91544
FLRs_05gd_A1.out	3.6	5	A1	0.92043	0.00040	0.92123
FLRs_05gd_A2.out	3.6	5	A2	0.91335	0.00044	0.91423
FLRs_05gd_B2.out	3.6	5	B2	0.91304	0.00046	0.91396
FLRs_06gd_A1.out	3.8	6	A1	0.91807	0.00050	0.91907
FLRs_06gd_A3.out	3.8	6	A3	0.91919	0.00046	0.92011
FLRs_06gd_B2.out	3.8	6	B2	0.91962	0.00045	0.92052
FLRs_07gd_A1.out	3.9	7	A1	0.91680	0.00046	0.91772
FLRs_07gd_A2.out	3.9	7	A2	0.91669	0.00044	0.91757
FLRs_07gd_B3.out	3.9	7	B3	0.91214	0.00046	0.91306
FLRs_08gd_A1.out	4.1	8	A1	0.91598	0.00044	0.91686
FLRs_08gd_B2.out	4.1	8	B2	0.91602	0.00041	0.91684
FLRs_08gd_D1.out	4.1	8	D1	0.91573	0.00044	0.91661
FLRs_09gd_A1.out	4.2	9	A1	0.91535	0.00045	0.91625
FLRs_09gd_A2.out	4.2	9	A2	0.91121	0.00045	0.91211
FLRs_09gd_B3.out	4.2	9	B3	0.90798	0.00044	0.90886
FLRs_10gd_A1.out	4.4	10	A1	0.91104	0.00046	0.91196
FLRs_10gd_B2.out	4.4	10	B2	0.91242	0.00042	0.91326
FLRs_10gd_B4.out	4.4	10	B4	0.91047	0.00050	0.91147
FLRs_11gd_A1.out	4.6	11	A1	0.91520	0.00054	0.91628
FLRs_11gd_A2.out	4.6	11	A2	0.91331	0.00044	0.91419
FLRs_11gd_A3.out	4.6	11	A3	0.91092	0.00042	0.91176
FLRs_12gd_A2.out	4.8	12	A2	0.91032	0.00045	0.91122
FLRs_12gd_B2.out	4.8	12	B2	0.91117	0.00045	0.91207
FLRs_12gd_B4.out	4.8	12	B4	0.91193	0.00047	0.91287
FLRs_13gd_A2.out	5.0	13	A2	0.91337	0.00051	0.91439
FLRs_13gd_A3.out	5.0	13	A3	0.91117	0.00045	0.91207
FLRs_13gd_A4.out	5.0	13	A4	0.91044	0.00043	0.91130

Table 6-79 11x11 Gadolinia-Urania Analysis Results

Filename	^{235}U wt%	# Gd rods	Axial Pattern			k_{eff}	σ	k_{eff} + 2σ
			Bottom	Middle	Top			
5wt_13gd.out	**5.0**	**13**	**C3**	**B1**	**A2**	**0.93710**	**0.00050**	**0.93810**
48wt_12gd_fullA2.out	4.8	12	B2	A2	A2	0.93550	0.00046	0.93642
48wt_12gd_fullB2.out	4.8	12	B2	A2	B2	0.93576	0.00048	0.93672
48wt_12gd_fullB4.out	**4.8**	**12**	**B2**	**A2**	**B4**	**0.93599**	**0.00047**	**0.93693**
46wt_11gd_B1-A1-A1.out	**4.6**	**11**	**B1**	**A1**	**A1**	**0.93582**	**0.00047**	**0.93676**
46wt_11gd_B1-B2-A1.out	4.6	11	B1	B2	A1	0.93548	0.00050	0.93648
46wt_11gd_B2-A1-A1.out	4.6	11	B2	A1	A1	0.93493	0.00047	0.93587
46wt_11gd_B2-B2-A1.out	4.6	11	B2	B2	A1	0.93476	0.00042	0.93560
44wt_10gd_fullA1.out	4.4	10	A2	A2	A1	0.93413	0.00048	0.93509
44wt_10gd_fullB2.out	**4.4**	**10**	**A2**	**A2**	**B2**	**0.93471**	**0.00044**	**0.93559**
42wt_09gd.out	**4.2**	**9**	**B1**	**A1**	**A1**	**0.93341**	**0.00045**	**0.93431**
41wt_08gd_fullA1.out	4.1	8	B1	A2	A1	0.93683	0.00046	**0.93775**
41wt_08gd_fullB2.out	4.1	8	B1	A2	B2	0.93662	0.00042	0.93746
41wt_08gd_fullD1.out	4.1	8	B1	A2	D1	0.93589	0.00043	0.93675
39wt_07gd_fullA1.out	**3.9**	**7**	**A3**	**A1**	**A1**	**0.93417**	**0.00046**	**0.93509**
39wt_07gd_fullA2.out	3.9	7	A3	A1	A2	0.93403	0.00047	0.93497
38wt_06gd_A2_A1_A3.out	3.8	6	A2	A1	A3	0.93579	0.00046	0.93671
38wt_06gd_A2_A1_B2.out	**3.8**	**6**	**A2**	**A1**	**B2**	**0.93684**	**0.00043**	**0.93770**
38wt_06gd_A2_B1_B2.out	3.8	6	A2	B1	B2	0.93620	0.00045	0.93710
38wt_06gd_A2_B3_A3.out	3.8	6	A2	B3	A3	0.93662	0.00050	0.93762
38wt_06gd_A2_B3_B2.out	3.8	6	A2	B3	B2	0.93545	0.00050	0.93645
38wt_06gd_A3_A1_B2.out	3.8	6	A3	A1	B2	0.93551	0.00051	0.93653
38wt_06gd_A3_B3_A3.out	3.8	6	A3	B3	A3	0.93520	0.00048	0.93616
36wt_05gd_botA1.out	3.6	5	A1	A1	A1	0.93372	0.00048	0.93468
36wt_05gd_botA2.out	**3.6**	**5**	**A2**	**A1**	**A1**	**0.93420**	**0.00043**	**0.93506**
36wt_05gd_botB3.out	3.6	5	B3	A1	A1	0.93364	0.00046	0.93456
35wt_04gd_A2-A1-A1.out	3.5	4	A2	A1	A1	0.93596	0.00048	0.93692
35wt_04gd_A2-A1-A3.out	3.5	4	A2	A1	A3	0.93602	0.00050	0.93702
35wt_04gd_A2-A3-A1.out	3.5	4	A2	A3	A1	0.93499	0.00043	0.93585
35wt_04gd_A2-A3-A3.out	**3.5**	**4**	**A2**	**A3**	**A3**	**0.93664**	**0.00044**	**0.93752**
33wt_03gd.out	**3.3**	**3**	**A1**	**A1**	**A1**	**0.93355**	**0.00047**	**0.93449**
32wt_02gd_A1-A1-A1.out	3.2	2	A1	A1	A1	0.93268	0.00046	0.93360
32wt_02gd_A1-A4-A1.out	3.2	2	A1	A4	A1	0.93236	0.00043	0.93322
32wt_02gd_A1-A4-A3.out	3.2	2	A1	A4	A3	0.93310	0.00045	0.93400
32wt_02gd_A2-A4-A3.out	3.2	2	A2	A4	A3	0.93276	0.00044	0.93364
32wt_02gd_A4-A1-A3.out	3.2	2	A4	A1	A3	0.93285	0.00043	0.93371
32wt_02gd_A4-A4-A1.out	**3.2**	**2**	**A4**	**A4**	**A1**	**0.93320**	**0.00042**	**0.93404**
32wt_02gd_A4-A4-A3.out	3.2	2	A4	A4	A3	0.93290	0.00054	0.93398
29wt_00gd.out	**2.9**	**0**	**---**	**---**	**---**	**0.93500**	**0.00048**	**0.93596**
5-5-33wt_13-13-3gd.out	**5 / 5 / 3.3 [a]**	**13 / 13 / 3 [a]**	**C3**	**B1**	**A1**	**0.93855**	**0.00044**	**0.93943**

[a] Values provided for each lattice region as bottom / middle / top.

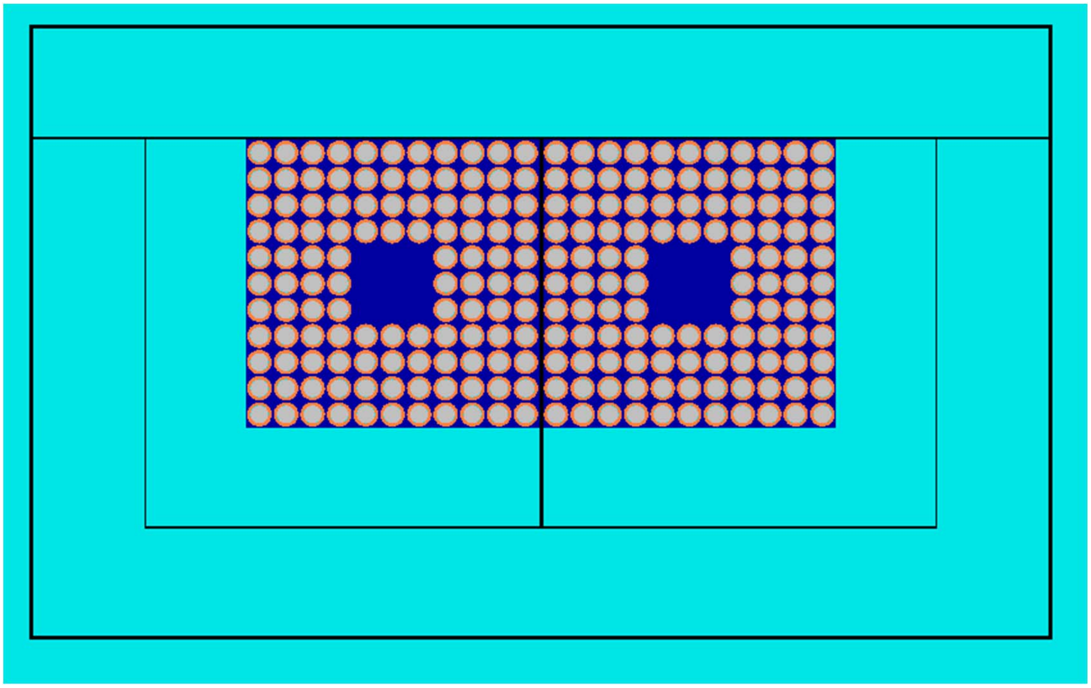

Figure 6-55 Fuel Assembly Orientation 1

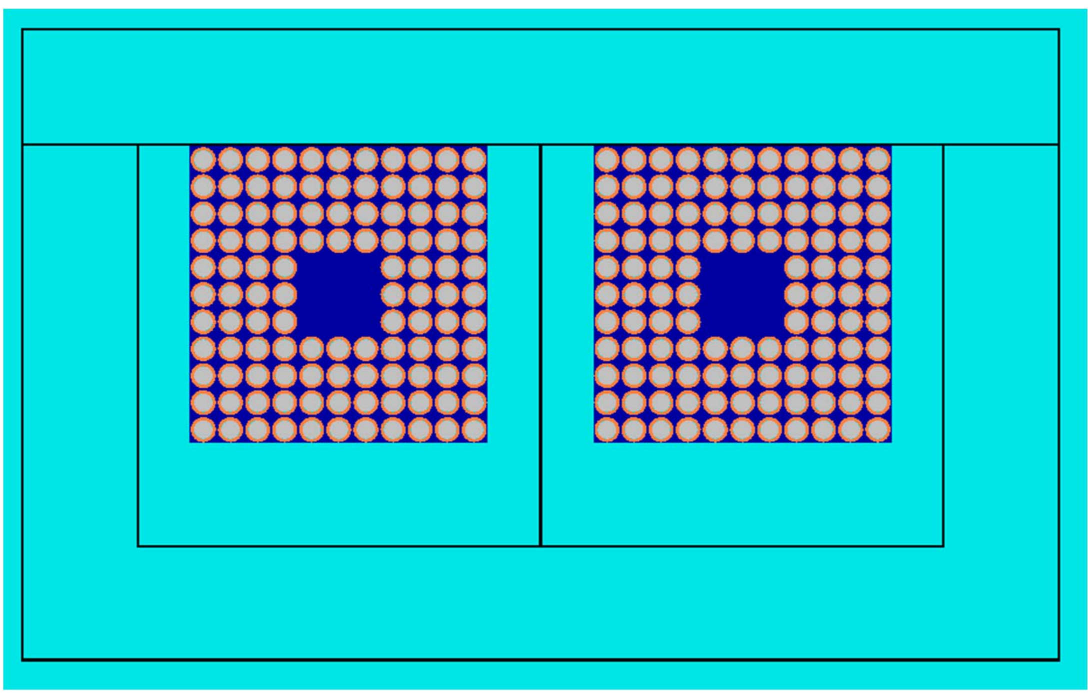

Figure 6-56 Fuel Assembly Orientation 2

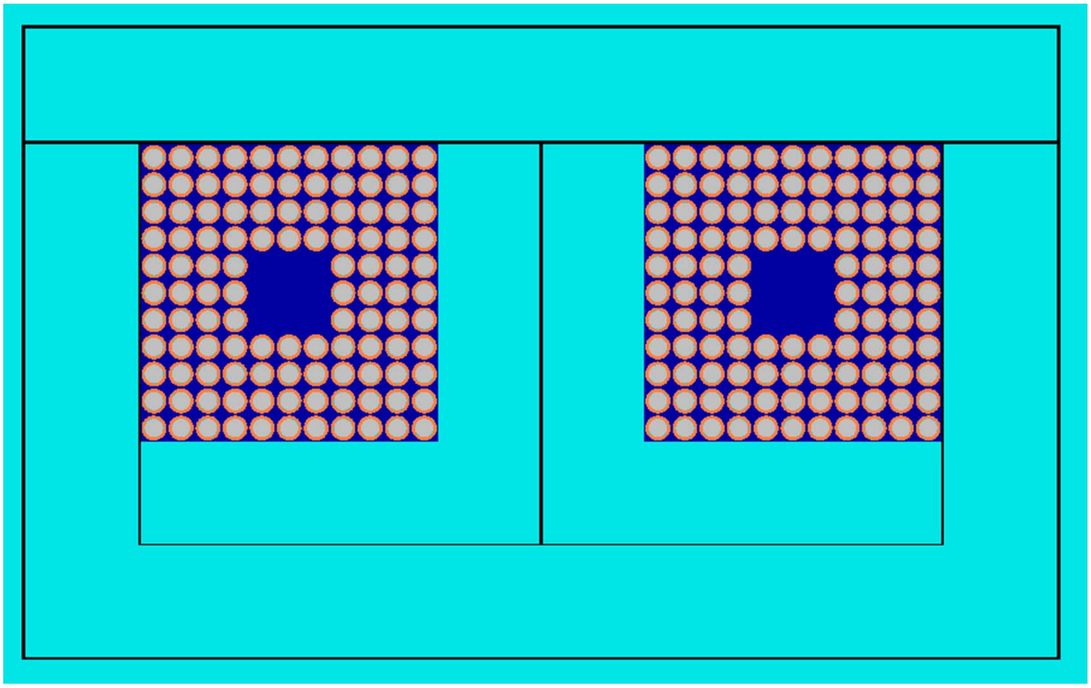

Figure 6-57 Fuel Assembly Orientation 3

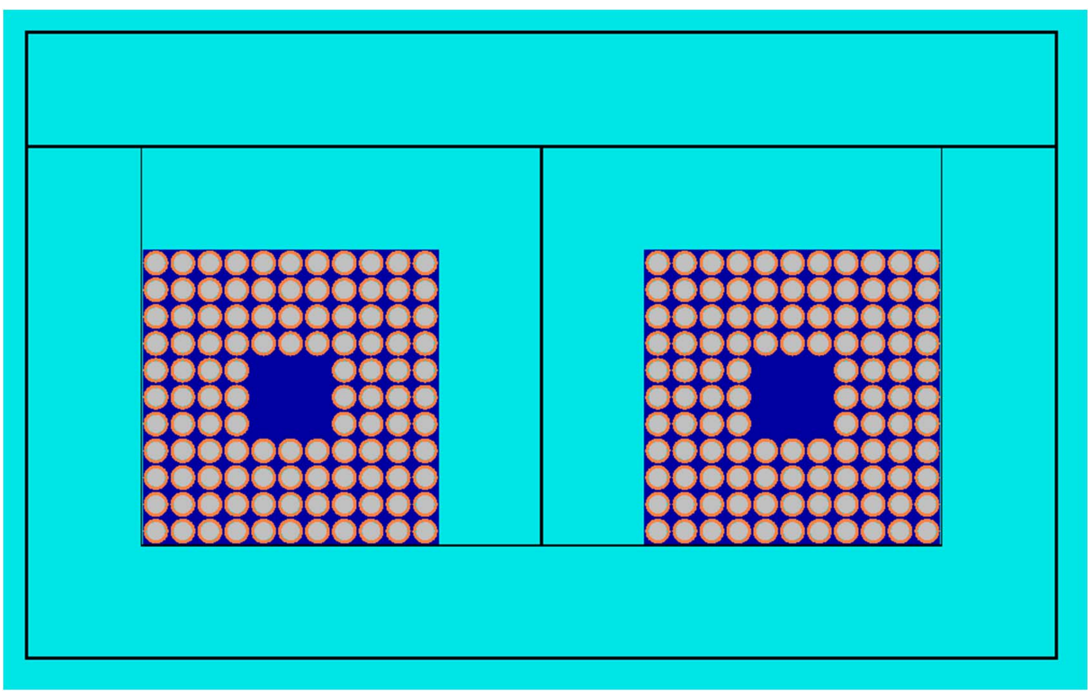

Figure 6-58 Fuel Assembly Orientation 4

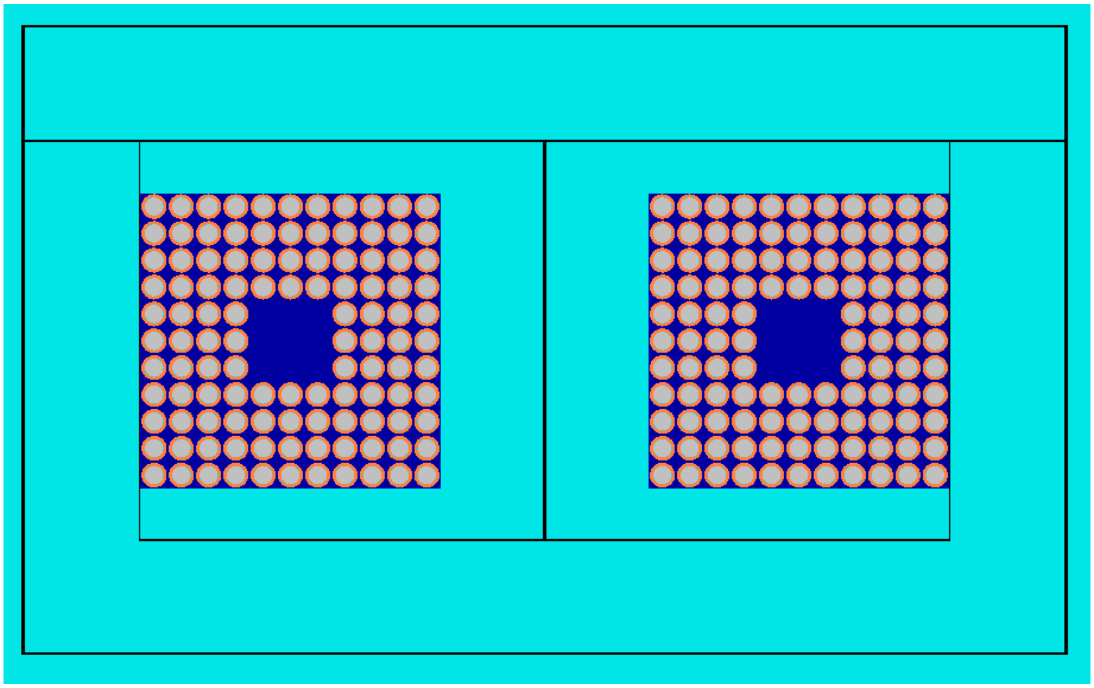

Figure 6-59 Fuel Assembly Orientation 5

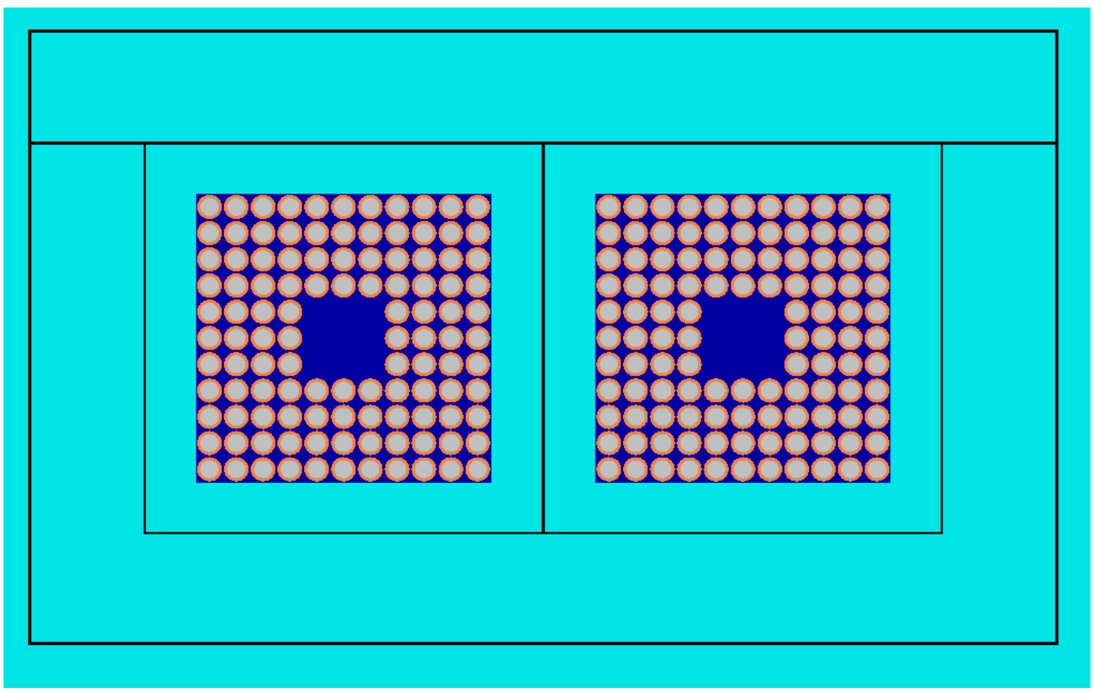

Figure 6-60 Fuel Assembly Orientation 6

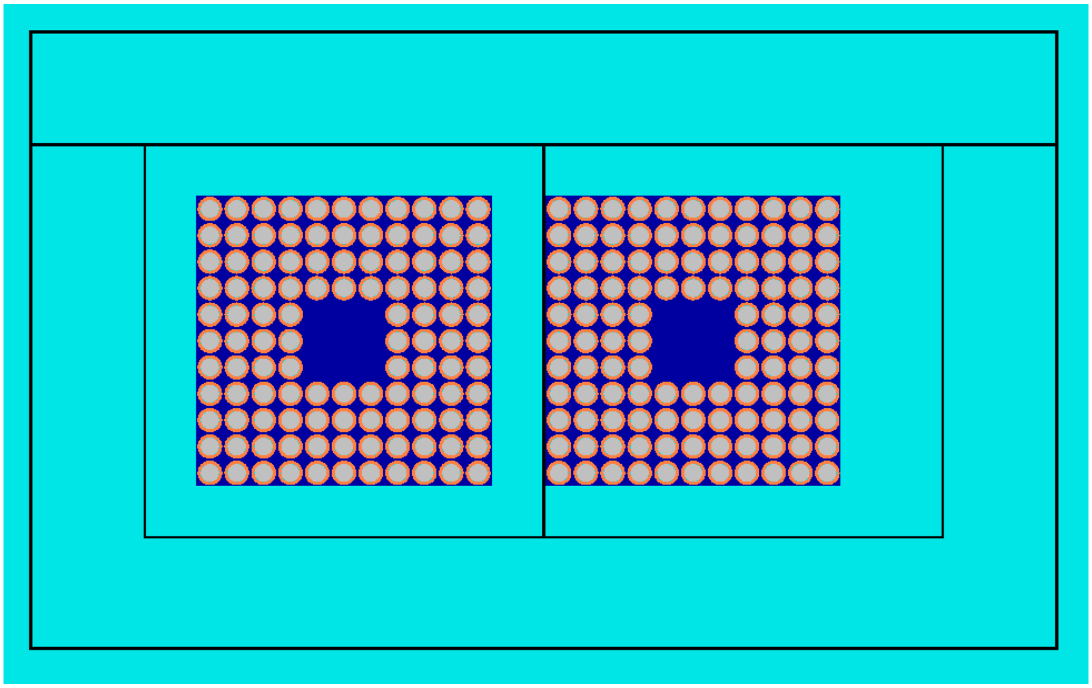

Figure 6-61 Fuel Assembly Orientation 7

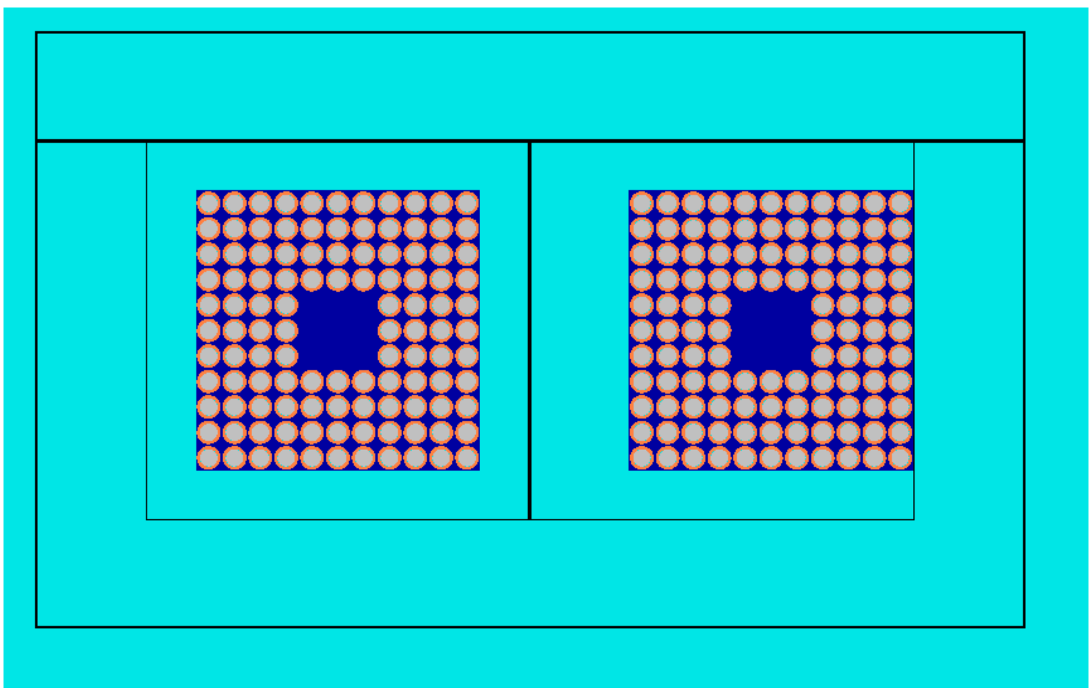

Figure 6-62 Fuel Assembly Orientation 8

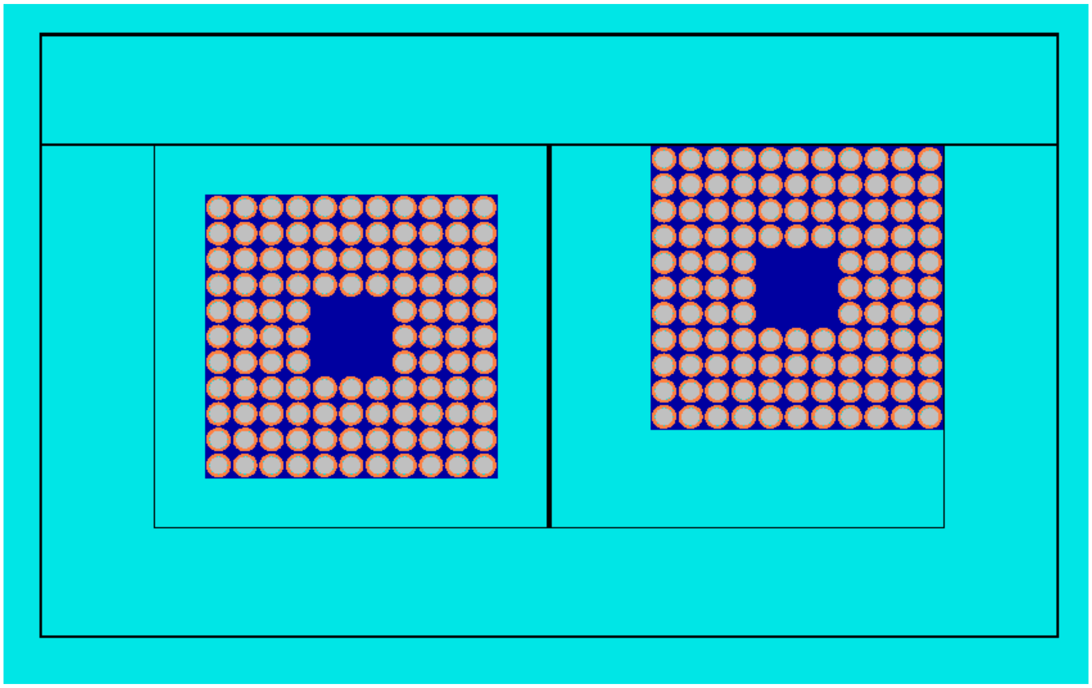

Figure 6-63 Fuel Assembly Orientation 9

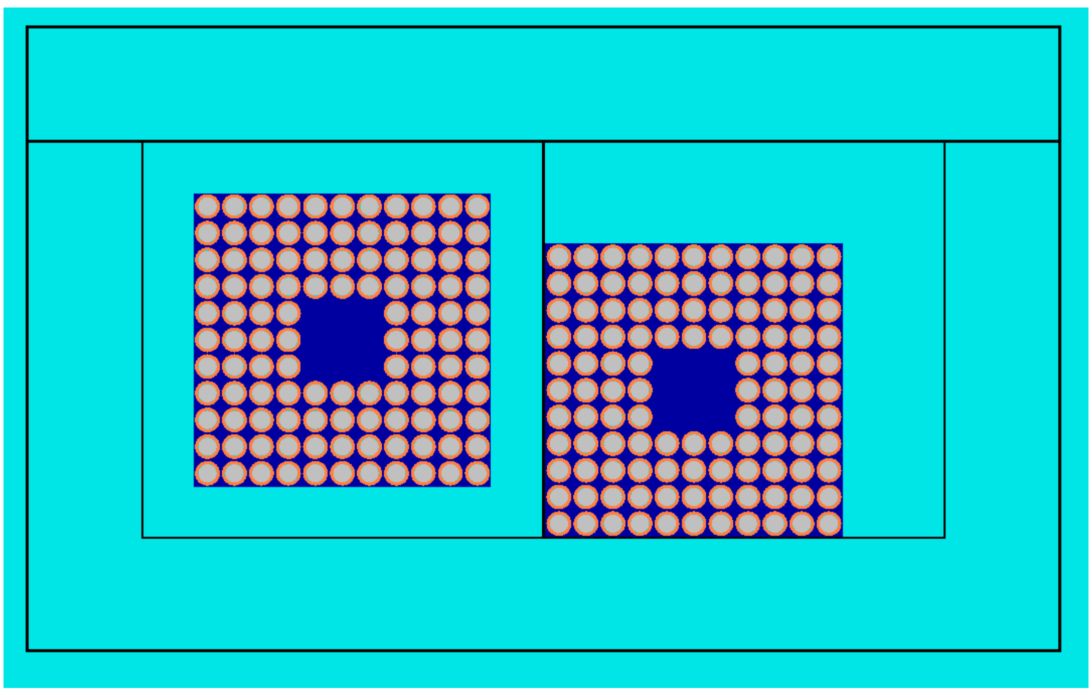

Figure 6-64 Fuel Assembly Orientation 10

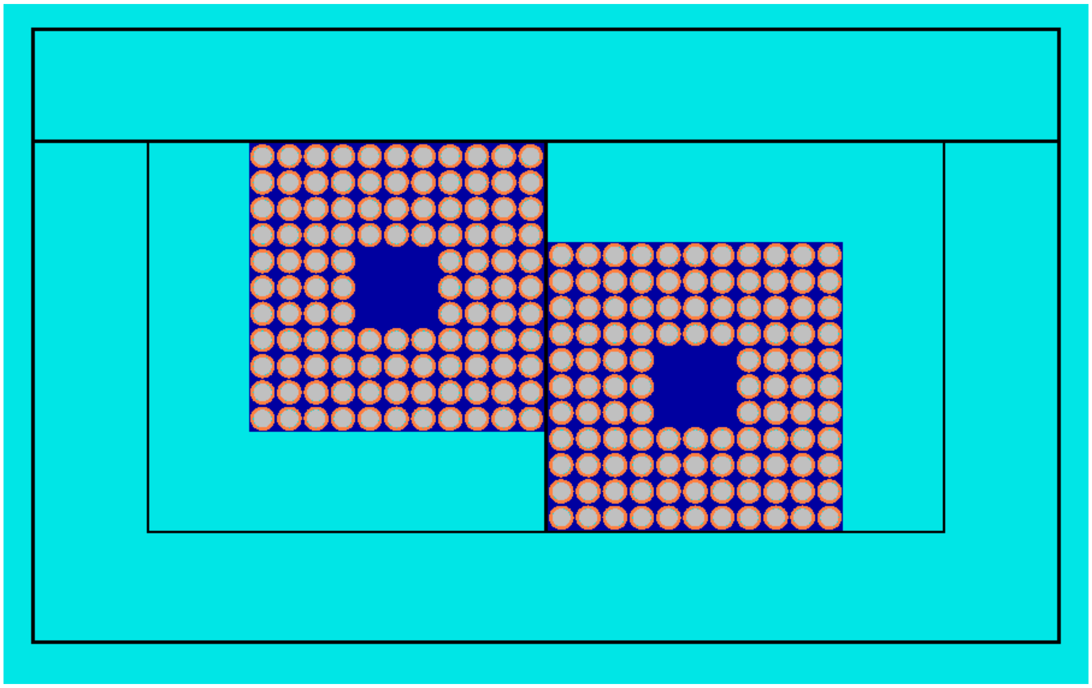

Figure 6-65 Fuel Assembly Orientation 11

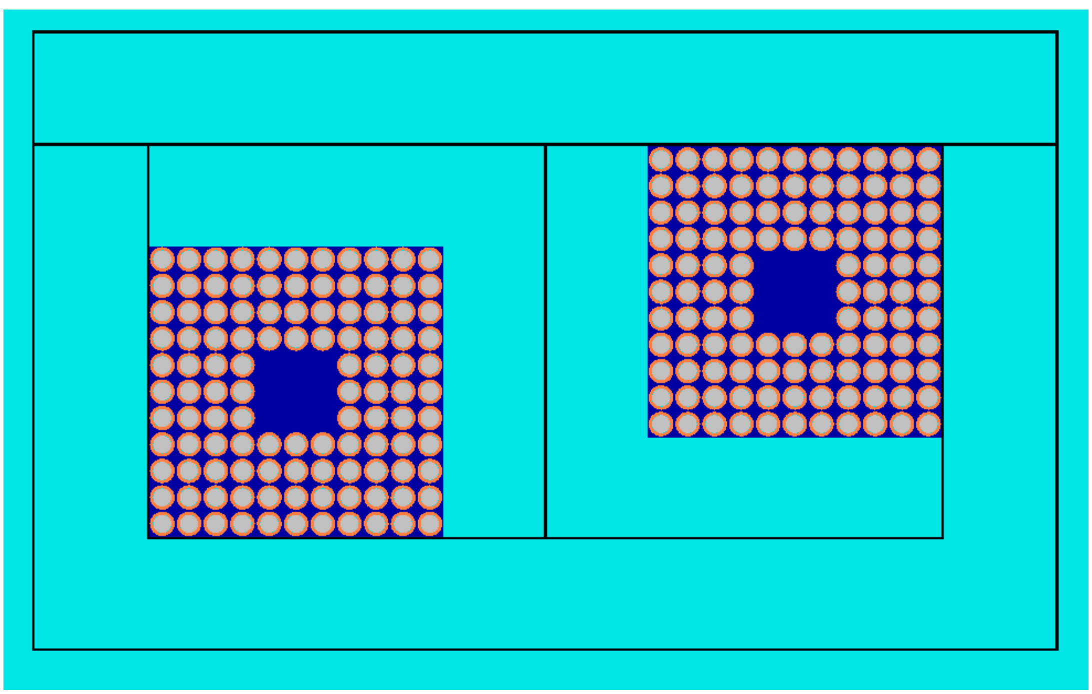

Figure 6-66 Fuel Assembly Orientation 12

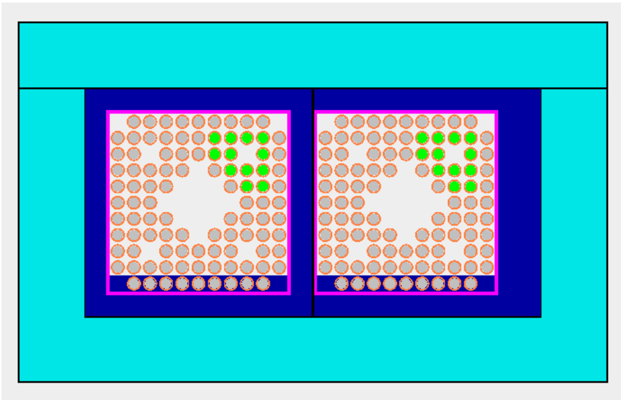

1 Fuel Row Covered with H_2O

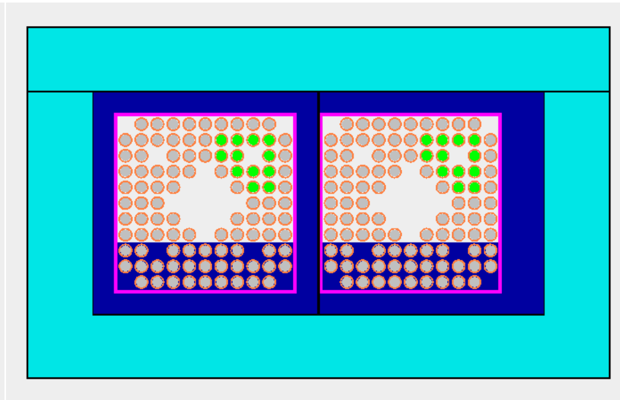

3 Fuel Rows Covered with H_2O

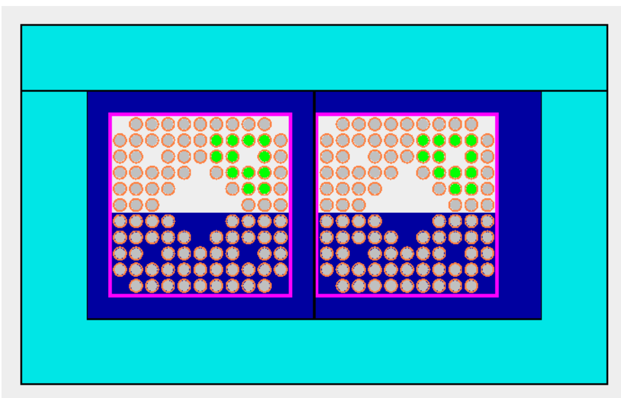

5 Fuel Rows Covered with H_2O

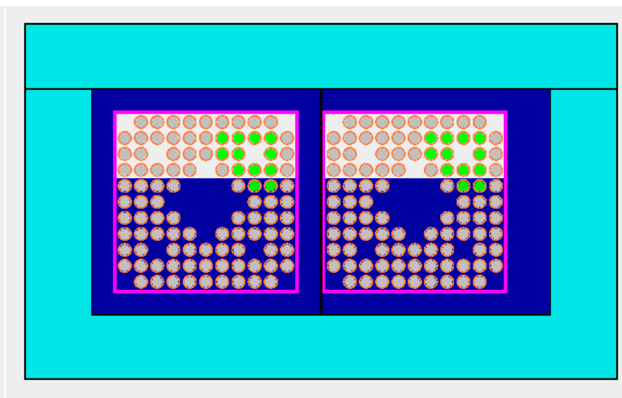

7 Fuel Rows Covered with H_2O

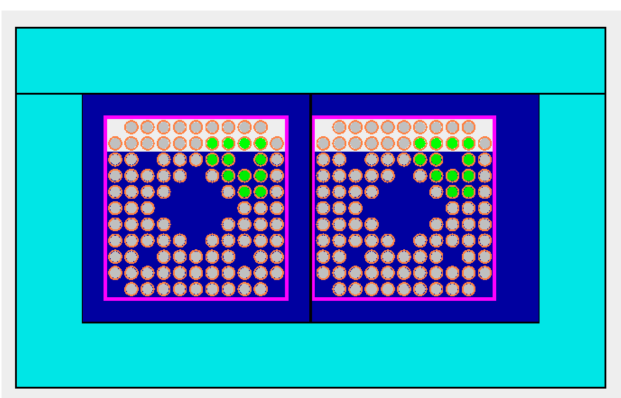

9 Fuel Rows Covered with H_2O

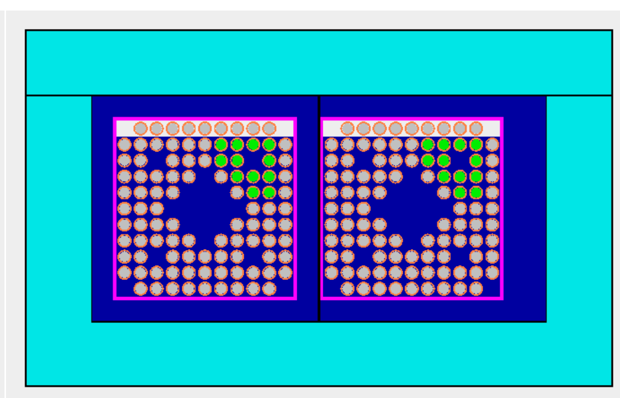

10 Fuel Rows Covered with H_2O

Figure 6-67 Inner Container Partial Flooding

Bottom Axial Layer (Full and Partial Length Rods):

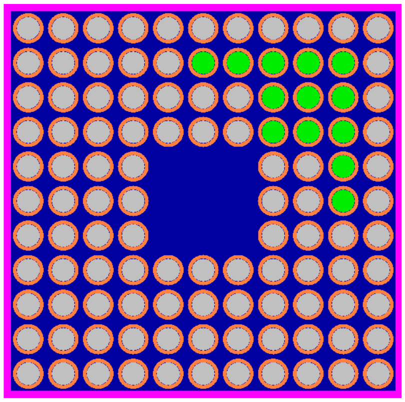

A2

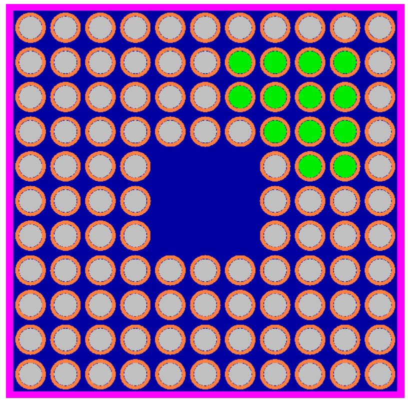

C3

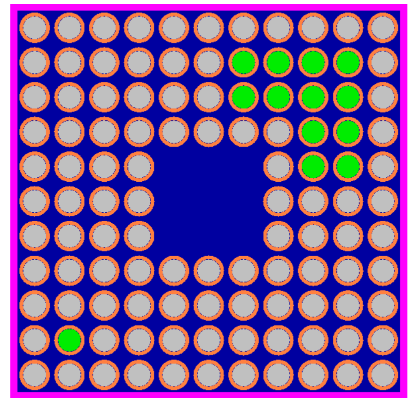

F1

Middle Axial Layer (Full and Long Partial Length Rods):

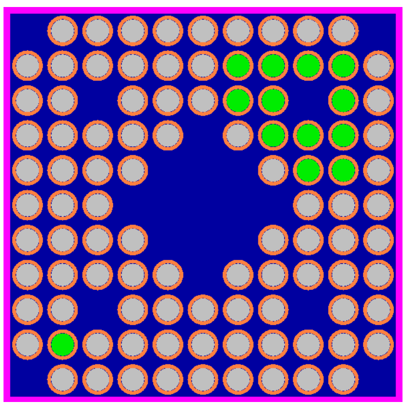

A3

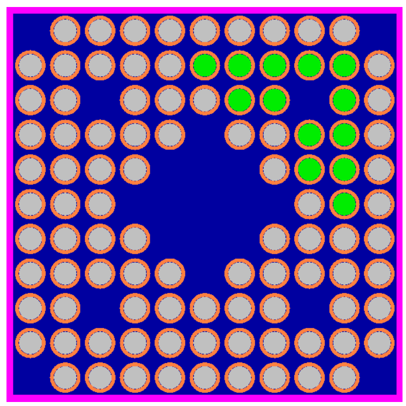

B1

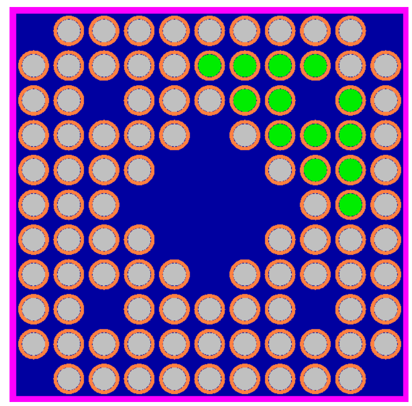

B2

Top Axial Layer (Full Length Rods Only):

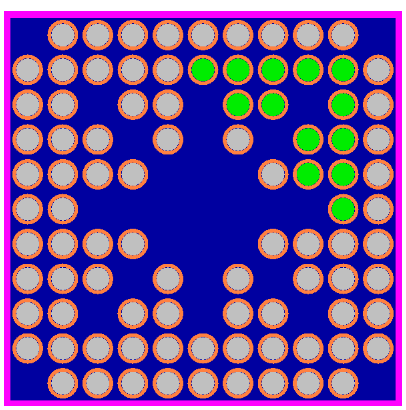

A2

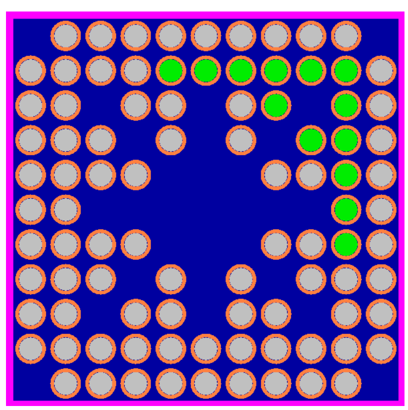

A3

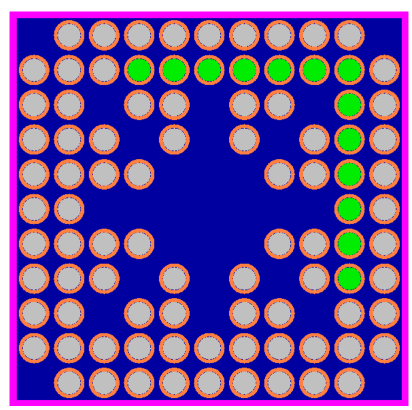

A4

Figure 6-68 Most Reactive Gadolinia-Urania Fuel Rod Patterns: 5.0 wt% ^{235}U, 13 Gd Rods

Bottom Axial Layer (Full and Partial Length Rods):

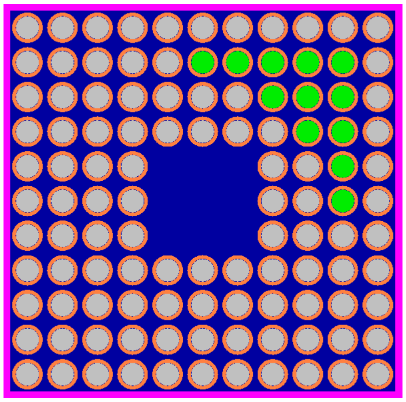

A2

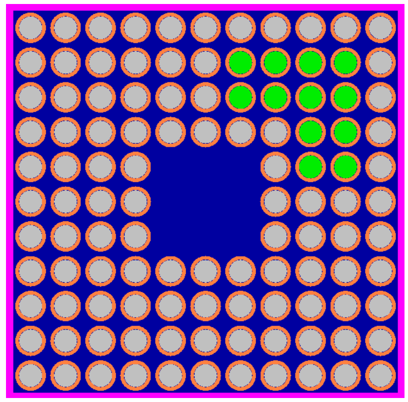

B2

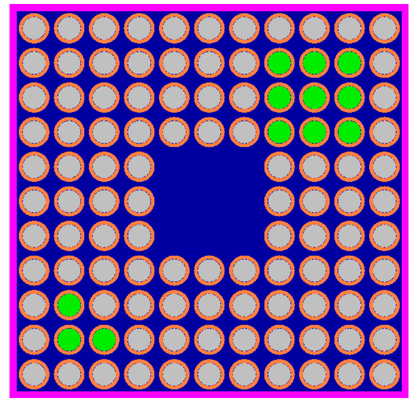

D2

Middle Axial Layer (Full and Long Partial Length Rods):

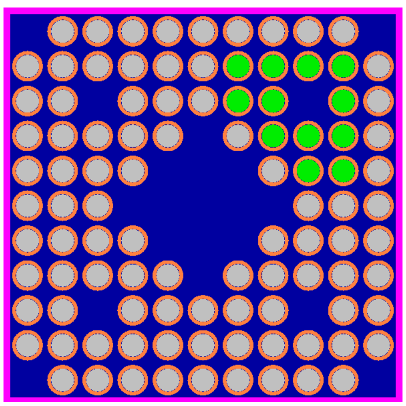

A2

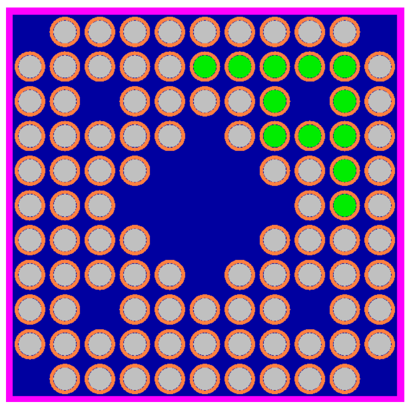

B1

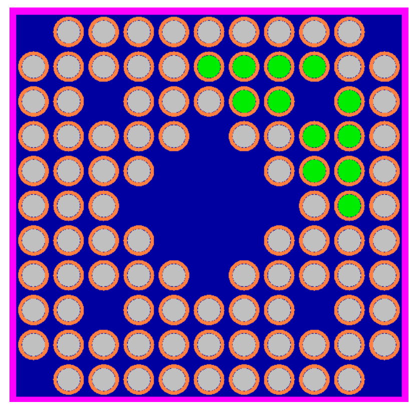

C4

Top Axial Layer (Full Length Rods Only):

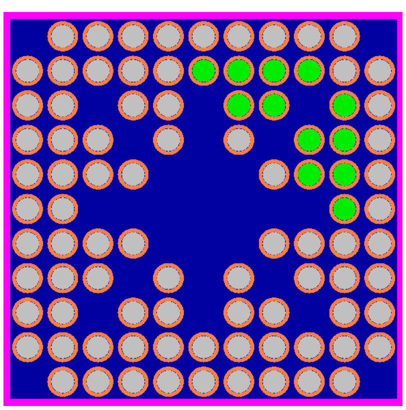

A2

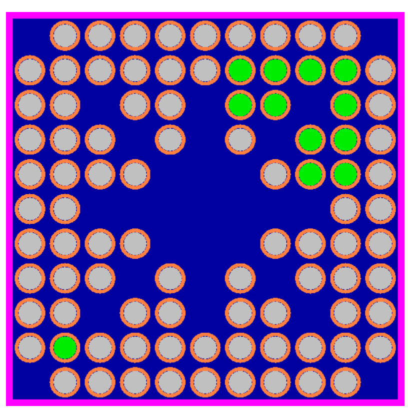

B2

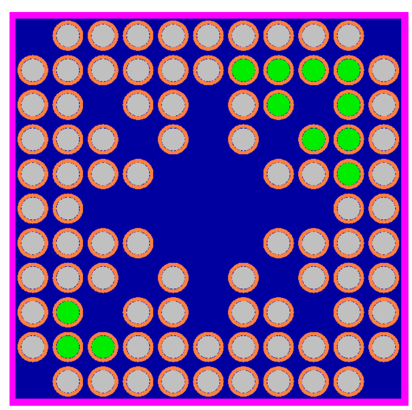

B4

Figure 6-69 Most Reactive Gadolinia-Urania Fuel Rod Patterns: 4.8 wt% ^{235}U, 12 Gd Rods

Bottom Axial Layer (Full and Partial Length Rods):

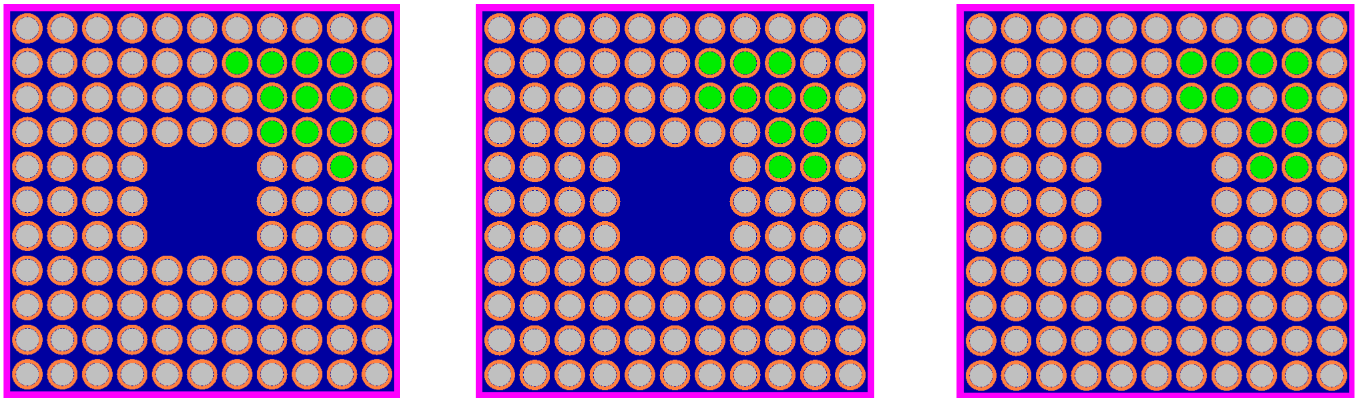

B1 B2 B3

Middle Axial Layer (Full and Long Partial Length Rods):

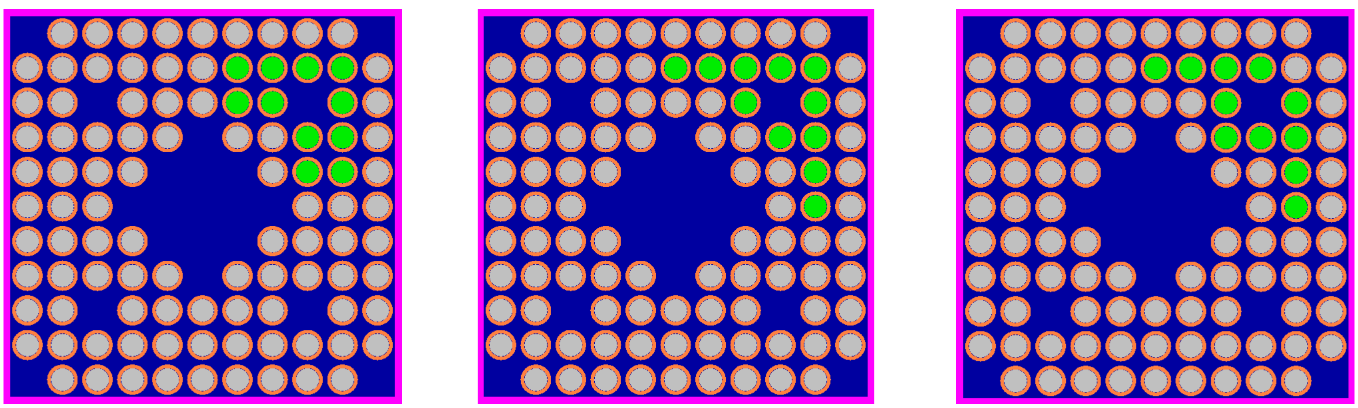

A1 B2 D3

Top Axial Layer (Full Length Rods Only):

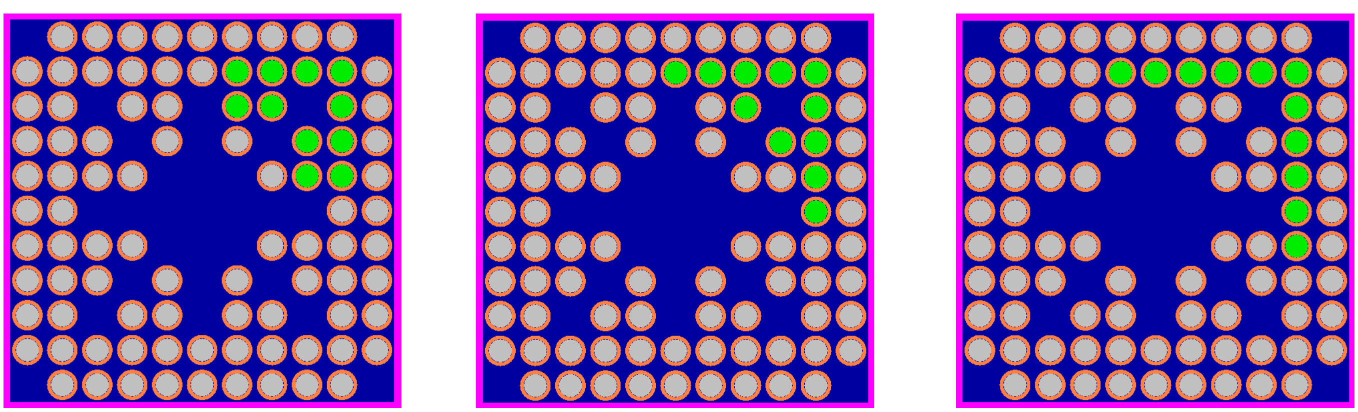

A1 A2 A3

Figure 6-70 Most Reactive Gadolinia-Urania Fuel Rod Patterns: 4.6 wt% ^{235}U, 11 Gd Rods

Bottom Axial Layer (Full and Partial Length Rods):

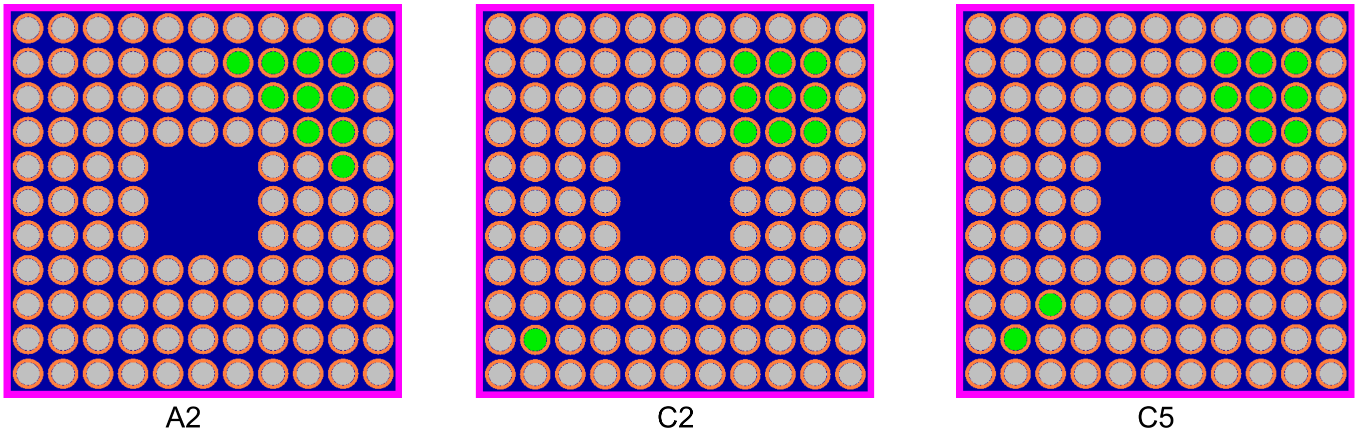

Middle Axial Layer (Full and Long Partial Length Rods):

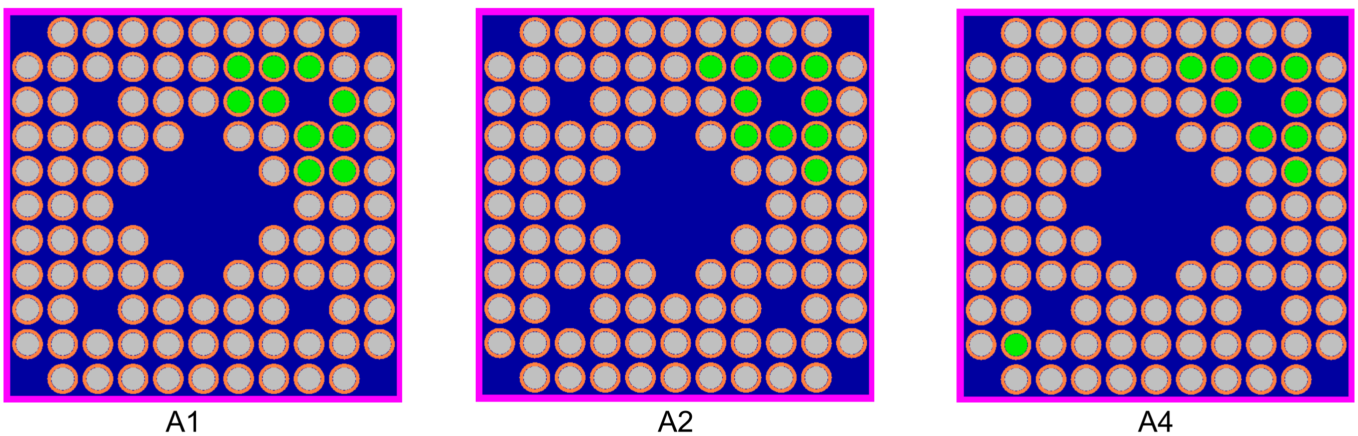

Top Axial Layer (Full Length Rods Only):

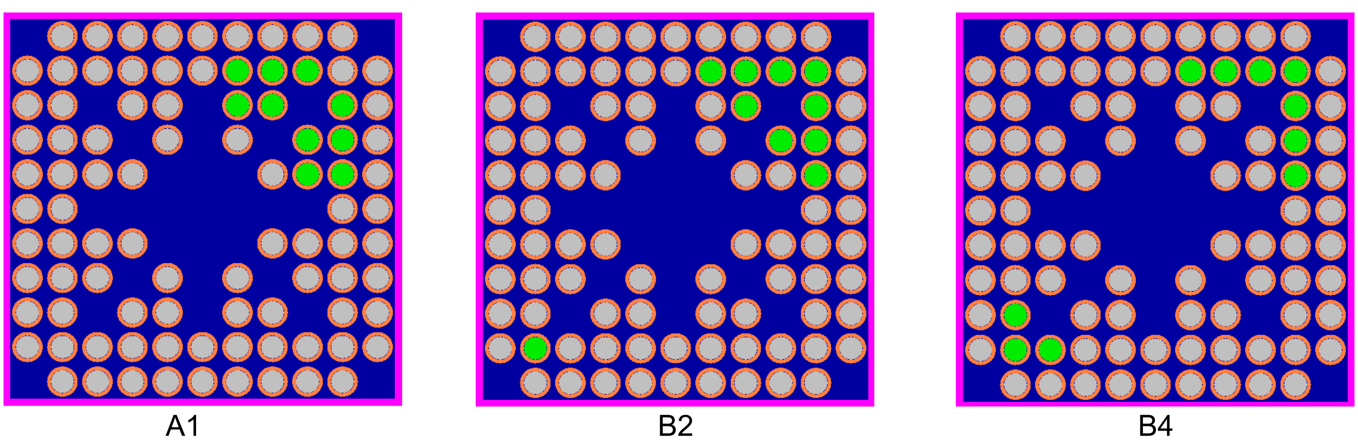

Figure 6-71 Most Reactive Gadolinia-Urania Fuel Rod Patterns: 4.4 wt% ^{235}U, 10 Gd Rods

Bottom Axial Layer (Full and Partial Length Rods):

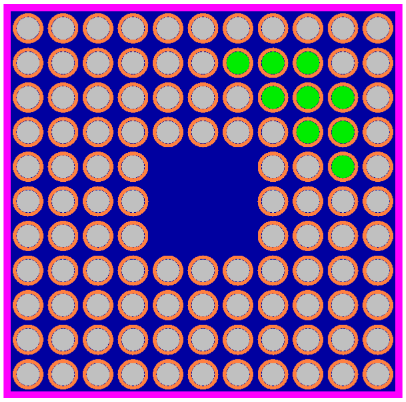
A2

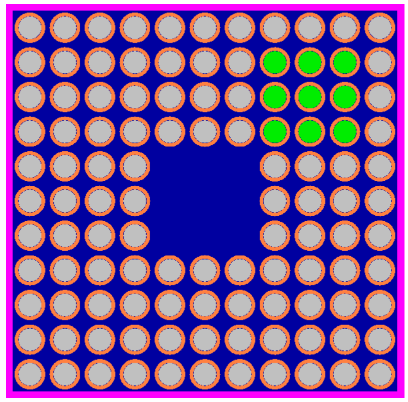
B1

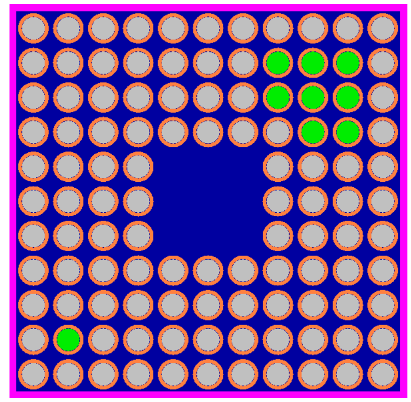
B3

Middle Axial Layer (Full and Long Partial Length Rods):

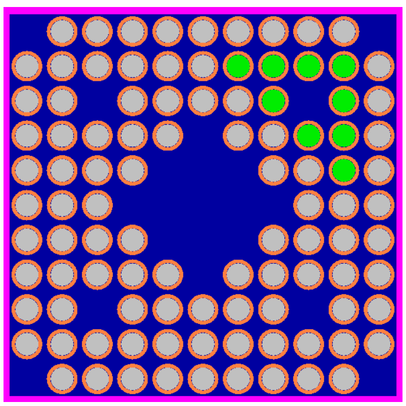
A1

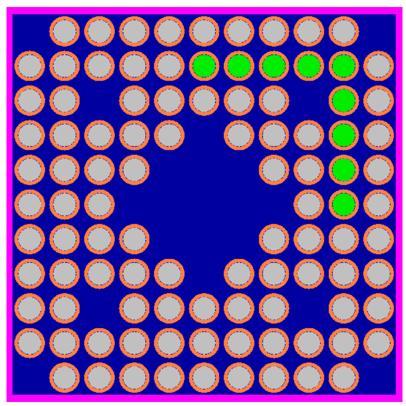
B1

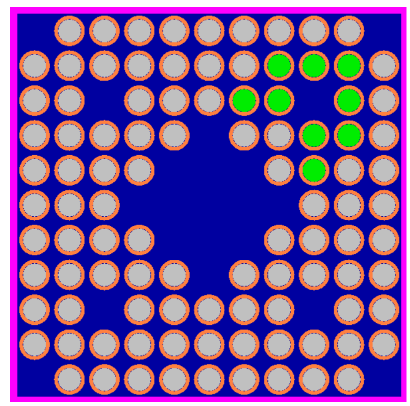
C2

Top Axial Layer (Full Length Rods Only):

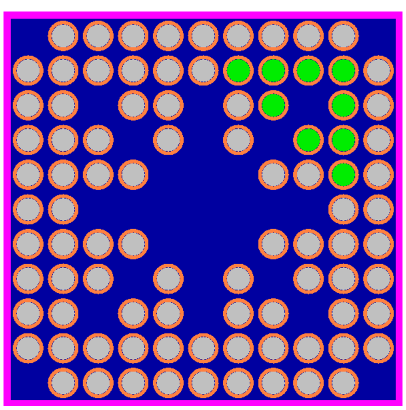
A1

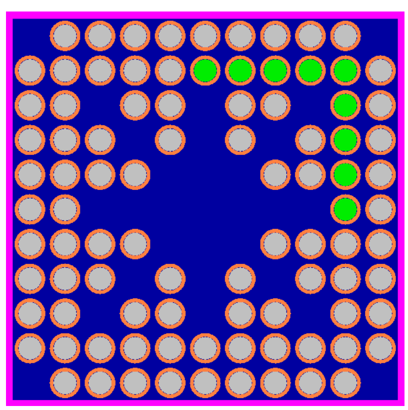
A2

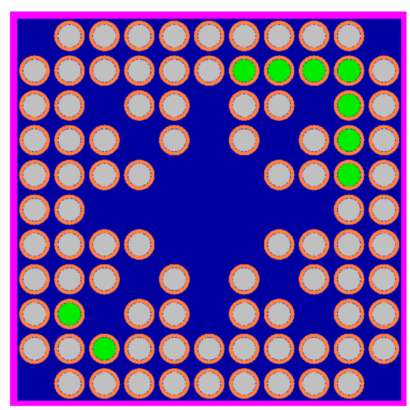
B3

Figure 6-72 Most Reactive Gadolinia-Urania Fuel Rod Patterns: 4.2 wt% ^{235}U, 9 Gd Rods

Bottom Axial Layer (Full and Partial Length Rods):

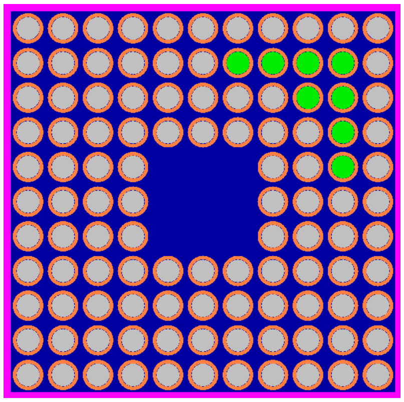
A2

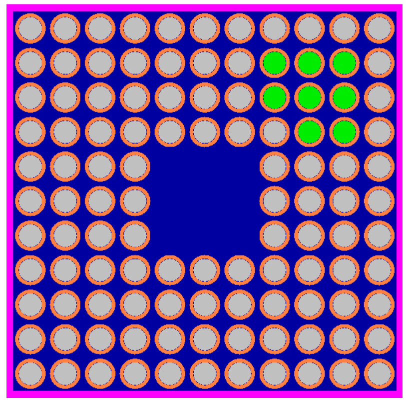
B1

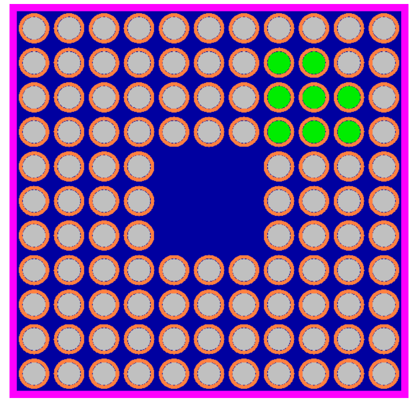
E1

Middle Axial Layer (Full and Long Partial Length Rods):

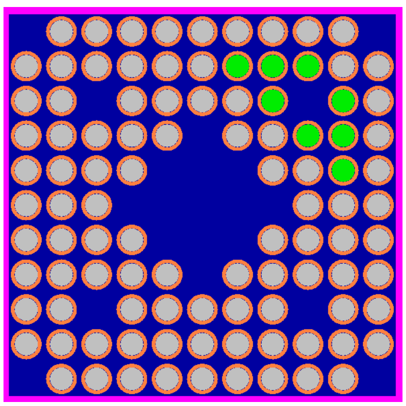
A1

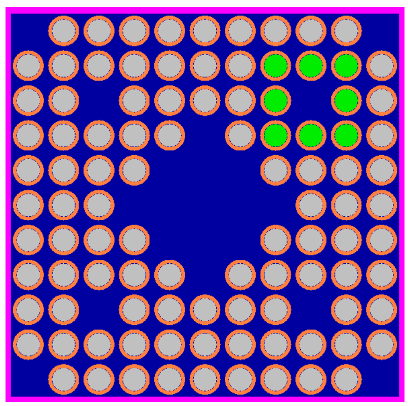
A2

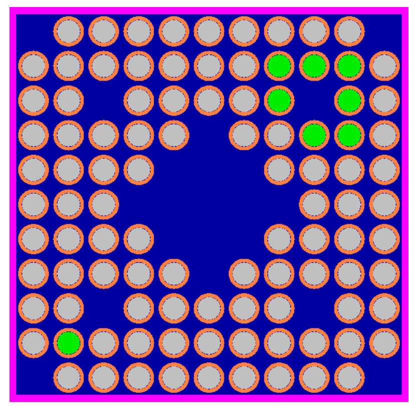
A3

Top Axial Layer (Full Length Rods Only):

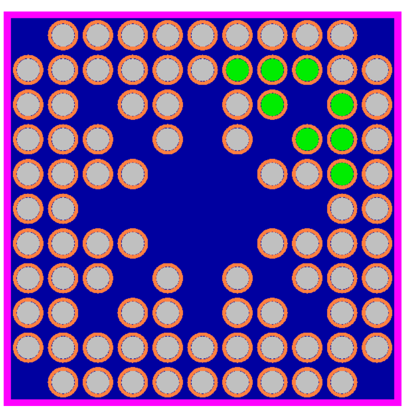
A1

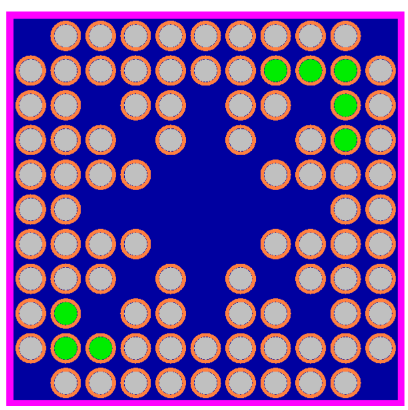
B2

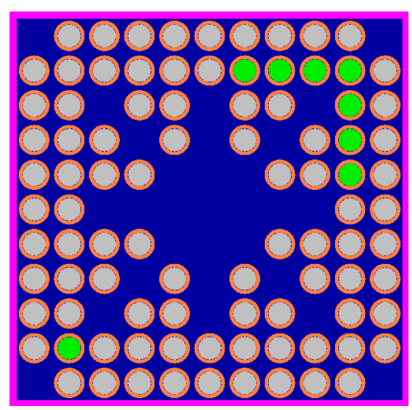
D1

Figure 6-73 Most Reactive Gadolinia-Urania Fuel Rod Patterns: 4.1 wt% ^{235}U, 8 Gd Rods

Bottom Axial Layer (Full and Partial Length Rods):

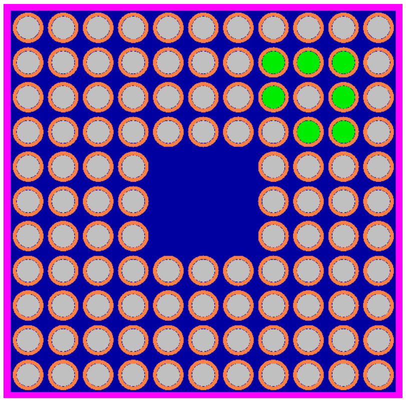
A1

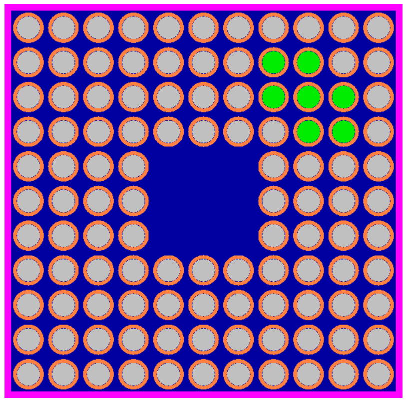
A3

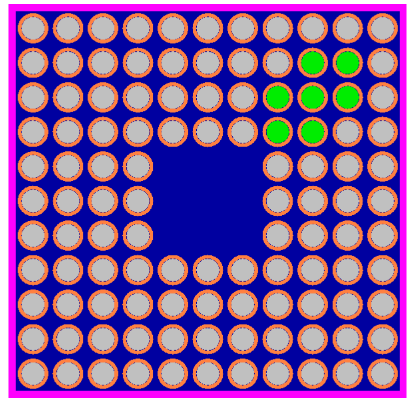
E1

Middle Axial Layer (Full and Long Partial Length Rods):

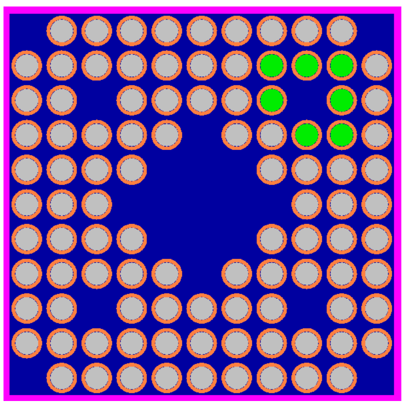
A1

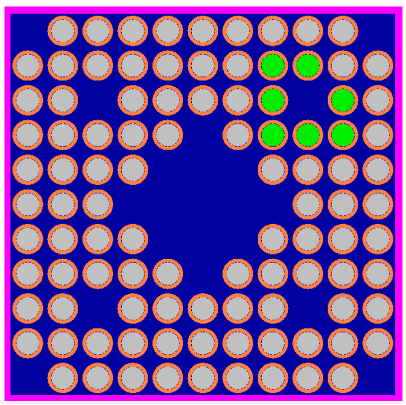
A2

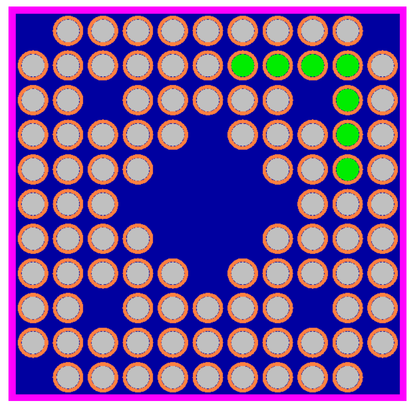
B1

Top Axial Layer (Full Length Rods Only):

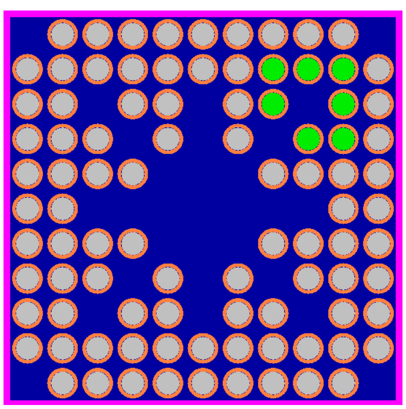
A1

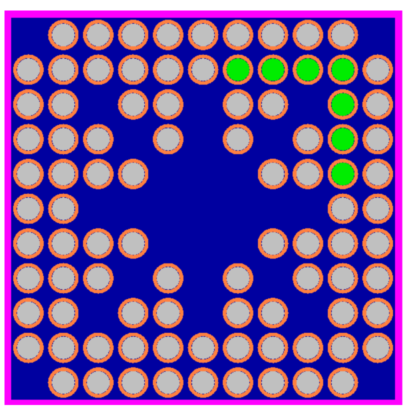
A2

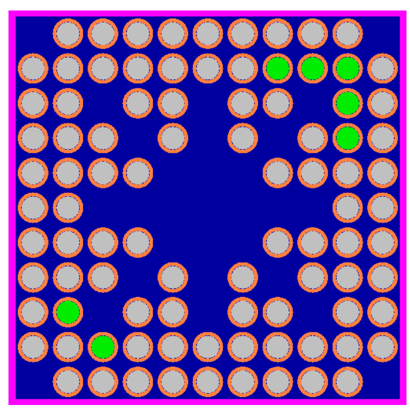
B3

Figure 6-74 Most Reactive Gadolinia-Urania Fuel Rod Patterns: 3.9 wt% ^{235}U, 7 Gd Rods

Bottom Axial Layer (Full and Partial Length Rods):

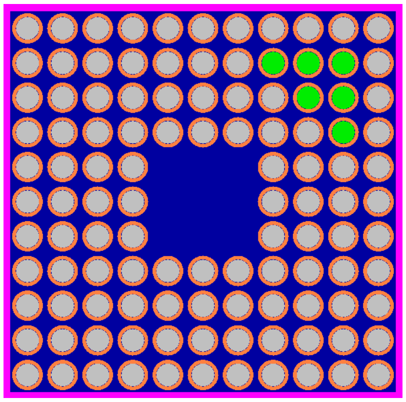

A2

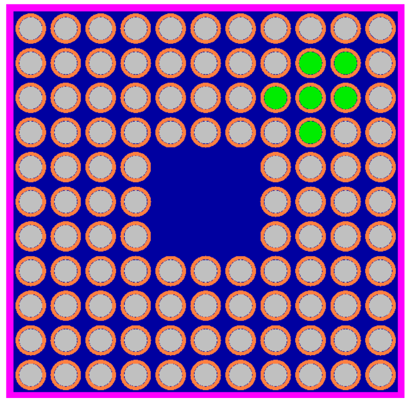

A3

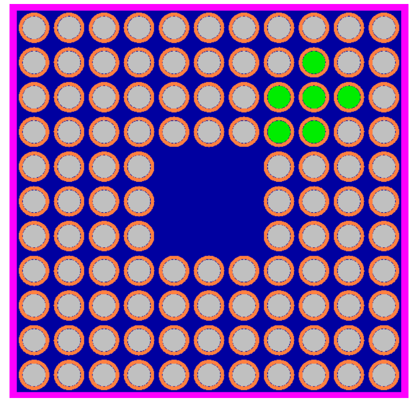

E1

Middle Axial Layer (Full and Long Partial Length Rods):

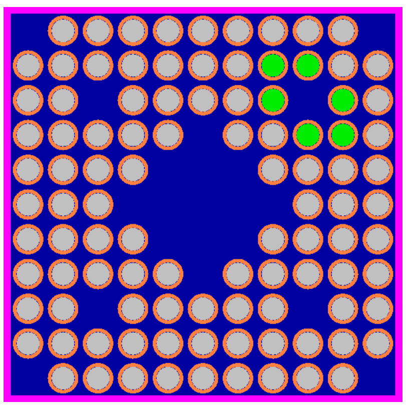

A1

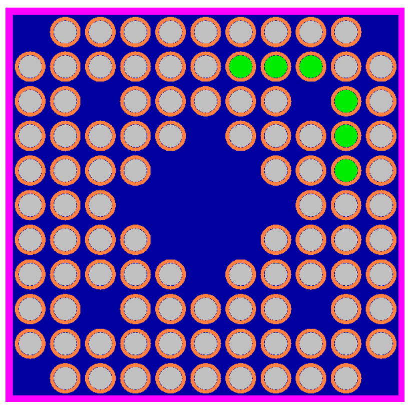

B1

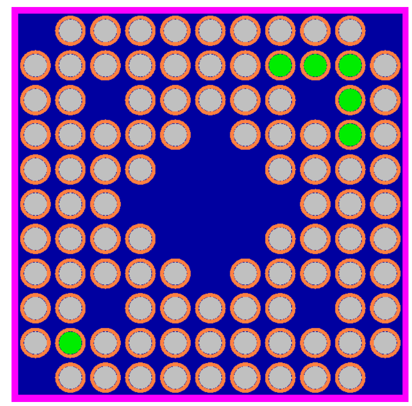

B3

Top Axial Layer (Full Length Rods Only):

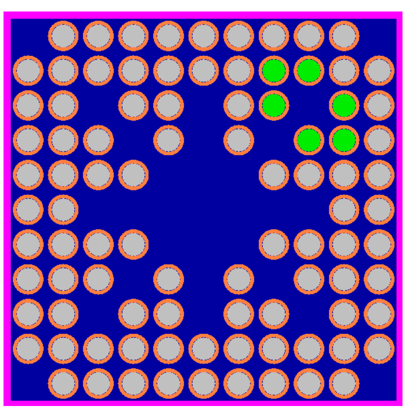

A1

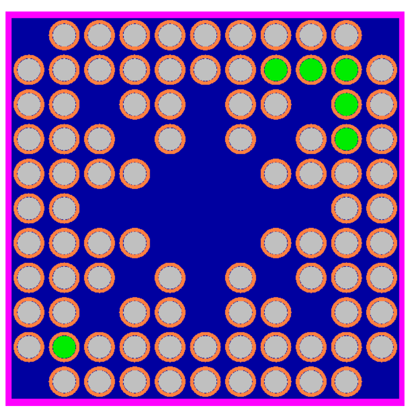

A3

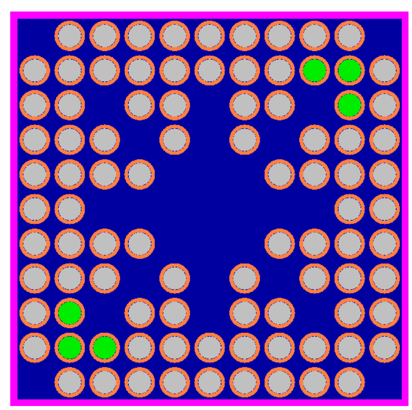

B2

Figure 6-75 Most Reactive Gadolinia-Urania Fuel Rod Patterns: 3.8 wt% ^{235}U, 6 Gd Rods

Bottom Axial Layer (Full and Partial Length Rods):

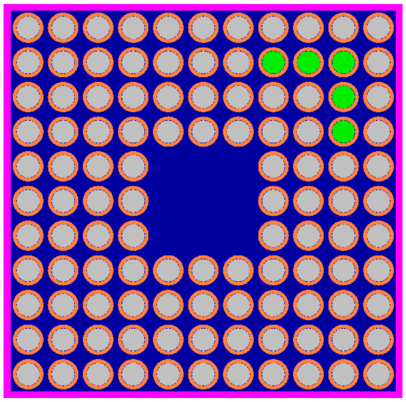
A1

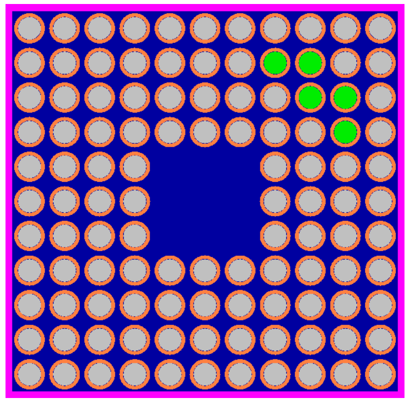
A2

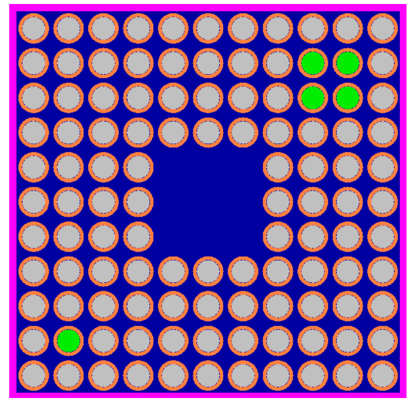
B3

Middle Axial Layer (Full and Long Partial Length Rods):

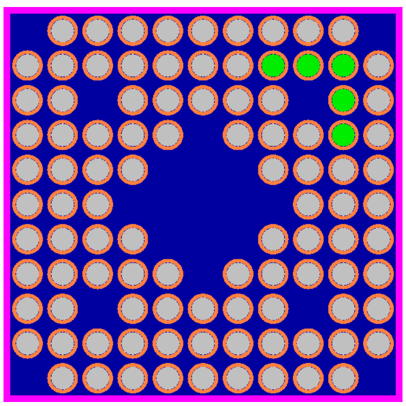
A1

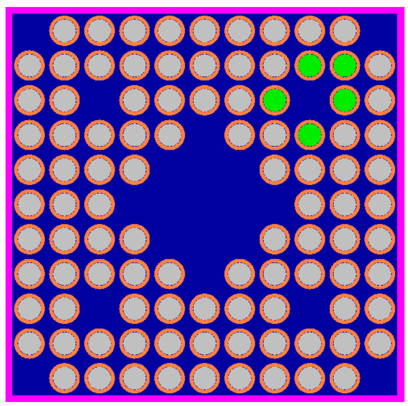
A2

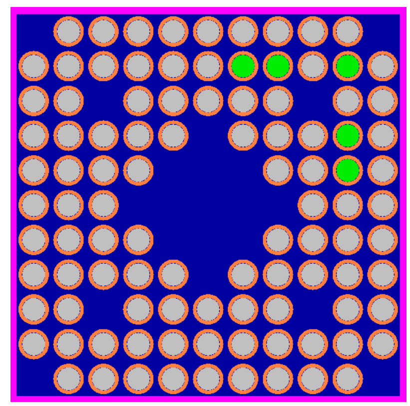
C1

Top Axial Layer (Full Length Rods Only):

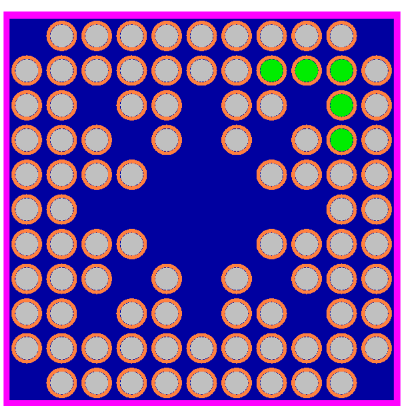
A1

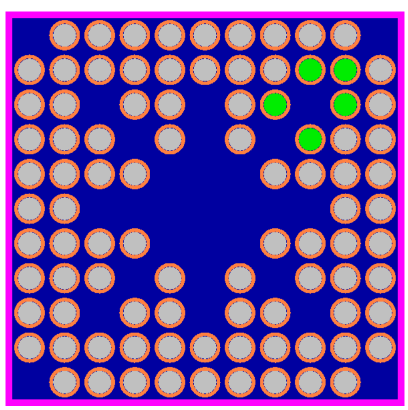
A2

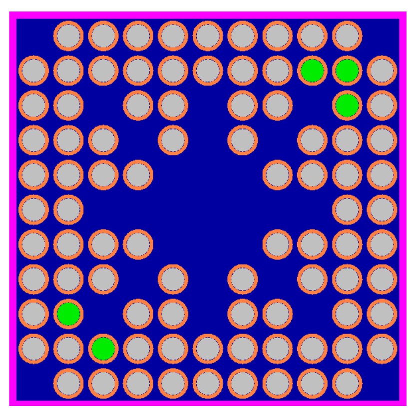
B2

Figure 6-76 Most Reactive Gadolinia-Urania Fuel Rod Patterns: 3.6 wt% ^{235}U, 5 Gd Rods

Bottom Axial Layer (Full and Partial Length Rods):

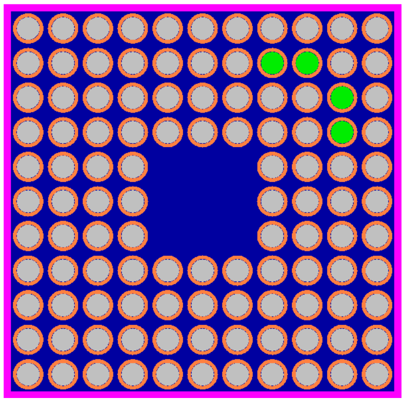

A1

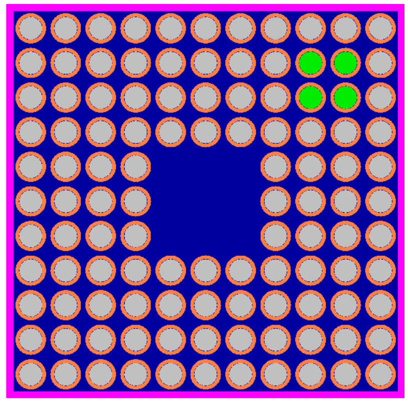

A2

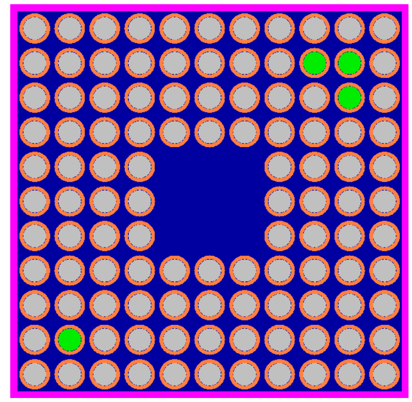

B3

Middle Axial Layer (Full and Long Partial Length Rods):

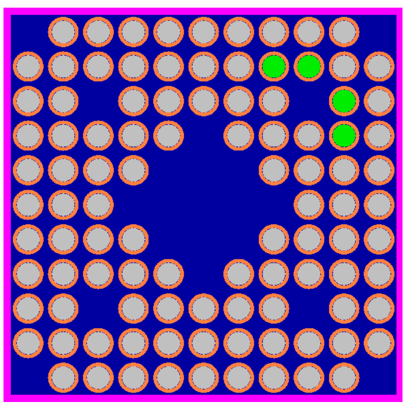

A1

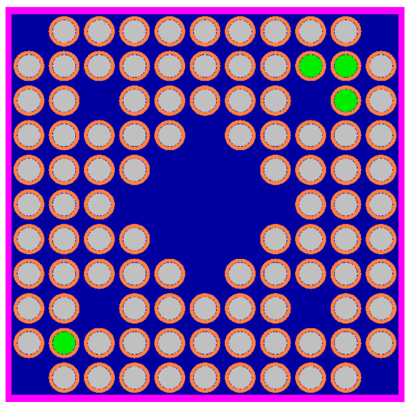

A3

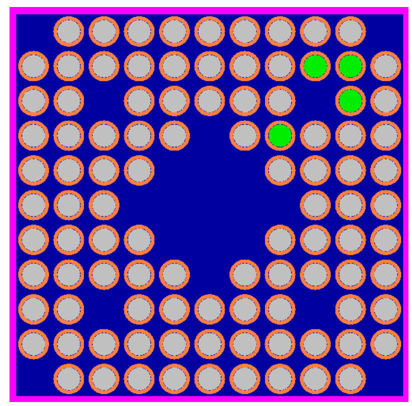

A4

Top Axial Layer (Full Length Rods Only):

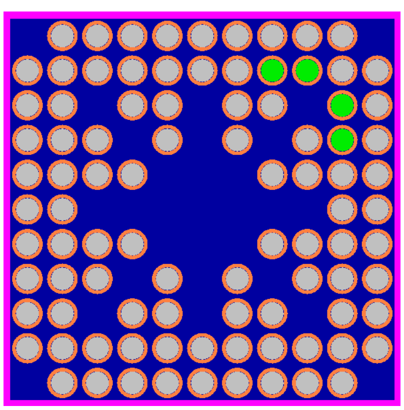

A1

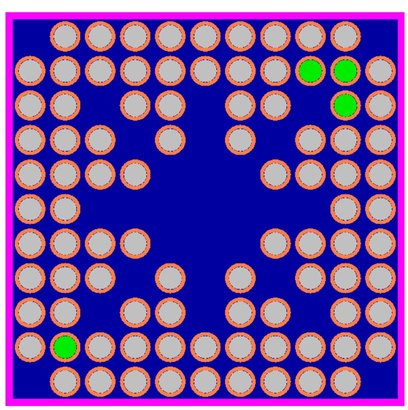

A3

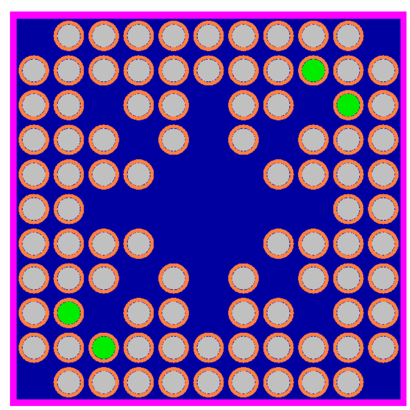

B1

Figure 6-77 Most Reactive Gadolinia-Urania Fuel Rod Patterns: 3.5 wt% ^{235}U, 4 Gd Rods

Bottom Axial Layer (Full and Partial Length Rods):

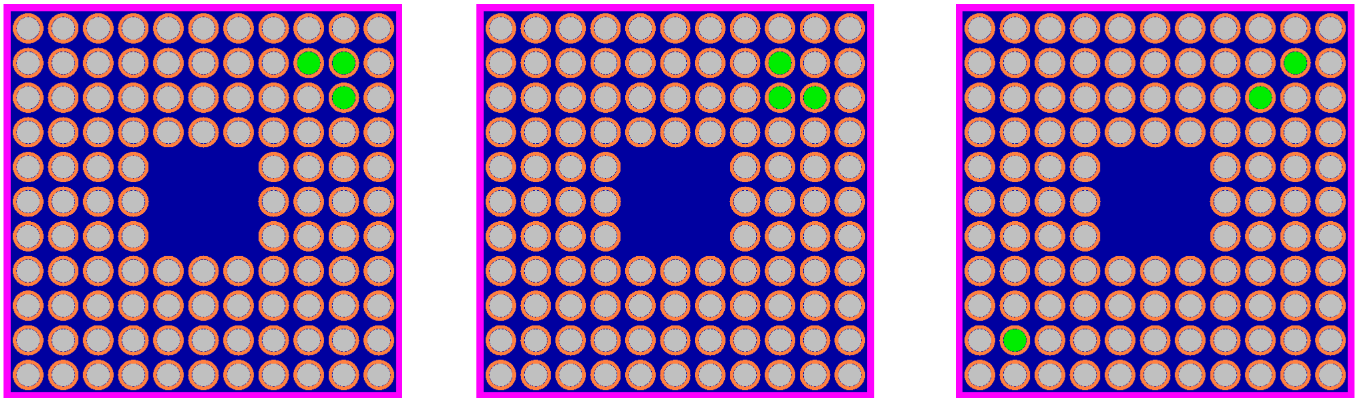

A1 A2 B3

Middle Axial Layer (Full and Long Partial Length Rods):

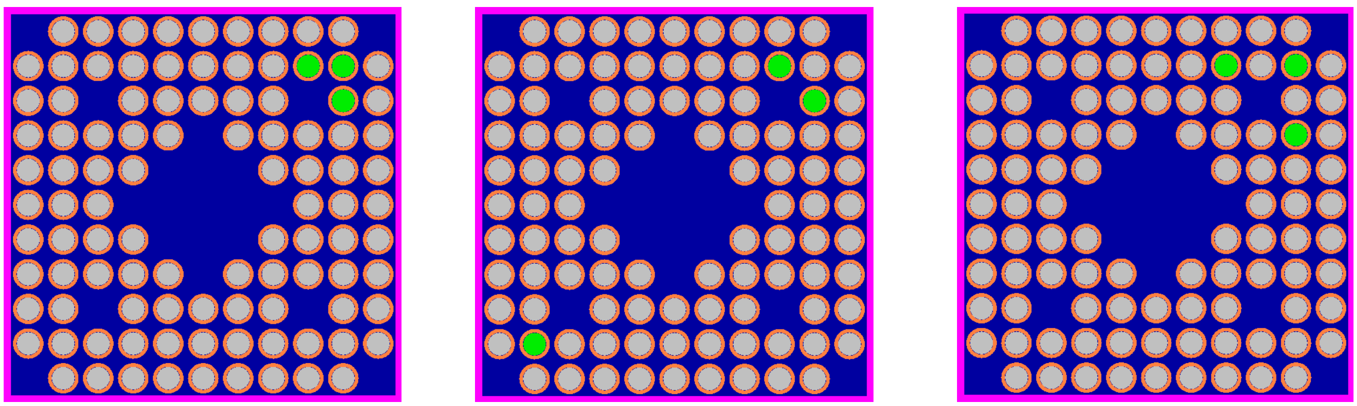

A1 B1 B2

Top Axial Layer (Full Length Rods Only):

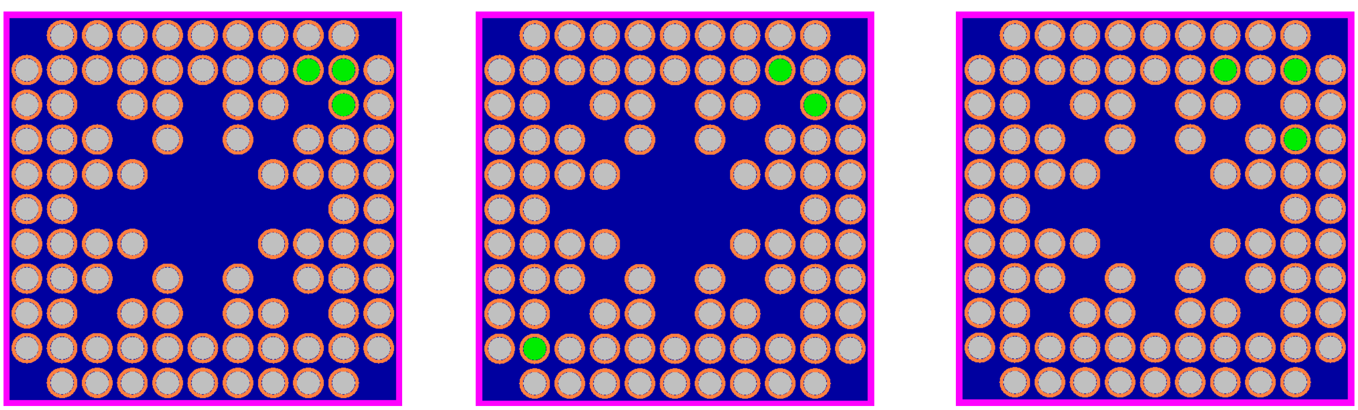

A1 A3 B1

Figure 6-78 Most Reactive Gadolinia-Urania Fuel Rod Patterns: 3.3 wt% ^{235}U, 3 Gd Rods

Bottom Axial Layer (Full and Partial Length Rods):

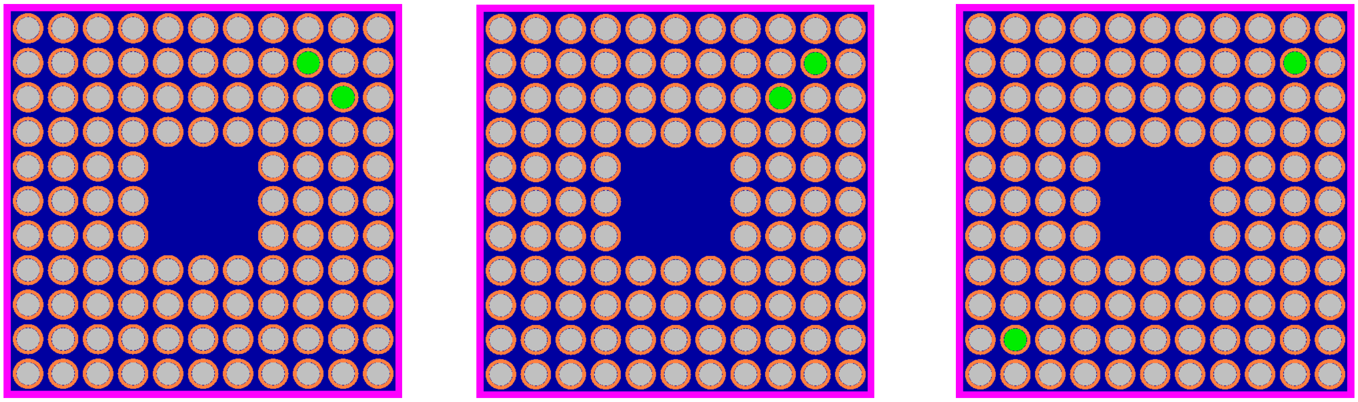

A1 A2 A4

Middle Axial Layer (Full and Long Partial Length Rods):

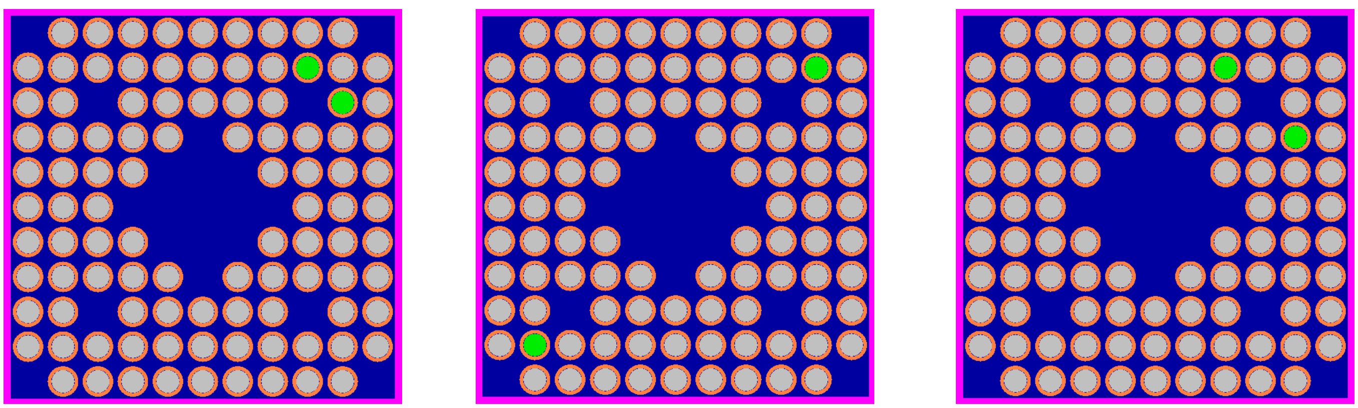

A1 A4 B2

Top Axial Layer (Full Length Rods Only):

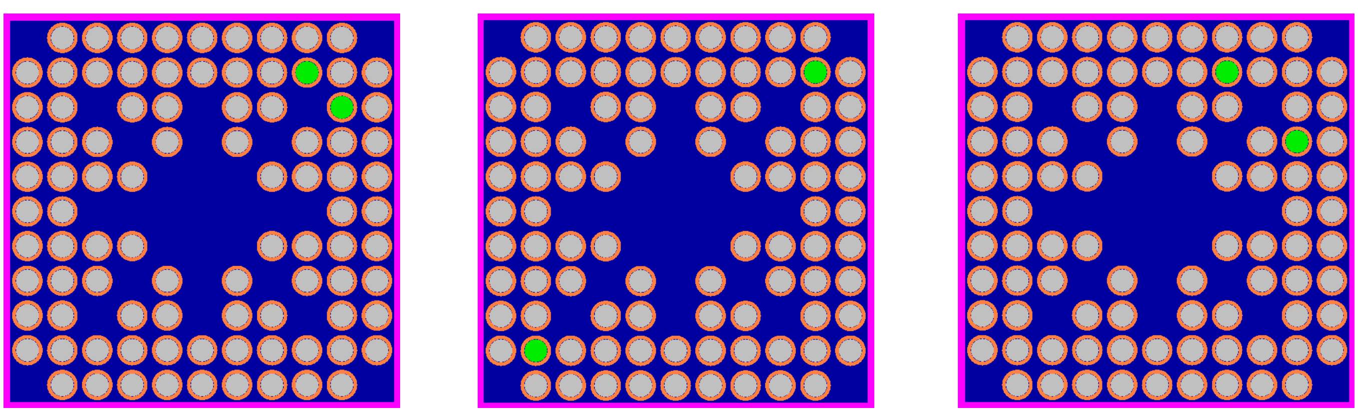

A1 A3 B1

Figure 6-79 Most Reactive Gadolinia-Urania Fuel Rod Patterns: 3.2 wt% ^{235}U, 2 Gd Rods

6.12.4. *Single Package Evaluation*

This section describes the evaluation of a single package model under NCT and HAC.

The fuel assembly model is described in Section 6.12.3.1.1, *Fuel Assembly Model*, and is based on the parametric study performed in Section 6.12.3.5, *Parameter Selection for 11x11 Fuel Assembly Model*.

6.12.4.1. NCT Single Package Evaluation

In the NCT single package evaluation, the package is modeled using NCT geometry, as described in Section 6.12.3.1.2, *Single Package NCT Model with 11x11 Fuel*. Because the fuel is undamaged under NCT, the nominal fuel rod pitch of 1.195 cm is used. Also, the full-thickness polyethylene liner is in place, which centers the fuel assemblies in each compartment.

In the NCT models, the 10.2 kg of polyethylene allowed per fuel assembly is modeled as homogenized with the water between the fuel rods, in the water holes resulting from partial-length fuel rods, and within the center water channel. The volume fractions for the polyethylene and water materials in the moderator are calculated as follows:

Total Assembly Volume = [(# Fuel Rod Number/side) * (fuel rod pitch)]^2 * (Full length Fuel Rod Length)]

$Volume_{assy}$ = (11 rods/side * 1.195 cm)^2 * 385 cm = 66524.54 cm^3

Fuel Rod Volume per Assembly = # fuel rods * π(Fuel Rod Outer Clad)^2*Fuel Rod Length

Full length: $Volume_{fuel\_rod\_full} = 92 * \pi * (0.465cm)^2 * 385cm = 24060.48\ cm^3$

Long Partial length: $Volume_{fuel\_rod\_ LPLR} = 8 * \pi * (0.465cm)^2 * 236.8cm = 1286.85\ cm^3$

Short Partial length: $Volume_{fuel\_rod\_ SPLR} = 12 * \pi * (0.465cm)^2 * 155.1cm = 1264.30\ cm^3$

$Volume_{fuel} = Volume_{fuel\_rod\_full} + Volume_{fuel\_rod\_ LPLR} + Volume_{fuel\_rod\_ SPLR}$

$Volume_{fuel} = 24060.48\ cm^3 + 1286.85\ cm^3 + 1264.30\ cm^3 = 26611.63\ cm^3$

Water + Polyethylene Volume per Assembly = $Volume_{assy}$ - $Volume_{fuel}$

$Volume_{h2o+poly} = 66524.54\ cm^3 - 26611.63\ cm^3 = 39912.92\ cm^3$

Total Polyethylene Volume = Total Polyethylene Mass / Polyethylene Density

$Volume_{poly} = 10.2\ kg / (0.949\ g / cm^3) = 10748.16\ cm^3$

Water Volume Fraction = [(Water + Polyethylene Volume) – (Polyethylene Volume)]/(Water + Polyethylene Volume)

$VF_{h2o} = (39912.92cm^3 – 10748.16cm^3) / (39912.92cm^3) = \mathbf{0.73071}$

Polyethylene Volume Fraction = Polyethylene Volume/(Water + Polyethylene Volume)

$VF_{poly} = 10748.16cm^3 / (39912.92cm^3) = \mathbf{0.26929}$

In the NCT model, void is modeled in the pellet-to-cladding gap.

Since the foam liner remains intact for NCT, the full thickness liner is used in the model. A moderator density study, in which the density of the water within the inner container is varied, is performed for the single package model for both channeled and un-channeled fuel assemblies. The region between the inner and outer containers is modeled as full-density water to maximize reflection.

Results from the NCT single package model are provided in Table 6-80 11x11 Single Package NCT Results. The most reactive configuration is observed for the channeled fuel assemblies for a moderator density of 1.0 g/cm^3 within the inner container. The maximum k_{eff} + 2σ value for the single package normal conditions of transport case is 0.63166, which is far below the USL of 0.94094. This case also meets the requirements of 71.55(b). Therefore, criticality safety is established for the NCT single package TN-B1 container.

The assembly containing varying axial enrichment was also considered in the final configuration for the NCT single package model. The k_{eff} + 2σ value calculated for the 5-5-3.3wt% assembly was 0.63085, which is lower than that found for the assembly with uniform axial enrichment. Therefore, criticality safety is maintained for the NCT single package TN-B1 container for assemblies having varying axial enrichment.

6.12.4.2. HAC Single Package Evaluation

In the HAC single package evaluation, the package is modeled using HAC geometry, as described in Section 6.12.3.1.3, *Single Package HAC Model with 11x11 Fuel*. Because the fuel could be damaged under HAC, the fuel rod pitch is expanded 5% to 1.2548 cm. In the HAC models, the 10.2 kg of polyethylene is assumed to be smeared into the fuel rod cladding. The fuel assemblies are allowed to move within the inner container compartments. Also, water is modeled in the pellet-to-cladding gap.

The Alumina Silicate thermal insulation is modeled between the inner and outer walls. This is consistent with the physical condition of the TN-B1 shipping container after being subjected to the tests specified in 10 CFR Part 71 (see Sections 3.2.2 and 3.5.2).

In an initial series of cases, the polyethylene foam liner is assumed to completely burn away. Full density water that provides more reflection capability is assumed to flood the TN-B1 inner container fuel compartment. Since the foam liner is assumed to burn away, the most reactive assembly orientation from Section 6.12.3.5.1, *Fuel Assembly Orientation Study*, is used: orientation 7 with the assembly in the right compartment shifted toward the center of the container. An evaluation to determine the most reactive configuration regarding the presence of the assembly channel is performed. The results are provided in Table 6-81 11x11 Single Package HAC Results, Channel Study. The most reactive configuration for the HAC single package model is found for the unchanneled assemblies.

Next, a moderator density study is performed without the fuel channel. Full density water is modeled within the outer container to maximize reflection and the moderator density is varied only within the inner container. Results are provided in Table 6-82 11x11 Single Package HAC Results, Complete Foam Burn. The maximum k_{eff} + 2σ value is 0.76705.

Because the HAC array cases are more reactive with liner partial foam burn rather than complete foam burn (see Section 6.12.3.5.10, *Polyethylene Foam Liner Study*), additional cases are investigated in which only partial foam burn is modeled. For each of the orientations shown below, a study is performed for both a channeled and unchanneled fuel assembly:

1. Both assemblies centered within the compartment.
2. The assembly in the left compartment centered and the assembly in the right compartment shifted toward the left.
3. Both assemblies shifted toward the center of the package.

Results for these three configurations are provided in Table 6-83 11x11 Single Package HAC Results, Partial Foam Burn, Centered Assemblies, Table 6-84 11x11 Single Package HAC Results, Partial Foam Burn, Right Assembly Shifted, and Table 6-85 11x11 Single Package HAC Results, Partial Foam Burn, Both Assemblies Shifted. It is observed that for the HAC single package, complete foam burn is more reactive than partial foam burn, as the liner region is acting primarily as a reflector. Conversely, in the HAC array, lower-density foam in this region increases neutron interactions between packages because the neutron mean free path is much higher in the low-density foam compared to water, thus increasing the reactivity.

The maximum $k_{eff} + 2\sigma$ value for the HAC single package is 0.76705 (complete foam burn), which is far below the USL of 0.94094. Therefore, criticality safety is established for the HAC single package TN-B1 container.

The assembly containing varying axial enrichment was also considered in the final configuration for the HAC single package model. The $k_{eff} + 2\sigma$ value calculated for the 5-5-3.3wt% assembly was 0.76703, which is lower than that found for the assembly with uniform axial enrichment. Therefore, criticality safety is maintained for the HAC single package TN-B1 container for assemblies having varying axial enrichment.

A second modeling approach in which the melted polyethylene is smeared into the moderator instead of the clad material was considered. Using the uniform axial configuration, the $k_{eff} + 2\sigma$ value calculated for this approach was 0.76595, which is lower than that found for the modeling approach in which the polyethylene is smeared into the clad.

6.12.4.3. Single Package Results

The NCT and HAC single package results are provided in Table 6-80 11x11 Single Package NCT Results through Table 6-85 11x11 Single Package HAC Results, Partial Foam Burn, Both Assemblies Shifted.

Table 6-80 11x11 Single Package NCT Results

Filename	Moderator Density (g/cm^3)	Fuel Channel?	k_{eff}	σ	k_{eff} + 2σ
NCT_single_pkg_dens000_ch.out	0.00	yes	0.39691	0.00035	0.39761
NCT_single_pkg_dens002_ch.out	0.02	yes	0.40084	0.00034	0.40152
NCT_single_pkg_dens004_ch.out	0.04	yes	0.40647	0.00035	0.40717
NCT_single_pkg_dens006_ch.out	0.06	yes	0.41135	0.00035	0.41205
NCT_single_pkg_dens008_ch.out	0.08	yes	0.41558	0.00034	0.41626
NCT_single_pkg_dens010_ch.out	0.10	yes	0.42054	0.00038	0.42130
NCT_single_pkg_dens020_ch.out	0.20	yes	0.44513	0.00038	0.44589
NCT_single_pkg_dens040_ch.out	0.40	yes	0.49541	0.00041	0.49623
NCT_single_pkg_dens060_ch.out	0.60	yes	0.54417	0.00039	0.54495
NCT_single_pkg_dens080_ch.out	0.80	yes	0.58873	0.00042	0.58957
NCT_single_pkg_dens100_ch.out	**1.0**	**yes**	**0.63082**	**0.00042**	**0.63166**
NCT_single_pkg_dens000_nc.out	0.00	no	0.39511	0.00035	0.39581
NCT_single_pkg_dens002_nc.out	0.02	no	0.39933	0.00033	0.39999
NCT_single_pkg_dens004_nc.out	0.04	no	0.40421	0.00032	0.40485
NCT_single_pkg_dens006_nc.out	0.06	no	0.40812	0.00037	0.40886
NCT_single_pkg_dens008_nc.out	0.08	no	0.41323	0.00036	0.41395
NCT_single_pkg_dens010_nc.out	0.10	no	0.41763	0.00035	0.41833
NCT_single_pkg_dens020_nc.out	0.20	no	0.44306	0.00036	0.44378
NCT_single_pkg_dens040_nc.out	0.40	no	0.49112	0.00042	0.49196
NCT_single_pkg_dens060_nc.out	0.60	no	0.53836	0.00044	0.53924
NCT_single_pkg_dens080_nc.out	0.80	no	0.58375	0.00043	0.58461
NCT_single_pkg_dens100_nc.out	1.0	no	0.62383	0.00045	0.62473

Table 6-81 11x11 Single Package HAC Results, Channel Study

Filename	Fuel Channel?	k_{eff}	σ	k_{eff} + 2σ
HAC_single_pkg_5wt13gd_NL_shft_ch.out	yes	0.75955	0.00046	0.76047
HAC_single_pkg_5wt13gd_NL_shft_un.out	**no**	**0.76615**	**0.00045**	**0.76705**

Table 6-82 11x11 Single Package HAC Results, Complete Foam Burn

Filename	Moderator Density (g/cm^3)	k_{eff}	σ	k_{eff} + 2σ
HAC_single_dens000.out	0.00	0.40245	0.00032	0.40309
HAC_single_dens002.out	0.02	0.40749	0.00037	0.40823
HAC_single_dens004.out	0.04	0.41194	0.00034	0.41262
HAC_single_dens006.out	0.06	0.41873	0.00034	0.41941
HAC_single_dens008.out	0.08	0.42450	0.00039	0.42528
HAC_single_dens010.out	0.10	0.43117	0.00036	0.43189
HAC_single_dens020.out	0.20	0.46946	0.00044	0.47034
HAC_single_dens040.out	0.40	0.55640	0.00041	0.55722
HAC_single_dens060.out	0.60	0.63868	0.00045	0.63958
HAC_single_dens080.out	0.80	0.70904	0.00049	0.71002
HAC_single_dens100.out	**1.0**	**0.76615**	**0.00045**	**0.76705**

Table 6-83 11x11 Single Package HAC Results, Partial Foam Burn, Centered Assemblies

Filename	Fuel Channel?	Polyethylene liner thickness (cm)	k_{eff}	σ	k_{eff} + 2σ
HAC_single_liner_000_cc.out	yes	0.00	0.74267	0.00044	0.74355
HAC_single_liner_020_cc.out	yes	0.20	0.73742	0.00048	0.73838
HAC_single_liner_040_cc.out	yes	0.40	0.73191	0.00048	0.73287
HAC_single_liner_060_cc.out	yes	0.60	0.72604	0.00045	0.72694
HAC_single_liner_080_cc.out	yes	0.80	0.71675	0.00047	0.71769
HAC_single_liner_100_cc.out	yes	1.00	0.70796	0.00046	0.70888
HAC_single_liner_120_cc.out	yes	1.20	0.69876	0.00046	0.69968
HAC_single_liner_140_cc.out	yes	1.40	0.68730	0.00045	0.68820
HAC_single_liner_160_cc.out	yes	1.60	0.67801	0.00046	0.67893
HAC_single_liner_full_cc.out	yes	1.657	0.67415	0.00043	0.67501
HAC_single_liner_000_cn.out	no	0.00	0.74453	0.00044	0.74541
HAC_single_liner_020_cn.out	no	0.20	0.74112	0.00047	0.74206
HAC_single_liner_040_cn.out	no	0.40	0.73562	0.00052	0.73666
HAC_single_liner_060_cn.out	no	0.60	0.72960	0.00043	0.73046
HAC_single_liner_080_cn.out	no	0.80	0.72258	0.00046	0.72350
HAC_single_liner_100_cn.out	no	1.00	0.71394	0.00047	0.71488
HAC_single_liner_120_cn.out	no	1.20	0.70495	0.00047	0.70589
HAC_single_liner_140_cn.out	no	1.40	0.69502	0.00045	0.69592
HAC_single_liner_160_cn.out	no	1.60	0.68508	0.00046	0.68600
HAC_single_liner_180_cn.out	no	1.80	0.67373	0.00046	0.67465
HAC_single_liner_full_cn.out	no	1.911	0.66622	0.00044	0.66710

Table 6-84 11x11 Single Package HAC Results, Partial Foam Burn, Right Assembly Shifted

Filename	Fuel Channel?	Polyethylene liner thickness (cm)	k_{eff}	σ	k_{eff} + 2σ
HAC_single_liner_000_o7c.out	yes	0.00	0.75663	0.00051	0.75765
HAC_single_liner_020_o7c.out	yes	0.20	0.74806	0.00048	0.74902
HAC_single_liner_040_o7c.out	yes	0.40	0.73805	0.00044	0.73893
HAC_single_liner_060_o7c.out	yes	0.60	0.72806	0.00045	0.72896
HAC_single_liner_080_o7c.out	yes	0.80	0.71742	0.00043	0.71828
HAC_single_liner_100_o7c.out	yes	1.00	0.70778	0.00049	0.70876
HAC_single_liner_120_o7c.out	yes	1.20	0.69759	0.00049	0.69857
HAC_single_liner_140_o7c.out	yes	1.40	0.68722	0.00048	0.68818
HAC_single_liner_160_o7c.out	yes	1.60	0.67707	0.00041	0.67789
HAC_single_liner_full_o7c.out	yes	1.657	0.67415	0.00043	0.67501
HAC_single_liner_000_o7n.out	no	0.00	0.76504	0.00045	0.76594
HAC_single_liner_020_o7n.out	no	0.20	0.75573	0.00046	0.75665
HAC_single_liner_040_o7n.out	no	0.40	0.74562	0.00051	0.74664
HAC_single_liner_060_o7n.out	no	0.60	0.73538	0.00048	0.73634
HAC_single_liner_080_o7n.out	no	0.80	0.72495	0.00048	0.72591
HAC_single_liner_100_o7n.out	no	1.00	0.71591	0.00051	0.71693
HAC_single_liner_120_o7n.out	no	1.20	0.70519	0.00047	0.70613
HAC_single_liner_140_o7n.out	no	1.40	0.69323	0.00048	0.69419
HAC_single_liner_160_o7n.out	no	1.60	0.68341	0.00042	0.68425
HAC_single_liner_180_o7n.out	no	1.80	0.67444	0.00044	0.67532
HAC_single_liner_full_o7n.out	no	1.911	0.66622	0.00044	0.66710

Table 6-85 11x11 Single Package HAC Results, Partial Foam Burn, Both Assemblies Shifted

Filename	Fuel Channel?	Polyethylene liner thickness (cm)	k_{eff}	σ	k_{eff} + 2σ
HAC_single_liner_000_INc.out	yes	0.00	0.75356	0.00046	0.75448
HAC_single_liner_020_INc.out	yes	0.20	0.74478	0.00045	0.74568
HAC_single_liner_040_INc.out	yes	0.40	0.73510	0.00053	0.73616
HAC_single_liner_060_INc.out	yes	0.60	0.72556	0.00048	0.72652
HAC_single_liner_080_INc.out	yes	0.80	0.71580	0.00046	0.71672
HAC_single_liner_100_INc.out	yes	1.00	0.70685	0.00049	0.70783
HAC_single_liner_120_INc.out	yes	1.20	0.69602	0.00043	0.69688
HAC_single_liner_140_INc.out	yes	1.40	0.68519	0.00045	0.68609
HAC_single_liner_160_INc.out	yes	1.60	0.67717	0.00046	0.67809
HAC_single_liner_full_INc.out	yes	1.657	0.67415	0.00043	0.67501
HAC_single_liner_000_INn.out	no	0.00	0.76073	0.00047	0.76167
HAC_single_liner_020_INn.out	no	0.20	0.75191	0.00046	0.75283
HAC_single_liner_040_INn.out	no	0.40	0.74247	0.00042	0.74331
HAC_single_liner_060_INn.out	no	0.60	0.73316	0.00046	0.73408
HAC_single_liner_080_INn.out	no	0.80	0.72331	0.00045	0.72421
HAC_single_liner_100_INn.out	no	1.00	0.71371	0.00044	0.71459
HAC_single_liner_120_INn.out	no	1.20	0.70294	0.00048	0.70390
HAC_single_liner_140_INn.out	no	1.40	0.69257	0.00045	0.69347
HAC_single_liner_160_INn.out	no	1.60	0.68392	0.00047	0.68486
HAC_single_liner_180_INn.out	no	1.80	0.67264	0.00048	0.67360
HAC_single_liner_full_INn.out	no	1.911	0.66622	0.00044	0.66710

6.12.5. *Evaluation of Package Arrays Under Normal Conditions of Transport*

6.12.5.1. Configuration

The NCT package array model is described in Section 6.12.3.1.4, *NCT Array Model with 11x11 Fuel*. The NCT model consists of a 21x3x24 array of containers, surrounded by a 30.48-cm layer of full density water for reflection. The container array is fully flooded with water at a density needed to achieve the most reactive configuration. The model is comprised of both the inner and outer containers fabricated from Stainless Steel. The inner container has Alumina Silicate thermal insulation between the inner and outer walls. No credit is taken for any of the structural steel between the inner and outer containers.

The worst-case fuel assembly parameters from Section 6.12.3.5, *Parameter Selection for 11x11 Fuel Assembly Model*, are used in the package array model. Nominal pitch is utilized to reflect the NCT condition. The package array evaluation is made for the most reactive lattice with axial uniform enrichment: average lattice enrichment of 5.0 wt% and thirteen 2.0 wt% gadolinia fuel rods. Void is modeled in the pellet-to-cladding gap.

For the NCT package array evaluation, the fuel assemblies are held centered within the inner container compartments by the polyethylene liner. The top and sides of the liner are modeled with 0.08 g/cm^3 polyethylene, while the bottom liner is modeled with 0.16 g/cm^3 polyethylene. The maximum allowable polyethylene equivalent mass (10.2 kg) is smeared into the water region surrounding the fuel rods, in the water holes resulting from partial-length fuel rods, and within the center water channel. The volume fractions for the polyethylene and water materials in the moderator are provided in Section 6.12.3.6.1, *NCT Single Package Evaluation*.

Since the foam liner remains intact for NCT, the full thickness liner is used in the model. A moderator density study, in which the density of the water within the inner and outer containers is varied, is performed for the package array model for both channeled and un-channeled fuel assemblies.

Results from the NCT package array model are provided in Table 6-86 11x11 NCT Array Results. The most reactive configuration is observed for the channeled fuel assemblies. The reactivity peaks with no water within the package, although moderation is provided by the 10.2 kg of polyethylene. The maximum $k_{eff} + 2\sigma$ value obtained for the package array for normal conditions of transport case is 0.85383, which is below the USL of 0.94094. Therefore, criticality safety of the TN-B1 shipping container is demonstrated under normal conditions of transport.

The assembly containing varying axial enrichment was also considered in the final configuration for the NCT package array model. The $k_{eff} + 2\sigma$ value calculated for the 5-5-3.3wt% assembly was 0.84759, which is lower than that found for the assembly with uniform axial enrichment. Therefore, criticality safety is maintained for the NCT single package TN-B1 container for assemblies having varying axial enrichment.

6.12.5.2. Results

The NCT array results are provided in Table 6-86 11x11 NCT Array Results.

Table 6-86 11x11 NCT Array Results

Filename	Moderator Density (g/cm^3)	Fuel Channel?	k_{eff}	σ	k_{eff} + 2σ
NCT_array_pkg_dens000_ch.out	**0.00**	**yes**	**0.85303**	**0.00040**	**0.85383**
NCT_array_pkg_dens002_ch.out	0.02	yes	0.79296	0.00042	0.79380
NCT_array_pkg_dens004_ch.out	0.04	yes	0.74358	0.00045	0.74448
NCT_array_pkg_dens006_ch.out	0.06	yes	0.70552	0.00041	0.70634
NCT_array_pkg_dens008_ch.out	0.08	yes	0.67097	0.00039	0.67175
NCT_array_pkg_dens010_ch.out	0.10	yes	0.64318	0.00042	0.64402
NCT_array_pkg_dens020_ch.out	0.20	yes	0.55071	0.00039	0.55149
NCT_array_pkg_dens040_ch.out	0.40	yes	0.51469	0.00037	0.51543
NCT_array_pkg_dens060_ch.out	0.60	yes	0.54575	0.00043	0.54661
NCT_array_pkg_dens080_ch.out	0.80	yes	0.58996	0.00040	0.59076
NCT_array_pkg_dens100_ch.out	1.00	yes	0.63123	0.00049	0.63221
NCT_array_pkg_dens000_nc.out	0.00	no	0.83671	0.00041	0.83753
NCT_array_pkg_dens002_nc.out	0.02	no	0.78267	0.00036	0.78339
NCT_array_pkg_dens004_nc.out	0.04	no	0.73327	0.00039	0.73405
NCT_array_pkg_dens006_nc.out	0.06	no	0.69606	0.00040	0.69686
NCT_array_pkg_dens008_nc.out	0.08	no	0.66290	0.00037	0.66364
NCT_array_pkg_dens010_nc.out	0.10	no	0.63378	0.00042	0.63462
NCT_array_pkg_dens020_nc.out	0.20	no	0.53825	0.00039	0.53903
NCT_array_pkg_dens040_nc.out	0.40	no	0.50125	0.00038	0.50201
NCT_array_pkg_dens060_nc.out	0.60	no	0.53365	0.00040	0.53445
NCT_array_pkg_dens080_nc.out	0.80	no	0.57891	0.00041	0.57973
NCT_array_pkg_dens100_nc.out	1.00	no	0.62302	0.00042	0.62386

6.12.6. *Evaluation of Package Arrays Under Hypothetical Accident Conditions*

6.12.6.1. Configuration

The parameter study documented in Section 6.12.3.5, *Parameter Selection for 11x11 Fuel Assembly Model*, is performed for an HAC array of 10x1x10 packages. Therefore, the cases documented in that section are part of the HAC array analysis. The conclusions are summarized below:

- Assembly orientation 6 (fuel assemblies centered for partial foam burn)
- 0.254 cm thick fuel assembly zirconium channel included
- Zirconium water channel not included

- 10.2 kg polyethylene per fuel assembly (smeared into the cladding)
- Pitch increased 5% to 1.2548 cm
- Pellet diameter of 0.820 cm
- Cladding inner diameter of 0.840 cm
- Cladding outer diameter of 0.930 cm
- Fuel assemblies fully flooded (i.e, no uncovered fuel rods)
- Thermal insulator modeled as Alumina-Silica
- Polyethylene foam liner modeled as partially burned with a thickness of 1.2 cm
- Enrichment of 5.0% with 13 gadolinia-urania rods with the loading pattern shown in Figure 6-52 Bounding Fuel Assembly Model for the uniform axial enrichment.

The maximum k_{eff} + 2σ value for the HAC package array case with uniform axial enrichment from Table 6-79 11x11 Gadolinia-Urania Analysis Results is 0.93810, which is below the USL of 0.94094. This case is developed with full-water moderation of the inner container and void between the inner and outer containers, which is assumed to be the most reactive moderation condition. This assumption is proven in the following sets of cases.

In the first set of cases, the moderator density within the inner container is varied while void is modeled between the inner and outer containers. In the second set of cases, the moderator density within the inner container is modeled as full-density water while variable density water is modeled between the inner and outer containers. The results are provided in Table 6-87 11x11 HAC Array Results. It is observed that the most reactive condition is with a fully moderated inner container and void outer container. When water is added to the outer container, the reactivity drops considerably, as the water in the outer container effectively isolates the packages from one another.

Note that in the calculations uranium in the mixture is modeled as only U-235 and U-238. However, as indicated in Table 1-3, 3.04×10^{-9} gPu-239/gU may be present in the fuel matrix. Because Pu-239 is fissile, it is added to the worst-case package array HAC model with uniform axial enrichment.

The results indicate no statistically significant difference between the cases with and without plutonium. The k_{eff} + 2σ for the case with plutonium is 0.93871. The k_{eff} + 2σ for the case without plutonium is 0.93810. Therefore, the plutonium is justifiably neglected in the TN-B1 evaluation.

As noted in Section 6.12.3.5.11 and Table 6-79 11x11 Gadolinia-Urania Analysis Results, the assembly containing varying axial enrichment resulted in a slightly higher reactivity than did the assembly with axial uniform enrichment. The maximum k_{eff} + 2σ value for the HAC package array case with varying axial enrichment from Table 6-79 11x11 Gadolinia-Urania Analysis Results is 0.93943, which is below the USL of 0.94094. This case is developed with full-water moderation of the inner container and void between the inner and outer containers, which is assumed to be the most reactive moderation condition. Therefore, criticality safety is maintained for the HAC package array for assemblies having varying axial enrichment.

A second modeling approach in which the melted polyethylene is smeared into the moderator instead of the clad material was considered. Using the varying axial enrichment configuration, the $k_{eff} + 2\sigma$ value calculated for this approach was 0.94068, which is higher than that found for the modeling approach in which the polyethylene is smeared into the clad. This value remains below the USL of 0.94094 and criticality safety is maintained for the HAC package array.

6.12.6.2. Results

Results for the HAC array cases are provided in Table 6-87 11x11 HAC Array Results.

Table 6-87 11x11 HAC Array Results

Filename	Inner Container Moderator Density (g/cm^3)	Outer Region Water Density (g/cm^3)	k_{eff}	σ	k_{eff} + 2σ
HAC_array_dens000.out	0.00	0.00	0.62068	0.00040	0.62148
HAC_array_dens002.out	0.02	0.00	0.63438	0.00036	0.63510
HAC_array_dens004.out	0.04	0.00	0.64665	0.00036	0.64737
HAC_array_dens006.out	0.06	0.00	0.65966	0.00037	0.66040
HAC_array_dens008.out	0.08	0.00	0.67109	0.00040	0.67189
HAC_array_dens010.out	0.10	0.00	0.68278	0.00047	0.68372
HAC_array_dens020.out	0.20	0.00	0.73465	0.00045	0.73555
HAC_array_dens040.out	0.40	0.00	0.81370	0.00052	0.81474
HAC_array_dens060.out	0.60	0.00	0.87019	0.00050	0.87119
HAC_array_dens080.out	0.80	0.00	0.90958	0.00044	0.91046
HAC_array_dens100.out	**1.0**	**0.00**	**0.93710**	**0.00050**	**0.93810**
HAC_array_outH2O_dens000.out	**1.0**	**0.00**	**0.93710**	**0.00050**	**0.93810**
HAC_array_outH2O_dens002.out	1.0	0.02	0.91440	0.00047	0.91534
HAC_array_outH2O_dens004.out	1.0	0.04	0.88722	0.00045	0.88812
HAC_array_outH2O_dens006.out	1.0	0.06	0.86099	0.00047	0.86193
HAC_array_outH2O_dens008.out	1.0	0.08	0.83691	0.00045	0.83781
HAC_array_outH2O_dens010.out	1.0	0.10	0.81614	0.00075	0.81764
HAC_array_outH2O_dens020.out	1.0	0.20	0.75097	0.00046	0.75189
HAC_array_outH2O_dens040.out	1.0	0.40	0.70736	0.00045	0.70826
HAC_array_outH2O_dens060.out	1.0	0.60	0.69956	0.00045	0.70046
HAC_array_outH2O_dens080.out	1.0	0.80	0.69831	0.00046	0.69923
HAC_array_outH2O_dens100.out	1.0	1.0	0.69970	0.00044	0.70058

6.12.7. *Transport of 11x11 Rods*

The analysis for transport of 8x8, 9x9, and 10x10 fuel assembly rods within the TN-B1 is documented in *Section 6.7, Fuel Rod Transport in the TN-B1*. However, a review of Table 6-2 TN-B1 Fuel Rod Loading Criteria indicates the 11x11 fuel rod is outside the criteria set in terms of theoretical density and fuel rod outer diameter. All other parameters fall within the values provided for the 10x10 UO_2 fuel rods. Therefore, studies are conducted to allow transport of the 11x11 fuel assembly UO_2 fuel rods in the TN-B1 container. Two configurations are investigated, which include the loose fuel rods and fuel rods contained in a 5-inch stainless steel pipe. It was shown in Section 6.7, *Fuel Rod Transport in the TN-B1*, that these two configurations bound the configurations in which fuel rods are bundled together or contained within a protective case.

Fuel parameters modeled to reflect the 11x11 rod worst-case parameters are shown below:

UO_2 pellet density = 10.763 g/cm^3
UO_2 enrichment = 5.0 wt% ^{235}U
Pellet diameter = 0.820 cm
Rod outer diameter = 0.930 cm
Cladding thickness = 0.00 cm
Fuel length = 385 cm

Similar to Section 6.7, *Fuel Rod Transport in the TN-B1*, a 6-mil layer of polyethylene encircles each fuel rod in the model to bound protective packing material that may be used for fuel rod transport. Moderator is modeled between the fuel and polyethylene. The cladding is conservatively modeled as water to further increase moderation. Water is modeled in the pellet/cladding gap.

The approach is to investigate 25 loose rods in each liner cavity and 30 rods in each pipe component under HAC array conditions, and select the most reactive rod configuration for the single package and NCT array analyses.

6.12.7.1. **11x11 Fuel Rods Loose or Bundled**

In the following analysis, the fuel rods are placed loose within the liner without any hardware to restrict movement. Twenty-five (25) fuel rods per compartment, or 50 fuel rods per package, are considered. This analysis bounds fuel rods that are bundled together, as bundled fuel rods would have significantly less moderation than loose rods, and credit could not be taken for the bundles remaining intact in an accident.

The package array model under HAC is used for the loose fuel rod calculations since it is demonstrated to be more reactive than the NCT package array model for the 11x11 fuel assembly. The inner container is initially filled with 60% density water since this was determined to be the optimum density for moderation in the original loose rod analysis, see Table 6-23 Fuel

Rod Maximum Quantity at Reduced Moderator Densities, and system behavior will be similar for the 11x11 rod. The outer container has no water, which facilitates leakage of neutrons into neighboring containers. Twenty-five (25) worst-case fuel rods are arranged in a square pitch inside each TN-B1 transport compartment.

A fuel rod pitch sensitivity study is performed for the 11x11 loose fuel rods in which the fuel rod pitch is varied from close packed to filling the inner compartment, as shown in Figure 6-80 Twenty-five 11x11 Fuel Rods in the TN-B1 Container. The results are provided in Table 6-88 Fuel Rod Pitch Sensitivity Study Results with 11x11 Fuel Rods. The maximum reactivity for 25 11x11 fuel rods in the TN-B1 package HAC array occurs for a fuel rod pitch of 3.20 cm. Because reactivity decreases for a larger pitch of 3.52 cm, optimum moderation is achieved for a 3.20 cm pitch.

The fuel rod pitch sensitivity study is initially performed using a water density of 0.60 g/cm^2 since this was found to be the limiting case the original analysis. To ensure that this moderator density produces the highest reactivity for the 11x11 rods, a moderator density study is performed. A rod pitch of 3.20 cm is used for the density study. The results are provided in Table 6-89 Moderator Density Sensitivity Study Results with 11x11 Fuel Rods. These results demonstrate that a moderator density of 0.60 g/cm^3 produces the highest reactivity for 25 11x11 fuel rods in the TN-B1 package array.

Finally, a study considering the polyethylene liner within the inner container is performed. The most reactive fuel rod pitch of 0.320 cm is used along with a moderator density of 0.60 g/cm^3. The liner thickness is varied from no liner to the maximum liner that could accommodate the fuel rod array used. Thicker liners would require a smaller rod pitch, which would lower the system reactivity. The foam liner is modeled with a density of 0.08 g/cm^3 on the top and sides and 0.16 g/cm^3 on the bottom. The results are provided in Table 6-90 Polyethylene Liner Sensitivity Study Results with 11x11 Fuel Rods. These results show that a 0.4 cm thick polyethylene liner produces the highest reactivity for 25 11x11 fuel rods in the TN-B1 package array, with k_{eff} +2σ = 0.72725. It is noted that there is very little variation in the results for the different liner thicknesses.

Compared to the 11x11 fuel assembly (maximum k_{eff} +2σ = 0.93810), the reactivity of 25 loose rods is comparatively quite low due to insufficient fissile mass.

Table 6-88 Fuel Rod Pitch Sensitivity Study Results with 11x11 Fuel Rods

Filename	Fuel Rod Pitch (cm)	k_{eff}	σ	k_{eff} + 2σ
atrium11_pitch_097_MOD.out	0.970	0.42032	0.00037	0.42106
atrium11_pitch_120_MOD.out	1.200	0.47105	0.00037	0.47179
atrium11_pitch_160_MOD.out	1.600	0.55238	0.00042	0.55322
atrium11_pitch_200_MOD.out	2.000	0.62411	0.00047	0.62505
atrium11_pitch_240_MOD.out	2.400	0.67726	0.00044	0.67814
atrium11_pitch_280_MOD.out	2.800	0.71075	0.00044	0.71163
atrium11_pitch_301_MOD.out	3.0056	0.71942	0.00046	0.72034
atrium11_pitch_320_MOD.out	**3.200**	**0.72369**	**0.00043**	**0.72455**
atrium11_pitch_352_MOD.out	3.520	0.71850	0.00039	0.71928

Table 6-89 Moderator Density Sensitivity Study Results with 11x11 Fuel Rods

Filename	Moderator Density (g/cm^3)	k_{eff}	σ	k_{eff} + 2σ
atrium11_dens000_MOD.out	0.00	0.19803	0.00020	0.19843
atrium11_dens010_MOD.out	0.10	0.38208	0.00034	0.38276
atrium11_dens020_MOD.out	0.20	0.53767	0.00045	0.53857
atrium11_dens040_MOD.out	0.40	0.68478	0.00040	0.68558
atrium11_pitch_320_MOD.out	**0.60**	**0.72369**	**0.00043**	**0.72455**
atrium11_dens080_MOD.out	0.80	0.71880	0.00041	0.71962
atrium11_dens100_MOD.out	1.00	0.69309	0.00040	0.69389

Table 6-90 Polyethylene Liner Sensitivity Study Results with 11x11 Fuel Rods

Filename	Polyethylene Liner Thickness (cm)	k_{eff}	σ	k_{eff} + 2σ
looseRods_liner_000.out	0.00	0.72386	0.00042	0.72470
looseRods_liner_020.out	0.20	0.72532	0.00042	0.72616
looseRods_liner_040.out	**0.40**	**0.72635**	**0.00045**	**0.72725**
looseRods_liner_060.out	0.60	0.72565	0.00044	0.72653
looseRods_liner_080.out	0.80	0.72477	0.00046	0.72569
looseRods_liner_full.out	0.8125	0.72512	0.00041	0.72594

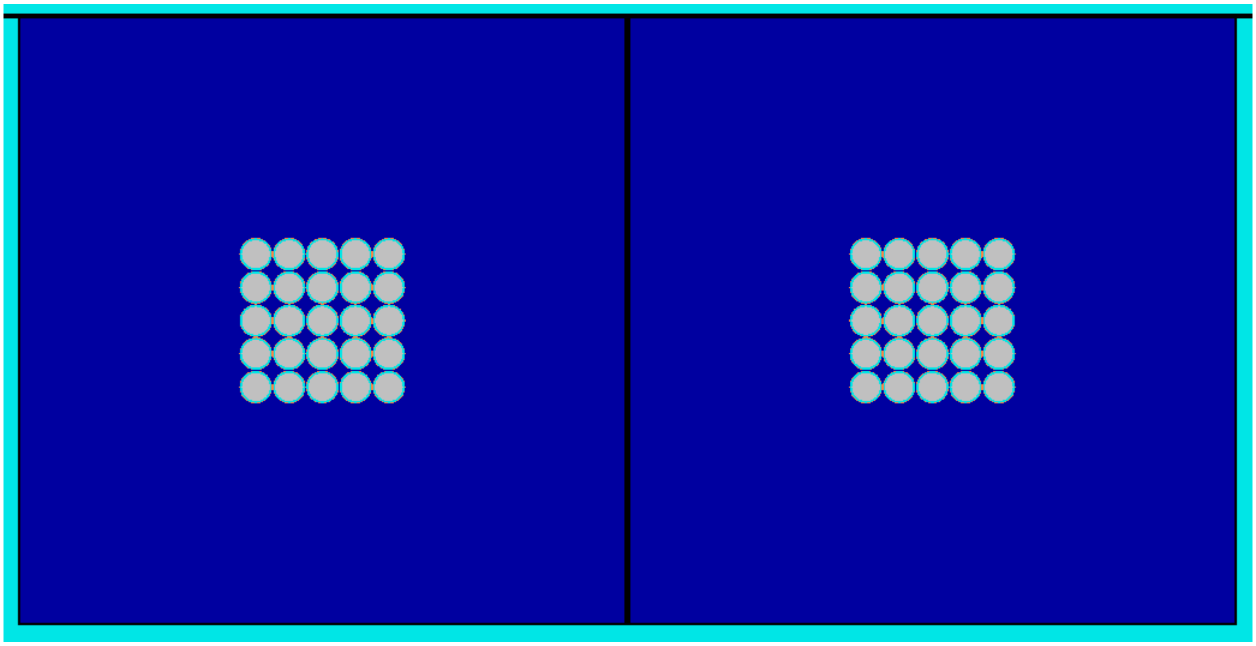

Close-packed loose fuel rods

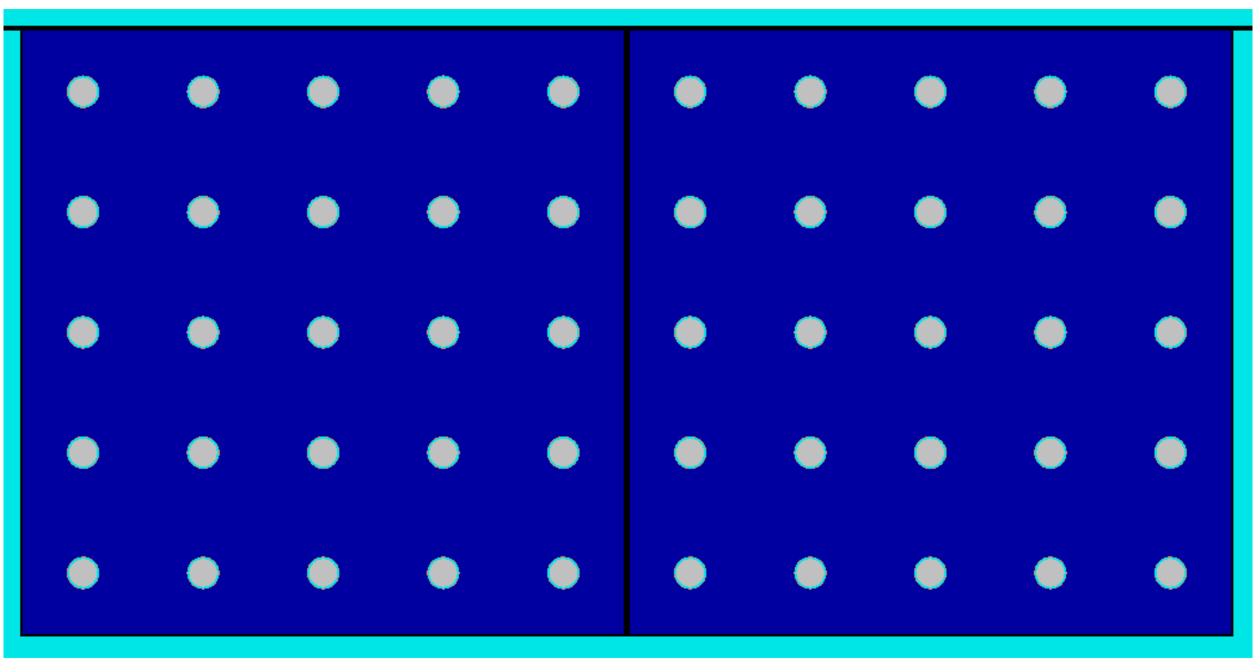

Maximum-pitch loose fuel rods

Figure 6-80 Twenty-five 11x11 Fuel Rods in the TN-B1 Container

6.12.7.2. 11x11 Fuel Rods in 5-in Pipe or Protective Case

In the following analysis, the fuel rods are placed in a 5-in stainless steel pipe. Thirty (30) fuel rods per pipe, or 60 fuel rods per package, are considered. This analysis bounds fuel rods transported in a protective case, as the protective case has a much smaller cross sectional area than the pipe and would allow significantly less moderation.

The package array model under HAC is used for the fuel rod in a stainless steel pipe calculations since it is demonstrated to be more reactive than the NCT package array model for the 11x11 fuel assembly. The volume inside the pipe is filled with water. The inner compartment volume outside the pipe as well as the volume in the outer container is initially modeled with no material present to maximize neutron interactions among packages in the array. This configuration is consistent with complete liner foam burn. The pipe's stainless steel wall is neglected for conservatism.

A 5-in schedule 40 pipe has an outer diameter of 5.563-in and a wall thickness of 0.258-in. The pipe is modeled as a moderator-filled cylinder with a 5.563-in diameter, which allows additional volume for pitch expansion because the pitch is allowed to expand until the outer diameter of the pipe is reached. The number of rods allowed in a pipe is limited to 30, consistent with the 10x10 fuel rod design. A triangular pitch is used in the models, similar to the 10x10 rod analysis, and a fuel rod pitch sensitivity study is performed. The fuel rod pitch is varied from close packed to filling the pipe, as shown in Figure 6-81 Thirty 11x11 Fuel Rods in a 5-in Stainless Steel Pipe. The results are given in Table 6-91 Fuel Rod Pitch Sensitivity Study Results with 11x11 Fuel Rods in a Pipe. The maximum reactivity for 30 fuel rods per pipe is found with a fuel rod pitch of 2.3606 cm, which is the maximum possible pitch.

The fuel rod pitch sensitivity study is executed using a water density of 1.0 g/cm^3. To ensure that this moderator density produces the highest reactivity for the 11x11 rods, a moderator density study is performed. A rod pitch of 2.3606 cm is used for the moderator density study. The results are provided in Table 6-92 Moderator Density in Pipe Sensitivity Study Results with 11x11 Fuel Rods. These results show that a moderator density of 1.0 g/cm^3 produces the highest reactivity for 30 11x11 fuel rods in the pipe within the TN-B1 package array.

Because the rods in the pipe are likely undermoderated, it is possible that reducing the number of rods within the pipe may increase reactivity by increasing moderation. Using the maximum reactivity configuration from above (fuel rod pitch of 2.3606 cm, density of 1.0 g/cm^3), several calculations are performed to show that 30 rods remain bounding. First, two rods are removed from near center for a total of 28 rods in the pipe. Next, four rods are removed from the periphery for a total of 26 rods in the pipe. Removing these rods also allows the pitch to increase slightly. Calculations are performed for the original pitch, corresponding to 30 rods, and with the maximum pitch allowed with 26 rods. Finally, 22 rods are considered by removing four periphery rods and four interior rods. This configuration is considered for both the original pitch corresponding to 30 rods and the maximum pitch allowed with 22 rods. The configurations at maximum pitch are shown in Figure 6-82 Configurations for Sensitivity Study on Number of 11x11 Fuel Rods in a 5-in Stainless Steel Pipe. Results are provided in Table 6-93 Number of Rods Sensitivity Study Results with 11x11 Fuel in Pipe and indicate that reducing the number of rods in the pipe decreases reactivity.

The outer diameter of the pipe is 5.563-in, which is significantly less than the width of the fuel compartment of the TN-B1 container. Thus, the location of the pipe within the compartment is considered. Only the horizontal positioning of the pipe is varied since it is shown in the 11x11 fuel assembly orientation study (see Section 6.12.3.5.1, Fuel Assembly Orientation Study) that reactivity is not sensitive to the vertical variation. The original configuration has both pipes centered horizontally and nearly flush with the bottom of the compartment, as illustrated in Figure 6-81 Thirty 11x11 Fuel Rods in a 5-in Stainless Steel Pipe. Configurations considered in this sensitivity study are provided in Figure 6-83 Configurations for Sensitivity Study on Placement of the 5-in Stainless Steel Pipe. Results are given in Table 6-94 Pipe Placement Sensitivity Study Results and demonstrate that shifting both pipes toward the center of the container (case shift2) produces the highest reactivity.

A study considering the polyethylene liner within the inner container is also performed. The most reactive fuel rod pitch of 2.3606 cm is used along with a moderator density of 1.0 g/cm^3. The liner thickness is varied from no liner to the maximum liner that could accommodate the pipe. The foam liner is modeled with a density of 0.08 g/cm^3 on the top and sides and 0.16 g/cm^3 on the bottom. It is observed when the liner has completely burned away (see Table 6-94 Pipe Placement Sensitivity Study Results) that maximum reactivity occurs when both pipes are shifted toward the center of the container (shifted in). Thus, when the liner is modeled, two pipe orientations are investigated: (1) pipes centered within their compartment, and (2) pipes shifted in. It is noted that for the study with the pipes shifted in, the location of the pipe shifts with the liner thickness. The results for the liner study are provided in Table 6-95 Polyethylene Liner Sensitivity Study Results with 11x11 Fuel Rods in Pipe and indicate that the most reactive configuration occurs when the liner has completely burned away with the pipes shifted in. It is noted that there is very little variation in the results for the different liner thicknesses.

Finally, a second moderator density study is performed in which moderator is modeled outside the pipe but within the inner container with varying density. The most reactive model from the polyethylene liner study is used for this study: both pipes shifted in and no foam liner present. The results for the study are provided in Table 6-96 Inner Container (Outside Pipe) Moderator Density Sensitivity Study. The results indicate that adding moderator with a density of $\leq$0.1 g/cm^3 outside of the pipe increases reactivity. The maximum $k_{eff} + 2\sigma$ is 0.82035 for 0.1 g/cm^3 water in this region.

Table 6-91 Fuel Rod Pitch Sensitivity Study Results with 11x11 Fuel Rods in a Pipe

Filename	Fuel Rod Pitch (cm)	k_{eff}	σ	k_{eff} + 2σ
30rods_pipe_pitch0961_MOD.out	0.9606	0.48115	0.00043	0.48201
30rods_pipe_pitch1261_MOD.out	1.2606	0.58817	0.00045	0.58907
30rods_pipe_pitch1561_MOD.out	1.5606	0.68463	0.00044	0.68551
30rods_pipe_pitch1861_MOD.out	1.8606	0.75785	0.00047	0.75879
30rods_pipe_pitch2048_MOD.out	2.0484	0.78662	0.00048	0.78758
30rods_pipe_pitch2161_MOD.out	2.1606	0.79855	0.00046	0.79947
30rods_pipe_pitch2361_MOD.out	**2.3606**	**0.80614**	**0.00047**	**0.80708**

Table 6-92 Moderator Density in Pipe Sensitivity Study Results with 11x11 Fuel Rods

Filename	Moderator Density (g/cm^3)	k_{eff}	σ	k_{eff} + 2σ
30rods_pipe_dens00_MOD.out	0.00	0.21700	0.00022	0.21744
30rods_pipe_dens01_MOD.out	0.10	0.30569	0.00028	0.30625
30rods_pipe_dens02_MOD.out	0.20	0.41873	0.00036	0.41945
30rods_pipe_dens04_MOD.out	0.40	0.60063	0.00040	0.60143
30rods_pipe_dens06_MOD.out	0.60	0.71187	0.00049	0.71285
30rods_pipe_dens08_MOD.out	0.80	0.77393	0.00045	0.77483
30rods_pipe_pitch2361_MOD.out	**1.00**	**0.80614**	**0.00047**	**0.80708**

Table 6-93 Number of Rods Sensitivity Study Results with 11x11 Fuel in Pipe

Filename	# Rods	Pitch, cm	k_{eff}	σ	k_{eff} + 2σ
atrium11_22rods_pipe.out	22	2.3606	0.70613	0.00043	0.70699
atrium11_22rods_pipe_maxPitch.out	22	2.5326	0.69620	0.00042	0.69704
atrium11_26rods_pipe.out	26	2.3606	0.76348	0.00044	0.76436
atrium11_26rods_pipe_maxPitch.out	26	2.5326	0.76328	0.00045	0.76418
atrium11_28rods_pipe.out	28	2.3606	0.78038	0.00049	0.78136
30rods_pipe_pitch2361_MOD.out	**30**	**2.3606**	**0.80614**	**0.00047**	**0.80708**

Table 6-94 Pipe Placement Sensitivity Study Results

Filename	Left pipe placement [a]	Right pipe placement [a]	k_{eff}	σ	k_{eff} + 2σ
30rods_pipe_pitch2361_MOD.out	center	center	0.80614	0.00047	0.80708
pipe_shift_up.out	up	up	0.80580	0.00043	0.80666
pipe_shift1.out	center	in	0.80947	0.00044	0.81035
pipe_shift2.out	**in**	**in**	**0.81502**	**0.00048**	**0.81598**
pipe_shift3.out	center	out	0.80487	0.00046	0.80579
pipe_shift4.out	out	out	0.80268	0.00044	0.80356

[a] Refers to horizontal position for all cases except pipe_shift_up. Pipe_shift_up shifts the pipes vertically to the center of the compartment.

Table 6-95 Polyethylene Liner Sensitivity Study Results with 11x11 Fuel Rods in Pipe

Filename	Polyethylene Liner Thickness (cm)	k_{eff}	σ	k_{eff} + 2σ
Pipes centered in compartments				
liner_000_cntr_void.out	0.00	0.80563	0.00044	0.80651
liner_020_cntr_void.out	0.20	0.80736	0.00044	0.80824
liner_040_cntr_void.out	0.40	0.80834	0.00046	0.80926
liner_060_cntr_void.out	0.60	0.80886	0.00044	0.80974
liner_080_cntr_void.out	0.80	0.80879	0.00049	0.80977
liner_100_cntr_void.out	1.00	0.80915	0.00042	0.80999
liner_120_cntr_void.out	1.20	0.81128	0.00046	0.81220
liner_140_cntr_void.out	1.40	0.81179	0.00050	0.81279
liner_160_cntr_void.out	1.60	0.81144	0.00048	0.81240
liner_full_cntr_void.out	1.74	0.81198	0.00046	0.81290
Pipes shifted in towards center of container [a]				
liner_000_shift2_void.out	**0.00**	**0.81557**	**0.00047**	**0.81651**
liner_020_shift2_void.out	0.20	0.81443	0.00056	0.81555
liner_040_shift2_void.out	0.40	0.81373	0.00041	0.81455
liner_060_shift2_void.out	0.60	0.81281	0.00047	0.81375
liner_080_shift2_void.out	0.80	0.81336	0.00043	0.81422
liner_100_shift2_void.out	1.00	0.81343	0.00042	0.81427
liner_120_shift2_void.out	1.20	0.81293	0.00046	0.81385
liner_140_shift2_void.out	1.40	0.81259	0.00047	0.81353
liner_160_shift2_void.out	1.60	0.81278	0.00046	0.81370
liner_full_shift2_void.out	1.74	0.81198	0.00046	0.81290

[a] For these cases, the pipes are shifted towards the center of the package as in “shift2” of Figure 6-83; however, the pipes are centered vertically in the compartment instead of being shifted to the bottom of the compartment.

Table 6-96 Inner Container (Outside Pipe) Moderator Density Sensitivity Study

Filename	Moderator Density (g/cm^3)	k_{eff}	σ	$k_{eff} + 2σ$
liner_000_shift2_void.out [a]	0.00	0.81557	0.00047	0.81651
mod_in_pipe10_dens002.out:	0.02	0.81657	0.00043	0.81743
mod_in_pipe10_dens004.out:	0.04	0.81709	0.00046	0.81801
mod_in_pipe10_dens006.out:	0.06	0.81827	0.00049	0.81925
mod_in_pipe10_dens008.out:	0.08	0.81871	0.00046	0.81963
mod_in_pipe10_dens010.out:	**0.10**	**0.81947**	**0.00044**	**0.82035**
mod_in_pipe10_dens020.out:	0.20	0.81481	0.00045	0.81571
mod_in_pipe10_dens040.out:	0.40	0.80142	0.00047	0.80236
mod_in_pipe10_dens060.out:	0.60	0.78567	0.00046	0.78659
mod_in_pipe10_dens080.out:	0.80	0.76915	0.00041	0.76997
mod_in_pipe10_dens100.out:	1.0	0.75750	0.00044	0.75838

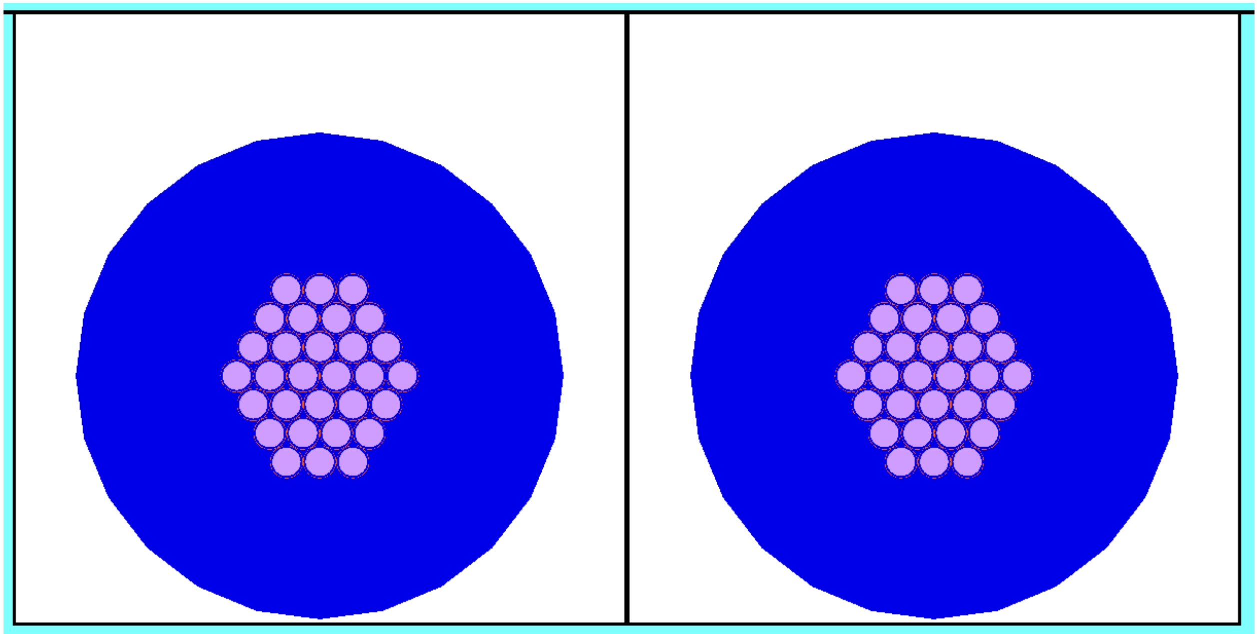

Close-packed fuel rods in pipe

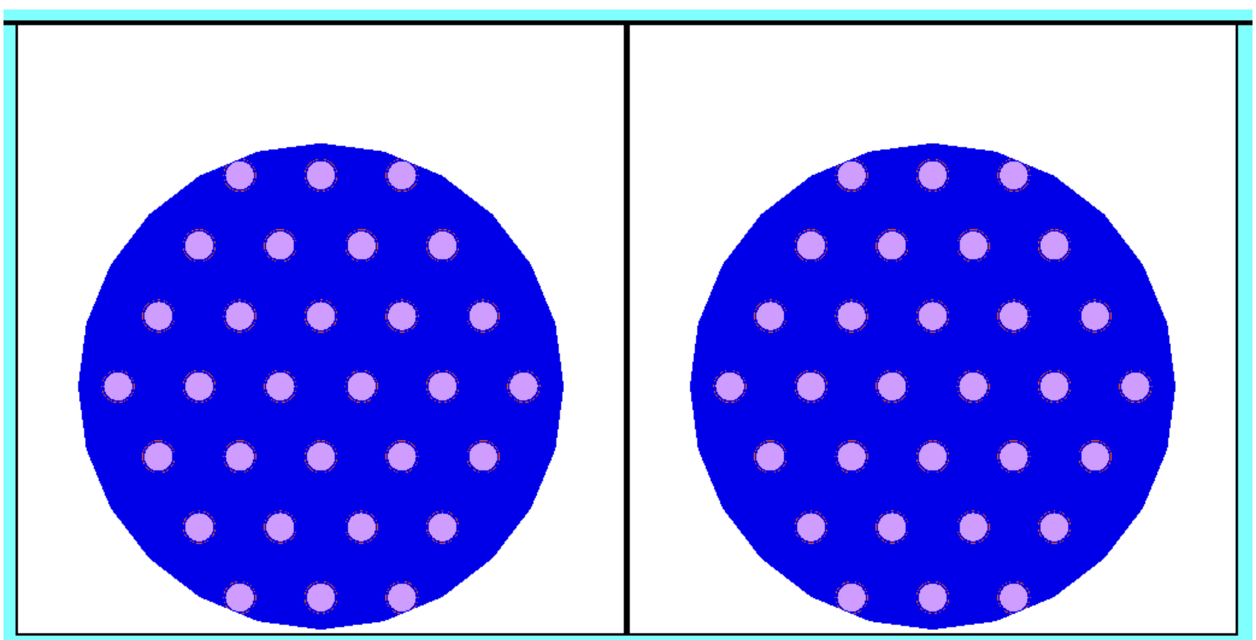

Maximum-pitch fuel rods in pipe

Figure 6-81 Thirty 11x11 Fuel Rods in a 5-in Stainless Steel Pipe

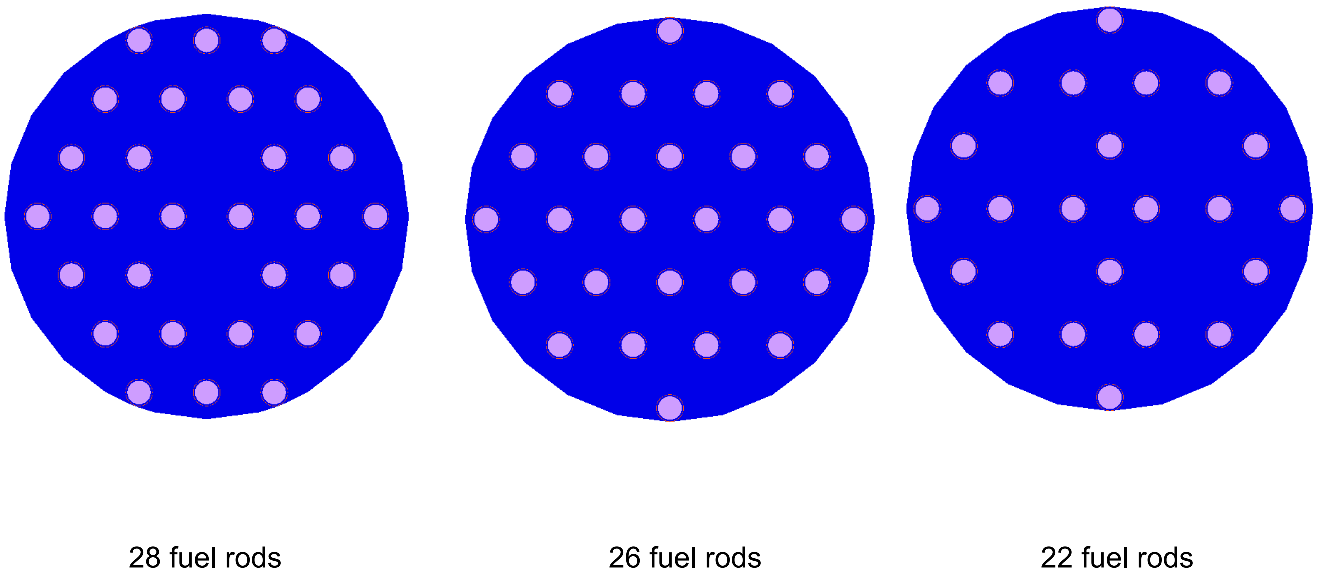

Figure 6-82 Configurations for Sensitivity Study on Number of 11x11 Fuel Rods in a 5-in Stainless Steel Pipe

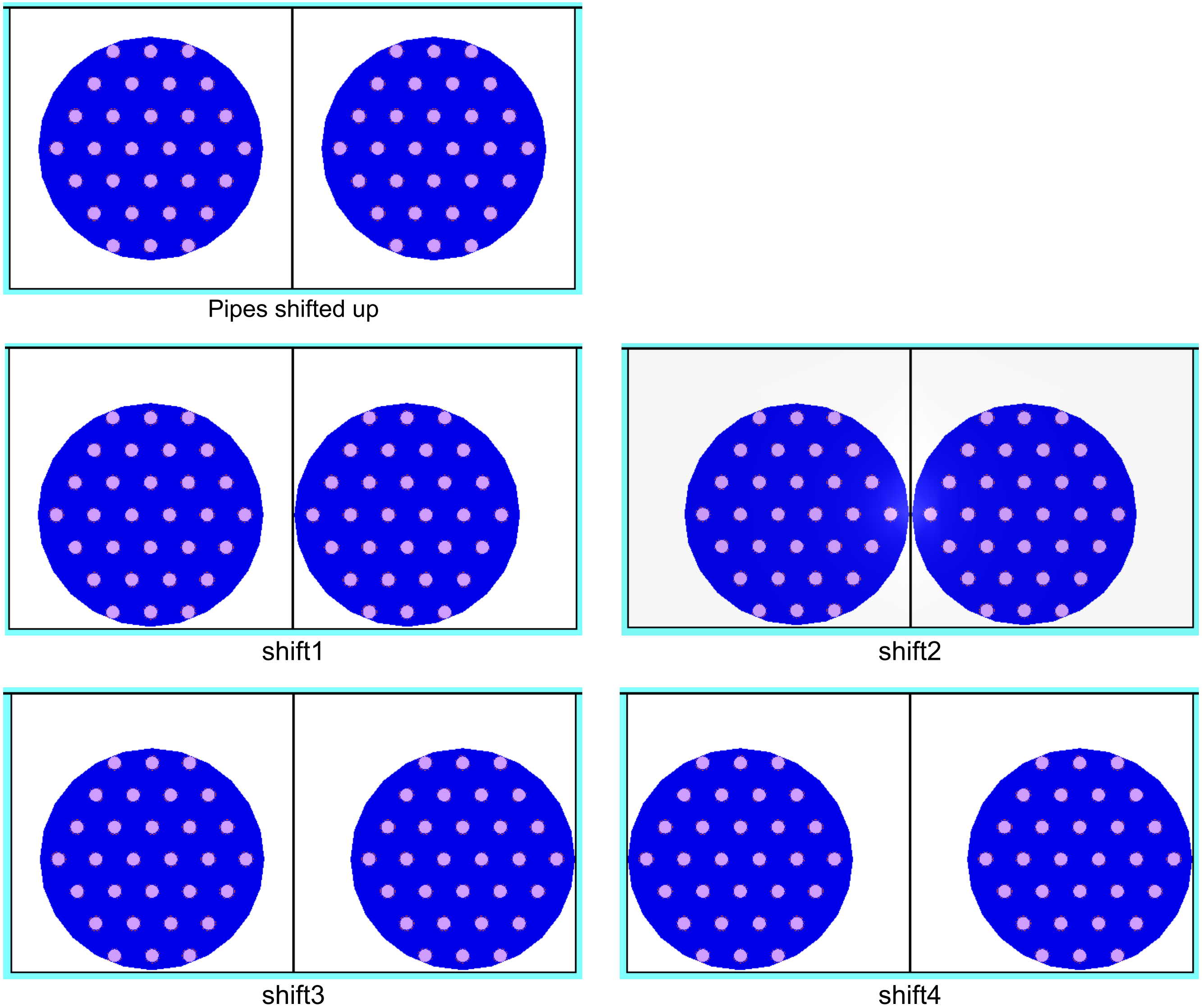

Figure 6-83 Configurations for Sensitivity Study on Placement of the 5-in Stainless Steel Pipe

6.12.7.3. Single Package Evaluation for 11x11 Rods

This section describes the evaluation of a single package model under NCT and HAC. Fuel parameters modeled to reflect the 11x11 rod worst-case parameters shown below:

UO_2 pellet density = 10.763 g/cm^3

UO_2 enrichment = 5.0 wt% ^{235}U

Pellet diameter = 0.820 cm

Rod outer diameter = 0.930 cm

Cladding thickness = 0.00 cm

Fuel length = 385 cm

A 6-mil layer of polyethylene encircles each fuel rod. Comparing the most reactive HAC array results from the loose rod analysis (k_{eff} +2σ = 0.72725, see Section 6.12.7.1) and pipe analysis (k_{eff} + 2σ = 0.82035, see Section 6.12.7.2), the pipe analysis is significantly more reactive than the loose rod analysis. Therefore, single package cases are performed only for 30 rods in the 5-in pipe. The NCT and HAC single package models are the same basic models used for the 11x11 fuel assembly analysis, with the fuel assembly replaced with the pipe. The single package model is enveloped with a 30.48-cm layer of full density water for reflection.

NCT Single Package

For the NCT single package evaluation, the stainless steel pipes are held centered within the inner container compartments by the polyethylene liner. The top and sides of the liner are modeled with 0.08 g/cm^3 polyethylene, while the bottom liner is modeled with 0.16 g/cm^3 polyethylene. A liner thickness of 1.74 cm is used, which corresponds to available space between the walls of the compartment and the pipe. The space between the pipe and the liner is filled with moderator.

A moderator density study, in which the density of the water within the inner container is varied, is performed for the NCT single package model. Results from the NCT single package model are provided in Table 6-97 TN-B1 NCT Single Package Evaluation with 11x11 Fuel Rods. The maximum k_{eff} + 2σ value for the single package normal conditions of transport case is 0.59235 for a moderator density of 1 g/cm^3, which is far below the rod USL of 0.94047. Therefore, criticality safety is established for the NCT single package TN-B1 container with 11x11 fuel rods.

HAC Single Package

For the HAC single package evaluation, the polyethylene foam liner is assumed to burn away and the pipes are allowed to move within the inner container compartments. Thus, the most reactive pipe configuration from Section 6.12.7.2, 11x11 Fuel Rods in 5-in Pipe or Protective Case, is used: shift2 with both pipes shifted toward the center of the container.

The Alumina Silicate thermal insulation is modeled between the inner and outer walls. This is consistent with the physical condition of the TN-B1 shipping container after being subjected to the tests specified in 10 CFR Part 71 (see Sections 3.2.2 and 3.5.2).

Two moderator density studies are performed for the most reactive configuration determined above. For the first study, the moderator density is varied within the inner container. For the second study, the moderator density in the pipe is fixed at 1.0 g/cm^3 while the density outside the pipe but within the inner container is varied.

Results from the HAC single package model are provided in Table 6-98 TN-B1 HAC Single Package Evaluation with 11x11 Fuel Rods, Moderator Density Varied within Pipe and Inner Container for the moderator density study in which all water within the pipe and inner container is uniformly varied. Results of fixing the moderator density in the pipe at 1.0 g/cm^3 and varying the water density outside the pipe are provided in Table 6-99 TN-B1 HAC Single Package Evaluation with 11x11 Fuel Rods: Moderator Density Varied Outside Pipe. The maximum k_{eff} + 2σ value for the single package HAC case is 0.66400 and occurs with maximum density water inside the pipe and inner container. This result is far below the rod USL of 0.94047. Therefore, criticality safety is established for the HAC single package TN-B1 container with 11x11 fuel rods.

Table 6-97 TN-B1 NCT Single Package Evaluation with 11x11 Fuel Rods

Filename	Moderator Density (g/cm^3)	k_{eff}	σ	k_{eff} + 2σ
NCT_single_pipe_dens000.out	0.00	0.23555	0.00027	0.23609
NCT_single_pipe_dens002.out	0.02	0.23929	0.00027	0.23983
NCT_single_pipe_dens004.out	0.04	0.24207	0.00027	0.24261
NCT_single_pipe_dens006.out	0.06	0.24581	0.00027	0.24635
NCT_single_pipe_dens008.out	0.08	0.25086	0.00030	0.25146
NCT_single_pipe_dens010.out	0.10	0.25585	0.00027	0.25639
NCT_single_pipe_dens020.out	0.20	0.28698	0.00031	0.28760
NCT_single_pipe_dens040.out	0.40	0.37263	0.00036	0.37335
NCT_single_pipe_dens060.out	0.60	0.45991	0.00039	0.46069
NCT_single_pipe_dens080.out	0.80	0.53590	0.00039	0.53668
NCT_single_pipe_dens100.out	**1.0**	**0.59145**	**0.00045**	**0.59235**

Table 6-98 TN-B1 HAC Single Package Evaluation with 11x11 Fuel Rods, Moderator Density Varied within Pipe and Inner Container

Filename	Moderator Density (g/cm^3)	k_{eff}	σ	k_{eff} + 2σ
HAC_single_pipe_dens000_shift.out	0.00	0.23969	0.00025	0.24019
HAC_single_pipe_dens002_shift.out	0.02	0.24037	0.00025	0.24087
HAC_single_pipe_dens004_shift.out	0.04	0.24167	0.00027	0.24221
HAC_single_pipe_dens006_shift.out	0.06	0.24368	0.00026	0.24420
HAC_single_pipe_dens008_shift.out	0.08	0.24749	0.00026	0.24801
HAC_single_pipe_dens010_shift.out	0.10	0.25197	0.00029	0.25255
HAC_single_pipe_dens020_shift.out	0.20	0.29275	0.00030	0.29335
HAC_single_pipe_dens040_shift.out	0.40	0.41304	0.00036	0.41376
HAC_single_pipe_dens060_shift.out	0.60	0.52597	0.00041	0.52679
HAC_single_pipe_dens080_shift.out	0.80	0.60853	0.00042	0.60937
HAC_single_pipe_dens100_shift.out	**1.0**	**0.66316**	**0.00042**	**0.66400**

Table 6-99 TN-B1 HAC Single Package Evaluation with 11x11 Fuel Rods: Moderator Density Varied Outside Pipe

Filename	Moderator Density (g/cm^3)	k_{eff}	σ	k_{eff} + 2σ
HAC_single_pipe_dens000_in100.out	0.00	0.57214	0.00044	0.57302
HAC_single_pipe_dens002_in100.out	0.02	0.57475	0.00043	0.57561
HAC_single_pipe_dens004_in100.out	0.04	0.57776	0.00047	0.57870
HAC_single_pipe_dens006_in100.out	0.06	0.58142	0.00041	0.58224
HAC_single_pipe_dens008_in100.out	0.08	0.58505	0.00043	0.58591
HAC_single_pipe_dens010_in100.out	0.10	0.58731	0.00043	0.58817
HAC_single_pipe_dens020_in100.out	0.20	0.60136	0.00040	0.60216
HAC_single_pipe_dens040_in100.out	0.40	0.62405	0.00043	0.62491
HAC_single_pipe_dens060_in100.out	0.60	0.64117	0.00043	0.64203
HAC_single_pipe_dens080_in100.out	0.80	0.65417	0.00044	0.65505
HAC_single_pipe_dens100_shift.out	**1.0**	**0.66316**	**0.00042**	**0.66400**

6.12.7.4. NCT Array Evaluation for 11x11 Rods

The NCT package array model is the same basic model used for the 11x11 fuel assembly analysis, with the fuel assembly replaced with the pipe. The model consists of a 21x3x24 array of containers, surrounded by a 30.48-cm layer of full density water for reflection. The container array is fully flooded with water at a density sufficient for maximum reactivity.

Fuel parameters modeled to reflect the 11x11 rod worst-case parameters shown below:

- UO_2 pellet density = 10.763 g/cm^3
- UO_2 enrichment = 5.0 wt% ^{235}U
- Pellet diameter = 0.820 cm
- Rod outer diameter = 0.930 cm
- Cladding thickness = 0.00 cm
- Fuel length = 385 cm

A 6-mil layer of polyethylene encircles each fuel rod. Comparing the most reactive HAC array results from the loose rod analysis (k_{eff} +2σ = 0.72725, see Section 6.12.7.1) and pipe analysis (k_{eff} + 2σ = 0.82035, see Section 6.12.7.2), the pipe analysis is significantly more reactive than the loose rod analysis. Therefore, NCT array cases are performed only for 30 rods in the 5-in pipe.

For the NCT package array evaluation, the fuel assemblies are held centered within the inner container compartments by the polyethylene liner. A liner thickness of 1.74 cm is used, which corresponds to available space between the walls of the compartment and the pipe. The space between the pipe and the liner is filled with moderator. The top and sides of the liner are modeled with 0.08 g/cm^3 polyethylene, while the bottom liner is modeled with 0.16 g/cm^3 polyethylene.

A moderator density study, in which the density of the water within the inner and outer containers is uniformly varied, is performed for the package array model. Results from the NCT package array model with 11x11 fuel rods are provided in Table 6-100 TN-B1 NCT Package Array Evaluation with 11x11 Fuel Rods. The maximum k_{eff} + 2σ value for the package array NCT case is 0.59384 and occurs for full density water, which is far below the rod USL of 0.94047. Therefore, criticality safety is established for the TN-B1 container package array with 11x11 fuel rods for the NCT array.

Table 6-100 TN-B1 NCT Package Array Evaluation with 11x11 Fuel Rods

Filename	Moderator Density (g/cm^3)	k_{eff}	σ	k_{eff} + 2σ
NCT_array_pipe_dens000.out	0.00	0.49959	0.00032	0.50023
NCT_array_pipe_dens002.out	0.02	0.53972	0.00036	0.54044
NCT_array_pipe_dens004.out	0.04	0.52833	0.00037	0.52907
NCT_array_pipe_dens006.out	0.06	0.51110	0.00035	0.51180
NCT_array_pipe_dens008.out	0.08	0.48967	0.00037	0.49041
NCT_array_pipe_dens010.out	0.10	0.46815	0.00037	0.46889
NCT_array_pipe_dens020.out	0.20	0.38906	0.00033	0.38972
NCT_array_pipe_dens040.out	0.40	0.38840	0.00036	0.38912
NCT_array_pipe_dens060.out	0.60	0.46283	0.00040	0.46363
NCT_array_pipe_dens080.out	0.80	0.53585	0.00042	0.53669
NCT_array_pipe_dens100.out	**1.0**	**0.59300**	**0.00042**	**0.59384**

6.12.7.5. HAC Array Evaluation for 11x11 Rods

The loose rod evaluation documented in Section 6.12.7.1, *11x11 Fuel Rods Loose or Bundled* and Section 6.12.7.2, *11x11 Fuel Rods in 5-in Pipe or Protective Case*, are for a 10x1x10 HAC array. Comparing the most reactive HAC array results from the loose rod analysis (k_{eff} +2σ = 0.72725) and pipe analysis (k_{eff} + 2σ = 0.82035), the pipe analysis is significantly more reactive than the loose rod analysis.

The most reactive pipe configuration is with a moderator density of 1.0 g/cm^3 inside the pipe and 0.10 g/cm^3 within the inner container, outside the pipe. The polyethylene foam liner is assumed to have burned away, which allows the pipes to relocate toward the center of the package. The region between the inner and outer container is conservatively modeled as void. The maximum k_{eff} + 2σ value for the HAC package array case is 0.82035, which is below the USL of 0.94047. Therefore, criticality safety of the TN-B1 shipping container with 11x11 fuel rods is demonstrated for the HAC array.

6.12.8. *Fissile Material Packages for Air Transport*

This package is not intended for the air transport of fissile material.

6.12.9. *Benchmark Evaluation for SCALE 6.1.3*

The 11x11 fuel assembly and fuel rod analyses are performed using the KENO V.a module of SCALE 6.1.3. Therefore, the SCALE 4.4a benchmarking evaluation documented in Section 6.10, *Benchmark Evaluations*, is repeated using SCALE 6.1.3. The SCALE 6.1.3 benchmark evaluation uses the 238 group ENDF/B-VII cross section library with CENTRM resonance processing.

A USL of 0.94094 is justified for the 11x11 fuel assembly, and a USL of 0.94047 is justified for the 11x11 fuel rod analysis.

6.12.9.1. Applicability of Benchmark Experiments

A total of 58 experiments are selected for benchmarking SCALE 6.1.3 as it is applied to the current evaluation. The 27 experiments originally used in the TN-B1 criticality analysis (see Section 6.10, *Benchmark Evaluations*) are retained in the current analysis:

- 14 configurations: These configurations are water moderated U(4.31 wt. %)O_2 fuel rods in 2.54 cm square-pitched arrays reflected by aluminum, steel, borated steel, zircaloy or boral plates. These experiments use an open top carbon steel tank configuration with acrylic support plates, polyethylene lattice plates and aluminum plates as support structure.
- 13 configurations: These configurations are borated water moderated U(2.459 wt. %)O_2 fuel rods in 1.636 cm square-pitched arrays. 12 experiments replaced some of the fuel rods with U(4.02 wt. %)O_2 fuel rods and/or U(1.94 wt%)O_2-4 wt% Gd_2O_3 rods. These experiments use an aluminum tank and aluminum plates as support structure.

An additional 31 experiments from the International Handbook of Evaluated Criticality Safety Benchmark Experiments (ICSBEP) (Reference 17) are selected to supplement the original 27 experiments identified above. The additional experiments are:

- 8 configurations (cases 1-8) from LEU-COMP-THERM-001: These configurations are water moderated U(2.35 wt. %)O_2 fuel rods in 2.032 cm square-pitched arrays. These experiments use an open top carbon steel tank configuration with acrylic support plates, polyethylene lattice plates and aluminum plates as support structure.
- 4 configurations (cases 1-3, 5) from LEU-COMP-THERM-002: These configurations are water moderated U(4.31 wt. %)O_2 fuel rods in 2.54 cm square-pitched arrays. These experiments use an open top carbon steel tank configuration with acrylic support plates, polyethylene lattice plates and aluminum plates as support structure.
- 3 configurations (cases 1, 16, 17) from LEU-COMP-THERM-008: These configurations are borated water moderated U(2.459 wt. %)O_2 fuel rods in 1.636 cm square-pitched arrays. These experiments use an aluminum tank and aluminum plates as support structure.

- 12 configurations (cases 10-17, 19-22) from LEU-COMP-THERM-017: These configurations are water moderated U(2.35 wt. %)O_2 fuel rods in square pitched arrays reflected by steel. These experiments use an open top carbon steel tank configuration with acrylic support plates, polyethylene lattice plates and aluminum plates as support structure.
- 2 configurations (cases 1-2) from LEU-COMP-THERM-042: These configurations are water moderated, square-pitched arrays of U(2.35 wt. %)O_2 fuel rods separated by absorption plates made of steel (case 1) or borated steel (case 2) and reflected by steel walls. These experiments use open top carbon steel tank configuration with acrylic support plates, polyethylene lattice plates and aluminum plates as support structure.
- 2 configurations (cases 1-2) from LEU-COMP-THERM-050: These configurations are water moderated, square-pitched arrays of U(4.738 wt. %)O_2 fuel rods with a central zircaloy tank that contains water. These experiments use stainless steel tank configuration with aluminum alloy (AG3M) and stainless steel as support structure.

Table 6-101 Data for Selected Experiments summarizes pertinent data from each of the experiments selected to be included in the USL calculations. Table 6-102 Experiment Keff shows the experiment k_{eff} and associated uncertainty for all selected experiments. When available, the experiment k_{eff} and uncertainty values given Table 6-102 Experiment Keff are the benchmark values from the references. The benchmark values are determined in the ICSBEP evaluation by accounting for modeling approximations and simplifications.

The cases are run for 1550 generations, 2000 neutrons per generation, and 50 generations skipped. The results are summarized in Table 6-103 SCALE 6.1.3 Results. This table also includes parameters of interest in the USL evaluation: enrichment, moderator-to-fuel volume ratio, pin pitch, energy of the average lethargy of fission (EALF), and average energy group causing fission (AFG).

6.12.9.2. Bias Determination

A set of Upper Subcritical Limits is determined using the results from the critical experiments and the USL Method 1, Confidence Band with Administrative Margin. The USL Method 1 applies a statistical calculation of the method bias and its uncertainty plus an administrative margin (0.05 Δk) to a linear fit of the critical experiment benchmark data. The USLs are determined as a function of the critical experiment system parameters; enrichment, water-to-fuel volume ratio, pin pitch, EALF, and AFG.

While the original TN-B1 benchmarking also included a USL equation as a function of hydrogen-to-U-235 ratio, the additional experiments did not include this data. It is not expected that this parameter would result in a considerably better correlation of the data than the other parameters considered; therefore, a USL equation is not determined as a function of hydrogen-to-U-235 ratio for the current analysis.

The USL method has the tacit assumption that the experimental k is 1.0000 (Reference 7). Likewise, it does not account for the uncertainty in the experimental values. NUREG/CR-6698 (Reference 18) discusses a process for which a different value of the experiment k_{eff} is considered, as well as the experimental uncertainty. The document has the following definitions for the calculated values used for the bias evaluation:

$$k_{norm} = \frac{k_{calc}}{k_{exp}}$$

$$\sigma_{norm} = \sqrt{\sigma_{calc}^2 + \sigma_{exp}^2}$$

The above equations normalize the calculated to experimental data to account for uncertainties in the experiment values. K_{norm} and σ_{norm} for each case are provided in Table 6-104 Data Needed for Calculation of USL for SCALE 6.1.3 and are used to generate the USL equations. Table 6-104 also summarizes the data from Table 6-101 through Table 6-103 needed for the USL calculations.

Using the data in Table 6-104, a set of USL equations are generated using the USLSTATS code provided with SCALE 6.1.3. This is run using a 0.05 Δk margin. The USLSTATS computed results for each parameter are:

- The following equation is determined for the USL as a function of enrichment:
  USL = 0.9404 + (6.8308×10^{-4})x for all x.
  The variance of the equation fit is 2.2323×10^{-6}.
  The applicable range for enrichment is $2.35 \leq x \leq 4.738$ ^{235}U wt%
- The following equation is determined for the USL as a function of water-to-fuel volume ratio:
  USL = 0.9403 + (8.5180×10^{-4})x for all x.
  The variance of the equation fit is 2.0192×10^{-6}.
  The applicable range for water-to-fuel ratio is $1.60 \leq x \leq 3.8832$
- The following equation is determined for the USL as a function of pin pitch:
  USL = 0.9385 + (2.0457×10^{-3})x for all x.
  The variance of the equation fit is 1.9479×10^{-6}.
  The applicable range for pin pitch is $1.30 \leq x \leq 2.54$ cm
- The following equation is determined for the USL as a function of average energy of the lethargy causing fission:
  USL = 0.9440 - (9.1167×10^{-3})x for all x.
  The variance of the equation fit is 2.1023×10^{-6}.
  The applicable range for average energy of lethargy causing fission is $0.0936 \leq x \leq 0.3547$ eV

- The following equation is determined for the USL as a function of the average energy group causing fission:
  USL = 0.9126 + (1.4681×10^{-4})x for all x.
  The variance of the equation fit is 2.0426×10^{-6}.
  The applicable range for average energy group causing fission is $193.58 \leq x \leq 209.32$

Of the preceding equations, the USL as a function of pin pitch is the best correlation to the data since the variance of the equation fit is the smallest (Reference 7, Section 4.1.3). Therefore, the USL as a function of pin pitch is used to determine a minimum USL for the 11x11 fuel assembly for use with the TN-B1 shipping container. Figure 6-84: USL as a Function of Pin Pitch shows the USL as a function of pin pitch. The nominal pin pitch used in the 11x11 fuel assembly criticality analyses is 1.195 cm. Although the 1.195 cm pin pitch falls outside the range of applicability, ANSI/ANS-8.1 (Reference 6) allows the range of applicability to be extended beyond the range of conditions represented by the benchmarks, as long as that extrapolation is not large. As outlined in (Reference 7), k(x)-w(x) is used to extend the USL curve beyond the range of applicability. Figure 6-84: USL as a Function of Pin Pitch displays the USL curve extrapolation using k(x)-w(x); the extrapolated USL value corresponding to the 1.195 cm pin pitch is 0.94094. Since the extrapolated value results in a lower USL than the minimum pin pitch within the range of applicability would produce (0.94116), the USL corresponding to the 1.195 cm pin pitch is selected. Therefore, the USL for the TN-B1 shipping container with 11x11 fuel assemblies is 0.94094.

It is also noted that the most reactive 11x11 fuel assembly is for the HAC cases where the pitch is increased by 5%. Increasing the pin pitch would bring the value closer to the range of applicability but would also increase the USL. Thus, using the lower USL corresponding to the nominal pitch is conservative.

This USL value is not directly applicable to the 11x11 fuel rod analysis since the pin pitch is not maintained. Per Section 6.12.7, *Transport of 11x11 Rods*, the pin pitch for the fuel rod study varies from 0.970 cm to 3.520 cm for the loose rods and from 0.9606 cm to 2.3606 cm for the rods in the pipe.

The USL corresponding to the smallest pin pitch in the fuel rod analysis is 0.94047. The smallest pin pitch corresponds to the lowest USL. Use of a lower USL for configurations with larger pitch values is conservative. Therefore, an upper subcritical limit of 0.94047 is used for comparison of all fuel rod configurations to ensure subcriticality.

The following equation is used to develop the keff for the transportation of fuel in the TN-B1 shipping container:

$$k_{eff} = k_{case} + 2\sigma$$

where:

k_{case} = KENO V.a (SCALE 6.1.3) k_{eff} for a particular case of interest

σ = uncertainty in the calculated KENO V.a (SCALE 6.1.3) k_{eff} for a particular case of interest

The k_{eff} for each container configuration analyzed in the TN-B1 shipping container criticality analysis is compared to the USL of 0.94094 for the 11x11 fuel assembly or 0.94047 for the 11x11 fuel rod analysis to ensure subcriticality.

Table 6-101 Data for Selected Experiments

Experiment Name	Assembly Separation (cm)	Boron Conc. (ppm)	Enrichment (^{235}U wt%)	Mod/fuel ratio	Pin Pitch (cm)	Comments
See Section 6.11.10.1						
c004	10.62	-	4.31	3.8832	2.54	no absorber plates
c005b	9.64	-	4.31	3.8832	2.54	0.625 cm Al plates
c006b	9.59	-	4.31	3.8832	2.54	0.625 cm Al plates
c007a	8.63	-	4.31	3.8832	2.54	0.302 cm SS 304L plates
c008b	8.09	-	4.31	3.8832	2.54	0.302 cm SS 304L plates
c009b	6.95	-	4.31	3.8832	2.54	0.298 cm SS 304L plates with 1.05 wt% B
c010b	5.47	-	4.31	3.8832	2.54	0.298 cm SS 304L plates with 1.05 wt% B
c011b	6.77	-	4.31	3.8832	2.54	0.298 cm SS 304L plates with 1.62 wt% B
c012b	4.63	-	4.31	3.8832	2.54	0.298 cm SS 304L plates with 1.62 wt% B
c013b	8.52	-	4.31	3.8832	2.54	0.485 cm SS 304L plates
c014b	7.45	-	4.31	3.8832	2.54	0.485 cm SS 304L plates
c029b	9.77	-	4.31	3.8832	2.54	0.652 cm Zircaloy-4 plates
c030b	9.73	-	4.31	3.8832	2.54	0.652 cm Zircaloy-4 plates
c031b	6.55	-	4.31	3.8832	2.54	0.723 cm Boral plates, 28.7 wt% B
See Section 6.11.10.2 [a]						
core01	-	1337.9	2.459	1.9385	1.6358	4808-2.46 wt%
core03	-	1239.3	2.457	1.9282	1.6358	4788-2.46 wt%, 20 Gd
core05	-	1208.0	2.456	1.9385	1.6358	4780-2.46 wt%, 28 Gd
core05a	-	1191.3	2.456	1.9385	1.6358	4776-2.46 wt%, 32 Gd
core05b	-	1207.1	2.456	1.9385	1.6358	4780-2.46 wt%, 28 Gd
core08	-	1170.7	2.455	1.9385	1.6358	4772-2.46 wt%, 36 Gd
core10	-	1177.1	2.455	1.9278	1.6358	4772-2.46 wt%, 36 Gd
core12a	-	1899.3	2.747	1.8714	1.6358	3920-2.46 wt%, 888-4.02 wt%
core14	-	1653.8	2.735	1.8735	1.6358	3920-2.46 wt%, 860-4.02 wt%, 28 Gd
core16	-	1579.4	2.732	1.8741	1.6358	3920-2.46 wt%, 852-4.02 wt%, 36 Gd
core18	-	1776.8	2.778	1.8866	1.6358	3676-2.46 wt%, 944-4.02 wt%
core19	-	1628.3	2.771	1.8878	1.6358	3676-2.46 wt%, 928-4.02 wt%, 16 Gd
core20	-	1499.0	2.764	1.8891	1.6358	3676- 2.46 wt%, 912-4.02 wt%, 32 Gd

Table 6–101 Data for Selected Experiments Continued

Experiment Name	Assembly Separation (cm)	Boron Conc. (ppm)	Enrichment (^{235}U wt%)	Mod/fuel ratio	Pin Pitch (cm)	Comments
LEU-COMP-THERM-001, Table 10-2						
-001	-	-	2.35	2.918	2.032	
-002	11.92	-	2.35	2.918	2.032	
-003	8.41	-	2.35	2.918	2.032	
-004	10.05	-	2.35	2.918	2.032	
-005	6.39	-	2.35	2.918	2.032	
-006	8.01	-	2.35	2.918	2.032	
-007	4.46	-	2.35	2.918	2.032	
-008	7.57	-	2.35	2.918	2.032	
LEU-COMP-THERM-002, Table 10-2						
-001	-	-	4.31	3.882	2.540	contains partial rows
-002	-	-	4.31	3.882	2.540	contains partial rows
-003	-	-	4.31	3.882	2.540	contains partial rows
-005	7.11	-	4.31	3.882	2.540	13x8 array
LEU-COMP-THERM-008, Table 10-2						
-001	-	1511	2.459	1.841	1.636	no water rods
-016	-	1158	2.459	1.841	1.636	water rods in lines
-017	-	921	2.459	1.841	1.636	water rods in lines
LEU-COMP-THERM-017, Table 10-2						
-010	9.89	-	2.35	2.918	2.032	steel plates
-011	10.44	-	2.35	2.918	2.032	steel plates
-012	10.44	-	2.35	2.918	2.032	steel plates
-013	9.60	-	2.35	2.918	2.032	steel plates
-014	8.75	-	2.35	2.918	2.032	steel plates
-015	8.57	-	2.35	1.600	1.684	steel plates
-016	9.17	-	2.35	1.600	1.684	steel plates
-017	9.10	-	2.35	1.600	1.684	steel plates
-019	8.87	-	2.35	1.600	1.684	steel plates
-020	8.65	-	2.35	1.600	1.684	steel plates
-021	8.13	-	2.35	1.600	1.684	steel plates
-022	7.26	-	2.35	1.600	1.684	steel plates
LEU-COMP-THERM-042, Table 10-2						
-001	8.28	-	2.35	1.600	1.684	steel plates
-002	4.80	-	2.35	1.600	1.684	borated steel plates
LEU-COMP-THERM-050, Table 10-2						
-001	-	-	4.738	2.032	1.300	center water tank
-002	-	-	4.738	2.032	1.300	center water tank

[a] Enrichment listed for these experiments are the average of all rods in the core. The number of rods for each enrichment is listed in the “comments” column with the ^{235}U enrichment of the Gd rods being 1.94 wt%.

Table 6-102 Experiment K_{eff}

Case	k_{eff} [a]	σ
See Table 6-43		
c004	0.9997	0.0020
c005b	0.9997	0.0020
c006b	0.9997	0.0020
c007a	0.9997	0.0020
c008b	0.9997	0.0020
c009b	0.9997	0.0020
c010b	0.9997	0.0020
c011b	0.9997	0.0020
c012b	0.9997	0.0020
c013b	0.9997	0.0020
c014b	0.9997	0.0020
c029b	0.9997	0.0020
c030b	0.9997	0.0020
c031b	0.9997	0.0020
See Table 6-47		
core01	1.0002	0.0005
core03	1.0000	0.0006
core05	0.9999	0.0006
core05a	0.9999	0.0006
core05b	0.9999	0.0006
core08	1.0083	0.0012
core10	1.0001	0.0009
core12a	1.0000	0.0007
core14	1.0030	0.0009
core16	1.0001	0.0010
core18	1.0002	0.0011
core19	1.0002	0.0010
core20	1.0002	0.0010

Case	k_{eff} [a]	σ
LEU-COMP-THERM-001, Section 3.5		
-001	0.9998	0.0031
-002	0.9998	0.0031
-003	0.9998	0.0031
-004	0.9998	0.0031
-005	0.9998	0.0031
-006	0.9998	0.0031
-007	0.9998	0.0031
-008	0.9998	0.0031
LEU-COMP-THERM-002, Section 3.5		
-001	0.9997	0.0020
-002	0.9997	0.0020
-003	0.9997	0.0020
-005	0.9997	0.0020
LEU-COMP-THERM-008, Section 3.5		
-001	1.0007	0.0012
-016	1.0007	0.0012
-017	1.0007	0.0012
LEU-COMP-THERM-017, Section 3.5		
-010	1.0000	0.0031
-011	1.0000	0.0031
-012	1.0000	0.0031
-013	1.0000	0.0031
-014	1.0000	0.0031
-015	1.0000	0.0028
-016	1.0000	0.0028
-017	1.0000	0.0028
-019	1.0000	0.0028
-020	1.0000	0.0028
-021	1.0000	0.0028
-022	1.0000	0.0028
LEU-COMP-THERM-042, Section 3.5		
-001	1.0000	0.0016
-002	1.0000	0.0016
LEU-COMP-THERM-050, Section 3.5		
-001	1.0004	0.0010
-002	1.0004	0.0010

[a] When available, the experiment k_{eff} and uncertainty values given in this table are the benchmark values from the references. The benchmark values are determined in the ICSBEP evaluations by accounting for modeling approximations and simplifications.

Table 6-103 SCALE 6.1.3 Results

Experiment	Enrichment (^{235}U wt%)	Mod/fuel ratio	Pitch (cm)	EALF (eV)	AFG	k_{eff}	σ
TN-B1 original set							
c004	4.31	3.8832	2.54	0.1117	207.75	0.9970	0.0005
c005b	4.31	3.8832	2.54	0.1117	207.74	0.9980	0.0005
c006b	4.31	3.8832	2.54	0.1119	207.73	0.9981	0.0005
c007a	4.31	3.8832	2.54	0.1120	207.72	0.9983	0.0005
c008b	4.31	3.8832	2.54	0.1121	207.70	0.9966	0.0005
c009b	4.31	3.8832	2.54	0.1125	207.67	0.9983	0.0004
c010b	4.31	3.8832	2.54	0.1133	207.58	0.9985	0.0005
c011b	4.31	3.8832	2.54	0.1127	207.64	0.9968	0.0005
c012b	4.31	3.8832	2.54	0.1133	207.57	0.9982	0.0005
c013b	4.31	3.8832	2.54	0.1119	207.72	0.9972	0.0005
c014b	4.31	3.8832	2.54	0.1125	207.67	0.9970	0.0005
c029b	4.31	3.8832	2.54	0.1115	207.77	0.9982	0.0005
c030b	4.31	3.8832	2.54	0.1117	207.74	0.9983	0.0005
c031b	4.31	3.8832	2.54	0.1131	207.60	0.9987	0.0005
core01	2.459	1.9385	1.6358	0.2460	198.01	0.9962	0.0004
core03	2.457	1.9282	1.6358	0.2452	198.04	0.9959	0.0004
core05	2.456	1.9385	1.6358	0.2447	198.06	0.9961	0.0004
core05a	2.456	1.9385	1.6358	0.2446	198.06	0.9964	0.0004
core05b	2.456	1.9385	1.6358	0.2453	198.03	0.9955	0.0004
core08	2.455	1.9385	1.6358	0.2450	198.04	0.9965	0.0004
core10	2.455	1.9278	1.6358	0.2451	198.03	0.9960	0.0003
core12a	2.747	1.8714	1.6358	0.3547	193.58	0.9971	0.0005
core14	2.735	1.8735	1.6358	0.3355	194.24	0.9965	0.0005
core16	2.732	1.8741	1.6358	0.3287	194.49	0.9962	0.0004
core18	2.778	1.8866	1.6358	0.3525	193.66	0.9977	0.0005
core19	2.771	1.8878	1.6358	0.3406	194.06	0.9973	0.0004
core20	2.764	1.8891	1.6358	0.3289	194.48	0.9970	0.0004
LEU-COMP-THERM-001							
-001	2.35	2.918	2.032	0.097	208.94	0.9982	0.0004
-002	2.35	2.918	2.032	0.096	209.05	0.9968	0.0005
-003	2.35	2.918	2.032	0.095	209.16	0.9965	0.0004
-004	2.35	2.918	2.032	0.096	209.07	0.9978	0.0004
-005	2.35	2.918	2.032	0.094	209.22	0.9955	0.0004
-006	2.35	2.918	2.032	0.095	209.12	0.9976	0.0004
-007	2.35	2.918	2.032	0.094	209.32	0.9965	0.0006
-008	2.35	2.918	2.032	0.095	209.19	0.9963	0.0004
LEU-COMP-THERM-002							
-001	4.31	3.882	2.540	0.113	207.60	0.9978	0.0005
-002	4.31	3.882	2.540	0.113	207.62	0.9995	0.0005
-003	4.31	3.882	2.540	0.113	207.64	0.9976	0.0005
-005	4.31	3.882	2.540	0.112	207.76	0.9985	0.0005
LEU-COMP-THERM-008							
-001	2.459	1.841	1.636	0.280	196.49	0.9969	0.0004
-016	2.459	1.841	1.636	0.228	198.96	0.9985	0.0004
-017	2.459	1.841	1.636	0.199	200.56	0.9972	0.0004

Table 6-103 SCALE 6.1.3 Results (continued)

Experiment	Enrichment (^{235}U wt%)	Mod/fuel ratio	Pitch (cm)	EALF (eV)	AFG	k_{eff}	σ
LEU-COMP-THERM-017							
-010	2.35	2.918	2.032	0.100	208.54	0.9973	0.0004
-011	2.35	2.918	2.032	0.098	208.74	0.9970	0.0005
-012	2.35	2.918	2.032	0.097	208.90	0.9979	0.0004
-013	2.35	2.918	2.032	0.095	209.09	0.9980	0.0004
-014	2.35	2.918	2.032	0.095	209.19	0.9977	0.0004
-015	2.35	1.600	1.684	0.178	201.72	0.9972	0.0004
-016	2.35	1.600	1.684	0.172	202.13	0.9977	0.0005
-017	2.35	1.600	1.684	0.167	202.50	0.9984	0.0004
-019	2.35	1.600	1.684	0.162	202.82	0.9978	0.0005
-020	2.35	1.600	1.684	0.161	202.93	0.9967	0.0004
-021	2.35	1.600	1.684	0.159	203.04	0.9970	0.0005
-022	2.35	1.600	1.684	0.158	203.12	0.9964	0.0005
LEU-COMP-THERM-042							
-001	2.35	1.600	1.684	0.169	202.34	0.9968	0.0005
-002	2.35	1.600	1.684	0.176	201.86	0.9961	0.0004
LEU-COMP-THERM-050							
-001	4.738	2.032	1.300	0.200	200.35	0.9978	0.0005
-002	4.738	2.032	1.300	0.191	200.90	0.9965	0.0005

Table 6-104 Data Needed for Calculation of USL for SCALE 6.1.3

Experiment	Enrichment (^{235}U wt%)	Mod/fuel ratio	Pitch (cm)	EALF (eV)	AFG	k_{norm} [a]	σ_{norm} [b]
TN-B1 original set							
c004	4.31	3.8832	2.54	0.1117	207.75	0.9973	0.0021
c005b	4.31	3.8832	2.54	0.1117	207.74	0.9983	0.0021
c006b	4.31	3.8832	2.54	0.1119	207.73	0.9984	0.0021
c007a	4.31	3.8832	2.54	0.1120	207.72	0.9986	0.0021
c008b	4.31	3.8832	2.54	0.1121	207.70	0.9969	0.0021
c009b	4.31	3.8832	2.54	0.1125	207.67	0.9986	0.0020
c010b	4.31	3.8832	2.54	0.1133	207.58	0.9988	0.0021
c011b	4.31	3.8832	2.54	0.1127	207.64	0.9971	0.0021
c012b	4.31	3.8832	2.54	0.1133	207.57	0.9985	0.0021
c013b	4.31	3.8832	2.54	0.1119	207.72	0.9975	0.0021
c014b	4.31	3.8832	2.54	0.1125	207.67	0.9973	0.0021
c029b	4.31	3.8832	2.54	0.1115	207.77	0.9985	0.0021
c030b	4.31	3.8832	2.54	0.1117	207.74	0.9986	0.0021
c031b	4.31	3.8832	2.54	0.1131	207.60	0.9990	0.0021
core01	2.459	1.9385	1.6358	0.2460	198.01	0.9960	0.0006
core03	2.457	1.9282	1.6358	0.2452	198.04	0.9959	0.0007
core05	2.456	1.9385	1.6358	0.2447	198.06	0.9962	0.0007
core05a	2.456	1.9385	1.6358	0.2446	198.06	0.9965	0.0007
core05b	2.456	1.9385	1.6358	0.2453	198.03	0.9956	0.0007
core08	2.455	1.9385	1.6358	0.2450	198.04	0.9882	0.0013
core10	2.455	1.9278	1.6358	0.2451	198.03	0.9959	0.0010
core12a	2.747	1.8714	1.6358	0.3547	193.58	0.9971	0.0009
core14	2.735	1.8735	1.6358	0.3355	194.24	0.9935	0.0010
core16	2.732	1.8741	1.6358	0.3287	194.49	0.9961	0.0011
core18	2.778	1.8866	1.6358	0.3525	193.66	0.9975	0.0012
core19	2.771	1.8878	1.6358	0.3406	194.06	0.9971	0.0011
core20	2.764	1.8891	1.6358	0.3289	194.48	0.9968	0.0011
LEU-COMP-THERM-001							
-001	2.35	2.918	2.032	0.097	208.94	0.9984	0.0031
-002	2.35	2.918	2.032	0.096	209.05	0.9970	0.0031
-003	2.35	2.918	2.032	0.095	209.16	0.9967	0.0031
-004	2.35	2.918	2.032	0.096	209.07	0.9980	0.0031
-005	2.35	2.918	2.032	0.094	209.22	0.9957	0.0031
-006	2.35	2.918	2.032	0.095	209.12	0.9978	0.0031
-007	2.35	2.918	2.032	0.094	209.32	0.9967	0.0031
-008	2.35	2.918	2.032	0.095	209.19	0.9965	0.0031

Table 6-104 Data Needed for Calculation of USL for SCALE 6.1.3 (continued)

Experiment	Enrichment (^{235}U wt%)	Mod/fuel ratio	Pitch (cm)	EALF (eV)	AFG	k_{norm} [a]	σ_{norm} [b]
LEU-COMP-THERM-002							
-001	4.31	3.882	2.540	0.113	207.60	0.9981	0.0021
-002	4.31	3.882	2.540	0.113	207.62	0.9998	0.0021
-003	4.31	3.882	2.540	0.113	207.64	0.9979	0.0021
-005	4.31	3.882	2.540	0.112	207.76	0.9988	0.0021
LEU-COMP-THERM-008							
-001	2.459	1.841	1.636	0.280	196.49	0.9962	0.0013
-016	2.459	1.841	1.636	0.228	198.96	0.9978	0.0013
-017	2.459	1.841	1.636	0.199	200.56	0.9965	0.0013
LEU-COMP-THERM-017							
-010	2.35	2.918	2.032	0.100	208.54	0.9973	0.0031
-011	2.35	2.918	2.032	0.098	208.74	0.9970	0.0031
-012	2.35	2.918	2.032	0.097	208.90	0.9979	0.0031
-013	2.35	2.918	2.032	0.095	209.09	0.9980	0.0031
-014	2.35	2.918	2.032	0.095	209.19	0.9977	0.0031
-015	2.35	1.600	1.684	0.178	201.72	0.9972	0.0028
-016	2.35	1.600	1.684	0.172	202.13	0.9977	0.0028
-017	2.35	1.600	1.684	0.167	202.50	0.9984	0.0028
-019	2.35	1.600	1.684	0.162	202.82	0.9978	0.0028
-020	2.35	1.600	1.684	0.161	202.93	0.9967	0.0028
-021	2.35	1.600	1.684	0.159	203.04	0.9970	0.0028
-022	2.35	1.600	1.684	0.158	203.12	0.9964	0.0028
LEU-COMP-THERM-042							
-001	2.35	1.600	1.684	0.169	202.34	0.9968	0.0017
-002	2.35	1.600	1.684	0.176	201.86	0.9961	0.0016
LEU-COMP-THERM-050							
-001	4.738	2.032	1.300	0.200	200.35	0.9974	0.0011
-002	4.738	2.032	1.300	0.191	200.90	0.9961	0.0011

[a] $k_{norm} = k_{calc} / k_{exp}$, where k_{calc} is shown in Table 6-103 and k_{exp} is given in Table 6-102.

[b] $\sigma_{norm} = \sqrt{\sigma_{calc}^2 + \sigma_{exp}^2}$, where σ_{calc} is shown in Table 6-103 and σ_{exp} is given in Table 6-102.

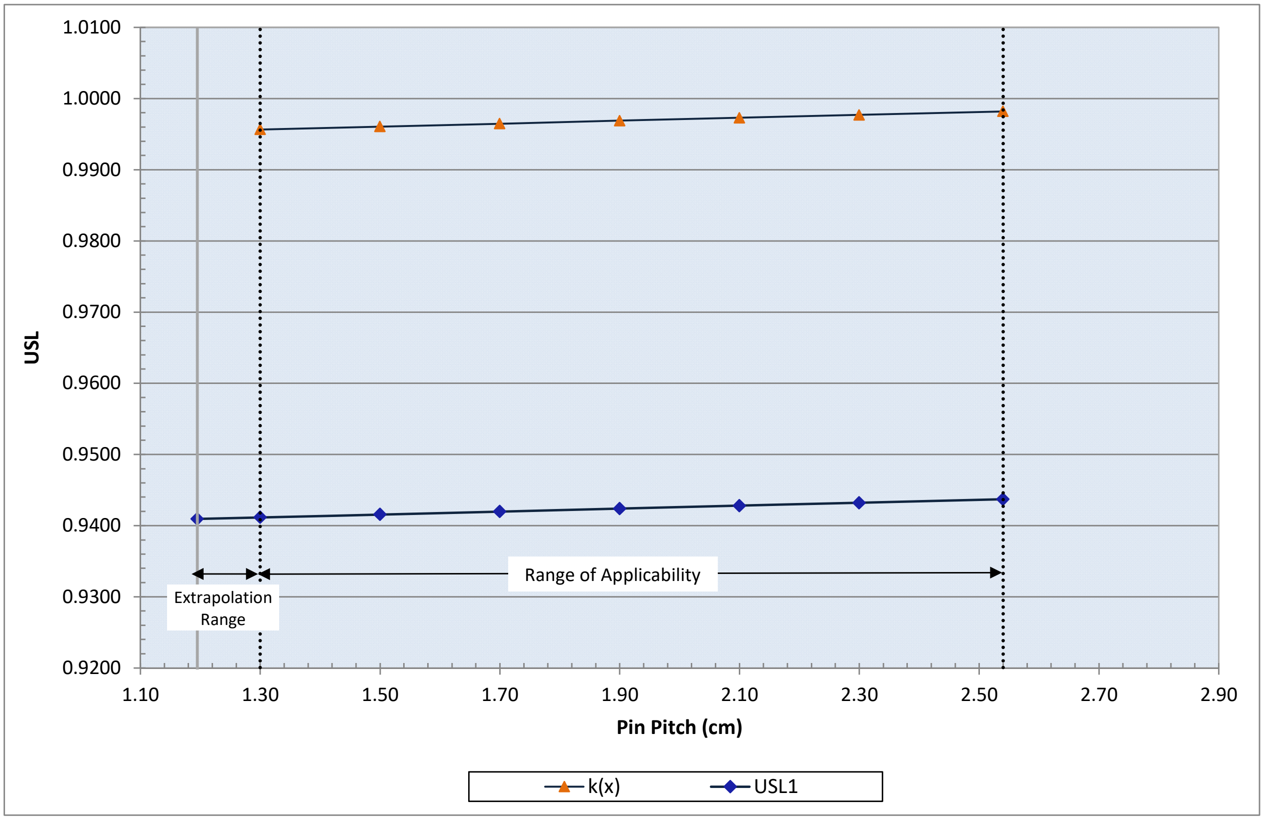

Figure 6-84: USL as a Function of Pin Pitch

6.12.10. *Sample Input Files*

Sample input files are provided for the most reactive 11x11 fuel assembly and 11x11 rod cases.

6.12.10.1. 11x11 Fuel Assembly, HAC Array, Case “5wt_13gd”

```
=csas5
     TN-B1 container, hac, 5.0wt, 13 gad rods
v7-238
read composition
 uo2         1 den=10.763 1 293                                  material 1, UO2 (see Section 6.12.3.2
                                 92235 5                                               and Table 6-60)
                                 92238 95   end
 zr          2 0.31309 293   end
 polyethylene 2 den=0.949 0.68691 293   end
 h2o         3 0.01 293   end
 atomuo2         4  10.763  2                             material 4, entry 1, UO2 (see Section 6.12.3.2
                                 92000 1                                               and Table 6-60)
                                 8016 2
                       0.9784 293
                                 92235 5
                                 92238 95   end
 atomgd2o3       4  7.407  2                            material 4, entry 2, Gd2O3 (see Section 6.12.3.2
                                 64000 2                                               and Table 6-60)
                                 8016 3
                       0.0216 293   end
 h2o         5 1 293   end
 ss304       6 1 293   end
 h2o         7 den=1 1 293   end
 polyethylene 8 den=0.08 1 293   end
 polyethylene 9 den=0.16 1 293   end
 atomal2o3       10  0.25  2
                                 13027 2
                                 8016 3
                       0.49 293   end
 atomsio2        10  0.25  2
                                 14000 1
                                 8016 2
                       0.51 293   end
 zr          12 0.31309 293   end
 polyethylene 12 den=0.949 0.68691 293   end
 h2o         17 den=1 1 293   end
 h2o         18 den=1 1 293   end
 h2o         19 den=1 1 293   end
 zr          15 1 293   end
end composition
read celldata
  latticecell squarepitch fuelr=0.4100 1 gapr=0.420 18 cladr=0.5510 2 hpitch=0.6274 7 end
  latticecell squarepitch fuelr=0.4100 4 gapr=0.420 19 cladr=0.5510 12 hpitch=0.6274 17 end
end celldata
read parameter
 tme=400
 gen=1550
 npg=2000
 nsk=50
 htm=no
end parameter
```

```
read geometry
unit 1
com="container inner box"
 cuboid 6 1   0.0875  -0.0875    225.2  -228.34    8.829   -8.829
 cuboid 7 1   17.713  -17.713    225.2  -228.34    8.829   -8.829
  hole 4 -8.9002   0   0
  hole 5  8.9002   0   0
 cuboid 6 1     17.8    -17.8    225.2  -228.34    8.829  -8.9165
 cuboid 10 1   22.798  -22.798    225.2  -228.34    8.829  -13.839
 cuboid 6 1   22.798  -22.798   225.34  -228.48    8.829  -13.979
 cuboid 10 1   22.798  -22.798   225.34  -233.44    8.829  -13.979
 cuboid 6 1   22.938  -22.938   225.48  -233.58    8.829  -13.979
unit 2
com="inner box lid"
 cuboid 10 1   22.798  -22.798   229.39  -229.39     2.48    -2.48
 cuboid 6 1   22.938  -22.938   229.53  -229.53     2.62    -2.62
unit 3
com="inner box with ends and lid"
  array 1       0       0       0
unit 4
com="foam polyethylene for left assembly compartment"
 cuboid 7 1   7.1556  -7.1556    225.2  -228.34    7.1556  -7.1556
  hole 70   -6.9014   -192.5    -6.9014
 cuboid 7 1   7.6126  -7.6126    225.2  -228.34    7.629   -7.629
 cuboid 8 1   8.8126  -8.8126    225.2  -228.34    8.829   -7.629
 cuboid 9 1   8.8126  -8.8126    225.2  -228.34    8.829   -8.829
unit 5
com="foam polyethylene for right assembly compartment"
 cuboid 7 1   7.1556  -7.1556    225.2  -228.34    7.1556  -7.1556
  hole 70   -6.9014   -192.5    -6.9014
 cuboid 7 1   7.6126  -7.6126    225.2  -228.34    7.629   -7.629
 cuboid 8 1   8.8126  -8.8126    225.2  -228.34    8.829   -7.629
 cuboid 9 1   8.8126  -8.8126    225.2  -228.34    8.829   -8.829
unit 10
com="5 w/o fuel pins w/o gad - lower level"
 ycylinder 1 1  0.4100    155.1        0
 ycylinder 7 1   0.420    155.1        0
 ycylinder 2 1  0.5510    155.1        0
 cuboid 7 1   0.6274  -0.6274    155.1        0   0.6274  -0.6274
unit 11
com="5 w/o fuel pins w/o gad - middle level"
 ycylinder 1 1  0.4100     81.7        0
 ycylinder 7 1   0.420     81.7        0
 ycylinder 2 1  0.5510     81.7        0
 cuboid 7 1   0.6274  -0.6274     81.7        0   0.6274  -0.6274
unit 12
com="5 w/o fuel pins w/o gad - upper level"
 ycylinder 1 1  0.4100    148.2        0
 ycylinder 7 1   0.420    148.2        0
 ycylinder 2 1  0.5510    148.2        0
 cuboid 7 1   0.6274  -0.6274    148.2        0   0.6274  -0.6274
unit 20
com="space within fuel assembly lattice - lower level"
 cuboid 7 1   0.6274  -0.6274    155.1        0   0.6274  -0.6274
unit 21
com="space within fuel assembly lattice - middle level"
 cuboid 7 1   0.6274  -0.6274     81.7        0   0.6274  -0.6274
unit 22
com="space within fuel assembly lattice - upper level"
 cuboid 7 1   0.6274  -0.6274    148.2        0   0.6274  -0.6274
```

```
unit 40
com="5 w/o fuel pins w/ gad - lower level"
 ycylinder 4 1  0.4100    155.1        0
 ycylinder 7 1   0.420    155.1        0
 ycylinder 2 1  0.5510    155.1        0
 cuboid 7 1   0.6274  -0.6274    155.1        0   0.6274  -0.6274
unit 41
com="5 w/o fuel pins w/ gad - middle level"
 ycylinder 4 1  0.4100     81.7        0
 ycylinder 7 1   0.420     81.7        0
 ycylinder 2 1  0.5510     81.7        0
 cuboid 7 1   0.6274  -0.6274     81.7        0   0.6274  -0.6274
unit 42
com="5 w/o fuel pins w/ gad - upper level"
 ycylinder 4 1  0.4100    148.2        0
 ycylinder 7 1   0.420    148.2        0
 ycylinder 2 1  0.5510    148.2        0
 cuboid 7 1   0.6274  -0.6274    148.2        0   0.6274  -0.6274
unit 50
com="lower level assembly"
  array 2       0        0        0
unit 51
com="middle level fuel assembly"
  array 3       0        0        0
unit 52
com="upper level fuel assembly"
  array 4       0        0        0
unit 70
com="complete fuel assembly"
  array 5       0        0        0
 replicate 15 1   0.254    0.254    0.00    0.00    0.254    0.254 1
unit 400
com="outer container body and lid"
 cuboid 0 1   35.788  -35.788   247.96  -253.19     29.5    -31.9
  hole 3 -22.938  -229.53  -14.024
 cuboid 6 1   35.963  -35.963  248.135  -253.365   29.675  -32.075
global unit 500
com="global unit 500 references array 10"
  array 10       0        0        0
 replicate 5 1   30.48    30.48    30.48    30.48    30.48    30.48 1
end geometry
read array
ara=1 nux=1 nuy=1 nuz=2
 com=''
 fill
    1
    2  end fill
ara=2 nux=11 nuy=1 nuz=11
 com=''
 fill
   10   10   10   10   10   10   10   10   10   10   10
   10   10   10   10   10   10   10   10   10   10   10
   10   10   10   10   10   10   10   10   10   10   10
   10   10   10   10   10   10   10   10   10   10   10
   10   10   10   10   20   20   20   10   10   10   10
   10   10   10   10   20   20   20   10   10   10   10
   10   10   10   10   20   20   20   10   40   40   10
   10   10   10   10   10   10   10   40   40   40   10
   10   10   10   10   10   10   40   40   40   40   10
   10   10   10   10   10   10   40   40   40   40   10
```

```
   10   10   10   10   10   10   10   10   10   10   10  end fill
ara=3 nux=11 nuy=1 nuz=11
 com=''
 fill
   21   11   11   11   11   11   11   11   11   11   21
   11   11   11   11   11   11   11   11   11   11   11
   11   11   21   11   11   11   11   11   21   11   11
   11   11   11   11   11   21   11   11   11   11   11
   11   11   11   11   21   21   21   11   11   11   11
   11   11   11   21   21   21   21   21   11   41   11
   11   11   11   11   21   21   21   11   41   41   11
   11   11   11   11   11   21   11   11   41   41   11
   11   11   21   11   11   11   41   41   21   41   11
   11   11   11   11   11   41   41   41   41   41   11
   21   11   11   11   11   11   11   11   11   11   21  end fill
ara=4 nux=11 nuy=1 nuz=11
 com=''
 fill
   22   12   12   12   12   12   12   12   12   12   22
   12   12   12   12   12   12   12   12   12   12   12
   12   12   22   12   12   22   12   12   22   12   12
   12   12   12   22   12   22   12   22   12   12   12
   12   12   12   12   22   22   22   12   12   12   12
   12   12   22   22   22   22   22   22   22   42   12
   12   12   12   12   22   22   22   12   42   42   12
   12   12   12   22   12   22   12   22   42   42   12
   12   12   22   12   12   22   42   42   22   42   12
   12   12   12   12   12   42   42   42   42   42   12
   22   12   12   12   12   12   12   12   12   12   22  end fill
ara=5 nux=1 nuy=3 nuz=1
 fill
   52
   51
   50  end fill
ara=10 nux=10 nuy=1 nuz=10
 com=''
 fill
  400  400  400  400  400  400  400  400  400  400
  400  400  400  400  400  400  400  400  400  400
  400  400  400  400  400  400  400  400  400  400
  400  400  400  400  400  400  400  400  400  400
  400  400  400  400  400  400  400  400  400  400
  400  400  400  400  400  400  400  400  400  400
  400  400  400  400  400  400  400  400  400  400
  400  400  400  400  400  400  400  400  400  400
  400  400  400  400  400  400  400  400  400  400
  400  400  400  400  400  400  400  400  400  400  end fill
end array
read bnds
 +xb=vacuum
 -xb=vacuum
 +yb=vacuum
 -yb=vacuum
 +zb=vacuum
 -zb=vacuum
  end bnds
end data
end
```

6.12.10.2. 11x11 Fuel Rod Analysis, HAC Array, Case "mod_in_pipe10_dens010"

```
'Input generated by GeeWiz SCALE 6.1 Compiled on Tue Sep  6 15:23:32 2011
=csas5
     TN-B1 container, 11, hac, worst case model, 2.0484 cm pitch, rods in pipe
v7-238
read composition
 uo2         1 den=10.763 1 293                                material 1, UO2 (see Section 6.12.3.2
                                 92235 5                                        and Table 6-60)
                                 92238 95   end
 polyethylene 2 den=0.949 1 293   end
 h2o         3 den=1.00 1 293   end
 h2o         5 1 293   end
 ss304       6 1 293   end
 h2o         7 den=0.10 1 293   end
 h2o         8 den=1.00 1 293   end
 atomal2o3       10  0.25  2
                                 13027 2
                                 8016 3
                       0.49 293   end
 atomsio2        10  0.25  2
                                 14000 1
                                 8016 2
                       0.51 293   end
end composition
read celldata
  latticecell triangpitch fuelr=0.41 1 gapr=0.465 3 cladr=0.48024 2 hpitch=1.1803 8 end
end celldata
read parameter
 tme=400
 gen=1550
 npg=2000
 nsk=50
 htm=no
end parameter
read geometry
unit 1
com="container inner box"
 cuboid 6 1   0.0875  -0.0875    225.2  -228.34    8.829   -8.829
 cuboid 7 1   17.713  -17.713    225.2  -228.34    8.829   -8.829
  hole 4 -8.9003   0   0
  hole 5  8.9003   0   0
 cuboid 6 1     17.8    -17.8    225.2  -228.34    8.829  -8.9165
 cuboid 10 1   22.798  -22.798    225.2  -228.34    8.829  -13.839
 cuboid 6 1   22.798  -22.798   225.34  -228.48    8.829  -13.979
 cuboid 10 1   22.798  -22.798   225.34  -233.44    8.829  -13.979
 cuboid 6 1   22.938  -22.938   225.48  -233.58    8.829  -13.979
unit 2
com="inner box lid"
 cuboid 10 1   22.798  -22.798   229.39  -229.39     2.48    -2.48
 cuboid 6 1   22.938  -22.938   229.53  -229.53     2.62    -2.62
unit 3
com="inner box with ends and lid"
  array 1       0        0        0
unit 4
```

```
com="foam polyethylene for left assembly compartment"
 cuboid 7 1   8.8126  -5.3274    225.2  -228.34    7.07  -7.07
  hole 70   1.7426   -192.5    0
 cuboid 7 1   8.8126  -8.8126    225.2  -228.34    8.829   -8.829
unit 5
com="foam polyethylene for right assembly compartment"
 cuboid 7 1   5.3274  -8.8126    225.2  -228.34    7.07  -7.07
  hole 70   -1.7426   -192.5    0
 cuboid 7 1   8.8126  -8.8126    225.2  -228.34    8.829   -8.829
unit 10
com="5 w/o fuel pins w/o gad"
 ycylinder 1 1 0.41      385.0        0
 ycylinder 3 1 0.465     385.0        0
 ycylinder 2 1 0.48024   385.0        0
unit 70
com="5-inch ss pipe"
 ycylinder 3 1   7.065   385.0        0
  hole 10    -5.9015     0     0
  hole 10    -3.5409     0     0
  hole 10    -1.1803     0     0
  hole 10    1.18030     0
  hole 10    3.54090     0
  hole 10    5.90150     0
  hole 10    -3.5409     0     -4.0887
  hole 10    -1.1803     0     -4.0887
  hole 10    1.18030     -4.0887
  hole 10    3.54090     -4.0887
  hole 10    -3.5409     0     4.0887
  hole 10    -1.1803     0     4.0887
  hole 10    1.18030     4.0887
  hole 10    3.54090     4.0887
  hole 10    -4.7212     0     -2.0443
  hole 10    -2.3606     0     -2.0443
  hole 10    0     0     -2.0443
  hole 10    2.36060     -2.0443
  hole 10    4.72120     -2.0443
  hole 10    -4.7212     0     2.0443
  hole 10    -2.3606     0     2.0443
  hole 10    0     0     2.0443
  hole 10    2.36060     2.0443
  hole 10    4.72120     2.0443
  hole 10    -2.3606     0     -6.1330
  hole 10    0     0     -6.1330
  hole 10    2.36060     -6.1330
  hole 10    -2.3606     0     6.1330
  hole 10    0     0     6.1330
  hole 10    2.36060     6.1330
unit 400
com="outer container body and lid"
 cuboid 0 1   35.788  -35.788   247.96  -253.19     29.5    -31.9
  hole 3 -22.938  -229.53  -14.024
 cuboid 6 1   35.963  -35.963  248.135  -253.365   29.675  -32.075
global unit 500
  array 10       0        0        0
 replicate 5 1   30.48    30.48    30.48    30.48    30.48    30.48 1
end geometry
read array
```

```
ara=1 nux=1 nuy=1 nuz=2
 fill
    1
    2  end fill
ara=10 nux=10 nuy=1 nuz=10
 fill
  400  400  400  400  400  400  400  400  400  400
  400  400  400  400  400  400  400  400  400  400
  400  400  400  400  400  400  400  400  400  400
  400  400  400  400  400  400  400  400  400  400
  400  400  400  400  400  400  400  400  400  400
  400  400  400  400  400  400  400  400  400  400
  400  400  400  400  400  400  400  400  400  400
  400  400  400  400  400  400  400  400  400  400
  400  400  400  400  400  400  400  400  400  400
  400  400  400  400  400  400  400  400  400  400  end fill
end array
read bnds
 +xb=vacuum
 -xb=vacuum
 +yb=vacuum
 -yb=vacuum
 +zb=vacuum
 -zb=vacuum
  end bnds
end data
end
```

6.12.11. *Additional Analyses for Increased Fuel Channel and Assembly Orientation*

This section documents the additional criticality calculations performed for the 11x11 fuel assembly to address the following conditions:

- Increased fuel channel thickness to 0.320 cm
- Fuel assembly orientation within the package varied with consideration to location of the Gd rods in the limiting assembly configuration (see Figure 6-85)
- Added explicit consideration of preferential flooding in the NCT array configuration
- Added consideration of material change for inner container liner
- SCALE code errors for H1-Poly cross section

To be consistent with the USL generated in Section 6.12.9. *Benchmark Evaluation for SCALE 6.1.3* for the 11x11 fuel assembly criticality analysis, SCALE 6.1.3 is used for the calculations in this section. In February 2021, ORNL issued an error notice pertinent to SCALE 6.1.3 which consisted of an incorrect H1-Poly incoherent elastic scattering cross section that can cause an underprediction in k-eff. An adjustment to the results for the most reactive configurations found for the TN-B1 package is applied in Section 6.12.11.5 Adjustment for H1-Poly Cross Section on Most Reactive Configurations.

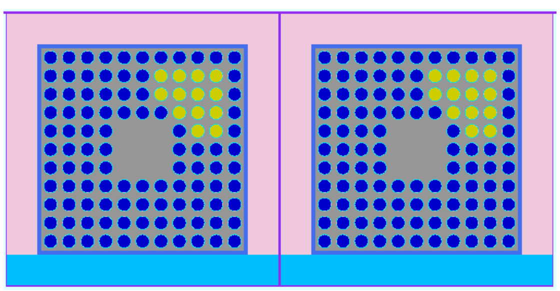

No rotation of left assembly

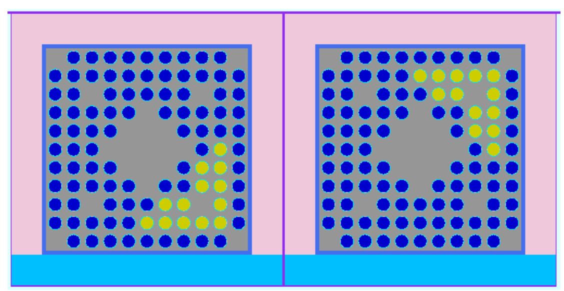

Left assembly rotated 90°

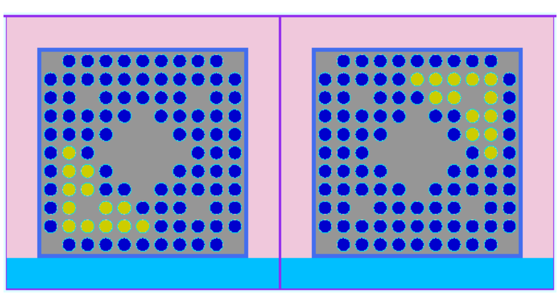

Left assembly rotated 180°

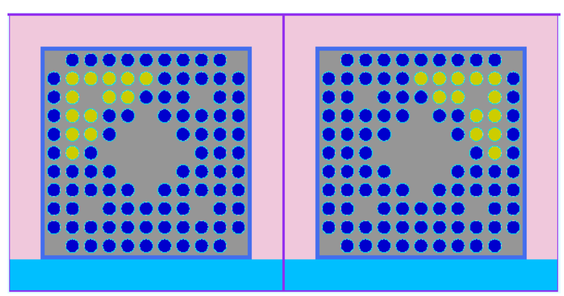

Left assembly rotated 270°

Figure 6-85: Left Assembly Rotation Relative to Right Assembly within Package

6.12.11.1. **NCT Single Package Evaluation**

The most reactive configuration for the NCT single package model was described in Section 6.12.4.1. NCT Single Package Evaluation. This configuration has the following characteristics:

- All axial layers containing 5 wt% U-235 and 13 gadolinia-urania rods,
- Full foam liner, which centers the assemblies,
- Void in the pellet-to-cladding gap, and
- Moderator density of 1.0 g/cm^3 within the inner container.

Using this configuration, the fuel channel thickness was varied from 0.254 cm to 0.320 cm. These results are given in Table 6-105 TN-B1 NCT Single Package Evaluation for Channel Thickness and show that reactivity increases with increasing fuel channel thickness. Therefore, the remainder of the calculations in this section use a channel thickness of 0.320 cm.

The most reactive assembly orientation from Figure 6-85 Left Assembly Rotation Relative to Right Assembly within Package was determined for both the channeled and unchanneled models as well as for the all-5 wt% assemblies and the 5-5-3.3 wt% assemblies. The results are show in Table 6-106 TN-B1 NCT Single Package Evaluation for Assembly Orientation. The most reactive configuration is found to be for the all 5-wt% channeled assemblies in which the left assembly is rotated 270° relative to the right assembly. The $k_{eff} + 2\sigma$ value for this configuration is 0.64602.

Table 6-105 TN-B1 NCT Single Package Evaluation for Channel Thickness

Filename	Fuel Channel Thickness (cm)	k_{eff}	σ	k_{eff} + 2σ
NCT_single_channel_0254.out	0.254	0.64362	0.00028	0.64418
NCT_single_channel_0275.out	0.275	0.64427	0.00029	0.64485
NCT_single_channel_0295.out	0.295	0.64437	0.00027	0.64491
NCT_single_channel_0315.out	0.315	0.64486	0.00029	0.64544
NCT_single_channel_0320.out	0.320	0.64528	0.00029	**0.64586**

Table 6-106 TN-B1 NCT Single Package Evaluation for Assembly Orientation

Filename	Left Assembly Rotation	Fuel Channel?	Fuel Axially Varied?	k_{eff}	σ	k_{eff} + 2σ
NCT_single_pkg_000.out	0°	yes	no	0.63174	0.00046	0.63266
NCT_single_pkg_090.out	90°	yes	no	0.62913	0.00044	0.63001
NCT_single_pkg_180.out	180°	yes	no	0.64401	0.00046	0.64493
NCT_single_pkg_270.out	**270°**	**yes**	**no**	**0.64510**	**0.00046**	**0.64602**
NCT_single_pkg_000.out	0°	yes	yes	0.63171	0.00040	0.63251
NCT_single_pkg_090.out	90°	yes	yes	0.62983	0.00043	0.63069
NCT_single_pkg_180.out	180°	yes	yes	0.64331	0.00040	0.64411
NCT_single_pkg_270.out	270°	yes	yes	0.64445	0.00045	0.64535
NCT_single_pkg_000.out	0°	no	no	0.62348	0.00043	0.62434
NCT_single_pkg_090.out	90°	no	no	0.62077	0.00046	0.62169
NCT_single_pkg_180.out	180°	no	no	0.63590	0.00042	0.63674
NCT_single_pkg_270.out	270°	no	no	0.63766	0.00047	0.63860
NCT_single_pkg_000.out	0°	no	yes	0.62326	0.00048	0.62422
NCT_single_pkg_090.out	90°	no	yes	0.62198	0.00042	0.62282
NCT_single_pkg_180.out	180°	no	yes	0.63545	0.00048	0.63641
NCT_single_pkg_270.out	270°	no	yes	0.63697	0.00047	0.63791

6.12.11.2. HAC Single Package Evaluation

The most reactive configuration for the HAC single package model was described in Section 6.12.4.2. HAC Single Package Evaluation. This configuration has the following characteristics:

- All axial layers containing 5 wt% U-235 and 13 gadolinia-urania rods,
- No fuel channel,
- Complete foam burn,
- Water in the pellet-to-cladding gap, and
- Modeling approach in which the polyethylene is smeared into the clad.

Using this configuration, the most reactive assembly orientation from Figure 6-85 Left Assembly Rotation Relative to Right Assembly within Package was determined for the unchanneled model using both the all-5 wt% assemblies and the 5-5-3.3 wt% assemblies. The results are given in Table 6-107 TN-B1 HAC Single Package Evaluation for Assembly Orientation, Unchanneled Assemblies. The most reactive configuration is found to be for the 5-5-3.3wt% assemblies in which the left assembly is rotated 270° relative to the right assembly. The $k_{eff} + 2\sigma$ value for this configuration is 0.79422.

The partial foam burn sensitivity study discussed in 6.12.4.2. HAC Single Package Evaluation is repeated for the unchanneled and channeled assemblies in which the left assembly is rotated 270° relative to the right assembly and for fuel channel thicknesses of 0.254 cm, 0.285 cm, and 0.320 cm. Results for these configurations are provided in Table 6-108 11x11 Single Package HAC Results, Partial Foam Burn, Centered Assemblies (270° Left Assembly Rotation), Table 6-109 11x11 Single Package HAC Results, Partial Foam Burn, Right Assembly Shifted (270° Left Assembly Rotation), and Table 6-110 11x11 Single Package HAC Results, Partial Foam Burn, Both Assemblies Shifted (270° Left Assembly Rotation). The most reactive configuration for the HAC single package is confirmed to be for the unchanneled assemblies with complete foam burn.

Table 6-107 TN-B1 HAC Single Package Evaluation for Assembly Orientation, Unchanneled Assemblies

Filename	Left Assembly Rotation	Fuel Axially Varied?	k_{eff}	σ	$k_{eff} + 2σ$
HAC_single_pkg_000.out	0°	no	0.76615	0.00045	0.76705
HAC_single_pkg_090.out	90°	no	0.76217	0.00048	0.76313
HAC_single_pkg_180.out	180°	no	0.79244	0.00046	0.79336
HAC_single_pkg_270.out	270°	no	0.79285	0.00045	0.79375
HAC_single_pkg_000.out	0°	yes	0.76615	0.00044	0.76703
HAC_single_pkg_090.out	90°	yes	0.76294	0.00044	0.76382
HAC_single_pkg_180.out	180°	yes	0.79176	0.00054	0.79284
HAC_single_pkg_270.out	**270°**	**yes**	**0.79328**	**0.00047**	**0.79422**

Table 6-108 11x11 Single Package HAC Results, Partial Foam Burn, Centered Assemblies (270° Left Assembly Rotation)

Filename	Channel thickness (cm)	Polyethylene liner thickness (cm)	k_{eff}	σ	k_{eff} + 2σ
HAC_single_liner_000_cn.out	N/A	0.00	0.76870	0.00047	0.76964
HAC_single_liner_020_cn.out	N/A	0.20	0.76420	0.00048	0.76516
HAC_single_liner_040_cn.out	N/A	0.40	0.75992	0.00049	0.76090
HAC_single_liner_060_cn.out	N/A	0.60	0.75273	0.00046	0.75365
HAC_single_liner_080_cn.out	N/A	0.80	0.74590	0.00050	0.74690
HAC_single_liner_100_cn.out	N/A	1.00	0.73726	0.00046	0.73818
HAC_single_liner_120_cn.out	N/A	1.20	0.72550	0.00047	0.72644
HAC_single_liner_140_cn.out	N/A	1.40	0.71496	0.00047	0.71590
HAC_single_liner_160_cn.out	N/A	1.60	0.70344	0.00045	0.70434
HAC_single_liner_180_cn.out	N/A	1.80	0.69057	0.00045	0.69147
HAC_single_liner_full_cn.out	N/A	1.911	0.68504	0.00044	0.68592
HAC_single_liner_000_cc.out	0.254	0.00	0.76787	0.00046	0.76879
HAC_single_liner_020_cc.out	0.254	0.20	0.76234	0.00047	0.76328
HAC_single_liner_040_cc.out	0.254	0.40	0.75500	0.00053	0.75606
HAC_single_liner_060_cc.out	0.254	0.60	0.74827	0.00050	0.74927
HAC_single_liner_080_cc.out	0.254	0.80	0.73935	0.00050	0.74035
HAC_single_liner_100_cc.out	0.254	1.00	0.72957	0.00046	0.73049
HAC_single_liner_120_cc.out	0.254	1.20	0.71859	0.00045	0.71949
HAC_single_liner_140_cc.out	0.254	1.40	0.70651	0.00045	0.70741
HAC_single_liner_160_cc.out	0.254	1.60	0.69378	0.00044	0.69466
HAC_single_liner_full_cc.out	0.254	1.657	0.69004	0.00046	0.69096
HAC_single_liner_000_cc.out	0.285	0.00	0.76780	0.00038	0.76856
HAC_single_liner_020_cc.out	0.285	0.20	0.76145	0.00039	0.76223
HAC_single_liner_040_cc.out	0.285	0.40	0.75531	0.00037	0.75605
HAC_single_liner_060_cc.out	0.285	0.60	0.74741	0.00037	0.74815
HAC_single_liner_080_cc.out	0.285	0.80	0.73745	0.00045	0.73835
HAC_single_liner_100_cc.out	0.285	1.00	0.72804	0.00037	0.72878
HAC_single_liner_120_cc.out	0.285	1.20	0.71751	0.00037	0.71825
HAC_single_liner_140_cc.out	0.285	1.40	0.70563	0.00042	0.70647
HAC_single_liner_160_cc.out	0.285	1.60	0.69343	0.00035	0.69413
HAC_single_liner_full_cc.out	0.285	1.626	0.69056	0.00035	0.69126
HAC_single_liner_000_cc.out	0.320	0.00	0.76686	0.00038	0.76762
HAC_single_liner_020_cc.out	0.320	0.20	0.76128	0.00040	0.76208
HAC_single_liner_040_cc.out	0.320	0.40	0.75462	0.00040	0.75542
HAC_single_liner_060_cc.out	0.320	0.60	0.74713	0.00040	0.74793
HAC_single_liner_080_cc.out	0.320	0.80	0.73779	0.00039	0.73857
HAC_single_liner_100_cc.out	0.320	1.00	0.72719	0.00036	0.72791
HAC_single_liner_120_cc.out	0.320	1.20	0.71568	0.00040	0.71648
HAC_single_liner_140_cc.out	0.320	1.40	0.70325	0.00035	0.70395
HAC_single_liner_full_cc.out	0.320	1.591	0.69205	0.00040	0.69285

Table 6-109 11x11 Single Package HAC Results, Partial Foam Burn, Right Assembly Shifted (270° Left Assembly Rotation)

Filename	Channel thickness (cm)	Polyethylene liner thickness (cm)	k_{eff}	σ	k_{eff} + 2σ
HAC_single_liner_000_o7n.out	N/A	0.00	0.79250	0.00047	0.79344
HAC_single_liner_020_o7n.out	N/A	0.20	0.78234	0.00043	0.78320
HAC_single_liner_040_o7n.out	N/A	0.40	0.77172	0.00050	0.77272
HAC_single_liner_060_o7n.out	N/A	0.60	0.75999	0.00048	0.76095
HAC_single_liner_080_o7n.out	N/A	0.80	0.74856	0.00051	0.74958
HAC_single_liner_100_o7n.out	N/A	1.00	0.73714	0.00047	0.73808
HAC_single_liner_120_o7n.out	N/A	1.20	0.72548	0.00046	0.72640
HAC_single_liner_140_o7n.out	N/A	1.40	0.71316	0.00045	0.71406
HAC_single_liner_160_o7n.out	N/A	1.60	0.70311	0.00047	0.70405
HAC_single_liner_180_o7n.out	N/A	1.80	0.69046	0.00042	0.69130
HAC_single_liner_full_o7n.out	N/A	1.911	0.68504	0.00044	0.68592
HAC_single_liner_000_o7c.out	0.254	0.00	0.78714	0.00051	0.78816
HAC_single_liner_020_o7c.out	0.254	0.20	0.77323	0.00045	0.77413
HAC_single_liner_040_o7c.out	0.254	0.40	0.76270	0.00049	0.76368
HAC_single_liner_060_o7c.out	0.254	0.60	0.75137	0.00053	0.75243
HAC_single_liner_080_o7c.out	0.254	0.80	0.74008	0.00049	0.74106
HAC_single_liner_100_o7c.out	0.254	1.00	0.72834	0.00049	0.72932
HAC_single_liner_120_o7c.out	0.254	1.20	0.71629	0.00050	0.71729
HAC_single_liner_140_o7c.out	0.254	1.40	0.70417	0.00043	0.70503
HAC_single_liner_160_o7c.out	0.254	1.60	0.69451	0.00046	0.69543
HAC_single_liner_full_o7c.out	0.254	1.657	0.69004	0.00046	0.69096
HAC_single_liner_000_o7c.out	0.285	0.00	0.78584	0.00038	0.78660
HAC_single_liner_020_o7c.out	0.285	0.20	0.77228	0.00038	0.77304
HAC_single_liner_040_o7c.out	0.285	0.40	0.76082	0.00037	0.76156
HAC_single_liner_060_o7c.out	0.285	0.60	0.74954	0.00041	0.75036
HAC_single_liner_080_o7c.out	0.285	0.80	0.73835	0.00041	0.73917
HAC_single_liner_100_o7c.out	0.285	1.00	0.72676	0.00042	0.72760
HAC_single_liner_120_o7c.out	0.285	1.20	0.71634	0.00038	0.71710
HAC_single_liner_140_o7c.out	0.285	1.40	0.70388	0.00039	0.70466
HAC_single_liner_160_o7c.out	0.285	1.60	0.69293	0.00035	0.69363
HAC_single_liner_full_o7c.out	0.285	1.626	0.69056	0.00035	0.69126
HAC_single_liner_000_o7c.out	0.320	0.00	0.78600	0.00042	0.78684
HAC_single_liner_020_o7c.out	0.320	0.20	0.77101	0.00040	0.77181
HAC_single_liner_040_o7c.out	0.320	0.40	0.76062	0.00035	0.76132
HAC_single_liner_060_o7c.out	0.320	0.60	0.74912	0.00039	0.74990
HAC_single_liner_080_o7c.out	0.320	0.80	0.73729	0.00037	0.73803
HAC_single_liner_100_o7c.out	0.320	1.00	0.72565	0.00036	0.72637
HAC_single_liner_120_o7c.out	0.320	1.20	0.71471	0.00035	0.71541
HAC_single_liner_140_o7c.out	0.320	1.40	0.70295	0.00038	0.70371
HAC_single_liner_full_o7n.out	0.320	1.591	0.69205	0.00040	0.69285

Table 6-110 11x11 Single Package HAC Results, Partial Foam Burn, Both Assemblies Shifted (270° Left Assembly Rotation)

Filename	Channel thickness (cm)	Polyethylene liner thickness (cm)	k_{eff}	σ	k_{eff} + 2σ
HAC_single_liner_000_INn.out	N/A	0.00	0.78222	0.00049	0.78320
HAC_single_liner_020_INn.out	N/A	0.20	0.77303	0.00046	0.77395
HAC_single_liner_040_INn.out	N/A	0.40	0.76174	0.00046	0.76266
HAC_single_liner_060_INn.out	N/A	0.60	0.75206	0.00051	0.75308
HAC_single_liner_080_INn.out	N/A	0.80	0.74042	0.00048	0.74138
HAC_single_liner_100_INn.out	N/A	1.00	0.73072	0.00049	0.73170
HAC_single_liner_120_INn.out	N/A	1.20	0.71969	0.00044	0.72057
HAC_single_liner_140_INn.out	N/A	1.40	0.70998	0.00044	0.71086
HAC_single_liner_160_INn.out	N/A	1.60	0.69905	0.00047	0.69999
HAC_single_liner_180_INn.out	N/A	1.80	0.69002	0.00048	0.69098
HAC_single_liner_full_INn.out	N/A	1.911	0.68504	0.00044	0.68592
HAC_single_liner_000_INc.out	0.254	0.00	0.77417	0.00048	0.77513
HAC_single_liner_020_INc.out	0.254	0.20	0.76427	0.00047	0.76521
HAC_single_liner_040_INc.out	0.254	0.40	0.75497	0.00045	0.75587
HAC_single_liner_060_INc.out	0.254	0.60	0.74367	0.00044	0.74455
HAC_single_liner_080_INc.out	0.254	0.80	0.73419	0.00046	0.73511
HAC_single_liner_100_INc.out	0.254	1.00	0.72428	0.00048	0.72524
HAC_single_liner_120_INc.out	0.254	1.20	0.71302	0.00053	0.71408
HAC_single_liner_140_INc.out	0.254	1.40	0.70243	0.00049	0.70341
HAC_single_liner_160_INc.out	0.254	1.60	0.69419	0.00042	0.69503
HAC_single_liner_full_INc.out	0.254	1.657	0.69004	0.00046	0.69096
HAC_single_liner_000_INc.out	0.285	0.00	0.77388	0.00038	0.77464
HAC_single_liner_020_INc.out	0.285	0.20	0.76387	0.00041	0.76469
HAC_single_liner_040_INc.out	0.285	0.40	0.75406	0.00037	0.75480
HAC_single_liner_060_INc.out	0.285	0.60	0.74340	0.00040	0.74420
HAC_single_liner_080_INc.out	0.285	0.80	0.73259	0.00036	0.73331
HAC_single_liner_100_INc.out	0.285	1.00	0.72325	0.00039	0.72403
HAC_single_liner_120_INc.out	0.285	1.20	0.71214	0.00042	0.71298
HAC_single_liner_140_INc.out	0.285	1.40	0.70227	0.00036	0.70299
HAC_single_liner_160_INc.out	0.285	1.60	0.69221	0.00039	0.69299
HAC_single_liner_full_INc.out	0.285	1.626	0.69056	0.00035	0.69126
HAC_single_liner_000_INc.out	0.320	0.00	0.77237	0.00037	0.77311
HAC_single_liner_020_INc.out	0.320	0.20	0.76309	0.00039	0.76387
HAC_single_liner_040_INc.out	0.320	0.40	0.75212	0.00038	0.75288
HAC_single_liner_060_INc.out	0.320	0.60	0.74233	0.00041	0.74315
HAC_single_liner_080_INc.out	0.320	0.80	0.73196	0.00038	0.73272
HAC_single_liner_100_INc.out	0.320	1.00	0.72164	0.00040	0.72244
HAC_single_liner_120_INc.out	0.320	1.20	0.71161	0.00041	0.71243
HAC_single_liner_140_INc.out	0.320	1.40	0.70188	0.00036	0.70260
HAC_single_liner_full_INn.out	0.320	1.591	0.69205	0.00040	0.69285

6.12.11.3. Evaluation of Package Arrays Under Normal Conditions of Transport

The most reactive configuration for the NCT package array model was described in Section 6.12.5. *Evaluation of Package Arrays Under Normal Conditions of Transport*. This configuration has the following characteristics:

- All axial layers containing 5 wt% U-235 and 13 gadolinia-urania rods,
- Full foam liner, which centers the assemblies, and
- Void in the pellet-to-cladding gap.

For the NCT array, the fuel channel thickness was varied from 0.254 cm to 0.320 cm using a model in which the left assembly was rotated 270° relative to the right assembly. The model consisted of an 12x2x10 array with 1.0 g/cm^3 moderator in the inner container and no moderator between the inner and outer containers. The results are given in Table 6-111 TN-B1 NCT Package Array Evaluation for Channel Thickness and show that reactivity remains statistically the same over the range of channel thicknesses.

The most reactive assembly orientation from Figure 6-85 Left Assembly Rotation Relative to Right Assembly within Package was determined for both the channeled and unchanneled models as well as for the all-5 wt% assemblies and the 5-5-3.3 wt% assemblies. Calculations were performed for channel thicknesses of 0.254 cm, 0.300 cm, and 0.320 cm. The results are show in Table 6-112 TN-B1 NCT Package Array Evaluation for Assembly Orientation. The most reactive configuration is found to be for the 5-5-3.3-wt% unchanneled assemblies in which the left assembly is rotated 270° relative to the right assembly. The $k_{eff} + 2\sigma$ value for this configuration is 0.92917.

A moderator density study in which the moderator within the inner container was varied with no moderator present in the outer container and in which the moderator within the outer container was varied with 1.0 g/cm^3 density moderator present in the inner container using the unchanneled 5-5-3.3-wt% assemblies. The results are provided in Table 6-113 TN-B1 NCT Package Array Evaluation for Moderator Density and confirm that the most reactive configuration is found when there is 1.0 g/cm3 density moderator in the inner container and void between the inner and outer containers.

An additional study was performed for the NCT array in which the arrangement of the containers was varied, relative to the placement of the Gd rods. The four array variations considered are given in Figure 6-86 Configurations for Array Variation Study (shown as a 2x2 package subset) along with the nomenclature used for the calculations. The results are presented in Table 6-114 TN-B1 NCT Package Array Evaluation for Array Variation. The highest reactivity was found for the HHHH array variation, which corresponds to the variation used in the previous calculations.

Table 6-111 TN-B1 NCT Package Array Evaluation for Channel Thickness

Filename	Fuel Channel Thickness (cm)	k_{eff}	σ	k_{eff} + 2σ
NCT_array_ch0254.out	0.254	0.92789	0.00040	0.92869
NCT_array_ch0270.out	0.270	0.92761	0.00033	0.92827
NCT_array_ch0285.out	0.285	0.92745	0.00041	0.92827
NCT_array_ch0300.out	0.300	0.92765	0.00036	0.92837
NCT_array_ch0315.out	0.315	0.92760	0.00038	0.92836
NCT_array_ch0320.out	0.320	0.92774	0.00042	0.92858

Table 6-112 TN-B1 NCT Package Array Evaluation for Assembly Orientation

Filename	Left Assembly Rotation	Fuel Channel Thickness (cm)	Fuel Axially Varied?	k_{eff}	σ	k_{eff} + 2σ
NCT_array_000.out	0°	N/A	no	0.91909	0.00046	0.92001
NCT_array_090.out	90°	N/A	no	0.91588	0.00042	0.91672
NCT_array_180.out	180°	N/A	no	0.92598	0.00044	0.92686
NCT_array_270.out	270°	N/A	no	0.92689	0.00045	0.92779
NCT_array_000.out	0°	N/A	yes	0.92068	0.00046	0.92160
NCT_array_090.out	90°	N/A	yes	0.92055	0.00048	0.92151
NCT_array_180.out	180°	N/A	yes	0.92660	0.00046	0.92752
NCT_array_270.out	270°	N/A	yes	0.92829	0.00044	**0.92917**
NCT_array_000.out	0°	0.254	no	0.91721	0.00041	0.91803
NCT_array_090.out	90°	0.254	no	0.91621	0.00047	0.91715
NCT_array_180.out	180°	0.254	no	0.92616	0.00053	0.92722
NCT_array_270.out	270°	0.254	no	0.92763	0.00056	0.92875
NCT_array_000.out	0°	0.254	yes	0.92043	0.00050	0.92143
NCT_array_090.out	90°	0.254	yes	0.91939	0.00044	0.92027
NCT_array_180.out	180°	0.254	yes	0.92746	0.00045	0.92836
NCT_array_270.out	270°	0.254	yes	0.92770	0.00046	0.92862
NCT_array_000.out	0°	0.300	no	0.91756	0.00043	0.91842
NCT_array_090.out	90°	0.300	no	0.91626	0.00040	0.91706
NCT_array_180.out	180°	0.300	no	0.92514	0.00039	0.92592
NCT_array_270.out	270°	0.300	no	0.92732	0.00039	0.92810
NCT_array_000.out	0°	0.300	yes	0.92116	0.00037	0.92190
NCT_array_090.out	90°	0.300	yes	0.91958	0.00038	0.92034
NCT_array_180.out	180°	0.300	yes	0.92743	0.00035	0.92813
NCT_array_270.out	270°	0.300	yes	0.92765	0.00036	0.92837
NCT_array_000.out	0°	0.320	no	0.91773	0.00039	0.91851
NCT_array_090.out	90°	0.320	no	0.91624	0.00040	0.91704
NCT_array_180.out	180°	0.320	no	0.92457	0.00038	0.92533
NCT_array_270.out	270°	0.320	no	0.92593	0.00038	0.92669
NCT_array_000.out	0°	0.320	yes	0.92052	0.00038	0.92128
NCT_array_090.out	90°	0.320	yes	0.91925	0.00033	0.91991
NCT_array_180.out	180°	0.320	yes	0.92715	0.00039	0.92793
NCT_array_270.out	270°	0.320	yes	0.92774	0.00042	0.92858

Table 6-113 TN-B1 NCT Package Array Evaluation for Moderator Density

Filename	Inner Moderator Density (g/cm^3)	Outer Moderator Density (g/cm^3)	k_{eff}	σ	k_{eff} + 2σ
NCT_array_dens000_nc.out	0.00	N/A	0.70537	0.00046	0.70629
NCT_array_dens002_nc.out	0.02	N/A	0.71312	0.00040	0.71392
NCT_array_dens004_nc.out	0.04	N/A	0.72110	0.00039	0.72188
NCT_array_dens006_nc.out	0.06	N/A	0.72723	0.00040	0.72803
NCT_array_dens008_nc.out	0.08	N/A	0.73430	0.00043	0.73516
NCT_array_dens010_nc.out	0.10	N/A	0.74037	0.00042	0.74121
NCT_array_dens020_nc.out	0.20	N/A	0.77235	0.00044	0.77323
NCT_array_dens040_nc.out	0.40	N/A	0.82360	0.00045	0.82450
NCT_array_dens060_nc.out	0.60	N/A	0.86766	0.00042	0.86850
NCT_array_dens080_nc.out	0.80	N/A	0.90150	0.00048	0.90246
NCT_array_dens100_nc.out	**1.00**	**N/A**	**0.92829**	**0.00044**	**0.92917**
NCT_array_outDens000_nc.out	**1.00**	**0.00**	**0.92829**	**0.00044**	**0.92917**
NCT_array_outDens002_nc.out	1.00	0.02	0.89756	0.00045	0.89846
NCT_array_outDens004_nc.out	1.00	0.04	0.86418	0.00047	0.86512
NCT_array_outDens006_nc.out	1.00	0.06	0.83250	0.00046	0.83342
NCT_array_outDens008_nc.out	1.00	0.08	0.80496	0.00045	0.80586
NCT_array_outDens010_nc.out	1.00	0.10	0.78040	0.00048	0.78136
NCT_array_outDens020_nc.out	1.00	0.20	0.69825	0.00045	0.69915
NCT_array_outDens040_nc.out	1.00	0.40	0.64575	0.00048	0.64671
NCT_array_outDens060_nc.out	1.00	0.60	0.63662	0.00048	0.63758
NCT_array_outDens080_nc.out	1.00	0.80	0.63687	0.00045	0.63777
NCT_array_outDens100_nc.out	1.00	1.00	0.63785	0.00047	0.63879

Table 6-114 TN-B1 NCT Package Array Evaluation for Array Variation

Filename	Configuration	k_{eff}	σ	k_{eff} + 2σ
NCT_array_270_nc_HHHH.out	**HHHH**	**0.92829**	**0.00044**	**0.92917**
NCT_array_270_nc_HHLL.out	HHLL	0.92786	0.00045	0.92876
NCT_array_270_nc_HLHL.out	HLHL	0.92742	0.00044	0.92830
NCT_array_270_nc_HLLH.out	HLLH	0.92648	0.00048	0.92744

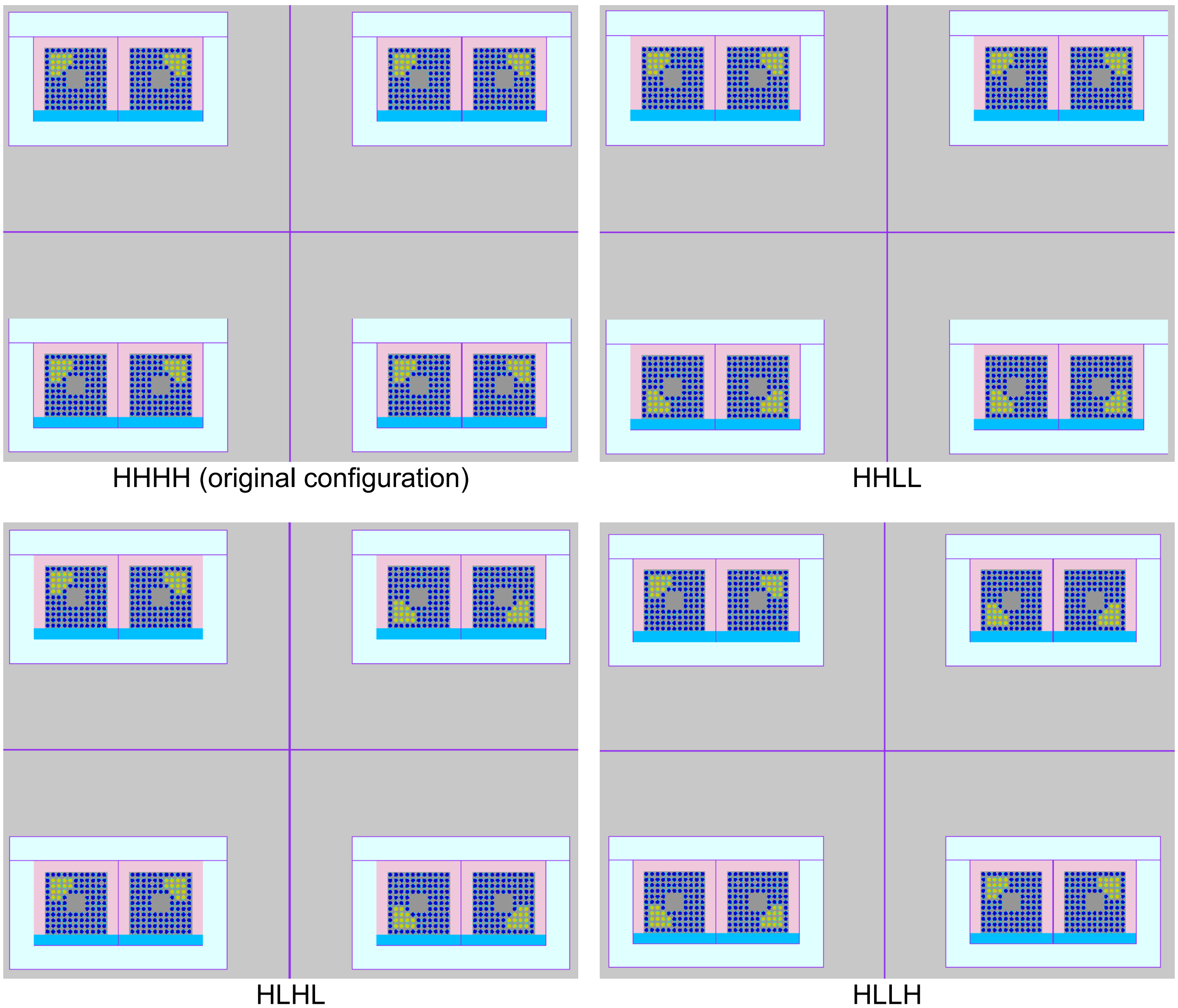

Figure 6-86: Configurations for Array Variation Study

(Gadolinia rods are depicted in yellow)

6.12.11.4. Evaluation of Package Arrays Under Hypothetical Accident Conditions

The most reactive configuration for the NCT package array model was described in Section 6.12.6. *Evaluation of Package Arrays Under Hypothetical Accident Conditions*. This configuration has the following characteristics:

- Axially varying enrichment (5-5-3.3 wt% U-235 and 13-13-3 gadolinia-urania rods),
- Partially burned foam liner with a thickness of 1.2 cm, and
- Water in the pellet-to-cladding gap.

For the HAC array, the fuel channel thickness was varied from 0.254 cm to 0.320 cm using a model in which the left assembly was rotated 270° relative to the right assembly. The model consisted of an 10x1x7 array with 1.0 g/cm^3 moderator in the inner container and no moderator between the inner and outer containers. The results are given in Table 6-115 TN-B1 HAC Package Array Evaluation for Channel Thickness and show that reactivity increases slightly as channel thickness increases.

Since the fuel channel thickness affects the thickness of the liner within the HAC array, the sensitivity study from Section 6.12.3.5.10. *Polyethylene Foam Liner Study* was repeated for channel thicknesses of 0.254 cm and 0.320 cm. For all calculations in this study, the left assembly was rotated 270° relative the right assembly; therefore, the no-channel liner study was also repeated here. Results for the liner study are shown in Table 6-116 TN-B1 HAC Package Array Liner Sensitivity Study (270° Left Assembly Rotation, Centered Assemblies) and Table 6-117 TN-B1 HAC Package Array Liner Sensitivity Study (270° Left Assembly Rotation, Assembly in Right Compartment Shifted). The highest system reactivity is seen for a centered configuration with a 0.320-cm-thick fuel channel, and a 0.8-cm-thick polyethylene liner.

Using the most reactive configuration from the liner study, the most reactive assembly orientation from Figure 6-85 Left Assembly Rotation Relative to Right Assembly within Package was determined. The results are given in Table 6-118 TN-B1 HAC Package Array Evaluation for Assembly Rotation and confirm that the highest reactivity is found for the configuration in which the left assembly is rotated 270° relative to the right assembly.

A moderator density study in which the moderator within the inner container was varied with no moderator present in the outer container and in which the moderator within the outer container was varied with 1.0 g/cm^3 density moderator present in the inner container using the 0.32-cm-thick fuel channeled assemblies, with a 0.8-cm-thick liner. The results are provided in Table 6-119 TN-B1 HAC Package Array Evaluation for Moderator Density and confirm that the most reactive configuration is found when there is 1.0 g/cm^3 density moderator in the inner container and void between the inner and outer containers.

An additional study was performed for the HAC array in which the arrangement of the containers was varied, relative to the placement of the Gd rods. The four array variations considered are given in Figure 6-86 Configurations for Array Variation Study (shown as a 2x2 package subset) along with the nomenclature used for the calculations. The results are presented in Table 6-120 TN-B1 HAC Package Array Evaluation for Array Variation. The highest reactivity was found for the HHHH array variation, which corresponds to the variation used in the previous calculations.

Table 6-115 TN-B1 HAC Package Array Evaluation for Channel Thickness

Filename	Fuel Channel Thickness (cm)	k_{eff}	σ	k_{eff} + 2σ
HAC_fuel_channel_0254.out	0.254	0.91438	0.00030	0.91498
HAC_fuel_channel_0275.out	0.275	0.91419	0.00031	0.91481
HAC_fuel_channel_0295.out	0.295	0.91494	0.00026	0.91546
HAC_fuel_channel_0315.out	0.315	0.91528	0.00029	0.91586
HAC_fuel_channel_0320.out	0.320	0.91583	0.00029	0.91641

Table 6-116 TN-B1 HAC Package Array Liner Sensitivity Study (270° Left Assembly Rotation, Centered Assemblies)

Filename	Fuel Channel Thickness (cm)	Polyethylene liner thickness (cm)	k_{eff}	σ	k_{eff} + 2σ
poly_liner_000_cn.out	N/A	0	0.90865	0.00029	0.90923
poly_liner_020_cn.out	N/A	0.2	0.91504	0.00030	0.91564
poly_liner_040_cn.out	N/A	0.4	0.92061	0.00030	0.92121
poly_liner_060_cn.out	N/A	0.6	0.92502	0.00030	0.92562
poly_liner_080_cn.out	N/A	0.8	0.92823	0.00026	0.92875
poly_liner_100_cn.out	N/A	1.0	0.92966	0.00027	0.93020
poly_liner_120_cn.out	N/A	1.2	0.93038	0.00032	0.93102
poly_liner_140_cn.out	N/A	1.4	0.92789	0.00031	0.92851
poly_liner_160_cn.out	N/A	1.6	0.92469	0.00028	0.92525
poly_liner_180_cn.out	N/A	1.8	0.91939	0.00028	0.91995
poly_liner_full_cn.out	N/A	1.911	0.91523	0.00029	0.91581
poly_liner_000_cc.out	0.254	0	0.91379	0.00033	0.91445
poly_liner_020_cc.out	0.254	0.2	0.92061	0.00027	0.92115
poly_liner_040_cc.out	0.254	0.4	0.92496	0.00028	0.92552
poly_liner_060_cc.out	0.254	0.6	0.92745	0.00031	0.92807
poly_liner_080_cc.out	0.254	0.8	0.92945	0.00030	0.93005
poly_liner_100_cc.out	0.254	1.0	0.92955	0.00030	0.93015
poly_liner_120_cc.out	0.254	1.2	0.92803	0.00032	0.92867
poly_liner_140_cc.out	0.254	1.4	0.92488	0.00029	0.92546
poly_liner_160_cc.out	0.254	1.6	0.91830	0.00032	0.91894
poly_liner_full_cc.out	0.254	1.657	0.91379	0.00033	0.91445
poly_liner_000_cc.out	0.320	0	0.91607	0.00030	0.91667
poly_liner_020_cc.out	0.320	0.2	0.92113	0.00028	0.92169
poly_liner_040_cc.out	0.320	0.4	0.92586	0.00031	0.92648
poly_liner_060_cc.out	0.320	0.6	0.92847	0.00029	0.92905
poly_liner_080_cc.out	0.320	0.8	0.93067	0.00029	0.93125
poly_liner_100_cc.out	0.320	1.0	0.92985	0.00029	0.93043
poly_liner_120_cc.out	0.320	1.2	0.92738	0.00032	0.92802
poly_liner_140_cc.out	0.320	1.4	0.92254	0.00028	0.92310
poly_liner_full_cc.out	0.320	1.59	0.91663	0.00027	0.91717

Table 6-117 TN-B1 HAC Package Array Liner Sensitivity Study (270° Left Assembly Rotation, Assembly in Right Compartment Shifted)

Filename	Fuel Channel Thickness (cm)	Polyethylene liner thickness (cm)	k_{eff}	σ	$k_{eff} + 2σ$
poly_liner_000_sn.out	N/A	0	0.91962	0.00030	0.92022
poly_liner_020_sn.out	N/A	0.2	0.92244	0.00033	0.92310
poly_liner_040_sn.out	N/A	0.4	0.92384	0.00030	0.92444
poly_liner_060_sn.out	N/A	0.6	0.92525	0.00031	0.92587
poly_liner_080_sn.out	N/A	0.8	0.92615	0.00029	0.92673
poly_liner_100_sn.out	N/A	1.0	0.92709	0.00034	0.92777
poly_liner_120_sn.out	N/A	1.2	0.92629	0.00031	0.92691
poly_liner_140_sn.out	N/A	1.4	0.92540	0.00029	0.92598
poly_liner_160_sn.out	N/A	1.6	0.92258	0.00029	0.92316
poly_liner_180_sn.out	N/A	1.8	0.91805	0.00030	0.91865
poly_liner_full_sn.out	N/A	1.911	0.91505	0.00028	0.91561
poly_liner_000_sc.out	0.254	0	0.92123	0.00028	0.92179
poly_liner_020_sc.out	0.254	0.2	0.92335	0.00029	0.92393
poly_liner_040_sc.out	0.254	0.4	0.92515	0.00033	0.92581
poly_liner_060_sc.out	0.254	0.6	0.92616	0.00029	0.92674
poly_liner_080_sc.out	0.254	0.8	0.92741	0.00033	0.92807
poly_liner_100_sc.out	0.254	1.0	0.92605	0.00030	0.92665
poly_liner_120_sc.out	0.254	1.2	0.92474	0.00035	0.92544
poly_liner_140_sc.out	0.254	1.4	0.92197	0.00027	0.92251
poly_liner_160_sc.out	0.254	1.6	0.91798	0.00031	0.91860
poly_liner_full_sc.out	0.254	1.657	0.91595	0.00031	0.91657
poly_liner_000_sc.out	0.320	0	0.92185	0.00030	0.92245
poly_liner_020_sc.out	0.320	0.2	0.92359	0.00029	0.92417
poly_liner_040_sc.out	0.320	0.4	0.92520	0.00030	0.92580
poly_liner_060_sc.out	0.320	0.6	0.92651	0.00031	0.92713
poly_liner_080_sc.out	0.320	0.8	0.92704	0.00030	0.92764
poly_liner_100_sc.out	0.320	1.0	0.92686	0.00031	0.92748
poly_liner_120_sc.out	0.320	1.2	0.92400	0.00030	0.92460
poly_liner_140_sc.out	0.320	1.4	0.92114	0.00029	0.92172
poly_liner_full_sc.out	0.320	1.59	0.91663	0.00027	0.91717

Table 6-118 TN-B1 HAC Package Array Evaluation for Assembly Rotation

Filename	Left Assembly Rotation	k_{eff}	σ	k_{eff} + 2σ
HAC_array_pkg_000.out	0°	0.91751	0.00030	0.91811
HAC_array_pkg_090.out	90°	0.91792	0.00031	0.91854
HAC_array_pkg_180.out	180°	0.92956	0.00029	0.93014
HAC_array_pkg_270.out	**270°**	**0.93067**	**0.00029**	**0.93125**

Table 6-119 TN-B1 HAC Package Array Evaluation for Moderator Density

Filename	Inner Moderator Density (g/cm^3)	Outer Moderator Density (g/cm^3)	k_{eff}	σ	k_{eff} + 2σ
HAC_array_inDens000.out	0.00	N/A	0.57026	0.00024	0.57074
HAC_array_inDens002.out	0.02	N/A	0.58635	0.00024	0.58683
HAC_array_inDens004.out	0.04	N/A	0.60140	0.00024	0.60188
HAC_array_inDens006.out	0.06	N/A	0.61626	0.00027	0.61680
HAC_array_inDens008.out	0.08	N/A	0.63039	0.00025	0.63089
HAC_array_inDens010.out	0.10	N/A	0.64407	0.00025	0.64457
HAC_array_inDens020.out	0.20	N/A	0.70568	0.00029	0.70626
HAC_array_inDens040.out	0.40	N/A	0.79754	0.00029	0.79812
HAC_array_inDens060.out	0.60	N/A	0.85991	0.00032	0.86055
HAC_array_inDens080.out	0.80	N/A	0.90158	0.00031	0.90220
HAC_array_inDens100.out	**1.00**	**N/A**	**0.93067**	**0.00029**	**0.93125**
HAC_array_outDens000.out	**1.00**	**0.00**	**0.93067**	**0.00029**	**0.93125**
HAC_array_outDens002.out	1.00	0.02	0.90773	0.00029	0.90831
HAC_array_outDens004.out	1.00	0.04	0.88492	0.00027	0.88546
HAC_array_outDens006.out	1.00	0.06	0.86350	0.00030	0.86410
HAC_array_outDens008.out	1.00	0.08	0.84464	0.00031	0.84526
HAC_array_outDens010.out	1.00	0.10	0.82866	0.00029	0.82924
HAC_array_outDens020.out	1.00	0.20	0.77626	0.00030	0.77686
HAC_array_outDens040.out	1.00	0.40	0.74364	0.00029	0.74422
HAC_array_outDens060.out	1.00	0.60	0.73780	0.00028	0.73836
HAC_array_outDens080.out	1.00	0.80	0.73696	0.00030	0.73756
HAC_array_outDens100.out	1.00	1.00	0.73779	0.00030	0.73839

Table 6-120 TN-B1 HAC Package Array Evaluation for Array Variation

Filename	Configuration	k_{eff}	σ	$k_{eff} + 2σ$
HAC_array_270_ch_HHHH.out	**HHHH**	**0.93067**	**0.00029**	**0.93125**
HAC_array_270_ch_HHLL.out	HHLL	0.92956	0.00030	0.93016
HAC_array_270_ch_HLHL.out	HLHL	0.92983	0.00029	0.93041
HAC_array_270_ch_HLLH.out	HLLH	0.93031	0.00026	0.93083

6.12.11.5. Adjustment for H1-Poly Cross Section on Most Reactive Configurations

In February 2021, ORNL issued an error notice pertinent to SCALE 6.1.3 which consisted of an incorrect H1-Poly incoherent elastic scattering cross section that can cause an underprediction in k-eff. This section applies an adjustment to the most reactive configuration results in Section 6.12.11.1 through Section 6.12.11.4 to account for the H1-Poly cross section error.

The process for determining the adjustment is outlined below:

1. Calculate keff of configuration with SCALE 6.2.2 and continuous energy cross sections based on ENDF/B-VII.1 (ce_v7.1)
2. Calculate keff of configuration with SCALE 6.2.2 and the fixed continuous energy cross sections based on ENDF/B-VII.1 provided by ORNL (ce_fixed)
3. Calculate the difference the “bad” and “fixed” cross section sets and the associated uncertainty: $\Delta k_{poly} \pm \sigma_{poly}$, where $\Delta k_{poly} = k_{bad} - k_{fixed}$ and $\sigma_{poly} = \text{sqrt}(\sigma^2_{bad} + \sigma^2_{fixed})$
4. Calculate $k_{penalty}$ = absolute value of ($\Delta k_{poly} - 3\sigma_{poly}$), rounded up to the nearest 0.001.
5. Add the absolute value of $k_{penalty}$ to the SCALE 6.1.3 mult-group calculation:

$$k_{final}\ (\text{multi-group}) = k_{6.1.3} + 2 * \sigma_{6.1.3} + k_{penalty}$$

For the HAC configurations, the H1-Poly cross section adjustment is performed for both modeling approaches: polyethylene smeared into the clad and polyethylene smeared into the moderator, see Section 6.12.6.1. Configuration.

For the HAC package array, the calculations were performed for both the 5-5-3.3wt% assemblies and the all-5wt% assemblies.

Results for the NCT configurations are shown in Table 6-121 Adjustments on Reactivity Results for H1-Poly Cross Section Error, NCT. Results for the HAC configurations are shown in Table 6-122 Adjustments on Reactivity Results for H1-Poly Cross Section Error, HAC. The maximum k_{eff} + 2σ result, including the H1-Poly cross section error penalty, are as follows:

- NCT, single package: 0.64902
- HAC, single package: 0.79722
- NCT, package array: 0.93017
- HAC, package array: 0.93419

All values remain below the USL of 0.94094 and criticality safety is maintained for the single package and package array under NCT and HAC.

Table 6-121 Adjustments on Reactivity Results for H1-Poly Cross Section Error, NCT

Filename	SCALE version, cross section set used	k_{eff}	σ
NCT, single package			
NCT_single_pkg_270.out	6.1.3, multi-group	0.64510	0.00046
NCT_single_pkg_badCE.out	6.2.2, original cont. energy	0.64589	0.00015
NCT_single_pkg_fixedCE.out	6.2.2, fixed cont. energy	0.64800	0.00016
$\Delta k_{poly} \pm \sigma_{poly}$		-0.00211 ± 0.00022	
$k_{penalty}$		0.003	
NCT, single package k_{final} (multi-group)		**0.64902**	
NCT, package array			
NCT_array_270.out	6.1.3, multi-group	0.92829	0.00044
NCT_array_270_nc_12x2x10_badCE.out	6.2.2, original cont. energy	0.92845	0.00015
NCT_array_270_nc_12x2x10_fixedCE.out	6.2.2, fixed cont. energy	0.92803	0.00015
$\Delta k_{poly} \pm \sigma_{poly}$		0.00042 ± 0.00021	
$k_{penalty}$		0.001	
NCT, package array k_{final} (multi-group)		**0.93017**	

Table 6-122 Adjustments on Reactivity Results for H1-Poly Cross Section Error, HAC

Filename	SCALE version, cross section set used	k_{eff}	σ
HAC, single package, polyethylene material smeared with clad			
HAC_single_pkg_270.out	6.1.3, multi-group	0.79328	0.00047
HAC_single_pkg_badCE.out	6.2.2, original cont. energy	0.79342	0.00013
HAC_single_pkg_fixedCE.out	6.2.2, fixed cont. energy	0.79512	0.00013
$\Delta k_{poly} \pm \sigma_{poly}$		-0.00170 ± 0.00018	
$k_{penalty}$		0.003	
HAC, single package k_{final} (multi-group)		**0.79722**	
HAC, single package, polyethylene material smeared with moderator			
HAC_single_homPOLY.out	6.1.3, multi-group	0.79129	0.00050
HAC_single_homPOLY _badCE.out	6.2.2, original cont. energy	0.79261	0.00014
HAC_single_homPOLY _fixedCE.out	6.2.2, fixed cont. energy	0.79328	0.00013
$\Delta k_{poly} \pm \sigma_{poly}$		-0.00067 ± 0.00019	
$k_{penalty}$		0.002	
HAC, single package k_{final} (multi-group)		0.79429	
HAC, package array, polyethylene material smeared with clad, 5-5-3.3wt% assemblies			
HAC_pkg_array_outDens000.out	6.1.3, multi-group	0.93067	0.00029
HAC_pkg_array_10x1x7_badCE.out	6.2.2, original cont. energy	0.93017	0.00015
HAC_pkg_array_10x1x7_fixedCE.out	6.2.2, fixed cont. energy	0.93114	0.00016
$\Delta k_{poly} \pm \sigma_{poly}$		-0.00097 ± 0.00022	
$k_{penalty}$		0.002	
HAC, package array k_{final} (multi-group)		0.93325	
HAC, package array, polyethylene material smeared with moderator, 5-5-3.3wt% assemblies			
HAC_pkg_array_modApp.out	6.1.3, multi-group	0.93088	0.00033
HAC_pkg_array_modApp_badCE.out	6.2.2, original cont. energy	0.93099	0.00015
HAC_pkg_array_modApp_fixedCE.out	6.2.2, fixed cont. energy	0.93150	0.00014
$\Delta k_{poly} \pm \sigma_{poly}$		-0.00051 ± 0.00021	
$k_{penalty}$		0.002	
HAC, package arrayk_{final} (multi-group)		0.93354	
HAC, package array, polyethylene material smeared with clad, all-5wt% assemblies			
HAC_array_pkg_270_all5.out	6.1.3, multi-group	0.93155	0.00032
HAC_pkg_array_10x1x7_badCE.out	6.2.2, original cont. energy	0.93144	0.00015
HAC_pkg_array_10x1x7_fixedCE.out	6.2.2, fixed cont. energy	0.93250	0.00016
$\Delta k_{poly} \pm \sigma_{poly}$		-0.00106 ± 0.00021	
$k_{penalty}$		0.002	
HAC, package array k_{final} (multi-group)		**0.93419**	
HAC, package array, polyethylene material smeared with moderator, all-5wt% assemblies			
HAC_pkg_array_modApp_all5.out	6.1.3, multi-group	0.93249	0.00029
HAC_pkg_array_modApp_badCE.out	6.2.2, original cont. energy	0.93238	0.00016
HAC_pkg_array_modApp_fixedCE.out	6.2.2, fixed cont. energy	0.93271	0.00015
$\Delta k_{poly} \pm \sigma_{poly}$		-0.00033 ± 0.00022	
$k_{penalty}$		0.001	
HAC, package array k_{final} (multi-group)		0.93407	

6.12.11.6. Adjustment for Change in Inner Container Liner Material

The liner within the inner container was modeled as polyethylene with a density of 0.08 g/cm^3 on the top and sides and 0.16 g/cm^3 on the bottom to represent natural rubber. To accommodate different rubber specifications for the liner, polyethylene with density up to 1.362 g/cm^3 is evaluated. The polyethylene specification bounds materials with 14.3 weight percent of Hydrogen. Various rubber bulk densities and hydrogen desities are provided in Table 6-123.

The most reactive HAC array configuration from Table 6-122 Adjustments on Reactivity Results for H1-Poly Cross Section Error, HAC was used to vary the liner density from the original value to 1.362 g/cm^3. The results are provided in Table 6-124 TN-B1 Inner Container Liner Material Sensitivity Study and shows the maximum reactivity is found for a liner density of 0.28 g/cm^3 on the sides and top and 0.56 g/cm^3 on the bottom.

The optimal liner density was then used to repeat the liner sensitivity study from Table 6-116 TN-B1 HAC Package Array Liner Sensitivity Study (270° Left Assembly Rotation, Centered Assemblies) for the most reactive configuration (i.e., centered configuration with a 0.320-cm-thick fuel channel, and a 0.8-cm-thick polyethylene liner). Results for this sensitivity are found in Table 6-125 TN-B1 HAC Package Array Liner Sensitivity Study with Optimal Liner Density. The maximum reactivity is found for a 1.4-cm-thick liner.

The results from the most reactive configurations in Table 6-116 TN-B1 HAC Package Array Liner Sensitivity Study (270° Left Assembly Rotation, Centered Assemblies) and Table 6-125 TN-B1 HAC Package Array Liner Sensitivity Study with Optimal Liner Density are used to determine an adjustment to account for different inner container liner materials. The process for determining the adjustment is outlined below:

1. Calculate the difference the “orig” and “optimal” liner densities and the associated uncertainty: $\Delta k_{liner} \pm \sigma_{liner}$, where $\Delta k_{liner} = k_{orig} – k_{optimal}$ and $\sigma_{liner} = sqrt(\sigma^2_{orig} + \sigma^2_{optimal})$
2. Calculate k_{liner_adj} = absolute value of (Δk_{liner} - 3σ_{liner}), rounded up to the nearest 0.001.

Thus

Δk_{liner} = 0.93067 – 0.93316 = -0.00249

σ_{liner} = sqrt(0.00029^2+0.00031^2) = 0.00042

k_{liner_adj} = abs(-0.00249-3*0.00042) = 0.004

This adjustment is calculated for the HAC array model since that model resulted in the most limiting and bounding k_{eff} value. However, this adjustment isolates the effect of the liner material and is applied to all limiting NCT and HAC models to obtain the bounding k_{eff} values found in Table 6-3 Criticality Evaluation Summary for the 11x11 assemblies.

The maximum k_{eff} + 2σ result, including the H1-Poly cross section error penalty and the liner material adjustment, are as follows:

- NCT, single package: 0.65302
- HAC, single package: 0.80122
- NCT, package array: 0.93417
- HAC, package array: 0.93819

All values remain below the USL of 0.94094 and criticality safety is maintained for the single package and package array under NCT and HAC.

Table 6-123 TN-B1 Inner Container Liner Material Sensitivity Study

Material	Bulk Density (g/cc)	% Hydrogen by Weight	Hydrogen Density (g/cc)
Polyethylene (C_2H_4)	0.92	14.3	0.132
Synthetic Rubber (*C_2H_4)	1.362	*14.3	*0.195
Natural Rubber (C_5H_8)	0.95	11.8	0.112
Neoprene (C_4H_5Cl)	1.23	5.65	0.069
Water (H_2O)	0.9982	11.1	0.111

**Synthetic rubber conservatively assumed to have the same % hydrogen by weight and chemical formula as polyethylene*

Table 6-124 TN-B1 Inner Container Liner Material Sensitivity Study

Filename	Liner Density (g/cm^3), Top/Sides	Liner Density (g/cm^3), Bottom	k_{eff}	σ	k_{eff} + 2σ
HACarray_1.5_poly_0.08_.out	0.08	0.16	0.9318	0.0003	0.9324
HACarray_1.5_poly_0.18_.out	0.18	0.36	0.9329	0.0003	0.9335
HACarray_1.5_poly_0.28_.out	0.28	0.56	0.9337	0.0003	0.9343
HACarray_1.5_poly_0.38_.out	0.38	0.76	0.9329	0.0003	0.9335
HACarray_1.5_poly_0.48_.out	0.48	0.96	0.9299	0.0003	0.9305
HACarray_1.5_poly_0.58_.out	0.58	1.16	0.9275	0.0003	0.9281
HACarray_1.5_poly_0.68_.out	0.68	1.36	0.9245	0.0003	0.9251
HACarray_1.5_poly_0.78_.out	0.78	1.56	0.9205	0.0003	0.9211
HACarray_1.5_poly_0.88_.out	0.88	1.76	0.9169	0.0003	0.9175
HACarray_1.5_poly_0.98_.out	0.98	1.96	0.9122	0.0003	0.9128
HACarray_1.5_poly_1.08_.out	1.08	2.16	0.9073	0.0002	0.9077
HACarray_1.5_poly_1.18_.out	1.18	2.36	0.9034	0.0003	0.904
HACarray_1.5_poly_1.28_.out	1.28	2.56	0.8980	0.0003	0.8986
HACarray_1.5_poly_1.362_.out	1.362	2.724	0.8946	0.0002	0.8950
HACarray_1.5_poly_opt_0.08_.out	0.08	0.08	0.9307	0.0003	0.9313
HACarray_1.5_poly_opt_0.18_.out	0.18	0.18	0.9327	0.0003	0.9333
HACarray_1.5_poly_opt_0.28_.out	0.28	0.28	0.9329	0.0003	0.9335
HACarray_1.5_poly_opt_0.38_.out	0.38	0.38	0.9327	0.0003	0.9333
HACarray_1.5_poly_opt_0.48_.out	0.48	0.48	0.9307	0.0003	0.9313
HACarray_1.5_poly_opt_0.58_.out	0.58	0.58	0.929	0.0003	0.9296
HACarray_1.5_poly_opt_0.68_.out	0.68	0.68	0.9274	0.0003	0.9280
HACarray_1.5_poly_opt_0.78_.out	0.78	0.78	0.9248	0.0003	0.9254
HACarray_1.5_poly_opt_0.88_.out	0.88	0.88	0.9214	0.0003	0.9220
HACarray_1.5_poly_opt_0.98_.out	0.98	0.98	0.9172	0.0003	0.9178
HACarray_1.5_poly_opt_1.08_.out	1.08	1.08	0.9142	0.0003	0.9148
HACarray_1.5_poly_opt_1.18_.out	1.18	1.18	0.9095	0.0003	0.9101
HACarray_1.5_poly_opt_1.28_.out	1.28	1.28	0.9061	0.0003	0.9067
HACarray_1.5_poly_opt_1.362_.out	1.362	1.362	0.9021	0.0003	0.9027

Table 6-125 TN-B1 HAC Package Array Liner Sensitivity Study with Optimal Liner Density

Filename	Fuel Channel Thickness (cm)	Polyethylene liner thickness (cm)	k_{eff}	σ	$k_{eff} + 2\sigma$
poly_liner_000_cc.out	0.320	0	0.91607	0.00030	0.91667
poly_liner_020_cc.out	0.320	0.2	0.92089	0.00028	0.92145
poly_liner_040_cc.out	0.320	0.4	0.92494	0.00031	0.92556
poly_liner_060_cc.out	0.320	0.6	0.92861	0.00029	0.92919
poly_liner_080_cc.out	0.320	0.8	0.93169	0.00032	0.93233
poly_liner_100_cc.out	0.320	1.0	0.93290	0.00029	0.93348
poly_liner_120_cc.out	0.320	1.2	0.93311	0.00029	0.93369
poly_liner_140_cc.out	0.320	1.4	0.93316	0.00031	**0.93378**
poly_liner_full_cc.out	0.320	1.59	0.93160	0.00031	0.93222

6.12.11.7. **Additional Considerations for 11x11 Fuel Rod Transport**

The analysis for transport of the 11x11 fuel rods is documented in Section 6.12.7. *Transport of 11x11 Rods*. This section augments that analysis by considering preferential flooding in the NCT package array configuration. Since the final model for both HAC and NCT are loose rods inserted into a pipe in a symmetric configuration, no fuel assembly orientation or fuel channel thickness sensitivities are needed.

Using the most reactive configuration for the NCT loose rod study, the moderator density between the inner and outer containers was varied from void to full density. The moderator density within the inner container is 1.0 g/cm^3. For consistency with the assembly NCT array package from Section 6.12.11.3. Evaluation of Package Arrays Under Normal Conditions of Transport, the array size was set to 12x2x10.

Results for the preferential flooding study for the NCT rod transport array are provided in Table 6-126 TN-B1 NCT Rod Transport Array Evaluation for Preferential Flooding and show that the highest reactivity is found when there is no moderation between the inner and outer containers.

An adjustment is needed for the rod transport models to account for the H1-Poly cross section error. This adjustment is applied to the most reactive configuration results for the fuel rod transport models determined for the single package models (Section 6.12.7.3. Single Package Evaluation for 11x11 Rods), the HAC array model (Section 6.12.7.5. HAC Array Evaluation for 11x11 Rods), and the NCT array model (Section 6.12.11.4. Transport of 11x11 Rods, NCT Array). The process for determining the H1-Poly cross section error adjustment is the same as that in 6.12.11.5. Adjustment for H1-Poly Cross Section on Most Reactive Configurations.

Results for the fuel rod transport configurations are shown in Table 6-127 Adjustments on Reactivity Results for H1-Poly Cross Section Error, Fuel Rod Transport. The maximum $k_{eff} + 2\sigma$ result, including the H1-Poly cross section error penalty and the liner material adjustment, are as follows:

- NCT, single package: 0.59735
- HAC, single package: 0.67000
- NCT, package array: 0.80598
- HAC, package array: 0.82635

All values remain below the USL of 0.94047 and criticality safety is maintained for the single package and package array under NCT and HAC for fuel rod transport.

Table 6-126 TN-B1 NCT Rod Transport Array Evaluation for Preferential Flooding

Filename	Density between containers (g/cm^3)	k_{eff}	σ	k_{eff} + 2σ
NCT_array_pipe_outVoid.out	0.00	0.80006	0.00046	**0.80098**
NCT_array_pipe_out002.out	0.02	0.76619	0.00048	0.76715
NCT_array_pipe_out004.out	0.04	0.73708	0.00048	0.73804
NCT_array_pipe_out006.out	0.06	0.71380	0.00041	0.71462
NCT_array_pipe_out008.out	0.08	0.69427	0.00044	0.69515
NCT_array_pipe_out010.out	0.10	0.67769	0.00041	0.67851
NCT_array_pipe_out020.out	0.20	0.63092	0.00041	0.63174
NCT_array_pipe_out040.out	0.40	0.60003	0.00040	0.60083
NCT_array_pipe_out060.out	0.60	0.59400	0.00041	0.59482
NCT_array_pipe_out080.out	0.80	0.59286	0.00053	0.59392
NCT_array_pipe_out100.out	1.00	0.59306	0.00041	0.59388

Table 6-127 Adjustments on Reactivity Results for H1-Poly Cross Section Error, Fuel Rod Transport

Filename	SCALE version, cross section set used	k_{eff}	σ
NCT, single package			
NCT_single_pipe_dens100.out	6.1.3, multi-group	0.59145	0.00045
CE_bad/NCT_single_pipe_dens100.out	6.2.2, original cont. energy	0.59249	0.00013
CE_fixed/NCT_single_pipe_dens100.out	6.2.2, fixed cont. energy	0.59234	0.00012
	$\Delta k_{poly} \pm \sigma_{poly}$	0.00015 ± 0.00018	
	$k_{penalty}$	0.001	
	NCT, single package k_{final} (multi-group)	**0.59335**	
HAC, single package			
HAC_single_pipe_dens100_shift.out	6.1.3, multi-group	0.63316	0.00042
CE_bad/HAC_single_pipe_dens100_shift.out	6.2.2, original cont. energy	0.66322	0.00012
CE_fixed/HAC_single_pipe_dens100_shift.out	6.2.2, fixed cont. energy	0.66393	0.00012
	$\Delta k_{poly} \pm \sigma_{poly}$	-0.00071 ± 0.00017	
	$k_{penalty}$	0.002	
	HAC, single package k_{final} (multi-group)	**0.66600**	
NCT, package array			
NCT_array_pipe_outVoid.out	6.1.3, multi-group	0.80006	0.00046
CE_bad/NCT_array_pipe_outVoid	6.2.2, original cont. energy	0.80086	0.00014
CE_fixed/NCT_array_pipe_outVoid	6.2.2, fixed cont. energy	0.79972	0.00013
	$\Delta k_{poly} \pm \sigma_{poly}$	0.00114 ± 0.00019	
	$k_{penalty}$	0.001	
	NCT, package array k_{final} (multi-group)	**0.80198**	
HAC, package array			
mod_in_pipe_dens010.out	6.1.3, multi-group	0.81947	0.00044
CE_bad/mod_in_pipe_dens010.out	6.2.2, original cont. energy	0.81760	0.00013
CE_fixed/mod_in_pipe_dens010.out	6.2.2, fixed cont. energy	0.81857	0.00013
	$\Delta k_{poly} \pm \sigma_{poly}$	-0.00097 ± 0.00018	
	$k_{penalty}$	0.002	
	HAC, package array k_{final} (multi-group)	**0.82235**	

6.13. APPENDIX C: ≤ 8.0 WT.% ^{235}U FUEL ASSEMBLY CRITICALITY ANALYSIS

This appendix, Appendix C, documents the criticality analysis of the TN-B1 package with a payload of two ATRIUM 11 (i.e., 11x11 lattice) fuel assemblies having one or more lattices with lattice-average enrichments greater than 5.0 and no greater than 8.0 wt% ^{235}U. The requirements and limits documented in Section 6 of the previously approved TN-B1 SAR for enrichments no greater than 5 wt% are still applicable to fuel with enrichments no greater than 5.0 wt% ^{235}U. Appendix C also documents the criticality analysis for (1) up to 25 loose or bundled ATRIUM 11, ATRIUM 10XM, or pressurized water reactor (PWR) 17x17, type 3 fuel rods or (2) up to 30 ATRIUM 11, ATRIUM 10XM, or PWR 17x17, type 3 fuel rods transported in a 5-inch stainless steel pipe or “protective case”. The format of Appendix C follows the same general outline of the main body of the report and references the main body of the report for information common to both analyses.

The criticality analysis documented in this section is performed using SCALE 6.2.4 [24] and its ENDF/B-VII.1 252-neutron-energy-group cross sections. All calculations were performed using the default SCALE multi-group cross-section processing approach. SCALE CENTRM/PMC calculations are used to perform problem-specific resonance self-shielded cross-section calculations for all fuel rods. Resonance self-shielded cross-section calculations for materials that are not modeled with the fuel pins are performed using the SCALE BONAMI code.

During preparation of this analysis, the SCALE development team published two error reports that could potentially impact the TN-B1 analysis using SCALE 6.2.4. These error reports were downloaded from *https://www.ornl.gov/content/scale-v624*, on May 4, 2021.

The first one is 2021-02-26-SCALE User Notice Rev. 3, “SCALE h1-poly incoherent elastic scattering can cause k-eff under prediction approaching 1% in criticality problems with polyethylene as the primary moderator,” published on February 26, 2021 [34]. Since there is a significant amount of polyethylene modeled in some of the criticality calculations, this error could significantly impact the TN-B1 analysis. This is addressed in Section 6.13.5.

The second error report is 2021-04-01-SCALE User Notice Rev. 14, “Memory error with SCALE 3D general geometry package leading to an incorrect model when shapes are truncated by CHORDs,” published on April 1, 2021 [35]. Note this error does not affect CSAS5 which uses KENO V.a, and none of the criticality calculations performed to support the TN-B1 SAR update, utilized geometry defined using SCALE “chords”. Consequently, this error does not impact the TN-B1 SAR update analysis nor prior SAR work using CSAS5.

The following analyses demonstrate that the TN-B1 package complies fully with the requirements of 10CFR §71 [28] for the revised TN-B1 fuel contents. The nuclear criticality safety requirements for Type B fissile packages are satisfied for a single package and package array configurations under normal conditions of transport (NCT) and hypothetical accident conditions (HAC). A comprehensive description of the TN-B1 packaging is provided in Sections 1 and 6 of Reference [25]. This section supplements the previous SAR by providing a description of the packaging and contents that is sufficient for understanding the features of the TN-B1 that maintain criticality safety for the transported nuclear fuel.

Specifically, this criticality evaluation presents the following information [36]:

- Description of the contents and packaging.
- Description of the calculation models, including sketches with dimensions and materials, pointing out the differences between the models and actual package design, with explanation of how the differences affect the calculations.

- Description of the most reactive content loading and the most reactive configuration of the contents, the packaging, and the package array in the criticality evaluation.
- Description of the codes and cross-section data used.
- Discussion of software capabilities and limitations of importance to the criticality safety evaluations.
- Description of validation procedures used to justify the bias and uncertainties associated with the calculation method, including use of the administrative subcritical margin of 0.05 Δk to set an upper safety limit (USL) of 0.9318 and 0.9292 for the different packaging contents as discussed in Section 6.13.10.
- Demonstration that the effective neutron multiplication factor (k_{eff}) calculated in the safety analysis is less than the USL after consideration of appropriate bias and uncertainties for the following:
  - A single package with optimum moderation within the package, close water reflection, and the most reactive configuration consistent with the effects of either normal conditions of transport or hypothetical accident conditions, whichever is more reactive.
  - An array of 5N undamaged packages (packages subject to normal conditions of transport) with nothing between the packages and close water reflection of the array.
  - An array of 2N damaged packages (packages subject to hypothetical accident conditions) if each package were subjected to the tests specified in 10 CFR §71.73, with optimum interspersed moderation and close water reflection of the array.
- Calculation of the Criticality Safety Index (CSI) values based on the value of N determined in the array analyses. The evaluation supports the following CSI values for the specified fissionable loads:
  - ATRIUM 11 fuel assemblies with the specified maximum lattice average enrichments with each assembly containing a minimum number of UO_2+Gd_2O_3 fuel rods with minimum Gd_2O_3 loading such that the maximum CSI is less than or equal to 3.3.

Wt% ^{235}U	#Gd rods	wt% Gd_2O_3	CSI
≤ 8.0	21	4.0	3.2
≤ 7.5	19	4.0	3.2
≤ 7.0	17	4.0	3.2
≤ 6.5	15	4.0	3.2
≤ 6.1	13	4.0	3.2
≤ 5.8	13	2.0	3.2

  - ATRIUM 11 fuel rods with enrichments no greater than 8.0 wt% ^{235}U
    - Up to 25 loose or bundled fuel rods, CSI = 1.0
    - Up to 30 fuel rods in a 5-inch stainless steel pipe or a protective carrier (described in Section 1.2.3.4.7 of the currently approved TN-B1 SAR revision [25]), CSI = 2.3
  - ATRIUM 10XM fuel rods with enrichments no greater than 5.0 wt% ^{235}U
    - Up to 25 loose or bundled fuel rods, CSI = 1.0
    - Up to 30 fuel rods in a 5-inch stainless steel pipe or a protective carrier (described in Section 1.2.3.4.7), CSI = 1.0

- PWR 17x17, type 3 fuel rods with enrichments no greater than 8.0 wt% ^{235}U
  - Up to 25 loose or bundled fuel rods, CSI = 1.0
  - Up to 30 fuel rods in a 5-inch stainless steel pipe or a protective carrier (described in Section 1.2.3.4.7), CSI = 2.5

6.13.1. *Description of Criticality Design*

6.13.1.1. Design Features

The design features of the TN-B1 package are unchanged from the description in Sections 6.1.1 and 6.12.1.1, *Design Features* [25]. The primary purpose of this update to the TN-B1 SAR is to increase the maximum allowed enrichment for ATRIUM 11 fuel assemblies and for individual ATRIUM 11 fuel rods to 8 wt% ^{235}U, and to add limits for transport of individual ATRIUM 10XM fuel rods with a maximum enrichment of 5.0 wt% ^{235}U or individual PWR 17x17, type 3 fuel rods with a maximum enrichment of 8.0 wt% ^{235}U. The ATRIUM 11 fuel assemblies and various individual fuel rods are described in Section 6.13.2.

6.13.1.2. Summary Table of Criticality Evaluation

Sensitivity studies are performed by evaluating the TN-B1 package with various fuel materials and determining the most conservative configurations for the normal and hypothetical accident conditions for an individual package and package arrays. For the ATRIUM 11 assembly evaluations, the package array size is fixed such that a maximum CSI of less than 3.3 is maintained under NCT or HAC conditions, and the maximum enrichment per minimum Gd rod loading is determined. The results for the bounding cases defined through the sensitivity studies, rounded to four decimal places, are shown in

The results show that the Upper Safety Limit (USL) of 0.9318 and 0.9292 for the different packaging contents discussed in Section 6.13.10 is satisfied. The results also show that the NCT array results yield more restrictive acceptable loadings for transportation (e.g., for a Gd rod loading of 13 Gd rods with 2 wt% Gd_2O_3, the NCT array maximum allowable enrichment is 5.8 wt% ^{235}U versus 6.3 wt% ^{235}U under HAC conditions). Acceptable loadings for each enrichment and Gd rod combination are highlighted in yellow.

Table 6-128 Summary Table for TN-B1 with Various Loads

Fuel Load	Normal Conditions of Transport			Hypothetical Accident Conditions		
	Single	Array		Single	Array	
	$k_{eff}+2\sigma$*	No. Packages	$k_{eff}+2\sigma$*	$k_{eff}+2\sigma$*	No. Packages	$k_{eff}+2\sigma$*
ATRIUM 11 assemblies enrichment (# $UO_2+Gd_2O_3$ rods, wt% Gd_2O_3)						
≤ 8.0 (13, 2.0)**	0.7514	1	--	0.8513	1	--
≤ 8.0 wt% ^{235}U (21, 4.0)		81	0.9252		32	--
≤ 8.0 (19, 4.0)		81	--		32	0.9255
≤ 7.6 (17, 4.0)		81	--		32	0.9307
≤ 7.5 (19, 4.0)		81	0.9292		32	--
≤ 7.0 (17, 4.0)		81	0.9299		32	--
≤ 7.0 (15, 4.0)		81	--		32	0.9289
≤ 6.6 (13, 4.0)		81	--		32	0.9304
≤ 6.7 (15, 2.0)		81	--		32	0.9301
≤ 6.5 (15, 4.0)		81	0.9308		32	--
≤ 6.3 (13, 2.0)		81	--		32	0.9300
≤ 6.1 (13, 4.0)		81	0.9311		32	--
≤ 5.8 (13, 2.0)		81	0.9295		32	--
ATRIUM 11 rods, ≤ 8.0 wt% ^{235}U						
25 loose rods	0.6647	256	0.8904	0.6832	100	0.8652
30 rods in 5-inch ss-pipe	0.7014	110	0.9285	0.7630	81	0.9240
ATRIUM 10 rods, ≤ 5.0 wt% ^{235}U						
25 loose rods	0.6181	256	0.8255	0.6328	100	0.8024
30 rods in 5-inch ss-pipe	0.6531	264	0.8978	0.7114	100	0.8690
PWR 17x17, type 3 rods, ≤ 8.0 wt% ^{235}U						
25 loose rods	0.6656	256	0.8937	0.6838	100	0.8681
30 rods in 5-inch ss-pipe	0.7043	100	0.9241	0.7655	81	0.9266

* Also includes polyethylene cross-section error penalty (see Section 6.13.5)

** Used maximum enrichment with minimum Gd rod loading to bound single package evaluations

6.13.1.3. Criticality Safety Index

The Criticality Safety Index (CSI) to be used when transporting the various new loads is calculated as prescribed in 10 CFR §71.59 [28]. The CSI value for a package is equal to the greater of $50/(N_{HAC}/2)$ or $50/(N_{NCT}/5)$, where N_{HAC} and N_{NCT} are the number of packages, under hypothetical accident conditions (HAC) and normal conditions of transport (NCT) that can be optimally stacked and still meet the USL. CSI values are rounded up to the next highest tenth, for example, a calculated CSI value of 1.22 becomes 1.3. Table 6-129 presents the additional CSI values determined for the TN-B1 package update. For the ATRIUM 11 assemblies, the maximum enrichment per minimum Gd rod loading is determined for fixed NCT and HAC array sizes. The NCT array loadings bound the HAC array loadings, but the calculated CSI_{HAC} is greater than the CSI_{NCT}, and is used for the package CSI.

Table 6-129 CSI Values Determined for TN-B1 Update

Fuel Load	Normal Conditions of Transport		Hypothetical Accident Conditions		CSI
	No. Packages	CSI_{NCT}	No. Packages	CSI_{HAC}	
ATRIUM 11 assemblies enrichment (# UO_2+Gd_2O_3 rods, wt% Gd_2O_3)					
≤ 8.0 wt% ^{235}U (21, 4.0)	81	3.1	--	--	3.2
≤ 8.0 (19, 4.0)	--	--	32	3.2	
≤ 7.6 (17, 4.0)	--	--	32	3.2	
≤ 7.5 (19, 4.0)	81	3.1	--	--	3.2
≤ 7.0 (17, 4.0)	81	3.1	--	--	3.2
≤ 7.0 (15, 4.0)	--	--	32	3.2	
≤ 6.6 (13, 4.0)	--	--	32	3.2	
≤ 6.7 (15, 2.0)	--	--	32	3.2	
≤ 6.5 (15, 4.0)	81	3.1	--	--	3.2
≤ 6.3 (13, 2.0)	--	--	32	3.2	
≤ 6.1 (13, 4.0)	81	3.1	--	--	3.2
≤ 5.8 (13, 2.0)	81	3.1	--	--	3.2
ATRIUM 11 rods, ≤ 8 wt% ^{235}U					
25 loose rods	256	1.0	100	1.0	1.0
30 rods in 5-inch ss-pipe*	110	2.3	81	1.3	2.3
ATRIUM 10 rods, ≤ 5.0 wt% ^{235}U					
25 loose rods	256	1.0	100	1.0	1.0
30 rods in 5-inch ss-pipe*	264	1.0	100	1.0	1.0
PWR 17x17, type 3 rods, ≤ 8 wt% ^{235}U					
25 loose rods	256	1.0	100	1.0	1.0
30 rods in 5-inch ss-pipe*	100	2.5	81	1.3	2.5

* 5-inch schedule 40 ss pipe or protective carrier

6.13.2. *Fissile Material Contents*

The TN-B1 package will be used to carry heterogeneous uranium compounds in the form of fuel rods. These rods will be transported as ATRIUM 11 BWR fuel assemblies or individual ATRIUM 11, ATRIUM 10XM, or PWR 17x17, type 3 fuel rods. For ATRIUM 11 assemblies, the lattice average uranium enrichment shall not be greater than 8.0 wt% ^{235}U. Individual ATRIUM 11 and PWR 17x17, type 3 fuel rods shall not have uranium enrichments greater than 8.0 wt% ^{235}U and ATRIUM 10XM fuel rods shall not have uranium enrichment greater than 5.0 wt% ^{235}U. The ATRIUM 11 fuel assemblies will have mixed uranium dioxide and gadolinia (UO_2-Gd_2O_3) fuel rods (also referred to as Gd rods) within the lattice that are be relied upon for additional criticality control during transportation. The uranium isotopic distribution considered in the models for this evaluation is shown in Table 6-130.

Table 6-130 Modeled Uranium Isotopic Distributions

Fuel Type	Minimum Gadolinia Requirements*	Isotope	Modeled wt%
ATRIUM 11 Assemblies	21 @ 4.0 wt%	^{235}U	≤ 8.0
		^{238}U	≥ 92.0
	19 @ 4.0 wt%	^{235}U	≤ 7.5
		^{238}U	≥ 92.5
	17 @ 4.0 wt%	^{235}U	≤ 7.0
		^{238}U	≥ 93.0
	15 @ 4.0 wt%	^{235}U	≤ 6.5
		^{238}U	≥ 93.5
	13 @ 4.0 wt%	^{235}U	≤ 6.1
		^{238}U	≥ 93.9
	13 @ 2.0 wt%	^{235}U	≤ 5.8
		^{238}U	≥ 94.2
ATRIUM 11 Rods	none	^{235}U	8.0
		^{238}U	92.0
ATRIUM 10XM Rods	none	^{235}U	5.0
		^{238}U	95.0
PWR 17x17, Type 3 Rods	none	^{235}U	8.0
		^{238}U	92.0

* Gadolinia content modeled at 75% credit for conservatism

6.13.2.1. BWR Fuel Assemblies

Other than raising the maximum lattice average enrichment, the ATRIUM 11 fuel assembly described in Section 6.12 of the latest TN-B1 SAR update [25] has not changed. See Table 6-61 for ATRIUM 11 fuel assembly data. Figure 6-51 shows the locations of the full-length, long part-length, and short part-length fuel rods in the ATRIUM 11 fuel assembly.

6.13.2.2. Individual Fuel Rods

This analysis also covers transport of individual ATRIUM 11, ATRIUM 10XM, and PWR 17x17, type 3 fuel rods. Note that the ATRIUM 11 and ATRIUM 10XM fuel rods may be part-length rods. Only full-length rods are evaluated as maximizing the total uranium in an optimum moderation situation maximizes k_{eff}. Table 6-131 provides descriptions of these fuel rods.

Table 6-131 Fuel Rod Data

Description	Units	Value
ATRIUM 11 Rods		
Fuel Pellet Outer Diameter	cm	≤ 0.820
Fuel Pellet Density	g/cm^3	≤ 10.7627
Clad Inner Diameter	cm	≤ 0.840
Clad Outer Diameter	cm	≥ 0.930
Clad Material		Zr alloy
Active Fuel Length	cm	≤ 385
Polyethylene Sleeve Thickness	cm	≤ 0.0152
ATRIUM 10XM Rods		
Fuel Pellet Outer Diameter	cm	≤ 0.899
Fuel Pellet Density	g/cm^3	≤ 10.7627
Clad Inner Diameter	cm	≤ 0.904
Clad Outer Diameter	cm	≥ 1.028
Clad Material		Zr alloy
Active Fuel Length	cm	≤ 385
Polyethylene Sleeve Thickness	cm	≤ 0.0152
PWR 17x17, Type 3 Rods		
Fuel Pellet Outer Diameter	cm	≤ 0.8265
Fuel Pellet Density	g/cm^3	≤ 10.7627
Clad Inner Diameter	cm	≤ 0.8407
Clad Outer Diameter	cm	≥ 0.9449
Clad Material		Zr alloy
Active Fuel Length	cm	≤ 381
Polyethylene Sleeve Thickness	cm	≤ 0.0152

6.13.3. *Modeling Considerations*

The package model features are unchanged from those documented in the previous revision of the SAR [25]. The models developed for these calculations are conservative representations of the package that include all of the physical features that are important to criticality safety and the updated fuel assembly and fuel rod contents. This section describes the packaging with contents models.

6.13.3.1. TN-B1 Package Models

The TN-B1 package models for NCT and HAC have not changed. See Section 6.3 of the latest TN-B1 SAR update [25] for details.

As was previously assumed for the last SAR revision, it is again assumed that the package leaks under both HAC and NCT conditions and optimum moderation is evaluated. Preferential flooding of different volumes within the package is considered for both NCT and HAC single package and array models. Additionally, full and partial burning of the polyethylene foam pads lining the inside of the fuel storage volume is considered for HAC array and single package models. Additional load-specific considerations are presented in the next sections. All models are reflected on all sides by a 30.48 cm thick layer of full density water.

The HAC and NCT models differ from each other in two ways. First, the top of the outer steel box in the HAC models is 2.4 cm shorter than for the NCT models. Second, the HAC models have an optimum amount of polyethylene foam pad removed. This material is considered to be burned and the burned polyethylene may be replaced with either water or reduced density polyethylene. Physical removal of the polyethylene permits a wider range of fuel assembly, loose rod array or storage pipe locations within the damaged package. Studies are performed to identify the worst-case locations in the HAC array and single package models.

6.13.3.2. TN-B1 Loaded with ATRIUM 11 Fuel Assemblies

In general, modeling of the ATRIUM 11 fuel assemblies in the TN-B1 has not changed from what is described in Section 6.12. New analysis includes determination of the most reactive multiple Gd rod loading patterns, determination of the most reactive orientation of each of the two assemblies that may be transported, determination of the most reactive location within the inner volume for HAC models, determination of most reactive selective flooding conditions, and the most reactive modeling of polyethylene within the fuel assembly.

6.13.3.3. Gd Rod Loading Pattern

The prior work documented in the previous revisions to the TN-B1 SAR focused on determining how many Gd rods and at what Gd_2O_3 loading would be needed to support use of a CSI value of 1.0 for the fuel assembly designs and covered up to 5 wt% ^{235}U. Scoping studies performed for this TN-B1 update indicated that, above 5 wt% ^{235}U, the ATRIUM 11 fuel assembly limits would require an increased Gd rod loading as the enrichment increased. Gd rod loadings were evaluated at 2 wt% Gd_2O_3 and 4 wt% Gd_2O_3 and searching for combinations that allow a maximum CSI of 3.3 as a function of enrichment. Analysis was performed to determine the most reactive Gd rod pattern or patterns for ATRIUM 11 assemblies with enrichments above 5 wt% ^{235}U that maintain a maximum CSI of 3.3 for enrichments up to 8.0 wt% ^{235}U.

The design requirements specify that the Gd rods must be placed symmetrically with respect to the assembly major diagonal and that the required Gd rods shall not be placed in an assembly peripheral location. In addition to these, for enrichments above 5 wt% ^{235}U, it is also required that each face of the enriched lattices must contain a minimum of one equivalent Gd rod in the second and tenth row/column locations. The word *equivalent* is used because ATRIUM 11 Gd rods at positions (2,2), (2,10), (10,2), and (10,10) will also meet this requirement. Examination of prior work documented in the TN-B1 indicates that the most reactive condition is produced by moving the Gd rods as close together as possible, thereby maximizing shielding of Gd rods by other Gd rods and maximizing k_{eff}, and by avoiding placement of Gd rods near empty (i.e., water filled) lattice positions, thereby avoiding placement of Gd rods in higher thermal neutron flux locations. Since gadolinium is primarily a thermal neutron absorber, avoiding higher thermal neutron flux reduces neutron absorption and maximizes k_{eff}. With those guiding principles, the most reactive 13, 15, 17, 18, 19, and 21 Gd rod patterns were determined to be as shown in Figure 6-87. Several variations were tried at each axial level at 8 wt% ^{235}U and varied Gd rod loadings to determine the most reactive configuration.

In the figure, the green dots are the Gd rods, the orange dots are the UO_2 rods, and the empty white squares are lattice vacancies for the central 3x3 water channel and for empty lattice locations left above part-length fuel rods.

The Gd rod patterns shown in Figure 6-87 were used for all ATRIUM 11 assembly criticality calculations. It should be noted that to maximize package reactivity, various rotations of these patterns were evaluated. These Gd rod patterns are bounding and not necessarily something that will be used in fuel design and fabrication.

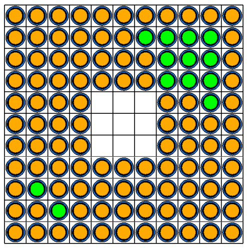

13 Gd Rod (Bottom Lattice)

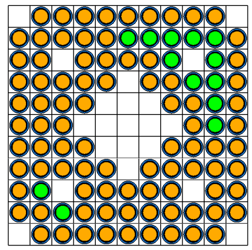

13 Gd Rod (Middle Lattice)

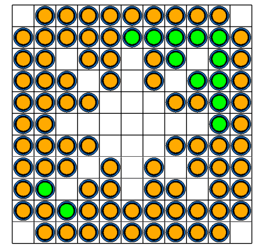

13 Gd Rod (Top Lattice)

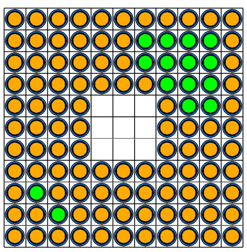

15 Gd Rod (Bottom Lattice)

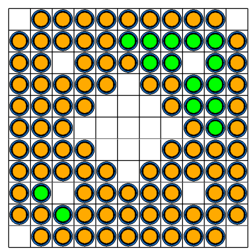

15 Gd Rod (Middle Lattice)

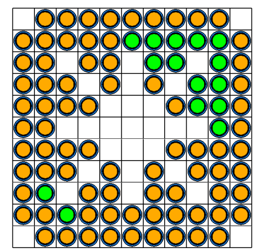

15 Gd Rod (Top Lattice)

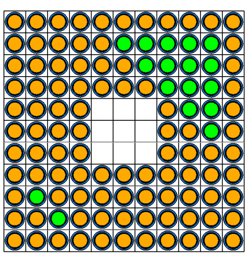

17 Gd Rod (Bottom Lattice)

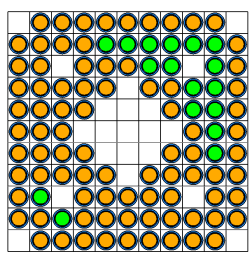

17 Gd Rod (Middle Lattice)

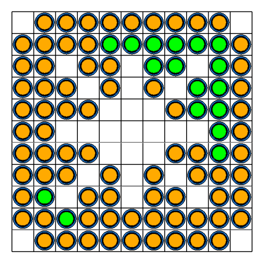

17 Gd Rod (Top Lattice)

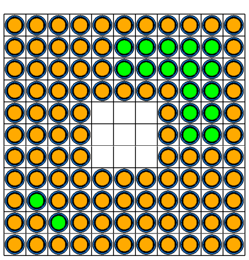

18 Gd Rod (Bottom Lattice)

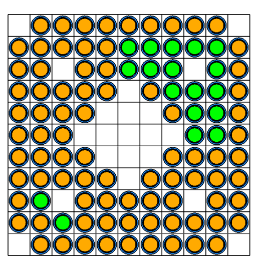

18 Gd Rod (Middle Lattice)

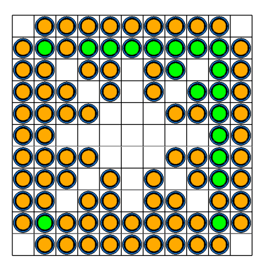

18 Gd Rod (Top Lattice)

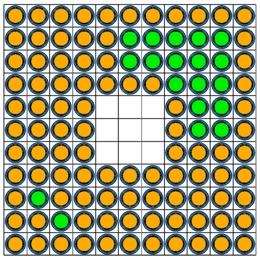
19 Gd Rod (Bottom Lattice)

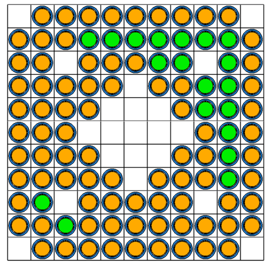
19 Gd Rod (Middle Lattice)

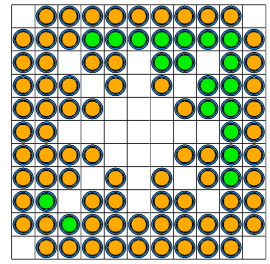
19 Gd Rod (Top Lattice)

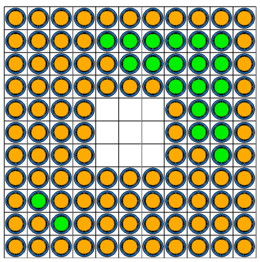
21 Gd Rod (Bottom Lattice)

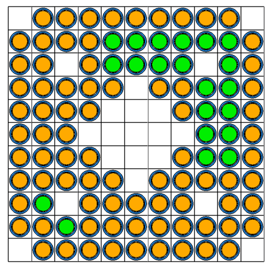
21 Gd Rod (Middle Lattice)

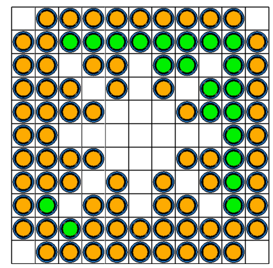
21 Gd Rod (Top Lattice)

Figure 6-87 Most Reactive Rod Lattice Configurations; top, middle and bottom

6.13.3.4. Fuel Assembly Orientation

Sensitivity studies were performed to find the most reactive fuel assembly orientations within the TN-B1 package. These studies were performed for each of the Gd rod configurations with 8.0 wt% ^{235}U and included consideration that k_{eff} may be maximized by locating the Gd rods in the two assemblies differently. In all cases, k_{eff} was maximized by locating the Gd rods toward the top of the package and away from the horizontal center. Table 6-132 shows the results of the various configurations with the TN-B1 loaded with 8.0 wt% fuel assemblies with 19 Gd rods. Similar results were obtained for the other Gd rod loading configurations. Figure 6-88 shows the most reactive configuration, in which the Gd groups in both assemblies are up (i.e., toward the top) and out (i.e., on the side farther from the package center).

Table 6-132 Study of Most Reactive Assembly Orientations

Assembly Gd Rod Group Positions				$k_{eff} + 2\sigma$
Left Assembly		Right Assembly		
Up	Out	Up	Out	0.97840
Down	Out	Up	Out	0.97754
Down	Out	Down	Out	0.97699
Up	Out	Up	In	0.96579
Down	Out	Down	In	0.96431
Up	In	Down	In	0.95650
Down	In	Down	In	0.95498
Up	In	Down	In	0.95465

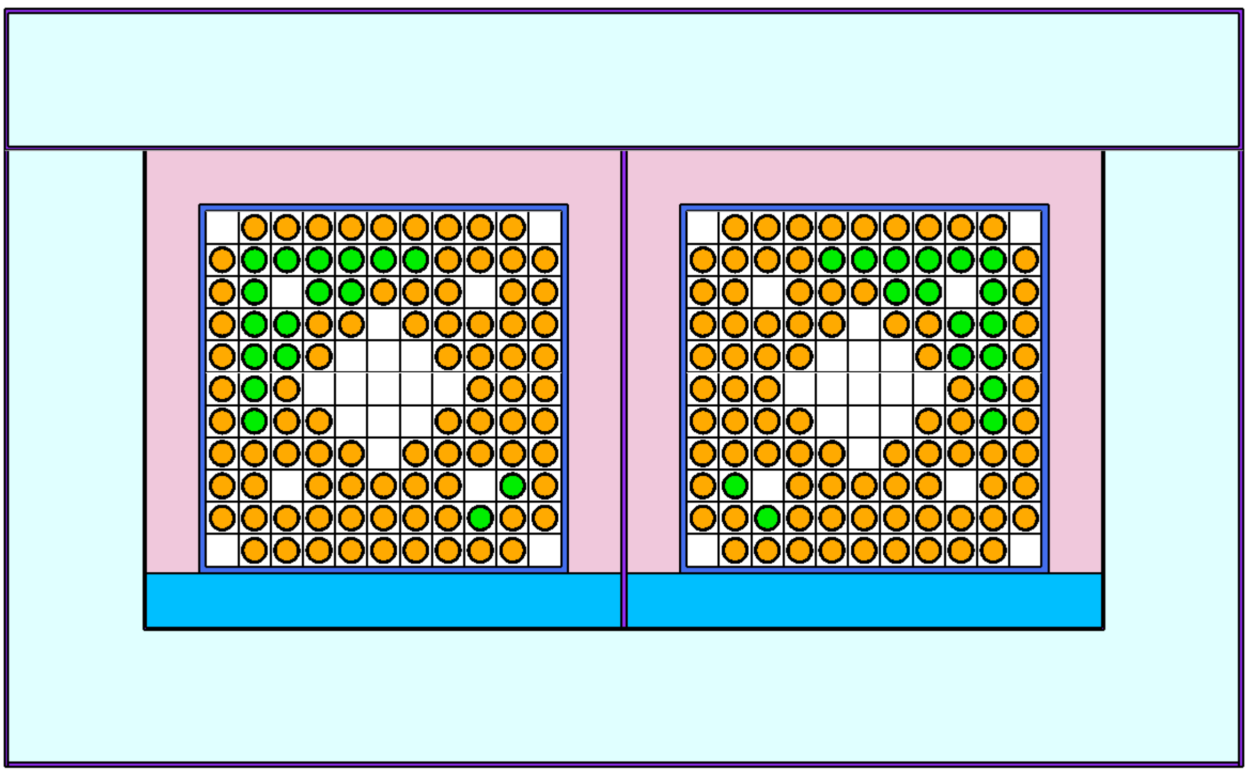

Figure 6-88 Most Reactive Assembly Orientation

The lattice orientation configuration shown in Figure 6-88 is used for the ATRIUM 11 assembly NCT and HAC models (number of Gd rods varies, but the assembly rotational orientation is the consistent).

6.13.3.5. Positioning of the fuel in the TN-B1 with and without fuel channels

Sensitivity studies were performed for both HAC and NCT arrays with and without fuel channels and for different Gd rod loading configurations to identify the most reactive location of the fuel assemblies within the interior storage compartments. The HAC array studies also included consideration of partial loss of the polyethylene pads in a fire. The results from the positioning studies are presented in the sections describing the results for each NCT and HAC limiting configuration.

6.13.3.6. Preferential flooding of the TN-B1 package

Consistent with the guidance in several references (e.g., 29, 30, and 36), preferential flooding was considered in both NCT and HAC models. Evaluation of preferential flooding involves identifying various regions in the package that may or may not flood and may or may not drain, following flooding, in such way as to maximize reactivity. Note that flooding under NCT was not physically tested. Consequently, optimal package flooding is considered for all HAC and NCT models.

Calculations performed for the TN-B1 SAR update demonstrated that for ATRIUM 11 fuel assemblies in HAC and NCT arrays, reactivity is maximized when the region between the inner and outer package walls is empty and the internal storage area is flooded with full density water. Partial flooding of the inner container has already been adequately addressed in Section 6.12.3.5.8, with results presented in Table 6-73. This work demonstrated that the assembly was most reactive when the inner container was fully flooded.

6.13.3.7. Flooding between packages in HAC array

In HAC conditions, the analysis must consider whether or not adding space or water between packages will increase reactivity. Calculations performed for the prior TN-B1 SAR update demonstrated that adding water or space between packages in the HAC array reduces reactivity.

6.13.3.8. Polyethylene on fuel rods

As is discussed in detail in Section 6.12 of the current TN-B1 SAR, in addition to the peripheral polyethylene foam pads, there may be a significant amount (i.e., ≤ 10.2 kg / assembly) of polyethylene used in the TN-B1 package to support and protect the fuel assemblies in the package. Calculations documented in the current TN-B1 SAR were used to prepare models in which the polyethylene melted into a layer on the fuel rods, was homogenized with the clad, or was homogenized with the water in the assembly.

Calculation of material models for these three modeling approaches is provided in Section 6.13.4.3. Due to limitations in SCALE associated with performing resonance self-shielded multi-group cross-section calculations, for the cross-section calculations the polyethylene must be homogenized either with the clad or the moderator. Inclusion of the polyethylene in the resonance calculations ensures that the energy dependent neutron flux entering the fuel material is as accurate as is practical.

In reality, the polyethylene will not be homogeneously mixed with water or with the clad material. To ensure a conservative approach, calculations were performed for ATRIUM 11 assembly models using five different approaches, including the following:

(1) polyethylene homogenized with water in assembly

(2) polyethylene homogenized with fuel rod clad

(3) polyethylene modeled in a layer on the clad, but homogenized with clad for resonance calculations

(4) polyethylene modeled in a layer on the clad, but homogenized with moderator for resonance calculations

(5) polyethylene replaced with water

Results from these approaches for 8 wt% ^{235}U fuel assemblies in a HAC array model are presented in Table 6-133.

Table 6-133 Polyethylene Modeling Study Results

Polyethylene Modeling Methods	K_{eff}	σ_{keff}
layer on clad, homogenized with clad for cross-sections	0.92229	0.00010
layer on clad, homogenized with water for cross-sections	0.92219	0.00010
homogenized with water	0.92195	0.00010
homogenized with clad	0.92100	0.00010
replaced with water	0.91541	0.00010

These results demonstrate that for modeling 8 wt% ^{235}U ATRIUM 11 fuel assemblies in HAC array conditions, the most reactive modeling approach is to model the polyethylene in a layer on the outside of each fuel rod and perform cross-section resonance calculations with the polyethylene homogenized with the clad. A similar set of calculations was performed for each Gd loading configuration and for both HAC and NCT arrays and single packages to determine the most reactive modeling approach for each enrichment and configuration.

6.13.3.9. TN-B1 Loaded with “Loose” Fuel Rods

Up to 25 fuel rods (i.e., ATRIUM 11, ATRIUM 10XM or PWR 17x17, type 3 rods) may be transported in each side of the TN-B1, without use of additional packaging such as the 5-inch ss-pipe or the protective rod carrier. It is likely that some strapping or other packaging will restrain these rods into a close packed bundle. However, the criticality analysis assumes that the fuel rods are completely “loose”. Each of the fuel rods may be enclosed in a polyethylene sleeve that is no thicker than 6 mils (0.006 inches). The analysis approach documented in Sections 6.3.1.3, 6.7 and 6.12.3.1.6 of the TN-B1 SAR [25] is used for this update.

Variations from the previously documented approach include increasing the maximum enrichment of the ATRIUM 11 to 8.0 wt% ^{235}U, adding limits for the ATRIUM 10XM fuel rods with enrichment up to 5 wt% ^{235}U, and adding limits for PWR 17x17, type 3 fuel rods with enrichment up to 8 wt% ^{235}U. The analysis documented in this appendix further examines the impact of how the polyethylene sleeves are modeled, similar to what is shown in Table 6-133. Additionally, the impact of liner density between nominal and maximum values is evaluated.

While shipment of 10x10 fuel rods was discussed in the earlier work, the ATRIUM 10XM fuel rod has a minimum clad outer diameter of 0.978 cm, which is slightly smaller than the minimum outer diameter of 1.00 cm shown for the 10x10 (UO_2) fuel type shown in Table 6-2 of the latest TN-B1 SAR update [25]. Additionally, the PWR 17x17, type 3 fuel rod is significantly smaller than the “Generic PWR (UO_2)” rod described in Table 6-2 of the latest TN-B1 SAR update [25].

The analysis for loose fuel rods involves performing calculations for a square 5x5 array of maximum enrichment fuel pins with varied pin pitch and moderator density to identify the pin pitch and moderator density that maximize k_{eff}. Additional calculations are performed to quantify the impact of different polyethylene pad thickness or density for HAC cases and the worst-case location of the optimized arrays within their storage volume. Details of these calculations are provided in the sections addressing demonstration of maximum reactivity. Figure 6-89 shows the limiting case for 25 loose ATRIUM 11 fuel rods in the HAC array configuration.

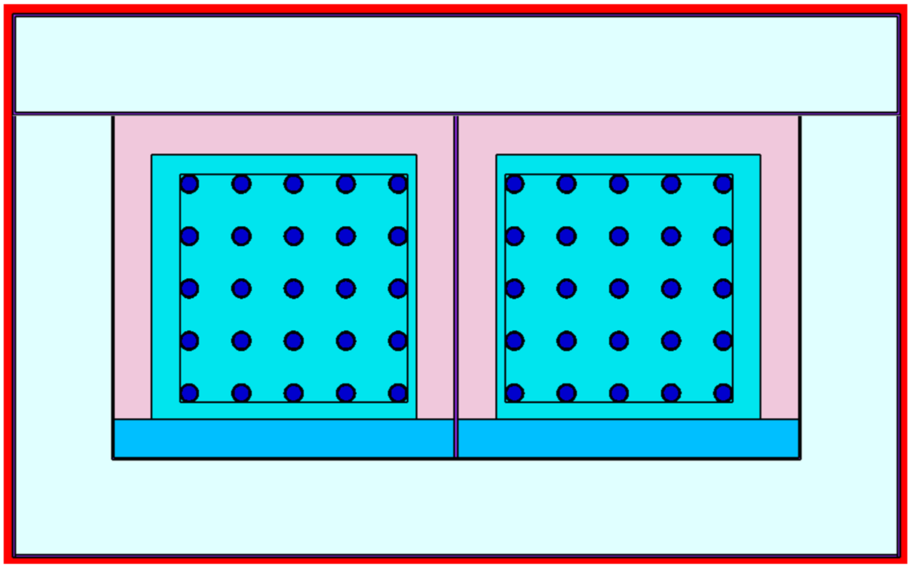

Figure 6-89 Loose ATRIUM 11 fuel rods in limiting HAC configuration

6.13.3.10. TN-B1 Loaded with Fuel Rods in 5-inch Schedule 40 SS Pipe

Up to 30 fuel rods (i.e., ATRIUM 11, ATRIUM 10XM or PWR 17x17, type 3 rods) may be transported in either a 5-inch schedule 40 stainless steel (ss) pipe or in the protective carrier, described in Section 1.2.3.4.7 of the latest TN-B1 SAR update [25], in each side of the TN-B1. Consistent with the existing TN-B1 SAR, detailed criticality analysis of the protective carrier is not performed because, due to its having a cross-sectional area that is significantly smaller than the inside of the 5-inch ss pipe model, the analysis of the pipe adequately bounds protective carrier configurations. Each of the fuel rods may be enclosed in a polyethylene sleeve that is no thicker than 6 mils (0.006 inches). The analysis approach documented in Sections 6.3.1.3, 6.7 and 6.12.3.1.6 of the TN-B1 SAR [25] is used for this update.

The analysis of fuel rods in the ss pipe involves modeling triangular pitched arrays of 30 fuel rods inside the dimension representing the outer diameter of a standard 5-inch schedule 40 ss pipe. The pitch is varied from tightly packed pins out to where the outer most pins reach the limiting pipe radius. The pitch is further increased while manually moving the outermost fuel pins such that they are still within the pipe outer diameter. The manual movement of outer fuel pins created some local areas with decreased average pin pitch. A few rods were removed or moved from “crowded” areas to demonstrate that removing pins will not increase k_{eff}. Other than the geometry restriction and potential impact on preferential flooding, the stainless steel of the pipe is conservatively not modeled.

These calculations are used to find the limiting fuel rod arrangement for the highest enrichment of each fuel rod type. Additional calculations were performed to determine:

- Optimal water density for water that is outside the pipe, but still inside the inner transport volumes
- Optimal pitch with and without polyethylene sleeves
- Liner density impact (nominal and high-density liner)
- For HAC packages, optimal location for pipes within internal storage volumes
- For HAC packages, optimal pad thickness

Details of these calculations are provided in the sections addressing demonstration of maximum reactivity. Figure 6-90 shows the limiting HAC array configuration for 30 ATRIUM 11, 8.0 wt% ^{235}U fuel rods in the 5-inch ss pipe.

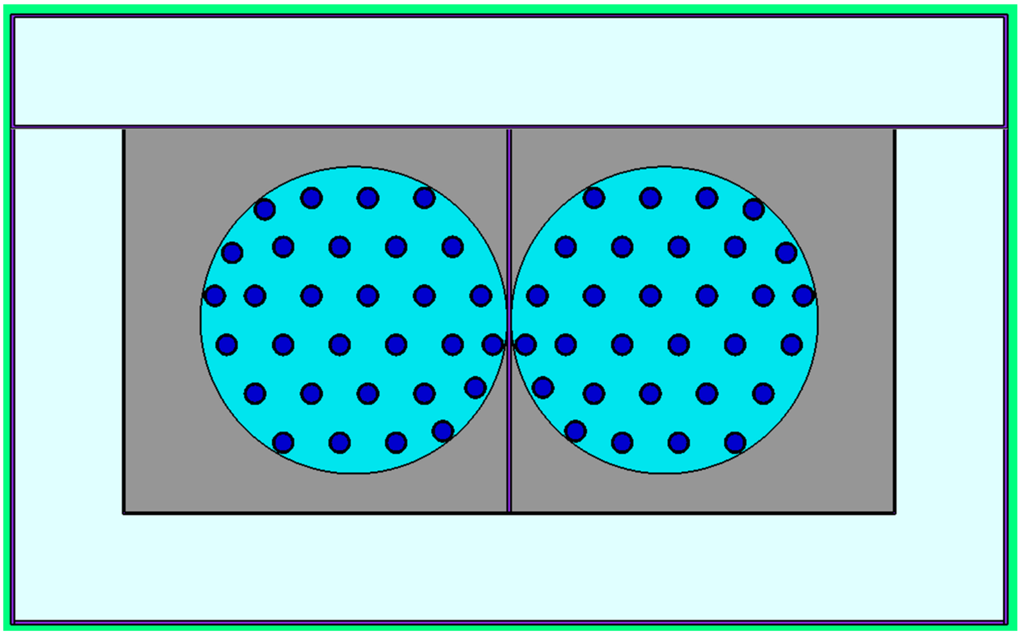

Figure 6-90 Limiting model for 30 ATRIUM 11, 8.0 wt% ^{235}U fuel rods in SS pipe

6.13.4. *Material Properties for Package Models*

6.13.4.1. Fuel Composition Calculations

Fuel compositions for the TN-B1 SAR Update work were calculated as described in this section.

Fuel compositions were calculated for enrichments between 5.5 and 8.0 wt% ^{235}U and for both UO_2 fuel rods and fuel rods containing a mixture of UO_2 and Gd_2O_3.

- **Fuel Rod Compositions for Fuel Rods Containing only UO_2**

Consistent with the approach described in Section 6.12.3.2 of [25], the UO_2 fuel compositions used were calculated assuming fuel density equal to 98.2% of the UO_2 maximum theoretical density (MTD).

The following equations were used to calculate the UO_2 compositions:

UO_2 density in (g/cm^3) = ρ_{UO2} (%MTD) = MTD_{UO2} * %MTD / 100

Where: MTD_{UO2} is the maximum theoretical density of UO_2. The commonly accepted value for MTD_{UO2} is 10.96 g UO_2/cm^3.

%MTD is the % of MTD assumed for UO_2 fuel to be transported in the TN-B1. This analysis uses 98.2% for the calculation of CSI values.

ρ_{UO2} (98.2) = 10.96 * 98.2 / 100 = 10.7627 g/cm^3

^{238}U wt% = 100% - ^{235}U wt%

The UO_2 density, the ^{235}U wt%, and ^{238}U wt% are the direct inputs for the SCALE computer code system. The trace presence of ^{234}U and ^{236}U are conservatively ignored.

This approach includes an unquantified conservatism. For purposes of this analysis, it was assumed that the MTD of UO_2 did not change with enrichment. In reality, the commonly used maximum theoretical density of 10.96 g/cm^3 is for natural uranium. A ^{235}U atom is the same size as a ^{238}U atom. Since the ^{235}U atom has 3 fewer neutrons, it weighs about 1.3 % less than a ^{238}U atom. Consequently, as uranium is enriched and ^{238}U atoms are replaced with ^{235}U atoms, the density of the uranium and, consequently, the UO_2 are reduced. At 8 wt% ^{235}U the UO_2 MTD could be reduced from 10.96 to 10.9511 g UO_2/cm^3.

- **Fuel Rod Compositions for Fuel Rods Containing UO_2 and Gd_2O_3**

All ATRIUM 11 fuel assemblies shipped in the TN-B1 container and having enrichments greater than 5 weight percent (wt%) ^{235}U, must have a minimum number of UO_2+Gd_2O_3 fuel rods in each lattice (i.e., top, middle and bottom lattice) that has a lattice average enrichment greater than 5 wt% ^{235}U. The fuel in each of these rods must contain a minimum number and wt% Gd_2O_3 loading per lattice ^{235}U enrichment. The overall density of the fuel in these UO_2+Gd_2O_3 fuel rods was calculated as a linear combination of the maximum theoretical densities of UO_2 and Gd_2O_3, reduced by applying the specified percent of maximum theoretical density. The following equations were used to calculate the SCALE inputs for the fuel compositions used in the UO_2+Gd_2O_3 fuel rods.

$$\rho_{UO2+Gd2O3}(Gd_2O_3\ wt\%, \%MTD) =$$

$$[(MTD_{Gd2O3} * Gd_2O_3\ wt\%/100) + (MTD_{UO2} * \{100 - Gd_2O_3\ wt\%\}/100)\ ]*\%MTD/100$$

Where: Gd_2O_3 wt% is the weight percent of the Gd_2O_3 in the UO_2+Gd_2O_3 mixture

MTD_{Gd2O3} is the maximum theoretical density of Gd_2O_3, 7.407 g Gd_2O_3 per cm^3 (from Section 6.12.3.2).

MTD_{UO2} is the maximum theoretical density of UO_2. The commonly accepted value for MTD_{UO2} is 10.96 g UO_2/cm^3.

%MTD is the % of MTD assumed for UO_2+Gd_2O_3 fuel to be transported in the TN-B1. This analysis, consistent with the last SAR update, uses 98.2% for criticality calculations.

For fuel with 4 wt% Gd_2O_3, and at 98.2% of MTD,

$$\rho_{UO2+Gd2O3}(4, 98.2) = [(4*7.407/100)+(100-4)*10.96/100]*98.2/100$$

$$\rho_{UO2+Gd2O3}(4, 98.2) = 10.6232\ g\ Gd_2O_3+UO_2\ /cm^3$$

The other SCALE CSAS5 inputs for the UO_2+Gd_2O_3 fuel mixture are the ^{235}U enrichment, ^{238}U wt%, fraction mixture density assigned to UO_2, and fraction of mixture density assigned to Gd_2O_3.

For this SAR revision, all fuel with enrichments greater than 5 wt% ^{235}U required inclusion of a minimum number of fuel rods having at least 2 or 4 wt% Gd_2O_3. Consequently, for the UO_2 in the UO_2+Gd_2O_3 rods, a multiplier of 0.98 or 0.96 is applied to the calculated UO_2+Gd_2O_3 mixture density. Similarly for the Gd_2O_3, a multiplier of 0.02 or 0.04 is applied to the calculated mixture and is further reduced by 25% to 0.015 or 0.030 to reduce credit for Gd_2O_3, as recommended by NRC Staff, to 75% of the minimum required.

This reduction to 75% of the required minimum neutron absorber content is expected by the Nuclear Regulatory Commission Staff reviewers as is noted in Section 7.4.7.2 of NUREG-2216, *Standard Review Plan for Transportation Packages for Spent Fuel and Radioactive Material*. Consequently, the multiplier applied to the mixture density to model Gd_2O_3 is 0.015 (=0.02*0.75) or 0.030 (=0.04*0.75). The removed 25% of Gd_2O_3 is not replaced with UO_2 as adding more uranium is unnecessarily conservative.

Table 6-134 below provides a collection of data used to model the fuel in the SCALE input. Table 6-135 and Table 6-136 provide fuel number densities calculated by SCALE computer code based on the inputs from Table 6-134.

Table 6-134 Fuel Composition Description

UO_2 Fuel Rods	
UO_2 Maximum Theoretical Density (MTD)	10.96 g UO_2 / cm^3
% of MTD Used	98.2 %
SCALE UO_2 Density Input	10.7627 g UO_2/cm^3
wt% ^{235}U Enrichment	>5.0 to 8.0 wt% ^{235}U
wt% ^{238}U	100.0 – wt% ^{235}U
UO_2 + Gd_2O_3 Fuel Rods	
UO_2 MTD	10.96 g UO_2 / cm^3
wt% ^{235}U Enrichment	>5.0 to 8.0 wt% ^{235}U
wt% ^{238}U	100.0 – wt% ^{235}U
Gd_2O_3 MTD	7.407 g Gd_2O_3 / cm^3
wt% Gd_2O_3 in UO_2 + Gd_2O_3	4 wt% Gd_2O_3; 2 wt% Gd_2O_3
% of Gd_2O_3 credited	75 % (3.0 wt% Gd_2O_3 input; 1.5 wt% Gd_2O_3 input)
UO_2 + Gd_2O_3 MTD	10.7468 g UO_2 + Gd_2O_3 / cm^3
% of MTD Used	98.2 %
SCALE UO_2 + 100% Gd_2O_3 Density Input (4 or 2)	10.6232; 10.6929 g UO_2 + Gd_2O_3 / cm^3
UO_2 density multiplier for UO_2+Gd_2O_3 density	0.96; 0.98
Gd_2O_3 density multiplier for UO_2+Gd_2O_3 density	0.030; 0.015
UO_2 + Gd_2O_3 density with 25% Gd_2O_3 removed	10.4638; 10.5325 g UO_2 + Gd_2O_3 / cm^3

Table 6-135 Compositions for UO_2 Fuel

Material	Density (g/cm^3)	Constituent	Atomic Density (atoms/b-cm)
$U(5.8)O_2$	10.7627	^{235}U	1.40974E-03
		^{238}U	2.26069E-02
		^{16}O	4.79166E-02
		^{17}O	1.82527E-05
$U(6.1)O_2$		^{235}U	1.48265E-03
		^{238}U	2.25348E-02
		^{16}O	4.79182E-02
		^{17}O	1.82533E-05
$U(6.3)O_2$		^{235}U	1.53126E-03
		^{238}U	2.24868E-02
		^{16}O	4.79193E-02
		^{17}O	1.82537E-05
$U(6.5)O_2$		^{235}U	1.57986E-03
		^{238}U	2.24387E-02
		^{16}O	4.79204E-02
		^{17}O	1.82541E-05
$U(6.6)O_2$		^{235}U	1.60417E-03
		^{238}U	2.24147E-02
		^{16}O	4.79209E-02
		^{17}O	1.82543E-05
$U(6.7)O_2$		^{235}U	1.62847E-03
		^{238}U	2.23906E-02
		^{16}O	4.79215E-02
		^{17}O	1.82545E-05
$U(7.0)O_2$		^{235}U	1.70138E-03
		^{238}U	2.23185E-02
		^{16}O	4.79231E-02
		^{17}O	1.82551E-05
$U(7.5)O_2$		^{235}U	1.82289E-03
		^{238}U	2.21984E-02
		^{16}O	4.79258E-02
		^{17}O	1.82562E-05
$U(7.6)O_2$		^{235}U	1.84720E-03
		^{238}U	2.21743E-02
		^{16}O	4.79263E-02
		^{17}O	1.82564E-05
$U(8.0)O_2$		^{235}U	1.94440E-03
		^{238}U	2.20782E-02
		^{16}O	4.79285E-02
		^{17}O	1.82572E-05

Table 6-136 Compositions for UO_2 + x wt% Gd_2O_3 Fuel

Material	Density (g/cm^3)	Constituent	Atomic Density (atoms/b-cm)
U(5.8)O_2 + Gd_2O_3 (2.0)	10.6394	^{235}U	1.37259E-03
		^{238}U	2.20111E-02
		^{152}Gd	1.06583E-06
		^{154}Gd	1.16175E-05
		^{155}Gd	7.88712E-05
		^{156}Gd	1.09087E-04
		^{157}Gd	8.34010E-05
		^{158}Gd	1.32376E-04
		^{160}Gd	1.16495E-04
		^{16}O	4.74512E-02
		^{17}O	7.88712E-05
U(6.1)O_2 + Gd_2O_3 (4.0)	10.5170	^{235}U	1.40490E-03
		^{238}U	2.13530E-02
		^{152}Gd	2.11776E-06
		^{154}Gd	2.30836E-05
		^{155}Gd	1.56714E-04
		^{156}Gd	2.16753E-04
		^{157}Gd	1.65715E-04
		^{158}Gd	2.63026E-04
		^{160}Gd	2.31471E-04
		^{16}O	4.69897E-02
		^{17}O	1.56714E-04
U(6.3)O_2 + Gd_2O_3 (2.0)	10.6394	^{235}U	1.49090E-03
		^{238}U	2.18941E-02
		^{152}Gd	1.06583E-06
		^{154}Gd	1.16175E-05
		^{155}Gd	7.88712E-05
		^{156}Gd	1.09087E-04
		^{157}Gd	8.34010E-05
		^{158}Gd	1.32376E-04
		^{160}Gd	1.16495E-04
		^{16}O	4.74538E-02
		^{17}O	7.88712E-05
U(6.5)O_2 + Gd_2O_3 (4.0)	10.5170	^{235}U	1.49701E-03
		^{238}U	2.12619E-02
		^{152}Gd	2.11776E-06
		^{154}Gd	2.30836E-05
		^{155}Gd	1.56714E-04
		^{156}Gd	2.16753E-04
		^{157}Gd	1.65715E-04
		^{158}Gd	2.63026E-04
		^{160}Gd	2.31471E-04
		^{16}O	4.69918E-02
		^{17}O	1.56714E-04

Table 6-136 Compositions for UO2 + x wt% Gd2O3 Fuel (continued)

Material	Density (g/cm^3)	Constituent	Atomic Density (atoms/b-cm)
U(6.6)O_2 + Gd_2O_3 (4.0)	10.5170	^{235}U	1.52004E-03
		^{238}U	2.12392E-02
		^{152}Gd	2.11776E-06
		^{154}Gd	2.30836E-05
		^{155}Gd	1.56714E-04
		^{156}Gd	2.16753E-04
		^{157}Gd	1.65715E-04
		^{158}Gd	2.63026E-04
		^{160}Gd	2.31471E-04
		^{16}O	4.69923E-02
		^{17}O	1.56714E-04
U(6.7)O_2 + Gd_2O_3 (2.0)	10.6929	^{235}U	1.58555E-03
		^{238}U	2.18005E-02
		^{152}Gd	1.06583E-06
		^{154}Gd	1.16175E-05
		^{155}Gd	7.88712E-05
		^{156}Gd	1.09087E-04
		^{157}Gd	8.34010E-05
		^{158}Gd	1.32376E-04
		^{160}Gd	1.16495E-04
		^{16}O	4.74559E-02
		^{17}O	1.80772E-05
U(7.0)O_2 + Gd_2O_3 (4.0)	10.5170	^{235}U	1.61215E-03
		^{238}U	2.11481E-02
		^{152}Gd	2.11776E-06
		^{154}Gd	2.30836E-05
		^{155}Gd	1.56714E-04
		^{156}Gd	2.16753E-04
		^{157}Gd	1.65715E-04
		^{158}Gd	2.63026E-04
		^{160}Gd	2.31471E-04
		^{16}O	4.69943E-02
		^{17}O	1.56714E-04
U(7.5)O_2 + Gd_2O_3 (4.0)	10.5170	^{235}U	1.72730E-03
		^{238}U	2.10342E-02
		^{152}Gd	2.11776E-06
		^{154}Gd	2.30836E-05
		^{155}Gd	1.56714E-04
		^{156}Gd	2.16753E-04
		^{157}Gd	1.65715E-04
		^{158}Gd	2.63026E-04
		^{160}Gd	2.31471E-04
		^{16}O	4.69969E-02
		^{17}O	1.56714E-04

Table 6-136 Compositions for UO2 + x wt% Gd2O3 Fuel (continued)

Material	Density (g/cm^3)	Constituent	Atomic Density (atoms/b-cm)
$U(7.6)O_2 + Gd_2O_3$ (4.0)	10.5170	^{235}U	1.75032E-03
		^{238}U	2.10115E-02
		^{152}Gd	2.11776E-06
		^{154}Gd	2.30836E-05
		^{155}Gd	1.56714E-04
		^{156}Gd	2.16753E-04
		^{157}Gd	1.65715E-04
		^{158}Gd	2.63026E-04
		^{160}Gd	2.31471E-04
		^{16}O	4.69974E-02
		^{17}O	1.56714E-04
$U(8.0)O_2 + Gd_2O_3$ (4.0)	10.5170	^{235}U	1.84243E-03
		^{238}U	2.09204E-02
		^{152}Gd	2.11776E-06
		^{154}Gd	2.30836E-05
		^{155}Gd	1.56714E-04
		^{156}Gd	2.16753E-04
		^{157}Gd	1.65715E-04
		^{158}Gd	2.63026E-04
		^{160}Gd	2.31471E-04
		^{16}O	4.69994E-02
		^{17}O	1.56714E-04

6.13.4.2. Non-Fuel Compositions

All non-fuel material compositions used in this appendix are described in Section 6.12, *Appendix B: 11x11 Fuel Assembly Criticality Analysis*. Due to small changes in the SCALE standard composition library, some of the non-fuel compositions have changed negligibly from those provided in Table 6-60. Consequently, updated values are provided below in Table 6-137. Compositions for polyethylene homogenized with clad or with water are addressed in Section 6.13.4.3.

Table 6-137 Non-Fuel Compositions

Material	Density (g/cm^3)	Constituent	Atomic Density (atoms/b-cm)
Zirconium	6.49	Zr-90	2.20431E-02
		Zr-91	4.80708E-03
		Zr-92	7.34772E-03
		Zr-94	7.44626E-03
		Zr-96	1.19963E-03
Nominal density liner (Polyethylene Foam-4 pcf)	0.08	H-1(in poly)	6.86950E-03
		C	3.43475E-03
Nominal density liner (Polyethylene Foam-9 pcf)	0.16	H-1(in poly)	1.37390E-02
		C	6.86950E-03
High density liner	0.28	H-1(in poly)	2.40432E-02
		C	1.20216E-02
High density liner	0.56	H-1(in poly)	4.80865E-02
		C	2.40432E-02
Polyethylene (full density)	0.949	H-1(in poly)	8.14894E-02
		C	4.07447E-02
Aluminum Silicate [Al_2O_3(49%)+SiO_2(51%)]	0.25	O-16	4.72705E-03
		Al-27	1.44724E-03
		Si-28	1.17870E-03
		Si-29	5.98790E-05
		Si-30	3.95189E-05
Full Density Water	1.0	H-1 (in water)	6.68482E-02
		H-2 (in water)	7.68843E-06
		O-16	3.33467E-02
		O-17	1.27026E-05
SS-304	7.94	C	3.18487E-04
		Si-28	1.57010E-03
		Si-29	7.97625E-05
		Si-30	5.26416E-05
		P-31	6.94688E-05
		Cr-50	7.59178E-04
		Cr-52	1.46400E-02
		Cr-53	1.66006E-03
		Cr-54	4.13224E-04
		Mn-55	1.74072E-03
		Fe-54	3.42190E-03
		Fe-56	5.37166E-02
		Fe-57	1.24055E-03
		Fe-58	1.65094E-04
		Ni-58	5.26873E-03
		Ni-60	2.02951E-03
		Ni-61	8.82212E-05
		Ni-62	2.81288E-04
		Ni-64	7.16357E-05

6.13.4.3. Polyethylene Compositions

In addition to the peripheral polyethylene pads, there may be, as is noted in Section 6.12, as much as 10.2 kg of polyethylene in and around each fuel assembly. For the TN-B1 work, this polyethylene is modeled in three different ways. These include (1) a full density layer of polyethylene on the outside of each fuel rod, (2) a homogenized clad + polyethylene zone on each fuel rod, and (3) polyethylene and water homogenized within the envelope of the fuel assembly model. This section describes generation of the SCALE input values for each approach. The accuracy of each of these methods was checked using the SCALE output to calculate the mass of polyethylene per assembly, which compared well with the target 10.2 kg of polyethylene.

- **Full Density Polyethylene Layer**

In this model the polyethylene is added as a layer on the outside of each fuel rod. This was accomplished by calculating the sum of the length of each full and part-length fuel rod in the ATRIUM 11 assembly. As modeled, there is 39,175.6 cm of fuel rod in each assembly. Using the total length of the fuel rods, the 0.465 cm outer radius of the fuel rod clad, a polyethylene density of 0.949 g/cm^3, and the total mass of polyethylene, the outer radius of the polyethylene layer is calculated to be 0.551 cm.

In this model for ATRIUM 11 fuel assemblies, the resonance self-shielding calculations are performed using the homogenized clad and polyethylene model or the homogenized moderator and polyethylene model described below. It is done this way because the SCALE latticecell resonance self-shielding cross-section calculation approach does not support multiple material zones outside the clad. Homogenizing the polyethylene with the clad or moderator for cross section calculations yields a good approximation for the flux entering the fuel pellet zone.

The composition calculated by SCALE for full density polyethylene is provided in Table 6-137.

- **Homogenized Clad and Polyethylene**

In this model, the two cylinders of clad and polyethylene are homogenized into a single zone, having an interior radius equal to the clad inner radius (0.42 cm) and an exterior radius equal to the polyethylene zone outer radius (0.551 cm) described in the first polyethylene model. Each composition is input as full density material that is reduced by its pre-homogenized fraction of cross-sectional area of a fuel rod. For the ATRIUM 11 assemblies, the clad cross-sectional area is 0.12511 cm^2, the polyethylene cross-sectional area is 0.27450 cm^2, and the total clad+polyethylene area is then 0.39961 cm^2. These areas were used to calculate a clad volume fraction multiplier of 0.31309 and a polyethylene volume fraction multiplier of 0.68691.

The composition calculated by SCALE for the homogenized clad and polyethylene mixture is provided in Table 6-138.

Table 6-138 Composition for Homogenized Clad and Polyethylene Mixture

Homogenized Polyethylene and Clad			
Polyethylene		Constituent	Atomic Density (atoms/b-cm)
Density	0.949 g/cm^3	H-1 (in poly)	5.59759E-02
Vol. Fraction	0.68691	C	2.79879E-02
Clad (zirconium)		Zr-90	6.90149E-03
Density	6.49 g/cm^3	Zr-91	1.50505E-03
Vol. Fraction	0.31309	Zr-92	2.30050E-03
		Zr-94	2.33135E-03
		Zr-96	3.75591E-04

- **Homogenized Water and Polyethylene**

In this final model, the polyethylene is homogenized with the water that is within outer envelope of the ATRIUM 11 assembly. Different compositions are needed for the normal conditions of transport (NCT) and hypothetical accident conditions (HAC) models because the pin pitch and assembly width are increased for the HAC models to account for hypothetical fuel assembly deformation in an accident.

For the HAC model, the compositions are calculated using the total fuel rod length (39,175.6 cm), the clad outer radius (0.465 cm) and the total assembly volume 73,349.16 cm^3 [= (11*1.2548cm)^2*385 cm]. The volume of the fuel rods is 26,611.63 cm^3 [= π * 0.465^2 * 39175.6] leaving a total water-plus-polyethylene volume of 46,737.53 cm^3 [=73349.16 - 26611.63]. The total polyethylene volume, 10,748.16 cm^3, is calculated using the 10.2 kg of polyethylene and a polyethylene density of 0.949 g/cm^3. The remainder of the volume, 35,983.84 cm^3 [=46737.53 - 10748.16], is water. Using these volumes, the volume fraction reduction for the HAC models for homogenization of polyethylene is 0.2300 [=10748.16 ÷ 46737.53] and the water volume fraction is 0.7700 [=1 - 0.2300].

For the NCT model, the compositions are calculated using the total fuel rod length (39,175.6 cm), the clad outer radius (0.465 cm) and the total assembly volume [66,524.54 cm^3 = (11*1.195cm)^2*385 cm]. The volume of the fuel rods is 26,611.63 cm^3, leaving a total water-plus-polyethylene volume of 39,912.92 cm^3. The total polyethylene volume (10,748.16 cm^3) is calculated using the 10.2 kg of polyethylene and a polyethylene density of 0.949 g/cm^3. The remainder of the volume (29,164.76 cm^3) is water. Using these volumes, the volume fraction reduction for NCT models for homogenization of polyethylene is 0.26929 and the water volume fraction is 0.73071.

In HAC and NCT models, the fuel resonance processing calculations are performed using either a homogenized clad and polyethylene model or a homogenized water and polyethylene model. It is done this way because the SCALE latticecell approach does not support multiple material zones outside the clad. This approach yields a good approximation for the flux entering the fuel pellet zone.

The composition calculated by SCALE for the homogenized moderator and full density water mixtures is provided in Table 6-139.

Table 6-139 Compositions for Homogenized Polyethylene and Water Mixtures

Homogenized Polyethylene and Water for HAC Models			
Polyethylene		Constituent	Atomic Density (atoms/b-cm)
Density	0.949 g/cm^3	H-1 (in poly)	1.87426E-02
Vol. Fraction	0.2300	C	9.37128E-03
Water		H-1 (in water)	5.14731E-02
Density	1 g/cm^3	H-2 (in water)	5.92009E-06
Vol. Fraction	0.7700	O-16	2.56770E-02
		O-17	9.78102E-06
Homogenized Polyethylene and Water for NCT Models			
Polyethylene		Constituent	Atomic Density (atoms/b-cm)
Density	0.949 g/cm^3	H-1 (in poly)	2.19443E-02
Vol. Fraction	0.26929	C	1.09721E-02
Water		H-1 (in water)	5.14731E-02
Density	1 g/cm^3	H-2 (in water)	5.61801E-06
Vol. Fraction	0.73071	O-16	2.43668E-02
		O-17	9.28193E-06

- **Polyethylene Sleeves on Loose Rods**

Some loose rods models include a 6 mil (i.e., 0.006 inches) thick layer of full density polyethylene. Composition for this material is provided in Table 6-137, “Polyethylene (full density).”

- **Peripheral Polyethylene Foam Pads Around Fuel**

The polyethylene material models used for the peripheral polyethylene foam pads are evaluated at nominal (0.08 g/cm^3 sides and 0.16 g/cm^3 bottom) and high-density (0.28 g/cm^3 sides and 0.56 g/cm^3 bottom) to account for different rubber densities, the same as was used in the prior work documented in Section 6.12.11.6 of the most recent revision of the TN-B1 SAR. Compositions for these materials is provided in Table 6-137, under “nominal density liner” to represent polyethylene foam, and “high density liner” to represent higher density materials.

6.13.5. *Computer Codes and Cross-Section Libraries (including SCALE error notices)*

The 252 neutron-energy-group ENDF/B-VII.1 library is utilized in this analysis with the CSAS5 code sequence available in SCALE 6.2.4. The use of this cross-section library and computer code is validated using 187 critical benchmark experiments with adequate similarities to the TN-B1 package. Section 6.13.10 describes the code validation and determination of the Upper Safety Limits (USL) for this evaluation.

The applicability and completeness of the validation are addressed in Section 6.13.10, in which it is verified that the validation benchmarks adequately represent the range of parameters for the TN-B1 package and the USLs are applicable to the results to which they are compared.

As was noted in Section 6.13, a SCALE user notice [34] was issued February 26, 2021, entitled "SCALE h1-poly incoherent elastic scattering can cause k-eff under prediction approaching 1% in criticality problems with polyethylene as the primary moderator." Since there is a significant amount of polyethylene modeled in some of the criticality calculations, this error could significantly impact the TN-B1 analysis.

This issue was addressed for the TN-B1 SAR update work by performing CSAS5 continuous energy (CE) calculations with both erroneous, distributed with SCALE, and corrected, distributed by download by the SCALE development team, polyethylene cross sections for the final criticality safety index calculation. Case-specific "bias+3σ" penalties were calculated and applied in calculation of the maximum k_{eff} values.

An additional SCALE user notice [35] was issued on April 1, 2021, entitled "Memory error with SCALE 3D general geometry package leading to an incorrect model when shapes are truncated by CHORDs." None of the criticality calculations, performed to support the TN-B1 SAR update, utilized geometry defined using SCALE "chords". Consequently, this error does not impact the TN-B1 SAR update analysis.

Criticality calculations were run with varying numbers of neutron generations (GEN), generations skipped (NSK), and neutron histories per generations (NPG). In most cases a minimum standard deviation (SIG) of 0.0002 is used to terminate each calculation. These parameters were all varied such that ALL k_{eff} distribution normality and Shannon Entropy Convergence Tests (SECT) were passed for ALL calculations. Generally, failed normality tests were corrected by making small changes to the NPG and rerunning the calculations. Failed SECT 1 was fixed by decreasing NSK and increasing NPG. Failed SECT 2 were corrected by increasing NSK and NPG. Note that occasionally satisfying both SECT 1 and 2 was difficult and resulted in some unusual parameter values for NPG and NSK.

Passing all three SECTs and the generation k_{eff} distribution normality tests ensures that the calculation is well converged and that the k_{eff} standard deviation values are representative of a normal distribution (e.g., there is an approximately 95% probability that the true {i.e. resulting from running an infinite number of neutron histories} "calculated" mean k_{eff} value is within +/- two standard deviations of the calculated and reported "best estimate" mean k_{eff} value).

6.13.6. *Demonstration of Maximum Reactivity*

The discussion provided in this section describes work performed to demonstrate that the maximum reactivity has been quantified for each loading configuration and model. It is organized first by package load type (i.e., ATRIUM 11 assembly, or loose fuel rods, or loose fuel rods in a 5-inch schedule 40 ss pipe) and then by the four required model types (i.e., HAC array, NCT array, HAC single package, and NCT single package).

6.13.6.1. **ATRIUM 11 (11x11) Fuel Assembly Analysis**

6.13.6.1.1. *ATRIUM 11 Assembly HAC Array Models*

In general, this update uses the same HAC array models that were described in the currently approved TN-B1 SAR revision and in the update documented in Section 6.12. Figures 6-6 through 6-8 in the latest TN-B1 SAR update [25] show the basic HAC model. Additional parameter studies, listed below, were performed to determine the most reactive HAC array model for the TN-B1 package loaded with ATRIUM 11 fuel assemblies at various enrichments above 5 wt% ^{235}U.

- The most reactive Gd rod pattern was determined.
- The most reactive assembly rotation was determined for each assembly.
- The most reactive polyethylene pad thicknesses, with and without fuel channel, were determined.
- The most reactive polyethylene modeling approach was determined for each enrichment.
- The most reactive assembly positions, with and without fuel channel, were determined.
- The most reactive preferential flooding distribution was determined.
- Other miscellaneous considerations were investigated.
- Polyethylene cross-section-error penalties were calculated.

The results of these studies are presented below.

As was noted in the prior analysis of 11x11 fuel assemblies, when flooded with full density water the assemblies are still under moderated. Increasing the enrichment and leaving the volume of water in the assembly unchanged causes the assembly to be even more under moderated at higher enrichments. Consequently, maximum reactivity is obtained for ATRIUM 11 (11x11) fuel assemblies models with the TN-B1 inner container flooded with full density water.

- Gd Rod Pattern

This update to the TN-B1 SAR requires use of different Gd rod patterns and loadings in any lattice of an assembly where the lattice average enrichment exceeds 5.0 wt% ^{235}U. In addition to the discussion already provided in Section 6.13.3.3, variations from the patterns shown in Figure 6-87 were explored both with and without fuel channels, for the various enrichments, and in a HAC array model. The minor differences between the HAC and NCT models do not impact the determination of the most reactive Gd rod pattern. The patterns presented in Figure 6-87 are, in all cases, the limiting patterns. These limiting patterns are used in the criticality analysis for all ATRIUM 11 assemblies in all HAC array, HAC single package, NCT array and NCT single package calculations.

- Assembly Orientation in the TN-B1

Since the fuel bundle lattice designs are not fully symmetric, it is possible that rotating the design or physically rotating an assembly of the same design could result in a higher package or array reactivity. A study was performed using the limiting Gd rod patterns and loadings, with the two assemblies in various rotational positions. The most limiting orientation of the two assemblies in the TN-B1 is shown in Figure 6-88. Results for various configurations are provided in Table 6-132. The orientation study was performed for each Gd rod configuration and loading using 8.0 wt% ^{235}U to bound the results. The most reactive results are those where the Gd rods are located toward the upper outside corners of the TN-B1 package. Gd rods in either assembly nearer the center of the package reduce neutronic communication between the two assemblies in the package.

The minimum number of Gd rods, in the limiting Gd rod pattern and loading, in the limiting rotational orientation are used for ATRIUM 11 assemblies in all HAC array, HAC single package, NCT array and NCT single package calculations. A target CSI of 3.3 is used to determine maximum lattice ^{235}U wt% loadings per Gd rod configuration that are acceptable for transport.

- Polyethylene Pad Thickness

Under normal conditions, 1.8-cm-thick lower density polyethylene pads (see Section 6.1.1.1) provide cushioning for the assembly during transport. In HAC conditions, it is necessary to consider that some or all of the polyethylene pads may be burned away. Calculations were performed for different Gd rod loadings and configurations, both with and without the fuel channel to determine the pad thicknesses that maximize k_{eff} for the HAC array models. A nominal fuel channel thickness of 0.254 cm and maximum channel thickness of 0.320 cm were also evaluated. A liner density of 0.28 g/cm^3 on the sides and top and 0.56 g/cm^3 on the bottom was used for these studies based on results presented in Section 6.12.11.6. Table 6-140 presents the polyethylene pad thicknesses that maximize k_{eff}. Figure 6-91 through Figure 6-95 show the configuration dependent results. Note that the thick channel configurations are slightly more limiting for Gd rod loadings with 17 Gd rods or less, and the no channel configuration are slightly more limiting for 18 Gd rods and above.

Table 6-140 Optimal Pad Thickness for ATRIUM 11 Fuel Assemblies

# Gd rods	Pad Thickness (cm)		
	With nominal channel (ch254)	With thick channel (ch320)	no channel
13	0.8, 1.0*	**0.8**	1.2
15	0.8	**0.8**	1.2
17	0.8	**0.8**	1.2
18	0.8	0.8	**1.1**
19	0.8	0.8	**1.0**

* Statistically equivalent maximum k_{eff}

Note that the optimal pad thickness varies significantly with Gd Rod loading and with the presence of the fuel channel. These enrichment- and configuration-dependent polyethylene pad thicknesses are used for the HAC array models.

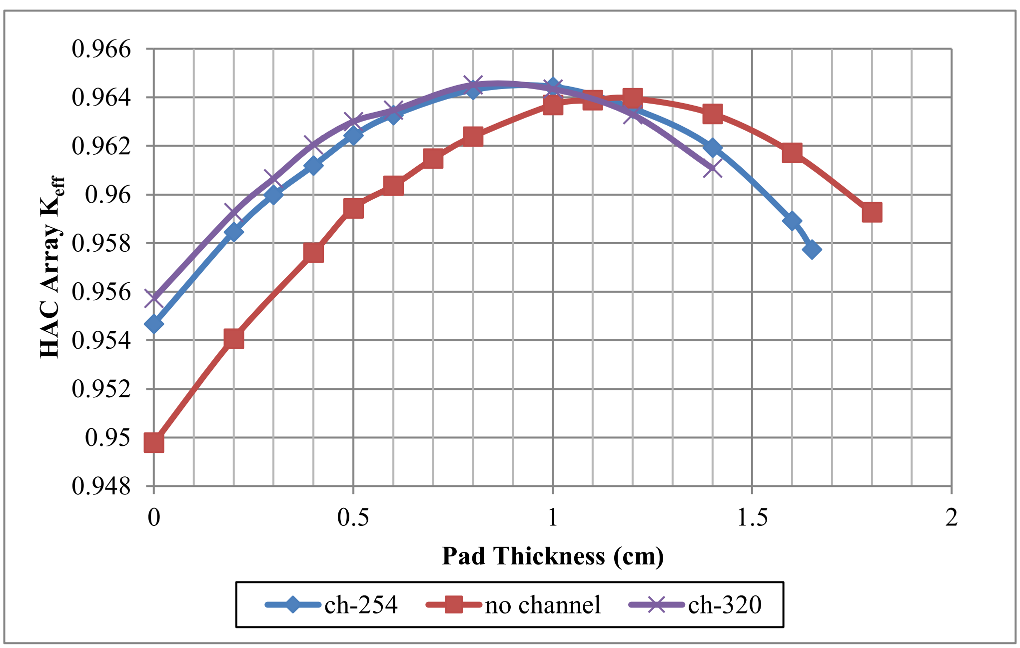

Figure 6-91 Pad Thickness Study for 13 Gd Rod Fuel Assemblies

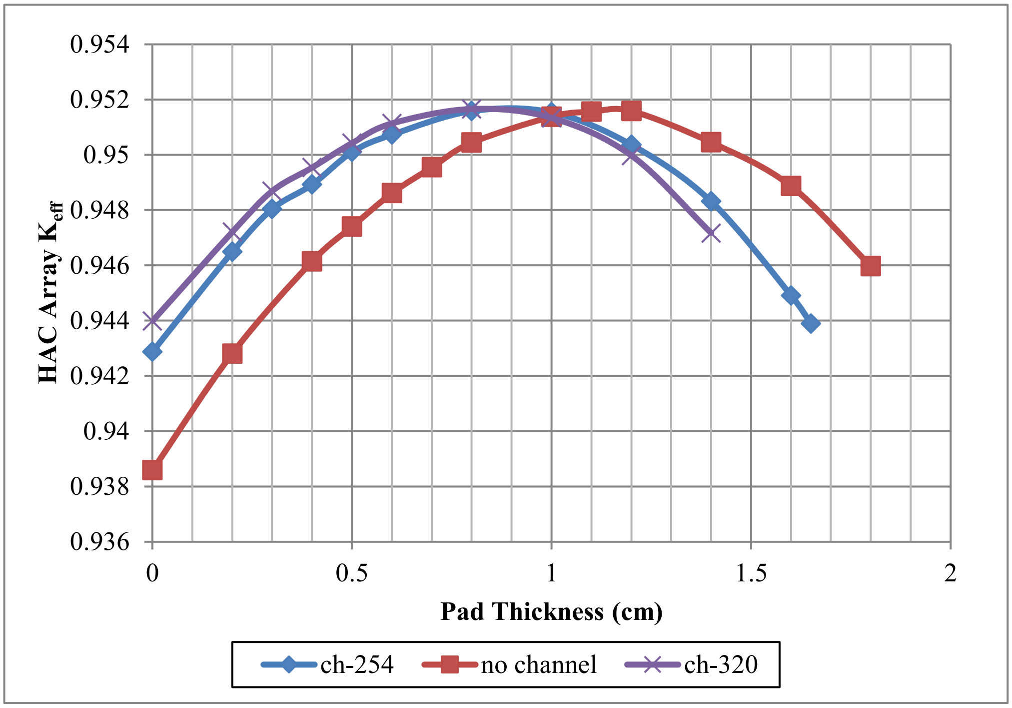

Figure 6-92 Pad Thickness Study for 15 Gd Rod Fuel Assemblies

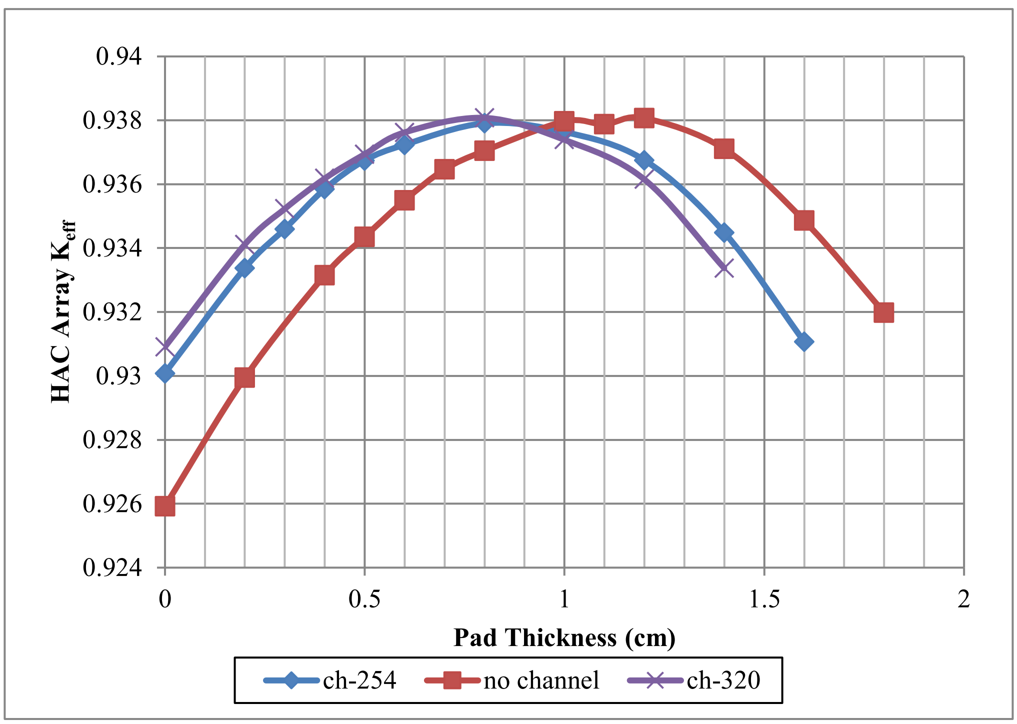

Figure 6-93 Pad Thickness Study for 17 Gd Rod Fuel Assemblies

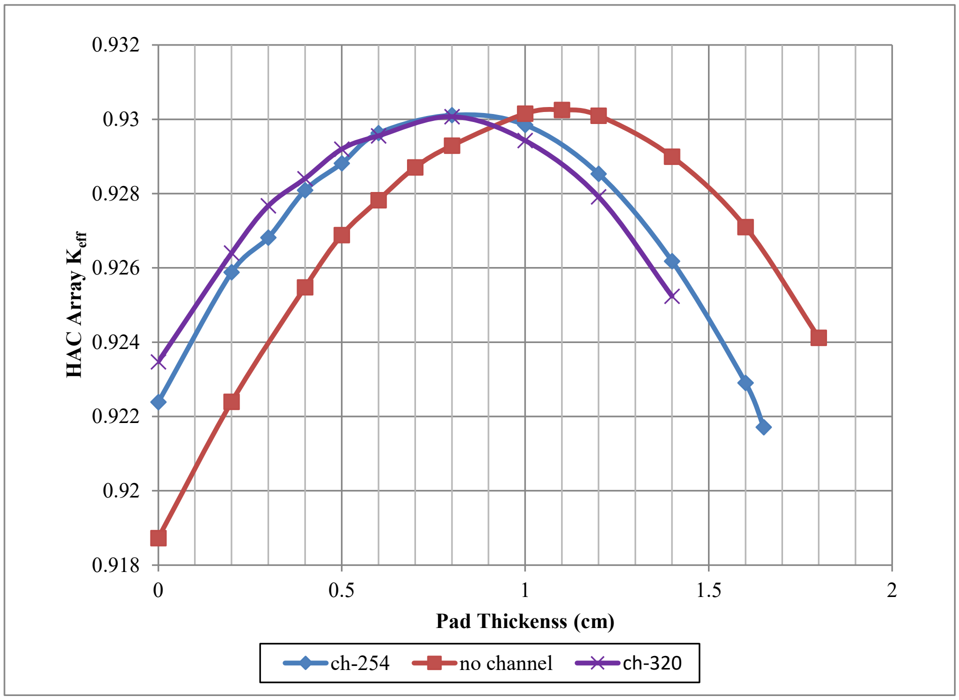

Figure 6-94 Pad Thickness Study for 18 Gd Rod Fuel Assemblies

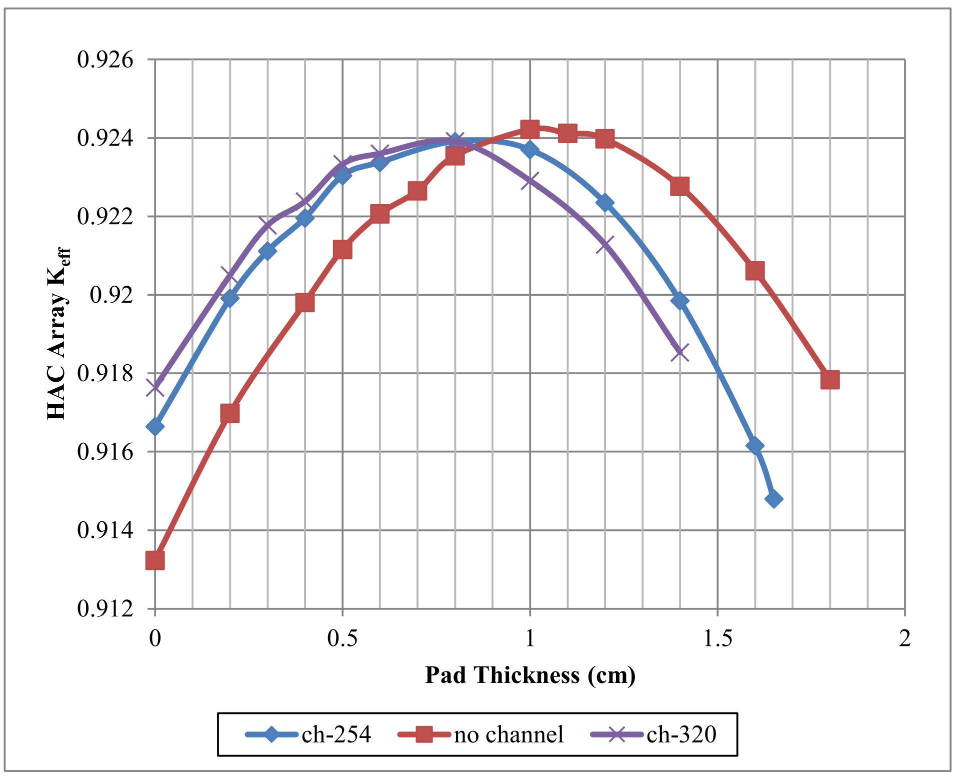

Figure 6-95 Pad Thickness Study for 19 Gd Rod Fuel Assemblies

- Most Reactive Polyethylene Modeling Approach

There may be up to 10.2 kg of polyethylene present in and around each ATRIUM 11 fuel assembly. It is not clear exactly where this polyethylene will end up under HAC or what is the best way to model the polyethylene for HAC or NCT. As was discussed in Section 6.13.3.8, studies have been performed using various modeling approaches to determine which approach yields the highest k_{eff} for a given model. The most reactive modeling method varies with enrichment and model configuration because the degree to which the assemblies are under moderated varies with enrichment and model configuration. The changing moderation level changes the importance of moderation provided by the polyethylene.

The k_{eff} results for various modeling approaches for HAC model arrays are presented in Table 6-141. In this table, "Layer/Clad" means the polyethylene is modeled as homogenized with the clad for resonance cross-section calculations, but is explicitly modeled as a layer on the fuel rod for the k_{eff} calculation. "Layer/Mod" means the polyethylene is modeled as homogenized with the assembly water for the resonance cross-section calculations and modeled as a layer on the fuel rod for the k_{eff} calculation. "Homog w/Water" means the polyethylene is homogenized with the assembly water for both resonance cross-section and k_{eff} calculations. "Homog w/Clad" means the polyethylene is homogenized with the clad for both resonance cross-section and k_{eff} calculations. "Replaced w/Water" means the polyethylene in the assembly is replaced with water for both resonance cross-section and k_{eff} calculations. While the polyethylene cross-section-error penalty has not been included in this table, it has been included in the maximum k_{eff} values presented later in this section.

The results for various enrichments are not comparable to each other because they have different array sizes, each of which is expected to be close to the array size that will be used for HAC CSI calculations. The polyethylene modeling method combined with its model-specific polyethylene cross-section-error penalty (PCSEP) that yields the highest k_{eff} value for each enrichment is used for the HAC array CSI calculations for that enrichment.

Table 6-141 Comparison of Polyethylene Modeling Methods for HAC Arrays

wt% ^{235}U	Gd Rods	Layer/Clad	Layer/Mod	Homog w/Water	Homog w/Clad	Replaced w/Water
8.0	18@4 wt%	**0.92831**	0.92790	0.92805	0.92689	0.92119
8.0	13@4 wt%	**0.96063**	0.96057	0.96029	0.95943	0.95353
8.0	15@4 wt%	**0.94843**	0.94804	0.94812	0.94722	0.94129
8.0	17@4 wt%	**0.93586**	0.93549	0.93542	0.93459	0.92873
7.5	17@4 wt%	**0.92392**	0.92335	0.92367	0.92263	0.91675
7.0	15@4 wt%	**0.92412**	0.92381	0.92367	0.92296	0.91721
6.5	13@4 wt%	**0.92265**	0.92232	0.92240	0.92152	0.91562
8.0	19@4 wt%	**0.92229**	0.92219	0.92195	0.92100	0.91541

Use of the "Layer/Clad" method for modeling the 10.2 kg of polyethylene per assembly for all enrichments yields limiting values.

- Most Reactive Assembly Positions, With and Without Fuel Channel

Under HAC, an optimal amount of the padding around the assemblies is assumed to have been burned away and is replaced with water. As was shown earlier in this section, the optimal pad thickness varies with Gd rod loading and with the presence of the fuel channel. This leaves variable room within the inner container for the assemblies to move around. Studies were performed to identify the most reactive locations for the assemblies, for each Gd rod loading configuration, with the optimal pad thickness, and with and without channels. The k_{eff} values from the location study for 8.0 wt% ^{235}U fuel containing 18 Gd rods at 4 wt% Gd_2O_3 without a fuel channel is provided below as Figure 6-96. In this figure, the left-most column shows the Z-Gap distance, in cm, of the bottom of the assembly down to the top of the bottom polyethylene pad in the TN-B1 package. The bottom-most row shows the X-Gap distance, in cm, from the outside vertical pad to the side of the assembly. At position (1.6223, 1.655) both assemblies are at the top and moved horizontally all the way toward the center. Calculations were performed for positions around the periphery and vertically and horizontally through the center. Results were used to guide additional calculations to clearly identify the assembly location where the peak reactivity occurred. In Figure 6-96, the (0.81115, 0.8275) location would place the assemblies in the center of each cell of the TN-B1 internal container. In this example, the highest k_{eff} value occurred when the assemblies were positioned in the (1.0, 1.1) location. Additional calculations were performed for nearby positions to demonstrate that the peak reactivity value had been captured.

Distance (cm) of the bottom of the assembly to the top of the bottom polyethylene pad										
1.655	0.9172	0.9218	0.9252	0.9282	0.9297	0.9300		0.9295	0.9271	0.9238
1.4	0.9181	0.9225			0.9306			0.9298		0.9240
1.2	0.9188	0.9231			0.9306	0.9309		0.9297		0.9242
1.1				0.9289	0.9308	**0.9312**	0.9306	0.9302	0.9278	0.9239
1	0.9185	0.9233			0.9304	0.9309		0.9300		0.9241
0.8275	0.9185	0.9229	0.9261	0.9284	**0.9301**	0.9309		0.9300	0.9273	0.9234
0.6	0.9174	0.9218			0.9295	0.9296		0.9291		0.9230
0.4	0.9168	0.9209			0.9283			0.9274		0.9214
0.2	0.9152	0.9192			0.9269			0.9264		0.9195
0	0.9135	0.9171	0.9206	0.9233	0.9250	0.9254		0.9241	0.9222	0.9179
	0	0.2	0.4	0.6	0.81115	1	1.1	1.2	1.4	1.6223
	Distance (cm) from the outside vertical pad to the side of the assembly									

Figure 6-96 Location Study for 8.0 wt% Fuel (18@4wt% Gd rods), without Fuel Channel in HAC Array

The results from the assembly location studies are presented below in Table 6-142. The data presented in this table are used to create the HAC array models used to calculate the HAC array maximum enrichment, minimum Gd rod loading criteria to maintain a maximum CSI value of 3.3. For Gd rod loadings that contain less than 18 Gd rods, inclusion of the fuel channel increased k_{eff}. At Gd rod loadings containing 18 Gd rods and higher, removal of the fuel channel maximized k_{eff}. Differences between channeled and unchanneled results are small to negligible and need to account for PCSEP for final comparison to the USL.

Table 6-142 Most Reactive Assembly Locations in HAC Array Models

wt% ^{235}U #@Gd_2O_3	Fuel Channel Present?	Pad Thick (cm)	X-Gap (cm)	Z-Gap (cm)	k_{eff}	σ_{keff}
5.5	**yes**	**0.8**	**1.0**	**1.0**	**0.90303**	**0.00019**
13@2 wt%	no	1.2	0.9	0.8	0.90247	0.00019
6	**yes**	**0.8**	**1.0**	**1.2**	**0.91993**	**0.00019**
13@2 wt%	no	Bounded by channel results				
6.5	**yes**	**0.8**	**1.0**	**1.0**	**0.92673**	**0.00019**
13@4 wt%	no	Bounded by channel results				
7	**yes**	**0.8**	**1.0**	**1.0**	**0.92779**	**0.00019**
15@4 wt%	no	Bounded by channel results				
7.5	**yes**	**0.8**	**0.79115**	**1.2**	**0.92696**	**0.00019**
17@4 wt%	no	Bounded by channel results				
8.0	yes	0.8	0.9	1.2	0.93108	0.00019
18@4 wt%	**no**	**1.1**	**1.0**	**1.1**	**0.93120**	**0.00019**
8.0	yes	0.8	1.0	1.2	0.92482	0.00019
19@4 wt%	**no**	**1.0**	**1.2**	**1.3**	**0.92541**	**0.00019**

- Most Reactive Preferential Flooding Distribution

The various guidance documents and NRC standard review plans [28, 29, 30 and 36] recommend consideration of the impact of what is termed “preferential flooding.” Evaluation of preferential flooding involves identifying regions within a package that may flood and determining the optimal moderation level in each of these regions. Empty volumes must be assumed floodable unless HAC/NCT testing proves that the volumes will not flood.

For the transport of ATRIUM 11 assemblies, the floodable regions include the internal container fuel storage compartments and the volume between the internal and external TN-B1 containers. Flooding of these two regions must be considered to be independent. It is possible that a package could flood completely and then have the outer volume drain. The results presented in Section 6.12.6.2 demonstrate that the most reactive preferential flooding configuration for ATRIUM 11 assemblies in HAC arrays is for the internal compartments to be fully flooded with full density water and for the volume between the inner and outer containers to be empty. This is the optimum configuration because the assemblies are under moderated, even when flooded with full density water, and the water in the outer volume limits or prevents neutron movement between packages.

One additional consideration mandated by 10 CFR §71.59(a)(2) is that the HAC array would be subcritical with optimum interspersed moderation. This amounts to evaluating optimal spacing and flooding between packages in the HAC array. Since adding water between packages is neutronically the same as adding water in the TN-B1 outer volume, the results presented in Section 6.12.6.2 demonstrate that any space and water added between the packages will reduce k_{eff}.

- Other Miscellaneous Considerations

Beyond the issues already addressed, a couple of other issues deserve discussion. These are (1) the impact of mixed arrays within one fuel bundle and (2) the worth of the Gd_2O_3 in the ATRIUM 11 assemblies.

Due to axial variation of lattice average enrichment frequently seen in boiling water reactor (BWR) fuel assembly designs, it is possible that lattices with different lattice average enrichments and different Gd_2O_3 requirements may be present in the same fuel assembly. Of concern is the fact that for lattices with enrichments up to 5 wt% ^{235}U the Gd_2O_3 requirements were reduced for lower enrichments. Gd_2O_3 requirements (i.e., number of Gd rods and Gd_2O_3 content of Gd rods) were designed to support a CSI value of 1.0 for all lattices with lattice average enrichments not greater than 5 wt%. In some cases, a lower enrichment lattice with its lower Gd rod requirements may be more reactive than a higher enrichment lattice. Consequently, extra evaluation was required to demonstrate that mixing lattices with differing enrichments and Gd_2O_3 requirements will not result in higher reactivity than was evaluated for assemblies that had a single lattice average enrichment. This analysis was performed and documented in the NRC review process for a previous TN-B1 SAR update.

For this TN-B1 update covering lattice average enrichments above 5 wt% ^{235}U, all CSI values are greater than 1.0 and minimum Gd rod loadings were used to identify maximum lattice enrichments per loading to maintain a constant CSI. Since the CSI value is kept constant for each ^{235}U enrichment above 5 wt% ^{235}U, mixing of various enrichment lattices within an assembly is covered by meeting the minimum Gd rod loading requirements per lattice region.

The other consideration to discuss is the margin associated with the reduction in Gd_2O_3 in the TN-B1 analysis. Consistent with NRC recommendations, the Gd_2O_3 credited in the analysis of the ATRIUM 11 fuel assemblies has been reduced 25% from the minimum required wt% Gd_2O_3. A study was performed to quantify the sensitivity of the TN-B1 package k_{eff} value to the Gd_2O_3 content at the Gd rod loading/enrichment threshold limits. These studies showed that reducing the Gd_2O_3 content from 2.0 to 1.5 wt% Gd_2O_3 increased k_{eff} by ~0.004 Δk for the 13 Gd rod configuration, but increased to 0.0043 Δk for 15 Gd rods. A similar trend with increasing Gd rod quantity was observed for the 4.0 to 3.5 wt% Gd_2O_3 content change going from 0.0037 Δk for the 13 Gd rod loading to 0.0053 for the 19 Gd rod loading.

- o Polyethylene cross-section-error penalties were calculated

Due to the polyethylene cross-section error reported [34] by the SCALE development team, a polyethylene cross-section-error penalty (PCSEP) is calculated for the limiting and near limiting cases and is included when determining the largest acceptable (i.e., k_{eff} + $2\sigma_{keff}$ + PCSEP < USL) array sizes. The PCSEP is determined by performing model-specific continuous energy (CE) CSAS5 calculations with both the erroneous and corrected CE cross sections. The PCSEP is then calculated as the bias (i.e., $\Delta k = k_{corr} - k_{error}$) + 3 standard deviations (i.e., $3^*\sigma_{bias} = 3^*\{\sigma_{corr}^2 + \sigma_{error}^2\}^{1/2}$). This PCSEP is calculated for limiting cases and for near limiting cases where the penalty might vary. In some cases, the PCSEP did change which case was considered limiting. CE calculations were used for calculation of the PCSEP because corrected multi-energy group cross sections were not provided by the SCALE development team. Use of the PCSEP is considered acceptable because (1) the purpose of the PCSEP is to quantify only the reactivity worth of polyethylene cross-section errors, (2) calculation of the PCSEP is performed on a model specific basis, (3) the penalty is calculated on a 3σ basis, and (4) some of the effect of the polyethylene errors will also be captured in the validation, which should include significant contribution from critical experiments with polyethylene. Thus, there should be conservative overlap of the PCSEP with the validation bias and bias uncertainty.

The information presented in this section is used to generate the HAC array models that are used in the calculation to establish enrichment and minimum Gd rod loadings for a maximum CSI value of 3.3 that are documented in Section 6.13.6.2.

6.13.6.1.2. *ATRIUM 11 Assembly NCT Array Models*

The NCT array models were developed from the TN-B1 HAC array models described in preceding sections of this report. The only differences are (1) that the upper part of the outer container is 2.4 cm taller (2) the peripheral polyethylene foam pads used to cushion the fuel assemblies remain intact (i.e., no pad loss due to fire) for NCT, and (3) the fuel rod spacing (i.e., pin pitch) within the assembly is reduced to the undamaged value described in Section 6.12.3.1.1. The basic NCT package model is shown in Figures 6-3 through 6-5 of the latest TN-B1 SAR update [25].

Preferential (i.e., optimal) flooding (i.e., fully flooded interior compartments and empty volume between the inner and outer containers) is still considered throughout the package under NCT. Since there is no moderator in the outer volume, the change in the outer dimension of the outer container has only a small impact on k_{eff}, which is due to increased neutron leakage between the packages in the array. The presence of intact polyethylene pads removes the ability of the assemblies to move around within the internal storage volumes and, consequently, the assemblies are modeled in the center of the storage volume. The most reactive Gd rod loading and orientation are not affected by the HAC to NCT package model changes.

There may be up to 10.2 kg of polyethylene, which does not include the cushioning foam pads, present in and around each assembly. This polyethylene is modeled using the five models discussed in Section 6.13.6.1.1 and the most reactive polyethylene model is used. The results from the NCT array polyethylene model study are provided in Table 6-143. Excluding the fuel channel maximized k_{eff} for all enrichment and Gd rod loading combinations. For the no fuel channel models, modeling the polyethylene as a layer on the fuel rods for the k_{eff} calculation and as homogenized with the clad for the cross-section resonance calculations maximized k_{eff} for all enrichments and Gd loadings.

Table 6-143 NCT Array Channel and Polyethylene Modeling Study

^{235}U wt%	Gd Rod loading	Fuel Channel Present?	Array	K_{eff} values Layer/Clad	Layer/Mod	Homog w/water	Homog w/Clad	Replaced w/Water
5.8	13@2 wt%	No	9x1x9	**0.9291**	0.9254	0.9246	0.9244	0.9145
	13@2 wt%	Yes		0.9167	0.9154	0.9150	0.9154	0.9030
6.1	13@4 wt%	No	9x1x9	**0.9301**	0.9295	0.9299	0.9285	0.9213
	13@4 wt%	Yes		0.9268	0.9280	0.9284	0.9254	0.9187
6.5	15@4 wt%	No	9x1x9	**0.9295**	0.9292	0.9288	0.9282	0.9209
	15@4 wt%	Yes		0.9257	0.9268	0.9267	0.9260	0.9173
7	17@4 wt%	No	9x1x9	**0.9293**	0.9288	0.9287	0.9278	0.9205
	17@4 wt%	Yes		0.9270	0.9265	0.9258	0.9253	0.9166
7.5	19@4 wt%	No	9x1x9	**0.9282**	0.9278	0.9275	0.9267	0.9189
	19@4 wt%	Yes		0.9070	0.9246	0.9244	0.9238	0.9150
8	21@4 wt%	No	9x1x9	**0.9240**	0.9233	0.9233	0.9218	0.9153
	21@4 wt%	Yes		0.9203	0.9192	0.9196	0.9181	0.9112

Since the ATRIUM 11 (11x11) fuel assemblies are under moderated, decreasing the assembly fuel rod pitch decreases reactivity. Since the decrease is uniform across the lattices and along the length of the assembly, this change does not impact identification of the most reactive Gd rod pattern and fuel assembly orientation.

The information presented in this section is used to generate the NCT array model that establishes Gd rod loading pattern combinations as a function of enrichment such that k_{eff} < USL and the CSI remains below 3.3.

The PCSEP described near the end of Section 6.13.6.1.1 is calculated and applied in the described manner to the NCT array results.

6.13.6.1.3. *ATRIUM 11 Assembly HAC Single Package Model*

The requirements of 10 CFR § 71.55 include that individual packages remain subcritical under HAC conditions. To demonstrate subcriticality of a single package, the HAC array model with 8 wt% ^{235}U fuel was reduced to a single package, the volume between the TN-B1 inner and outer containers was filled with full density water and the cushioning pads were replaced with full density water to maximize neutron reflection. A location study, similar to that shown in Figure 6-96, was performed, both with and without fuel channels, to identify the assembly locations that maximized k_{eff}. Results for the HAC single package model are provided in Table 6-144.

The PCSEP described near the end of Section 6.13.6.1.1 is calculated and applied in the described manner to the HAC single package results.

Table 6-144 HAC Single Package Results

Fuel Channel Present?	X-Gap (cm)	Z-Gap (cm)	k_{eff}	σ_{keff}	PCSEP
No	3.1	2.1	0.84878	0.00019	0.00211
Yes (ch254)	2.6	1.8	0.84044	0.00017	0.00222
Yes (ch320)	2.4	1.6075	0.83822	0.00015	0.00199

The maximum calculated k_{eff} for the HAC single package was found to be 0.84878 + 0.00019. The PCSEP calculated, as described in Section 6.13.5, for this model is calculated to be 0.00211. The maximum k_{eff} for ATRIUM 11 assembly HAC single package model is thus 0.84878 + 2*0.00019 + 0.00211 = 0.85127, which is well below the USL of 0.9318 from Section 6.13.11 and is thus considered subcritical. HAC single package results were calculated for the maximum enrichment (8.0 wt% ^{235}U) with the lowest Gd rod loading combination (13@2 wt%) to bound all results.

6.13.6.1.4. *ATRIUM 11 Assembly NCT Single Package Model*

The requirements of 10 CFR § 71.55 require that individual packages remain subcritical under NCT conditions. To demonstrate subcriticality of a single package, the NCT array model with 8 wt% ^{235}U fuel and a Gd rod loading of 13 Gd rods with 2 wt% Gd_2O_3 was reduced to a single package, the volume between the TN-B1 inner and outer containers was filled with full density water to maximize neutron reflection. For the NCT model the intact cushioning pads are modeled as present. Since the pads are present, the fuel assemblies are modeled as centered in each side of the inner TN-B1 inner container.

While not expected to change, calculations were performed that confirmed the more reactive Gd rod pattern, and assembly orientations were unchanged from those identified for the HAC arrays. Additionally, a study was performed, similar to that discussed in Section 6.13.3.8, to identify the most reactive assembly polyethylene modeling approach for a single package. The most reactive configuration was found to be without the fuel channel and with the polyethylene modeled as a layer on the fuel rods for k_{eff} calculation and homogenized with the assembly moderator for cross-section resonance calculations. The maximum calculated k_{eff} for the NCT single package was found to be 0.74735 + 0.00019. The PCSEP calculated, as described in Section 6.13.5, for this model is calculated to be 0.00363. The maximum k_{eff} for ATRIUM 11 assembly NCT single package model is thus 0.74735 + 2*0.00019 + 0.00363 = 0.7514, which is well below the USL of 0.9318 from Section 6.13.10 and is thus considered subcritical. NCT single package results were calculated for only the maximum enrichment (8.0 wt% ^{235}U) with the lowest Gd rod loading combination (13@2 wt%) to bound all results.

6.13.6.2. CSI calculation for ATRIUM 11 (11x11) Assemblies with Enrichments Above 5 wt% ^{235}U

The requirements of 10 CFR § 71.59 include calculation of the criticality safety index (CSI) values for both arrays of packages under NCT and HAC. This is accomplished using the most reactive array configurations documented in Sections 6.13.6.1.1 and 6.13.6.1.2 to identify package array sizes that are demonstrably subcritical.

Normally, this is accomplished by modeling various size package arrays and comparing the array k_{eff} values to the upper subcritical limit from validation to determine array sizes suitable for calculation of the CSI values. This process is modified slightly for the TN-B1 update work. As was discussed in Section 6.13.3.3, for assembly enrichments above 5 wt% ^{235}U, a target maximum CSI of 3.3 was desired, so the array sizes are fixed with a search for maximum enrichment for a given Gd rod loading pattern that maintains k_{eff} < USL. Additionally, as discussed in Section 6.13.5, the SCALE development team has discovered errors in the hydrogen-in-polyethylene cross sections distributed with SCALE. It is non-conservative to use hydrogen-in-water cross sections in place of the hydrogen-in-polyethylene cross sections. To correct for the erroneous hydrogen-in-polyethylene cross sections for this work, a penalty value is calculated using the corrected continuous-energy (CE) cross sections distributed by the SCALE development team. The CE cross sections are used because the SCALE team declined to provide corrected multi-group cross sections. For the work documented in this report, the k_{eff} value for the limiting arrays is calculated using both corrected and uncorrected CE cross sections. The difference between the two k_{eff} values is then increased by three standard deviations to yield a k_{eff} penalty.

The calculated array k_{eff} values are increased by two of standard deviations and by the PCSEP. The result must be less than the applicable USL. The PCSEP is calculated for the limiting HAC and NCT array at each limiting enrichment determined for the corresponding Gd rod loading per array configuration (i.e., HCTA or NCTA). Any negative PCSEP values are discarded.

$$PCSEP = \text{maximum of } [k_{corr} - k_{err} + 3*(\sigma_{kcorr}^2 + \sigma_{kerr}^2)^{0.5}] \text{ or } [0.0]$$

- CSI enrichment limits for ATRIUM 11 Assemblies in Limiting HAC Arrays

Table 6-145 provides the maximum enrichment with minimum Gd rod loading requirements per limiting array configuration, the calculated k_{eff} values and standard deviations, PCSEP, maximum k_{eff} values, applicable USLs and CSI values for the limiting HAC arrays. For HAC arrays, CSI = 50 / (N_{HAC}/2) round up to the nearest 0.1.

Table 6-145 CSI Enrichment Limits for ATRIUM 11 Assemblies in HAC Arrays

wt% ^{235}U	Min. Gd Rods	Array Description	N_{HAC}	k_{eff}	σ_{keff}	Poly Penalty	Max. k_{eff}	USL	CSI
6.3	13@2 wt%	4x1x8	32	0.92879	0.00019	0.00084	0.9300	0.9318	3.2
6.7	15@2 wt%	4x1x8	32	0.92879	0.00019	0.00098	0.9301	0.9318	3.2
6.6	13@4 wt%	4x1x8	32	0.92964	0.00019	0.00034	0.9304	0.9318	3.2
7	15@4 wt%	4x1x8	32	0.92754	0.00019	0.00102	0.9289	0.9318	3.2
7.6	17@4 wt%	4x1x8	32	0.92900	0.00019	0.00128	0.9307	0.9318	3.2
8	19@4 wt%	4x1x8	32	0.92410	0.00019	0.00103	0.9255	0.9318	3.2

- CSI enrichment limits for ATRIUM 11 Assemblies in NCT Arrays

Table 6-146 provides the maximum enrichment with minimum Gd rod loading requirements per limiting array configuration, the calculated k_{eff} values and standard deviations, PCSEP, maximum k_{eff} values, applicable USLs and CSI values for the limiting NCT arrays. For NCT arrays, CSI = 50 / (N_{NCT}/5) round up to the nearest 0.1.

Table 6-146 CSI Enrichment Limits for ATRIUM 11 Assemblies in NCT Arrays

wt% ^{235}U	Min. Gd Rods	Array Description	N_{NCT}	k_{eff}	σ_{keff}	Poly Penalty	Max. k_{eff}	USL	CSI
5.8	13@2 wt%	9x1x9	81	0.92914	0.00019	0.00000	0.9295	0.9318	3.1
6.1	13@4 wt%	9x1x9	81	0.9301	0.00019	0.00066	0.9311	0.9318	3.1
6.5	15@4 wt%	9x1x9	81	0.9295	0.00019	0.00094	0.9308	0.9318	3.1
7	17@4 wt%	9x1x9	81	0.92929	0.00019	0.00027	0.9299	0.9318	3.1
7.5	19@4 wt%	9x1x9	81	0.92817	0.00019	0.00062	0.9292	0.9318	3.1
8	21@4 wt%	9x1x9	81	0.92399	0.00019	0.00080	0.9252	0.9318	3.1

- Overall CSI Values for ATRIUM 11 Assemblies

Table 6-147 combines the information from Table 6-145 and Table 6-146 to produce the overall limiting array loading configurations of ATRIUM 11 assemblies by lattice average enrichment. The overall enrichment limit per Gd rod loading is the lower of the NCT and HAC array results.

Table 6-147 Overall CSI Values for ATRIUM 11 Assemblies

Min. Gd Rods	NCT Array Description	N_{NCT}	CSI	Enr. Limit wt% ^{235}U	HAC Array Description	N_{HAC}	CSI	Enr. Limit wt% ^{235}U	Overall Enr. Limit wt% ^{235}U
13@2 wt%	9x1x9	81	3.1	5.8	4x1x8	32	3.2	6.3	5.8
13@4 wt%	9x1x9	81	3.1	6.1	4x1x8	32	3.2	6.6	6.1
15@4 wt%	9x1x9	81	3.1	6.5	4x1x8	32	3.2	7.0	6.5
17@4 wt%	9x1x9	81	3.1	7.0	4x1x8	32	3.2	7.6	7.0
19@4 wt%	9x1x9	81	3.1	7.5	4x1x8	32	3.2	8.0	7.5
21@4 wt%	9x1x9	81	3.1	8.0	4x1x8	32	3.2	N/A	8.0

N/A indicates no calculation needed as Gd rod loading exceeds minimum required for given enrichment

6.13.7. *Fuel Rods – Loose*

For transport of loose fuel rods that are NOT in a 5-inch SS pipe or protective case, the analysis approach for this update is generally the same as was used in the last update to the TN-B1 SAR [25]. This is described in Sections 6.12.3.1.6, 6.12.3.4.2, 6.12.7, and 6.12.11.7. Variation of the analysis method is described in the next few paragraphs.

- Analysis covers up to 25 ATRIUM 11 fuel rods with fuel enriched to no greater than 8 wt% ^{235}U, up to 25 ATRIUM 10XM fuel rods with fuel enriched to no greater than 5 wt% ^{235}U, or up to 25 PWR 17x17, type 3 fuel rods with fuel enriched to no greater than 8 wt% ^{235}U.

The last update to the TN-B1 SAR included analysis for ATRIUM 11 fuel rods with enrichments up to 5 wt% ^{235}U. This new analysis expands the analysis to increase the maximum enrichment from 5 to 8 wt% ^{235}U. Additionally, the two additional fuel rod types are also included. These are ATRIUM 10XM fuel rods with enrichments up to 5 wt% ^{235}U and PWR 17x17, type 3 rods with enrichments up to 8 wt% ^{235}U. All three fuel rods are described in Table 6-131. For all fuel rod types, the clad and gap are modeled as water. This reduces the fuel rod model to a cylinder of fuel pellet material, surrounded by water out to the clad outer radius, followed by a 0.006 inch-thick layer of polyethylene or water.

- Polyethylene sleeves

The prior analysis included a 6 mil (i.e., 0.006 inches) thick sleeve of polyethylene on all individual fuel rods. This new analysis performed additional studies that demonstrated that, near optimum moderation conditions, replacing the polyethylene with water may increase k_{eff}. Consequently, calculations for all limiting models are performed both with and without the 6 mil polyethylene sleeves.

- Polyethylene cross-section error penalty

As was discussed in Section 6.13.5, part-way through the TN-B1 SAR update project, the SCALE development team issued a SCALE software error notice [34] indicating that the hydrogen-in-polyethylene cross sections, both in multi-group and continuous energy formats were significantly incorrect. The SCALE development team provided corrected continuous energy (CE) cross sections for hydrogen bound to carbon in polyethylene, but declined to provide corrected multi-group cross sections. For the SAR update, PCSEP are calculated for all near limiting cases to conservatively capture the impact of the cross section errors. The penalty is calculated by performing model-specific CE calculations, with both the erroneous and corrected CE cross sections. The penalty is then calculated as change in k_{eff} plus three standard deviations. Negative penalties are conservatively discarded.

6.13.7.1. HAC Array Models

As was modeled in the prior analysis for both the NCT and HAC models, the fuel rods are modeled in a square 5x5 array of fuel rods that are spaced to maximize reactivity. For all three fuel types, a moderation study similar that shown in Figure 6-97 was performed to find the optimal water density and fuel pin spacing. In all cases, flooding the inner fuel storage volume with full density water maximized k_{eff}. Additionally, the liner material was evaluated at nominal (0.08 g/cm^3 sides and 0.16 g/cm^3 bottom) and high density (0.28 g/cm^3 sides and 0.56 g/cm^3 bottom) and the results demonstrated that the nominal-density liner was more limiting than the high-density liner.

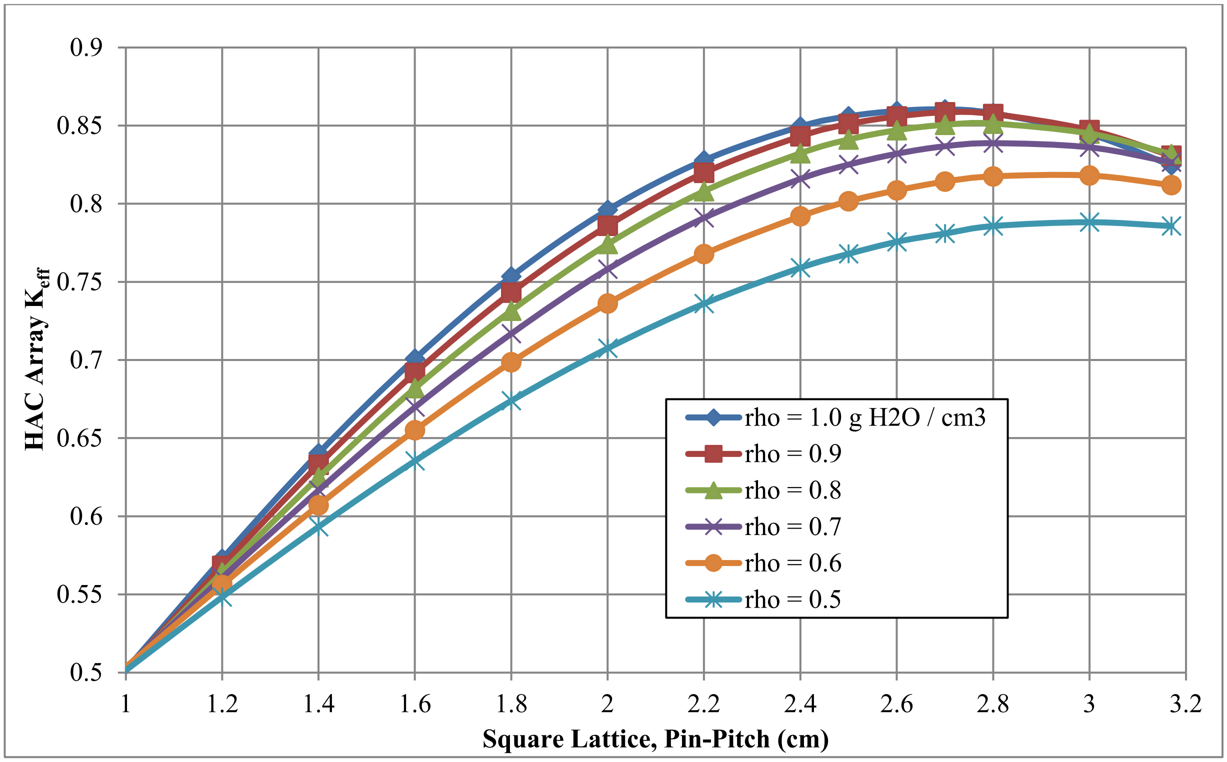

Figure 6-97 Moderation Study for 25 Loose 8 wt% ^{235}U ATRIUM 11 Rods

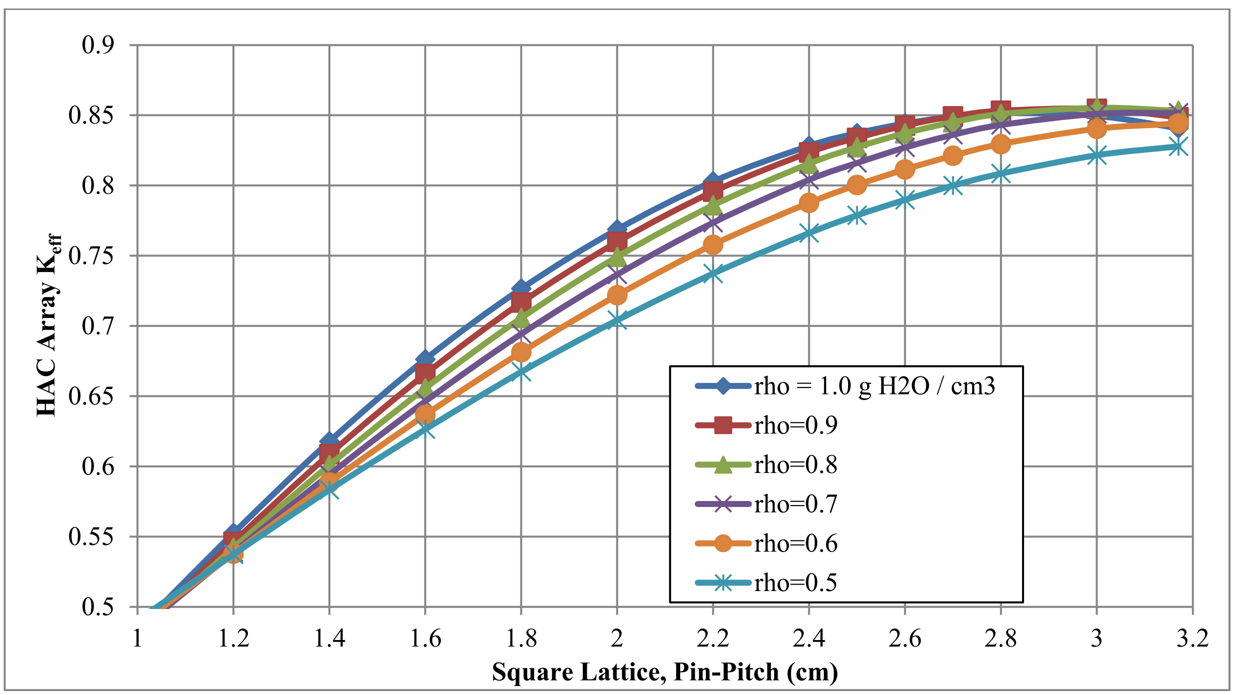

Figure 6-98: Moderation Study for 25 Loose 8 wt% ^{235}U ATRIUM 11 Rods with High-Density Liner

The optimum moderation pin-pitch was identified for each fuel rod type. The limiting pin pitch values are 2.7 cm for the 8 wt% ATRIUM 11 rods, 2.6 cm for the 5 wt% ATRIUM 10XM rods, and 2.7 cm for the 8 wt% PWR 17x17, type 3 rods. These studies also revealed that replacing the polyethylene sleeves with water increased the maximum k_{eff} for all three fuel rod types.

For HAC, it is assumed that some or all of the cushioning polyethylene pads are removed due to burning or melting. A pin-pitch optimum moderation study was also performed with varied peripheral polyethylene pad thicknesses. Figure 6-99 shows that the maximum k_{eff} value is obtained for the ATRIUM 11 rods with the full pad thickness.

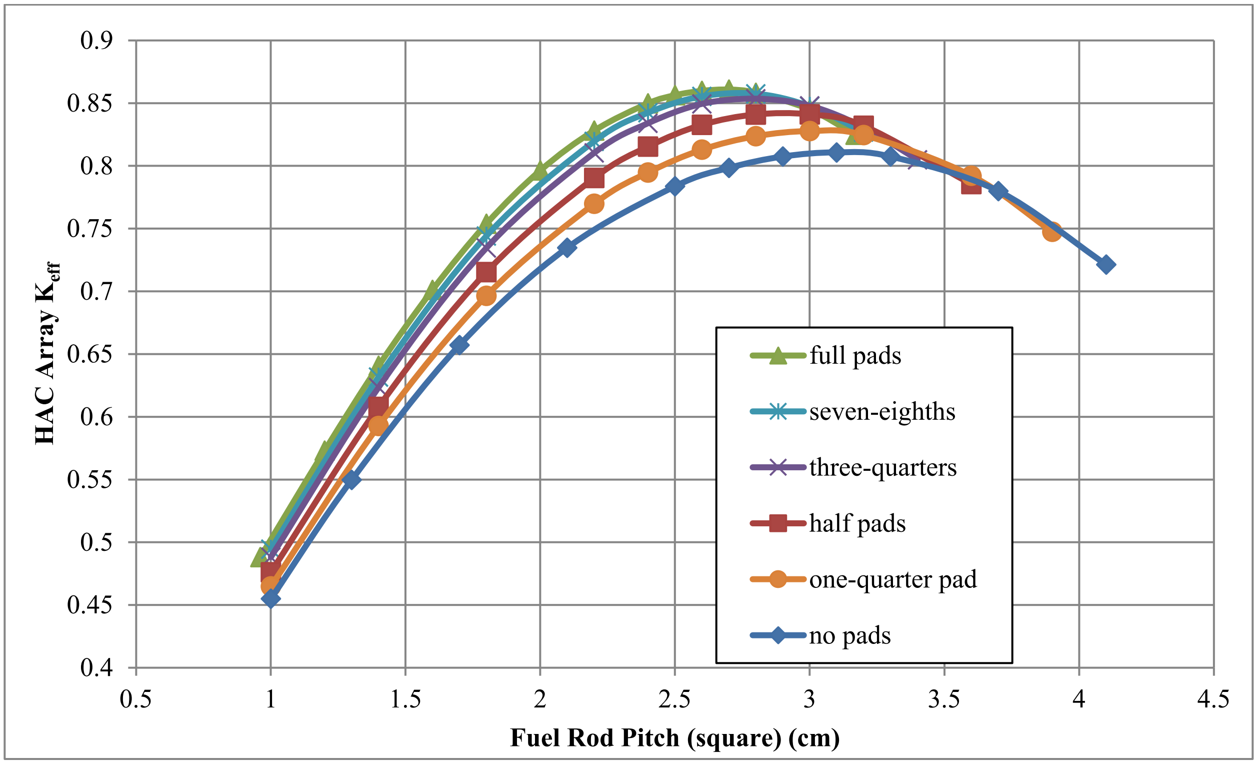

Figure 6-99 ATRIUM 11 Optimum Moderation Study with Varied Pad Thickness

An additional sensitivity study was performed that demonstrated that reducing the polyethylene pad density reduced k_{eff}.

Sensitivity studies were also performed to identify the optimal location of the optimal-pitch array within the TN-B1 storage volume, both with and without the peripheral cushioning polyethylene pads. In all cases, the maximum k_{eff} occurred with the full thickness cushioning pad present. One additional study was performed with the ATRIUM 11 rods to examine the impact of changing pad thickness and location simultaneously. In this study, the optimized 5x5 pin arrays in the adjacent storage locations were moved toward each other and the pad thickness was reduced to permit closer approach of the arrays to each other. Note from Figure 6-100 that maximum k_{eff} is achieved before pad thinning is started.

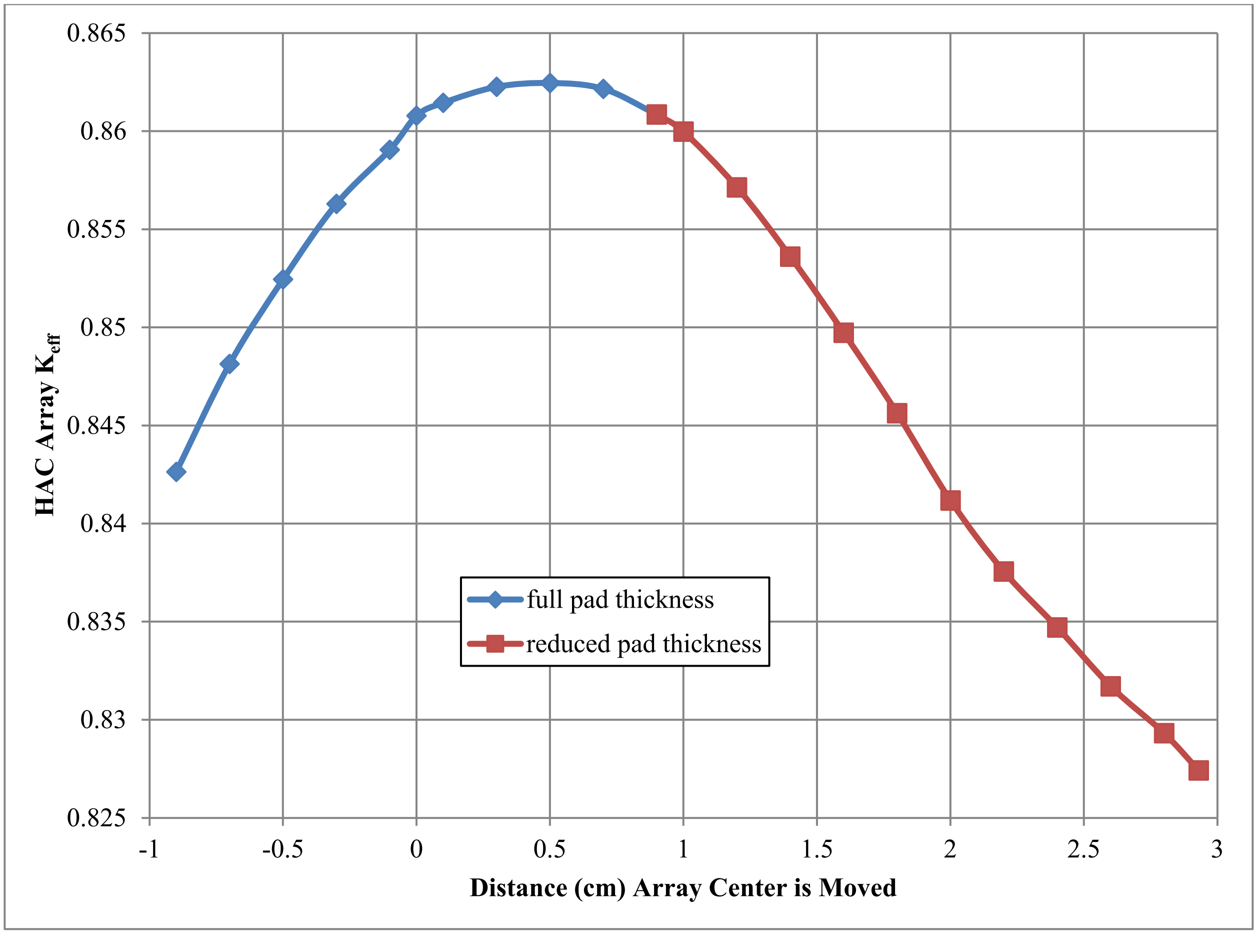

Figure 6-100 Sensitivity Study for Location and Pad Thickness

Similar to what was done for ATRIUM 11 fuel assemblies and is presented in Figure 6-96, sensitivity studies were performed both with and without pads to identify the most reactive position for the fuel pin array within the storage volume.

Based on the sensitivity studies and on the ATRIUM 11 fuel assembly studies, the most reactive HAC array loose rod models are:

- TN-B1 central storage volumes flooded with full density water
- Volume between outer and inner TN-B1 containers empty
- Full thickness of peripheral polyethylene cushioning pads present at nominal density
- 25 full-length fuel rods in a 5x5 square-pitched array
- Fuel rod gap and clad modeled as full density water.
- Maximum reactivity evaluated both with and without polyethylene sleeve to capture potential impact of PCSEP.
- No credit taken for Gd_2O_3 that may be in some of the fuel rods

- ATRIUM 11 fuel rods
  - Lattice average enrichment ≤ 8.0 wt% ^{235}U
  - Pin pitch = 2.7 cm (optimum moderation)
  - Center of the 5x5 array moved horizontally 0.5 cm from the cell center toward the package center
  - Center of the 5x5 array moved down 0.1 cm from the cell center.
- ATRIUM 10XM fuel rods
  - Lattice average enrichment ≤ 5.0 wt% ^{235}U
  - Pin pitch = 2.6 cm (optimum moderation)
  - Center of the 5x5 array moved horizontally 0.5 cm from the cell center toward the package center
  - Center of the 5x5 array moved down 0.1 cm from the cell center.
- PWR 17x17, type 3 fuel rods
  - Lattice average enrichment ≤ 8.0 wt% ^{235}U
  - Pin pitch = 2.7 cm (optimum moderation)
  - Center of the 5x5 arrays moved horizontally 0.4 cm from the cell center toward the package center
  - Center of the 5x5 arrays moved down 0.1 cm from the cell center.

These models are used for HAC array calculations used to calculate CSI values (see Section 6.13.7.5) for loose rods. The PCSEP was evaluated and included for limiting and near limiting configurations.

6.13.7.2. NCT Array Models

The only differences between the HAC and NCT array models are that the top of the TN-B1 outer container is 2.4 cm shorter for the HAC packages than for the NCT packages.

Since the region between the TN-B1 inner and outer packages is conservatively modeled as empty, the small change in the outer package dimension does not affect the optimal moderation conditions within each package in any way. This was confirmed by performing the array location sensitivity studies for the ATRIUM 11 and PWR 17x17 fuel rods in the NCT array model. The location of the peak k_{eff} value is unchanged between the HAC and NCT array models.

The NCT array models are used to calculate the CSI values (see Section 6.13.7.5) for loose rods. The PCSEP was evaluated and included for limiting and near limiting configurations.

6.13.7.3. HAC Single Package Model

Per the requirements of 10 CFR §71.55, a single HAC package under optimal moderation conditions must be subcritical. The HAC single package model was generated using the HAC array model.

The base model included full density/thickness polyethylene pads and 6 mil polyethylene sleeves on each rod. Sensitivity studies were then performed for ATRIUM 11 fuel rods with the sleeves replaced with water, with the pads replaced with water and with both pads and sleeves replaced with water. The results from the studies are presented in Table 6-148.

Table 6-148 ATRIUM 11 Loose Rod HAC Single Package Sensitivity Study

Sleeve Material	Pad Material	k_{eff}	σ_{keff}
water	water	0.68233	0.00019
polyethylene	water	0.68161	0.00015
water	polyethylene	0.63140	0.00019
polyethylene	polyethylene	0.63043	0.00019
water	HD polyethylene	0.66424	0.00019
polyethylene	HD polyethylene	0.66318	0.00019

For the single package model, replacing the relatively low-density (nominal) polyethylene pads with full-density water significantly improves neutron reflection and increases k_{eff}. This effect is also shown with the use of the high-density (HD) pads, but replacing the pads with water is more limiting. Replacing the polyethylene sleeves with water also increases k_{eff}. However, addition of the PCSEP raises the maximum k_{eff} for the model with polyethylene sleeves to be limiting.

HAC single package models were created for each fuel type, with and without sleeves, with pads replaced with full density water. These models included the optimum moderation pitch and location from the limiting HAC array model. All single package and array models were reflected by 30.48 cm of full density water.

The HAC single package results are presented in Table 6-149. All results are significantly below the applicable USL values of 0.9318 and 0.9292 for the different packaging contents discussed in Section 6.13.10. The “Max. K_{eff}“ value is the calculation k_{eff} + 2 σ_{keff} + PCSEP.

Table 6-149 Loose Rods, HAC and NCT Single Package Results

Fuel Rod Design	HAC Single Package				NCT Single Package			
	k_{eff}	σ_{keff}	PCSEP	Max. k_{eff}	k_{eff}	σ_{keff}	PCSEP	Max. k_{eff}
ATRIUM 11	0.68161	0.00015	0.00133	0.6832	0.66434	0.00019	0.00000	0.6647
ATRIUM 10XM	0.63109	0.00019	0.00138	0.6328	0.61770	0.00019	0.00000	0.6181
PWR 17x17	0.68199	0.00017	0.00149	0.6838	0.66526	0.00019	0.00000	0.6656

6.13.7.4. NCT Single Package Model

Per the requirements of 10 CFR §71.55, a single NCT package under optimal moderation conditions must be subcritical. The NCT single package model was generated using the limiting NCT array model.

The NCT single package models were created for each fuel type, with polyethylene pads at nominal- and high-density, and with and without polyethylene sleeves. These models included the optimum moderation pitch and location from the limiting NCT array model. All single package and array models were reflected by 30.48 cm of full density water.

The NCT single package results, including evaluation of the PCSEP, for loose rods are presented in Table 6-149. All results are significantly below the applicable USL value of 0.9318 and 0.9292 for the different packaging contents discussed in Section 6.13.10.

6.13.7.5. CSI Calculations for Loose Rods

The size of the package arrays in the HAC array models described in Section 6.13.6.1.1 and the NCT array models described in Section 6.13.6.1.2 were varied to find the maximum array sizes yielding k_{eff} + 2 σ_{keff} + PCSEP values that were below the applicable USL from Section 6.13.10.

Table 6-150 describes the subcritical HAC and NCT arrays, the number of packages in each array, k_{eff} value and uncertainty, the PCSEP, maximum k_{eff} value, applicable USL, and the CSI_{HAC}, CSI_{NCT} and overall CSI values for the loose rod packages. The CSI values are calculated, consistent with the requirements of 10 CFR § 71.59, as described in Section 6.13.1.3.

For the reader's convenience:

CSI_{HAC} = 50 / (N_{HAC}/2), rounded up to nearest tenth

CSI_{NCT} = 50 / (N_{NCT}/5), rounded up to nearest tenth

CSI = greater of CSI_{HAC} and CSI_{NCT}

Table 6-150 CSI Calculations for Loose Rods

Fuel Rod Design	HAC Array	N_{HAC}	k_{eff}	σ_{keff}	PCSEP	Max. K_{eff}	USL	CSI_{HAC}
ATRIUM 11	10x1x10	100	0.86480	0.00019	0	0.8652	0.9318	1.0
ATRIUM 10XM	10x1x10	100	0.80202	0.00019	0	0.8024	0.9292	1.0
PWR 17x17	10x1x10	100	0.86776	0.00019	0	0.8681	0.9292	1.0
Fuel Rod Design	**NCT Array**	**N_{NCT}**	**k_{eff}**	**σ_{keff}**			**USL**	**CSI_{NCT}**
ATRIUM 11	16x1x16	256	0.89000	0.00019	0	0.8904	0.9318	1.0
ATRIUM 10XM	16x1x16	256	0.82508	0.00019	0	0.8255	0.9292	1.0
PWR 17x17	16x1x16	256	0.89328	0.00019	0	0.8937	0.9292	1.0

Fuel Rod Design	Overall CSI
ATRIUM 11	1.0
ATRIUM 10XM	1.0
PWR 17x17	1.0

6.13.8. *Fuel Rods – in SS Pipe*

The final transport configuration considered in this TN-B1 SAR update is the transport of up to 30 fuel rods in either a 5-inch schedule 40 stainless steel pipe, see Section 1.2.3.4.6 of the currently approved TN-B1 SAR revision [25] or in the protective carrier described in Section 1.2.3.4.7 of the currently approved TN-B1 SAR revision [25]. Fuel rods covered in this update are:

- ATRIUM 11 rods with enrichments greater than 5.0 and no greater than 8.0 wt% ^{235}U. Transport of ATRIUM 11 fuel rods with enrichments up to 5.0 wt% ^{235}U is covered in Section 6.12 of the most recent update to the TN-B1 SAR [25]
- ATRIUM 10XM rods with enrichments no greater than 5.0 wt% ^{235}U
- PWR 17x17, type 3 rods with enrichment no greater than 8.0 wt% ^{235}U

The ATRIUM 11, ATRIUM 10XM and PWR 17x17, type 3 rods within in the scope of this analysis are described in Table 6-131.

The analysis in this section evaluates fuel rods in a 5-inch schedule 40 ss pipe. For the analysis, the fuel rods are restrained within the nominal outer diameter of the pipe (i.e., 5.563 inches) and the steel wall of the pipe is not modeled. In this model, the 30 fuel rods are spread out within the 156.8 cm^2 area inside the pipe.

From Section 6.7.4 of the currently approved TN-B1 SAR revision [25], the protective case is 8.9 cm by 8.0 cm, yielding a cross-sectional area of 71.2 cm^2. Due to the significantly smaller cross-sectional area of the protective case compared to the pipe diameter and the relatively large 2.6-cm optimal pin pitch found in the analysis, transport of rods in the protective case is bounded by the analysis of rods transported in the ss pipe.

For the rods-in-pipe analysis, sensitivity studies were performed to:

- Determine the optimum triangular pitch for fuel rods in the pipe
- Determine the optimum water density for water that is inside the fuel transport area and outside the pipe
- Determine the optimal model for the polyethylene sleeves
- For HAC models,
  - o determine the optimal peripheral pad thicknesses and
  - o determine the optimal pipe locations within the internal transport volume.

As was demonstrated in the currently approved TN-B1 SAR revision [25] analysis, use of the maximum pellet outer diameter and minimum outer clad diameter maximizes k_{eff}. Development of models and demonstration of maximum reactivity are addressed in the remaining subsections of this section.

6.13.8.1. HAC Array Models

This section describes development of maximum reactivity HAC array models. Due to model similarities, many of the optimum model features determined for the HAC array models are applicable to the HAC single package models, and the NCT array and single package models. Studies were performed to establish the following.

- Optimal Fuel Rod Arrangement Within the Pipe
- Optimal Water Density Within the Inner Storage Container, but Outside the Pipe

- Optimal Cushioning Pad Thickness and limiting density (nominal or high)
- Optimal Location of the Pipe Within the Inner Storage Container

The base HAC package model remains as was shown in Figures 6-6 through 6-8. The differences being that the fuel assemblies shown in Figure 6-8 are replaced with a conservative model for a 5-inch schedule 40 ss pipe loaded with up to 30 fuel rods and the peripheral cushioning pads, shown in Figure 6-5 for the NCT model, may still be present. The model for the 5-inch schedule 40 ss pipe is conservative because the nominal outer diameter of 5.563 inches was used as the inner diameter within which the fuel rods are restrained and the 0.258-inch thick neutron absorbing steel pipe wall is not modeled.

The first sensitivity study was performed to establish the optimum pitch for a triangular-pitched array of 30 fuel rods within the pipe. For the purposes of this study, full density water was used within the pipe and 0.25 g/cm^3 water was modeled in the package interior, but outside of the pipe. The 0.25 g/cm^3 value was used because some early sensitivity studies indicated that to be the optimum value when the pipe was centered and the NCT peripheral pads were present. An additional sensitivity study is documented later in this report to update the value for the final HAC array models. Additionally, both nominal- and high-density liner (HDL) is evaluated. Consistent with the HAC array model for the ATRIUM 11 fuel assemblies, the volume between the TN-B1 inner and outer containers was modeled as empty. The package array used for this study is a closely packed 10x1x10 stack of packages reflected by 30.48 cm of full density water. Figure 6-101 and Table 6-151 provide the results for the ATRIUM 11 fuel rod optimum pitch study. The optimal pin pitch was found to be 2.6 cm for the ATRIUM 11 fuel rods with a nominal liner. Similar studies were performed for the ATRIUM 10XM and PWR 17x17, type 3 rods, yielding optimum pin pitch of 2.6 cm for all three fuel rod designs.

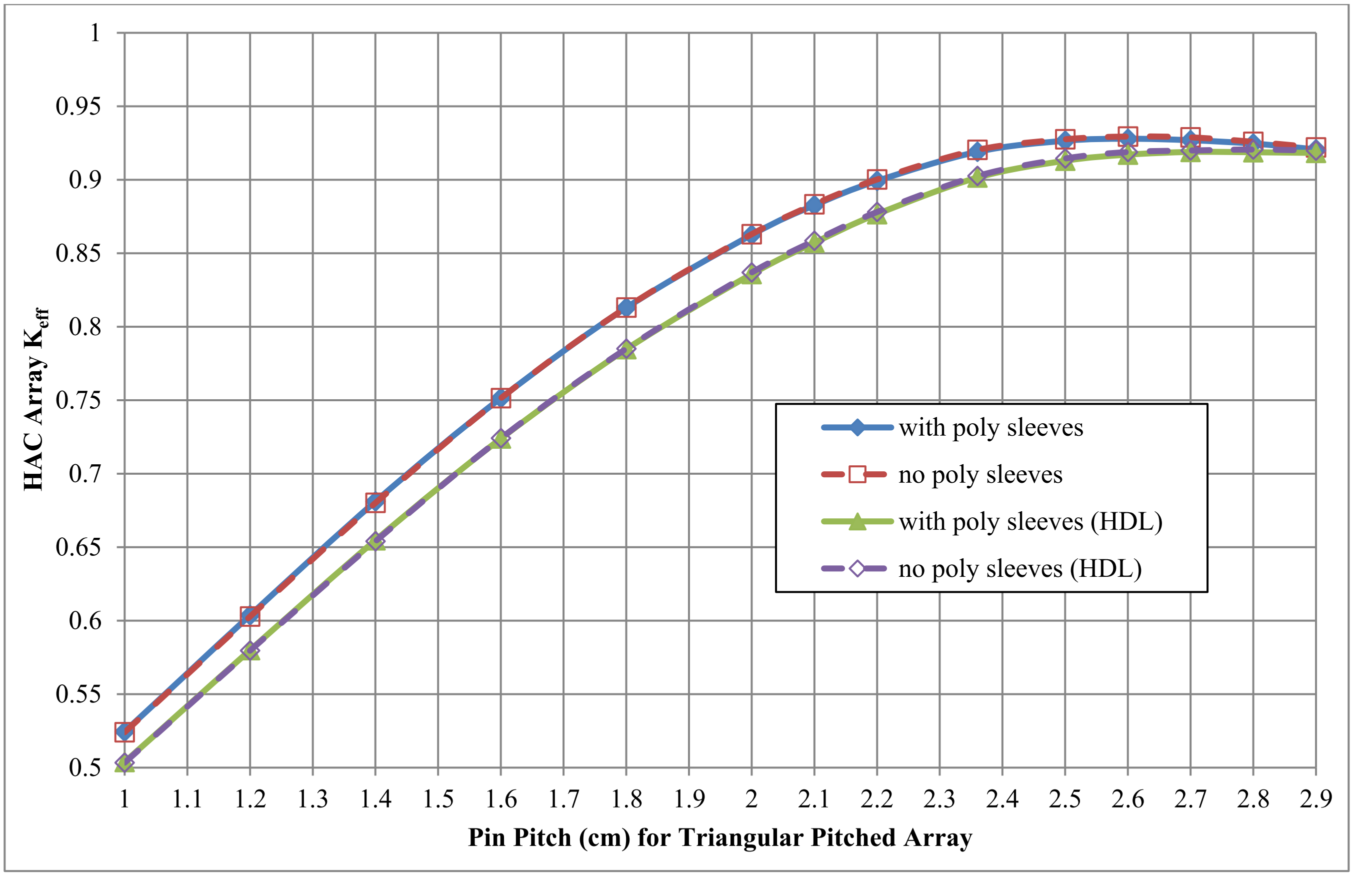

Figure 6-101 Optimum Moderation Pin Pitch Study for ATRIUM 11 Fuel Rods in Pipe

Table 6-151 Optimum Pitch Study Results

pin pitch (cm)	with poly sleeve		without poly sleeve		with poly sleeve (HDL)		without poly sleeve (HDL)	
	k_{eff}	σ_{keff}	k_{eff}	σ_{keff}	k_{eff}	σ_{keff}	k_{eff}	σ_{keff}
1	0.52450	0.00018	0.52404	0.00019	0.50385	0.00018	0.50338	0.00019
1.2	0.60375	0.00018	0.60281	0.00019	0.57993	0.00019	0.57963	0.00019
1.4	0.68114	0.00019	0.68020	0.00018	0.65476	0.00018	0.65401	0.00019
1.6	0.75151	0.00019	0.75147	0.00019	0.72400	0.00019	0.72421	0.00019
1.8	0.81295	0.00019	0.81313	0.00019	0.78468	0.00019	0.78514	0.00019
2	0.86255	0.00019	0.86295	0.00019	0.83591	0.00019	0.83697	0.00019
2.1	0.88273	0.00019	0.88332	0.00019	0.85722	0.00019	0.85858	0.00019
2.2	0.89932	0.00019	0.90030	0.00019	0.87667	0.00019	0.8781	0.00019
2.36	0.91911	0.00019	0.92038	0.00019	0.90151	0.00019	0.90262	0.00019
2.5	0.92657	0.00019	0.92759	0.00018	0.91299	0.00019	0.91455	0.00019
2.6	**0.92796**	**0.00019**	**0.9294**	**0.00019**	0.91711	0.00019	0.9189	0.00018
2.7	0.92691	0.00019	0.92888	0.00019	**0.91896**	**0.00019**	0.91994	0.00019
2.8	0.92465	0.00019	0.92590	0.00019	0.91874	0.00019	**0.92064**	**0.00019**
2.9	0.92074	0.00018	0.92209	0.00019	0.91832	0.00019	0.91989	0.00019

The pin-pitch sensitivity study was conducted starting with the fuel pins in a tightly packed bundle of 30 fuel rods. The fuel rod center to center pitch was increased in increments until reaching 2.36 cm, which is the largest triangular pitched array that could fit within the pipe model without adjustment. For pitches above 2.36 cm, the fuel rods that would have extended outside the pipe were moved back into the pipe. Figure 6-90 shows the fuel rod arrangement for the ATRIUM 11 optimum pin pitch fuel rod array. Additional cases were run for the 2.6 and 2.8 cm pitch cases in which the two outermost rods from each fuel array were removed to demonstrate that removing rods from a slightly overcrowded area near the array periphery would not increase k_{eff}.

The next sensitivity study performed investigated the most reactive peripheral pad thickness. Results from this study are presented in Figure 6-102. The results shown by the “Pipe Centered” curve in this figure demonstrate that if the pipe and fuel rods remain in the center of the storage volume, reducing the pad from full thickness reduces k_{eff}. However, if the pipe is moved toward the horizontal center of the package with the reduced pad thickness, k_{eff} is increased. Consequently, the most reactive pipe and pad configuration is with the pad removed and the pipes in each side of the package moved toward each other. This is the configuration shown in Figure 6-90.

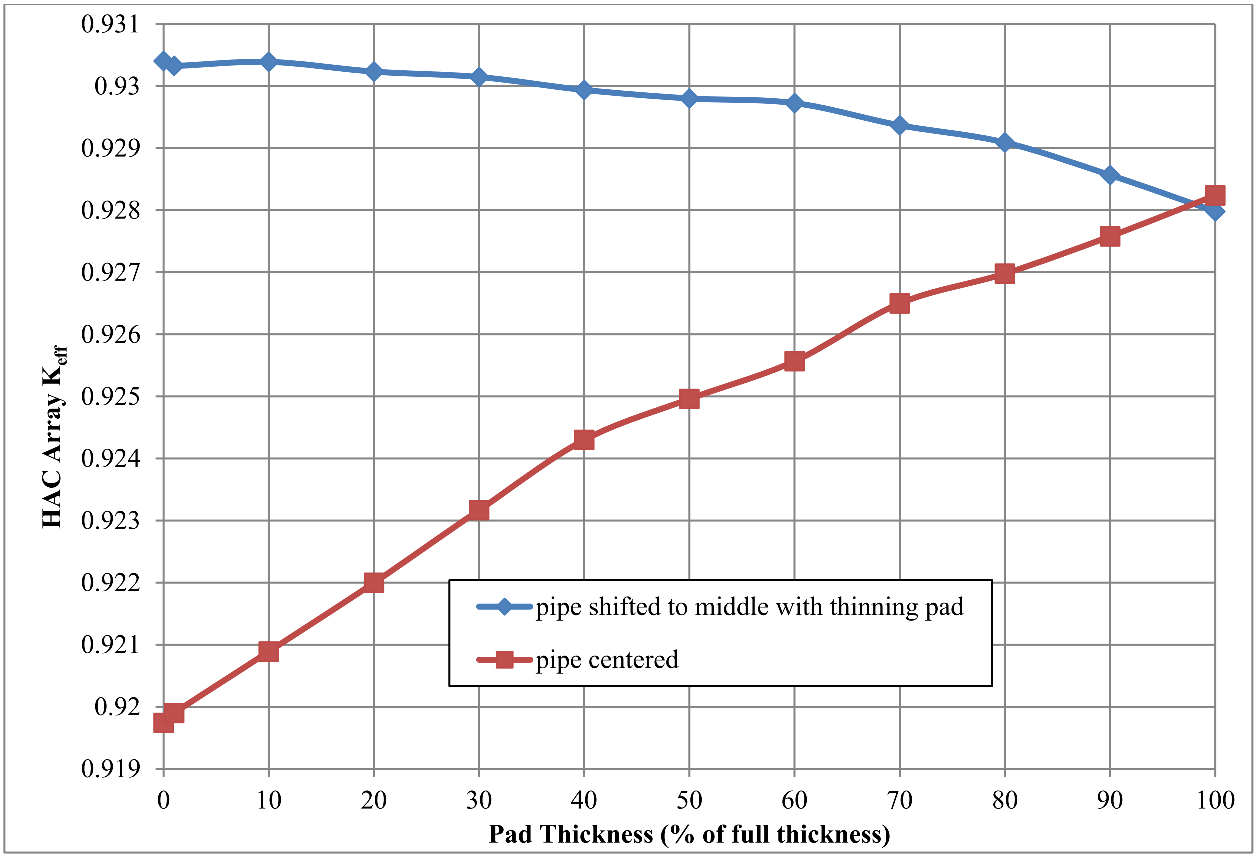

Figure 6-102 Pad Thickness Studies for ATRIUM 11 Fuel Rods

To further clarify and confirm the results from the pad thickness studies, an additional study was performed with the location of the pipe varied within the storage cell with the pads removed. Figure 6-103 demonstrates that the most reactive configuration is with the pads removed and the pipes moved to the center partition and centered vertically within the storage volume. The values provided in the figure are the HAC array k_{eff} values for each array location.

		Distance (cm) Pipe Centers are Moved Horizontally Toward Package Center									
		0	0.2	0.4	0.6	0.8	1	1.2	1.4	1.6	1.746
Distance (cm) Pipe Centers Are Moved Vertically From Storage Volume Center	1.74										0.92929
	1.6										0.93005
	1.3										0.93029
	1										0.93107
	0.7										0.93097
	0.4										0.93186
	0.2										0.93159
	0	0.92121	0.92217	0.92351	0.92505	0.92585	0.92736	0.92842	0.92958	0.93039	**0.93195**
	-0.2										0.93188
	-0.4										0.93186
	-0.7										0.93123
	-1										0.93094
	-1.3										0.93010
	-1.6										0.92954
	-1.74										0.92934

Figure 6-103 HAC Array Pipe Location Study for ATRIUM 11 Fuel Rods

Similar studies were performed for the ATRIUM 10XM and PWR 17x17, type 3 rods. The same location was seen as limiting for the ATRIUM 10XM fuel rods. The limiting location for the PWR fuel rods was lowered vertically by 0.2 cm. While this variation is likely due to Monte Carlo method statistical noise, this location is still used for the HAC array CSI calculations for PWR 17x17, type 3 fuel rods.

The studies documented to this point have set (1) the optimum moderation pin pitch and fuel rod configuration within the pipes, (2) the optimum pad thickness is no pads, (3) that modeling the polyethylene sleeves as water is bounding, and (4) have identified the most reactive pipe positions within the storage volume. An additional sensitivity study was performed with the limiting pipe and pad configurations to determine the optimal water density for the water inside the storage volume, but outside the pipe. Note that since the optimum moderation study was performed with full density water inside the pipe, reduction of the water density in the pipe would increase the optimum moderation fuel rod pitch and move additional rods outside the pipe, thereby reducing k_{eff}.

Results from the sensitivity study for water outside the pipe for ATRIUM 11 fuel rods are presented in Figure 6-104. This study demonstrated that the optimum water density for the water outside the pipe is 0.12 g/cm^3 for the ATRIUM 11 fuel. Similar studies determined that the optimal density was 0.13 g/cm^3 for the ATRIUM 10XM rods and 0.11 g/cm^3 for the PWR 17x17, type 3 fuel rods.

To capture the potential impact of the PCSEP on the calculation of maximum reactivity, the limiting models were evaluated both with and without the 6 mil polyethylene sleeves and the maximum k_{eff} values were adjusted with the PCSEP where appropriate.

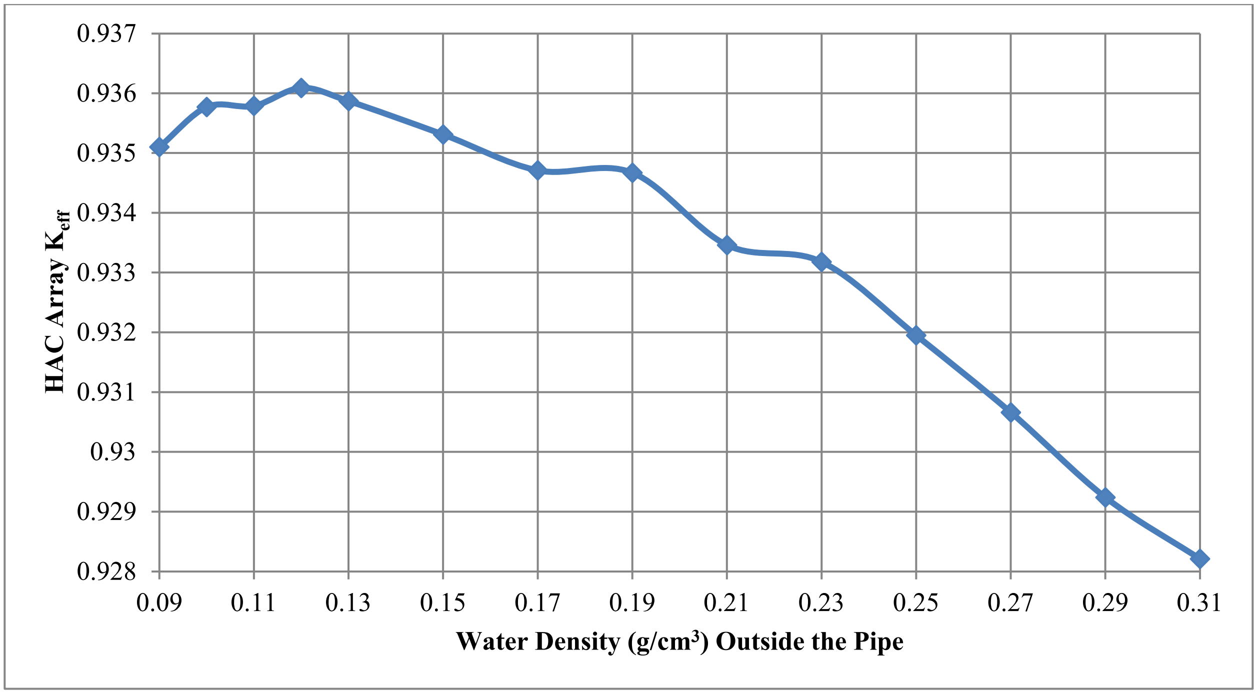

Figure 6-104 Sensitivity Study for Water Density Outside Pipes for ATRIUM 11 Fuel Rods

The optimal configurations documented in this section were used in the HAC array CSI calculations documented in Section 6.13.8.5.

6.13.8.2. NCT Array Models

The differences between the NCT and HAC package array models is that the height of the top of the outer container is increased 2.4 cm for the NCT models and the full thickness of the peripheral cushioning pads is used in the NCT models. For the NCT array models the pipe is held in the center of the storage volume by the pads. This does not affect the optimum moderation configuration of the rods in the pipe.

However, the optimum density of the water outside the pipes may vary significantly from that determined for the HAC models. Consequently, sensitivity studies were performed for the water density outside the pipes for each fuel type. The optimum water density is 0.06 g/cm^3 for the ATRIUM 11 rods, 0.07 g/cm^3 for the ATRIUM 10XM rods, and 0.05 g/cm^3 for the PWR 17x17, type 3 fuel rods.

To capture the potential impact of the PCSEP on the calculation of maximum reactivity, the limiting models were evaluated both with and without the 6 mil polyethylene sleeves and the maximum k_{eff} values were adjusted with the PCSEP where appropriate.

The optimal configurations documented in this section were used in the NCT array CSI calculations documented in Section 6.13.8.5.

6.13.8.3. HAC Single Package Model

The HAC single package model is derived from the HAC array model. The following changes are made to maximize neutron reflection. The empty space between the TN-B1 inner and outer packages is filled with full density water and, consistent with the sensitivity study shown in Figure 6-105, the density of the water that is inside the inner container and outside the pipe is raised to 1.0 g/cm³. The results for these single package models are presented in Table 6-152.

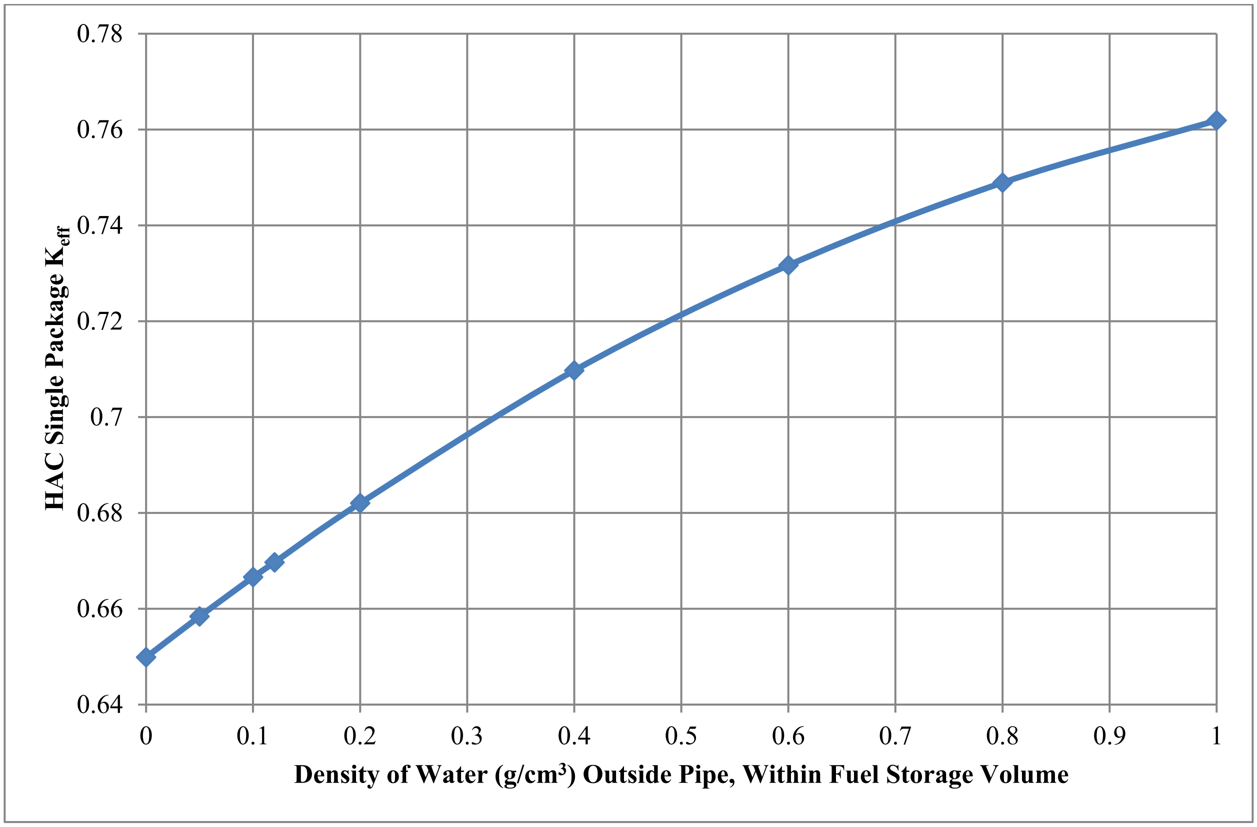

Figure 6-105 Sensitivity Study for Water Outside Pipe

Table 6-152 Loose Rods in Pipe, HAC and NCT Single Package Results

Fuel Rod	HAC Single Package				NCT Single Package			
Design	k_{eff}	σ_{keff}	PCSEP	Max. k_{eff}	k_{eff}	σ_{keff}	PCSEP	Max. k_{eff}
ATRIUM 11	0.76104	0.00019	0.00159	0.7630	0.70106	0.00019	0.00000	0.7014
ATRIUM 10XM	0.70926	0.00019	0.00173	0.7114	0.65273	0.00019	0.00000	0.6531
PWR 17x17	0.76355	0.00019	0.00161	0.7655	0.70325	0.00019	0.00065	0.7043

To capture the potential impact of the PCSEP on the calculation of maximum reactivity, the limiting models were evaluated both with and without the 6 mil polyethylene sleeves and the maximum k_{eff} values were adjusted with the PCSEP where appropriate.

The HAC single package results are all well below the applicable USL from Section 6.13.10 and are all considered subcritical.

6.13.8.4. NCT Single Package Model

The NCT single package model is derived from the NCT array model. Only the following changes were made to maximize neutron reflection. The empty space between the TN-B1 inner and outer packages is filled with full density water and, consistent with sensitivity study performed for the HAC single package model, the density of the water that is inside the inner container and outside the pipe is raised to 1.0 g/cm^3. The results for these single package models are presented in Table 6-152.

To capture the potential impact of the PCSEP on the calculation of maximum reactivity, the limiting models were evaluated both with and without the 6 mil polyethylene sleeves and the maximum k_{eff} values were adjusted with the PCSEP where appropriate.

The NCT single package results are all well below the applicable USL from Section 6.13.10 and are all considered subcritical.

6.13.8.5. CSI Calculations for Loose Rods in SS Pipe

The size of the package arrays in the HAC array models described in Section 6.13.8.1 and the NCT array models described in Section 6.13.8.2 were varied to find the maximum array sizes yielding k_{eff} + 2 σ_{keff} + PCSEP values that were below the applicable USL from Section 6.13.10.

Table 6-153 describes the subcritical HAC and NCT arrays, the number of packages in each array, k_{eff} value, and the HAC, NCT and overall CSI values for the loose rod packages. The CSI values are calculated, consistent with the requirements of 10 CFR § 71.59, as described in Section 6.13.1.3.

For the reader's convenience:

CSI_{HAC} = 50 / (N_{HAC}/2), rounded up to nearest tenth

CSI_{NCT} = 50 / (N_{NCT}/5), rounded up to nearest tenth

CSI = greater of CSI_{HAC} and CSI_{NCT}

Table 6-153 CSI Calculations for Loose Rods in Pipes

Fuel Rod Design	HAC Array	N_{HAC}	k_{eff}	σ_{keff}	PCSEP	Max. K_{eff}	USL	CSI_{HAC}
ATRIUM 11	9x1x9	81	0.92357	0.00019	0.00000	0.9240	0.9318	1.3
ATRIUM 10XM	10x1x10	100	0.86687	0.00019	0.00178	0.8690	0.9292	1.0
PWR 17x17	9x1x9	81	0.92624	0.00019	0.00000	0.9266	0.9292	1.3
Fuel Rod Design	**NCT Array**	**N_{NCT}**	**k_{eff}**	**σ_{keff}**	**PCSEP**	**Max. K_{eff}**	**USL**	**CSI_{NCT}**
ATRIUM 11	10x1x11	110	0.92812	0.00019	0.00000	0.9285	0.9318	2.3
ATRIUM 10XM	11x2x12	264	0.89741	0.00019	0.00000	0.8978	0.9292	1.0
PWR 17x17	10x1x10	100	0.92367	0.00019	0.00000	0.9241	0.9292	2.5
Fuel Rod Design	**Overall CSI**							
ATRIUM 11	2.3							
ATRIUM 10XM	1.0							
PWR 17x17	2.5							

6.13.9. *Fissile Material Packages for Air Transport*

This package is not intended for the air transport of fissile material.

6.13.10. *Validation*

The computer code used for these criticality calculations has been benchmarked against applicable criticality experiments. Use of SCALE 6.2.4 is validated in CALC-3023904 [31]. The application models and the benchmark evaluations use the same code and nuclear data to calculate k_{eff} values.

6.13.10.1. Applicability of Benchmark Experiments

The primary objective of computational method validation is to establish the relationship between reality and calculated results. For validation of criticality calculations, this is accomplished with comparisons between measured critical conditions and calculated k_{eff} values of laboratory critical experiments (LCEs). The generally accepted guidance for critical experiment selection is that the critical experiments should be as similar to the application model as is practical and that the same computational method should be used for both critical experiment and application models.

The SCALE computer code system includes calculation sequences (i.e., TSUNAMI-1D, -2D, and -3D) that can be used to calculate the sensitivity of the k_{eff} value of a system to variation of the nuclear data used in the k_{eff} calculation. The fundamental principle evaluated, which can be evaluated with any criticality code, is how the response (e.g., system k_{eff}) changes with minor variations (i.e., perturbations) to input parameters used to calculate k_{eff}. The SCALE-generated sensitivities are calculated as a function of nuclide, nuclear reaction, and neutron energy group using first-order linear perturbation theory (Ref. [24], Section 6). As calculated by TSUNAMI, sensitivity is the fractional change in k_{eff} due to a fractional change in a nuclear data value, or S ≡ (Δk/k)/(Δσ/σ). A sensitivity of +1.0 means a 1.0 % increase in the value of the nuclear data will result in a 1.0% increase in the system k_{eff} value.

TSUNAMI-3D calculations are performed for two application models to generate sensitivity data files (SDFs) for use in identifying applicable critical benchmark experiments for use in validation. The application models consist of TN-B1 package configurations for 1) an array of packages containing ATRIUM 11 fuel assemblies with ^{235}U enrichments no greater than 8.0 wt% ^{235}U under hypothetical accident conditions, and 2) an array of packages containing loose PWR 17x17, type 3 fuel rods with ^{235}U enrichments no greater than 8.0 wt% ^{235}U. The ATRIUM 10 loose fuel rod configurations with ^{235}U enrichments no greater than 5.0 wt% are sufficiently similar to these application models such that the identified applicable benchmark experiments would be the same or sufficiently similar. Ref. [24] recommends that direct perturbation calculations be used to confirm the validity of the sensitivity coefficients generated.

Direct perturbation calculations were performed using an ATRIUM 11 fuel assembly HAC array application model. To reduce computer memory and run time requirements, the array model was represented with an infinite array of packages. Confirmation of the similarity between the infinite array and the finite array near limiting model was demonstrated using TSUNAMI-IP (c_k = 0.95). Direct perturbation calculated sensitivity coefficients were generated as described in Ref. [24] (Section 6) using the following equation:

$$S_{k,\alpha} = \frac{\alpha}{k} \times \frac{dk}{d\alpha} = \frac{\alpha}{k} \times \frac{k_{\alpha^+} - k_{\alpha^-}}{\alpha^+ - \alpha^-}$$

Where α^+ and α^- represent the increased and decreased values respectively, or the input quantity α and k_{α^+} and k_{α^-} represent the corresponding values of k_{eff}. Direct perturbation calculated sensitivity coefficients for ^{235}U and ^{1}H were 0.201 and 0.054, respectively. Tsunami-3D calculated sensitivity coefficients for comparison were 0.182 and 0.062 for ^{235}U and ^{1}H, respectively. Hence, the mesh size used for the application model SDF was considered sufficient. For the PWR rod model, the direct perturbation calculated sensitivity coefficients for ^{235}U and ^{1}H were 0.220 and 0.258, respectively. Tsunami-3D calculated sensitivity coefficients for comparison were 0.209 and 0.207 for ^{235}U and ^{1}H, respectively. Hence, the mesh size used for the application model SDF was considered sufficient.

TSUNAMI-IP is used to compare the application model SDFs against the SDFs available in the International Handbook of Evaluated Criticality Safety Benchmark Experiments (IHECSBE) [37] to assist with identification of applicable critical benchmark experiments for computational validation. Note that the SDFs from the IHECSBE are only used for screening what is available, final selection is based on expert judgement and ensuring coverage of the range of parameters of the application model. Per [38], at least 15 to 20 very highly correlated systems (c_k ≥0.90) or 25 to 40 moderately correlated systems (c_k ≥0.80) should be included in the benchmark evaluations.

The critical experiment set includes experiments with gadolinium and boron neutron absorbers, polyethylene, and enrichments above 5.0 wt% ^{235}U. The similarity of a benchmark to the application is characterized by the correlation coefficient, c_k, which is calculated by TSUNAMI-IP. A total of 187 critical experiments are selected for calculation of the USL for the ATRIUM 11 fuel assembly application model, and a total of 154 critical experiments are selected for calculation of the USL for the PWR loose rod application model. Selected benchmarks are shown in Table 6-154. For the ATRIUM fuel assembly benchmark set 20 of 187 benchmarks used for calculation of the USL have correlation coefficients above 0.90; and 121 of 154 are above 0.90 for the PWR loose rod configuration benchmark set. The critical configurations are from the following IHECSBE evaluations:

- LEU-COMP-THERM (LCT)-001, 002, 003, 004, 009, 010, 012, 013, 014, 039, 078, 079, 080

Descriptions of the selected critical experiments are provided in [37] with summary data derived from the experiment descriptions shown in

Table 6-155 and Table 6-156. All 187 critical configurations are modeled and analyzed with SCALE.

Table 6-154 Table of Selected Critical Benchmark Experiments

Experiment Identifier	Benchmark k_{eff}	σ	Calculated k_{eff}	σ	c_k ATRIUM 11 assemblies	c_k PWR rods
LCT-001-001	0.9998	0.0031	0.9986	0.0005	0.8840	0.9055
LCT-001-002	0.9998	0.0031	0.9982	0.0005	0.8858	0.9035
LCT-001-003	0.9998	0.0031	0.9982	0.0005	0.8862	0.9013
LCT-001-004	0.9998	0.0031	0.9984	0.0005	0.8860	0.9034
LCT-001-005	0.9998	0.0031	0.9969	0.0005	0.8862	0.8998
LCT-001-006	0.9998	0.0031	0.9984	0.0005	0.8863	0.9024
LCT-001-007	0.9998	0.0031	0.9980	0.0005	0.8858	0.8989
LCT-001-008	0.9998	0.0031	0.9976	0.0005	0.8861	0.9002
LCT-002-001	0.9997	0.0020	0.9968	0.0005	0.8738	0.9137
LCT-002-002	0.9997	0.0020	0.9998	0.0005	0.8746	0.9142
LCT-002-003	0.9997	0.0020	0.9994	0.0005	0.8770	0.9155
LCT-002-004	0.9997	0.0020	0.9987	0.0005	0.8887	0.9229
LCT-002-005	0.9997	0.0020	0.9974	0.0005	0.8917	0.9238
LCT-003-001	1.0000	0.0039	0.9901	0.0005	0.8729	<0.8
LCT-003-002	1.0000	0.0039	0.9900	0.0005	0.8707	<0.8
LCT-003-003	1.0000	0.0039	0.9898	0.0005	0.8716	<0.8
LCT-003-004	1.0000	0.0039	0.9895	0.0005	0.8723	<0.8
LCT-003-005	1.0000	0.0039	0.9898	0.0005	0.8743	<0.8
LCT-003-006	1.0000	0.0039	0.9883	0.0005	0.8779	0.8981
LCT-003-007	1.0000	0.0039	0.9902	0.0005	0.8764	0.8961
LCT-003-008	1.0000	0.0039	0.9913	0.0005	0.8769	0.8973
LCT-003-009	1.0000	0.0039	0.9845	0.0005	0.8791	<0.8
LCT-003-010	1.0000	0.0039	0.9852	0.0005	0.8778	0.8966
LCT-003-011	1.0000	0.0039	0.9869	0.0005	0.8811	<0.8
LCT-003-012	1.0000	0.0039	0.9852	0.0005	0.8624	<0.8
LCT-003-013	1.0000	0.0039	0.9888	0.0005	0.8799	<0.8
LCT-003-014	1.0000	0.0039	0.9875	0.0005	0.8804	<0.8

Experiment Identifier	Benchmark k_{eff}	σ	Calculated k_{eff}	σ	c_k ATRIUM 11 assemblies	c_k PWR rods
LCT-003-015	1.0000	0.0039	0.9876	0.0004	0.8797	<0.8
LCT-003-016	1.0000	0.0039	0.9864	0.0005	0.8798	<0.8
LCT-003-017	1.0000	0.0039	0.9882	0.0005	0.8786	<0.8
LCT-003-018	1.0000	0.0039	0.9875	0.0005	0.8786	<0.8
LCT-003-019	1.0000	0.0039	0.9873	0.0005	0.8772	<0.8
LCT-003-020	1.0000	0.0039	0.9883	0.0005	0.8748	<0.8
LCT-003-021	1.0000	0.0039	0.9863	0.0005	0.8773	<0.8
LCT-003-022	1.0000	0.0039	0.9973	0.0005	0.8762	<0.8
LCT-003-023	1.0000	0.0039	N/A	N/A	N/A	<0.8
LCT-004-001	0.9998	0.0033	0.9937	0.0005	0.8648	0.9054
LCT-004-002	0.9998	0.0033	0.9932	0.0005	0.8676	0.9057
LCT-004-003	0.9998	0.0033	0.9942	0.0005	0.8673	0.9061
LCT-004-004	0.9998	0.0033	0.9941	0.0005	0.8682	0.9103
LCT-004-005	0.9998	0.0033	0.9925	0.0005	0.8682	0.9107
LCT-004-006	0.9998	0.0033	0.9928	0.0005	0.8708	0.9162
LCT-004-007	0.9998	0.0033	0.9917	0.0005	0.8775	0.9125
LCT-004-008	0.9998	0.0035	0.9918	0.0005	0.8749	0.9153
LCT-004-009	0.9998	0.0035	0.9934	0.0005	0.8845	0.9188
LCT-004-010	0.9998	0.0035	0.9984	0.0005	0.8893	0.9280
LCT-004-011	0.9998	0.0035	0.9882	0.0005	0.9026	0.9270
LCT-004-012	0.9998	0.0035	0.9851	0.0005	0.9089	0.9180
LCT-004-013	0.9998	0.0035	0.9901	0.0005	0.8828	0.9157
LCT-004-014	0.9998	0.0035	0.9892	0.0005	0.8799	0.9172
LCT-004-015	0.9998	0.0035	0.9893	0.0005	0.8815	0.9169
LCT-004-016	0.9998	0.0035	0.9899	0.0005	0.8805	0.9191
LCT-004-017	0.9998	0.0035	0.9896	0.0005	0.8856	0.9175
LCT-004-018	0.9998	0.0035	0.9899	0.0005	0.8828	0.9187
LCT-004-019	0.9998	0.0035	0.9915	0.0005	0.8857	0.9250
LCT-004-020	0.9998	0.0035	0.9879	0.0005	0.8978	0.9701

Experiment Identifier	Benchmark k_{eff}	σ	Calculated k_{eff}	σ	c_k ATRIUM 11 assemblies	c_k PWR rods
LCT-009-001	1.0000	0.0021	0.9995	0.0005	0.9024	0.9332
LCT-009-002	1.0000	0.0021	0.9980	0.0005	0.8910	0.9245
LCT-009-003	1.0000	0.0021	0.9984	0.0005	0.8925	0.9252
LCT-009-004	1.0000	0.0021	0.9997	0.0005	0.8908	0.9234
LCT-009-005	1.0000	0.0021	0.9995	0.0005	0.8941	0.9248
LCT-009-006	1.0000	0.0021	0.9987	0.0005	0.8840	0.9196
LCT-009-007	1.0000	0.0021	1.0003	0.0005	0.8841	0.9196
LCT-009-008	1.0000	0.0021	0.9993	0.0005	0.8892	0.9219
LCT-009-009	1.0000	0.0021	0.9987	0.0005	0.8923	0.9234
LCT-009-010	1.0000	0.0021	0.9998	0.0005	0.8875	0.9211
LCT-009-011	1.0000	0.0021	0.9984	0.0005	0.8857	0.9200
LCT-009-012	1.0000	0.0021	0.9993	0.0005	0.8867	0.9205
LCT-009-013	1.0000	0.0021	0.9991	0.0005	0.8892	0.9217
LCT-009-014	1.0000	0.0021	0.9984	0.0005	0.8853	0.9199
LCT-009-015	1.0000	0.0021	0.9994	0.0005	0.8885	0.9214
LCT-009-016	1.0000	0.0021	0.9991	0.0005	0.8893	0.9223
LCT-009-017	1.0000	0.0021	0.9987	0.0005	0.8879	0.9212
LCT-009-018	1.0000	0.0021	0.9993	0.0005	0.8899	0.9226
LCT-009-019	1.0000	0.0021	1.0008	0.0005	0.8890	0.9219
LCT-009-020	1.0000	0.0021	0.9993	0.0005	0.8913	0.9229
LCT-009-021	1.0000	0.0021	1.0000	0.0005	0.8891	0.9219
LCT-009-022	1.0000	0.0021	0.9994	0.0005	0.8911	0.9228
LCT-009-023	1.0000	0.0021	0.9995	0.0005	0.8866	0.9208
LCT-009-024	1.0000	0.0021	0.9989	0.0005	0.8892	0.9217
LCT-009-025	1.0000	0.0021	0.9990	0.0005	0.8849	0.9197
LCT-009-026	1.0000	0.0021	0.9993	0.0005	0.8868	0.9216
LCT-009-027	1.0000	0.0021	0.9994	0.0005	0.8864	0.9209
LCT-010-001	1.0000	0.0021	1.0041	0.0005	0.8885	0.9162
LCT-010-002	1.0000	0.0021	1.0051	0.0005	0.8905	0.9188

Experiment Identifier	Benchmark k_{eff}	σ	Calculated k_{eff}	σ	c_k ATRIUM 11 assemblies	c_k PWR rods
LCT-010-003	1.0000	0.0021	1.0037	0.0005	0.8933	0.9208
LCT-010-004	1.0000	0.0021	0.9973	0.0005	0.8968	0.9248
LCT-010-005	1.0000	0.0021	1.0000	0.0005	0.8911	0.8920
LCT-010-006	1.0000	0.0021	0.9998	0.0005	0.9011	0.9111
LCT-010-007	1.0000	0.0021	1.0010	0.0005	0.8998	0.9176
LCT-010-008	1.0000	0.0021	0.9973	0.0005	0.8996	0.9196
LCT-010-009	1.0000	0.0021	1.0004	0.0005	0.9271	0.9406
LCT-010-010	1.0000	0.0021	1.0007	0.0005	0.9239	0.9412
LCT-010-011	1.0000	0.0021	1.0014	0.0005	0.9217	0.9402
LCT-010-012	1.0000	0.0021	1.0004	0.0005	0.9148	0.9365
LCT-010-013	1.0000	0.0021	0.9978	0.0005	0.9055	0.9302
LCT-010-014	1.0000	0.0028	1.0013	0.0005	0.9076	0.9271
LCT-010-015	1.0000	0.0028	1.0013	0.0005	0.9065	0.9274
LCT-010-016	1.0000	0.0028	1.0021	0.0005	0.9113	0.9300
LCT-010-017	1.0000	0.0028	1.0009	0.0005	0.9021	0.9255
LCT-010-018	1.0000	0.0028	1.0003	0.0005	0.8995	0.9246
LCT-010-019	1.0000	0.0028	1.0008	0.0005	0.8939	0.9203
LCT-010-020	1.0000	0.0028	1.0021	0.0005	0.8856	0.9121
LCT-010-021	1.0000	0.0028	1.0018	0.0005	0.8821	0.9113
LCT-010-022	1.0000	0.0028	1.0015	0.0005	0.8833	0.9136
LCT-010-023	1.0000	0.0028	1.0009	0.0005	0.8888	0.9173
LCT-010-024	1.0000	0.0028	0.9986	0.0005	0.8942	<0.8
LCT-010-025	1.0000	0.0028	1.0000	0.0005	0.8935	<0.8
LCT-010-026	1.0000	0.0028	1.0007	0.0005	0.8964	0.9132
LCT-010-027	1.0000	0.0028	1.0002	0.0005	0.8930	0.9136
LCT-010-028	1.0000	0.0028	1.0012	0.0005	0.8951	0.9166
LCT-010-029	1.0000	0.0028	1.0000	0.0005	0.8935	0.9173
LCT-010-030	1.0000	0.0028	0.9990	0.0005	0.8948	0.9196
LCT-012-001	1.0000	0.0034	0.9878	0.0005	0.8877	<0.8

Experiment Identifier	Benchmark k_{eff}	σ	Calculated k_{eff}	σ	c_k ATRIUM 11 assemblies	c_k PWR rods
LCT-012-002	1.0000	0.0034	0.9880	0.0005	0.8761	<0.8
LCT-012-003	1.0000	0.0034	0.9888	0.0005	0.8763	<0.8
LCT-012-004	1.0000	0.0034	0.9874	0.0005	0.8739	<0.8
LCT-012-005	1.0000	0.0034	0.9887	0.0005	0.8748	<0.8
LCT-012-006	1.0000	0.0034	0.9896	0.0005	0.8748	<0.8
LCT-012-007	1.0000	0.0034	0.9897	0.0005	0.8752	<0.8
LCT-012-008	1.0000	0.0049	0.9876	0.0005	0.8750	<0.8
LCT-012-009	1.0000	0.0034	0.9887	0.0005	0.8756	<0.8
LCT-012-010	1.0000	0.0034	0.9893	0.0005	0.8760	<0.8
LCT-013-001	1.0000	0.0018	1.0017	0.0005	0.9181	0.9382
LCT-013-002	1.0000	0.0018	1.0013	0.0005	0.9081	0.9297
LCT-013-003	1.0000	0.0018	1.0012	0.0005	0.9106	0.9298
LCT-013-004	1.0000	0.0018	1.0018	0.0005	0.9112	0.9304
LCT-013-005	1.0000	0.0032	0.9999	0.0005	0.9074	0.9288
LCT-013-006	1.0000	0.0018	1.0014	0.0005	0.9048	0.9281
LCT-013-007	1.0000	0.0018	1.0010	0.0005	0.9073	0.9288
LCT-014-001	1.0000	0.0019	0.9998	0.0005	0.8889	0.9202
LCT-014-002	1.0000	0.0077	0.9869	0.0005	0.8928	0.9194
LCT-014-005	1.0000	0.0069	1.0036	0.0005	0.8607	<0.8
LCT-014-006	1.0000	0.0033	1.0041	0.0005	0.8789	<0.8
LCT-014-007	1.0000	0.0051	1.0011	0.0005	0.8736	<0.8
LCT-039-001	1.0000	0.0014	0.9962	0.0005	0.8698	0.9110
LCT-039-002	1.0000	0.0014	0.9975	0.0005	0.8710	0.9123
LCT-039-003	1.0000	0.0014	0.9974	0.0005	0.8689	0.9115
LCT-039-004	1.0000	0.0014	0.9971	0.0005	0.8698	0.9122
LCT-039-005	1.0000	0.0009	0.9984	0.0005	0.8705	0.9131
LCT-039-006	1.0000	0.0009	0.9982	0.0005	0.8692	0.9125
LCT-039-007	1.0000	0.0012	0.9969	0.0005	0.8660	0.9090
LCT-039-008	1.0000	0.0012	0.9975	0.0005	0.8669	0.9099

Experiment Identifier	Benchmark k_{eff}	σ	Calculated k_{eff}	σ	c_k ATRIUM 11 assemblies	c_k PWR rods
LCT-039-009	1.0000	0.0012	0.9979	0.0005	0.8668	0.9101
LCT-039-010	1.0000	0.0012	0.9986	0.0005	0.8667	0.9107
LCT-039-011	1.0000	0.0013	0.9953	0.0005	0.8683	0.9100
LCT-039-012	1.0000	0.0013	0.9962	0.0005	0.8682	0.9102
LCT-039-013	1.0000	0.0013	0.9965	0.0005	0.8687	0.9108
LCT-039-014	1.0000	0.0013	0.9973	0.0005	0.8665	0.9093
LCT-039-015	1.0000	0.0013	0.9967	0.0005	0.8649	0.9083
LCT-039-016	1.0000	0.0013	0.9979	0.0005	0.8676	0.9102
LCT-039-017	1.0000	0.0013	0.9959	0.0005	0.8671	0.9099
LCT-078-001	0.9995	0.0010	0.9973	0.0005	0.8485	0.8969
LCT-078-002	0.9999	0.0010	0.9975	0.0005	0.8482	0.8967
LCT-078-003	0.9990	0.0010	0.9959	0.0005	0.8477	0.8964
LCT-078-004	0.9986	0.0010	0.9965	0.0005	0.8482	0.8968
LCT-078-005	0.9980	0.0010	0.9956	0.0005	0.8476	0.8963
LCT-078-006	0.9974	0.0010	0.9955	0.0005	0.8476	0.8963
LCT-078-007	0.9994	0.0010	0.9977	0.0005	0.8478	0.8966
LCT-078-008	0.9987	0.0010	0.9970	0.0005	0.8471	0.8960
LCT-078-009	0.9978	0.0010	0.9951	0.0005	0.8478	0.8965
LCT-078-010	0.9969	0.0010	0.9953	0.0005	0.8478	0.8965
LCT-078-011	0.9994	0.0010	0.9969	0.0005	0.8484	0.8969
LCT-078-012	0.9993	0.0010	0.9972	0.0005	0.8492	0.8975
LCT-078-013	0.9993	0.0010	0.9971	0.0005	0.8488	0.8972
LCT-078-014	0.9991	0.0010	0.9969	0.0005	0.8483	0.8968
LCT-078-015	0.9996	0.0010	0.9976	0.0005	0.8470	0.8970
LCT-079-001	0.9999	0.0010	0.9974	0.0005	0.8677	0.9084
LCT-079-002	1.0002	0.0010	0.9981	0.0005	0.8671	0.9079
LCT-079-003	1.0005	0.0010	0.9982	0.0005	0.8708	0.9102
LCT-079-004	1.0004	0.0010	0.9987	0.0005	0.8712	0.9102
LCT-079-005	1.0004	0.0010	0.9990	0.0005	0.8751	0.9126

Experiment Identifier	Benchmark k_{eff}	σ	Calculated k_{eff}	σ	c_k ATRIUM 11 assemblies	c_k PWR rods
LCT-079-006	0.9994	0.0007	0.9986	0.0005	0.8763	0.9171
LCT-079-007	1.0003	0.0007	0.9990	0.0005	0.8772	0.9177
LCT-079-008	1.0008	0.0007	1.0007	0.0005	0.8818	0.9205
LCT-079-009	1.0003	0.0007	0.9997	0.0005	0.8828	0.9211
LCT-079-010	1.0009	0.0007	1.0020	0.0005	0.8889	0.9238
LCT-080-001	0.9976	0.0010	0.9953	0.0005	0.8462	0.8914
LCT-080-002	0.9982	0.0010	0.9957	0.0005	0.8461	0.8913
LCT-080-003	0.9984	0.0010	0.9962	0.0005	0.8460	0.8913
LCT-080-004	0.9981	0.0010	0.9952	0.0005	0.8464	0.8916
LCT-080-005	0.9979	0.0010	0.9953	0.0005	0.8467	0.8919
LCT-080-006	0.9975	0.0010	0.9964	0.0005	0.8468	0.8919
LCT-080-007	0.9993	0.0010	0.9970	0.0005	0.8469	0.8922
LCT-080-008	0.9987	0.0010	0.9972	0.0005	0.8460	0.8914
LCT-080-009	0.9982	0.0010	0.9962	0.0005	0.8460	0.8915
LCT-080-010	0.9972	0.0010	0.9955	0.0005	0.8466	0.8919
LCT-080-011	0.9984	0.0010	0.9977	0.0005	0.8479	0.8958

Table 6-155 Comparison of critical benchmark experiment properties to TN-B1 with ATRIUM 11 assemblies

Critical Benchmark Experiments					
	All	**Boron Neutron Absorber**	**Gadolinium Neutron Absorber**	**Boron and Gadolinium Absorber**	**TN-B1 Package (11x11)**
Number of benchmark cases	187	17	50	6	--
Water-to-fuel volume ratio	0.52 – 3.88	1.1 – 3.88	1.6	1.6	0.898 – 1.175
Lattice pitch (cm)	0.8 – 2.8	1.684 – 2.54	1.684 – 1.892	1.684	1.195 – 1.255
H-to-X	42 – 137	66 – 137	66 – 137	137	34.4 – 50.0
Clad OD (cm)	0.635 – 1.415	1.27 – 1.415	1.27 – 1.415	1.27	1.102
Fuel OD (cm)	0.526 – 1.265	1.118 – 1.265	1.118 – 1.265	1.1176	0.82
^{235}U Density in Fuel (a/b-cm)	4.88E-04 – 1.60E-03	4.88E-04 – 1.01E-03	4.88E-04 – 1.01E-03	4.88E-04	≤ 1.94E-03
^{235}U Enrichment (wt% ^{235}U/U)	2.35 – 6.9	2.35 – 4.31	2.35 – 4.31	2.35	5.5 – 8.0
EALF (eV)	0.109 – 0.821	0.13 – 0.765	0.176 – 0.353	0.213 – 0.224	0.239 – 0.448 (for License- Basis Single Container and Array Cases)

Table 6-156: Comparison of critical benchmark experiment properties to TN-B1 with PWR rods

Critical Benchmark Experiments		TN-B1 Package (PWR rods)
Number of benchmark cases	154	--
Water-to-fuel volume ratio	0.52 – 3.88	0.476
Lattice pitch (cm)	0.8 – 2.8	2.6 (triangular)
H-to-X	42 – 137	34.4
Clad OD (cm)	0.635 – 1.415	0.9754
Fuel OD (cm)	0.526 – 1.265	0.8265
^{235}U Density in Fuel (a/b-cm)	4.88E-04 – 1.60E-03	≤ 1.94E-03
^{235}U Enrichment (wt% ^{235}U/U)	2.35 – 6.9	8.0
EALF (eV)	0.109 – 0.699	0.091-0.975 (for License- Basis Single Container and Array Cases)

6.13.11. *Determination of the Upper Safety Limit*

The methodology employed for determination of the upper safety limit (USL) is consistent with that described in References [26] and [27]. Calculation of k_{eff} is performed for each benchmark case described in Section 6.13.10.1 (modeled in KENO-V with the v7-252 group library and utilizing the CSAS5 option of SCALE 6.2.4). For the critical benchmark experiments that are slightly super or subcritical, an adjustment to the k_{eff} value calculated with KENO-V (k_{ca1c}) is done as suggested in Reference [26]. This adjustment is done by normalizing the (k_{ca1c}) value to the experimental value (k_{exp}). This normalization does not affect the inherent bias in the calculation due to very small differences in k_{eff}. To normalize, the following formula applies:

$$k_{norrn}=k_{ca1c}/k_{exp} \quad (1)$$

The normalized k_{eff} values are first tested for trending against several neutronic or physical parameters (Energy of average lethargy of a neutron causing fission [EALF], enrichment, hydrogen to fissile isotope [H/X], and pitch to diameter ratio [P/D]) from each subset using a linear regression fit in order to determine whether a trend does exist and which parameters exhibit the strongest trends. The regression analysis was performed using USLSTATS. Figure 6-106 shows the trend results for EALF for the 187 benchmark set.

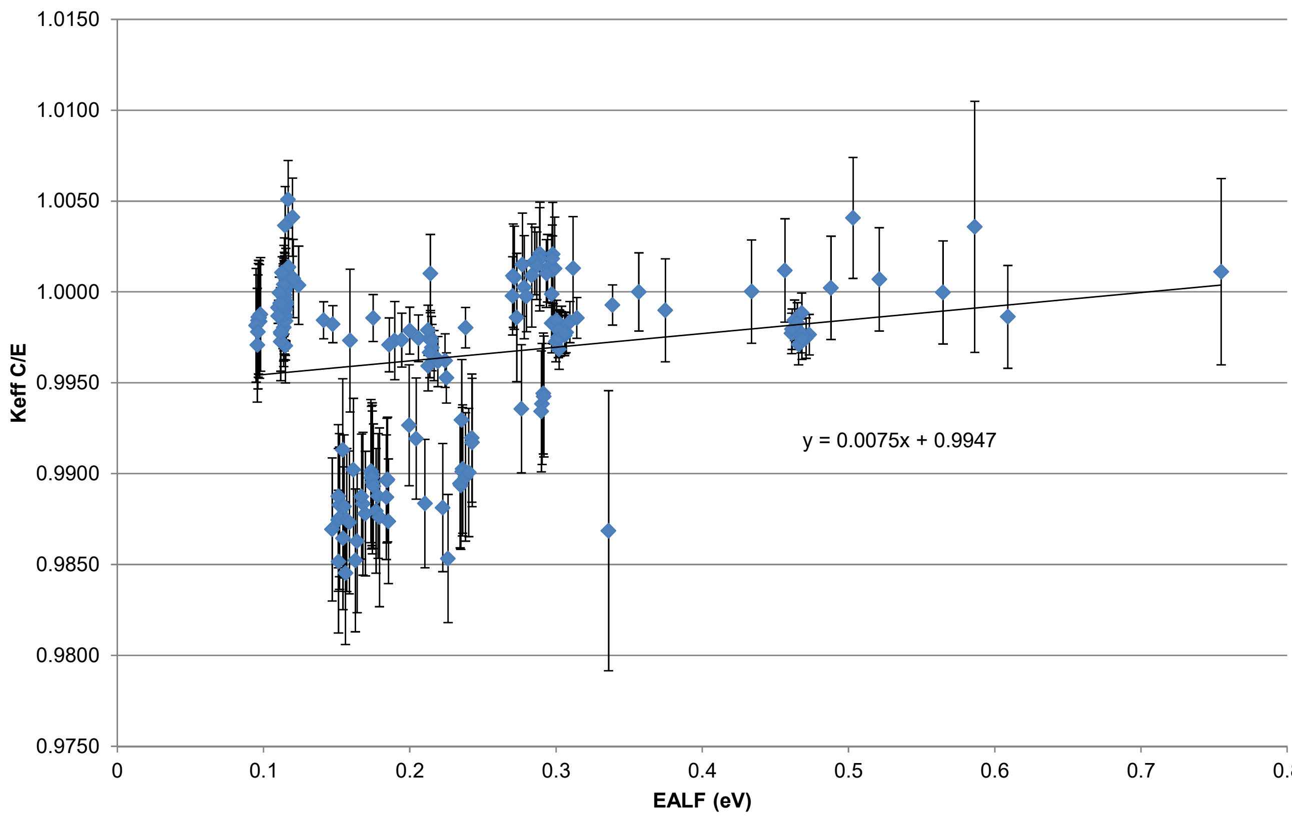

Figure 6-106 Normalized k_{eff} versus EALF trend (187 experiments)

Many techniques can be used to calculate bias and bias uncertainty. Some examples are provided in references [26] and [27]. Care must be taken to ensure that the application of the statistical method meets all assumptions and prerequisites associated with the method. For example, many methods rely on an assumption that the population of critical experiments is normally distributed. If the distribution is not normal, the uncertainty associated with the 95% probability and 95% confidence levels may be significantly in error. Typically, nonparametric methods are used when distribution normality cannot be established.

Neither application model data set follows a normal distribution so a non-parametric technique is used to establish the USLs [26]. A more specific description of the method is presented in [26], resulting in the determination of the degree of confidence that a fraction of the true population of data lies above the smallest value observed. The more data are available in the sample, the higher the degree of confidence. Non-parametric techniques do not require reliance upon distributions, but are rather an analysis of ranks. Therefore, the k_{eff} values in a sample are ranked from the smallest to the largest.

The critical benchmark sample size is 187 for the ATRIUM 11 fuel assembly application model. For this sample population size the rank index for a one-sided distribution-free tolerance limit with 95% confidence that 95% of the population is covered is 4 [37, Table A-31]. For the PWR, type 3 fuel rod application model, the critical benchmark sample size is 154. For this sample population size the rank index for a one-sided distribution-free tolerance limit with 95% confidence that 95% of the population is covered is 3 [37, Table A-31].

For non-parametric data analysis, the USL is determined as follows:

$$USL = K_L - \Delta_{SM} - \Delta_{AOA} \quad (2)$$

where

K_L = Index (4 or 3) k_{eff} value – uncertainty in the index (4 or 3) k_{eff} value – Non-parametric margin (NPM)

K_L = 0.98533 – 0.00353 – 0 = 0.9818 (NPM is 0 because the sample size is not small) (ATRIUM-11 fuel)

K_L = 0.98686 – 0.00771 – 0 = 0.9792 (NPM is 0 because the sample size is not small) (PWR, type 3 fuel)

ΔSM = 0.05, administrative margin to ensure subcriticality

ΔAOA = 0, because extensions are not made to the area of applicability (nonparametric analysis)

The minimum value for the USL is 0.9318 or 0.9292 for the ATRIUM 11 fuel packages or the PWR fuel rod packages, respectively, which includes an administrative margin of 0.05. Because the ATRIUM 10XM fuel rods are limited to 5.0 wt% ^{235}U enrichment, they are bounded by the ATRIUM 11 and PWR loose rod evaluations. Hence the more limiting USL of 0.9292 will be applied to CSI determinations for the ATRIUM 10XM fuel.

6.13.12. *Sample Input Cases*

Example input files are provided in this section. Note that in the Tsunami-IP input file, that the experiment listing is abbreviated due to length.

6.13.12.1. Input for Licensing-Basis HAC Array Model

```
=csas5
TN-B1 container, hac, 8.0woU+4woG, 21 gad rods, assy defined separately
v7-252
read composition

' Mix 1,  Fuel, 8.00 wt% 235U, 98.20 %MTD
  uo2          1 den=10.7627  1         293.00  92235 8.00 92238 92.00  end
' Mix 4,   Fuel, 8.00 wt%235U, 98.20 %MTD, 4.00 wt% Gd2O3
  uo2          4 den=10.6232  9.6000E-1  293.00  92235 8.00 92238 92.00  end
  gd2o3        4 den=10.6232  3.0000E-2  293.00  end
  zr           2           1       293   end
  h2o          3 den=1.00   1       293   end
  h2o          5 den=1.00   1       293   end
  ss304        6           1       293   end
  h2o          7 den=1.00   1       293   end
  polyethylene  8 den=0.28   1       293   end
  polyethylene  9 den=0.56   1       293   end
  atomal2o3    10 0.25 2 13027 2 8016 3 0.49 293   end
  atomsio2     10 0.25 2 14000 1 8016 2 0.51 293   end
```

```
  zr           12           0.31309 293   end
  polyethylene 12 den=0.949  0.68691 293   end
  zr           15           0.31309 293   end
  polyethylene 15 den=0.949  0.68691 293   end
  h2o          17 den=1.00   1       293   end
  zr           15           1       293   end
  polyethylene 18 den=0.949  1       293   end
end composition
read celldata
  latticecell squarepitch
     fuelr=0.4100  1
      gapr=0.420   0
     cladr=0.551  12
    hpitch=0.5975  7 end
  latticecell squarepitch
     fuelr=0.4100  4
      gapr=0.420   0
     cladr=0.551  15
    hpitch=0.5975 17 end
end celldata
read parameter
    gen=10100 npg=50031 nsk=50 htm=no sig=0.0002
end parameter
read geometry
unit 1
 com="container inner box"
 cuboid    6 1    0.0875  -0.0875  225.2  -228.34    8.829   -8.829
 cuboid    0 1   17.713  -17.713   225.2  -228.34    8.829   -8.829
   hole    4 -8.9002   0   0
   hole    5  8.9002   0   0
 cuboid    6 1   17.8    -17.8     225.2  -228.34    8.829   -8.9165
 cuboid   10 1   22.798  -22.798   225.2  -228.34    8.829  -13.839
 cuboid    6 1   22.798  -22.798   225.34 -228.48    8.829  -13.979
 cuboid   10 1   22.798  -22.798   225.34 -233.44    8.829  -13.979
 cuboid    6 1   22.938  -22.938   225.48 -233.58    8.829  -13.979
unit 2
 com="inner box lid"
 cuboid   10 1   22.798  -22.798   229.39 -229.39    2.48    -2.48
 cuboid    6 1   22.938  -22.938   229.53 -229.53    2.62    -2.62
unit 3
 com="inner box with ends and lid"
 array     1      0       0       0
```

```
unit 4
 com="foam polyethylene for left assembly compartment"
 cuboid    0 1   6.8926  -6.8926   225.2  -228.34   6.8926  -6.8926
   hole   80    -6.5725  -192.5    -6.5725
 cuboid    8 1   8.8126  -8.8126   225.2  -228.34   8.829   -6.8926
 cuboid    9 1   8.8126  -8.8126   225.2  -228.34   8.829   -8.829
unit 5
 com="foam polyethylene for right assembly compartment"
 cuboid    0 1   6.8926  -6.8926   225.2  -228.34   6.8926  -6.8926
   hole   70    -6.5725  -192.5    -6.5725
 cuboid    8 1   8.8126  -8.8126   225.2  -228.34   8.829   -6.8926
 cuboid    9 1   8.8126  -8.8126   225.2  -228.34   8.829   -8.829
unit 10
 com="fuel pins w/o gad - lower level"
 ycylinder  1 1  0.4100          155.1       0
 ycylinder  0 1  0.420           155.1       0
 ycylinder  2 1  0.4650          155.1       0
 ycylinder 18 1  0.5510          155.1       0
 cuboid    3 1  0.5975  -0.5975   155.1       0   0.5975  -0.5975
unit 11
 com="fuel pins w/o gad - middle level"
 ycylinder  1 1  0.4100           81.7       0
 ycylinder  0 1  0.420            81.7       0
 ycylinder  2 1  0.4650           81.7       0
 ycylinder 18 1  0.5510           81.7       0
 cuboid    3 1  0.5975  -0.5975    81.7       0   0.5975  -0.5975
unit 12
 com="fuel pins w/o gad - upper level"
 ycylinder  1 1  0.4100          148.2       0
 ycylinder  0 1  0.420           148.2       0
 ycylinder  2 1  0.4650          148.2       0
 ycylinder 18 1  0.5510          148.2       0
 cuboid    3 1  0.5975  -0.5975   148.2       0   0.5975  -0.5975
unit 20
 com="space within fuel assembly lattice - lower level"
 cuboid    3 1  0.5975  -0.5975   155.1       0   0.5975  -0.5975
unit 21
 com="space within fuel assembly lattice - middle level"
 cuboid    3 1  0.5975  -0.5975    81.7       0   0.5975  -0.5975
unit 22
 com="space within fuel assembly lattice - upper level"
 cuboid    3 1  0.5975  -0.5975   148.2       0   0.5975  -0.5975
```

```
unit 40
 com="fuel pins w/ gad - lower level"
 ycylinder  4 1  0.4100           155.1       0
 ycylinder  0 1  0.420            155.1       0
 ycylinder  2 1  0.4650           155.1       0
 ycylinder 18 1  0.5510           155.1       0
 cuboid     3 1  0.5975  -0.5975    155.1       0   0.5975  -0.5975
unit 41
 com="fuel pins w/ gad - middle level"
 ycylinder  4 1  0.4100            81.7       0
 ycylinder  0 1  0.420             81.7       0
 ycylinder  2 1  0.4650            81.7       0
 ycylinder 18 1  0.5510            81.7       0
 cuboid     3 1  0.5975  -0.5975     81.7       0   0.5975  -0.5975
unit 42
 com="fuel pins w/ gad - upper level"
 ycylinder  4 1  0.4100           148.2       0
 ycylinder  0 1   0.420           148.2       0
 ycylinder  2 1  0.4650           148.2       0
 ycylinder 18 1  0.5510           148.2       0
 cuboid     3 1   0.5975  -0.5975   148.2       0   0.5975  -0.5975
unit 50
 com="lower level assembly"
 array     2      0       0       0
unit 51
 com="middle level fuel assembly"
 array     3      0       0       0
unit 52
 com="upper level fuel assembly"
 array     4      0       0       0
unit 60
 com="lower level assembly"
 array    12      0       0       0
unit 61
 com="middle level fuel assembly"
 array    13      0       0       0
unit 62
 com="upper level fuel assembly"
 array    14      0       0       0
unit 70
 com="complete fuel assembly"
 array     5      0       0       0
```

```
 replicate  3 1   0.320    0.320    0.00    0.00    0.320    0.320 1
unit 80
 com="complete fuel assembly"
 array     15       0        0        0
 replicate  3 1   0.320    0.320    0.00    0.00    0.320    0.320 1
unit 400
 com="outer container body and lid"
 cuboid     0 1   35.788  -35.788  247.96  -253.19    31.9    -31.9
   hole     3    -22.938 -229.53   -14.024
 cuboid     6 1   35.963  -35.963  248.135 -253.365   32.075  -32.075
global unit 500
 com="global unit 500 references array 10"
 array     100       0        0        0
 replicate  5 1   30.48    30.48    30.48    30.48    30.48    30.48 1
end geometry
read array
ara=1 nux=1 nuy=1 nuz=2
 fill 1 2  end fill
' 11x11 bottom array with 21 Gd rods, 9 water holes
  ara=2 nux=11 nuy=1 nuz=11
  fill    10 10 10 10 10 10 10 10 10 10 10
          10 10 40 10 10 10 10 10 10 10 10
          10 40 10 10 10 10 10 10 10 10 10
          10 10 10 10 10 10 10 10 10 10 10
          10 10 10 10 20 20 20 10 10 40 10
          10 10 10 10 20 20 20 10 10 40 10
          10 10 10 10 20 20 20 40 40 40 10
          10 10 10 10 10 10 40 40 40 40 10
          10 10 10 10 10 10 40 40 40 40 10
          10 10 10 10 40 40 40 40 40 40 10
          10 10 10 10 10 10 10 10 10 10 10   end fill
' 11x11 middle array with 21 Gd rods, 21 water holes
  ara=3 nux=11 nuy=1 nuz=11
  fill    21 11 11 11 11 11 11 11 11 11 21
          11 11 41 11 11 11 11 11 11 11 11
          11 41 21 11 11 11 11 11 21 11 11
          11 11 11 11 11 21 11 11 11 11 11
          11 11 11 11 21 21 21 11 41 41 11
          11 11 11 21 21 21 21 21 41 41 11
          11 11 11 11 21 21 21 11 41 41 11
          11 11 11 11 11 21 11 11 41 41 11
          11 11 21 11 41 41 41 41 21 41 11
```

```
        11 11 11 11 41 41 41 41 41 41 11
        21 11 11 11 11 11 11 11 11 11 21   end fill
' 11x11 top array with 21 Gd rods, 29 water holes
  ara=4 nux=11 nuy=1 nuz=11
  fill    22 12 12 12 12 12 12 12 12 12 22
        12 12 42 12 12 12 12 12 12 12 12
        12 42 22 12 12 22 12 12 22 42 12
        12 12 12 22 12 22 12 22 12 42 12
        12 12 12 12 22 22 22 12 12 42 12
        12 12 22 22 22 22 22 22 22 42 12
        12 12 12 12 22 22 22 12 42 42 12
        12 12 12 22 12 22 12 22 42 42 12
        12 12 22 12 12 22 42 42 22 42 12
        12 12 42 42 42 42 42 42 42 42 12
        22 12 12 12 12 12 12 12 12 12 22   end fill
  ara=5 nux=1 nuy=3 nuz=1
    fill  52  51  50 end fill
' 11x11 bottom array with 21 Gd rods, 9 water holes
  ara=12 nux=11 nuy=1 nuz=11
  fill    10 10 10 10 10 10 10 10 10 10 10
        10 10 10 10 10 10 10 10 40 10 10
        10 10 10 10 10 10 10 10 10 40 10
        10 10 10 10 10 10 10 10 10 10 10
        10 40 10 10 20 20 20 10 10 10 10
        10 40 10 10 20 20 20 10 10 10 10
        10 40 40 40 20 20 20 10 10 10 10
        10 40 40 40 40 10 10 10 10 10 10
        10 40 40 40 40 10 10 10 10 10 10
        10 40 40 40 40 40 40 10 10 10 10
        10 10 10 10 10 10 10 10 10 10 10   end fill
' 11x11 middle array with 21 Gd rods, 21 water holes
  ara=13 nux=11 nuy=1 nuz=11
  fill    21 11 11 11 11 11 11 11 11 11 21
        11 11 11 11 11 11 11 11 41 11 11
        11 11 21 11 11 11 11 11 21 41 11
        11 11 11 11 11 21 11 11 11 11 11
        11 41 41 11 21 21 21 11 11 11 11
        11 41 41 21 21 21 21 21 11 11 11
        11 41 41 11 21 21 21 11 11 11 11
        11 41 41 11 11 21 11 11 11 11 11
        11 41 21 41 41 41 41 11 21 11 11
        11 41 41 41 41 41 41 11 11 11 11
```

```
        21 11 11 11 11 11 11 11 11 11 21   end fill
' 11x11 top array with 21 Gd rods, 29 water holes
  ara=14 nux=11 nuy=1 nuz=11
  fill    22 12 12 12 12 12 12 12 12 12 22
        12 12 12 12 12 12 12 12 42 12 12
        12 42 22 12 12 22 12 12 22 42 12
        12 42 12 22 12 22 12 22 12 12 12
        12 42 12 12 22 22 22 12 12 12 12
        12 42 22 22 22 22 22 22 22 12 12
        12 42 42 12 22 22 22 12 12 12 12
        12 42 42 22 12 22 12 22 12 12 12
        12 42 22 42 42 22 12 12 22 12 12
        12 42 42 42 42 42 42 42 42 12 12
        22 12 12 12 12 12 12 12 12 12 22   end fill
  ara=15 nux=1 nuy=3 nuz=1
    fill  62  61  60 end fill
  ara=100 nux=9 nuy=1 nuz=9
    fill F400  end fill
end array
read bnds
 all=vacuum
end bnds
end data
end
```

6.13.12.2. INPUT FOR TSUNAMI-IP FILE

```
=shell
copy     C:\Users\jscaglione\runs\TN-B1\Mueller_copy-3-15-2022\sens_calcs\HAC80w15r6wc_4x1x5_varmesh03.sdf
scale6-3d_k6-1.sdf
end
=tsunami-ip
Similarity Assessment and Uncertainties, ATRIUM HAC
read parameter
  coverx=44groupcov
  cov_fix
  udcov_corr_type=zone
  udcov_fast=0.4
  udcov_inter=0.2
  udcov_therm=0.05
  use_dcov
  udcov=0.05
  use_icov
  uncert
```

```
  uncert_long
  c
  c_long
  cr
  cr_long
  html
  plot
  inptcase
  prtcomp
  usename
  values
end parameter
read applications
  scale6-3d_k6-1.sdf
end applications
read exps
...

end exps
read covariance
end covariance
read reactions
'  u-234 total
  u-235 total
'  u-236 total
  u-238 total
'  pu-238 total
'  pu-239 total
'  pu-240 total
'  pu-241 total
'  pu-242 total
'  np-237 total
'  am-241 total
'  am-243 total
  h-1 scatter
  h-1 capture
  o-16 total
  b-10 total
'  sm-149 total
'  nd-143 total
'  rh-103 total
'  sm-151 total
'  cs-133 total
  gd-155 total
'  sm-152 total
end reactions
read html
  bg_clr=papayawhip
  h1_clr=maroon
  h2_clr=navy
  txt_clr=black
  lnk_clr=mediumorchid
'  lnk_dec=underline
```

```
  vlnk_clr=green
  max_clr=blue
  cut_clr=red
end html
end
```

6.14. FILE LISTING

File listing is located in text file *File_List*.

6.15. REFERENCES

1. Davis, J. K., “RAJ-II Shipping Container Test”, Document Identifier 51-5032941-000, September 10, 2003.
2. Bierman, S.R., Durst, B. M., Clayton, E.D., “Critical Separation Between Subcritical Clusters of 4.29 Wt% U-235 Enriched UO_2 Rods in Water With Fixed Neutron Poisons,” Battelle Pacific Northwest Laboratories, NUREG/CR-0073(PNL-2695).
3. Dean, V.F., Evaluator, “Water-Moderated U(4.31)O_2 Fuel Rods in 2.54-cm Square- Pitched Arrays,” International Handbook of Evaluated Criticality Safety Benchmark Experiments,” NEA/NSC/DOC(95)03, Sept 2001, Nuclear Energy Agency.
4. Newman, L.W., “Urania Gadolinia: Nuclear Model Development and Critical Experiment Benchmark,” Babcock & Wilcox for DOE, DOE/ET/34212-41, BAW-1910, April 1984.
5. Newman, L.W., “Development and Demonstration of An Advanced Extended-Burnup Fuel Assembly Design Incorporating Urania-Gadolinia,” Babcock & Wilcox for DOE, DOE/ET/34212-41, BAW-1681-2, August 1982.
6. American National Standard for Nuclear Criticality Safety in Operations with Fissionable Materials Outside Reactors, ANSI/ANS-8.1-1998.
7. Lichtenwalter, J. J., Bowman, S. M., DeHart, M. D., and Hopper, C. M., Criticality Benchmark Guide for Light-Water-Reactor Fuel in Transportation and Storage Packages, NUREG/CR-6361, ORNL/TM-13211, U. S. Nuclear Regulatory Commission.
8. SCALE Standardized Computer Analyses for Licensing Evaluation, NUREG/CR-2000.

   ORNL/NUREG/CSD-2, Volumes 1, 2, and 3.
9. Baldwin, M.N. et al., Critical Experiments Supporting Close Proximity Water Storage of Power Reactor Fuel, BAW-1484-7, July 1979.
10. Hovler, G.S. et al., Critical Experiments Supporting Underwater Storage of Tightly Packed Configurations of Spent Fuel Pins, BAW-1645-4, November, 1981.
11. Transactions of the American Nuclear Society, Dissolution and Storage Experimental Program with U[4.75]O_2 Rods, Vol. 33, pg. 362.

12. Harding, R.S., Validation Report – SCALEPC-44A Consolidation Experiments, FANP Doc. 32-5012897-00.
13. Ao, Qi., GEH Criticality Safety Analysis – Shipment of Loose Rods in RAJ-II Shipping Container, Rev. 01, Doc, November 1, 2007.
14. GEMER Monte Carlo Validation Report: RA-3/RAJ-II Shipping Containers, rev. 0, Qi Ao, November, 2007.
15. Scale: A Comprehensive Modeling and Simulation Suite for Nuclear Safety Analysis and Design, ORNL/TM-2005/39, Version 6.1, Oak Ridge National Laboratory, June 2011.
16. Regulatory Guide 7.9, Standard Format and Content of Part 71 Applications for Approval of Packages for Radioactive Material, Rev. 2, March 2005, US Nuclear Regulatory Commission.
17. International Handbook of Evaluated Criticality Safety Benchmark Experiments (ICSBEP), NEA/NSC/DOC(95)03, NEA Nuclear Science Committee, September 2015.
18. Dean, J. C., Tayloe, Jr., R. W., Guide for Validation of Nuclear Criticality Safety Calculational Methodology, NUREG/CR-6698, U. S. Nuclear Regulatory Commission.
19. Calculation FS1-0015328, Rev. 2, Structural Analyses of the AREVA Atrium-11 LTA Fuel Assembly in the RAJ-II Container during Normal and Accident Transport Conditions.
20. FS1-0029527 Revision 1.0, "AREVA TN-B1 Docket No. 71-9372 Safety Analysis Report Supplement," AREVA, November 2016.
21. FS1-0027837 Revision 6.0, "Criticality Analysis for the TN-B1 Shipping Container with the ATRIUM-11 Fuel Design," Framatome, January 2022.
22. E04-10-004, Version 1.0, "TN-B1 Sensitivity Studies," Framatome, December 2021.
23. Certificate of Compliance, No. 9372, Rev. 3 for Package USA/9372/B(U)F-96, U. S. Nuclear Regulatory Commission, August 10, 2022.
24. W. A. Wieselquist, R. A. Lefebvre, and M. A. Jessee, Eds., "SCALE Code System", ORNL/TM-2005/39, Version 6.2.4, Oak Ridge National Laboratory, Oak Ridge, TN, April 2020.
25. B. Flanagan, "Framatome TN-B1, Docket No. 71-9372, Safety Analysis Report", FS1-0014159, Rev. 10.0, Framatome, January 27, 2022.
26. Dean, J.C. and Tayloe Jr., R.W., "Guide for Validation of Nuclear Criticality Safety Calculational Methodology," NUREG/CR-6698, prepared for the U.S. Nuclear Regulatory Commission by Science Applications International Corporation, January 2001.
27. J. J. Lichtenwalter, S. M. Bowman, M. D. DeHart, and C. M. Hopper, "Criticality Benchmark Guide for Light-Water-Reactor Fuel in Transportation and Storage Packages", NUREG/CR-6361 (ORNL/TM-13211), prepared for the US Nuclear Regulatory Commission by Oak Ridge National Laboratory, Oak Ridge, Tenn., March 1997.

28. Title 10, “Energy”, Code of Federal Regulations, Part 71, “Packaging and Transportation of Radioactive Material.”
29. “Standard Format and Content of Part 71 Applications for Approval of Packages for Radioactive Material”, Regulatory Guide 7.9, Revision 2, U. S. Nuclear Regulatory Commission, March 2005.
30. “Standard Review Plan for Transportation Packages for Spent Fuel and Radioactive Material”, NUREG-2216, U. S. Nuclear Regulatory Commission, August 2020.
31. Orano Federal Services Calculation, SD-SCALE-6.2.4-CALC-3023904, “Software Dedication Report for SCALE 6.2.4”, Revision 0.
32. “Department of Energy Fundamentals Handbook”, DOE-HDBK-1019/1-93 and DOE-HDBK-1019/2-93 (2 volumes), Nuclear Physics and Reactor Theory, January 1993.
33. Orano Federal Services Design Basis Requirements Document (DBRD), “Design Basis Requirements for License Evaluation for TN-B1 SAR”, DBR-3024178, Orano Federal Services, March 26, 2021.
34. 2021-02-26-SCALE User Notice Rev 3, “SCALE h1-poly incoherent elastic scattering can cause k-eff under prediction approaching 1% in criticality problems with polyethylene as the primary moderator,” published on February 26, 2021. Downloaded from https://www.ornl.gov/content/scale-v624, on May 4, 2021.
35. 2021-03-01-SCALE User Notice Rev. 14, “Memory error with SCALE 3D general geometry package leading to an incorrect model when shapes are truncated by CHORDs,” published April 1, 2021. Downloaded from https://www.ornl.gov/content/scale-v624, on May 4, 2021.
36. H. R. Dyer and C. V. Parks, “Recommendations for Preparing the Criticality Safety Evaluation of Transportation Packages,” NUREG/CR-5661 (ORNL/TM-11936), prepared by Oak Ridge National Laboratory for the U. S. Nuclear Regulatory Commission, Oak Ridge, TN., April 1997.
37. NEA/NSC/DOC(95)03, International Handbook of Evaluated Criticality Safety Benchmark Experiments, Nuclear Energy Agency, July 2019.
38. B. L. Broadhead et al., Sensitivity- and Uncertainty-Based Criticality Safety Validation Techniques, Nuclear Science and Engineering 146, pages 340-366, March 2004.
39. Natrella, M.G. 1963. Experimental Statistics. National Bureau of Standards Handbook 91. Washington, D.C.: U.S. Department of Commerce, National Bureau of Standards. https://nvlpubs.nist.gov/nistpubs/Legacy/hb/nbshandbook91.pdf.

7. PACKAGE OPERATIONS

This chapter provides general instructions for loading and unloading and operation of the TN-B1 package. Specific detailed procedures based on and consistent with this application are used for the operation of the package. These procedures are maintained by the user of the package and may provide additional detail regarding the handling and operation of the package. Due to the low specific activity and low abundance of gamma emitting radionuclides, dose rates from the contents of the package when used as a Type A or Type B package are minimal. As a result of the low dose rates, there are no special handling requirements for radiation protection.

7.1. PACKAGE LOADING

This section delineates the procedures for loading a payload into the TN-B1 packaging. Hereafter, reference to specific TN-B1 packaging components may be found in Appendix 1.4.1.

7.1.1. *Preparation for Loading*

Prior to loading the TN-B1 with fuel, the packaging is inspected to ensure that it is in unimpaired physical condition. The inspection looks for damage, dents, corrosion, and missing hardware. Acceptable conditions are defined by the drawings in Section 1.4.1 as described in Section 8.2.5. Acceptance criteria and detailed loading procedures derived from this application are specified in user written procedures. These user procedures are specific to the authorized content of the package. Since the primary containment is the sealed fuel rod, radiation and contamination surveys are not required prior to loading. There is no required moderator, neutron absorbers or gaskets that require testing or inspection.

Defects that require repair will be fixed prior to shipping in accordance with approved procedures consistent with the quality program.

When used as a Type B package, verification that the primary containment (i.e., fuel rods have been leak checked) will be performed prior to shipping.

7.1.2. *Loading of Contents*

7.1.2.1. Outer Container Lid Removal

1. Remove the lid bolts.
2. Attach slings to the four lid lift attachment points on the lid.
3. Remove the outer lid.

7.1.2.2. Inner Container Removal

1. Release the inner clamp by removing the eight clamp bolts.

2. Remove the inner container from the outer container, and move it onto the packing table. Ensure that the inner container is lifted using the inner container handles and not the inner container lid handles.
3. Remove the bolts of the inner container lid and take the lid off.

7.1.2.3. **Loading Fuel Assemblies into the TN-B1**

1. Clamp the inner container body to the packing table or up righting device, and remove the end lid.
2. Ensure that the following preparation work for packing has been completed if required.
    a. The separators have been inserted.
    b. The finger spring protectors have been attached.
    c. The foam has been put in place.
    d. The fuel assemblies have been covered with poly bags.
3. Stand the packing table upright. (The inner container body is fixed with clamps.)
4. Lift one fuel assembly and pack it in the inner container.
5. After packing one fuel assembly into the inner container, fit the securing fixtures of the fuel assembly. Then pack the other fuel assembly in the inner container
6. Lower the packing table back to the horizontal position from the upright position.
7. Attach the end lid of the inner container.
8. Check to ensure that the fuel assemblies are packaged in the container properly.
9. Attach the inner container lid and tighten the bolts securely (wrench tight or as defined in user procedures).
10. Place the inner container into the outer container.
11. Put on hold down clamps and tighten bolts.
12. Place the outer container lid on the package, and tighten the bolts securely (wrench tight or as defined in user procedures).
13. Install tamper-indicating devices on the outer container ends.

7.1.2.4. **Loading Loose Rods in the Protective Case into the TN-B1**

1. Insert poly endcap spacers over each end or the fuel rod endcap (optional).
2. Sleeve (optional) each rod to be packed with a maximum of 5 mil polyethylene sleeve/tubing.
3. Insert up to 30, 11x11 or 10x10 design rods, 26, 9x9 design rods or 22, 8x8 design rods into the protective case and fill any empty space with empty tubing.

4. Place cushioning foam pads in protective case as needed to prevent sliding during shipment (optional).
5. Close the protective case and tighten bolts wrench tight.

7.1.2.5. **Loading the Protective Case into the TN-B1**

1. Loose rods may be loaded in the protective case while either in the inner container or while removed from the inner container.
2. After packing the protective case(s) into the inner container, fit the securing fixtures for the case.
3. Check to ensure that the protective cases are packaged in the container properly.
4. Attach the inner container lid and tighten the bolts securely (wrench tight or as defined in user procedures).
5. Put on hold down clamps and tighten bolts.
6. Place the outer container lid on the package, and tighten the bolts securely (wrench tight or as defined in user procedures).
7. Install tamper-indicating devices on the outer container ends.
8. It is allowable to ship only one protective case in an TN-B1 inner.

7.1.2.6. **Loading Loose Rods in the 5-Inch Stainless Steel Pipe into the TN-B1**

1. Sleeve (optional) each rod to be packed with a maximum of 5 mil polyethylene sleeve/tubing. The ends of the sleeves should be closed in a manner such as knotting or taping with the excess polyethylene trimmed away.
2. Place a cushioning foam pad in the capped end of the pipe (optional).
3. Insert up to 30, 11x11 or 10X10 design rods, 26, 9x9 design rods or 22, 8x8 design rods into the pipe and fill the empty space with empty zircaloy tubing with welded end plugs on both ends.
4. Place cushioning foam pads against the rod ends to block the rods from sliding during shipment (optional).
5. Close pipe with end cap.
6. Lift each 5-inch stainless steel pipe and pack it in the inner container.
7. Check to ensure that the 5-inch stainless steel pipe(s) is packaged in the container properly.
8. Attach the inner container lid and tighten the bolts securely (wrench tight or as defined in user procedures).
9. Place the outer container lid on the package, and tighten the bolts securely (wrench tight or as defined in user procedures).

10. Install tamper-indicating devices on the outer container ends.
11. It is allowable to ship one or two 5-inch pipes containing rods in an TN-B1 inner.

7.1.2.7. Loading Loose Rods (25 Maximum Per Side) into the TN-B1

1. Sleeve (optional) each rod to be packed with a maximum of 5 mil polyethylene sleeve/tubing. The ends of the sleeves should be closed in a manner such as knotting or taping with the excess polyethylene trimmed away.
2. When only one rod per side is to be packed, no clamps are required. Block the rod in the lower corner of the container by evenly spacing 10 or more notched foam pads the length of the rod.
3. When 2 rods up to a maximum of 25 rods are to be packed, banding with steel clamps is not required for criticality safety purposes. If banding is chosen, position 10 or more open steel clamps evenly in each side of the inner container in which loose rods are place.
4. Place foam pads on top of the open clamps, lay the rods on top of the foam.
5. Close and tighten the clamps so the foam surrounds the array of rods. Tighten each clamp until the foam collapses slightly.
6. Place foam pads against the ends of the rods, above the rods and beside the rods to block the rods from moving during shipment.
7. Repeat the above steps for the other side of the inner container, if required.
8. Fill each side (if used) with foam pads so as to minimize movement during shipment.
9. Attach the inner container lid and tighten the bolts securely (wrench tight or as defined by user procedure).
10. Place the outer container lid on the package, and tighten the bolts securely (wrench tight as defined by user procedure).
11. Install tamper-indicating devices on the outer container ends.

7.1.3. *Preparation for Transport*

When used as a type B package leak testing of the rods (primary containment) is performed during the manufacturing process. Verification of successful leak testing is done prior to shipment. There are no surface temperature measurements required for this package.

Procedure: (These steps may be performed in any sequence.)

1. Complete the necessary shipping papers in accordance with Subpart C of 49 CFR 172.
2. Ensure that the TN-B1 package markings are in accordance with 10 CFR 71.85(c) and Subpart D of 49 CFR 172. Package labeling shall be in accordance with Subpart E of 49CFR 172. Package placarding shall be in accordance with Subpart F of 49 CFR 172.
3. Survey the surface of the package for potential contamination and dose rates.

4. Transfer the package to the conveyance and secure using tie-downs secured to the package.

7.2. PACKAGE UNLOADING

7.2.1. *Receipt of Package from Carrier*

Radiation and contamination surveys are performed upon receipt of the package and the packages are inspected for significant damage. There are no fission gases, coolants or solid contaminants to be removed.

7.2.2. *Removal of Contents*

After freeing the tie downs, the TN-B1 package is lifted from the carrier either by fork lift or by the use of lifting slings placed around the package. If lifted by forklift, the forks are placed at the designated lift locations and the package is lifted. If slings lift the package, a sling is placed under each end of the package at the lifting angles that prevent the sling from sliding. Care should be taken to ensure that the slings are placed in the correct location depending on whether the package is loaded or empty.

7.2.2.1. Outer Container Lid Removal

1. Remove the lid bolts.
2. Attach slings to the four sling fittings on the lid.
3. Remove the outer lid.

7.2.2.2. Inner Container Removal

1. Release the inner clamp by removing the eight clamp bolts.
2. Remove the inner container from the outer container, and move it onto the packing table. Ensure that the inner container is lifted using the appropriate inner container handles and not the inner container lid handles.
3. Remove the bolts of the inner container lid and take the lid off.

7.2.2.3. Unloading Fuel Assemblies from the TN-B1

1. Clamp the inner container body to the packing table or up righting device, and remove the end lid.
2. Stand the packing table upright. (The inner container body is fixed with clamps.)
3. Attach the lifting device to the assembly and remove the securing fixture.
4. Lift one fuel assembly at a time from the package.
5. Repeat for other assembly.

7.2.2.4. Removing / Unloading Protective Case or 5-Inch Stainless Steel Pipe from the TN-B1

1. Remove the outer container and inner container lids as described in Sections 7.2.2.1 and 7.2.2.2.
2. The inner container may be removed or left in place while removing the protective case or 5- inch pipe.
3. Remove the 5-inch stainless steel pipe with a sling or remove the cover from the protective case.
4. Remove the rods from the 5-inch pipe or protective case.

7.3. PREPARATION OF EMPTY PACKAGE FOR TRANSPORT

Empty TN-B1's are prepared and transported per the requirements of 49 CFR 173.428. Prior to shipping as an empty TN-B1, the packaging is surveyed to assure that contamination levels are less than the 49 CFR 173.433(a) limit. The TN-B1 is visually verified as being empty. The packaging is inspected to assure that it is in an unimpaired condition and is securely closed so that there will be no leakage of material under conditions normally incident to transportation. Any labels previously applied in conformance with subpart E of part 172 of this subchapter are removed, obliterated, or covered and the "Empty" label prescribed in 49 CFR 172.450 of this subchapter is affixed to the packaging.

7.4. OTHER OPERATIONS

The following are considered normal routine maintenance items and do not require QA or Engineering evaluation for replacement. Material must be of the same type as original equipment parts.

a. Wooden Bolster Assemblies

b. Bolster Bolting

c. Delrin Inserts

d. Polyethylene Container Guides

e. Gaskets

f. Shock Absorbers (Paper Honeycomb)

g. Fork Pocket Rubber Protective Pads

h. Outer Container Stopper #2 (Rubber Pad)

i. Safety Walk

j. Plastic Plugs

k. Lid Tightening Bolts (Outer, Inner and End Lid)

l. Inner Container End Face Lumber (Upper)

m. Inner Container End Face Lumber (Lower “Y” Block)

n. Inner Container Polyethylene Foam

o. Inner Container Rubber (cushioning material)

p. Heliserts

When deviations to items other than those listed above are identified, the TN-B1 shall be removed from service, and the item(s) shall be identified as non-conforming material, and dispositioned in accordance with written procedures including the 10 CFR 71, Subpart H approved QA Plan.

7.5. APPENDIX

No additional information is required. Loading and unloading this package is a relatively simple and routine operation. The weights, contamination levels and radiation dose rates do not impose significant hazards or operations outside normal material handling.

Note: The regulatory references provided, such as 49 CFR and 10 CFR, are the current requirements. If regulatory references change, the new references are applicable. This applies throughout the SAR.

8. ACCEPTANCE TESTS AND MAINTENANCE PROGRAM

8.1. ACCEPTANCE TESTS

Per the requirements of subpart G of 10 CFR 71, this section discusses the inspections and tests to be performed prior to first use of the TN-B1. The TN-B1 is manufactured under a Quality Assurance Program meeting the requirements of 10 CFR 71 subpart H.

8.1.1. *Visual Inspections and Measurements*

Prior to the first use of the TN-B1 for the shipment of licensed material, the TN-B1 will be inspected to ensure that it is conspicuously and durably marked with its model number, serial number, gross weight and package identification number assigned by NRC. Prior to applying the model number, it will be determined that the TN-B1 was fabricated in accordance with the drawings reference in the NRC Certificate of Compliance. Critical dimensions related to quality are called out in the Appendix 1.4.1 drawings as Critical to Quality (CTQ). Data for these dimensions is recorded and verified in accordance with the quality plan. Documentation of these measurements is compiled in a data pack. This data pack will be checked for completeness for each TN-B1 as part of the acceptance program. TN-B1's are inspected to ensure that there are no missing parts (nuts, bolts, gaskets, plugs, etc.) or components and that there is no shipping damage on receipt.

8.1.2. *Weld Examinations*

TN-B1 packaging materials of construction and welds shall be examined in accordance with the requirements delineated on the drawings in Appendix 1.4.1, per the requirements of 10 CFR 71.85(a). This includes 100% liquid penetrant examination of the specified areas of the first ten (10) production units. (Note that the first 10 TN-B1 production units were manufactured as RAJ-II units in 2004 and had the required 100% liquid penetrant examination performed on them, no other production units require liquid penetrant testing.)

The non-destructive examination personnel qualification and certification shall be in accordance with either The American Society for Non-destructive Testing (ASNT) SNT-TC-1A (recommended practice) or Japanese Society for Non-destructive Inspection (JSND) Japanese Industrial Standard (JIS) JIS Z 2305 latest revision.

Subsequent production units will be tested as defined in the manufacturing quality plan.

8.1.3. *Structural and Pressure Tests*

The TN-B1 is not pressurized and is structurally the same to the test units. There are no additional structural or pressure tests required.

8.1.4. *Leakage Tests*

No leak tests of the packaging are required. The fuel rod weld joints are examined at the time of fuel fabrication and leak tested to ensure they are sealed. The welding and leak testing of fuel rods is performed during manufacturing using a qualified process. This process assures that the fuel is acceptable for use in a nuclear reactor core and is tightly controlled. The acceptable leak rate is less than $1x10^{-7}$ atm-cc/s. The inner and outer container are not relied on for containment, and do not require leak testing.

8.1.5. *Component and Material Tests*

The TN-B1 packaging does not contain gaskets that perform a safety function or pressure boundary, and as such, do not require testing. The packaging does not contain neutron absorbers that would require testing. No component tests are required.

Material testing or certifications from the suppliers of material for this container must show compliance to the properties found in Tables 2-2 and 2-3, or to other properties that satisfactorily indicate compliance to the properties found in these tables and that are approved by the licensee.

8.1.6. *Shielding Tests*

The TN-B1 packaging does not contain shielding and therefore shielding tests are not required.

8.1.7. *Thermal Tests*

The alumina silicate thermal properties will be assured by procuring this material with a certified pedigree. This procurement is done consistent with the QA program.

8.1.8. *Miscellaneous Tests*

There are no additional or miscellaneous tests are required prior to the use of the TN-B1 packaging.

8.2. MAINTENANCE PROGRAM

8.2.1. *Structural and Pressure Tests*

Prior to each use of the TN-B1, the packaging is visually inspected to assure that the packaging is not damaged and that the components parts are in place. The packagings are constructed primarily from stainless steel making it corrosion resistant. Since the packaging is not relied on for containment, there are no pressure test requirements for the inner or outer containers that comprise the packaging. When used as a Type B package, each fuel rod is leak checked and the successful results of the test are checked before shipment.

The TN-B1 packaging is maintained consistent with a 10 CFR 71 subpart H QA program. Packagings that do not conform to the license drawings are removed from service until they are brought back into compliance. Repairs are performed in accordance with the approved procedures and consistent with the quality assurance program.

8.2.2. *Leakage Tests*

Containment is provided by the fuel rod for Type B shipments. The fuel rods are manufactured under a Quality Assurance program meeting the requirements of 10 CFR 71 Subpart H. Welds of the fuel rod end caps to the cladding arte conducted under a qualified process and verified for integrity using approved inspection procedures performed by qualified inspection personnel. There are no penetrations in the fuel cladding when shipped. The fuel cladding after loading with the pellets is pressurized with helium and the end plugs are welded on to close the rod. These welds are designed to with stand the rigorous operating environment of a nuclear reactor.

For 11x11 fuel rods, the closure weld process qualification includes the following: (1) transverse metallographic samples of the welds, upon examination of the samples a single discontinuity >0.005 inch is not permitted along the solid state bond line in the plane of polish and the sum of all discontinuities along the solid state bond line shall be ≤0.010 inch along the solid state bond line in the plane of the polish; and (2) meet the in-process inspections listed below. The critical parameters for welding; current, cladding tube extension, and electrode force are established during the weld qualification process.

For 11x11 fuel rods, the following in-process inspections are performed: (1) visual inspection of each completed weld to verify that the surface is free of folds, holes, cracks, porosity, and inclusions at a minimum of 1X magnification; (2) burst testing, per Framatome's proprietary burst testing procedure of representative welds, on cladding samples shall be conducted at room temperature during initial weld parameter qualification and on in-process samples during production. The burst strength shall be ≥ 17,400 psi (≥ 1,200 bar) and failure shall not occur along the solid state bond line at the original interface between the cladding and end cap. The failure location will be determined by visual inspection of the burst tested sample. Visual standards may be used to determine the failure location. Rod inspection requirements specified in the Product Specification (Reference 1) applicable to the containment boundary include 100% dimensional inspections to the applicable drawing (example, Reference 2), 100% helium leak check and initial fill pressure.

Burst test frequency for each welder will be as follows:

- Five consecutive at the beginning of the contract
- One after each repair or change of the welding machine that may impact the process
- One after interruption for more than twenty-four (24) hours
- One for every approximately 350 rods during the contract (367 rods maximum between tests).
- One at the end of the contract.

The critical parameters for welding; current, cladding tube extension, and electrode force are monitored and recorded for each weld.

Each completed fuel rod (of any design) is helium leak tested after fabrication to demonstrate that it is leak tight (<1x10^{-7} atm-cc/s). Neither the inner or outer container is credited with providing leak protection. Therefore no leak test of the packaging is required.

8.2.3. *Component and Material Tests*

There are no prescribed component tests or replacement requirements for this packaging. The packaging does not use neutron absorbers or shielding that would require testing or maintenance.

8.2.4. *Thermal Tests*

The alumina silicate thermal material is sealed within the stainless steel plates of the container wall. The packaging is visually inspected prior to use to assure that the alumina silicate is contained.

8.2.5. *Miscellaneous Tests*

There are no additional or miscellaneous tests are required for the use of this packaging. The TN-B1 packaging is inspected prior to each use and maintained consistent with the license drawings. The package is inspected to verify that the package remains within the tolerances specified on the drawings in Section 1.4.1. As noted on the drawings localized deformation in the shell is permitted up to 25mm if the internal structure of the package remains within tolerance. The packaging is repaired in accordance with drawings found in Section 1.4.1.

Foam cushioning material may have up to 2% of the total volume removed for packing purposes, handling or as a result of tears or punctures to the foam.

Small dents, tears and rounding of corners on paper honeycomb are acceptable providing the area is less than 2%. The corners of the individual pieces of paper honeycomb may be rounded to approximately a radius of 3 inches.

8.3. APPENDIX

No appendix for this section

8.4. REFERENCES

1. FS1-0019890 Revision 1.0, “Upset Shape Welded BWR Fuel Rod Assemblies” AREVA, February 2015.
2. FS1-0011596 Revision 2.0, “3-Segment Fuel Rod Assembly” AREVA, March 2014.